

# QUANTUM CHEMISTRY

---

THE STATE  
OF THE ART

---

ATLAS

# QUANTUM CHEMISTRY

---

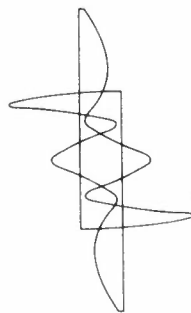
## THE STATE OF THE ART

---

PROCEEDINGS OF SRC ATLAS SYMPOSIUM No 4  
HELD AT  
ST CATHERINE'S COLLEGE OXFORD 8-10 APRIL 1974

EDITED BY

**V R SAUNDERS** AND **J BROWN**



**Copyright © Science Research Council  
and individual authors 1975**

**Published July 1975**

**Set on IBM composer in 10pt Press Roman  
and printed by Imediaprint Limited 01-253 6373**

**The Science Research Council does not accept any  
responsibility for loss or damage arising from the  
use of information contained in any of its reports or  
in any communication about its tests or investigations**

# Preface

The symposium 'Quantum Chemistry – The State of the Art' was sponsored and organized by the Science Research Council's Atlas Computer Laboratory as 'SRC Atlas Symposium No 4' and held at St. Catherine's College, Oxford, on 8-11 April 1974. The programme consisted of some forty papers presented to an international audience of approximately 100 scientists. The scope of the programme was deliberately kept as broad as possible, and covered the range of molecular scattering theory, correlated wavefunctions and Hartree-Fock theory and applications. It is our hope that the meeting provided a useful way of drawing together experts in each of these three important aspects of theoretical chemistry.

For the success of the meeting our thanks must first go to the director of the Atlas Computer Laboratory, Dr. J. Howlett CBE, for allowing the meeting to be the subject of the fourth Atlas symposium, and for allowing the administration group of the laboratory to be used for organizational purposes, and to Mr. C.L. Roberts MBE, head of the administration group, whose sound practical advice was always most welcome.

It is a particular pleasure to acknowledge the assistance rendered by Mrs. C. Davis, who acted as conference secretary, and to Miss E.S. Butler whose perfectionism has played such a vital part in the production of the present volume. Finally, our debt to Miss C. Brown of Imediaprint Limited must not be left unacknowledged. She has been responsible for the typesetting of the entire volume, an arduous task which has been completed with painstaking attention to detail from copy remarkable for its 'variable' quality.

V.R. Saunders  
J. Brown

Atlas Computer Laboratory  
Chilton Didcot Oxfordshire OX11 0QY

May 1975

# CONTENTS

## Scattering Theory

		Page
Review Notes on Molecular Scattering Theory	<i>M.S. Child</i>	1
Application of the Correspondence Principle to Vibrational and Rotational Excitation	<i>D. Richards</i>	3
Semiclassical Methods in Reactive and Non-reactive Collisions (not reproduced)	<i>W.H. Miller</i>	13
Canonical Integrals in Semiclassical Collision Theory	<i>J.N.L. Connor</i>	15
Cross Sections for the Rotationally Inelastic Scattering of $Ne + N_2$ : Application of the Exponential Semi-Classical Distorted Wave Approximation (Preliminary Results)	<i>S. Bosanac</i> <i>G.G. Balint-Kurti</i>	19
Proton-Molecule Collisions: Interacting Potentials and Inelastic Scattering	<i>F.A. Gianturco</i>	25
A Critical Look at Conjectures in the Theory of Autoionizing States of Atoms	<i>C.S. Sharma</i>	31
Experimental Results on Initial Energy Distributions in Simple Atom-Molecule Reactions Producing Hydrogen Fluoride	<i>P. Beadle</i> <i>N. Jonathan</i> <i>S. Okuda</i>	37
Procedure for Averaging Differential Cross Sections over the Experimental Angular Resolution	<i>S. Bosanac</i> <i>G.G. Balint-Kurti</i>	43
A Theoretical Study of Vibrational Self-Relaxation Rates of $HF$	<i>K. Smith</i> <i>M.J. Conneely</i> <i>A.R. Davies</i>	49
Reaction Pathways for the Triplet Methylene Abstraction $CH_3(^3B_1) + H_2 \rightarrow CH_3 + H$	<i>C.W. Bauschlicher, Jr.</i> <i>H.F. Schaefer III</i> <i>C.P. Baskin</i> <i>C.F. Bender</i>	57

## Correlated Wavefunctions

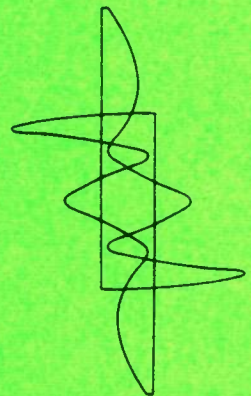
Computation of Correlation Energies of Closed Shell Systems. The Dimerization Energies of $BH_3$ and $LiH$	<i>R. Ahlrichs</i>	65
Quantum Chemistry and Dynamics: Connections with Experiment	<i>A.C. Wahl</i>	73

	Page
On the Direct Configuration Interaction Method from Molecular Integrals	<i>P. Siegbahn</i> 81
Electron Correlation in <i>BH</i> and <i>H<sub>4</sub></i> : A Numerical Comparison of Various Methods	<i>G.A. van der Velde</i> <i>W.C. Nieuwpoort</i> 87
Investigations of Molecular Electronic Structure using Spin Optimised Self Consistent Field Wavefunctions	<i>N.C. Pyper</i> <i>J. Gerratt</i> 93
Molecular Spectroscopic Constants by the Coupled Electron Pair Approach	<i>W. Meyer</i> 97
Calculation of Electron Affinities of Atoms in the Second Long Row	<i>C. Moser</i> <i>R.K. Nesbet</i> 101
Configuration Interaction by the Method of Bonded Functions: Some Preliminary Calculations	<i>G.H.F. Diercksen</i> <i>B.T. Sutcliffe</i> 103
Self Consistent Groups in Molecular Wavefunctions – An Effective Hamiltonian with Applications to Some Simple Systems	<i>S. Wilson</i> <i>J. Gerratt</i> 109
Studies in the Pair Replacement MC-SCF and Strongly Orthogonal Geminal Theories	<i>V.R. Saunders</i> <i>M.F. Guest</i> 119
Numerical Solution of First-Order Correlation Equations for Atoms	<i>C.S. Sharma</i> <i>G. Bowtell</i> 133
The Calculation of Three- and Four- Body Correlation Energies	<i>M.A. Robb</i> 137
Valence-Bond Calculations on <i>HF</i> and <i>LiH</i>	<i>R.N. Yardley</i> <i>G.G. Balint-Kurti</i> 141
Studies of Correlation Effects on Hydrogen Bonding and Ion Hydration	<i>G.H.F. Diercksen</i> <i>W.P. Kraemer</i> <i>B.O. Roos</i> 147
 <b>Hartree-Fock Theory and Applications</b>	
Cusped-Gaussian Molecular Wavefunctions	<i>E. Steiner</i> <i>B.C. Walsh</i> 151
The Simulated <i>Ab Initio</i> Molecular Orbital (SAMO) Method	<i>B.J. Duke</i> <i>B. O'Leary</i> 157
Approximate <i>Ab Initio</i> Calculations and the Method of Molecular Fragments	<i>D.F. Brailsford</i> 163

	Page
The Electronic Structure of Cadmium Dichloride by the Multiple Scattering $X\alpha$ Method	169
	<i>N.V. Richardson</i> <i>A.F. Orchard</i> <i>M.A. Whitehead</i>
Recent Developments in Hartree-Fock Theory	173
	<i>J.P. Dahl</i>
On Constrained Variational Calculations on Molecules	181
	<i>M.A. Whitehead</i> <i>G.D. Zeiss</i>
Direct Minimisation Schemes – Some Difficulties and Possible Resolutions	195
	<i>B.T. Sutcliffe</i> <i>D. Garton</i>
The Theoretical Interpretation of the Low Energy Photoelectron Spectra of Transition Metal Complexes	205
	<i>M.F. Guest</i> <i>I.H. Hillier</i>
<i>Ab Initio</i> Calculations of Transition Metal Complexes and Organometallics	211
	<i>A. Veillard</i>
Accurate Hartree-Fock Calculations on the Structure and Stability of Hydrated Diatomic Ions	217
	<i>W.P. Kraemer</i>
Can Hartree-Fock Limit Wavefunctions be calculated with Gaussian Basis Functions? – FH again	221
	<i>W. von Niessen</i> <i>G.H.F. Diercksen</i> <i>W.P. Kraemer</i>
Ground State Wavefunctions for Aromatic and Heteroaromatic Molecules	229
	<i>M.H. Palmer</i> <i>A.J. Gaskell</i> <i>R.H. Findlay</i> <i>S.M.F. Kennedy</i> <i>W. Moyes</i> <i>J. Nisbet</i>
Non Empirical LCAO SCF MO Investigations of Electronic Reorganisations accompanying Core Ionisations	235
	<i>D.T. Clark</i> <i>I. Scanlan</i> <i>J. Muller</i> <i>D.B. Adams</i>
Localised <i>versus</i> Delocalised Descriptions of the $n-\pi^*$ Excitations in <i>p</i> -Benzoquinone	243
	<i>H.T. Jonkman</i> <i>G.A. van der Velde</i> <i>W.C. Nieuwpoort</i>
The Shapes of $AX_2$ Molecules	247
	<i>J.C. Dobson</i>
A Study of the Structure and Properties of Clusters of Lithium Atoms	249
	<i>A.D. Tait</i>

## Participants

# SCATTERING THEORY





# Review Notes on Molecular Scattering Theory

M.S.Child\*

Exact numerical solution of the quantum mechanical equations of motion for all but the simplest model molecular collision problems would be prohibitive in computation time. Hence it may be helpful to give a brief review of the available approximation methods.

At the highest level we have the *close-coupling* approximation obtained by an expansion in unperturbed internal eigenfunctions  $\phi_n(\rho)$  with energies  $E_n$ .  $r$  and  $\rho$  are used throughout to denote collections of translational and internal coordinates respectively.

$$\Psi(r, \rho) = \sum_n \phi_n(\rho) \psi_n(r) \quad (1)$$

The resulting coupled equations may be abbreviated in the matrix form.

$$\left[ \frac{d^2}{dr^2} \mathbf{I} + \mathbf{k}^2 - \mathbf{U}(r) \right] \Psi(r) = 0, \quad (2)$$

where

$$k_{nn'}^2 = [2m(E - E_n)/\hbar^2] \delta_{nn'}, \quad U_{nn'}(r) = 2mV_{nn'}(r)/\hbar^2,$$

and  $V$  is the matrix of the interaction potential in the basis of internal states. This is an approximation only to the extent that it is necessary to truncate the basis set. An efficient programme due to Gordon [1] is available through QCPE.

First order perturbation solutions of (2) yield the *Born* and *Distorted Wave* approximations, according to which the scattering amplitude is given by

$$S_{nn'} = \frac{2}{(k_n k_{n'})^{1/2}} \int_0^\infty \psi_n^\circ(r) U_{nn'}(r) \psi_{n'}^\circ(r) dr \quad (3)$$

where the  $\psi_n^\circ(r)$  are solutions of (2), obtained in the Born approximation by neglecting the matrix  $U$ ; the diagonal elements  $U_{nn}(r)$  are retained in the

distorted wave method. Solutions of this form diverge as the Fourier component of  $U_{nn'}(r)$  at the de Broglie difference frequency in the product  $\psi_n^\circ(r) \psi_{n'}^\circ(r)$  increases.

Solutions of equations (2) by the amplitude density method [2] may be combined to yield an exponential form for the  $S$  matrix,

$$S = \exp(iA), \quad (4)$$

where  $A$  is a hermitian matrix. Truncation of a series for  $A$  by the first term yields the *exponential* approximation [3], according to which

$$A_{nn'} = \frac{2}{(k_n k_{n'})^{1/2}} \int_0^\infty \psi_n^\circ(r) U_{nn'}(r) \psi_{n'}(r) dr. \quad (5)$$

The necessary integrals are therefore identical to those which arise in the Born or distorted wave expressions, but the unitarity of the  $S$  matrix is necessarily preserved.

Other types of approximation are obtained by representing the collision as a time-dependent disturbance to the internal state, and the relation between this formulation and the time independent equations (2) above has recently been discussed [4-5]. An important limitation is that the translational motion in all channels of interest should be adequately described by a common trajectory  $r(t)$ . This classical path approach yields the following perturbation formulae.

$$S_{nn'} \simeq \frac{1}{\hbar} \int_{-\infty}^{\infty} V_{nn'}[r(t)] \exp(i\omega_{nn'} t) dt \quad (6)$$

and

$$S_{nn'} \simeq \frac{1}{\hbar} \int_{-\infty}^{\infty} \left[ V_{nn'}[r(t)] \exp\left(\frac{i}{\hbar} \int_0^t \{W_n[r(t')] - W_{n'}[r(t')]\} dt'\right) \right] dt, \quad (7)$$

\* Theoretical Chemistry Department, University of Oxford, 1 South Parks Road, Oxford, OX1 3TG

where

$$\hbar\omega_{nn'} = E_n - E_{n'}$$

$$W_n(r) = E_n + V_{nn'}(r)$$

Equations (6) and (7) are analogous to the Born and Distorted Wave approximations respectively. An exponential classical path approximation due to Magnus [6] is also available, namely

$$S \simeq \exp[iA],$$

$$A_{nn'} = -\frac{1}{\hbar} \int_{-\infty}^{\infty} V_{nn'}[r(t)] \exp(i\omega_{nn'}t) dt. \quad (8)$$

This reduces to the *sudden* approximation [7] if the  $\omega_{nn'}$  are set equal to zero. Equations somewhat similar to (6)-(8), but with classical Fourier components in place of the matrix elements  $V_{nn'}(r)$ , have been derived by correspondence principle arguments [8].

The above equations all assume a quantum description at least of the internal state. This has been replaced in an important recent series of papers by a strictly semi-classical argument, derived either from the Feynmann path integral [9] approach to quantum mechanics [10], or from the multidimension WKB solution of the time independent Schrödinger equation [11,12]. The results, which have been described as 'classical mechanics plus quantum superposition', show that the  $S$  matrix elements for classically allowed processes take the form

$$S_{nn'} = \sum_{\nu} \left[ P_{nn'}^{(\nu)} \right]^{1/2} e^{i\phi_{nn'}^{(\nu)}} \quad (9)$$

where  $P_{nn'}^{(\nu)}$  and  $\phi_{nn'}^{(\nu)}$  are the classical probability and classical action for the event in question, and the sum is taken over all trajectories leading to that event. Furthermore the theory may be extended into the classically forbidden region by working with solutions of Hamilton's classical equations of motion in the complex time and coordinate planes [13,14]. Problems arise at the classical threshold, but these may be handled by special integration techniques [15]. Applications to electronically non-adiabatic (surface-hopping) processes have also been discussed [16,17].

## References

- [1] GORDON, R.G. (1969). *J. Chem. Phys.*, **51**, 14.
- [2] CALOGERO, F. (1967). *Variable Phase Approach to Potential Scattering*, New York: Academic Press.
- [3] LEVINE, R.D. (1971). *Mol. Phys.*, **22**, 497.
- [4] DELOS, J.B., THORSON, W.R. and KNUDSON, S.K. (1972). *Phys. Rev.*, **A6**, 709.

- [5] BATES, D.R. and CROTHERS, D.S.F. (1970). *Proc. Roy. Soc. (London)*, **A315**, 465.
- [6] MAGNUS, W. (1954). *Commun. Pure and Appl. Math.*, **7**, 649.
- [7] BERNSTEIN, R.B. and KRAMER, K.H. (1966). *J. Chem. Phys.*, **44**, 4473.
- [8] PERCIVAL, I.C. and RICHARDS, D. (1970). *J. Phys. B.*, **3**, 1035.  
 ————— and ————— (1971). *Ibid.*, **4**, 918, 932.
- [9] FEYNMANN, R.P. and HIBBS, A.R. (1965). *Quantum Mechanics and Path Integrals*, New York: McGraw-Hill.
- [10] MILLER, W.H. (1970). *J. Chem. Phys.*, **53**, 1949, 3578.
- [11] MARCUS, R.A. (1971). *J. Chem. Phys.*, **54**, 3965.
- [12] CONNOR, J.N.L. and MARCUS, R.A. (1971). *J. Chem. Phys.*, **55**, 5636.
- [13] MILLER, W.H. and GEORGE, T.F. (1972). *J. Chem. Phys.*, **56**, 11.  
 ————— and ————— (1972). *Ibid.*, **57**, 2458.
- [14] STINE, J. and MARCUS, R.A. (1971). *Chem. Phys. Letters*, **15**, 536.
- [15] CONNOR, J.N.L. (1973). *Mol. Phys.*, **26**, 1217, 1371.  
 ————— (1973). *Discussions Faraday Soc.*, **55**, 51.
- [16] TULLY, J.C. and PRESTON, R.K. (1971). *J. Chem. Phys.*, **55**, 562.
- [17] MILLER, W.H. and GEORGE, T.F. (1972). *J. Chem. Phys.*, **56**, 5637.

# Application of the Correspondence Principle to Vibrational and Rotational Excitation

D.Richards\*

The physical ideas behind Heisenberg's form of the correspondence principle are described: it is shown how this correspondence principle provides semi-classical approximations to the excitation of excited systems when perturbed by time dependent fields.

A generalisation, the strong coupling correspondence principle (SCCP), is described.

Applications of the SCCP to both vibrational and rotational excitation are given, and where possible these results are compared with quantum mechanical calculations.

## Introduction

The correspondence principle methods described here have proved to be a powerful tool for the calculation of excitation cross sections. These methods are based upon Heisenberg's form of the correspondence principle, and the main assumption made is that classical perturbation theory - which is quite different from quantal perturbation theory - provides a good description of the classical collision. For transitions between highly excited states this is not a very restrictive condition, and its use has many computational advantages; when classical perturbation theory is not valid pure classical mechanics is often sufficient to obtain cross section since then quantal effects are often small. For transitions between low lying states semiclassical methods are not firmly established; new methods based upon correspondence identities are now being developed to deal with these transitions. These are briefly described later.

For atomic systems, where the interaction potentials are known, the correspondence principle methods described here together with pure classical calculations have been successfully used to understand the ranges of validity of the various theories and to obtain cross sections for wide ranges of relevant parameters, and processes, e.g. [1]. For molecular systems no such program has yet been carried through and the validity and accuracy of many approximations is still uncertain.

## The Correspondence Principle

The correspondence principle states that as the quantum numbers become large quantum mechanics goes into classical mechanics. However, the principle may be invoked in a variety of ways some of which are more useful than others. One of the more useful

is Heisenberg's form of the correspondence principle: here quantal matrix elements are approximated by Fourier components of the classical motion.

Since our approximations are based upon this correspondence principle we shall consider the physical ideas behind it before considering their applications. Only a one dimensional system will be considered, but the theory is essentially the same as for a many dimensional separable system the time variable being replaced by the angle variables [2]. No attempt will be made to prove mathematically any of the approximations.

First consider a bound particle moving in one dimension: its motion is periodic and of frequency  $\omega(E)$ , which usually depends upon the energy  $E$ . Thus the motion may be expressed as a Fourier series in time:

$$x(t) = \sum_{s=-\infty}^{\infty} X_s(E) \exp -is\omega t \quad (1a)$$

$$X_s(E) = \frac{\omega}{2\pi} \int_0^{2\pi/\omega} d\tau x(\tau) \exp is\omega\tau \quad (1b)$$

and any function of the dynamical variables may be expressed similarly.

According to classical radiation theory, an accelerating charge radiates energy as electromagnetic radiation. If the energy loss over one period of its motion is small the Fourier development of its motion, equation (1a), is still a good approximation and it can be shown [3] that the system will radiate at those frequencies present in the Fourier series (1a),

$$s \omega(E), \quad (2a)$$

\* *Mathematics Department, Open University, Walton Hall, Milton Keynes, Buckinghamshire, MK7 6AA*

and that the intensity of each frequency is

$$I_s = \frac{4e^2(s\omega)^4}{3c^3} |X_s(E)|^2. \quad (2b)$$

Now consider the equivalent quantal system with energy levels  $E_n$  and states  $|n\rangle$ . Suppose that it is in an excited level,  $n$ . Its behaviour is quite different from that of the classical system; it decays to a lower level,  $m$ , emitting a photon of frequency

$$\omega(m,n) = \frac{E_n - E_m}{\hbar}, \quad (m < n) \quad (3a)$$

and there is a known probability per unit time of a photon of each frequency being emitted. An ensemble of such systems will emit radiation at these frequencies, (3a), and with intensities, per atom:

$$I(n \rightarrow m) = \frac{4e^2 \omega(m,n)^4}{3c^3} |\langle m|x|n \rangle|^2. \quad (3b)$$

According to the correspondence principle an ensemble of classical and quantal systems would look the same if the quantum numbers are large. Thus we should expect the frequencies and intensities to be approximately the same:

$$\omega(m,n) = \frac{E_m - E_n}{\hbar} \simeq s\omega(E), \quad (4a)$$

$$\left. \begin{aligned} \langle m|x|n \rangle &\simeq X_s(E) \\ &\simeq \frac{\omega}{2\pi} \int_0^{2\pi/\omega} d\tau x(\tau) \exp is\omega\tau \end{aligned} \right\} (4b)$$

where  $s = n - m$ .

This is Heisenberg's form of the correspondence principle, named after him because of his use of it in his formulation of matrix mechanics [4].

There is some ambiguity present in these equations since the orbit of the classical system has not been specified. In fact it can not be specified uniquely since one classical orbit is being used to connect two quantal states of different energy. In practice it is best to use some mean of the initial and final orbit which is labelled by a quantum number  $n_c$ ; the relation between this quantum number and the energy of the orbit is determined from the Bohr-Sommerfeld quantisation conditions.

It is approximation (4b) and its generalisation to arbitrary functions,

$$\langle m|F(x)|n \rangle \simeq \frac{\omega}{2\pi} \int_0^{2\pi/\omega} d\tau F(x(\tau)) \exp is\omega\tau, \quad (5)$$

$(s = n - m)$

which is the basis of our approximation to quantal scattering amplitudes.

The accuracy of the approximations (4b) and (5) depends upon the system to which it is being applied. For harmonic oscillators and hydrogen atoms it is a better approximation than should be expected from the assumptions made, and is good even for small quantum numbers: this is a consequence of the Correspondence Identities [5,6].

As an elementary example consider the simple harmonic oscillator. Its classical motion is given by (unit mass)

$$x(t) = \left( \frac{n_c \hbar}{2\omega} \right)^{1/2} (e^{i\omega t} + e^{-i\omega t})$$

where the energy of the system is quantised using the Bohr-Sommerfeld quantisation rule:

$$n_c \hbar = \frac{1}{2\pi} \oint p dx = \frac{1}{2\pi} \oint dx (2E - \omega^2 x^2)^{1/2} = \frac{E}{\omega}$$

Thus a straight forward application of Heisenberg's form of the correspondence principle, equation (4b), gives the selection rules

$$\langle n|x|n' \rangle = 0 \quad n' \neq n \pm 1$$

and

$$\langle n|x|n \pm 1 \rangle = \left( \frac{n_c \hbar}{2\omega} \right)^{1/2}.$$

The quantal results are

$$\langle n|x|n+1 \rangle = \left( \frac{(n+1)\hbar}{2\omega} \right)^{1/2}.$$

$$\langle n|x|n-1 \rangle = \left( \frac{n\hbar}{2\omega} \right)^{1/2},$$

so that the agreement improves as  $n$  increases, as would be expected. In fact for this potential a judicious choice of  $n_c$  will give remarkably good agreement for small  $n$  and for matrix elements involving powers of  $x$  [7].

Another relevant example is the Morse potential

$$V(x) = D \{1 - \exp -a(x - x_e)\}^2 \quad (6)$$

For this potential exact quantal results are available and in the table below comparisons of these and the correspondence principle values are given.

In this example the correspondence principle becomes worse as the quantum number increases:

this is because the Morse potential supports a finite number of bound states and the correspondence principle implicitly supposes an infinite number, an approximation which gets worse as the quantum number increases.

(b) First order time dependent perturbation theory.

(c) The sudden approximation.

For our purposes the Born approximation is of little interest. The transition amplitude according to time dependent perturbation theory is

$$S(n',n) = -\frac{i}{\hbar} \int_{-\infty}^{\infty} dt \langle n' | V(x,t) | n \rangle \exp \frac{i(E_{n'} - E_n)t}{\hbar} \quad (7a)$$

$$\approx \frac{\omega}{2\pi} \int_0^{2\pi/\omega} d\tau \exp i s \omega \tau \left\{ -\frac{i}{\hbar} \int_{-\infty}^{\infty} dt V(x(t+\tau), t) \right\} \quad (7b)$$

( $s = n - n'$ )

where the correspondence principle approximations to the energy difference and matrix elements, equations (4a,b), have been used in obtaining the last equation.

The sudden approximation gives

$$S(n',n) = \langle n' | \exp -\frac{i}{\hbar} \int_{-\infty}^{\infty} dt V(x,t) | n \rangle \quad (8a)$$

$$\approx \frac{\omega}{2\pi} \int_0^{2\pi/\omega} d\tau \exp i \left\{ s \omega \tau - \frac{i}{\hbar} \int_{-\infty}^{\infty} dt V(x(\tau), t) \right\} \quad (8b)$$

( $s = n - n'$ )

Table 1: Values of  $a^2 s^2 \langle n | x | n+s \rangle^2$  for the Morse potential of equation (6) with about 50 bound states for  $s = 1, 2$  and various  $n$  (taken from [7]). The value of  $n_c$  is taken to be  $n_c = [(n+s)!/n!]^{1/s}$  following [7].

Transition	Quantal Value	Correspondence Principle	Percentage Difference
1 → 2	.020406	.020408	0.01
2 → 3	.030924	.030928	0.01
5 → 6	.063822	.063830	0.01
10 → 11	.12358	.12360	0.02
15 → 16	.19043	.19048	0.02
1 → 3	6.4440 (-4)	6.3051 (-4)	2
2 → 4	1.3162 (-3)	1.2877 (-3)	2
5 → 7	4.9142 (-3)	4.8023 (-3)	2
10 → 12	1.7289 (-2)	1.6849 (-2)	3
15 → 17	4.0169 (-2)	3.9005 (-2)	3

### Application to Scattering Theory

The direct application of these elementary ideas to scattering theory is straightforward if the scattering amplitude may be expressed directly as a matrix element; this is possible in three simple cases:

(a) Born approximation.

In equations (7) and (8),  $V(x,t)$  is the potential perturbing the bound system which has energy levels  $E_n$  and eigenstates  $|n\rangle$ .

These approximations, (7b) and (8b), are approximations to relatively simple quantal scattering amplitudes; they are useful if the quantum numbers are large since in general Fourier components are easier to calculate than matrix elements, and they have been used to obtain the excitation cross section of hydrogen atoms by charged particles [8-10].

From these two scattering amplitudes, (7b) and (8b), a generalisation may be obtained which has no closed form in quantum mechanics.

This generalisation is obtained by noting that in the sudden approximation (8b) the bound particle does not move during the collision - the classical position is a function of  $\tau$  only and not of  $t$ ; this is in contrast to perturbation theory (7b) and reflects the basic assumption of the sudden approximation.

The generalisation is simply:

$$S(n', n) = \frac{\omega}{2\pi} \int_0^{2\pi/\omega} d\tau \exp i \left\{ s\omega\tau - \frac{i}{\hbar} \int_{-\infty}^{\infty} dt V(x(t+\tau), t) \right\} \quad (9)$$

( $s = n - n'$ )

This, strong coupling correspondence principle (SCCP), can be obtained rigorously from the integral equation for the scattering amplitude [2] and is easily generalised to many dimensional separable systems. The one dimensional theory has been obtained independently [11], and a closely related quantal approximation has also been obtained [12].

Two major approximations are used in deriving equation (9). The first is the use of Heisenberg's form of the correspondence principle which restricts the use of (9) to transitions between highly excited states. The second is that classical perturbation theory must provide a good approximation to the classical collision; this is not the same as quantal perturbation theory and for highly excited states is generally much less restrictive, in fact the approximation of equation (9) is valid when quantal perturbation theory is totally inadequate.

The consequences of the assumption that classical perturbation theory is valid are two fold. First, this method can only be used when the classical constants of the bound motion change by relatively small amounts, although the changes in the equivalent quantum numbers may be large. Second, that the unperturbed classical orbit may be used in the calculation; since this can often be obtained in closed form the computations are considerably simplified so making these methods exceptionally easy to use. Further more, it should be added that when classical perturbation theory is invalid it is often unnecessary to use semiclassical techniques to obtain cross section data as quantal effects are often small or negligible. Also, when the change in quantum is large and when classical perturbation theory is valid it can be shown using a stationary phase argument that the probability obtained from the SCCP, equation (9), reduces to that obtained by classical perturbation theory.

Thus for large quantum numbers the region covered by classical perturbation theory is treated adequately using these correspondence principle methods; the remaining region can often be treated using exact classical trajectories using Monte Carlo methods. These two methods are complementary and have both been used to calculate the cross sections for collisions between charged particles and hydrogen atoms. These and other aspects of semiclassical methods were discussed by I.C. Percival at St. Catherine's College in 1970 [13].

For low quantum numbers, and when the classical action is comparable to  $\hbar$ , there is no formal justification for the use of classical or semiclassical mechanics. In these regions the application of classical

or semiclassical methods is always dependent on the particular classical and corresponding quantal representation used. However for certain problems there exist Correspondence Identities [5,6]. These are identities between the predictions of classical and quantum mechanics. They include such cases as the prediction by Rutherford, using classical mechanics, of the correct quantal differential cross section for scattering of a charged particle by a fixed charge.

There is also a 'Feynman Identity' for systems having a Lagrangian, at most quadratic in the coordinates and momenta. For such systems the propagator is given exactly in terms of the classical action in position,time representation (or momentum, time). This identity does not exist in energy representation.

Work is at present being carried out at Stirling by Clark and Percival to utilize the Feynman Identity in the field of Chemical Physics.

The main problems of applying semiclassical mechanics in this field occur in the neighbourhood of stationary points in the potential, for example

- (a) The low states of a bound system. Here the quanta of energy are comparable to the energy of the system.
- (b) In transition states where barrier penetration occurs.
- (c) In collision problems involving vibrational excitation where low quantum numbers are usually involved.

Near the stationary points it is normally valid to approximate the Hamiltonian of the system by a Hamiltonian quadratic in  $p, q$ . It is thus advantageous to choose the classical position,time (or momentum, time) representation for such problems and incorporate the Feynman Identity.

Although certain difficulties were encountered in the formulation, these have been overcome. The theory has, so far, only been applied to bound state problems and the following quantities have been evaluated.

- (a) Bound State Spectra.
- (b) Diagonal amplitudes due to a general time-dependent perturbation.
- (c) Transition probabilities due to a general time-dependent perturbation.

The formulation depends only on closed loops formed from classical paths and these may be represented by diagrams in position,time (or momentum,

time) space. It appears that it is the nature of these loops that prohibits the direct evaluation of the off-diagonal transition amplitudes, despite the fact that the probabilities can be calculated.

Calculations have been carried out using the Simple Harmonic Oscillator as a model with a time-dependent forcing term (this is the simplest model of vibrational excitation). All the quantities above (a, b and c) have been evaluated analytically and were found to be identical to the exact quantum mechanical solutions as required by the Feynman Identity.

In the near future it is expected that the formulation will be generalised to other processes and systems.

### Application to Vibrational Excitation

The simplest model of vibrational excitation is a simple harmonic oscillator forced by a time dependent potential. The strong coupling correspondence principle has been applied to this problem with potentials of the form

(a)  $x F(t)$

(b)  $x^2 F(t)$

see [14,15]. In both cases the solution to the quantal problem may be obtained in closed form.

First, consider case (a). The quantal transition probability may be expressed in terms of associated Laguerre polynomials and  $\Delta E^c$ , the phased averaged classical energy transfer; the SCCP probability is obtained in terms of Bessel functions of  $\Delta E^c$ , which is the appropriate asymptotic limit of the Laguerre polynomials. To be specific we take the time dependent part of the potential to be

$$F(t) = a \operatorname{sech}^2 bt$$

for which  $\Delta E^c$  may be obtained in closed form [14].

In figure 1 the probability for the  $0 \rightarrow 1$  transition has been plotted against  $\eta_0 = \Delta E^c / 2E_0$  where  $E_0$  is the ground state energy. The exact quantal and SCCP probabilities are shown together with the numerical solutions of Schrodinger's equation obtained by expressing the wavefunction as an expansion of  $N$  unperturbed wavefunctions, for various  $N$ . It is seen that the correspondence principle result breaks down for  $\eta_0 \approx 0.5$ , or when the mean classical energy transfer is equal to the initial energy. For larger  $\eta_0$  the correspondence principle gets worse, in keeping with the assumption that classical perturbation theory is still valid. However, even for such low quantum numbers the correspondence principle is as good as an 8-state quantal calculation.

For the  $5 \rightarrow 6$  transition, shown in figure 2, it is seen that the strong coupling correspondence principle is in good agreement with the exact result for all  $\eta_0$

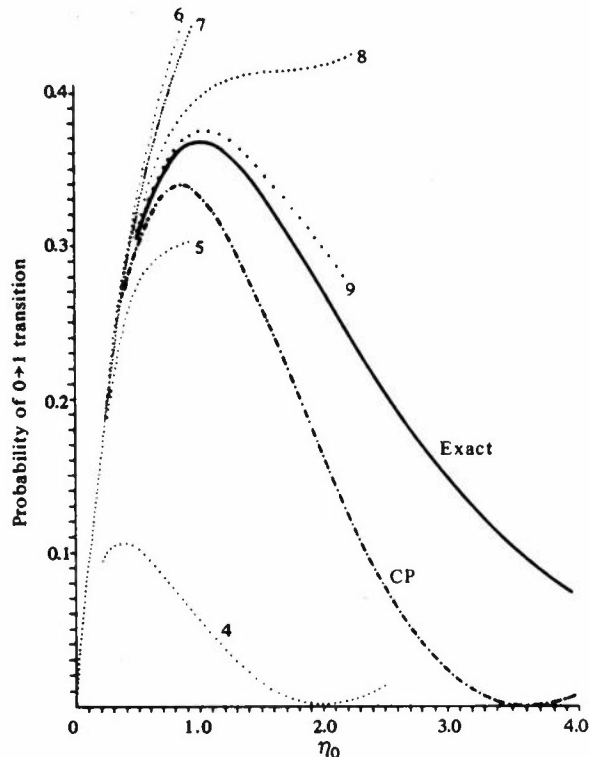


Figure 1: The transition probabilities for the  $0 \rightarrow 1$  transition shown as functions of the phase-averaged classical energy transfer  $\eta_0$ .

Exact, is the exact quantal probability; CP the correspondence principle probability and curves numbered 4, 5, ...9 are the 4, 5, ...9 state computer solutions [14]

shown, and that for a significant range of  $\eta_0$  it is better than a 16-state quantal calculation.

From these comparisons we see that the SCCP results are good whenever classical perturbation theory is valid, but as expected the results get progressively worse as the energy transfer increases. For the harmonic oscillator system we also see that correspondence principle methods are good even for low quantum numbers.

For a simple harmonic oscillator perturbed by a quadratic potential (case b) the results are not quite so encouraging due to the more rapid break down of classical perturbation theory. Again we take  $F(t)$  to be of the form of equation (10):

$$F(t) = \frac{1}{8} \left( \frac{E}{8} \right) \operatorname{sech}^2 \left( \left( \frac{E}{8} \right)^{1/2} t \right). \quad (11)$$

In figures 3 and 4 [15] we show the probability for the  $0 \rightarrow 2$  and  $2 \rightarrow 4$  transition plotted against  $E$ , defined in equation (11). It is seen that in both of

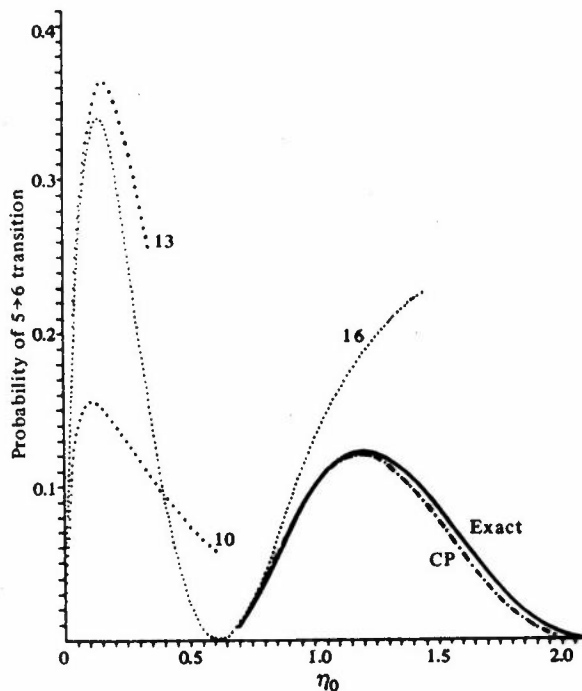


Figure 2: The transition probabilities for the  $5 \rightarrow 6$  transition shown as functions of the phased-averaged classical energy transfer  $\eta_0$ .

Exact, is the exact quantal probability; CP the correspondence principle probability and curves numbered 10, 13, ...16 are the 10, 13, ...16 state computer solutions [14]

these cases the SCCP is substantially in error for a significant range of  $E$ . The reason for this is that the bound orbit is significantly perturbed by the potential. If  $E$  is small the maximum magnitude of the force is small but its effect is spread over a long time; if  $E$  is large the force is large but strongly peaked in time. In either case the bound orbit is significantly affected.

In figures 3 and 4 the results of a modified strong coupling correspondence principle [15] are shown. This theory partially accounts for the distortion of the bound orbit and in this instance is a better approximation than the SCCP of equation (9).

This modified theory is not always significantly better; for the linearly perturbed oscillator the modified and unmodified theories are identical, and for charge particle-hydrogenic ion excitation and rotational excitation of diatomic molecules by atoms the bound orbit is not sufficiently perturbed, for most collisions, for such modifications to be necessary. However, the example of the quadratically perturbed harmonic oscillator shows that care must be exercised when applying these methods.

## Application to Rotational Excitation

The SCCP has been applied to the rotational excitation of diatomic molecules in  $\Sigma$  states by arbitrary spherically symmetric atoms [16]. The general formulation of the problem is presented in the above reference; here we shall only consider the rotational excitation of  $N_2$  by  $Ne$  for which close-coupling results are available [17].

In this case, following [17], the interaction potential may be taken to be

$$V(r_2(\mathbb{H})) = F_0(r_2) + F_2(r_2) P_2(\cos(\mathbb{H}))$$

where  $r_2$  is the radial distance between the incident atom and the centre of the molecule and  $\mathbb{H}$  the angle between the vector positions of the atom and the molecular axis.

One of the difficulties in applying time dependent scattering theory to this problem is that, through the angle  $\mathbb{H}$ , the interaction potential involves the coordinates of the molecule; since the molecule and the atom are treated asymmetrically in a time dependent theory there is no consistent way in which the effect of this part of the potential on the incident atom may

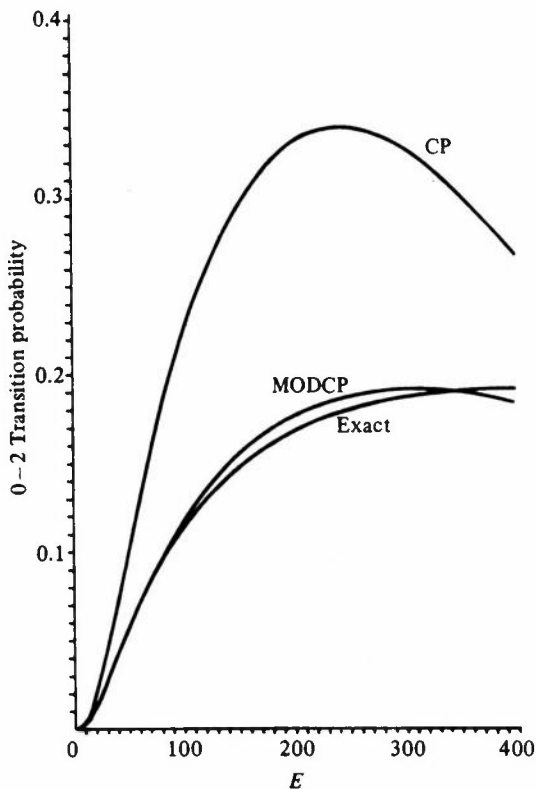


Figure 3: The  $0 \rightarrow 2$  transition probability, as a function of  $E$ , equation (11), for a harmonic oscillator perturbed by a potential  $x^2 F(t)$ . Exact is the exact quantal result, CP is the strong coupling correspondence principle result, equation (9), and MODCP is the modified correspondence principle result [15]



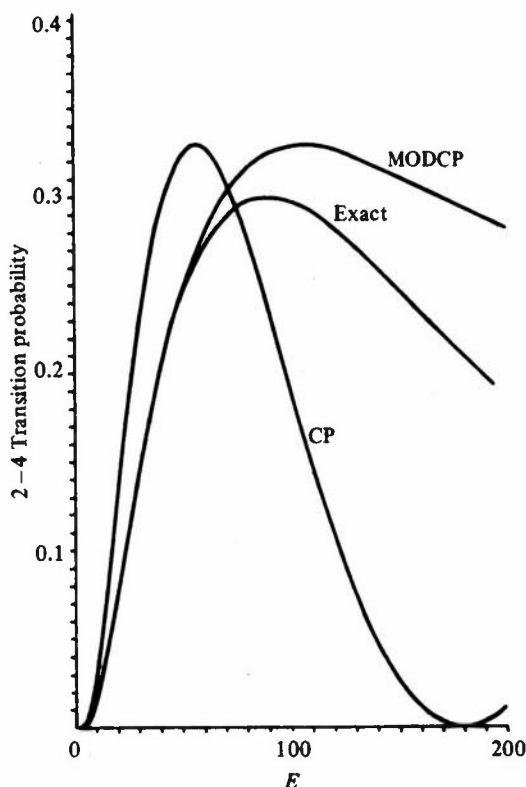


Figure 4: The 2 → 4 transition probability, as a function of  $E$ , equation (11), for a harmonic oscillator perturbed by a potential  $x^2 F(t)$ . Exact is the exact quantal result, CP is the strong coupling correspondence principle result, equation (9), and MODCP is the modified correspondence principle result [15]

be included. Thus it is necessary to suppose that the incident atom is only affected by the spherically symmetric part of the potential,  $F_0(r_2)$ . In general this is the dominant part of the potential and so no large errors are expected from this approximation.

Apart from this dynamical approximation the main approximations are the replacement of matrix elements by Fourier components, as in equation (5), and the replacement of the sum over degenerate angular momentum states by averages over a classical ensemble of molecules. By comparing various quantal approximations with their equivalent correspondence principle approximation it has been shown [16] that the relative error of these approximations decreases as  $(2j+1)^{-2}$ , where  $j$  is the quantum number of the rotor.

### Partial Cross Sections

It is possible to make more detailed comparisons of the partial cross sections by making a correspondence between the impact parameter,  $b$ , and the angular momentum of the incident atom, and between the total angular momentum quantum number and the

angle between the angular momentum of the rotor and the  $z$ -axis,  $\beta$ :

$$b = (\ell + \frac{1}{2})/k.$$

$$\cos \beta = \frac{J^2 - j^2 - \ell^2}{2j\ell}$$

where  $j$  is the initial rotational quantum number, and  $k$  the wave number of the incident atom with angular momentum quantum number  $\ell$ . With these correspondences it is possible to compare the partial cross

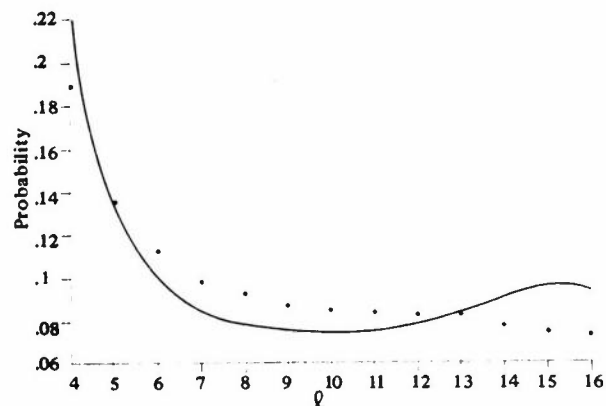


Figure 5: A comparison of the partial cross section  $S^J(j \rightarrow j')$  obtained from close-coupling calculations, indicated by the dots, and the probability obtained from the strong coupling correspondence principle, equation (9), indicated by the solid line. The total angular momentum quantum number is  $J = 10$ , the incident energy is  $E = 2.2\epsilon$  and the transition is  $j = 6 \rightarrow 8$

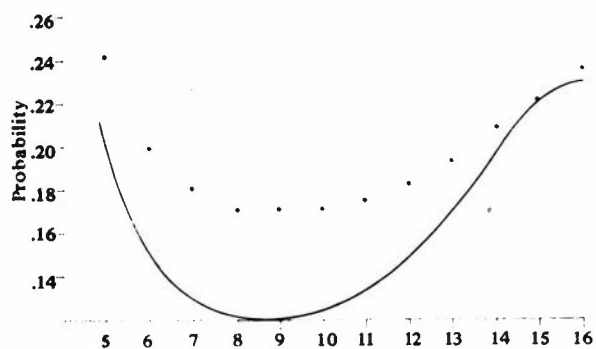


Figure 6: A comparison of the partial cross section  $S^J(j \rightarrow j')$  obtained from close-coupling calculations, indicated by the dots, and the probability obtained from the strong coupling correspondence principle, equation (9), indicated by the solid line. The total angular momentum quantum number is  $J = 10$ , the incident energy is  $E = 4.4\epsilon$  and the transition is  $j = 6 \rightarrow 8$

section  $S_Q^J(j \rightarrow j')$  obtained from the close-coupling calculation with the probability  $P_0(j \rightarrow j'; \cos \beta)$  obtained from the SCCP before averaging over the ensemble of molecules.

In figures 5 and 6 we show the partial cross sections for the  $6 \rightarrow 8$  transition for a total angular momentum,  $J = 10$ . The close coupling results are calculated using the  $j = 6$  and  $j = 8$  levels only using the method of Gordon [18]. These comparisons show that the strong coupling correspondence principle can predict the details of the cross section with reasonable accuracy.

At the low energy,  $E = 2.2\epsilon$  (figure 5), the agreement is good; this is reflected in the cross section given in table 2. At the higher energy,  $E = 4.4\epsilon$  the agreement is not so good; the reason for this is that the close coupling results are too large since at this energy more states need to be included; this conclusion is suggested by the results given in table 2.

### Total Cross Sections

The strong coupling correspondence principle calculations have been compared with the results of Burke *et al.* [17] for the  $2 \rightarrow 4$  transition (including contributions from both bi-parities); for other transitions the quantal close coupling equations were solved using the method of Gordon [18], QCPE program 187. The results are summarised in table 2.

Table 2: Comparison of the present calculations ( $\sigma^{\text{CP}}$ ) with close coupling results ( $\sigma^{\text{Q}}$ ). Results *a* are calculated using  $j$  and  $j'$  levels only: results *b* use levels 0,2,4 and 6.  $E$  is the energy of incident atom, in units of  $\epsilon$  the well depth of  $F_0(r_2)$

Transition	2 → 4			2 → 6		
$E(\epsilon)$	4.03	6.24	9.76	4.03	6.24	9.76
$\sigma^{\text{Q}}(\pi a_0^2)$	<i>a</i>	8.56	9.92	11.9		
	<i>b</i>	7.78	8.77	9.49	0.52	0.92
$\sigma^{\text{CP}}(\pi a_0^2)$	7.80	8.51	9.11	0.62	1.04	1.69

Transition	4 → 6			6 → 8	
$E(\epsilon)$	3.32	5.53	9.05	2.21	4.42
$\sigma^{\text{Q}}(\pi a_0^2)$	<i>a</i>			2.70	5.27
	<i>b</i>	5.93	7.14	8.82	
$\sigma^{\text{CP}}(\pi a_0^2)$	6.02	7.09	7.81	2.62	5.05

Starting with the  $2 \rightarrow 4$  results, the agreement of the correspondence principle with the larger basis

close coupling calculations is excellent. The success of the correspondence principle for such low quantum numbers is both surprising and encouraging. The results for  $2 \rightarrow 6$  transitions are quite satisfactory, the poorer agreement at lower energies almost certainly arising from the inadequacy of a mean orbit when the translational energy drops by about 40% in the collision.

For  $4 \rightarrow 6$  transitions the agreement is again excellent, except at the highest energy considered. Since the  $2 \rightarrow 4$  cross section at this energy changes considerably on going from the 2, 4 basis to the 0, 2, 4, 6 basis, it is quite likely that the close coupling results require at least the  $j = 8$  level to be included. Correspondence principle calculations show the  $4 \rightarrow 8$  cross section increasing from  $0.17\pi a_0^2$  at  $E = 3.32\epsilon$ , through  $0.55\pi a_0^2$  at  $5.53\epsilon$  to  $1.15\pi a_0^2$  at  $9.05\epsilon$ , suggesting that coupling to the  $j = 8$  level is significant at the higher energies.

Finally, for  $6 \rightarrow 8$  transitions good agreement is also obtained. Again the correspondence principle results lie below the close coupling calculations. As the introduction of further levels in the close coupling calculation is likely to reduce the cross section this would probably improve the agreement. Simply adding the  $j = 4$  and  $j = 10$  levels would give a 32 state calculation, taking about eight times as long as that reported here.

Subsequent calculations, which will be reported elsewhere, on  $0 \rightarrow 2$  transitions show that the SCCP gives remarkably accurate cross sections even for these low quantum numbers.

The 0–2–4–6 level close coupling calculations are about two orders of magnitude slower than the correspondence principle calculations, even though steps of 5 were taken in the total angular momentum quantum number.

### Conclusion

When classical perturbation theory adequately describes the classical collision we have shown that by applying Heisenberg's form of the correspondence principle appropriately accurate transition probabilities for transitions between highly excited states may be obtained. For such transitions the main inaccuracy of the theory is due to the breakdown of classical perturbation theory. For transitions between low quantum numbers the fundamental assumptions of this, and any semiclassical, theory are invalid even though these theories sometimes give remarkably accurate results in this region.

For transitions between highly excited states the theory described here is accurate and uses relatively little computer time, for example a large close coupling calculation can take up to two orders of magnitude longer to obtain a cross section 5% more accurate.

## Acknowledgements

I should like to thank A.P. Clark, A.S. Dickinson and I.C. Percival for discussion in preparing this talk. I am grateful to the S.R.C. for a relevant research grant and to the staff of the Atlas Computer Laboratory.

## References

- [1] PERCIVAL, I.C. (1972). *Atoms and Molecules in Astrophysics, Proceedings of the Twelfth Session of the Scottish Universities Summer School in Physics, 1971* (ed. T.R. Carson and M.J. Roberts), London and New York: Academic Press.
- [2] PERCIVAL, I.C. and RICHARDS, D. (1970). *J. Phys. B*, **3**, 1035-46.
- [3] LANDAU, L.D. and LIFSHITZ, E.M. (1971). *Classical Theory of Fields, Course in Theoretical Physics*, 2, Oxford: Pergamon.
- [4] HEISENBERG, W. (1925). *Z. Physik*, **33**, 879. Translation 1967 *Sources of Quantum Mechanics* (ed. B.L. van der Waerden), Amsterdam: North Holland.
- [5] PERCIVAL, I.C. (1969). *Physics of One and Two Electron Atoms* (ed. F. Bopp and H. Kleinpoppen), Amsterdam: North Holland.
- [6] NORCLIFFE, A. (1973). *Case Studies in Atomic Physics* (ed. E.W. McDaniel and M.R.C. McDowell), **4**, 1-55, Amsterdam: North Holland.
- [7] NACCACHE, P.F. (1972). *J. Phys. B*, **5**, 1308-19.
- [8] PERCIVAL, I.C. and RICHARDS, D. (1971). *J. Phys. B*, **4**, 918-31.
- [9] ——— and ——— (1971). *J. Phys. B*, **4**, 932-39.
- [10] RICHARDS, D. (1973). *J. Phys. B*, **6**, 832-36.
- [11] BEIGMAN, I. L., VAINSHTEIN, L. A. and SOBEL'MAN, I.L., (1969). *Zuhr. Eksp. i Teoret. Fiz.*, **57**, 1703-9. Translation 1970 *Soviet Phys. - JETP*, **30**, 920-3.
- [12] PRESNYAKOV, L.P. and URNOV, A.M. (1970). *J. Phys. B*, **3**, 1267-71.
- [13] PERCIVAL, I.C. (1971). *Atomic Physics 2, Proceedings of the Second International Conference on Atomic Physics, 21-24 July, Oxford* (ed. P.G.H. Sandars), London: Plenum Press.
- [14] CLARK, A.P. and DICKINSON, A.S. (1971). *J. Phys. B*, **4**, L112.
- [15] CLARK, A.P. (1973). *J. Phys. B*, **6**, 1153-64.
- [16] DICKINSON, A.S. and RICHARDS, D. (1974). *J. Phys. B*, **7**, 1916-1936.
- [17] BURKE, P.G., SCRUTTON, D., TAIT, J.H. and TAYLOR, A.J. (1969). *J. Phys. B*, **2**, 1155-68.
- [18] GORDON, R.G. (1969). *J. Chem. Phys.*, **51**, 14-25.

# Semiclassical Methods in Reactive and Non-reactive Collisions

W.H.Miller\*

In the last few years it has been shown how exact classical mechanics (i.e., numerically computed classical trajectories) can be used as input to a general semiclassical theory of complex (i.e., inelastic and reactive) molecular collision processes. This semiclassical model of 'classical dynamics' plus quantum superposition includes all quantum effects in molecular systems at least qualitatively, and the description is often quantitative. The primary emphasis of this paper will be the description of *classically forbidden* processes, i.e., those which do not occur via ordinary classical mechanics. This is essentially a generalization of the concept of tunneling to dynamical systems of more than one degree of freedom and is one of the most important aspects of this 'classical S-matrix' theory. Examples of reactive and non-reactive atom-diatom collisions are used to illustrate the ideas.

\* *Inorganic Material Research Division, Lawrence Berkeley Laboratory and Department of Chemistry, University of California, Berkeley, California 94720, USA*

# Canonical Integrals in Semiclassical Collision Theory

J.N.L.Connor\*

A basic problem in semiclassical collision theory is the derivation of uniform approximations for quantities such as  $S$  matrix elements and scattering amplitudes. The uniform approximations can be expressed in terms of certain canonical integrals and their derivatives. It is shown how the canonical integral is determined by the topological structure of the classical trajectories. The case of two and three nearly coincidental trajectories is considered in detail.

## Introduction

The semiclassical theory of molecular collisions involves an asymptotic solution of Schrödinger's equation. It requires real and complex valued solutions of Hamilton's equations [1-5]. An important part of the theory applies asymptotic methods to the evaluation of integrals. These asymptotic approximations can be written in terms of *canonical integrals*. This paper discusses how the topological structure of the classical trajectories determines the canonical integrals.

## Coalescing Trajectories

An  $S$  matrix element in semiclassical theory is represented by an integral of the form [2-5],

$$S(\alpha) = \int g(x) \exp[if(\alpha;x)] dx \quad (1)$$

in the one dimensional case. Similar integrals arise in the evaluation of scattering amplitudes [1]. In (1),  $\alpha$  is a set of parameters such as collision energy, final quantum numbers of the collision and any potential parameters.

When integral (1) is evaluated by asymptotic techniques, the main contribution comes from the saddle points of  $f$ . These are the real or complex points  $\{x_i\}, i = 1, 2, \dots, n$  satisfying

$$\frac{\partial f(\alpha;x)}{\partial x} = 0 \quad (2)$$

Physically the saddle points correspond to real or complex valued classical trajectories. Equation (2) shows the positions of the saddle points depend on  $\alpha$ .

As  $\alpha$  varies, so do the positions of the saddle points and for a certain value of  $\alpha$  they may come close together or coalesce. This is illustrated in figures 1 and 2.

Figure 1 shows a plot of the elastic deflection function against impact parameter [6,7]. The parameters are the collision energy and the scattering angle. There are three nearly coincident classical trajectories.

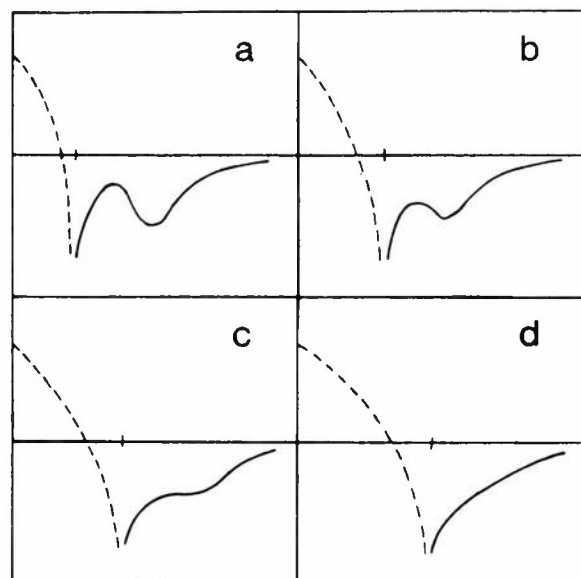


Figure 1: The elastic deflection function plotted against impact parameter for four values of the collision energy. The dashed line is a reactive deflection function. There are three saddle points.

\* Department of Chemistry, University of Manchester, Brunswick Street, Manchester, M13 9PL

Figure 2 shows a plot of the final action against initial angle for a collinear collision [8]. The parameters in this case are the collision energy and the final vibrational quantum number. This example has four coalescing trajectories.

The problem is to derive an asymptotic approximation that is valid regardless of whether the classical trajectories are close together or far apart.

### Uniform Approximation and Canonical Integrals

The simplest asymptotic method for evaluating integral (1) is the saddle point or stationary phase method:

$$S(\alpha) \sim (2\pi i)^{1/2} \sum_i \frac{g(x_i)}{[f''(\alpha; x_i)]^{1/2}} \exp [if'(\alpha; x_i)]. \quad (3)$$

The sum is over all contributing trajectories. Equation (3) is valid when all the trajectories are well separated from one another. For example, for two well separated real trajectories 1 and 2, the transition probability  $P = |S|^2$  becomes [5,9]

$$P = p_1 + p_2 + 2(p_1 p_2)^{1/2} \sin(\phi_2 - \phi_1), \quad (4)$$

where  $p_1$  and  $p_2$  are classical transition probabilities and  $\phi_1$  and  $\phi_2$  classical action integrals.

Equations (3) and (4) become invalid when the two trajectories approach one another (because  $f'' \rightarrow 0$ ). A uniform approximation for this case is [9]

$$P = \pi(p_1^{1/2} + p_2^{1/2})^2 \zeta^{1/2} Ai^2(-\zeta) + \pi(p_1^{1/2} - p_2^{1/2})^2 \zeta^{-1/2} Ai'^2(-\zeta) \quad (5)$$

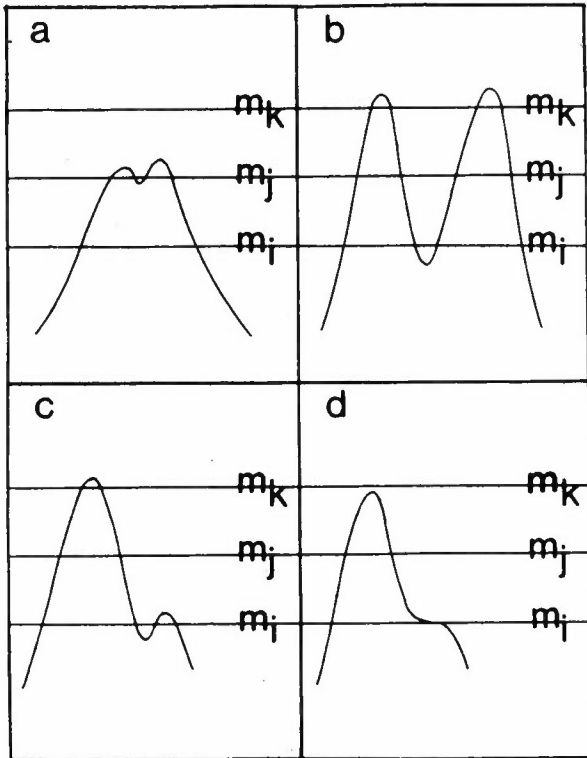


Figure 2: Final action-initial angle plots for a collinear collision at four values of the collision energy. There are four saddle points. The real saddle points lie where the horizontal lines intersect the action-angle points.

where

$$\zeta = [\frac{1}{4}(\phi_2 - \phi_1)]^{2/3}$$

and  $Ai(-\zeta)$  is the regular Airy function:

$$Ai(-\zeta) = (2\pi)^{-1} \int_{-\infty}^{\infty} \exp[i(-\zeta u + \frac{1}{3}u^3)] du. \quad (6)$$

Equation (5) is uniformly valid for two real trajectories close together or far apart. The regular Airy function is the canonical integral for this case.

Equation (5) becomes non-uniform however when three trajectories are close together. A uniform approximation for this case can be derived [7] in terms of the canonical integral

$$P(x,y) = \int_{-\infty}^{\infty} \exp[i(xu + yu^2 + u^4)] du. \quad (7)$$

Figure 3 shows a plot of  $|P(x,y)|$  and figure 4 one of  $\arg P(x,y)$ . Since  $P(-x,y) = P(x,y)$ , it is only necessary to plot the upper half plane.

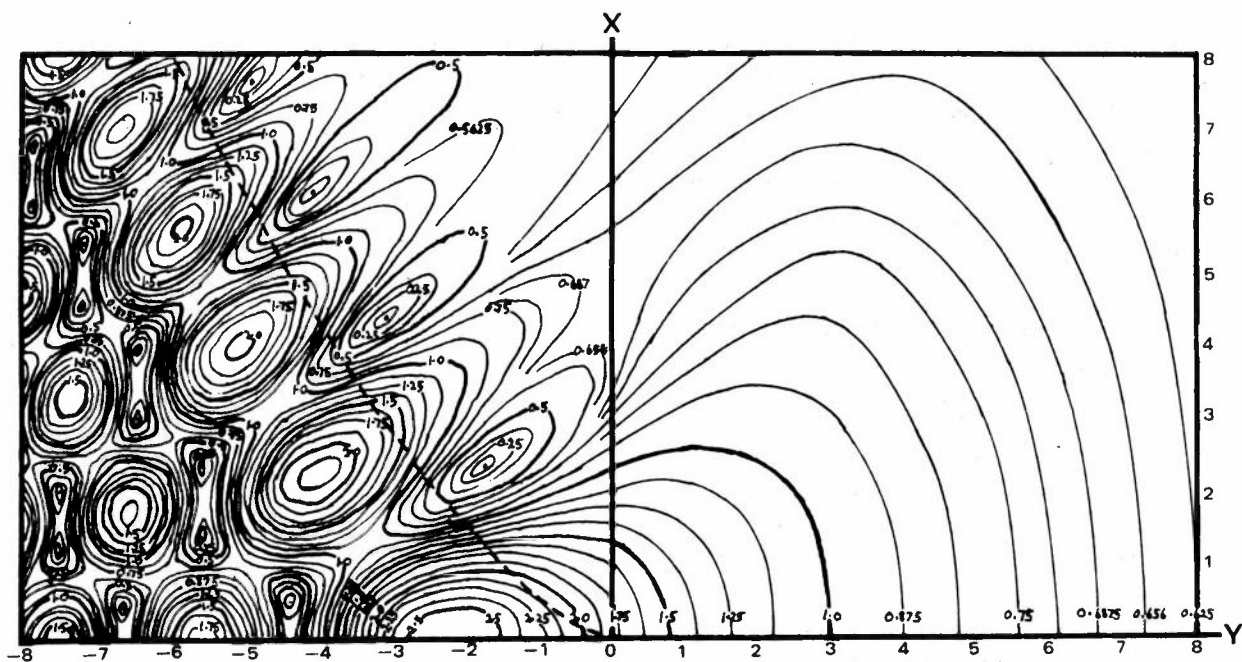


Figure 3: The modulus of  $P(x,y)$ .

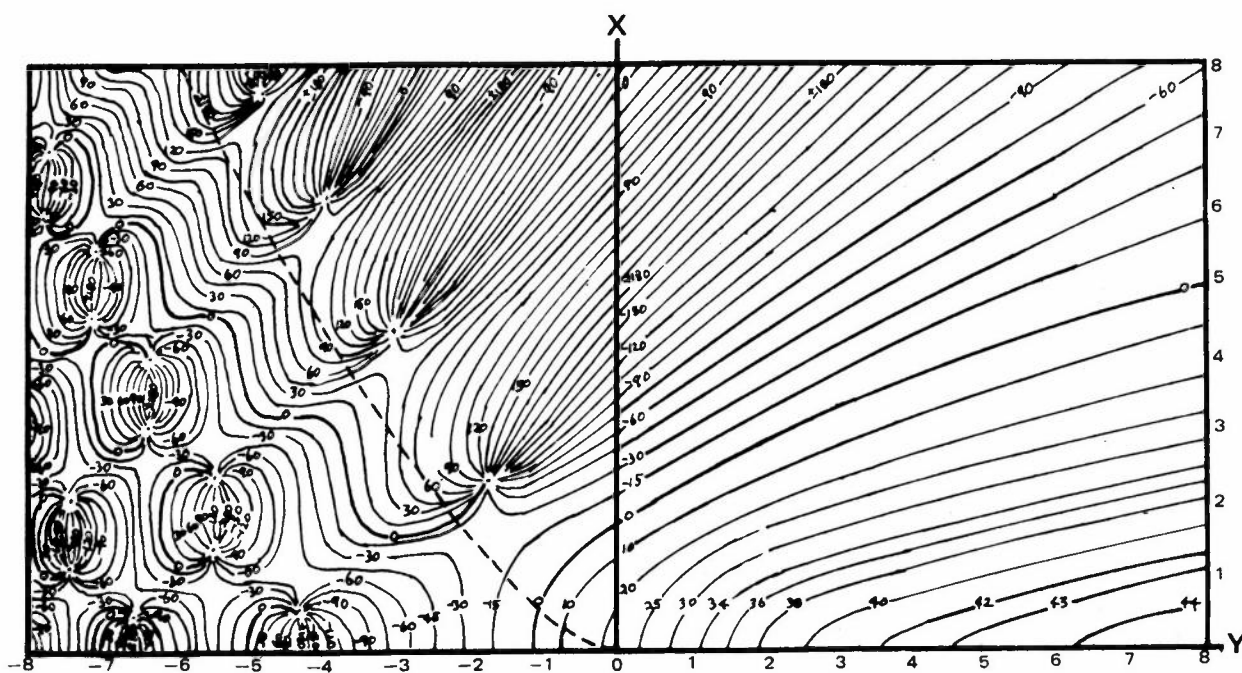


Figure 4: The phase of  $P(x,y)$  in degrees.

For  $n$  coalescing real or complex valued classical trajectories, the canonical integral is [8]

$$U(\xi_1, \xi_2, \dots, \xi_{n-1}) = \int_{-\infty}^{\infty} \exp [i(\xi_1 u + \xi_2 u^2 + \dots + \xi_{n-1} u^{n-1} + u^{n+1})] du. \quad (8)$$

The integral (8) includes (6) and (7) as special cases. It can be seen the number of coalescing trajectories determines the canonical integral.

An important property of equations (4) and (5) is they only involve quantities characterizing the classical trajectories. This is also true for uniform asymptotic approximations in terms of integrals (7) and (8).

The uniform approximations discussed above become invalid if  $g$  possesses zeroes, poles or branch points near a saddle point or if end point contributions to the integral are important. They also become invalid if  $f$  is a slowly varying function [10,11]. The use of non-uniform approximations may explain discrepancies that have been reported between semiclassical calculations and exact quantum results [12-15].

When an  $S$  matrix element is represented by a multidimensional integral, the derivation of uniform approximations is more difficult. For certain cases, the canonical integral is again integral (8) [8,16-20]. In general however the canonical integral is non separable and multidimensional [19,20].

## Conclusions

Semiclassical integral representations for  $S$  matrix elements and scattering amplitudes can be evaluated asymptotically in terms of a canonical integral. The canonical integral is determined by the number of coalescing real or complex valued classical trajectories. The uniform approximation involves only quantities characterizing the classical trajectories.

## References

- [1] BERRY, M.V. and MOUNT, K.E. (1972). *Rep. Prog. Phys.*, **35**, 315.
- [2] GEORGE, T.F. and ROSS, J. (1973). *Ann. Rev. Phys. Chem.*, **24**, 263.
- [3] SECREST, D. (1973). *Ann. Rev. Phys. Chem.*, **24**, 379.
- [4] CONNOR, J.N.L. (1973). *Ann. Rep. Chem. Soc.*, **70A**, 5.
- [5] MILLER, W.H. (1974). *Adv. Chem. Phys.*, **25**, 69.
- [6] CONNOR, J.N.L. and CHILD, M.S. (1970). *Mol. Phys.*, **18**, 653.
- [7] CONNOR, J.N.L. (1973). *Mol. Phys.*, **26**, 1217.
- [8] ————— (1974). *Mol. Phys.*, **27**, 853.
- [9] CONNOR, J.N.L. and MARCUS, R.A. (1971). *J. Chem. Phys.*, **55**, 5636.
- [10] STINE, J.R. and MARCUS, R.A. (1973). *J. Chem. Phys.*, **59**, 5145.
- [11] CONNOR, J.N.L. (1974). *Chem. Phys. Letters*, **25**, 611.
- [12] WU, S.F. and LEVINE, R.D. (1973). *Mol. Phys.*, **25**, 937.
- [13] BOWMAN, J.M. and KUPPERMANN, A. (1973). *Chem. Phys. Letters*, **19**, 166.
- [14] ————— and ————— (1973). *J. Chem. Phys.*, **59**, 6524.
- [15] TYSON, J.J., SAXON, R.P. and LIGHT, J.C. (1973). *J. Chem. Phys.*, **59**, 363.
- [16] DOLL, J.D. and MILLER, W.H. (1972). *J. Chem. Phys.*, **57**, 5019.
- [17] MARCUS, R.A. (1972). *J. Chem. Phys.*, **57**, 4903.
- [18] CONNOR, J.N.L. (1973). *Mol. Phys.*, **25**, 181.
- [19] ————— (1973). *Discussions Faraday Soc.*, **55**, 51.
- [20] ————— (1973). *Mol. Phys.*, **26**, 1371.



# Cross Sections for the Rotationally Inelastic Scattering of $Ne + N_2$ : Application of the Exponential Semi-Classical Distorted Wave Approximation (Preliminary Results)

S.Bosanac and G.G.Balint-Kurti\*

Exact quantum-mechanical close-coupling, and approximate calculations are presented for  $Ne + N_2$  collisions using a model potential. The calculations take account of the coupling only between the  $j = 0$  and  $j = 2$  rotational states of  $N_2$ . The approximate calculations are performed using an improved form of the exponential semi-classical distorted wave approximation which is outlined in the paper. Cross sections evaluated using the approximate method compare very well with the exact ones over the entire range of energies of chemical interest. Total and differential inelastic ( $j = 0 \rightarrow j = 2$ ) cross sections are presented and their variation with energy is examined. The present results disagree significantly with previously published results using the same potential

## Introduction and Theory

The  $Ne + N_2$  system has been studied by Burke *et al.* [1] who treated the system as a structureless atom colliding with a rigid rotor diatomic molecule. The potential is taken to be

$$V(\vec{R}, r) = \epsilon \left[ \left( \frac{R_m}{R} \right)^{12} - 2 \left( \frac{R_m}{R} \right)^6 \right] + \epsilon a_{12} \left( \frac{R_m}{R} \right)^{12} P_2(\cos \theta) - 2\epsilon a_6 \left( \frac{R_m}{R} \right)^6 P_2(\cos \theta) \quad (1)$$

where  $R$  is the distance from the atom to the centre of mass of the diatomic,  $\vec{R}$  is the corresponding vector,  $\hat{r}$  is a unit vector along the bond of the diatomic and  $\theta$  is the angle between  $\vec{R}$  and  $\hat{r}$ . These variables are illustrated in figure 1. There are four potential energy parameters [2]  $\epsilon, R_m, a_{12}$  and  $a_6$ . The first two are the well depth and the equilibrium distance of the spherically symmetric part of the potential, which is taken to be a Lennard-Jones potential.  $a_{12}$  and  $a_6$  are the so called anisotropy parameters.

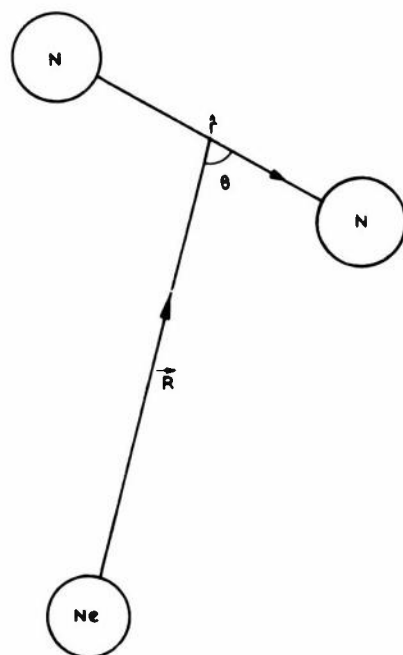


Figure 1: Definition of coordinates.

\* School of Chemistry, University of Bristol, Cantock's Close, Bristol, BS8 1TS  
(present address of S.B.) Institute 'Ruder Bošković', 41001 Zagreb, Bijenička C.54, Yugoslavia

Arthurs and Dalgarno [3] have discussed the atom-rigid rotor problem using the time-dependent Schrödinger equation. They expand the total wavefunction in terms of angular functions which are eigenfunctions of the total angular momentum  $J$ . In this way they obtain a set of coupled differential equations for the radial functions  $u_{j'\ell'}^{Jj\ell}(R)$ . These equations are of the form

$$\left[ \frac{d^2}{dR^2} + \left( k_{j'}^2 - \frac{\ell'(\ell'+1)}{R^2} - U_{j'\ell',j'\ell'}^J(R) \right) \right] u_{j'\ell'}^{Jj\ell}(R) = \sum_{j''\ell'' \neq j'\ell'} U_{j'\ell',j''\ell''}^J(R) u_{j''\ell''}^{Jj\ell}(R) \quad (2)$$

where the  $U_{j'\ell',j''\ell''}^J(R)$  are essentially the matrix elements of the potential between the angular functions. The  $j$ 's are rotational quantum numbers for the diatomic and the  $\ell$ 's are the orbital angular momentum quantum numbers corresponding to the relative motion of the atom and diatomic molecule. There is a different set of such coupled equations for every total angular momentum quantum number  $J$  and each set in principle involves an infinite number of differential equations. In practice we truncate both the number of  $J$  values considered and the number of coupled differential equations for each value of  $J$ .

The boundary conditions on the radial functions  $u_{j'\ell'}^{Jj\ell}(R)$  are

$$\begin{aligned} u_{j'\ell'}^{Jj\ell}(R) &\underset{R \rightarrow 0}{\sim} 0 \\ u_{j'\ell'}^{Jj\ell}(R) &\underset{R \rightarrow \infty}{\sim} -\frac{1}{2i} \left[ e^{-i(k_j R - \ell' \pi/2)} \delta_{jj'} \delta_{\ell\ell'} \right. \\ &\quad \left. - \left( \frac{k_j}{k_{j'}} \right)^{1/2} S_{j'\ell',j\ell}^J e^{i(k_j R - \ell' \pi/2)} \right] \end{aligned} \quad (3)$$

Thus the  $S$  matrices (whose elements are  $S_{j'\ell',j\ell}^J$ ) may be found from the asymptotic behaviour of the radial functions. The total cross section  $\sigma_{j' \leftarrow j}^{\text{Tot}}$  may be expressed as a sum involving the squares of elements of the  $S$  matrix.

$$\sigma_{j' \leftarrow j}^{\text{Tot}} = \frac{\pi}{k_{j'}^2 (2j+1)} \cdot \sum_J (2J+1) \sum_{\ell\ell'} |\delta_{jj'} \delta_{\ell\ell'} - S_{j'\ell',j\ell}^J|^2 \quad (4)$$

The differential cross section may similarly be expressed as

$$\sigma_{j' \leftarrow j}(\theta) = \frac{1}{4k_{j'}^2} \cdot \frac{1}{(2j+1)} \cdot \sum_{mm'} |\sum_J (2J+1) T_{j'm',jm}^J d_{m'm}^J(\theta)|^2 \quad (5)$$

where:

$$T_{j'm',jm}^J = \sum_{\ell\ell'} i^{\ell-\ell'} |\delta_{jj'} \delta_{\ell\ell'} - S_{j'\ell',j\ell}^J| (jmJ - m|j\ell 0)(j'm'J - m'|j'\ell' 0) \quad (6)$$

The  $d_{m'm}^J(\theta)$  are simple angular functions which are the reduced representations of the rotation group and

$(jmJ - m|j\ell 0)$  etc. are Clebsch-Gordan coefficients [4]. The quantum numbers  $m$  and  $m'$  correspond to the components of the rotational angular momentum of the diatomic along the relative direction of motion of the reactants and products respectively. The use of angular functions referred to these axes is called the helicity representation [5,6].

Several numerical techniques have recently been developed for the efficient solution of a finite set of coupled differential equations such as those of equation (2). We have used a program written by R.G. Gordon [7] to perform the 'exact' close-coupling calculations discussed in this paper. The whole program, including the part which evaluates the cross sections (written by S.B.) was tested by reproducing exactly the total and differential cross sections reported by Hayes and Kouri [8] for the  $He + H_2$  system.

For problems involving atoms and molecules of moderately large mass the number of  $J$  values needed and the number of coupled channels required for each  $J$  value often becomes so large as to make the exact solution of equation (2) impractical. One frequently used method of approximating the solutions of equation (2) for such cases is the Distorted Wave Born (DW) approximation [9]. In this method the coupling terms in equation (2) (i.e. the terms on the right-hand side of the equation) are ignored and the solution of the equation

$$\left[ \frac{d^2}{dR^2} + \left( k_j^2 - \frac{\ell(\ell+1)}{R^2} - U_{j\ell,j\ell}^J(R) \right) \right] \chi_{j\ell}^J(R) = 0 \quad (7)$$

with boundary conditions

$$\begin{aligned} \chi_{j\ell}^J(r) &\underset{R \rightarrow 0}{\sim} 0 \\ &\underset{R \rightarrow \infty}{\sim} \sin(k_j R - \ell \pi/2 + \delta_{j\ell}) \end{aligned} \quad (8)$$

is found [10]. The  $S$  matrix elements, which are needed to calculate the cross sections, may then be approximated as

$$S_{j'q',j\ell}^J = e^{i\delta_{j'q'}} \left[ \delta_{jj'} \delta_{\ell\ell'} - \frac{2i(1-\delta_{jj'}\delta_{\ell\ell'})}{\sqrt{k_j k_{j'}}} \int_0^\infty \chi_{j'q'}(R) U_{j'q',j\ell}^J(R) \chi_{j\ell}(R) dR \right] e^{i\delta_{j\ell}} \quad (9)$$

In the Distorted Wave Born (DW) approximation we avoid the necessity of solving the set of coupled differential equations, equation (2), and instead have to solve several uncoupled equations, equation (7), and then take integrals over the solutions to obtain the  $S$  matrix elements needed to evaluate the cross sections. One of the principle drawbacks of the DW approximation is that the  $S$  matrices calculated in this way are not in general unitary, as is required by the condition that the total number of particles should be conserved. An Exponential Distorted Wave (EDW) procedure, in which the approximate  $S$  matrix is unitary, has been proposed [11]. In this procedure the  $S$  matrix is written as:

$$S_{j'q',j\ell}^J = e^{i\delta_{j'q'}} \left[ e^{iA^J} \right]_{j'q',j\ell} e^{i\delta_{j\ell}} \quad (10)$$

where  $A^J$  is a Hermitian matrix with zero diagonal elements and whose off diagonal elements are given by

$$A_{j'q',j\ell}^J = -\frac{2}{\sqrt{k_j k_{j'}}} \int_0^\infty \chi_{j'q'}(R) U_{j'q',j\ell}^J(R) \chi_{j\ell}(R) dR \quad (11)$$

Clearly when the exponential in equation (10) is expanded in a power series the first two terms give the same result as the DW approximation, equation (9). The higher terms can be shown to correspond to parts of the higher order terms in the Distorted Wave Born series [12].

In the present work we use an exponential semi-classical distorted wave approximation (ESCDW) in which equations (10) and (11) are used to calculate the  $S$  matrix but the further approximation is made that the distorted waves  $\chi_{j\ell}(R)$  are evaluated using a semi-classical JWKB type approximation. A preliminary study, using a very similar approximation has been published [13]. The method used here differs from [13] in that the distorted waves are represented as linear combinations of Airy functions in the region from well inside the innermost classical turning point to well beyond the outermost one. In this region the wavefunction had the form

$$\chi_{j\ell}(R) = \alpha 2\pi^{1/2} q_{j\ell}(R)^{1/4} |P_{j\ell}(R)|^{-1/2} Ai(q_{j\ell}(R)) + \beta \pi^{1/2} q_{j\ell}(R)^{1/4} |P_{j\ell}(R)|^{-1/2} Bi(q_{j\ell}(R)) \quad (12)$$

$$\text{where } p_{j\ell}(R)^2 = k_j^2 - \frac{(\ell+1/2)^2}{R^2} - U_{j\ell,j\ell}^J(R)$$

$$\text{and } q_{j\ell}(R) = - \left[ \frac{3}{2} \int_{R_0}^R |P_{j\ell}(R)| dR \right]^{2/3}$$

and  $R_0$  is a turning point. When raising the right hand side of the expression for  $q_{j\ell}(R)$  to the power of 2/3, the quantity in the square brackets should first be squared and then the third root taken.

These wavefunctions are continuous in the neighbourhood of the turning points and in regions where the JWKB method is valid they go over smoothly to the correct JWKB wavefunction [14]. They have been used in the present work to provide an approximate description of the shape resonances which can arise when the effective potential (i.e. including the centrifugal term) has three classical turning points and the two colliding particles can be temporarily trapped inside the centrifugal barrier. The coefficients  $\alpha$  and  $\beta$  are determined by the boundary condition at small  $R$ . The precise details of how the distorted waves are calculated and some other technical aspects of the calculations will be reported at greater length elsewhere [15].

## Results and Discussion

The semi-classical JWKB approximation is designed to provide a good description of the scattering in the short wave length or high energy limit. In order to test the validity of the ESCDW approximation in one of the situations where it might be expected to be the least valid, we examined the scattering of  $Ne+N_2$  in the very low energy region where there were three classical turning points in channels with  $j=2$ . Only rotational states  $j=0$  and  $j=2$  were included in the calculations (i.e. 4 coupled channels) and a sufficiently large number of  $J$  values were considered to ensure convergence of the total cross sections to better than 1%. (This corresponded to  $J$  values up to  $J=20$  for low relative kinetic energies  $E = .0016 eV$  and  $J=100$  for  $E = 0.136 eV$ .)

Figure 2 compares the exact close coupling calculation results and the ESCDW results for the  $j=0 \rightarrow j=2$  total inelastic cross section in the energy range  $0.00158 \text{ eV}$  to  $.00174 \text{ eV}$ . This energy range is just above the threshold for the  $j=0 \rightarrow j=2$  excitation. The asymptotic kinetic energy of the particles in the lower channel ( $j=0$ ) corresponds to a wavelength about equal to  $R_m$  (the characteristic range parameter of the potential), while in the higher channel ( $j=2$ ) the asymptotic wavelength is considerably larger than  $R_m$ . These calculations therefore constitute an extremely severe test of the semi-classical aspect of the ESCDW approximation. We see from figure 2 that the agreement between the exact and ESCDW calculations is, in fact, remarkably good [15]. The maxima in the cross section arise from the shape resonances in the upper channels ( $j=2$ ) [1].

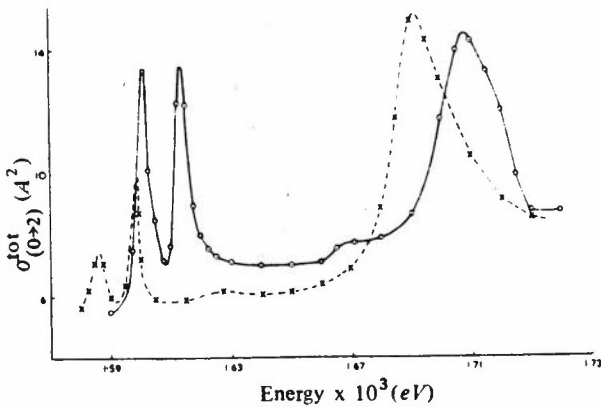


Figure 2: Comparison of total inelastic cross sections for  $j=0 \rightarrow j=2$  transition as calculated by exact close coupling method (---) and ESCDW approximation (—) in small energy range just above threshold.  $E = .00158 \text{ eV} - .00174 \text{ eV}$ .

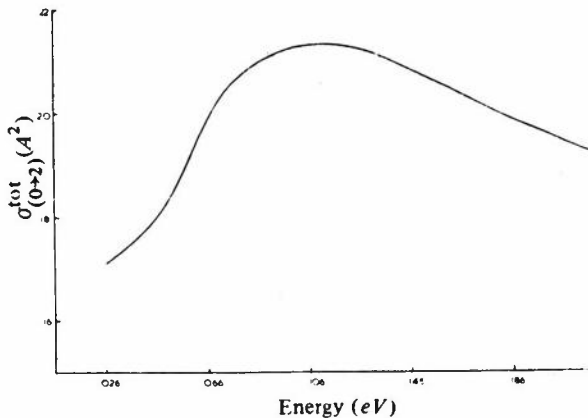


Figure 3: Variation of the total inelastic  $j=0 \rightarrow j=2$  cross section with energy. The calculations were performed using the ESCDW method.

In figure 3 the variation of the total  $j=0 \rightarrow j=2$  inelastic cross section, as calculated using the ESCDW approximation, is shown over a much larger energy range. The agreement between the exact and ESCDW cross sections was checked at an energy of  $0.136 \text{ eV}$ . They were found to agree within 6.8% ( $19.7 \text{ \AA}$  [2] for the exact as compared with  $21.0 \text{ \AA}$  [2] for the ESCDW). The cross sections shown in figure 3 are about an order of magnitude larger than those reported for the same system in [1]. At the lower energies corresponding to figure 2, the cross sections reported here are of the same order of magnitude as those of [1] but differ from them in detail.

Figure 4 shows a differential inelastic cross section, for the  $j=0 \rightarrow j=2$  transition, calculated using the ESCDW approximation at an energy of  $.001601 \text{ eV}$ , which corresponds to the first shape resonance in figure 2. The quasi-bound state which gives rise to this resonance is in the channel  $J=7, j=2, \ell=9$ . The differential cross section consists of a series of regularly spaced maximum. The minimum in intensity at around  $\theta = 70^\circ$  is thought to arise from an interference effect with the neighbouring resonance in the channel  $J=11, j=2, \ell=7$ . In figure 5 the differential cross section is shown at an energy of  $0.046 \text{ eV}$ . The structure of the cross section is now much more complex than in figure 4. This arises from the fact that the contributions from many channels are now of comparable importance.

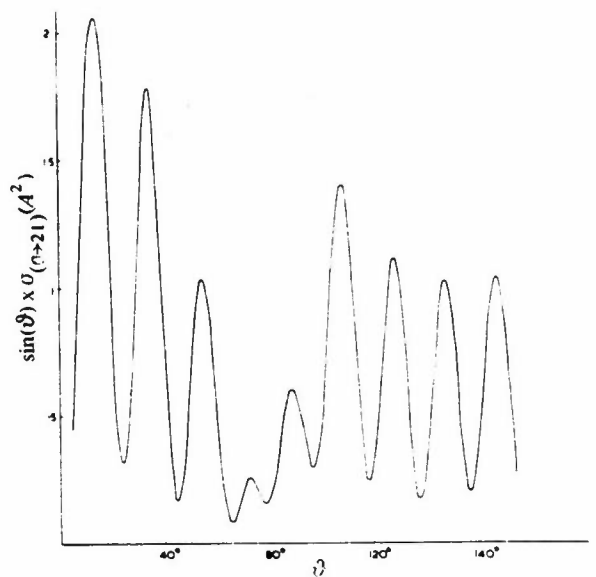


Figure 4: Differential cross section for  $j=0 \rightarrow j=2$  transition at  $E = 0.001601 \text{ eV}$ .

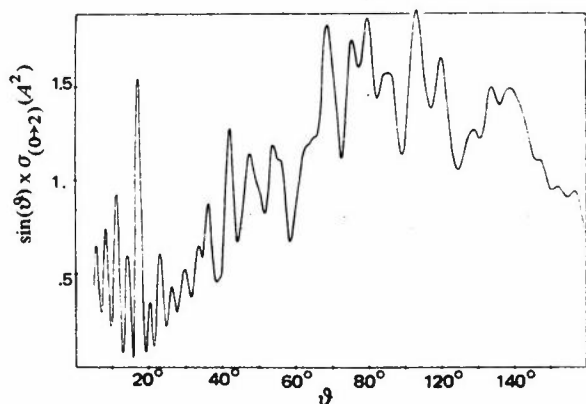


Figure 5: Differential cross section for  $j=0 \rightarrow j=2$  transition at  $E = 0.046 \text{ eV}$ .

### Conclusion

In this paper we have presented the first application of an exponential type approximation to the calculation of actual cross sections. We show that for the calculation of rotationally inelastic cross sections for the  $\text{Ne} + \text{N}_2$  system in the present four channel approximation (i.e.  $j=0$  and  $j=2$  only), the ESCDW method yields results in quantitative agreement with exact close coupling calculations. This agreement is found to hold good from extremely low energies to well above those corresponding to room temperature.

The results presented here should be regarded as a partial test of the validity of the ESCDW approximation. From a very preliminary investigation of the effect of including more coupled channels (i.e. rotational states  $j=0, 2$  and  $4$ ) it is thought that the  $j=0 \rightarrow j=2$  cross sections will be significantly reduced in magnitude, at least in the higher energy range. The elastic cross sections seem to be relatively insensitive to the inclusion of additional channels. Clearly a much more extensive investigation of the effect of including more coupled channels is needed, and this is currently being undertaken.

For the four channel calculations reported here the present computer programs for calculating the ESCDW cross sections are somewhat faster than those used to calculate the exact close coupling results. When a larger number of coupled channels are included (and for many systems a far greater number will be needed), the time needed to perform the exact calculations should increase as  $N^3$ , where  $N$  is the number of coupled channels [7]. The time needed to perform the ESCDW calculations is expected to increase only as  $N^2$ , and it is therefore in such situations when there are a large number of coupled channels, that the main computational advantages of approximations such as the ESCDW are expected to be realised.

### Acknowledgements

The authors wish to thank Professor R.D. Levine for suggesting the type of approximation used in this paper. They are indebted to the S.R.C. for financial support and for the provision of computer time and would like to express their gratitude to the staff of the Atlas Computer Laboratory and of the Rutherford Laboratory computer for their assistance.

### References

- [1] BURKE, P.G., SCRUTTON, D., TAIT, J.H. and TAYLOR, A.J. (1969). *J. Phys. B*, **2**, 1155.
- [2] The values of the potential energy parameters were
 

$\epsilon$	$= 4.92703093 \times 10^{-3} \text{ eV}$
$R_m$	$= 3.6309367 \text{ \AA}$
$a_{12}$	$= 0.375$
$a_6$	$= 0.176$
- [3] ARTHURS, A.M. and DALGARNO, A. (1960). *Proc. Roy. Soc. (London)*, **A256**, 540.
- [4] EDMONDS, A.R. (1960). *Angular Momentum in Quantum Mechanics*, Princeton University Press.
- [5] MILLER, W.H. (1969). *J. Chem. Phys.*, **50**, 407.
- [6] NEWTON, R.G. (1966). *Scattering Theory of Waves and Particles*, New York: McGraw-Hill.
- GOLDBERGER, M.L. and WATSON, K.M. (1964). *Collision Theory*, New York: Wiley.
- [7] GORDON, R.G. (1969). *J. Chem. Phys.*, **51**, 14. A program, written by R.G. Gordon and based on the method of the above paper is distributed by Quantum Chemistry program exchange, Indiana University. (QCPE 187).
- [8] HAYES, E.F., WELLS, C.A. and KOURI, D.J. (1971). *Phys. Rev.*, **A4**, 1017.
- [9] GORDON, R.G. (1973). *Discussions Faraday Soc.*, **55**, 22.
- [10] The decoupling procedure used here corresponds to the distortion decoupling method of LEVINE, R.D., JOHNSON, B.R., MUCKERMANN, J.T. and BERNSTEIN, R.B. (1968). *J. Chem. Phys.*, **49**, 56.
- [11] LEVINE, R.D. and BALINT-KURTI, G.G. (1970). *Chem. Phys. Letters*, **6**, 101.
- [12] BALINT-KURTI, G.G. (unpublished work).
- [13] BALINT-KURTI, G.G. and JOHNSON, B.R. (1973). *Discussions Faraday Soc.*, **55**, 59.
- [14] MORSE, P.M. and FESCHBACH, H. (1953). *Methods of Theoretical Physics*, Chapter 9.3, New York: McGraw-Hill.
- [15] We are presently examining some minor improvements to our present treatment of the three turning point problem. These improvements may lead to slightly better agreement than that reported here, between the exact and approximate cross sections, in the very low energy region where shape resonances are important.

# Proton-Molecule Collisions : Interacting Potentials and Inelastic Scattering\*

F.A.Gianturco †

Gas phase protonation processes and, in general, proton encounters with molecular systems require both the knowledge of interacting potentials through all the regions of space and an efficient way of solving the coupled integro-differential equations, generated in the usual time-independent equation, which are necessary to obtain the relevant scattering observables of both reactive and pre-reactive processes. We are reporting a numerical treatment of the atom(proton)-diatom problem by considering it within a laboratory frame of reference and by having the target described as a rigid rotor [1]. The necessary potential surface has been computed by considering first its static part and by producing it *via* a suitable multipolar expansion of the relevant bound-state single-particle MO's of Hartree-Fock quality. The polarization effects have also been included by adopting a suitable functional form which would give the necessary cut-off within the inner molecular region.

## Reference

- [1] BURKE, P.G., GIANTURCO, F.A. and CHANDRA, N. (1974). *Mol. Phys.*, 27, 1121.

Until very recently experimental investigations of translational-rotational and/or vibrational energy transfers in biomolecular collisions were confined to various relaxation techniques [1]. For a more complete description of the process, however, one likes to have information which is more microscopic in nature and more sensitive to *local* dynamical variables like impact parameters, internal quantum states, initial and final, of the involved partners and differential distributions of the inelastic cross sections.

Whenever such information becomes available from crossed molecular beam experiments, our theoretical models usually require a stepping up in sophistication to explain the newly acquired data [2] and indeed the scattering of a proton by a molecule at very low energies clearly requires quantum mechanics for a complete description of the non-classical behaviour detected recently [3] in the angular distribution of the scattered protons.

In the course of the collision the integrated response of each individual molecular atom, assumed as interacting with the incoming proton, is in general different. This causes excitation of molecular degrees of freedom, which may also be the consequence of the electronic structure of the target having been altered by the passing third atom making the nuclei accelerate toward the new potential minimum [4]. For systems like  $N_2$  and  $CO$ , however, the changes of molecular internuclear distances upon protonation are probably only 1 to 2%, depending on the geometry [3], a result which implies that a rather small

stretching force was applied to the molecule in the field of the proton. Even when the Hydrogen Fluoride system is concerned, recent experiments [5] and the following computations [6,7] indicate an overall bond variation of 0.066 au, i.e. also around 2%, in going from the *HF* structure to the fluoronium ion.

The above results seem therefore to suggest a possible way for efficiently constructing the relevant potential surfaces that may then be employed within completely *a priori* scattering calculations in a three-dimensional, quantum-mechanical sense. If one looks at the parallel problem of electron moderation in gases, one sees that a fair, if still far from satisfactory, amount of information has recently been accumulated due to remarkable progress in experiments and also to concomitant theoretical developments [8]. The circumstances thus seem to make it worthwhile for us to carry out the analogy with proton collisions as far as is allowed by physical intuition and computational feasibility.

The most direct analogy is, of course, with the problem of slow positron scattering; however the proton potential surface in the Born-Oppenheimer sense is given by the same equations if one disregards charge-transfers thus suggesting that a great deal can be learned from this analogy. Some notable differences between electron and positron scattering have already been recognized and investigated, particularly for some simple atoms [9]. The disparity originates from the changed interaction between the target molecule (or atom) and the impinging projectile since the mean

\* Work supported by the Italian National Research Council (C.N.R.)

† Istituto di Chimica Fisica, Università di Pisa, via Risorgimento 35, 56100 Pisa, Italy

static molecular field seen by a positron is repulsive whereas it is attractive for an electron. Moreover, the all-important effects of electron exchange<sup>7</sup> with the bound particles are absent both in positron and proton scattering. Finally, the long-range part of the interactions, which has been known to play an important role in slow electron scattering, can generally be written as:

$$V(r;R) = -\frac{\alpha(R)e^2}{2r^2} \mp \frac{\mu(R)}{r^2} P_1(\cos \vartheta) - \left\{ \frac{\alpha'(R)e^2}{2r^4} \pm \frac{Q(R)e}{r^3} \right\} P_2(\cos \vartheta) + \dots \quad (1)$$

where the  $P_n$ 's are Legendre polynomials,  $\cos \vartheta = Rr/Rr$  and the upper and lower sign refer to an electron and proton, respectively. Further,  $\mu(R)$  and  $Q(R)$  respectively represent the electrostatic dipole and quadrupole moments of a diatom with bond distance  $R$ ;  $\alpha(R)$  and  $\alpha'(R)$  the spherical and non-spherical part of the dipole molecular polarizability. The above equation exemplifies a significant contrast of the two types of interaction: the electrostatic part changes its sign, whereas the polarization part remains the same on going from electron to proton (or positron).

An immediate consequence is that there should be a substantial difference between computed observables for those processes in which the two parts of the interaction are operative in an explicit manner. A good example is provided by the rotational excitation (or de-excitation) of an homonuclear molecule for which the third term with  $P_2(\cos \vartheta)$  in equation (1) is mainly responsible and where the same or opposite signs of the static and polarizability parts lead to very different results. For vibrational excitations the same argument can be applied, the

very differently, at different energies for different targets, a fact that has not yet been extensively investigated from a theoretical viewpoint.

For thermal energy scattering it is fairly straightforward to develop the quantum mechanical form of the dynamics involved for a proton impinging on a

rigid rotor. According to the standard treatment the problem is in fact reduced to solving a set of coupled equations [11].

$$\left\{ \frac{d^2}{dr^2} + K_i^2 - \frac{\ell_i(\ell_i + 1)}{r^2} \right\} F_i^J(r) = \sum_m V_{im}^J(r) F_m^J(r) \quad (2)$$

where the channel numbers  $(i, k)$  label both the rotational level of the target ( $j$ ) and the partial-wave angular momentum ( $\ell$ ). A good quantum number is given by the total angular momentum  $J$  and the relative energy for the system is embodied in the wave vector  $K_i$ .

Whenever a multipolar form can be used for the potential of equation (1) one can write:

$$V_{im}^J(r;R) = 2\mu \langle i | V(r;R) | m \rangle \\ = 2\mu \sum_{\lambda} V_{\lambda}(r;R) A_{\lambda}^J(j'\ell'; j\ell) \quad (3)$$

where the  $A$ -matrix can be written in the form:

$$A_{\lambda}^J(j'\ell'; j\ell) = (-)^{j'+\ell'-J} [(2j+1)(2\ell+1)]^{1/2} W(j\ell j'\ell'; J\lambda)(\ell\lambda\ell')_0 (j\lambda j')_0 \quad (4)$$

major modification being essentially the replacement of the molecular parameters  $\alpha'(R_0)$  and  $Q(R_0)$  by their derivatives with respect to  $R$ .

The rotational excitation of a strongly polar molecule appears to provide another interesting case. If the dipolar interaction, the second term in equation (1), plays a predominant role in the long-range region of interaction, cross sections for electrons and positrons will turn out to be the same within any first order theory (such as the Born approximation) and the proton-molecule cross sections will have a similar energy-dependence behaviour.

Moreover, because of the repulsive nature of the static potential for proton scattering, the resonances usually detected for low-energy electron scattering (representing properties of the combined system of  $n+1$  'molecular' electrons) should be less likely to appear; if they exist they should show themselves

For homonuclear diatomic system,  $\lambda$  only assumes even values; it then follows from the above Clebsch-Gordon coefficients that the relevant potential decouples equation (2) into at least four different sets corresponding to even-even, even-odd, odd-odd and odd-even values of  $(J, \ell)$ . Further decoupling is obtained from the chosen values of  $\lambda$  and the particular  $\{j\}$  set.

Each coupled set is solved for the open channel  $K$ -matrix whose eigenvalues give the channel phase shifts, since the standard eigenphase equation can be written as:

$$K = U^+ \tan \delta U \quad (5)$$

where  $U$  is a real orthogonal matrix and  $\tan \delta$  a

diagonal matrix. The partial cross section is then given *via* the  $T$ -matrix as:

$$\sigma_{j \rightarrow j'}^J = \frac{(2J+1)}{K_j^2(2j+1)} \sum_{\ell=|J-j|}^{J+j} \sum_{\ell'=|J-j'|}^{J+j'} |T^J(j'\ell'; j\ell)|^2 \quad (6)$$

with

$$T^J(j'\ell'; j\ell) = \delta_{jj'} \delta_{\ell\ell'} - S_{j'\ell' \rightarrow j\ell}^J \quad (7)$$

and

$$K_j^2 = K_0^2 - \frac{\mu}{1} \left\{ j(j+1) - j_0(j_0+1) \right\} \quad (8)$$

$j_0$  being the lowest rotational level included and  $k_0^2/2\mu$  the associated relative kinetic energy.

The total cross section for the relevant transition now becomes:

$$\sigma_{j \rightarrow j'} = \sum_J \sigma_{j \rightarrow j'}^J \quad (9)$$

Recognising that the electronic motion is rapid when compared to nuclear motion [12], one can assume an effective field depending upon nuclear coordinates, and hence regard the nuclei of the target+projectile system as adiabatically moving on a many-dimensional potential energy surface.

Instead of computing such a surface over the whole relevant space for scattering encounters from some *ab initio* model for the effective electronic Hamiltonian, one can attempt a possible partitioning of the various contributions in the following form:

$$V_{\text{eff}}(\mathbf{r}, R) \sim V_{\text{HF}} + V_{\text{Pol}} + V_{\text{cb}} + V_{\text{CT}} \quad (10)$$

Here the  $V_{\text{HF}}(\mathbf{r}', R)$  represents the potential generated at  $\mathbf{r}'$  by the electronic and nuclear charge distribution of the molecule as given by the Hartree-Fock bound

$$V_{\text{Pol}}(\mathbf{r}; R) = - \left\{ \frac{\alpha(R_0)e^2}{2r^4} + \frac{\alpha'(R_0)e^2}{2r^4} P_2(\cos \vartheta) \right\} [1 - \exp(-\gamma)] \quad (14)$$

orbitals:

$$\rho_{\text{HF}}(\mathbf{r}; R) = -\rho_{\text{HF}}^{\text{el}}(\mathbf{r}) + \sum_{\alpha} Z_{\alpha} \delta(|\mathbf{r} - R_{\alpha}|) \quad (11)$$

$$V_{\text{HF}}(\mathbf{r}'; R) = \sum_{\mu\nu} P_{\mu\nu} \langle \chi_{\mu} | \frac{q}{|\mathbf{r} - \mathbf{r}'|} | \chi_{\nu} \rangle + \sum \frac{Z_{\alpha} q}{|R - \mathbf{r}'|} \quad (12)$$

where  $q$  is a structureless point charge located at

$\mathbf{r}'$ ,  $P_{\mu\nu}$  an element of the bond-order matrix, and the indices  $\mu$  and  $\nu$  range over all orbitals on all centres  $\alpha$ .

$V_{\text{CT}}$  includes the contributions due to electronic charge transfer over the incoming proton, i.e. is a measure of the charge density variation on the target molecule during encounters. They are usually recognized to be small for strongly bonded systems [3] and will be tentatively disregarded in the present treatment.

$V_{\text{cb}}$  and  $V_{\text{Pol}}$  contain respectively the centrifugal barrier due to the various partial waves contributing to the target expansion and the polarization contributions already indicated in equation (1).

In order to represent properly the nuclear singularities contributing to the short-range interaction with the static mean field, we have performed a one-centre expansion of the bound Molecular Orbitals given by the MO-LCAO-SCF description of some typical diatomic systems like  $N_2$ ,  $CO$  and  $HF$  [13,14] and have used them to construct the static potential surface of equation (10):

$$V_{\text{HF}}(\mathbf{r}; R) = V_{\text{static}}(\mathbf{r}; R) = \sum_{\lambda=0}^{14} V_{\lambda}(\mathbf{r}; R) P_{\lambda}(\cos \vartheta) \quad (13)$$

Such a description was already shown to be very effective in treating electron-molecule scattering at low energies [14,15]. Moreover, it represents a collision-oriented version of the static potential model which recently has been given a great deal of attention [16,17].

It is, however, well known from electron-atom scattering studies [12], that the polarization force which arises from a temporary and partial excitation of the molecule during the encounter has an important influence on the scattering of slow charged particles. Therefore we have included such an effect, indicated by the second term on the right hand side of equation (10), by 'mimicking' its behaviour in the inner region of the molecule and smoothing out the usual 'switching' technique previously used [18].

where  $\gamma = (-\frac{r}{r_0})^6$ . The last term on the right represents a cut-off factor with one free parameter ( $r_0$ ), removing singularities from  $V_{\text{Pol}}(\mathbf{r}; R)$  which now behaves as  $r^2$  near to the origin. The parameter was adjusted for the point charge of the electron-scattering problem so that the experimental resonances of the elastic cross sections could be well reproduced with the given static potential [13,19]. In other words, equation (14) takes from other theoretical models the necessary knowledge to describe the perturbing effects



of a positive structureless charge approaching the target, i.e. the simplest basis for a protonation reaction potential.

The homonuclear diatomics are the simplest target molecule for which a systematic study of static potential surfaces can be performed. We began with the  $N_2$  system for which an extensive analysis of the cusp behaviour and asymptotic values of the multipolar coefficients had already been performed [14].

A critical examination [20] of SCF wavefunctions of various accuracies suggests that minimal basis sets (MBS) and semiempirical methods manage to reproduce, albeit qualitatively, only the first few terms of the expansion (3) and in spatial regions very close to the molecule, thus failing both in giving correct cusps and realistic long-range terms.

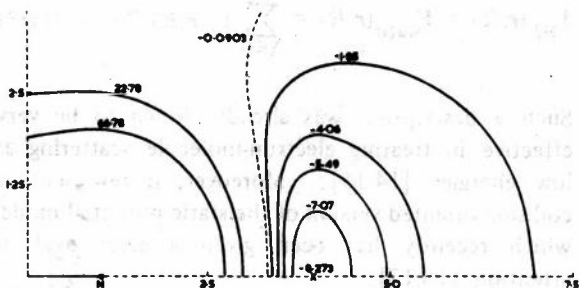


Figure 1: Proton potential energy surface (Kcal/mole) resulting from the static charge distribution of the ground-state  $N_2$  molecule.

Figure 1 shows the present results with only the  $V_{HF}$  term of equation (12). Chemical intuition is satisfied by the shallow basin existing along the bond distance and the steeply repulsive field closer to the nuclei: electronic attraction does not manage to offset the main repulsive character of the mean static field.

The large class of simple molecules possessing permanent dipole moment has received considerable attention in recent times, since in a quantum mechanical treatment the electric dipole field exhibits a critical binding property for non-neutral particles [21]. Moreover, because of the very long-range nature of this interaction, there is considerable contribution from partial waves with large  $\ell$  values so that in the inner region the lower partial wave modifications do not cause a drastic change in the total cross section.

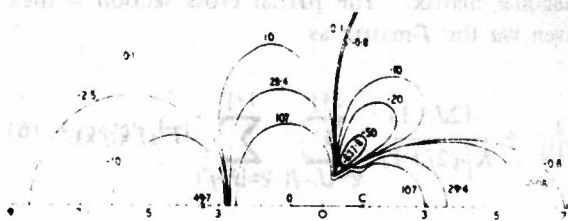


Figure 2: Same as figure 1 for the  $CO$  target system.

Figure 2 shows again our results for the  $CO$  molecule, using the rather extended basis set of STO's reported by McLean and Yoshimine [22] to construct the  $V_{HF}$  up to about 25 au from the centre of mass of the  $H^+-CO$  system. The lone-pair region of the Oxygen atom presents here a much deeper minimum than before (49.7 Kcal/mole at 3.44 Bohr radii from centre-of-mass), but the attractive well is by and large more evident for reaction paths impinging on the 'multiple' bond of the system: a steeper basin then appears, at about  $65^\circ$  and 2.302Å, with a minimum of 637.8 Kcal/mole. The different nuclei cause large changes of sign for the various multipolar components and this is also reflected in the overall behaviour of the static surface.

Polarization effects are obviously very important in the subreactive region we are examining, and this is shown by the changes on the adiabatic potential surface when such effects are included. The cut-off parameter was adjusted to be equal to 1.592 au, thus reproducing the experimental  $^2\Pi_g$  resonance of the  $e^- - N_2$  scattering [19] process. The physical simplifications here introduced implies negligible charge-transfer in going from positron to proton scattering, a fact already suggested by experiments [3,4] but which certainly needs further investigation.

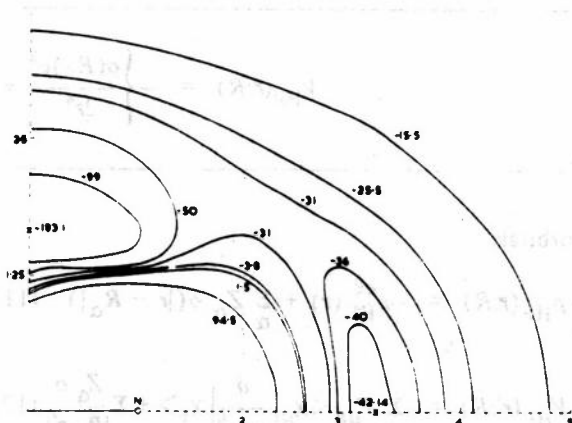


Figure 3: Polarization contributions to the static potential surface of the  $H^+-N_2$  system.

The results are reported in figure 3 where substantial differences appear from the case of figure 1: the more polarizable bond region has now become attractive thus overpowering the repulsive, anisotropic, character of the electric quadrupole term. The lone-pair region has been affected in an analogous manner thus deepening the previously shallow well. The minima now appear at  $\vartheta=0^\circ$  and  $90^\circ$ , with  $r=3.13$  au and  $1.68$  au respectively.

The method used for solving the coupled equations (2) within the Arthurs and Dalgarno formalism was the De Vogelaere method [23], a fourth-order step-by-step method based on difference formulas and already used for both neutral-molecule scattering [24] and electron-molecule collisions [15].

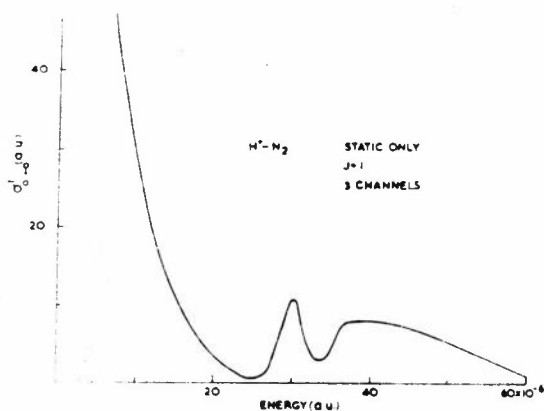


Figure 4: Energy behaviour of the partial cross section in the near threshold region for  $J=1$ . The matrix elements of equation (3) were computed via the potential surface of figure 1.

The effect of possible resonances at low energies is illustrated in an exploratory way by figure 4 on the  $J=1$  partial cross section when  $j=0$  and  $j=2$  rotational states are coupled: one sees that no resonances seem to be superimposed on an oscillating background contribution, contrary to what was found for neutral projectiles [24] or for electron scattering [19] but as expected from the main repulsive character of  $V_{HF}$ .

The relevant results for  $H^+-N_2$  when polarization contributions were included are reported in figure (5), and the marked increase of oscillations seems to indicate a greater presence of superimposed resonances when a more realistic form of the interaction is employed.

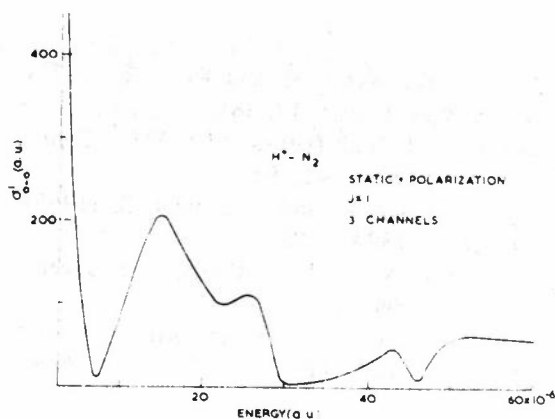


Figure 5: Same as figure 4, with  $V_{POL}$  included when computing the matrix elements of equation (3).

## References

- [1] BURNETT, G.M. and NORTH, A.M. (1969). *Transfer and Storage of Energy by Molecules*, 2, London: Wiley-Interscience.
- [2] HENGLEIN, A. (1966). *Advances in Chemistry Series, No. 58*, 63, Washington D.C.: American Chemical Society.
- [3] UDSETH, H., GIESE, C.F. and GENTRY, W.R. *Phys. Rev. A*, (in the press).
- [4] KAROBKIN, J. and SLAWSKY, Z.I. (1962). *J. Chem. Phys.*, **37**, 226.
- [5] COUZI, M., CARUNT, J.C., and HUONG, P.V. (1972). *J. Chem. Phys.*, **56**, 426.
- [6] DIERCKSEN, G.H.F., VON NIESSEN, W. and KRAEMER, W.P. (1973). *Theoret. Chim. Acta*, **31**, 205.
- [7] LISCHKA, M. (1973). *Theoret. Chim. Acta*, **31**, 39.
- [8] See for instance GOLDEN, D.E., LANE, N.F., TEMKIN, A. and GERYUOY, E. (1971). *Revs. Modern Phys.*, **43**, 642.
- [9] MASSEY, M.S.W., LAWSON, J. and THOMPSON, D.G. (1966). *Quantum Theory of Atoms Molecules and the Solid State - A Tribute to J.C. Slater* (ed. P.O. Lowdin), 203, New York: Academic Press.
- [10] TAKAYANGI, K. and INOKUTI, M. (1967). *J. Phys. Soc. Japan*, **23**, 1412.
- [11] ARTHURS, A.M. and DALGARNO, A. (1960). *Proc. Roy. Soc. (London)*, **A256**, 540.
- [12] GELTMAN, S. (1969). *Topics in Atomic Collision Theory*, 168, New York: Academic Press.
- [13] BURKE, P.G. and CHANDRA, N. (1972). *J. Phys. B*, **5**, 1969.
- [14] GIANTURCO, F.A. and CHANDRA, N. (1973). *Israel Acad. Sci. and Hum. Jerusalem*, (in the press).
- [15] \_\_\_\_\_ and \_\_\_\_\_ (1974). *Chem. Phys. Letters*, **24**, 326.

- [16] PACK, G.R., WANG, M. and REIN, R. (1972). *Chem. Phys. Letters*, **17**, 381.
- [17] SCROCCO, E. and TOMASI, J. (1973). *Topics in Current Chem.*, **42**, 95.
- [18] TAKAYANAGY, K. and GELTMAN, S. (1965). *Phys. Rev.*, **138A**, 1003.
- [19] CHANDRA, N. (1972). Thesis, The Queen's University, Belfast.
- [20] THRULAR, D.G., Van CATLEDGE, F.A. and DUNNING, T.M. (1973). *J. Chem. Phys.*,
  
- [21] BROWN, W.B. and ROBERTS, R.E. (1967). *J. Chem. Phys.*, **46**, 2006.
- [22] GIANTURCO, F.A. and TAIT, J.H. (1972). *Chem. Phys. Letters*, **12**, 589.
- [23] De VOGELAERE, R. (1955). *J. Research Natl Bur. Standards*, **54**, 119.
- [24] BURKE, P.G. *et al.* (1969). *J. Phys. B*, **2**, 1155.

# A Critical Look at Conjectures in the Theory of Autoionizing States of Atoms

C.S.Sharma\*

The present status of the theory of autoionizing states of atoms is reviewed with the particular aim of isolating and formulating precisely the outstanding weaknesses of the theory. Particular attention is paid to the following conjectures:

The autoionizing states are supposed to correspond to certain complex eigenvalues of the Hamiltonian, even though according to one of the most fundamental postulates of quantum theory a Hamiltonian is necessarily self-adjoint and therefore cannot have complex eigenvalues.

One of the weaknesses of the Feshbach formalism is that there is no way of defining the projection operators uniquely, but it is generally believed that the calculated energy provided the level-shift has been properly included is independent of the choice of the projection operator used in the calculation. The source of the belief is traced and the underlying argument is shown to be fallacious.

There are many derivations in the literature of the so-called golden rule for the calculation of the decay constant of an autoionizing state; some of these derivations are believed to be rigorous. It is shown that this belief is unfounded.

## Introduction

Hylleraas [1] obtained a value for the energy of the ground state of helium which differed by less than  $0.000\ 015\ eV$  from the mean experimental value at a time when the limits of experimental errors were ten times higher and this indeed was one of the finest triumphs of quantum theory. Calculations of much greater accuracy are now possible on most bound states of helium. However, when one comes to consider the doubly excited states of helium which give rise to the so called autoionizing states, the situation is not so happy. Some of the best calculations on such states have been done for the  $2s2p^1P$  state of helium: the difference between the best calculated and experimental values is  $0.012\ eV$  and the bounds on the experimental error ( $\pm 0.015\ eV$ ) have the same order of magnitude. The task of improving the accuracy of either the experimental or the theoretical value is fraught with difficulties of the most fundamental kind because the energy of an autoionizing state is not well-defined. The purpose of this work is to describe briefly the model on which the more successful calculations are based and then to discuss the difficulties in finding rigorous definitions of some of the concepts used in the model.

## The Model

The model which is relatively more successful in predicting the position of an autoionizing state is

based on the Feshbach *formalism* [2,3]. In this model the underlying Hilbert space is divided into two orthogonal subspaces so that the corresponding projection operators  $P$  and  $Q$  satisfy

$$P + Q = 1 \quad (1)$$

and

$$PQ = QP = 0 \quad (2)$$

If the operator  $QHQ$  where  $H$  is the Hamiltonian of the system has a point eigenvalue  $\epsilon$  in that interval of the real line which constitutes the continuous spectrum of  $H$ , then this eigenvalue *may be* associated with an autoionizing state and if it is then the energy of the autoionizing state is  $\epsilon + \Delta\epsilon$  where

$$\Delta\epsilon = \mathcal{P}\langle\Phi_0|QHP \frac{1}{\epsilon - QHQ - PHP} PHQ|\Phi_0\rangle \quad (3)$$

$\Phi_0$  is the eigenvector belonging to the point eigenvalue  $\epsilon$  and  $\mathcal{P}$  denotes that the Cauchy principal value is to be taken of the integral implicit in the expression on the right hand side. The projection operator  $Q$  is not uniquely defined, but it is generally believed that  $\epsilon + \Delta\epsilon$  is and only if this belief is well founded, the energy of the autoionizing state in this model can be said to be well defined. With the energy of an autoionizing state is associated a 'width'  $\Gamma$  and this is related to the decay constant of the autoionization.

\* Department of Mathematics, Birkbeck College, University of London, Malet Street, London, WC1E 7HX

The value of  $\Gamma$  in this formalism is given by the so called Fermi's golden rule:

$$\Gamma = 2\pi \langle \Phi_0 | QHP\delta(\mathcal{E} + \Delta\mathcal{E} - H)PHQ | \Phi_0 \rangle \quad (4)$$

For a judicious choice of  $Q$  the point eigenvalue  $\mathcal{E}$  corresponding to the autoionizing state is either the lowest or a low-lying eigenvalue (that is, it has only a finite number of point eigenvalues lying below it) and  $\mathcal{E}$  can be calculated with great accuracy by a variational calculation based on either the Hylleraas [1] or the Hylleraas-Undheim [4] variational principle. Until recently there has not been any mathematically satisfactory method (that is, a method which does not use an approximation not bounded by calculable error terms) for the calculation of  $\Delta\mathcal{E}$ . Sharma and Bowtell [5] have recently described a method for this calculation which seems to be fairly satisfactory. In this method the integral for  $\Delta\mathcal{E}$  is converted into another one involving the solution of a non-homogeneous differential equation and the singularity in the original integral manifests itself in the form of an undetermined additive term, which is the solution of the corresponding homogeneous problem, in the desired solution of the non-homogeneous problem. The new integral is free from singularities. Sharma and Bowtell [5] have developed a procedure for removing the unwanted homogeneous solution and their work provides a rather novel method for the evaluation of the Cauchy principal value of the integral in equation (3). The results of this method of calculation are justified not only by an improved agreement with experiment for each of the three cases for which all the numbers arising out of a single coupled set of calculations provide the values of  $\Delta\mathcal{E}$  but also by internal self-consistency (the theory tells us that two of the numbers calculated with the help of solutions of two different differential equations should have the same value and they do). Furthermore the procedure was developed with the help of purely mathematical arguments. In view of all this one could be tempted to say that this procedure is quite rigorous. However, it is a search for a genuinely rigorous justification of the method which has led the author to question certain aspects of the model.

Before concluding this section it should be pointed out that the author and his collaborators have developed their own algorithms for the calculation of both  $\mathcal{E}$  and  $\Gamma$  for autoionizing states of atoms, the first of these is described in [5] and the second will be described in due course elsewhere. Due to lack of facilities and resources it has not been possible to use these algorithms for the actual calculation of  $\mathcal{E}$  and  $\Gamma$  but since these methods are based on sound mathematical principles one can confidently predict that in due course they would become one of the standard algorithms for carrying out these calculations.

Since the criticism which the author wishes to make is of the most fundamental nature, it might be worthwhile to recapitulate briefly the mathematical and logical foundations on which the edifice of quantum theory is built.

Assuming that it is known *empirically* that laws governing observations on a quantum system are essentially probabilistic, that not all observables can be simultaneously observed and that certain aspects of the collective behaviour of an ensemble of non-interacting identical quantum systems can be described in terms of a single system which represents a kind of average system, one can, by mathematical and logical analysis, deduce the structure of the propositional calculus for the description of a system which behaves in accord with the above assumptions. The abstract mathematical structure which provides the basis of this description is called a  $\sigma$ -complete orthocomplemented weakly modular lattice. A study of lattice theory more or less immediately suggests that the lattice structure of a separable Hilbert space might provide a concrete realization of the structure of this particular lattice and a study of abstract Hilbert spaces confirms that this is so. Thus a Hilbert space provides a possible model for the description of a quantum system and if this model is adopted then the postulates of formal quantum statics follow rigorously from the description of a quantum system in terms of its propositional calculus. These postulates are:

(a) *There is a bijective correspondence between the states of a quantum system and the positive self-adjoint operators of unit trace on a Hilbert space  $\mathcal{H}$  of dimension  $\aleph_0$  over  $\mathbb{C}$ . The pure states are in bijective correspondence with the projection operators on one dimensional subspaces of  $\mathcal{H}$ . (Note that such projection operators are positive self-adjoint operators of unit trace and that it is this correspondence which enables one to represent a pure state by any unit vector in the range of the corresponding projection operator.)*

(b) *There is a bijective correspondence between the observables of the quantum system and self-adjoint operators on  $\mathcal{H}$ . If an observable corresponds to the operator  $A$  then the expectation value of the observable in a state which corresponds to the operator  $S$  is trace  $(AS)$ . (For a pure state  $S$  is a projection operator on a one-dimensional subspace, in this case if  $u$  is any unit vector satisfying  $Su = u$ , then it can be shown that the expectation value of the observable in this state is  $\text{Trace}(AS) = \langle u|A|u \rangle$ .)*

In order to get the postulate of quantum dynamics one assumes that the time evolutions of the probability distributions associated with the system are continuous and that the time evolution preserves convex combinations of states. After some work one arrives at

the postulate of quantum dynamics: *The time evolution of a quantum system is determined by a one-parameter unitary group  $U_t$  of automorphisms of the states  $S$  such that for each sequence  $\alpha_i$  in  $S$  and each real positive sequence  $\{\gamma_i\}$  with sum 1*

$$U_t(\sum_i \gamma_i \alpha_i) = \sum_i \gamma_i U_t(\alpha_i) \quad (5)$$

for all  $t \geq 0$ .

This brief description is based on the author's [6] exposition of the works of Birkhoff and von Neumann [7], Gleason [8] and Mackey [9]. This model is supposed to provide a good description of quantum phenomena only when relativistic effects are ignorable. It has not been proved that this model is the only possible one consistent with the basic assumptions, but this is the only model we have which has sound mathematical and logical foundations.

When calculations are done on the bound states of atoms, all the concepts and formulae used in the calculations are completely consistent with the above model. The purpose of the present paper is to show that many of the concepts and formulae used in the theory of autoionizing states are such that not only they cannot be reconciled with the above model but cannot be consistent with any mathematically meaningful model.

## The Complex Eigenvalue

The Feshbach model is a formalism and justifies itself by claiming formal equivalence with the complex eigenvalue theory which is supposed to have a better foundation. The idea of a complex eigenvalue is a very old one and is originally due to Gamow [10]. Since then perhaps more has been written on this subject in both mathematics and physics journals than on any other single problem of quantum theory. By analytically continuing Green's function of the resolvent of the Hamiltonian to the second sheet one gets an operator which has complex eigenvalues. The real part of a complex eigenvalue is supposed to define the energy and the imaginary part the width of the autoionizing state. This description is obviously inconsistent with the model described above: since the operator has a complex eigenvalue it cannot be self-adjoint and therefore it does not correspond to an observable. However, it is known by experience that calculations based on the complex eigenvalue theory (or an equivalent form of the theory) do provide good approximations to both the positions (on the energy spectrum) and the widths of these states. Furthermore the use of complex dynamical observables is quite common in both hydrodynamics and electrodynamics and therefore it could be possible to add an extra postulate to those of formal quantum theory to get a more powerful model. Though an

early attempt on these lines was tentatively made more than thirty years ago by Kemble [11], this extra postulate does not yet find a place in the standard elucidations of quantum theory. One finds that in most texts assumptions regarding the complex eigenvalue are invariably introduced surreptitiously through the back door.

As the author sees it the purpose of theoretical science is to establish bijections between physical reality and abstract mathematical structures and whenever this is done in a meaningful way one gets a good mathematical model for the description of physical reality. A concept is mathematically meaningful if and only if it is well-defined and something is well defined if and only if it has a *unique* meaning. It is precisely here that one meets the most fundamental difficulty. The Hamiltonian  $H$  of a single system is a single operator which is self-adjoint (or at least essentially so) and there is no way in which it can be made to yield a complex eigenvalue other than by making a change in  $H$ . The complex eigenvalues are not obtained by making a completely arbitrary change. One writes  $H$  as  $H = H_0 + H_1$  where both  $H_0$  and  $H_1$  are self-adjoint (or essentially self-adjoint), then a real parameter  $\epsilon$  is introduced in the second term to yield a family of operators  $H_0 + \epsilon H_1$  to which  $H$  belongs (for  $\epsilon = 1$ );  $\epsilon$  is then allowed to take complex values. This is a somewhat simplified account of how non self-adjoint operators are obtained for these problems. The most up to date and rigorous accounts follow one of the following two prescriptions:

- (a)  $H_1$  is factorized into two operators thus  $H_1 = AB$ , then  $A \frac{1}{H_0 + \epsilon H_1 - z} B$  is analytically continued to complex values of  $\epsilon$ , the poles of this continuation are called resonances [12,13].
- (b) A similarity transformation of  $H$  is made with the help of a dilatation  $U(\vartheta)$  defined on  $L^2(\mathbb{R}^n)$  by

$$(U(\vartheta)f)(r) = e^{3n\vartheta/2} f(e^\vartheta r) \quad (6)$$

for complex values of  $\vartheta$  this yields a non self-adjoint operator

$$H(\vartheta) = U(\vartheta) H U(\vartheta)^{-1} \quad (7)$$

which may have complex eigenvalues which are called resonances [14,15].

It becomes clear from the work of these authors that a complex eigenvalue is not an intrinsic property of the total Hamiltonian  $H$ , but of a pair  $(H, H_0)$  (note that once  $H_0$  is defined  $H_1$  gets defined too:  $H_1 = H - H_0$ ). Simon [15] argues that such a pair is well defined in two body scattering:  $H_0$  is the Hamiltonian when the two particles are an infinite distance apart. However, this concept cannot be easily extended when scattering involves more than two particles. For example in the case of  $He^2-e$

scattering the asymptotic Hamiltonian is (in natural atomic units):

$$H_0 = -\frac{1}{2}\nabla_1^2 - \frac{1}{2}\nabla_2^2 - \frac{Z}{r_1} \quad (8)$$

and then

$$H_1 = -\frac{Z}{r_2} + \frac{1}{r_{12}} \quad (9)$$

However, since it is impossible to distinguish between the first and the second electron it could be argued that  $H_0$  should be symmetric in  $r_1$  and  $r_2$ . Should we now take

$$H_0 = -\frac{1}{2}\nabla_1^2 - \frac{1}{2}\nabla_2^2 - \frac{Z}{r_1} - \frac{Z}{r_2} \quad (10)$$

or should it be

$$H_0 = -\frac{1}{2}\nabla_1^2 - \frac{1}{2}\nabla_2^2 - \frac{Z}{2r_1} - \frac{Z}{2r_2} \quad ? \quad (11)$$

In this case the pair  $(H, H_0)$  is not at all well defined and in the most successful calculations  $H_0$  includes part of  $\frac{1}{r_{12}}$  as well.

Thus the complex eigenvalue of the scattering problem is not well defined for a system consisting of more than two particles. What is worse that not all poles (see, for example, [16]) one gets in this way correspond to resonances. Unless these difficulties are circumvented, there cannot be a rigorous theory of resonances.

## $\mathcal{E} + \Delta\mathcal{E}$

It is generally believed that though the  $Q$ -operator of the Feshbach formalism is not uniquely defined and both  $\mathcal{E}$  and  $\Delta\mathcal{E}$  depend on  $Q$ ,  $\mathcal{E} + \Delta\mathcal{E}$  is unique. This belief corresponds to the hope that the complex eigenvalue is an intrinsic property of the total Hamiltonian  $H$  which according to Simon [15] is clearly not the case. What then is the source of this belief? Let us look at the corresponding problem for an isolated point eigenvalue  $\lambda$  of  $H$ . As long as  $H_0$  has a point eigenvalue  $\lambda_0$  which can be enclosed together with  $\lambda$  in a closed contour  $C$  in the complex plane in such a way that  $C$  neither encloses any other eigenvalue of either  $H$  or  $H_0$  nor passes through a point in the spectra of either  $H$  or  $H_0$ , a convergent perturbation expansion of  $\lambda$  exists and provided the calculations are carried out to sufficiently high orders no matter what  $H_0$  is chosen one will always get the same value of  $\lambda$  on summing the perturbation series [17,18]. An isolated point eigenvalue of  $H$ , of course, represents the energy of a bound state. It is analogy with this case which has led to the above mentioned belief. However, for the autoionizing case no contour

$C$  with the requisite properties exists; the formal perturbation series for different choice of  $H_0$  are necessarily different [19] and carrying out calculations to higher orders is not practicable. In all probability all higher order terms in the formal expansion diverge (there already is a singularity in  $\Delta\mathcal{E}$  which has to be removed by taking the Cauchy principal value). In fact if it could be proved that  $\mathcal{E} + \Delta\mathcal{E}$  is unique, this would be formally equivalent to proving that the resonance poles are intrinsic properties of the total Hamiltonian  $H$  thus contradicting the works of Howland [12,13] and Simon [15].

## The Golden Rule

While developing an algorithm for calculating the width according to the golden rule the author became interested in finding a derivation of the rule which could be acceptable to mathematics students as a deduction from the postulates of quantum theory. The author received advice from numerous kind experts: in each case he was directed to look up a perfectly rigorous proof by a named author and in each case he found a justification based on plausibility arguments. In view of the foregoing discussion the precise difficulties are evident:

- (a) One needs a perturbing term  $H_1$  which causes the transition and we have already seen that there is no unique way of defining  $H_1$ .
- (b) The golden rule does not have a prescription for going to higher order terms.
- (c) The rule needs the value of  $\mathcal{E} + \Delta\mathcal{E}$  which itself is not uniquely defined.

The width calculated by the golden rule thus depends heavily on the choice of  $H_1$  and as there is no unique way of making this choice  $\Gamma$  calculated by this rule is not well defined. It is needless to say that a rule for an ill-defined quantity cannot possibly have a rigorous derivation. Furthermore, in its more usual form the formula contains a continuum wavefunction (that is, a function with a  $\delta$ -function normalization): such wavefunctions are outside the realm of rigorous quantum mechanics; Though the form used in equation (4) circumvents this particular difficulty, for an actual calculation one still has to use such a wavefunction. An even more meaningful expression can be given in terms of spectral measures [15], but this does not make it either more rigorous or more amenable to actual computation. The golden rule is a formula which calculates to the lowest order the transition rate between two states under a perturbation; until the perturbation is well defined by the physical problem it is difficult to justify the validity of computations based on this rule except on purely empirical grounds. Finally the relation between line width and transition rate depends on a tenuous interpretation of the time-energy uncertainty relation and does not have a rigorous justification.

## Pure State or Mixed State

An isolated quantum system cannot have a width in its energy nor can it have a decay constant. Both these concepts are essentially statistical as are most of the concepts peculiar to scattering experiments. One is not talking about what happens when a single electron hits a  $He^+$  ion, but a whole ensemble of such occurrences. The autoionizing state, therefore, is quite likely a mixed state in which case it cannot be represented by a wavefunction (note that a linear superposition of wavefunctions does not give a mixed state but a pure one!). As explained above such a state can be represented only by a positive self-adjoint operator of unit trace. It is possible that this trace class operator  $A$  which represents such a state does not differ very much from the projection operator  $|\Phi_0\rangle\langle\Phi_0|$  on the subspace spanned by the eigenfunction  $\Phi_0$  of  $QHQ$  belonging to the eigenvalue  $\mathcal{E}$  for the more successful choice of  $Q$ . This might explain why the Feshbach formalism with a particular choice of  $Q$  consistently gives good answers. At present this is just another conjecture, but the author is trying to construct a model based on a mixed state representation of the autoionizing state. Whether or not such an attempt succeeds it is expected that at the end one will have gained a better understanding of the structure of a Hilbert space and a better insight into the phenomenon of autoionization.

## Concluding Remarks

The theory of autoionizing states contains a number of unresolved difficulties of the most fundamental kind. Nevertheless, the model most commonly used (the Feshbach formalism) is able to predict for helium both the positions and the widths of these states with accuracy comparable to that of experiment. Hence the model is directly useful to the experimentalist in locating a resonance and has phenomenological and empirical justifications. This suggests that the model though not deducible rigorously from the fundamental postulates of quantum theory is nevertheless a good description of an autoionizing state. It is, therefore, quite likely to have a heuristic value in the discovery of a more satisfactory model.

The author believes that it is a healthy attitude to have a somewhat sceptical attitude towards the theory one is using in one's calculations: this leads not only to a better understanding of the theory itself but often helps one in finding both better models and better algorithms for the computations. Quantum chemists are often criticized for carrying out lengthy calculations for the sake of calculations without looking carefully into precisely what or why they are calculating. It is hoped that this work will show that not all quantum chemists are guilty of this failing.

Before concluding the author would like to draw attention to a paper by Mayers *et al.* [20] which

has laid to rest another popular misunderstanding about autoionization and correlation. Many experts have been known to assert that correlation by keeping electrons apart lowers the energy and hence makes a system more stable. Therefore in the Hartree-Fock approximation where correlation is completely ignored all autoionizing states have 'run away' solutions. Mayers *et al.* [20] have shown convincingly that the contrary is true: in the Hartree-Fock approximation autoionizing states are bound states and it is a certain part of the correlation which causes these states to decay.

## References

- [1] HYLLERAAS, E.A. (1929). *Z. Physik*, **54**, 347.
- [2] FESHBACH, H. (1958). *Ann. Phys. N.Y.*, **6**, 357.
- [3] ——— (1962). *Ann. Phys. N.Y.*, **19**, 287.
- [4] HYLLERAAS, E.A. and UNDHEIM, B. (1930). *Z. Physik*, **65**, 759.
- [5] SHARMA, C.S. and BOWTELL, G. (1973). *Can. J. Phys.*, **51**, 1637.
- [6] SHARMA, C.S. (1972). *Mathematical Foundations of Non-relativistic Quantum Theory*. Duplicated lecture notes on an intercollegiate course given at the University of London (unpublished work).
- [7] BIRKHOFF, G. and von NEWMANN, J. (1936). *Ann. Math.*, **37**, 823.
- [8] GLEASON, A.M. (1957). *J. Math. and Mech.*, **6**, 885.
- [9] MACKEY, G. (1963). *The Mathematical Foundations of Quantum Mechanics*, New York: Benjamin.
- [10] GAMOW, G. (1928). *Z. Phys.*, **51**, 204.
- [11] KEMBLE, E.C. (1937). *The Fundamental Principles of Quantum Mechanics with Elementary Applications*, New York: Dover.
- [12] HOWLAND, J.S. (1972). *Bull. Am. Math. Soc.*, **78**, 280.
- [13] ——— (1972). *Puiseux Series for Resonances near an Embedded Eigenvalue*. University of Virginia reprint.
- [14] BALSLEV, E. and COMBES, J.M. (1971). *Comm. Math. Phys.*, **22**, 280.
- [15] SIMON, B. (1972). *Resonances in N-body Quantum Systems with Dilatation Analytic Potentials and the Foundations of Time-dependent Perturbation Theory*, Princeton University reprint (to be published).
- [16] NEWTON, R.G. (1966). *Scattering Theory of Waves and Particles*, New York: McGraw-Hill.
- [17] KATO, T. (1966). *Perturbation Theory for Linear Operators*, Heidelberg: Springer.
- [18] MESSIAH, A. (1961). *Quantum Mechanics Volume II*, Amsterdam: North-Holland.
- [19] SHARMA, C.S. (1968). *J. Phys. B*, **1**, 1016.
- [20] MAYERS, D.F., REBELO, I. and SHARMA, C.S. (1973). *Can. J. Phys.*, **51**, 1701.



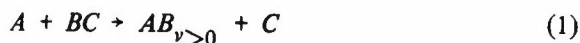
# Experimental Results on Initial Energy Distributions in Simple Atom-Molecule Reactions Producing Hydrogen Fluoride

P. Beadle, N. Jonathan and S. Okuda\*

The aim of this brief review paper is to bring to the attention of theoretical chemists the experimental information which is now available for energy distributions in some simple atom-molecule reactions. Particular emphasis is placed on reactions which produce hydrogen fluoride. Data from infrared chemiluminescence experiments for the reactions of atomic fluorine with hydrogen, methane, the hydrogen halides and other molecules, are presented and compared where possible with the results from molecular beam experiments. Initial vibrational and rotational energy distributions are given. These are discussed along with the relative rate constants. The need for trajectory calculations using 'good' potential surfaces is pointed out in the light of features of the experimental results.

## Introduction

The infrared chemiluminescence technique is one which provides complementary information to that obtained from molecular beam studies concerning initial energy distributions in simple atom-molecule reactions of the type



In certain cases it has also been possible to obtain some information regarding reaction mechanisms [1, 2,3]. Another use has been to place more accurate limits on bond dissociation energies. However, the major use is undoubtedly in providing accurate information on the initial vibrational and rotational energy distributions in reactions such as (1). In this respect the reactions which yield either hydrogen fluoride or deuterium fluoride are particularly important. Not only do they form the bases of efficient chemical laser systems, but also, because of the ease with which atomic fluorine abstracts either a hydrogen or deuterium atom from a molecule, they provide the most extensive series of reactions which can be studied. Under such circumstances it is possible to find a series of related reactions whereby the factors which may be of some importance in determining initial energy distributions may be varied in a systematic fashion. It is then possible to compare the information with predictions made using trajectory calculations and various semi-empirical potential energy surfaces. However, such an approach is not entirely satisfactory and the need for more detailed quantum mechanical calculations is evident. The main purpose of this paper is to point out various

experimental results which have been obtained and where perhaps better calculations are necessary.

## Experimental

The spectrometer used for detection of infra-red emission has been described on previous occasions [4, 5,6]. The reaction cells were designated as methods I and II by other workers [7].

Method I has been described in earlier work [4,5,6] and was of the basic flow-tube design. It consisted of a stainless steel tube with a Teflon liner. Infra-red emission was detected at four lithium fluoride windows placed equidistantly down the tube. Since time resolution of the emission was important, runs were only made under conditions in which the infra-red emission at the window which detected back diffusion, was less than 5%. The monochromator was mounted on rails running parallel to the flow-tube so that it could be reproducibly focused on any of the windows by a worm-screw assembly. The populations of the various vibrational energy levels were determined from the fundamental vibration-rotation spectra using the Einstein transition probabilities calculated by Cashion [8]. Since the flow-tube pressure was in the range 75-100 mtorr it was found that in all reactions studied except the  $F + HI$  reaction, that the rotational energy level populations followed a Boltzmann distribution corresponding to temperature in the range 300-350 K. Determination of initial vibrational energy level distributions was complicated by the short radiative lifetime of vibrationally excited hydrogen fluoride as well as by collisional deactivation. The technique used was to take measurements as a

\* Department of Chemistry, University of Southampton, Southampton, SO9 5NH

function of time down the flow-tube and to extrapolate relative populations back to zero time.

Method II used the 'arrested' relaxation technique. In this method the reactant gases were mixed at pressures of  $10^{-4}$ - $10^{-5}$  torr in a 24" reaction cell which was continuously evacuated by means of an oil diffusion pump and appropriate backing pump. The reaction cell was equipped with two pairs of gold-coated mirrors to increase the light gathering power of the system. The reaction volume was surrounded as far as practicable by a copper shield which was continuously cooled by liquid nitrogen. This technique helps to maintain low pressures because of cryogenic pumping of some gases and also helps to 'arrest' the relaxation process. The latter phenomenon occurs because energetically rich species are trapped for sufficient time at the walls so that

is interesting because it is one of the simplest atom-molecule reactions which can be studied by the infra-red chemiluminescence technique. Because hydrogen fluoride can be formed in high vibrational levels, this reaction provides a very thorough test of any potential energy surface used in trajectory calculations. This situation is to be contrasted with that found for many other reactions where only a few vibrational levels can be populated. Hence these do not provide very sensitive tests of theoretical models. Reaction (2) has been studied using both the 'arrested' relaxation [9] and the flow-tube [6] methods. The agreement between the experimental results for vibrational energy distributions is excellent as can be seen from table 1. The arrested relaxation method gave the fractions of available energy distributed between vibration, and rotation as  $f_{\text{vib}}:f_{\text{rot}} = 0.53:0.03$  whereas the flow-tube method gives  $f_{\text{vib}} = 0.58$ .

Table 1: Relative rate constants  $k(v')$  for the reaction  $H + F_2 \rightarrow HF + F$

	$k(0)$	$k(1)$	$k(2)$	$k(3)$	$k(4)$	$k(5)$	$k(6)$	$k(7)$	$k(8)$	$k(9)$	$k(10)$
flowtube method [6]	0.04	0.09	0.11	0.13	0.45	0.89	1.00	0.45	0.20	<0.04	<0.04
'arrested' relaxation [9]	<0.1	0.12	0.13	0.25	0.35	0.78	1.00	0.40	0.26	<0.16	-

they lose all their excess energy rather than undergo stepwise loss. The residence time of reactants in the cone of sight of the spectrometer is difficult to calculate because of problems of measuring pressure accurately and of knowing the effective volume of the system. The problems arise because one attempts to work with crude molecular beams of gases rather than with a diffusely mixed system. However, within these limitations, the residence time is thought to be <0.2 msec. The agreement between the product vibrational distributions measured for  $F + H_2$  by the two methods provides a useful check on the accuracy of the techniques.

In general the 'arrested' relaxation method is the more useful in that in addition to measurement of initial vibrational energy level distributions, it also provides estimates of the initial rotational distributions. However the flow-tube method provides a somewhat easier way of measuring vibrational distributions; Boltzmannization of rotational energy making summation of populations in the various vibration-rotation lines less difficult since in general problems of overlap are less in low  $J$  value levels.

## Results and Discussion

The reaction of atomic hydrogen with fluorine: The reaction

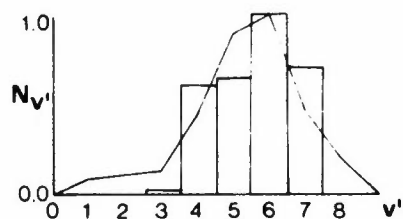
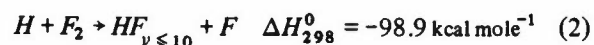


Figure 1: Experimental and calculated vibrational energy level populations for the  $H + F_2$  reaction

The energy distribution has been calculated using trajectory calculations of a modified LEPS form [6]. The vibrational level energy populations for the  $H + F_2$  system along with the experimental findings are given in figure 1. As can be seen, within the limitations of this semi-empirical approach the agreement is reasonable. The data for rotational energy level distributions became available after the trajectory calculations had been completed. It is interesting to compare these in figure 2. One of the features of the LEPS type surface was that it predicted a too narrow distribution of vibrational energies. As a consequence it was not possible to calculate rotational distributions in the first three excited vibrational levels. Figure 2 shows that experimentally there is little change in rotational energy or its distribution as the vibrational excitation decreases. Hence there must be a correspondingly large increase in the translational energy of the products. The experimental results are broadly in agreement with these findings.

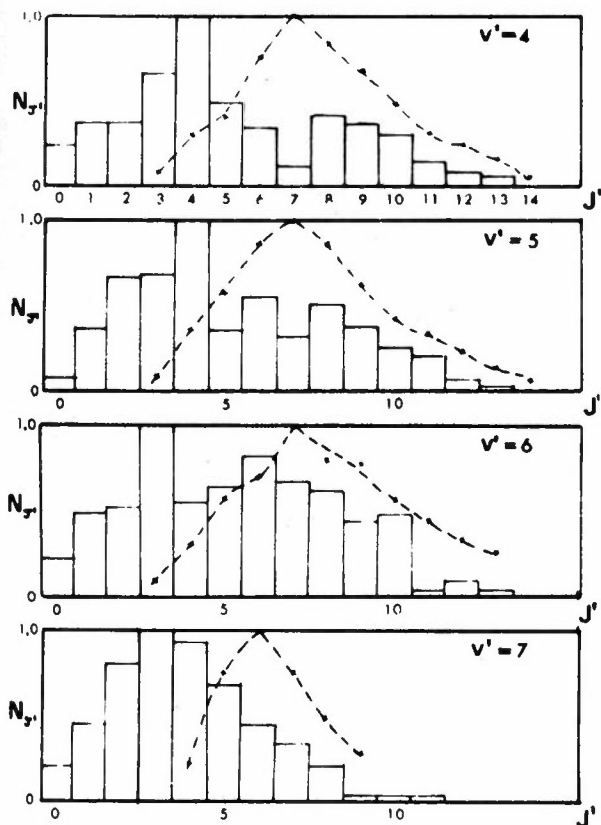


Figure 2: Experimental and calculated rotational level populations for the  $H + F_2$  reaction

We also believe that a test of a potential energy level surface should be the degree of accuracy with which it predicts the overall rate constant of the reaction, the  $A$  factor and activation energy. The values are given in table 2.

Table 2: Experimental and calculated kinetic data for the reaction  $H + F_2$

Rate Constant at 300 K $\text{cc.mol}^{-1}\text{s}^{-1}$	$A$ Factor $\text{cc.mol}^{-1}\text{s}^{-1}$	Activation Energy $\text{kcal mol}^{-1}$	Reference
$1.8 \times 10^{12}$	$10^{13.3}$	1.5	[10]
$2.1 \times 10^{12}$	$10^{14.1}$	2.4	[11]
$2.3 \times 10^{12}$	$10^{14.7}$	3.2	calculated

Within the accepted limitations of the LEPS type of potential energy surface, the agreement is satisfactory. However, there is a clear need for a less empirical surface which could be tested by the experimental data now available for this reaction.

The reactions of atomic fluorine with hydrogen, hydrogen chloride and methane: These particular reactions are interesting in that their exothermicities are very similar. In each case only  $v' \leq 3$  may be populated directly by reaction.

The reaction of  $F + H_2$  has been studied independently by other workers [12] using the 'arrested' relaxation technique. Their results for both vibrational and rotational energy level distributions are virtually identical with the ones presented here. In addition, the data are in very good agreement with those of flow-tube studies [4]. These results give us some confidence in the i.r. chemiluminescence methods. It should be added that the data are markedly different from those obtained by chemical laser studies [13].

Table 3: Summary of results from arrested relaxation

$F+$	$H_2$	$HCl$	$CH_4$
$f_{v'}$	0.70	0.58	0.67
$\langle E_{v'} \rangle$ $\text{kcal mol}^{-1}$	23.25	20.40	21.90
$f_R$	0.05	0.12	0.08
$\langle E_{R'} \rangle$ $\text{kcal mol}^{-1}$	1.56	4.36	2.59
$f_{T'}$	0.25	0.30	0.25
$\langle E_{T'} \rangle$ $\text{kcal mol}^{-1}$	8.32	10.53	8.18
$E_{TOTAL}$ $\text{kcal mol}^{-1}$	33.25	35.06	32.72

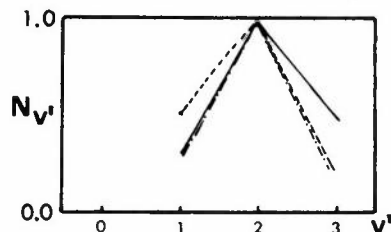


Figure 3: Relative vibrational energy level populations for the reactions  $F + H_2$ ,  $CH_4$  and  $HCl$ . —  $F + H_2$   
- - -  $F + CH_4$  - · - ·  $F + HCl$

A summary of the results obtained by the 'arrested' relaxation method is given in table 3. It can be seen that the fraction  $f_{v'}$  of available energy which enters vibration, is very similar in each of the three cases. However the actual distribution between the three excited vibrational levels is rather different as can be seen from figure 3. In the  $F + H_2$  case markedly more of the  $HF$  is formed in the  $v' = 3$  level than in the other two cases. In the case of the  $F + HCl$  reaction a considerably larger proportion of  $HF$  is formed in the  $v' = 1$  level. This accounts for the lower fraction of available energy which enters vibration for this reaction.

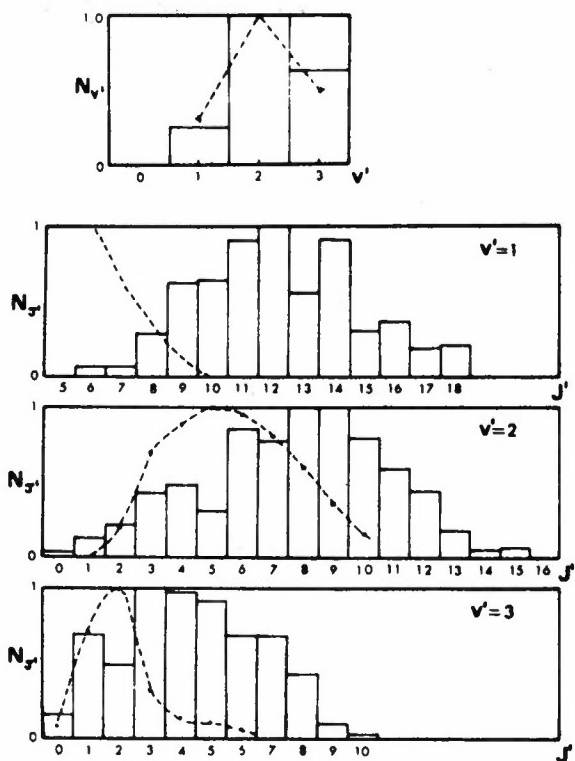


Figure 4: Experimental and calculated vibrational and rotational energy level populations for the  $F + H_2$  reaction

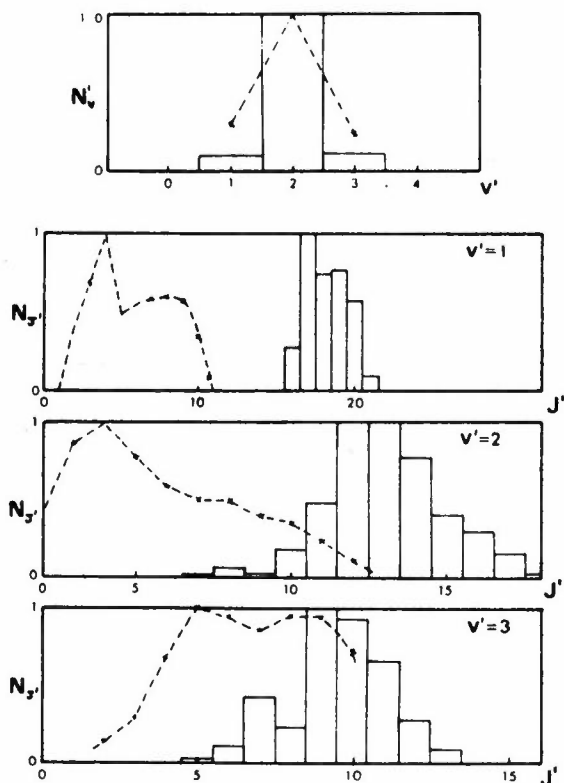


Figure 6: Experimental and calculated vibrational and rotational energy level populations for the  $F + CH_4$  reaction

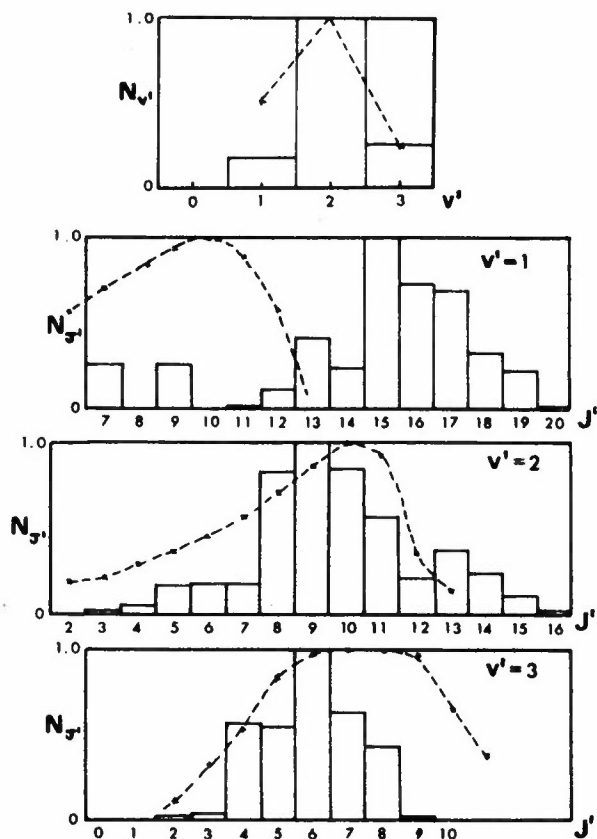


Figure 5: Experimental and calculated vibrational and rotational energy level populations for the  $F + HCl$  reaction

The differences between the reactions show up more markedly when one examines the experimental rotational energy level populations. The fraction  $f_{R'}$  of available energy rotation is small in each case, although considerably larger in the  $F + HCl$  reaction. The reasons for the difference in  $f_{R'}$  are obvious from figures 4, 5 and 6. There is a markedly greater population in the higher  $J$  levels for  $HCl$  reaction than the other two, although the same trend is evident for  $CH_4$  compared with  $H_2$ . However, perhaps the most significant feature which arises from the rotational analysis is the apparent double maxima in the methane case.

The reasons for this are not obvious but there is little doubt that it is a real effect. Studies of the reactions of atomic fluorine with  $C_2H_6$  show a similar double maxima and the effect is particularly obvious in the corresponding reaction with  $SiHCl_3$  [14].

The results of trajectory calculations are shown in figures 4, 5 and 6. The calculated vibrational energy level distributions are in satisfactory agreement with the experimental results but as we mentioned earlier, this is not a very severe test of a potential energy surface since only levels  $v' \leq 3$  can be populated. The rotational level populations are in much poorer agreement especially for the  $v' = 1$  levels and for the  $F + CH_4$  case. The former may be due to partial

collisional relaxation of  $HF^\dagger$  from higher levels although it is difficult to see why this should affect the  $\nu' = 1$  level significantly more than the others. There is no evidence from the calculations for the double maxima. Hence one cannot be sure whether these are due to general inadequacies in the chosen LEPS surface or to the treatment of the methyl group as a single particle. It is not clear whether all reactions in which the departing species  $C$  in reaction (1) is a multi-atom group, yield double maxima. An examination of the reactions of atomic fluorine with hydrogen bromide and hydrogen iodide might help to clarify this point. However, up to the present time the phenomenon has only been observed when  $C$  consists of more than one atom. Since double maxima are not observed in the  $HCl$  case, the mass of group  $C$  does not appear to be the determining factor and hence one suspects that the  $HBr$  and  $HI$  reactions will behave similarly to  $HCl$ .

Table 4: Calculated kinetic data for the reactions of atomic fluorine with hydrogen, methane and hydrogen chloride

Reaction	Rate constant at 300 K $\text{cc.mol}^{-1}\text{s}^{-1}$	A factor $\text{cc.mol}^{-1}\text{s}^{-1}$	Activation Energy $\text{kcal mol}^{-1}$
$F + H_2$	$2.2 \times 10^{12}$	$6.8 \times 10^{13}$	2.1
$F + HCl$	$3.1 \times 10^{11}$	$2.1 \times 10^{13}$	2.5
$F + CH_4$	$4.6 \times 10^{11}$	$1.1 \times 10^{13}$	0.8

The calculated kinetic data for the three reactions are shown in table 4. Unfortunately there are not good experimental data available for comparison. The relative rate constants for the three reactions have been measured to an estimated accuracy of  $\pm 10\%$  [5]. The calculated results for  $H_2$  and  $HCl$  fit in quite well but the value for  $CH_4$  is low by about a factor of 6. Hence once again we find the poorest agreement between calculations and observed data in the  $CH_4$  case.

The examples quoted illustrate the limitations of the classical trajectory calculations applied to this sort of problem. Although the general trend of energy distributions can be rationalized in terms of the semi-empirical surfaces and the type of energy release, and although such surfaces can be used to predict the effect of excess reactant energy, they fail to give a detailed picture. It is hoped that the information now forthcoming from the infra-red chemiluminescence studies and from molecular beam techniques will stimulate more work from the quantum mechanical standpoint.

#### Acknowledgements

The generous support of the Science Research Council in the form of equipment grants, various

Fellowships and computing facilities through the Atlas Computer Laboratory is gratefully acknowledged as is the support from the United States Air Force through the European Office of Aerospace Research.

#### References

- [1] PERONA, M.H., SETSER, D.W. and JOHNSON, R.L. (1969). *J. Phys. Chem.*, **73**, 2091.
- [2] CLOUGH, P. N. and THURS, B. A. (1968). *Chem. Comm.*, 1351.
- [3] CREEK, D. M., MELLIAR-SMITH, C. M. and JONATHAN, N. (1970). *J. Chem. Soc. A*, 646.
- [4] JONATHAN, N., MELLIAR-SMITH, C. M. and SLATER, D.H. (1971). *Mol. Phys.*, **20**, 93.
- [5] JONATHAN, N., MELLIAR-SMITH, C.M., OKUDA, S., SLATER, D.H. and TIMLIN, D. (1971). *Mol. Phys.*, **22**, 561.
- [6] JONATHAN, N., OKUDA, S and TIMLIN, D. (1972). *Mol. Phys.*, **24**, 1143.
- [7] ANLAUF, K.G., KUNTZ, P.J., MAYLOTTE, D.H., PACEY, P.D. and POLANYI, J.C. (1967). *Discussions Faraday Soc.*, **44**, 183.
- [8] CASHION, J.K. (1962). *Aeronautical Research Laboratories Technical Report*, ARL 62-412.
- [9] POLANYI, J. C. and SLOAN, J. J. (1972). *J. Chem. Phys.*, **57**, 4988.
- [10] LEVY, J.B. and COPELAND, B.K.W. (1968). *J. Phys. Chem.*, **72**, 3168.
- [11] DODONOV, A.E., GORDON, E.B., LAVROVSKAYA, G.K., MOROSOV, I.I., PONOMAREV, A.N. and TALROSE, V.L. (1970). *Int. J. Chem. Kinet.*, **2**, 66.
- [12] POLANYI, J.C. and WOODALL, K.B. (1972). *J. Chem. Phys.*, **57**, 1574.
- [13] PARKER, J.H. and PIMENTEL, G.C. (1969). *J. Chem. Phys.*, **51**, 91.
- [14] BEADLE, P. and JONATHAN, N., (unpublished work).

# Procedure for Averaging Differential Cross Sections over the Experimental Angular Resolution

S. Bosanac and G.G. Balint-Kurti\*

Differential cross sections for collisions of molecules in the thermal energy range normally oscillate rapidly with angle, the oscillations becoming more rapid with increasing relative kinetic energy. The angular resolution in crossed molecular beam experiments is generally insufficient to resolve these rapid oscillations. A method is proposed for averaging differential cross sections over small angular ranges without actually evaluating them at many angles. The method permits the calculation of averaged cross sections, which are much more directly comparable with the experimentally determined ones than those evaluated without averaging. Illustrative calculations are presented for three examples. One for elastic scattering ( $Ar + Kr$ ) and two for rotationally inelastic scattering ( $Ar + CsF$  and  $Ne + N_2$ ). When the differential cross section oscillates rapidly, as it does in the first two cases, it requires less computational effort to plot the relatively smoothly varying averaged differential cross section, than to plot the non-averaged cross section.

## Introduction

Differential cross sections for elastic and inelastic molecular collisions in the thermal energy range normally oscillate rapidly with angle [1, 2]. The angular frequency of the oscillations increases with relative kinetic energy and also, in general, with the masses of the collision partners. The detectors used to measure cross sections have finite apertures and are often unable to resolve these oscillations. A method is proposed for averaging the differential cross section over the angular resolution of the detector, without actually evaluating it at the large number of angles which would be needed to follow its oscillations. The theory underlying the method is given and three illustrative applications of the method are presented. The systems treated are the elastic scattering of  $Ar + Kr$  and the rotationally inelastic scattering in model systems which represent  $Ar + CsF$  and  $Ne + N_2$ .

The results show that although it is faster to calculate the non-averaged differential cross section than the averaged one at a single angle, in order to follow the oscillations of the non-averaged cross section it must be evaluated at very many more angles than the smoothly varying averaged cross section. The time required to plot the highly oscillatory non-averaged cross section may exceed manifold that required to plot the averaged one.

## Theory

The differential cross section, in the centre of mass reference frame, for the scattering of two atoms whose interaction potential is spherically symmetric, is given by [3]:

$$\sigma(\theta) = \frac{1}{4k^2} |\sum_{\ell} (2\ell + 1) T_{\ell}^{\ell} P_{\ell}(\cos\theta)|^2 \quad (1)$$

where  $\ell$  is the orbital angular momentum quantum number of the relative motion,  $k$  is related to the relative kinetic energy by  $k^2 = 2\mu E/\hbar^2$  and  $T_{\ell}^{\ell}$  is related to the phase shift by

$$T_{\ell}^{\ell} = -2ie^{i\delta_{\ell}} \sin \delta_{\ell} \quad (2)$$

The phase shifts  $\delta_{\ell}$  may be calculated by numerical solution of the Schrödinger equation or by approximate methods such as the JWKB method [4].

For inelastic collisions of an atom with a rigid rotor diatomic molecule, the differential cross section in the helicity representation is given by [5];

$$\sigma_{j'm' \leftarrow jm}(\theta) = \frac{1}{4k_j^2} |\sum_J (2J+1) T_{j'm',jm}^J d_{m'm}^J(\theta)|^2 \quad (3)$$

Each of the quantities in this equation are essentially generalisations of those for the elastic scattering case of equation (1). The angular functions  $d_{m'm}^J(\theta)$  are

\* School of Chemistry, University of Bristol, Cantock's Close, Bristol, BS8 1TS  
(present address of S.B.) Institute 'Ruder Bošković', 41001 Zagreb, Bijenička C.54, Yugoslavia

reduced representations of the rotation group [6]. The  $T$ -matrix elements  $T_{j'm',jm}^J$  are related to the more commonly encountered ones in the total angular momentum representation [7] by a matrix transformation involving the Clebsch-Gordan [8] coefficients:

$$T_{j'm',jm}^J = \sum_{\ell\ell'} i^{\ell-\ell'} T_{j'\ell',j\ell}^J (jmJ-m|jJ\ell 0) (j'm'J-m'|j'J\ell' 0) \quad (4)$$

The largest contributions to the differential cross section come from those total angular momentum ( $J$ ) values for which the term  $(2J+1)T_{j'm',jm}^J$  is close to its maximum value, (see equation (3)). The value of  $J$  for which this term is a maximum will be denoted by  $J_0$ . It is just a bit larger than the  $J$  value corresponding to the maximum in a partial integral cross section  $\sim J$  plot [9]. If we neglect all the terms in equation (3) except that arising from the maximum contribution to the sum, then the differential cross section can be written as:

$$\sigma_{j'm'\leftarrow jm}(\theta) \simeq \frac{(2J_0+1)^2}{4k_j^2} |T_{j'm',jm}^{J_0}|^2 |d_{m'm}^{J_0}(\theta)|^2 \quad (5)$$

For large  $J_0$  (and  $J_0 \gg m'$  and  $m$ ) the asymptotic form of  $d_{m'm}^{J_0}(\theta)$  may be used [5,10]:

$$d_{m'm}^{J_0}(\theta) \simeq \left(\frac{2}{\pi J_0}\right)^{1/2} \frac{\cos[J_0\theta + \theta/2 + \pi(m'-m-1/2)/2]}{(\sin\theta)^{1/2}} \quad (6)$$

When this is substituted into equation (5) we obtain:

$$\sigma_{j'm'\leftarrow jm}(\theta) \simeq \frac{(2J_0+1)^2 |T_{j'm',jm}^{J_0}|^2}{2k_j^2 \pi J_0} \frac{\cos^2[J_0\theta + \theta/2 + \pi(m'-m-1/2)/2]}{\sin\theta} \quad (7)$$

Thus the differential cross section (in this approximation is an oscillatory function with a period of

$$\Delta\theta \simeq \frac{\pi}{J_0} \quad (8)$$

Even when full account is taken of all the terms arising from the summation over  $J$  in equation (3), we expect the differential cross section to exhibit oscillations with approximately the above period. If the resolution of the detector ( $\Delta\theta_d$ ) is of the same

order as the angular period ( $\Delta\theta$ ), the rapid oscillations of the differential cross section will at least be damped and may not be observed at all. A recent report on molecular beams [11] indicates that the smallest attainable angular resolution should be between  $0.3^\circ$  and  $0.8^\circ$ , while a recent experimental paper [12] reports an angular resolution of  $\Delta\theta_d = 1.6^\circ$ . In the present paper we use this latter value as representative of a typically attainable resolution. The values of  $J_0$  for which  $\Delta\theta = 0.3^\circ$ ,  $0.8^\circ$  and  $1.6^\circ$  are  $J_0 \approx 600$ ,  $225$  and  $113$  respectively. Total angular momentum quantum numbers of this magnitude are often important in molecular scattering experiments.

If the angular resolution of the experiment is larger than or comparable to  $\Delta\theta$ , the period of the oscillations in the true differential cross section, then it will be necessary to average the calculated differential cross section over the experimental angle of resolution before a meaningful comparison between

experiment and calculations can be made. The averaged differential cross section is given by:

$$\bar{\sigma}_{j'm'\leftarrow jm}(\theta_0) = \frac{1}{\Delta\Omega_d} \int_{\Delta\Omega_d} \sigma_{j'm'\leftarrow jm}(\theta) d\Omega \quad (9)$$

where  $\Delta\Omega_d$  is the solid angle spanned by the aperture of the detector. As  $\sigma_{j'm'\leftarrow jm}(\theta)$  is a function of  $\theta$  only, the integration over  $\phi$  is trivially performed and we obtain:

$$\bar{\sigma}_{j'm'\leftarrow jm}(\theta_0) = \frac{1}{2 \sin\theta_0 \sin(\Delta\theta_d/2)} \int_{\theta_-}^{\theta_+} \sigma_{j'm'\leftarrow jm}(\theta) \sin\theta d\theta \quad (10)$$

where  $\theta_{\pm} = \theta_0 \pm \Delta\theta_d/2$ .

If the expression for the differential cross section equation (3) is substituted into the right hand side of equation (10), then the average differential cross section may be expressed as:

$$\bar{\sigma}_{j'm'\leftarrow jm}(\theta_0) = \frac{1}{8k_j^2 \sin\theta_0 \sin(\Delta\theta_d/2)} \sum_{J,J'} (2J+1)(2J'+1) T_{j'm',jm}^{J*} T_{j'm',jm}^J T_{m'm}^{JJ'}(\theta_0, \Delta\theta_d) \quad (11)$$

where

$$I_{m'm}^{JJ'}(\theta_0, \Delta\theta_d) = \int_{\theta_-}^{\theta_+} d_{m'm}^J(\theta) d_{m'm}^{J'}(\theta) \sin\theta d\theta \quad (12)$$

For sufficiently large  $J$  and  $J'$  the angular functions  $d_{m'm}^J(\theta)$  may be replaced by their asymptotic forms, equation (6). The integration in equation (12) may then be carried out analytically. If we denote the integral evaluated using these asymptotic forms by  $C_{m'm}^{JJ'}$ , we can write:

$$C_{m'm}^{JJ'}(\theta_0, \Delta\theta_d) = 2(JJ')^{-1/2} \pi^{-1} \left\{ (J-J')^{-1} \cos[(J-J')\theta_0] \sin[(J-J')\Delta\theta_d/2] + (-1)^{m-m'} (J+J'+1)^{-1} \sin[(J+J'+1)\theta_0] \sin[(J+J'+1)\Delta\theta_d/2] \right\} \quad (13)$$

Test calculations show that if  $J - |m| - |m'| > 11$ , and both  $|m|$  and  $|m'|$  are less than 3, then the asymptotic approximation of equation (6) is valid to better than 6%, for angles between  $14^\circ$  and  $166^\circ$ . The approximation becomes rapidly better as the angle moves towards the middle of the range and as  $J$  increases. For inelastic cross sections involving larger values of  $|m|$  it will be necessary to use the asymptotic form, equation (6), only for larger values of  $J$ . In the present calculations the analytic form of equation (13) is used when both  $J$  and  $J'$  satisfy the inequality  $J > 11 + |m| + |m'|$ . A test calculation on the  $j=0 \rightarrow j=2$  differential cross section for  $Ne + N_2$  (see figure 3

The notation used for the integral of equation (12) in the various different cases is:

$$\begin{aligned} I_{m'm}^{JJ'}(\theta, \Delta\theta_d) &= A_{m'm}^{JJ'}(\theta, \Delta\theta_d) \text{ for } J \text{ and } J' < 11 + |m| + |m'| \\ &= B_{m'm}^{JJ'}(\theta, \Delta\theta_d) \text{ for } J < 11 + |m| + |m'| < J' \\ &= C_{m'm}^{JJ'}(\theta, \Delta\theta_d) \text{ for } J \text{ and } J' \geq 11 + |m| + |m'| \end{aligned} \quad (14)$$

The averaged differential cross section, equation (11), may therefore be written as:

$$\begin{aligned} \bar{\sigma}_{j'm' \leftarrow jm}(\theta_0) &= \frac{1}{8k_j^2 \sin\theta_0 \sin(\Delta\theta_d/2)} \left\{ \sum_{J \geq J'}^{10 + |m| + |m'|} R_{m'm}^{JJ'} A_{m'm}^{JJ'}(\theta, \Delta\theta_d) (2 - \delta_{JJ'}) \right. \\ &+ \left. \sum_{J=0}^{10 + |m| + |m'|} \sum_{J'=11 + |m| + |m'|}^{\infty} R_{m'm}^{JJ'} B_{m'm}^{JJ'}(\theta, \Delta\theta_d) + \sum_{J > J' \geq 11 + |m| + |m'|}^{\infty} R_{m'm}^{JJ'} C_{m'm}^{JJ'}(\theta, \Delta\theta_d) (2 - \delta_{JJ'}) \right\} \quad (15) \end{aligned}$$

below) showed that it was only negligibly affected by imposing the more stringent condition that  $J > 20 + |m| + |m'|$ .

If either  $J$  or  $J'$  are smaller than  $11 + |m| + |m'|$ , alternative means must be used to evaluate the integral of equation (12). When both  $J$  and  $J'$  are small (i.e.  $J < 11 + |m| + |m'|$ ) the integral is denoted by  $A_{m'm}^{JJ'}$ , and it is evaluated using a two point Gaussian numerical integration rule [13]. This should give relatively accurate values as the limits of integration are much smaller than the period of oscillation of the integrand. For  $J=10$  the period of oscillation of the integrand is approximately  $18^\circ$  as compared with a range of integration of  $\Delta\theta_d = 1.6^\circ$  which we use here. When one of the  $J$  values is smaller and the other larger than  $11 + |m| + |m'|$  then the integrand is the product of a slowly varying function ( $d_{m'm}^J(\theta)$  for  $J < 11 + |m| + |m'|$ ) and a rapidly oscillating one, equation (6). In this case we use a four point Filon's integration formula [13] which is specially designed for such a situation, and denote the integral by  $B_{m'm}^{JJ'}$ .

where

$$R_{m'm}^{JJ'} = (2J+1)(2J'+1) \operatorname{Re}[T_{j'm',jm}^{J*} T_{j'm',jm}^J]$$

$\operatorname{Re}$  denotes the real parts of a complex number and  $\delta_{JJ'}$  is a Kronecker delta symbol. The most time consuming part of the calculation is the second summation (involving  $B_{m'm}^{JJ'}$ ), even though the third summation includes many more terms. This is because the various sines and cosines involved in evaluating  $C_{m'm}^{JJ'}$ , equation (13), can be computed and stored before the main calculation. If this is done each of the terms in the last summation becomes very simple to evaluate.

### Illustrative Applications

As a test of our averaging procedure we applied it first to the elastic scattering of  $Ar + Kr$ , for which both experimental results and calculated averaged differential cross sections have already been reported



[12]. We used the same potential (Schlier-type), angular resolution and energy as those used [12]. At this energy ( $0.061728 \text{ eV}$ ) 300 partial waves were required in the partial wave expansion, equation (1). The largest maximum in the partial integral cross section occurs at around  $\ell = 160$ , from which the angular oscillations in the differential cross section may be estimated to have a period  $\Delta\theta \approx 1.1^\circ$ . Both the averaged and non-averaged differential cross sections, calculated using a semi-classical approxi-

mation slightly better than the standard JWKB one [14], are shown in figure 1. The period of oscillation of the non-averaged cross section agrees roughly with our estimate. The broken line corresponds to the differential cross section averaged over the angular resolution of the detector ( $1.6^\circ$ ). This averaged cross section seems to be in good agreement with that reported by Parson *et al.* [12,15]. This example demonstrated that an averaging procedure is necessary before meaningful comparison can be made between theory and experiment.

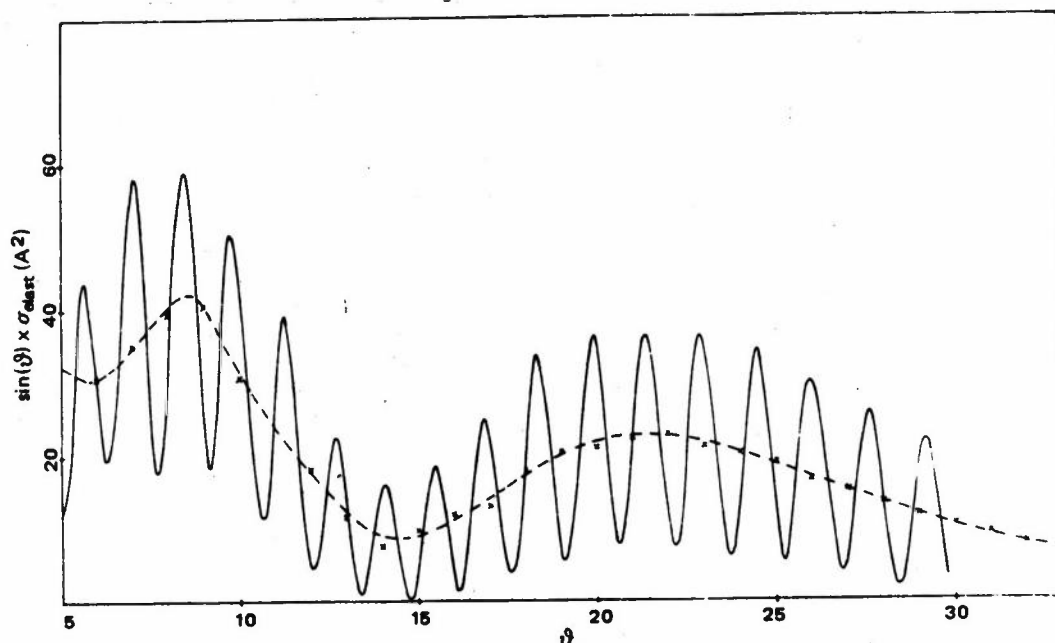


Figure 1: Differential scattering cross sections for  $Ar + Kr$  at  $E = 0.061728 \text{ eV}$ . The solid line corresponds to the non-averaged cross section while the broken line is the cross section averaged over the angular resolution of the detector ( $1.6^\circ$ ) [12].

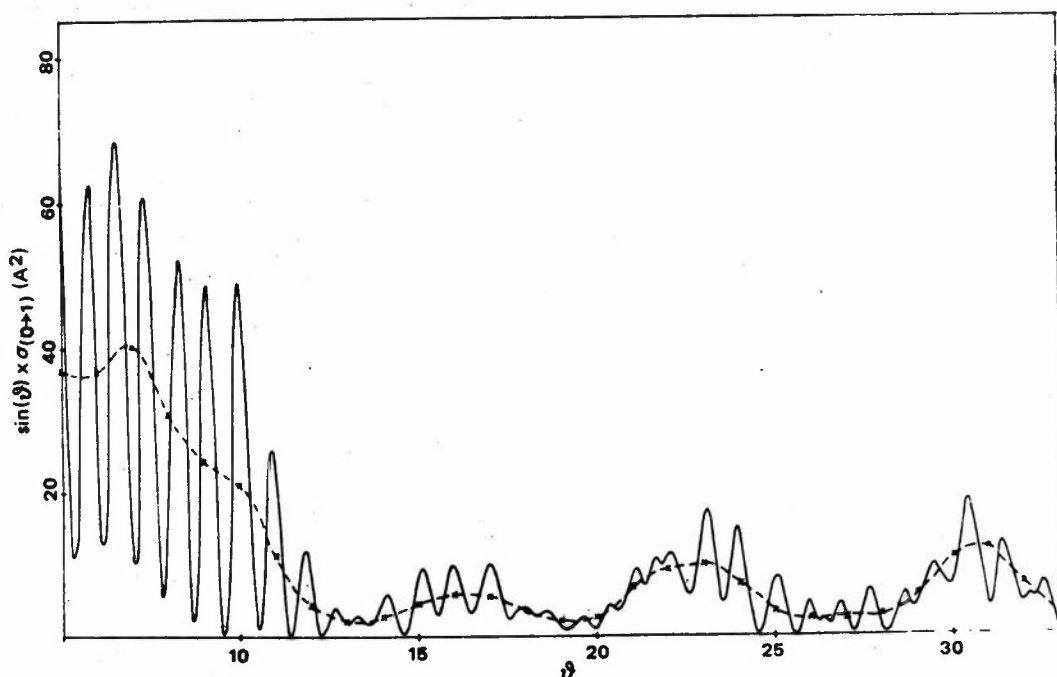


Figure 2: Rotationally inelastic ( $j=0 \rightarrow j=1$ ) differential cross sections for  $Ar + CsF$  at  $E = 0.04 \text{ eV}$ . The solid line is the non-averaged cross section while the broken line corresponds to the cross section averaged over an angular resolution of  $1.6^\circ$ . See [16] for details of the model used in the calculation.

Figure 2 shows averaged and non-averaged rotationally inelastic ( $j=0 \rightarrow j=1$ ) differential cross sections (summed over the final  $m'$  quantum numbers) for a model calculation [16] on  $Ar + CsF$  at an energy of  $E=0.04$  eV. The required  $T$  matrix elements were calculated using an exponential semi-classical distorted wave approximation [17] which will be discussed in a future publication. The number of  $J$  values needed for this case was 450 and the main maximum in the partial total inelastic cross section occurred at  $J=240$ . From this we would estimate that the oscillations in the cross section should have an angular period of about  $\Delta\theta \approx 0.75^\circ$ , which is close to the calculated period (figure 2, solid line) of  $\Delta\theta \approx 1.0^\circ$ . The broken line in figure 2 shows the inelastic differential cross section averaged over an angular resolution of  $1.6^\circ$ . The averaged differential cross section varies smoothly. The rapid oscillations of the true differential cross section cannot be observed using a detector of this resolving power. The time needed to evaluate a single point on the averaged differential cross section curve, equation (15), (excluding the time for the evaluation of the  $T_{j'm',jm}^j$  matrix elements) is about twice that required to evaluate a point on the non-averaged cross section curve, equation (3). As the non-averaged curve oscillates so rapidly, however, many more points (most probably at least six times as many) are needed to plot it as to plot the smoothly varying averaged curve.

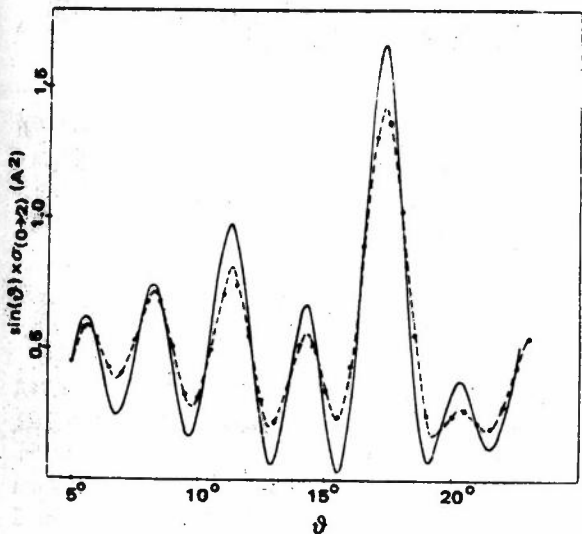


Figure 3: Rotationally inelastic ( $j=0 \rightarrow j=2$ ) differential cross sections for  $Ne + N_2$ . The solid line is the non-averaged cross section while the broken line corresponds to the cross section averaged over an angular resolution of  $1.6^\circ$ . See [18] for details of the model used in the calculation

When the angular resolution of the detector is smaller than the angular period of oscillation of the cross section, then the general form of the differential cross section will not be affected by the averaging procedure. Some of the details of the cross section, however, such as the heights of the peaks in the oscillations may well be affected. Figure 3 shows

the averaged and non-averaged rotationally inelastic ( $j=0 \rightarrow j=1$ ) differential cross sections (summed over the final  $m'$  quantum numbers) for a model calculation on  $Ne + N_2$  [18]. At the energy used in the calculation ( $E=0.046$  eV) 80 total angular momentum quantum numbers ( $J$ ) were required. The partial integral cross section had two maxima at about  $J=30$  and  $67$ . The figure shows oscillations with an angular frequency of about  $\Delta\theta \approx 3^\circ$  at low scattering angles. This is consistent with the qualitative concept that the low angle scattering is dominated by the large  $J$  partial waves, even though the maximum at larger  $J$  ( $=67$ ) makes a much smaller contribution to the total cross section. The averaging process does not significantly affect the form of the differential cross section, the peaks of the oscillations are, however, considerably damped.

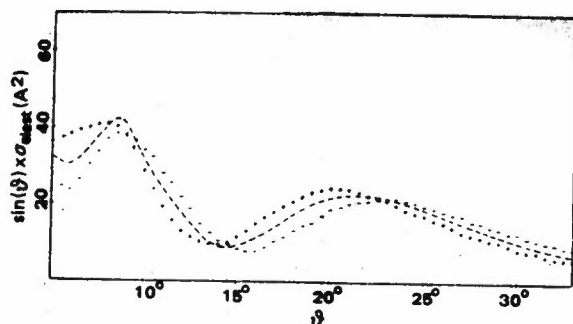


Figure 4: Differential cross sections for  $Ar + Kr$  at different energies. All the cross sections are averaged over an angular resolution of  $1.6^\circ$ . The relative kinetic energies corresponding to the different lines are  
 (---)  $E = 0.061728$  eV  
 (++++)  $E = 0.064728$  eV  
 (-----)  $E = 0.058728$  eV

Besides the size of the detector, there are several other factors contributing to the resolution in a crossed molecular beam experiment. There is the angular spread of the molecular beams and the fact that they are not mono-energetic, but have a distribution of velocities. When comparing theory with experiment, both of these factors should be taken properly into account. In some cases it is possible that the averaging over the angular resolution of the detector will be the dominant effect and that it will be permissible to largely ignore the averaging over the velocity distributions in the beams. In figure 4 the effect of a variation in the energy by about 5% either way on the  $Ar + Kr$  differential cross section is shown. The broken line corresponds to the averaged differential cross section at an energy of  $E=0.061728$  eV, the line with the plus signs is at  $E=0.064728$  eV and that with the minus signs at  $E=0.058728$  eV. The variation in the energy by 5% is seen to have a relatively small effect on the overall shape of the curve, and for this case the process of averaging over the angular resolution of the detector is seen to yield a cross section which, in the first approximation, may be directly compared with experiment.

## Conclusions

The procedure presented in the paper provides a method for the direct calculation of differential cross sections averaged over the angular resolution of the detector. Because the procedure does not involve following the details of the rapid oscillations of the non-averaged differential cross section, it should provide a faster and more convenient method of calculating differential cross sections for comparison with experiment. It is of special relevance to collisions between heavy molecules and/or collisions at high energies. In these cases the differential cross sections normally have angular oscillations which are too rapid for the detector to resolve.

## Acknowledgement

The authors thank the S.R.C. for financial support and for the provision of computer time. They would also like to express their gratitude to the staff of the Atlas Computer Laboratory and of the Rutherford Laboratory computer for their assistance.

## Editor's Note

Thanks are due to Taylor and Francis Limited and the editor of *Molecular Physics* for permission to reproduce this article.

## References

- [1] HUNDHAUSEN, E. and PAULY, H. (1965). *Z. Physik*, **187**, 305.
- [2] BERNSTEIN, R.B. and MUCKERMAN, J.T. (1967). *Adv. Chem. Phys.*, **12**, 389, see fig. 16.
- [3] SCHIFF, L.I. (1955). *Quantum Mechanics*, 104, New York: McGraw-Hill.
- [4] LANDAU, L.D. and LIFSHITZ, E.M. (1959). *Quantum Mechanics*, Section 106, Oxford: Pergamon.
- [5] MILLER, W.H. (1968). *J. Chem. Phys.*, **49**, 2373.
- [6] EDMONDS, A.R. (1960). *Angular Momentum in Quantum Mechanics*, Chapter 4, Princeton University Press.
- [7] ARTHURS, A.M. and DALGARNO, D. (1960). *Proc. Roy. Soc. (London)*, **A256**, 540.
- [8] The notation and phase conventions of Edmonds [6] are used here.
- [9] See for instance LESTER Jr., W.A. and SCHAEFER, J. (1973). *J. Chem. Phys.*, **59**, 3676.
- [10] The expression for the asymptotic form of  $d_{m,m}^j(\theta)$  may be obtained by first expressing it in terms of Jacobi Polynomials [6] and then using their asymptotic form as given in GRADSHTEYN, I.S. and RYZHIK, I.M. (1965). *Table of Integrals Series and Products*, 1037, New York: Academic Press.
- [11] TOENNIES, J.P. in *Physical Chemistry, an Advanced Treatise* (ed. H. Eyring, D. Henderson and W. Jost), (to be published).
- [12] PARSON, J.M., SCHAEFER, T.P., SISKA, P.E., TULLY, F.P., WONG, Y.C. and LEE, Y.T. (1970). *J. Chem. Phys.*, **53**, 3755.
- [13] (1965). *Handbook of Mathematical Functions* (ed. M. Abramowitz and I.A. Segun), New York: Dover.
- [14] This approximation made extensive use of Airy functions of the form
 
$$Ai\left[\frac{3}{2}\left(\int_{R_0}^R pdR\right)^{2/3}\right]$$
 BOSANAC, S. and BALINT-KURTI, G.G., *Mol. Phys.*, (in the press).
- [15] Parson *et al.* [12] do not say specifically how they averaged the cross section, but presumably their procedure involved evaluating the non-averaged cross section at a sufficient number of points to approximately follow the rapid oscillations. For this particular case this would involve at the very least four evaluations of the cross section for every one which we have to perform with the present averaging procedure.
- [16] The CsF was treated as a rigid rotor and the interaction potential recommended by DAVID, R., SPODEN, W. and TOENNIES, J.P. (1970). *J. Phys. B*, **6**, 897, was used. This potential was of the form:
 
$$V = \epsilon \left(\frac{R_m}{R}\right)^{12} [1 + q_{1,12} P_1(\cos\theta) + q_{2,12} P_2(\cos\theta)] - 2\epsilon \left(\frac{R_m}{R}\right)^6 [1 + q_{2,6} P_2(\cos\theta)] - \epsilon D \left(\frac{R_m}{R}\right)^7 \left[\frac{3}{5} P_1(\cos\theta) + \frac{2}{5} P_2(\cos\theta)\right]$$
 where  $\epsilon = 0.033 \times 10^{-21} J$ ;  $R_m = 9.74 \text{ \AA}$   $q_{1,12} = -2.5$ ;  $q_{2,12} = 0.9$ ;  $q_{2,6} = 0.3$  and  $D = 2.22$ , the calculations were performed using an improved version of the ESCDW approximation [17] and only rotational states  $j=0, 1$  and  $2$  were retained. The values of  $\epsilon$  and  $R_m$  are taken from BENNEWITZ, H.G., HAERTEN, R. and MULLER, G. (1969). *Z. Physik*, **226**, 139.
- [17] BALINT-KURTI, G.G. and JOHNSON, B.R. (1973). *Discussions Faraday Soc.*, **55**, 59. An improved version of this procedure was used here, BOSANAC, S. and BALINT-KURTI, G.G. *Mol. Phys.*, (in the press).
- [18] The  $N_2$  was treated as a rigid rotor and the interaction potential was taken from the work of BURKE, P.G., SCRUTTON, D., TAIT, J.H. and TAYLOR, A.J. (1969). *J. Phys. B*, **2**, 1155. The calculations were carried out using an improved form of the ESCDW approximation [17].

# A Theoretical Study of Vibrational Self-Relaxation Rates of $HF$

K.Smith\*, M.J.Conneely\*<sup>†</sup> and A.R.Davies<sup>‡</sup>

Calculations of  $HF$  vibrational self relaxation times have been performed using a theoretical model which treats the  $HF$  molecule as a simple harmonic oscillator and approximates the  $HF$ - $HF$  interaction with a Lennard-Jones potential. Results will be presented of  $Q_{01,00}(E)$  the vibrational de-excitation cross section and  $Q_{01,10}(E)$  the vibrational-vibrational cross section both as a function of energy, and  $\tau_{V-T}$  the vibrational self relaxation time as a function of temperature. These results are compared with experimental values.

## Introduction

**Experiments:** The vibrational relaxation rate of hydrogen fluoride is of current interest because of the extensive development of hydrogen fluoride chemical lasers [1]. To understand and predict the performance of these lasers a knowledge is required of the collisional deactivation cross sections of vibrationally excited hydrogen fluoride.

Airey and Fried [2] carried out the first measurement of the vibrational relaxation rate of  $HF$  ( $\nu=1$ ) upon collision with itself, using a laser fluorescence technique. They found that this self-relaxation rate was extremely fast at 350°K having a  $p\tau=10.5$   $\mu\text{sec Torr}$ . This method has also been used by Hancock and Green [3-5] and by Stephens and Cool [6]. The latter's measurement at 350°K, of  $p\tau$  is quoted in table 1 as 19  $\mu\text{sec} \cdot \text{atmos.}$ , while that of Hancock and Green [3,4] is given as 11.5  $\mu\text{sec} \cdot \text{atmos.}$  at 295°K. Green and Hancock [5] have studied the  $HF$  self-relaxation rate as a function of  $J$  line excitation frequency and found it to be independent of rotational level excitation over laser transitions  $P_{1 \rightarrow 0}(2) - P_{1 \rightarrow 0}(9)$ . (The theoretical model discussed in this paper neglects rotational motion of the colliding diatomic molecules). The laser fluorescence technique has also been used by Hinchey [7] to measure vibrational relaxation times for  $HF$ - $HF$  at 295°K and over the range 300°K-1000°K. His results coincide with the shock-tube data, to be discussed below, above 1000°K.

Shock tube studies of  $HF$  vibrational relaxation have been performed by Bott and Cohen [8] over the temperature range 1350 to 4000°K. They obtained a straight line Landau-Teller plot ( $P\tau$  versus  $T^{-1/3}$ ) with a slope of about 30°, and compared their data

with the predictions of three theories of V-T and V-R energy transfer. A similar experiment has been carried out by Blauer *et al.* [9] whose results were qualitatively the same as those of Airey and Fried [2], but smaller by a factor of three. Bott [10] has extended the temperature range of these results from 460 to 1030°K and at 295°K. A Landau-Teller plot of these results also exhibits a straight line, but with a negative slope of about 60°, with  $p\tau=19$   $\mu\text{sec Torr}$  at 295°K. This temperature range has also been investigated by Fried *et al.* [11] who obtained a straight line with a negative slope of about 45°. The various low-temperature results are presented in table 1.

Table 1: Low temperature experimental values of the  $HF(\nu=1)$  self-relaxation rate.

Temperature °K	$p\tau$ $\mu\text{sec Torr}$	Reference
350	10.5	[1]
350	19	[6]
296	19	[10]
294	11.5	[3,4]
294	$13.9 \pm 1.6$	[13]
290	20	[12]

In other words, it has been experimentally established that the self-relaxation rate of vibrationally excited  $HF$  has a markedly unusual temperature dependence — a minimum near 1000°K, and is extremely rapid. It should be emphasized, however, that no single experiment has been performed over the whole temperature range, see figure 1.

\* Centre for Computer Studies, University of Leeds, Leeds, LS2 9JT

<sup>†</sup> (present address) Department of Mathematical Physics, University College, Galway, Ireland

<sup>‡</sup> Department of Statistics and Computer Science, Royal Holloway College, University of London, Egham, Surrey, TW20 0EX

Osgood *et al.* [12] have reported a direct measurement of the V-V transfer rate out of  $\nu=2$ , that is

$$HF(\nu=2) + HF(\nu=0) \rightarrow 2HF(\nu=1) \quad (1)$$

This experiment yielded a value of 1.5  $\mu\text{sec Torr}$  for the V-V decay rate, compared with a value of  $2.2 \times 10^3 \text{ cc/mole. sec}$  obtained by Bott [10]. Bina and Jones [13] have interpreted their results on *HF* as resulting from VT de-excitation of *HF* ( $\nu=2$ ) level at a rate  $p\tau_2 = 6.6 \pm 1.7 \mu\text{sec Torr}$  and a second, and slower, decay from the VT collisional loss of *HF* ( $\nu=1$ ) at a rate  $p\tau_1 = 13.9 \pm 1.6 \mu\text{sec Torr}$ .

**Theory:** Two of these experimental groups, Fried *et al.* [11] and Bott [10], compared their results with a modified version of a theory developed by Shin [14,15]. The modification consists of multiplying Shin's expression for de-excitation of an oscillator,  $P_{10}$ , by  $\exp(\phi/kt)$ , where  $\phi$  is intended to simulate, in a crude way, the attractive dipole-dipole interaction between *HF* molecules. This so-called 'modified Shin theory' reproduces the qualitative result of the Landau-Teller maximum as seen in figure 1.

The existence of this considerable amount of data on *HF* self-relaxation rates does provide a stimulus to molecular collision theory to investigate the possibility of predicting these rates without recourse to the introduction of empirical parameters and functions such as  $\exp(\phi/kt)$ .

The theory of vibrational-vibrational energy transfer in diatomic-diatom collisions through 1968 has been reviewed by Rapp and Kassel [16]. These authors emphasized the semiclassical formulation of the problem based on head-on collisions in which the intermolecular potential is assumed to be an exponential function of the distance between the middle pair of atoms. This same model has been formulated within quantum mechanics by Riley and Kuppermann [17] who presented results for the collinear collision of two harmonic  $H_2$  molecules. Wilson [18] has developed a quantum mechanical theory for the collinear collision of two diatomic molecules in which the intermolecular potential is also just a function of the distance between the inner pair of atoms approximated as a series of constant steps outside an infinite potential barrier. He applied his model to diatomic molecules consisting of *H* and *D* atoms.

Although this paper describes a model which neglects rotation of the colliding partners, other workers, notably Shin [14,15,19] have constructed models for calculating vibrational-rotation energy transfer probabilities. Shin's work is based on a classical model consisting of a rotation-averaged oscillator and a rigid rotator. The interaction potential is assumed to be the sum of Morse potentials between the atoms of the different molecules

$$U = \sum_{i=1}^4 U(r_i) \quad (1)$$

where  $r_i$  are the inter-atom distances, and

$$U(r_i) = D[\exp(\ell-r_i/a) - 2 \exp(\ell/2-r_i/2a)] \quad (2)$$

where the parameters are determined by fitting the exponential to an empirical Lennard-Jones potential. The formula given by Shin [14] for the probability of vibrational de-excitation ( $1 \rightarrow 0$ ) through the V-R-T energy transfer mechanism did not include the effect of the dipole-dipole interaction. This effect leads to an  $r^{-6}$  potential which in turn modifies Shin's formula. When Shin [15,20] included this effect he was able to reproduce the qualitative features of a maximum in the Landau-Teller plot for *HF* self-relaxation observed experimentally. However, at high temperatures his calculated results are bigger than the experiments of Bott and Cohen [8] by a factor of three.

Calculations of V-V transfer probabilities in *CO-CO* collisions has been carried out by Jeffers and Kelley [21], who included both short-range and long-range forces. For the former, they assumed the collision to occur between collinear non-rotating *CO* molecules with a simple exponential as the intermolecular potential, see Rapp and Kassel [16], while for the latter they used the first Born approximation to calculate transition probabilities for dipole-dipole and dipole-quadrupole transitions as prescribed by Sharma and Brau [22,23]. They found that with increasing temperature, short-range interactions dominate.

The Sharma-Brau formulation is based on a model in which the translational motion of the colliding molecule is determined classically by a hard-sphere potential. The transfer of rotational and vibrational energies, which is treated quantum mechanically, is regarded as solely due to the *Coulomb interaction* between the molecules. Tam [24] has modified this theory by interchanging the order of taking the averages over the velocity distribution and the impact parameter, and applied it to *CO-CO* collisions, see Tam [25].

Kelley [26] has considered the collision between two harmonic oscillators in which a time-dependent interaction potential contains terms which are linear and quadratic in the oscillator coordinates. Explicit expressions for transition probabilities were derived for collinear collisions involving exponential potentials, but they were not used to calculate experimentally determined cross sections.

Berend and Thommarson [27] have programmed the classical equations of motion for a two-dimensional collision model. They have used an empirical interaction potential constructed from the six atom-atom functions. The interaction between the chemically bonded atoms was represented by Morse-functions, while the interaction between the non-bonded atom pairs was taken to be the sum of Morse and Coulombic

potential functions. The results of these authors are presented in figure 1 and are found to be in qualitative agreement with the experiments.

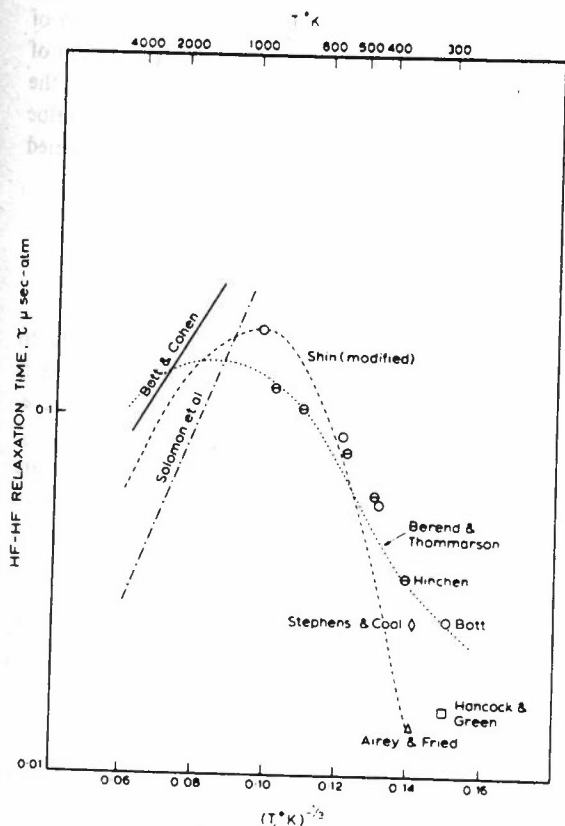


Figure 1: Comparison of experimental and theoretical values of the self-relaxation rate of HF on a Landau-Teller plot

A 'breathing sphere' model, in which one molecule is treated as a spherical body which is capable of changing its radius, while the incident molecule is represented as a point mass has been used by Marriott [28] for CO-CO collisions. The assumption on the intermolecular potential follows Schwartz *et al.* [29] by writing

$$V(R, r) = V_0 V(r) V_1(R) \quad (3)$$

where  $r$  is the intermolecular coordinate and  $R$  is the vibrational coordinate of the target diatomic. While  $V(r)$  is taken to be a Lennard-Jones (6,12) potential,  $V_1(R)$  is assumed to be adequately approximated by an exponential function whose parameters are obtained by fitting the magnitude and slope to the Lennard-Jones potential at the classical distance of closest approach. Later, Marriott [30] fitted the exponential function to the effective potential consisting of the centrifugal barrier and the Lennard-Jones potential. Calculations were carried out on CO-CO collisions [31] using this latter form. The model developed in this paper is an extension of Marriott's model to a pair of colliding breathing spheres.

In the following section we describe our theoretical model in detail and outline the various numerical tests we have carried out on the model to ensure our results are as correct as possible while in the next section we describe the HF-HF system. Following that we present our cross sections for both V-T and V-V energy transfer processes for HF-HF collisions. Then our calculations of the associated relaxation rates are presented, where we compare and contrast our results with previously published experimental and theoretical results. Finally we present a summary and conclusions in regard to the short-comings of our model.

### Theoretical Model

It will be assumed that the overall wavefunction for two colliding diatomic molecules,  $AB$  and  $HF$ , can be expanded in terms of a basis constructed from the product of simple harmonic oscillator functions, eigenvalues  $E_m$ , that is

$$\Psi(AB, HF, r) = \sum_{mn} \Psi_m(AB) \Psi_n(HF) F_{mn}(r) \quad (4)$$

When equation (4) is substituted into the non-relativistic Schrödinger equation for the system, the resulting equation pre-multiplied by a member of the basis, and the angular part of the expansion coefficients  $F_{mn}(r)$  are separated off, then we obtain the close-coupling radial equations for the system

$$\left[ \frac{d^2}{dr^2} - \frac{\ell(\ell+1)}{r^2} + k_{mn}^2 \right] F_{mn}^{\ell}(r) = \frac{2\mu}{\hbar^2} \sum_{m'n'} V_{mn, m'n'}(r) F_{m'n'}^{\ell}(r), \quad (5)$$

where

$$k_{mn}^2 = \frac{2\mu}{\hbar^2} (E - E_m - E_n), \quad (6)$$

$\mu$  is the reduced mass of the collision system, and

$$V_{mn, m'n'}(r) = \int d\tau \psi_m(AB) \psi_n(HF) V(AB, HF) \psi_{m'}(AB) \psi_{n'}(HF). \quad (7)$$

To evaluate these matrix elements we follow Schwartz *et al.* [29] and assume

$$V(AB, HF) = V_0 V(r) V_1(R_{AB}) V_2(R_{HF}), \quad (8)$$

where  $R_{AB}$  denotes the internal vector coordinate between the atoms of the molecule  $AB$ . To obtain an approximate representation for the potentials, Schwartz *et al.* [29] assumed that the intermolecular

potential can be approximated by an exponential function of the distance  $x$  between nearest atoms in a collinear collision: see also Mott and Massey [32], whose parameters are determined by fitting this exponential function to an empirically determined Lennard-Jones potential at the classical distance of closest approach [28]. The result is

$$V(AB, HF) \approx V_0 V(r) e^{-A_1 R_{AB}} e^{-A_2 R_{HF}}, \quad (9)$$

where

$$A_i = \frac{24\eta^{7/6}}{\sigma(2\eta-1)}(1-1/n_i),$$

$$\eta = \frac{1}{2}[1 + (1 + E_c/\epsilon)^{1/2}],$$

$n_i$  is the number of atoms in molecule  $i = 1(AB)$ ,  $i = 2(HF)$ ,  $E_c$  is the collision energy in eV, while  $\epsilon$  and  $\sigma$  are the Lennard-Jones force constants.

Equation (9) is substituted into equation (7) and the integrals over  $R_{AB}$  and  $R_{HF}$  can be performed, as in [28], to give

$$\begin{aligned} U_{mm'} &= \int dR_{AB} \psi_m(R_{AB}) e^{-A_1 R_{AB}} \psi_{m'}(R_{AB}) \\ &= e^{A_1^2/4\alpha^2} \left( \frac{m! m'}{2^{m+m'}} \right)^{1/2} (-1)^{m+m'} \\ &\times \sum_{t=0}^m \left[ \frac{2^t (A_1/\alpha)^{m+m'-2t}}{t!(m-t)!(m'-t)!} \right], \end{aligned} \quad (10)$$

where  $\alpha = (2\pi M\nu)^{1/2}$ ,  $M$  being the reduced mass of the oscillator, and  $\nu$  its fundamental frequency. Therefore, equation (7) can be written as

$$V_{mn, m'n'}(\dot{r}) = V_0 V(r) U_{mm'} U_{nn'}, \quad (7a)$$

where  $V(r)$  is taken to have a Lennard-Jones form and the constant  $V_0$  is normalized to ensure that the full intermolecular potential is normalized to the Lennard-Jones form when both molecules are in their ground vibrational states, that is  $V_0 = (U_{00})^{-2}$ .

From the asymptotic solutions to equation (5), the reactance matrix and consequently the cross sections can be determined in the usual way [33],

$$\begin{aligned} Q(m_1 m_2 \rightarrow m'_1 m'_2) \\ = \frac{\pi a_0^2}{(a_0 k_{m_1 m_2})^2} \sum_{\ell=0}^{\infty} (2\ell+1) |T_{m'_1 m'_2, m_1 m_2}^{\ell}|^2, \end{aligned} \quad (11)$$

where  $a_0$  is the first Bohr radius.

In this work we are particularly interested in V-T collisions, for example the de-excitation process  $Q(10 \rightarrow 00)$ , and V-V collisions, for example  $Q(10 \rightarrow 01)$ .

The numerical solution of equation (5) has been carried out using the algorithms described in Smith

*et al.* [34]. The analysis for the vibrator-vibrator problem differs from the structureless-vibrator problem only in the definitions of the wave number squared, equation (6), and the potential, equation (7a). Hand checks were carried out to ensure that this part of the code was correct. The numerical solution of the coupled system of ODE's and the extraction of the  $R$ -matrices and cross sections was identically the same as that used by Smith *et al.* [34] who describe in detail the numerical tests which had been carried out to ensure their correctness.

## HF-HF System

If the channels of equation (5) are ordered in increasing wave number, then it is seen that there is one elastic channel, associated with  $k_{00}$ , three degenerate inelastic channels associated with  $k_{11}$ ,  $k_{02}$ ,  $k_{20}$ , etc. The objective of this paper is to estimate the relaxation time for  $HF(\nu=1)$  molecules to return to the ground vibrational state. This can occur *via* several alternative paths, for example

$$HF(\nu=1) + HF(0) \rightarrow HF(0) + HF(0) + \Delta E = 3961 \text{ cm}^{-1}, \quad (12)$$

or

$$HF(\nu=1) + HF(\nu=1) \rightarrow HF(\nu=1) + HF(0) + \Delta E, \quad (13)$$

followed by equation (12), or

$$HF(\nu=1) + HF(\nu=1) \rightarrow HF(0) + HF(0) + 2\Delta E, \quad (14)$$

and, according to Hancock and Green [4], the experimentally measured rates are a summation of the several individual rates comprising both  $V \rightarrow V$  and  $V \rightarrow R, T$  energy transfer processes. In view of a near resonant match between  $\nu=1, J=4$  and  $\nu=0, J=14$  levels of  $HF$ , processes of the type

$$HF(\nu=1, J=4) + HF(0) \rightarrow HF(\nu=0, J=13) + HF(0), \quad (15)$$

might be important in  $HF$  vibrational relaxation.

Since both rotational and closed channel effects have been neglected in the present model, we have followed the consistent approach of including only three open channels associated with  $k_{00}$ ,  $k_{01}$ ,  $k_{10}$  and calculating relaxation times from reaction (12) as described in Smith *et al.* [34].

The model described in the previous section requires the energy separation of the vibrational levels of  $HF$ , that is  $\Delta E = 0.5133 \text{ eV}$ , the Lennard-Jones force constants,  $\sigma = 2.55 \text{ \AA}$  and  $\epsilon/k = 400^\circ \text{K}$ , the reduced mass of the oscillator,  $M = 0.95 m_p$ , and the reduced mass of the collision system,  $\mu = 10 m_p$ . Equations (5) are then solved for a given  $E_c$  for a sufficient number of  $\ell$  values to determine the total de-excitation cross section accurately.

Table 2: Relationships among the cross sections for elastic scattering,  $E$ , vibrational-translational energy transfer, V-T, and its inverse, T-V, related by detailed balance, and vibrational-vibrational energy transfer, V-V.

Initial States $m,n$	Final States $m',n'$					
	$k_0^2$	$k_{01}^2$		$k_{11}^2$		
	0,0	0,1	1,0	1,1	0,2	2,0
0,0	$E_1$	(T-V) <sub>1</sub>	(T-V) <sub>1</sub>	(T-V) <sub>2</sub>	(T-V) <sub>3</sub>	(T-V) <sub>3</sub>
0,1	(V-T) <sub>1</sub>	$E_2$	(V-V) <sub>1</sub>	(T-V) <sub>4</sub>	(T-V) <sub>5</sub>	(T-V) <sub>6</sub>
1,0	(V-T) <sub>1</sub>	(V-V) <sub>1</sub>	$E_2$	(T-V) <sub>4</sub>	(T-V) <sub>6</sub>	(T-V) <sub>5</sub>
1,1	(V-T) <sub>2</sub>	(V-T) <sub>4</sub>	(V-T) <sub>4</sub>	$E_3$	(V-V) <sub>2</sub>	(V-V) <sub>2</sub>
0,2	(V-T) <sub>3</sub>	(V-T) <sub>5</sub>	(V-T) <sub>6</sub>	(V-V) <sub>2</sub>	$E_4$	(V-V) <sub>3</sub>
2,0	(V-T) <sub>3</sub>	(V-T) <sub>6</sub>	(V-T) <sub>5</sub>	(V-V) <sub>2</sub>	(V-V) <sub>3</sub>	$E_4$

In table 2, we present the relationships among the various cross sections due to the identity between target and projectile. Cross sections (T-V) with the same suffix should be identical, while cross sections (T-V)<sub>*i*</sub> are related to their inverses (V-T)<sub>*i*</sub> by the detailed balance, that is

$$k_{mn}^2 Q_{mn,m'n'} = k_{m'n'}^2 Q_{m'n',mn}. \quad (16)$$

These relationships provided an explicit numerical check on the correctness of the code. The degree to which they are satisfied depends on the accuracy of the  $R$ -matrix which is real and symmetric. In general, the results we quote here are from  $R$ -matrices symmetric to four decimal places. However, for collision energies approaching the second excitation threshold, 1.0266 eV, and at very large  $\ell$  values, where the cross sections were very small,  $10^{-8}$ , the symmetry of  $R$  was lost.

### Cross Sections

In molecular collisions, many partial waves are required to calculate the total cross sections. However, the cross section does vary smoothly with  $\ell$  and so there is no need to solve equation (5) for each  $\ell$  value, but only a sufficient number to define the shape of the  $Q$  versus  $\ell$  curve. In table 3 we present the sequence of collision energies we used,  $E_c$ , and the values of the (V-T)<sub>1</sub> cross section at the peaks. From this table we see that for  $E_c \geq 4.0133$  eV, a second inner peak has appeared. We have plotted all the  $Q$  versus  $\ell$  curves and found them to be smooth. These curves are summed to give the total de-excitation cross section as shown in figure 2. This curve exhibits a shoulder at  $E_c = 4.0133$  eV. Since we cannot think of any mechanism which would induce such a shoulder in the energy behaviour of the cross section, then we conclude that either our method

produces too large cross sections at the lower energies or too small cross sections at the higher energies. We are in the process of trying to resolve this uncertainty.

Table 3: Dependence of the maxima of the V-T cross section  $Q_{10,00}$  in units of  $\pi a_0^2$  on  $\ell$  and  $E_c$

$E_c$ (eV)	$\ell$	$Q_{10,00}(\pi a_0^2)$	$\ell$	$Q_{10,00}$
1.0633	25	$0.19 \times 10^{-7}$		
1.1133	28	$0.38 \times 10^{-7}$		
1.3133	30	$0.33 \times 10^{-6}$		
1.5133	35	$0.16 \times 10^{-5}$		
2.0133	50	$0.17 \times 10^{-4}$		
2.5133	70	$0.61 \times 10^{-4}$		
4.0133	150	$0.25 \times 10^{-3}$	30	$0.015 \times 10^{-3}$
5.0133	200	$0.4 \times 10^{-3}$	75	$0.415 \times 10^{-3}$
6.0133	225	$0.52 \times 10^{-3}$	110	$1.025 \times 10^{-3}$
7.0133	265	$0.7 \times 10^{-3}$	150	$1.5 \times 10^{-3}$

As mentioned previously, the production runs of the present work have been carried out in the three-state close coupling approximation including the 0,0; 1,0; and 0,1 states of the collision partners. From table 2 we see that this enables us to calculate the

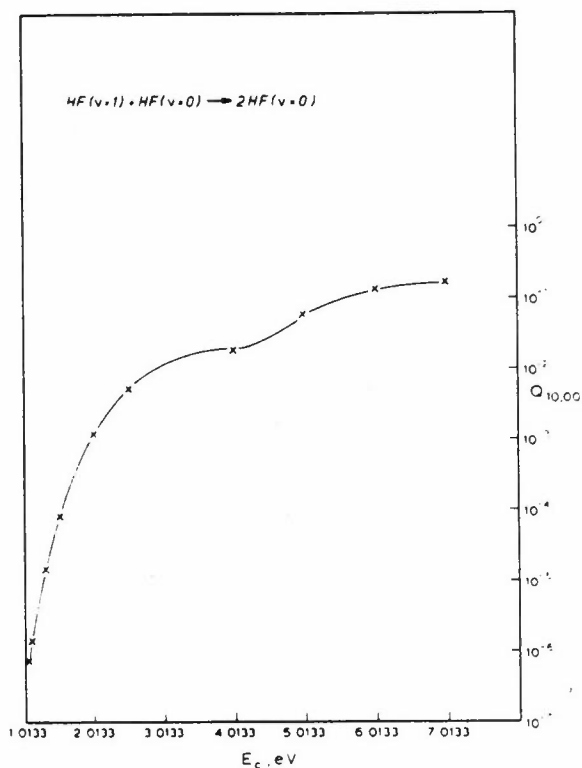


Figure 2: De-excitation cross section, in units of  $\pi a_0^2$ ,  $Q_{10,00}$ , as a function of the collision energy  $E_c$ , in a three-state close-coupling approximation



nine cross sections of the upper left hand corner  $3 \times 3$  matrix. In figure 2 we have plotted the  $(V-T)_1$  result and we did ensure that it equalled  $(T-V)_1$ , by reciprocity. We now turn to discuss the  $(V-V)_1$  cross section.

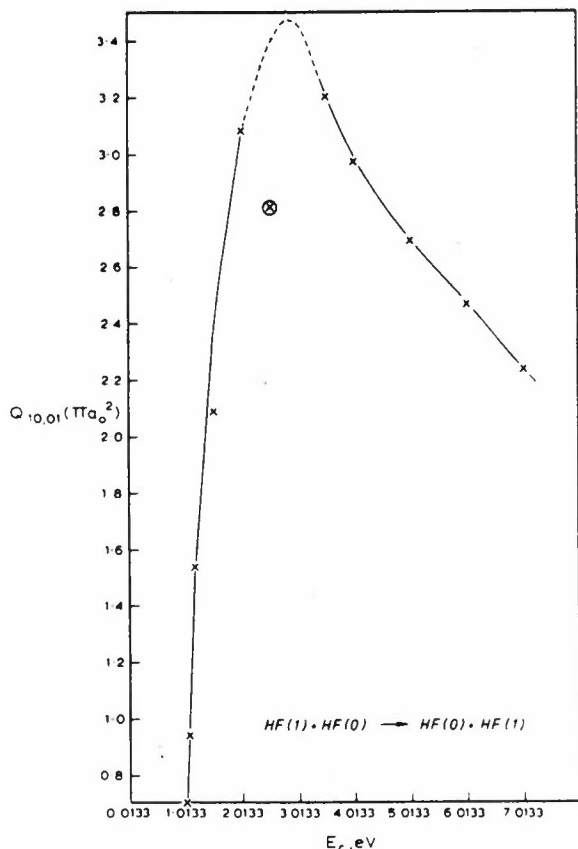


Figure 3: Vibrational-vibrational cross section, in units of  $\pi a_0^2$ ,  $Q_{10,01}$ , as a function of the collision energy  $E_c$ , in a three-state close-coupling approximation. The dashed part of the curve is interpolated from the results on either side of the peak. The circled cross indicated a calculated point which may not have converged in  $\ell$

We have found that the vibrational-vibrational energy transfer process converges in  $\ell$  much more slowly than the corresponding V-T cross sections. We have also found that they do not exhibit the huge variation over orders of magnitude that we presented in figure 2 for the V-T results. In figure 3 we present the V-V transfer cross sections for the process



We have drawn this curve so that it has a smooth peak, the dashed part of the curve, rather than draw it passing through the calculated point at  $E_c = 2.5133$  eV. This has been done because we found that convergence at high  $\ell$  was very slow and the  $R$ -matrices were becoming non-symmetric. We found, as in V-T, that the partial wave cross sections exhibited a

second peak at the higher energies. For V-V cross sections this peak contributes about 20% to the total cross sections. Consequently, if we assume that such a peak is present at high partial waves at  $E_c = 2.5133$ , then our calculated point would lie precisely on the dashed curve.

### Relaxation Rates

If it is assumed that the distribution of velocities of the HF molecules is Maxwellian, then the reaction rate coefficient is given by

$$\gamma_{if}(T) = 4\pi^2 a_0^2 \left( \frac{\mu}{2\pi kT} \right)^{3/2} N \int_0^\infty Q_{if}(v) e^{-\mu v^2/2kT} v^3 dv, \quad (18)$$

where  $N$  is the particle density at one atmosphere pressure at  $T^\circ K$ ,

$$N = \frac{N_0 P}{RT} \quad (19)$$

We have taken the following values for the constants,

Avogadro's number	$N_0 = 6.0228 \times 10^{23} \text{ cm}^{-3}$
1 atmos.	$P = 1.01325 \times 10^6 \text{ dynes}$
Gas constant	$R = 8.315 \times 10^7 \text{ ergs/mole/}^\circ K$
Boltzmann's constant	$k = 1.38033 \times 10^{-6} \text{ erg/}^\circ K$
Bohr radius	$a_0 = 0.5294 \times 10^{-8} \text{ cm}$
Proton mass	$m_p = 1836 \times 9.1055 \times 10^{-28}$

The cross section,  $Q_{if}$ , is given in units of  $\pi a_0^2$ .

When these constants are substituted into equation (18), and we change the integration variable to

$$x = m v^2 / 2kT, \quad (20)$$

then equation (18) becomes, in units of  $\text{sec}^{-1}$ ,

$$\gamma_{if}(T) = 0.93716 \times 10^{10} \times (\mu T)^{-1/2} \int_0^\infty Q_{if}(xkT) e^{-x} dx, \quad (21)$$

where  $\mu$  is in proton mass units, which agrees with Marriott [35].

Herzfeld and Litovitz [36] show that the internal energy of a simple harmonic oscillator has a single relaxation time related to the rate coefficients by

$$\tau_{\text{s.h.o.}}^{-1} = \gamma_{10} - \gamma_{01}, \quad (22)$$

provided the rate coefficients satisfy the ratios

$$\gamma_{\lambda+1, \lambda} / \gamma_{\lambda, \lambda-1} = \lambda + 1 / \lambda, \quad (23)$$

which they do in the distorted wave approximation of Wittman [37], but which they do not in the close-coupling approximation. Consequently, we

believe that it is inappropriate for us to use equation (22). Herzfeld and Litovitz [36] have given a two-state formula for the relaxation time, namely

$$\tau_2^{-1} = \gamma_{10} + \gamma_{01} \quad (24)$$

Our cross section calculations are based on a three state system. However, as yet, we have been unable to generalize equation (24) to calculate the relaxation times based on the V-T cross section of figure 2.

In figure 4 we present our values of the V-T relaxation time and it is seen to be orders of magnitude too large compared with the experimental values [8].

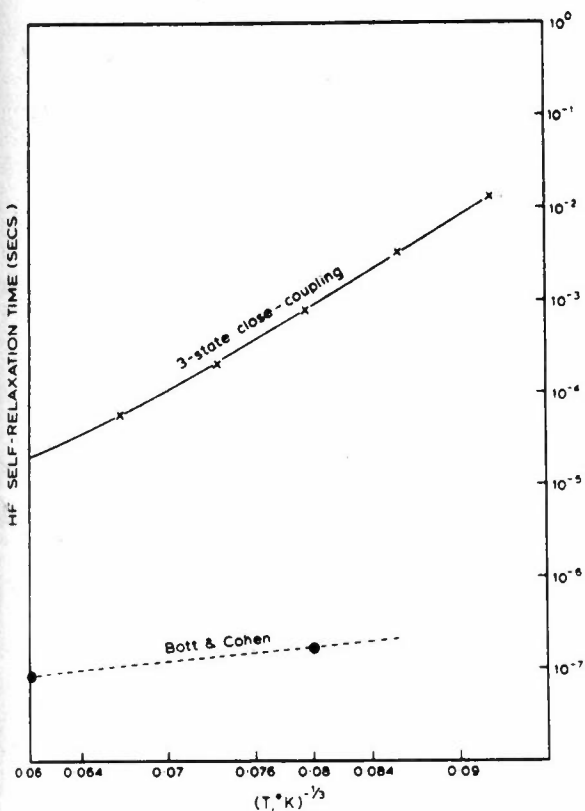


Figure 4: Comparison of theory (crosses) with experiment (dashed line)

### Summary and Conclusions

The gross disagreement between the predictions of the quantum mechanical three state close coupling approximation and the experimental results will be due in varying measures to the following approximations

- (a) we have assumed a Lennard-Jones interaction between the collision partners;
- (b) we have neglected rotational effects;
- (c) we have not solved the three state approximation for those values of  $E_c$  when closed channels are present;

- (d) we have not checked for convergence in the  $n$ -state approximation, at any  $E_c$  and  $l$ ;
- (e) we have probably used an invalid formula for  $\tau$ ;
- (f) we have neglected dimer formation.

Berend and Thommarson [27] found that when they neglected the hydrogen bonding (or dipole-dipole) interaction in the intermolecular potential they found an increase of 16-fold in the vibrational relaxation time at 300°K. This leads us to believe that the most crucial area for improvement in this quantum mechanical model is in replacing the Lennard-Jones (6,12) potential with realistic potentials.

### References

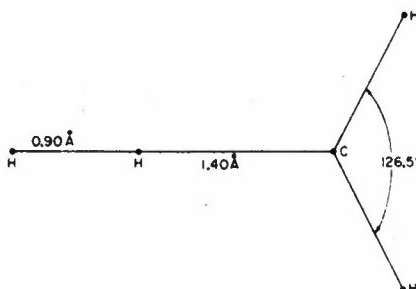
- [1] WISWALL, C.E., AMES, D.P. and MENNF, J.J. (1973). *IEEE J. Quant. Elec.*, **QE-9**, 181-188.
- [2] AIREY, J.R. and FRIED, S.F. (1971). *Chem. Phys. Letters*, **8**, 23-26.
- [3] HANCOCK, J.K. and GREEN, W.H. (1972). *J. Chem. Phys.*, **56**, 2474-2475.
- [4] ——— and ——— (1972). *J. Chem. Phys.*, **57**, 4515-4529.
- [5] GREEN, W.H. and HANCOCK, J.K. (1973). *IEEE J. Quant. Elec.*, **QE-9**, 50-58.
- [6] STEPHENS, R.R. and COOL, T.A. (1972). *J. Chem. Phys.*, **56**, 5863-5878.
- [7] HINCHEN, J.J. (1973). *J. Chem. Phys.*, **59**, 233-240.
- [8] BOTT, J.F. and COHEN, N. (1971). *J. Chem. Phys.*, **55**, 3698-3706.
- [9] BLAUER, J.A., SOLOMON, W.C., and OWENS, T.W. (1972). *Int. J. of Chem. Kinet.*, **4**, 293-306.
- [10] BOTT, J.F. (1972). *J. Chem. Phys.*, **57**, 96-102.
- [11] FRIED, S.F., WILSON, J. and TAYLOR, R.L. (1973). *IEEE J. Quant. Elec.*, **QE-9**, 59-64.
- [12] OSGOOD, R.M., JAVAN, A. and SACKETT, P.B. (1972). *Appl. Phys. Letters*, **20**, 469-472.
- [13] BINA, M.J. and JONES, C.R. (1973). *Appl. Phys. Letters*, **22**, 44-45.
- [14] SHIN, H.K. (1971). *J. Phys. Chem.*, **75**, 1079-1089.
- [15] ——— (1971). *Chem. Phys. Letters*, **10**, 81-85.
- [16] RAPP, D. and KASSAL, T. (1969). *Chem. Revs.*, **69**, 61-102.
- [17] RILEY, M.E. and KUPPERMANN, A. (1968). *Chem. Phys. Letters*, **1**, 537-538.
- [18] WILSON, D.J. (1970). *J. Chem. Phys.*, **53**, 2075-2078.
- [19] SHIN, H.K. (1970). *Chem. Phys. Letters*, **6**, 494-498.
- [20] ——— (1971). *Chem. Phys. Letters*, **11**, 628.
- [21] JEFFERS, W.Q. and KELLEY, J.D. (1971). *J. Chem. Phys.*, **55**, 4433-4437.
- [22] SHARMA, R.D. and BRAU, C.A. (1967). *Phys. Rev. Letters*, **19**, 1273.

- [23] ————— and ————— (1969).  
*J. Chem. Phys.*, **50**, 924.
- [24] TAM, W.G. (1972). *Chem. Phys. Letters*, **15**,  
113-115.
- [25] ————— (1972). *Can. J. Phys.*, **50**, 2691-  
2697.
- [26] KELLEY, J.D. (1972). *J. Chem. Phys.*, **56**,  
6108-6117.
- [27] BEREND, G.C. and THOMMARSON, R.L. (1973).  
*J. Chem. Phys.*, **58**, 3203-3208.
- [28] MARRIOTT, R. (1964). *Proc. Phys. Soc. (Lon-  
don)*, **83**, 159-169.
- [29] SCHWARTZ, R.N., SLAWSKY, Z.I. and HERZ-  
FELD, K.F. (1952). *J. Chem. Phys.*, **20**, 1591-  
1599.
- [30] MARRIOTT, R. (1964). *Proc. Phys. Soc. (Lon-  
don)*, **84**, 877-888.
- [31] GIANTURCO, F.A. and MARRIOTT, R. (1969).  
*J. Phys. B*, **2**, 1332-1335.
- [32] MOTT, N.F. and MASSEY, H.S.W. (1965).  
*Theory of Atomic Collisions* 3rd ed., 686,  
Oxford University Press.
- [33] SMITH, K. (1971). *The Calculation of Atomic  
Collision Processes*, 173, Wiley.
- [34] SMITH, K., ORMONDE, S., DAVIES, A.R. and  
TORRES, B.W. (1974). *J. Chem. Phys.*, **61**,  
2643-2650.
- [35] MARRIOTT, R. (1971). *Abstracts for VII  
I.C.P.E.A.C.*, 241, Amsterdam: North Holland.
- [36] HERZFELD, K.F. and LITOVITZ, T.A. (1959).  
*Absorption and Dispersion of Ultrasonic Waves*,  
New York: Wiley.
- [37] WITTEMAN, W.J. (1961). *J. Chem. Phys.*, **35**,  
1-10.

# Reaction Pathways for the Triplet Methylene Abstraction $CH_2(^3B_1) + H_2 \rightarrow CH_3 + H^*$

C.W.Bauschlicher Jr., H.F.Schaefer III<sup>†</sup>, C.P.Baskin and C.F.Bender<sup>‡</sup>

A non-empirical quantum mechanical study of the reaction of triplet methylene with molecular hydrogen has been carried out. A contracted gaussian basis set of double zeta quality was employed. Following the determination of each self-consistent-field wavefunction, configuration interaction was performed including all singly- and doubly-excited configurations (a total of 649). The potential surface was studied in three dimensions and a total of 780 points computed. From these data, several approximations to the minimum energy path have been computed and compared. The reaction exothermicity is computed to be 5.37 kcal/mole, in good agreement with experiment, 4.5 kcal/mole. The predicted barrier height is 15.5 kcal/mole, a result consistent with the lack of any observed reaction between  $CH_2(^3B_1)$  and  $H_2$  at 300°K. The predicted barrier is 4.2 kcal/mole less than that obtained by Carr using the bond-energy bond-order (BEBO) method. The saddle point geometry is predicted to be



## Introduction

Methylene reactions have become the topic of an increasing number of experimental [1-15] and theoretical [16-26] studies in recent years. And in fact the experimental studies have already yielded a wealth of valuable information about methylene reactions. For example, it now seems firmly established that triplet methylene abstracts hydrogen atoms from saturated hydrocarbons while the analogous reactions with singlet methylene yield insertion into CH bonds. One should note, however, that the interpretation of these experiments can be somewhat perilous. This is because in most cases the procedure used involves the photolysis of either ketene or diazomethane in the presence of the species with which a methylene reaction is desired. Although the elementary reactions of singlet and triplet methylene with the desired species will certainly occur to some degree, it is equally clear that a number of other chemical reactions may be taking place, e.g. the reaction of

methylene with ketene to give ethylene and carbon monoxide. Ideally, one would like to be able to cross a beam of triplet or singlet methylenes with a beam of the other reactant, e.g.  $H_2$ . Even though a methylene crossed molecular beam experiment may sound unlikely, there does appear to be a real possibility [27] that such an experiment will be carried out within the next several years. The potential importance of experiments of this kind with respect to the discernment of the dynamics of methylene reactions can hardly be overemphasized.

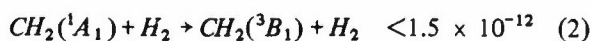
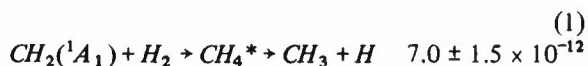
In a similar manner, the theoretical studies of methylene reactions, while being something less than the ultimate, have significantly advanced our understanding of the chemistry of this short-lived intermediate. For example, the extended Hückel calculations of Hoffmann [20] and, to a lesser degree, the MINDO work of Dewar [25] have given support to the contested two-step mechanism of Benson [28] for the singlet methylene insertion into methane.

\* Work performed under the auspices of the U.S. Atomic Energy Commission

† Lawrence Berkeley Laboratory and Department of Chemistry, University of California, Berkeley, California 94720, USA

‡ Lawrence Livermore Laboratory, University of California, Livermore, California 94550, USA

The prototype methylene reaction is  $CH_2 + H_2$ , hydrogen being the simplest partner molecule for which both abstraction and insertion reactions might occur. Among the several experimental studies [29-37] of this reaction, the most recent is that of Braun, Bass and Pilling [37]. With rate constants at 298°K given in  $cm^3/(molecule \cdot second)$ , they summarize their results as follows:



In fact, Braun *et al.* were unable to observe any reaction of triplet methylene with hydrogen at 300°K, and the figure given is an upper limit to the true rate constant. Recently Carr [22] has been able to rationalize this  $^3B_1$  nonreactivity using Johnston and Parr's empirical bond-energy bond-order method [38] for the calculation of activation energies. Carr predicts the activation energy for  $CH_2(^3B_1) + H_2 \rightarrow CH_3 + H$  to be quite high, 19.7 kcal/mole. Other computed abstraction activation energies ranged from 7.9 kcal/mole for  $C_3H_6$  to 44.2 kcal/mole for  $HCN$ . It is worth noting the Dewar's predicted activation energy [25] of 3.8 kcal/mole for  $CH_2(^3B_1) + CH_4 \rightarrow 2CH_3$  is qualitatively different from that of Carr, 25.6 kcal/mole.

Our *ab initio* theoretical study concerns the apparently slow  $CH_2(^3B_1) + H_2$  abstraction reaction. The method used, which explicitly considers electron correlation, is analogous to that adopted in our previous study [39] of isolated  $CH_2$ . That study unequivocally predicted the nonlinearity of methylene at a time when a linear structure had been almost universally accepted. The two primary goals of the present study were

- (a) to obtain a reliable ( $\pm 5$  kcal/mole) prediction of the activation energy and
- (b) to map out the minimum-energy-path for this simple reaction.

## Theoretical Approach

A double zeta basis set of contracted gaussian functions [49] was used in the present work. For the carbon atom, Huzinaga's (9s 5p) primitive gaussian basis [41] was contracted to (4s 2p) following Dunning [42]. In analogous fashion a (4s/2s) basis was chosen for each H atom. The hydrogen basis functions were scaled by a factor of 1.2, i.e. each gaussian exponent  $\alpha$  was multiplied by 1.44.

For  $C_{2v}$  approaches of the hydrogen molecule to  $^3B_1$  methylene, the self-consistent-field (SCF) wavefunction is of the form

$$1a_1^2 \ 2a_1^2 \ 1b_2^2 \ 3a_1^2 \ 4a_1 \ 1b_1 \quad (4)$$

The SCF wavefunctions were obtained using a method recently developed by Davidson [43]. In addition we have computed configuration interaction wavefunctions which include all (except that the  $1a_1$  orbital is always doubly occupied) singly- and doubly-excited configurations with respect to this SCF reference state. However, we have deleted those doubly-excited configurations which do not retain the open-shell spin coupling of the reference configuration. The deleted configurations  $i$  have identically zero Hamiltonian matrix elements  $H_{1i}$  with the SCF configuration [44,45]. A total of 649 configurations were included in the calculations.

Fortunately, the same SCF wavefunction (4) dissociates properly to SCF wavefunctions for the products  $CH_3 + H$ . Hence, the true wavefunction should be reasonably well-described by a single configuration along the entire minimum energy path. This being the case, our single- and double-excitation CI should be nearly comparable ( $\sim 95$ -98% of the correlation energy attainable from the chosen basis) to a full CI within the valence shell [40]. Three natural orbital iterations [46] were used in each calculation. Although in general such iterations tend to accelerate (lower total energy with fewer configurations) convergence of the CI expansion, the total energy was lowered relatively little (typically 0.003 hartrees) in the present cases, since the CI was initially nearly complete in a practical sense.

The accuracy of the potential surface should fall somewhere between that of our two surfaces [47,48] for  $F + H_2 \rightarrow FH + H$ . Although the basis set here is analogous to that used in our preliminary study [47], a more thorough level of CI was used in the present study. Both the  $F + H_2$  studies indicated the necessity of describing correlation effects in order to reliably predict the barrier height and exothermicity. Finally we note that the level of theory used in the present study seems [49] to predict equilibrium bond distances with a reliability of 0.03Å and bond angles to 2°.

## Geometries Considered

Intuition suggests that the minimum-energy-path for  $CH_2 + H_2$  should occur for a planar configuration in which the  $H-H$  molecule falls on the line bisecting the  $HCH$  methylene bond angle. However, Hoffmann has noted [50] that the surface may be rather flat with respect to a bending of the  $H_2$  out of this plane. Such a  $C_{2v}$  reaction path is also the only path fully consistent with the MINDO results of Bodor, Dewar and Wasson [25] for the analogous reaction  $CH_2(^3B_1) + CH_4 \rightarrow 2CH_3$ .

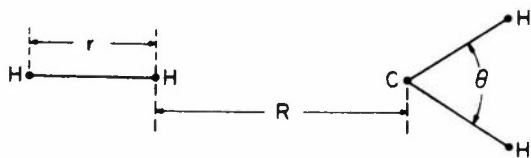
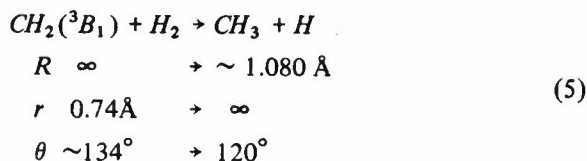


Figure 1: Coordinate system for  $CH_2(^3B_1) + H_2 \rightarrow CH_3 + H$

Therefore, we have restricted our study to the  $C_{2v}$  coordinate system shown in figure 1. In addition, the two methylene  $CH$  distances have been frozen at 2.06 bohrs = 1.090 Å. The remaining geometrical parameters are

- (a)  $R$ , the distance between the carbon atom and the closer of the two  $H$  atoms in  $H_2$ ;
- (b)  $r$ , the  $H-H$  separation in  $H_2$ ; and
- (c)  $\theta$ , the methylene bond angle.

As we go from reactants to products, these variables should change as follows:



This three-dimensional potential surface has been determined at 780 points. The  $R$  values considered were 100.0, 10.0, 6.0, 5.0, 4.0, 3.0, 2.8, 2.6, 2.5, 2.4, 2.3, 2.2, 2.1, 2.06 and 2.0 bohrs. The  $H-H$  separation  $r$  took the values 1.2, 1.4, 1.6, 1.8, 2.0, 2.2, 2.4, 2.6, 2.8, 3.0, 3.2, 3.4, 3.6, 3.8, 4.0, 5.0, 6.0, 10.0 and 100.0 bohrs. Bond angles  $\theta$  considered were  $110^\circ$ ,  $120^\circ$ ,  $130^\circ$  and  $140^\circ$ . It is apparent that not all points on this  $15 \times 19 \times 4 = 1140$  point grid were computed. Many points which were clearly far from the minimum energy path were omitted. However, near the saddle point, a number of additional  $R$  values were used. The 780 computed total energies, in hartrees and kcal/mole relative to separated  $CH_2 + H_2$ , are given in the appendix to our complete report [51] of this research.

## Results

Table 1 summarizes our results for the reactants (separated  $CH_2(^3B_1) + H_2$ ) and products (separated  $CH_3 + H$ ). The former results were obtained at  $R = 100.0$  bohrs and the latter at  $r = 100.0$  bohrs.

The methylene bond angle is predicted to be  $134.1^\circ$ , which is nearly identical to the  $134^\circ$  value obtained from the best available theoretical calculation [52], and consistent with experiment [53]  $136 \pm 5^\circ$ .

Table 1: Geometries and total energies of reactants and products

$CH_2(^3B_1) + H_2$	$E$	= -40.12866 hartrees
	$r(CH)$	= 1.090 Å
	$\theta(HCH)$	= $134.1^\circ$
	$r(HH)$	= 0.748 Å
$CH_3 + H$	$E$	= -40.13722 hartrees
	$r(CH)$	= 1.094 Å
	$\theta(HCH)$	= $120.2^\circ$

The predicted  $H_2$  equilibrium separation is 1.0007 Å longer than the exact result [54], 0.7414 Å.

Although the two methylene  $CH$  distances were everywhere constrained to be 2.060 bohr = 1.090 Å, the third  $CH$  bond distance of the methyl radical is a variable, determined to be 1.094 Å. In addition, our calculations predict the methylene bond angle to be  $120.2^\circ$ . However, this bond angle is uncertain by perhaps  $0.2^\circ$  since the calculations were carried out at  $10^\circ$  intervals. Hence, although slightly unsymmetrical, our methyl radical structure is essentially the same as the planar experimental  $CD_3$  structure of Herzberg [55] with  $r_0(CD) = 1079$  Å.

The reaction exothermicity is 0.00855 hartrees = 5.37 kcal/mole, in very good absolute agreement with the experimental value given by Carr [22], 4.5 kcal/mole. The latter value is obtained from  $D_e(H-H) = 109.5$  kcal/mole and  $D_e(CH_2-H) = 114.0$  kcal/mole.

The saddle point or transition state [56] is the energetically highest point on a continuous path connecting  $CH_2 + H_2$  with  $CH_3 + H$ . If several such points and paths occur, the true saddle point for the reaction is that which is energetically lowest. The saddle point for our three-dimensional potential energy surface was located by using the stationary property

$$\frac{\partial E}{\partial R} = \frac{\partial E}{\partial r} = \frac{\partial E}{\partial \theta} = 0 \quad (6)$$

With the obvious exception of the reactants, products and long range attractions, the predicted saddle point appears to be the only point on the *ab initio* surface which satisfies equation (6).

The predicted saddle point, seen in figure 2, occurs at  $R = 2.640$  bohrs = 1.397 Å,  $r = 1.702$  bohrs = 0.900 Å,  $\theta = 126.5^\circ$ . This geometry is intermediate between that of the products and reactants: the  $H-H$  separation is 0.152 Å or 20% longer than in  $H_2$ , while the  $H-C$  separation is 0.303 Å or 28% longer than in the isolated methyl radical. The fact that the transition state geometry is somewhat closer to the reactants than the products is consistent with Hammond's idea [57] that, in a highly exothermic reaction, the transition state should resemble the reactants.

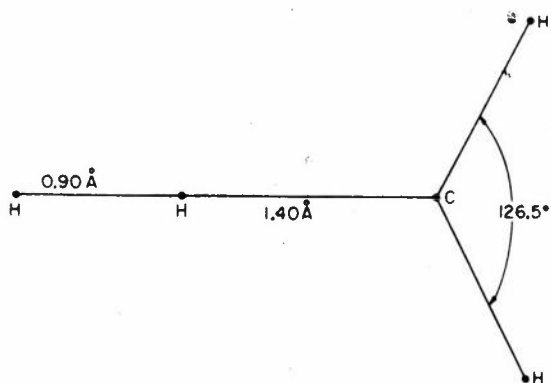


Figure 2: Transition state geometry for  $CH_2(^3B_1) + H_2 \rightarrow CH_3 + H$

The *ab initio* total energy at the saddle point is  $-40.10400$  hartrees, which lies  $15.5$  kcal/mole above  $CH_2(^3B_1) + H_2$ . This  $15.5$  kcal/mole barrier does not, of course, reflect the zero-point vibrational energies of the reactants and transition state. The barrier height defined in this way is sometimes called the classical activation energy [58]. The Arrhenius activation energy for  $CH_2(^3B_1) + H_2$  has not been measured, and the only related experimental information is the finding of Braun, Bass and Pilling [37] that no reaction was observed at  $300^\circ K$ . Our  $15.5$  kcal/mole barrier is sufficiently large to be consistent with their negative finding. As noted earlier, Carr [22] has used the empirical BEBO method to predict a barrier height of  $19.7$  kcal/mole. Although it is impossible to place error bars on our theoretical barrier height, based on earlier work [46,47], we intuitively feel that the  $15.5$  kcal/mole result should be within  $5$  kcal/mole of the exact result. Thus our study gives further [59] evidence of the usefulness of the BEBO method. The only example we are familiar with in which BEBO fails seriously is the  $F + HF \rightarrow FH + F$  reaction. There BEBO predicts a barrier of  $6$  kcal/mole [60], while the best *ab initio* calculations [61] imply a barrier  $\geq 18$  kcal/mole.

On the basis of our earlier work on the radical plus diatom reactions [47,48,61,62]  $F + H_2$ ,  $H + F_2$ , and  $F + HF$ , we were sceptical of the ability of single configuration SCF wavefunctions to describe the  $CH_2(^3B_1) + H_2$  potential surface. However, from a theoretical point of view, any information on the suitability of the Hartree-Fock approximation with respect to such reactions is extremely valuable. Therefore the relative energies and geometries of the reactants, saddle point and products were obtained from the SCF potential surface. The calculated exothermicity for  $CH_2(^3B_1) + H_2 \rightarrow CH_3 + H$  was found to be  $4.84$  kcal/mole, which is actually in somewhat better agreement with experiment [21],  $\sim 4.5$  kcal/mole, than the CI result,  $5.37$  kcal/mole. However, the barrier height is computed to  $25.1$  kcal/mole, or  $9.6$  kcal/mole higher than the CI result. Although the barrier height is not known experimentally, our previous experience [47, 48, 61, 62] would suggest that it may be close to or slightly lower

than the CI result, and hence that the SCF barrier may be much too high. The SCF saddle point geometry is  $R = 2.53$  bohrs,  $r = 1.69$  bohrs,  $\theta = 124.8^\circ$ . Thus the SCF and CI transition state geometries are quite similar, much more so than was the case [46, 47, 61] for  $F + H_2$  and  $H + F_2$ .

## Reaction Pathways

In both textbooks and the literature, one frequently finds terms such as 'reaction coordinate', 'reaction path', 'path of least energy', and 'minimum energy path' used interchangeably. We find this situation unfortunate, since there are at least two distinct procedures by which such a path might be obtained.

The most frequently used procedure is to choose a 'reaction coordinate', some geometrical parameter that varies significantly during the course of reaction. For the  $CH_2(^3B_1) + H_2$  reaction, either  $R$  (which goes from  $\infty$  to  $1.094\text{\AA}$ ) or  $r$  (which goes from  $0.748\text{\AA}$  to  $\infty$ ) would be reasonable choices.  $\theta$ , which goes from  $134^\circ$  to  $120^\circ$ , would probably not be a very good choice, since it does not undergo a large change during the reaction. Given a value of the 'reaction coordinate', one finds a point on the 'reaction path' by minimizing the total energy with respect to all other geometrical parameters [63]. Hereafter, our use of the terms 'reaction coordinate' and 'reaction path' will be strictly as defined above.

Under favourable conditions, a reaction coordinate will vary monotonically along the reaction path, and the energetically highest point on the reaction path will occur near the true saddle point. However, there are many exceptions to the favourable behaviour, an especially interesting example being the MINDO treatment of the interconversion of cyclobutene and butadiene [64]. Even if a reaction path does pass close by the saddle point, there are situations in which the reaction path will appear unrealistic. These situations generally occur when a small change in the chosen reaction coordinate is accompanied by large changes in other geometrical parameters. One example of such behaviour is noted by Dobson, Hayes and Hoffmann [20] in their study of  $CH_2(^1A_1) + CH_4$ .

There is at least one procedure [47,56] which defines the reaction pathway (an intentionally vague term) in a far more satisfactory manner. Rather than starting from either reactants or products, this procedure begins with the saddle point. From the saddle point, one follows the gradient  $\vec{\nabla} V$  of the potential energy in the direction of most negative curvature. Following the gradient leads in one direction to reactants and in the other direction to products, and we refer to the resulting path between products and reactants as the 'minimum energy path'. Note that although this definition is dependent on choice of coordinate system, one expects such dependence to be in general unimportant.

Table 2: Reaction paths for  $CH_2(^3B_1) + H_2 \rightarrow CH_3 + H$ . Bond distances are in bohr radii, bond angles in degrees and energies in kcal/mole.

Minimum Energy Path				<i>R</i> Reaction Coordinate				<i>r</i> Reaction Coordinate			
<i>R</i>	<i>r</i>	$\theta$	<i>E</i>	<i>R</i>	<i>r</i>	$\theta$	<i>E</i>	<i>R</i>	<i>r</i>	$\theta$	<i>E</i>
100.0	1.414	134.1	0.00	100.0	1.414	134.1	0.00	6.0	1.4	134.1	-0.02
6.0	1.412	134.1	-0.04	6.0	1.412	134.1	-0.04				
5.0	1.412	133.9	0.50	5.0	1.412	133.9	0.50				
4.5	1.412	133.8	1.35	4.5	1.412	133.8	1.35				
4.0	1.420	133.3	3.39	4.0	1.420	133.3	3.39				
3.8	1.428	132.9	4.66	3.8	1.428	132.9	4.66				
3.6	1.440	132.4	6.22	3.6	1.440	132.4	6.22				
3.4	1.452	131.9	8.05	3.4	1.452	131.9	8.05				
3.2	1.468	131.2	10.27	3.2	1.468	131.2	10.27				
3.0	1.524	130.0	12.72	3.0	1.504	130.0	12.63	6.0	1.5	134.1	0.81
2.8	1.612	128.1	14.82	2.8	1.572	128.2	14.70				
2.7	1.660	127.2	15.35	2.7	1.640	127.2	15.35	6.0	1.6	134.1	3.40
2.640	1.702	126.5	15.48	2.65	1.692	126.6	15.48	6.0	1.7	134.1	7.13
2.514	1.80	125.2	14.92	2.6	1.756	126.0	15.41	6.0	1.8	134.1	11.64
2.394	1.90	123.5	13.23	2.5	6.0	123.6	8.52	2.268	1.9	122.6	12.57
2.301	2.0	122.4	11.28	2.4	6.0	122.6	3.64	2.175	2.0	122.0	10.87
2.198	2.2	121.6	7.89	2.3	6.0	122.0	-0.54	2.155	2.2	121.3	7.68
2.140	2.4	120.9	4.82	2.2	6.0	121.3	-3.66	2.125	2.4	120.9	4.87
2.110	2.6	120.6	2.52	2.1	6.0	120.5	-5.29	2.103	2.6	120.6	2.54
2.095	2.8	120.4	0.63					2.090	2.8	120.3	0.63
2.085	3.0	120.3	-0.89					2.083	3.0	120.3	-0.89
2.073	3.5	120.2	-3.37					2.073	3.5	120.2	-3.37
2.068	4.0	120.2	-4.58					2.068	4.0	120.2	-4.58
2.068	5.0	120.2	-5.33					2.068	5.0	120.2	-5.33
2.068	6.0	120.2	-5.41	2.06	6.0	120.2	-5.40	2.068	6.0	120.2	-5.41
2.068	100.0	120.2	-5.37					2.068	100.0	120.2	-5.37

Table 2 gives the reaction path for reaction coordinate *R*, the reaction path for reaction coordinate *r*, and the minimum energy path. Let us first describe the 'minimum energy path', since this is the mathematical embodiment of what the chemist visualizes as the reaction pathway. Along the minimum energy path, all three variables *R*, *r* and  $\theta$  vary smoothly. On the reactants side, prior to *R* = 3.0, *R* is changing rapidly relative to the rather small changes in *r* and  $\theta$ . Around the saddle point, say between *R* = 3.0 and *r* = 2.0, all three geometrical parameters are changing significantly. Finally, from *r* = 2.0 to *r* = 100, small changes in *R* and  $\theta$  accompany large changes in *r*.

Inspection of table 2 makes it quite apparent that the choice of *R* as a reaction coordinate is appropriate for the reactant side of the minimum energy path, but not for the product side. The problem is that the value of *r* lurches from 1.756 to 6.0 as *R* changes from 2.6 to 2.5. As the minimum energy path shows, the 'correct value' of *r* for *R* = 2.5 is ~1.81 bohrs.

An opposite, but even more serious, breakdown occurs with respect to the choice of *r* as reaction coordinate. That is, on the product side (*r* > 2.0 bohrs), the reaction path obtained using *r* as reaction coordinate is quite similar to the minimum energy path. However, this reaction path also lurches,

between *r* = 1.9 and 1.8, and is inapplicable on the reactants side of the saddle point. Hence the saddle point position is not correctly predicted. In fact, inspection of table 2 would suggest that we have found a lower energy (~13 kcal barrier) route from  $CH_3 + H_2$  to  $CH_3 + H$ . The problem lies with the discontinuous change of *R* and  $\theta$  along this reaction path.

Recall that a point on the above reaction path is obtained, for a particular value of *r*, by minimizing the total energy with respect to *R* and  $\theta$ . Unfortunately, when *r* is in the range 1.6 - 1.9 bohrs, there are two distinct relative minima. The first occurs for *R* ≈ 2.3 bohrs,  $\theta$  ≈ 123° and the second for *R* ≈ 6.0 bohrs,  $\theta$  ≈ 134°. When *r* is greater than 1.84 bohrs, the first minima is the lower, but for *r* < 1.84, the second minima is lower. At *r* = 1.84 the two minima both have depth 13.59 kcal/mole, as illustrated in figure 3. Hence the reaction path based on *r* as reaction coordinate has a discontinuity at *r* = 1.84. This gives the mistaken impression that the barrier height is 13.59 kcal/mole. In fact, as figure 3 shows, a continuous reaction path between *r* = 1.841 and *r* = 1.839 would have to pass over a barrier of 18.50 kcal/mole.



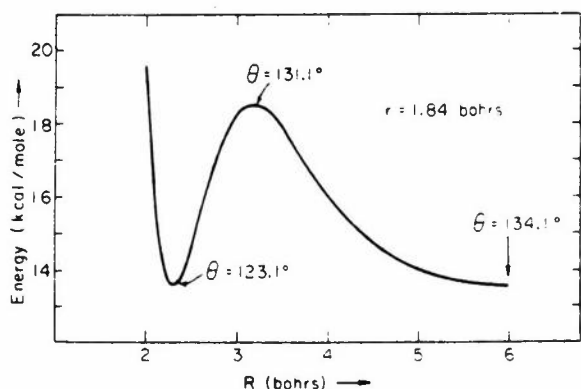


Figure 3: Illustration of the discontinuity of the reaction path obtained by choosing  $r$  as reaction coordinate. Each point on the curve corresponds to the value of  $R$  shown on the x-axis,  $r = 1.84$  bohrs, and the value of  $\theta$  for which the potential energy is minimised

If one must choose a reaction coordinate, a reasonable choice is  $(r - R)$ , which changes in a fairly smooth manner all along the minimum energy path. Although this conclusion is by no means unanticipated, the quantitative analysis made possible by table 2 seems to be of considerable value.

Finally, we must point out that there is no necessary relationship between the minimum energy path and the dynamics of a chemical reaction. That is, for any particular classical trajectory, the probability of following the minimum energy path is zero. Nevertheless, such a minimum energy path may be as close as one can come in a theoretical sense to the chemist's notion of a reaction mechanism. A reasonable alternative to this definition would be an 'average' or 'most probable' classical trajectory for the conditions of interest.

### Acknowledgements

We thank Professors Don Bunker and Roald Hoffmann for helpful discussions. This research was supported by the National Science Foundation, Grant GP - 31974.

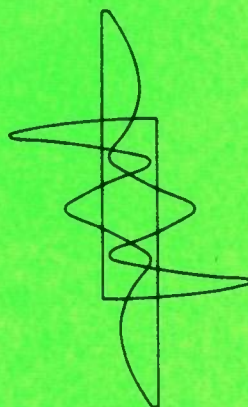
### References

- [1] FREY, H.M. (1964). *Prog. React. Kinet.*, **2**, 131.
- [2] Experimental references prior to 1971 are given by KIRMSE, W. (1971). *Carbene Chemistry*, New York: Academic Press.
- [3] MONTAGUE, D.C. and ROWLAND, F.S. (1971). *J. Am. Chem. Soc.*, **93**, 5381.  
\_\_\_\_\_ and \_\_\_\_\_ (1972). *Chem. Comm.*, 193.
- [4] ROTH, H.D. (1971). *J. Am. Chem. Soc.*, **93**, 1527, 4935.  
\_\_\_\_\_ (1972). *J. Am. Chem. Soc.*, **94**, 1400, 1761.

- [5] BELL, J.A. (1971). *J. Phys. Chem.*, **75**, 1537.
- [6] DEE, K., SETSER, D.W. and CLARK, W.G. (1971). *J. Phys. Chem.*, **75**, 2231, 2240.
- [7] BOLDT, P., THIELECKE, W. and LUTHE, H. (1971). *Chem. Ber.*, **104**, 353.
- [8] TAYLOR, G.W. and SIMONS, J.W. (1971). *Int. J. Chem. Kinet.*, **3**, 25.  
HASE, W.L. and SIMONS, J.W. (1971). *J. Organometal Chem.*, **32**, 47.  
\_\_\_\_\_ and \_\_\_\_\_ (1971). *J. Chem. Phys.*, **54**, 1277.  
HASE, W.L., PHILLIPS, R.J. and SIMONS, J.W. (1971). *Chem. Phys. Letters*, **12**, 161.  
HASE, W.L., JOHNSON, R.L. and SIMONS, J.W. (1972). *Int. J. Chem. Kinet.*, **4**, 1.  
GROWCOCK, F.B., HASE, W.L. and SIMONS, J.W. (1972). *J. Phys. Chem.*, **76**, 607.
- [9] MCNESBY, J.R. and KELLY, R.V. (1971). *Int. J. Chem. Kinet.*, **3**, 293.
- [10] REBBERT, R.E., LIAS, S.G. and AUSLOOS, P. (1971). *Chem. Phys. Letters*, **12**, 323.
- [11] HOFFMANN, R.W. (1971). *Agnew. Chem. Int. Ed. Engl.*, **10**, 529.
- [12] SEYFERTH, D. and HAAS, C. K. (1972). *J. Organometal Chem.*, **39**, C33.
- [13] CONLIN, R.T., GASPAR, P.P., LEVIN, R.H. and JONES, M. (1972). *J. Am. Chem. Soc.*, **94**, 7165.
- [14] POMERANTZ, M., ROSS, A.S. and GRUBER, G.W. (1972). *J. Am. Chem. Soc.*, **94**, 1403.
- [15] KISTIAKOWSKY, G. B. and SAUNDERS, B. B. (1973). *J. Phys. Chem.*, **77**, 427.
- [16] SKELL, P.S., VALENTY, S.J. and HUMER, P.W. (1973). *J. Am. Chem. Soc.*, **95**, 5041.
- [17] HOFFMANN, R. (1968). *J. Am. Chem. Soc.*, **90**, 1475.
- [18] KOLLMAR, H. (1970). *Tetrahedron Letters*, 3337.
- [19] HOFFMANN, R., GLETTTER, R. and MALLORY, F.B. (1970). *J. Am. Chem. Soc.*, **92**, 1460.
- [20] DOBSON, R.C., HAYES, D.M. and HOFFMANN, R. (1971). *J. Am. Chem. Soc.*, **93**, 6188.
- [21] BASCH, H. (1971). *J. Chem. Phys.*, **55**, 1700.
- [22] CARR, R.W. (1972). *J. Phys. Chem.*, **76**, 1581.
- [23] KOLLMAR, H. (1972). *Tetrahedron*, **28**, 5893.
- [24] FUJIMOTO, H., YAMABE, S. and FUJUI, K. (1972). *Bull. Chem. Soc. Japan*, **45**, 2424.
- [25] BODOR, N., DEWAR, M.J.S. and WASSON, J.S. (1972). *J. Am. Chem. Soc.*, **94**, 9095.
- [26] BODOR, N. and DEWAR, M.J.S. (1973). *J. Am. Chem. Soc.*, **94**, 9103.
- [27] HERSCHBACH, D.R., (personal communication).
- [28] BENSON, S.W. (1964). *Adv. Photochem.*, **2**, 1.  
MOORE, W.B. and BENSON, S.W. (1964). *Ibid.*, **2**, 219.
- [29] KIRKBRIDE, F.W. and NORRISH, R.G.W. (1933). *J. Chem. Soc.*, 119.
- [30] ROSENBLUM, C. (1938). *J. Am. Chem. Soc.*, **60**, 2819.  
\_\_\_\_\_ (1941). *J. Am. Chem. Soc.*, **63**, 3322.

- [31] BAWN, C. E. H. and MILSTEAD, J. (1939). *Trans. Faraday Soc.*, **35**, 889.
- [32] WIENER, H. and BURTON, M. (1953). *J. Am. Chem. Soc.*, **75**, 5815.
- [33] CHANMUGAN, J. and BURTON, M. (1956). *J. Am. Chem. Soc.*, **78**, 509.  
 \_\_\_\_\_ and \_\_\_\_\_ (1956). *Can. J. Chem.*, **34**, 1021.
- [34] GESSER, H. and STEACIE, E. W. R. (1956). *Can. J. Chem.*, **34**, 113.
- [35] HERZBERG, G. (1961). *Proc. Roy. Soc. (London)*, **A262**, 291.
- [36] BELL, J.A. and KISTIAKOWSKY, G.B. (1962). *J. Am. Chem. Soc.*, **84**, 3417.
- [37] BRAUN, W., BASS, A.M. and PILLING, M. (1970). *J. Chem. Phys.*, **52**, 5131.
- [38] JOHNSTON, H.S. and PARR, C. (1963). *J. Am. Chem. Soc.*, **85**, 2544.
- [39] BENDER, C.F. and SCHAEFER, H.F. (1970). *J. Am. Chem. Soc.*, **92**, 4984.
- [40] SCHAEFER, H. F. (1972). *The Electronic Structure of Atoms and Molecules: A Survey of Rigorous Quantum Mechanical Results*, Reading, Massachusetts: Addison-Wesley.
- [41] HUZINAGA, S. (1965). *J. Chem. Phys.*, **42**, 1293.
- [42] DUNNING, T.H. (1970). *J. Chem. Phys.*, **53**, 2823.
- [43] DAVIDSON, E.R. (1973). *Chem. Phys. Letters*, **21**, 565.
- [44] BUNGE, A. (1970). *J. Chem. Phys.*, **53**, 20.
- [45] McLEAN, A.D. and LIU, B. (1973). *J. Chem. Phys.*, **58**, 1066.
- [46] BENDER, C. F. and DAVIDSON, E. R. (1966). *J. Phys. Chem.*, **70**, 2675.
- [47] BENDER, C.F., PEARSON, P.K., O'NEIL, S.V. and SCHAEFER, H.F. (1972). *J. Chem. Phys.*, **56**, 4626.
- [48] BENDER, C.F., O'NEIL, S.V., PEARSON, P.K. and SCHAEFER, H.F. (1972). *Science*, **176**, 1412.
- [49] SCHAEFER, H.F. (1974). Status of *ab initio* molecular structure predictions, *Critical Evaluation of Chemical and Physical Structural Information*, Washington D.C.: National Academy of Sciences.
- [50] HOFFMANN, R., (personal communication).
- [51] BASKIN, C.P., BENDER, C.F., BAUSCHLICHER, C.W. and SCHAEFER, H.F. (1973). Lawrence Berkeley Laboratory Report No. LBL-2324, November.
- [52] McLAUGHLIN, D. R., BENDER, C. F. and SCHAEFER, H.F. (1972). *Theoret. Chim. Acta*, **25**, 352.
- [53] HERZBERG, G. and JOHNS, J. W. C. (1971). *J. Chem. Phys.*, **54**, 2276.  
 WASSERMANN, E., KUCK, V.J., HUTTON, R.S., ANDERSON, E.D. and YAGER, W.A. (1971). *J. Chem. Phys.*, **54**, 4120.
- [54] KOLOS, W. and WOLNIEWICZ, L. (1968). *J. Chem. Phys.*, **49**, 404.
- [55] HERZBERG, G. (1966). *Electronic Spectra of Polyatomic Molecules*, New York: Van Nostrand Reinold.
- [56] For a clear discussion, see McIVER, J.W. and KOMORNICKI, A. (1971). *Chem. Phys. Letters*, **10**, 303.  
 \_\_\_\_\_ and \_\_\_\_\_ (1972). *J. Am. Chem. Soc.*, **94**, 2625.
- [57] HAMMOND, G.S. (1955). *J. Am. Chem. Soc.*, **77**, 334.
- [58] KARPLUS, M. (1970). *Molecular Beams and Reaction Kinetics* (ed. C. Scylier), 378, New York: Academic Press.
- [59] TRUHLAR, D.G. (1972). *J. Am. Chem. Soc.*, **94**, 7584.
- [60] JOHNSTON, H.S. (1966). *Gas Phase Reaction Rate Theory*, New York: Ronald Press.
- [61] O'NEIL, S.V., SCHAEFER, H.F. and BENDER, C.F. (1974). *Proc. Natl. Acad. Sci. U.S.A.*, **71**, 104.
- [62] O'NEIL, S.V., PEARSON, P.K., SCHAEFER, H.F. and BENDER, C.F. (1973). *J. Chem. Phys.*, **58**, 1126.
- [63] EMPEDOCLES, P.B. (1960). *Int. J. Quantum Chem.*, **3S**, 47.
- [64] DEWAR, M.J.S. and KIRSCHNER, S. (1971). *J. Am. Chem. Soc.*, **93**, 4292.

# CORRELATED WAVEFUNCTIONS



# Computation of Correlation Energies of Closed Shell Systems. The Dimerization Energies of $BH_3$ and $LiH$

R. Ahlrichs\*

Results of rigorous computations employing extended Gaussian-type basis sets are reported for  $BH_3$ ,  $B_2H_6$ ,  $LiH$  and  $Li_2H_2$  in their respective equilibrium geometries. The dimerization energy of  $BH_3$  is calculated as  $-20.7$  kcal/mole within the Hartree-Fock approximation and as  $-36.6$  kcal/mole if electron correlation is included. The corresponding results for the dimerization of  $LiH$  are  $-47.3$  kcal/mole and  $-48.3$  kcal/mole. Partitioning of the correlation energy contributions allows the effect of electron correlation to be attributed to the increase of next neighbour bond interactions on the dimerization of  $BH_3$  and  $LiH$ . The difficulties of accurate computations of reaction energies are discussed in detail.

## Introduction

$B_2H_6$  is the simplest electron deficient compound known from experiment, whereas  $Li_2H_2$  may be considered as the simplest conceivable molecule of this class at all. Further small electron deficient compounds like  $Be_2H_4$  [1] and  $BeBH_5$  [2] have been investigated theoretically but are also not known experimentally, like  $Li_2H_2$ . Detailed investigations of the electron distribution [3] and the mechanism of binding in  $B_2H_6$  have been reported in the literature [4-8]. Of general interest for the understanding of the stability of electron deficient compounds is especially  $\Delta E_f$  of the reaction (1),



which is still rather uncertain. Experimental values between  $-25$  and  $-60$  kcal/mole are reported in the literature [9].

Hartree-Fock (HF) calculations with small Slater-type basis sets [10] or medium size Gaussian basis sets [8,11] yield  $\Delta E_f$  values of about  $-10$  kcal/mole, which is not in the most favourable range of experimental values. The effect of electron correlation on  $\Delta E_f$  was first investigated by Gélus, Ahlrichs, Staemmler and Kutzelnigg (GASK) [11] by means of the IEPA-PNO method [12] (IEPA = independent electron pair approximation, PNO = pair natural orbitals). Using a Gaussian basis of double zeta quality (5 *s*-, 2 *p*-groups on boron and 2 *s*-groups on hydrogen), GASK obtained a HF contribution of  $-8.5$  kcal/mole and a correlation energy contribution of  $-16.8$  kcal/mole to  $\Delta E_f$  (a *p*-set on hydrogen was

added for the computation of the correlation energy). The corresponding estimated exact values were  $-11.5$  and  $-25.2$  kcal/mole respectively, yielding a total  $\Delta E_f$  of  $-36$  kcal/mole.

The most accurate HF computations for  $BH_3$  and  $B_2H_6$  have been reported recently by Lipscomb and coworkers [3,13], who obtained a HF contribution of  $-19.0$  kcal/mole to  $\Delta E_f$ . It is then suggested [13], that GASK's estimate for the correlation contribution to  $\Delta E_f$  might be too large, since addition of the calculated value ( $-15.8$  kcal/mole) to the HF value of  $-19.0$  kcal/mole would give  $\Delta E_f = -35.8$  kcal/mole, which is close to a recent kinetic value [14] for  $\Delta E_f$ .

Kollman, Bender and Rothenberg (KBR) [15] have published the only theoretical investigation of  $Li_2H_2$ . They predict  $Li_2H_2$  to be most stable on the centrosymmetric  $D_{2h}$  structure. KBR [15] reported the following  $\Delta E_f$  values for the reaction (2)



HF approximation:  $\Delta E_f = -46.2$  kcal/mole  
including electron correlation:  $\Delta E_f = -45.8$  kcal/mole.

These authors thus predict the correlation energy in  $2 LiH$  to be larger than in  $Li_2H_2$ , in contrast to the result obtained by GASK [11] for  $B_2H_6$ . Unfortunately, KBR used a rather inappropriate basis set which recovered only about 50% of the total valence shell correlation energy. In consideration of this state of affairs it appeared worthwhile to repeat the computation of  $\Delta E_f$  for the reactions (1) and (2) with more extended basis sets than those used previously (by GASK [11] and KBR [15]) and employing

\* Institut für Physikalische Chemie und Elektrochemie, Universität Karlsruhe, Kaiserstrasse 12, 75 Karlsruhe, West Germany

a more refined method for the computation of correlation energies.

## Method

We used the HF approximation as starting point for the treatment of electron correlation. The difficulty in computing correlation energies by means of a conventional configuration interaction (CI) calculation is the large number of configurations that can be constructed and the slow convergence of the CI expansion. The present  $B_2H_6$  basis of 68 groups leads e.g. to 184,000 doubly substituted determinants (from the valence shell), which corresponds to 65,000 pure singlet functions or 9,000 spin and symmetry adapted configurations. The largest possible reduction of the number of doubly substituted configurations to be included in a CI is obtained if the latter is based on the so-called PNO's, which may be defined for arbitrary wavefunctions  $\Psi$  in the following way. Let us denote a spin irreducible pair [16] of occupied MO's and  $\Phi_u$  the part of  $\Psi$  in which all the double substitutions from the pair  $u$  are collected (in an obvious notation)

$$\Phi_u = \Phi_{\text{HF}} + \sum_{ij} c_{ij}^u \Phi_{ij}^u. \quad (3a)$$

(Throughout this paper we neglect singly substituted configurations). The PNO's  $\chi_u^i$  are then defined as the natural orbitals of  $\Phi_u$ . Let now  $\Phi_u^i$  denote the doubly substituted configuration with the replacement  $u \rightarrow \chi_u^i \chi_u^i$  if  $u$  is a singlet pair, or  $u \rightarrow \chi_u^i \chi_u^{i'}$  if  $u$  is a triplet pair, for the details the reader is referred to reference [11]. In terms of the  $\Phi_u^i$  one then has

$$\Phi_u = \Phi_{\text{HF}} + \sum_i c_u^i \Phi_u^i, \quad (3b)$$

i.e. the nondiagonal replacements  $\Phi_{ij}^u$  now have vanishing CI coefficients. The  $c_u^i$  and the energy contributions due to the  $\Phi_u^i$  furthermore form a rapidly decreasing series and it is usually sufficient to include 10-30 terms in equation (3b) to exhaust the basis set. Our final  $B_2H_6$  computation included 124 doubles only.

The disadvantage connected with the use of PNO's is their partial nonorthogonality

$$(\chi_u^i / \chi_v^j) \neq 0, \text{ if } u \neq v \quad (4)$$

whereas, of course,

$$(\chi_u^i / \chi_u^j) = \delta_{ij}. \quad (5)$$

The relationship (4) fortunately leads to minor complications only in the evaluation of matrix elements between arbitrary doubly substituted configurations.

Various methods have been proposed to obtain accurate approximations of the correct PNO's prior to the knowledge of the total wavefunction [17]. In the present study we have used a new method for this purpose [18] which is more accurate and less computer time consuming than the one used previously in our program [12,19].

The total correlation energy  $\mathcal{E}$  is obtained in three different degrees of approximation, which will now be discussed. For this purpose it is convenient to use a combined label  $a = (u, i)$ , i.e. we simply write  $\Phi_a$  for  $\Phi_u^i$ , etc. A partial summation  $\sum_{a \in u}$  is then understood to run over the HF term and all  $a = (u, i)$  for the given  $u$ . The CI coefficients  $c_a$  (with  $c_{\text{HF}} = 1$ ) and the pair correlation energies  $\mathcal{E}_u$  are within the IEPA obtained as solutions of the following set of equations, where  $H_{ab} = (\Phi_a | H | \Phi_b)$ ,

$$\sum_{b \in u} H_{ab} c_b = (E_{\text{HF}} + \mathcal{E}_u^{\text{IEPA}}) c_a, \quad a \in u. \quad (6)$$

The total correlation energy is then within this approximation given as

$$\mathcal{E}^{\text{IEPA}} = \sum_u \mathcal{E}_u^{\text{IEPA}}. \quad (7)$$

Next we perform a CI with  $\Phi_{\text{HF}}$  and all doubly substituted configurations, for which Meyer has suggested the name PNO-CI [20]:

$$\sum_b H_{ab} c_b = (E_{\text{HF}} + \mathcal{E}^{\text{PNO-CI}}) c_a. \quad (8)$$

The PNO-CI correlation energy  $\mathcal{E}^{\text{PNO-CI}}$  can, of course, also be divided into pair distributions such that equation (9) holds [20]

$$\mathcal{E}^{\text{PNO-CI}} = \sum_u \mathcal{E}_u^{\text{PNO-CI}}. \quad (9)$$

We finally perform a computation within the coupled electron pair approximation (CEPA), first proposed by Meyer [20]

$$\sum_b H_{ab} c_b = (E_{\text{HF}} + \mathcal{E}^{\text{CEPA}}) c_a, \quad a \in u, \quad (10)$$

$$\mathcal{E}^{\text{CEPA}} = \sum_u \mathcal{E}_u^{\text{CEPA}}.$$

As the just listed methods to obtain approximations to the true correlation energy have already been described in the literature [21], we shall not discuss them in detail here. A few comments, however, will be helpful for the discussion of the results presented in this paper.

(a) The PNO-CI is a variational calculation, whereas the IEPA and the CEPA are not.

(b) The PNO-CI wavefunction and correlation energy has an incorrect dependence on the number of

electrons [22]. This may e.g. be demonstrated by a consideration of a system of  $n$  noninteracting electron pairs, like  $He_n$  at sufficiently large internuclear distances. The exact wavefunction for this system is simply the antisymmetrized product of the corresponding helium wavefunctions, and it is easily verified that the PNO-CI wavefunction has vanishing overlap with the exact wavefunction in the limit  $n \rightarrow \infty$ . It can further be shown that  $\mathcal{E}^{\text{PNOCI}}$  increases only like  $\sqrt{n}$  for large  $n$ . These deficiencies of the PNO-CI are due to the fact that higher than doubly substituted terms are neglected in this treatment.

(c) The quadruple and higher substitutions are accounted for in an approximate way within the IEPA. This method thus yields, for the case under consideration, the correct  $n$ -dependence:  $\mathcal{E}^{\text{IEPA}}(He_n) = n\mathcal{E}^{\text{IEPA}}(He)$ , provided the IEPA-treatment starts from localized MO's. This difference between the IEPA and the PNO-CI is reflected in the corresponding equations (6) and (8) by the occurrence of  $\mathcal{E}_u^{\text{IEPA}}$  instead of the total correlation energy  $\mathcal{E}^{\text{PNOCI}}$ . The main drawback of the IEPA is the neglect of matrix elements  $H_{ab}$  for  $a \in u, b \in v$ , with  $u \neq v$ , which account for the interaction of the correlation functions of different electron pairs  $u$  and  $v$ .

(d) Inclusion of these matrix elements in the IEPA, equation (6), leads to the CEPA as given in equation (10). This method thus avoids the main shortcomings of the IEPA—neglect of certain matrix elements—and also those of the PNO-CI, since quadrupole and higher substitutions are accounted for in an approximate way. One can also say that the IEPA treats each electron pair in the field of the HF-MO's of the remaining electrons, whereas the CEPA considers each pair in the field of the correlated remaining electrons. Applications of the CEPA show in fact that this method yields more accurate potential curves, force constants etc. than the PNO-CI or the IEPA [20,23].

### Basis Set Considerations

As basis set we used linear combinations of Gaussian lobe functions. The construction of  $d$ - and  $f$ -type functions was performed as described in reference [25]. We started from a Huzinaga [26]  $9s, 5p$  basis for boron, contracted (5,1,1,1,1) and (3,1,1) basis for hydrogen. A set of polarization functions, i.e. a complete  $d$ -set on boron ( $\eta = 0.5$ ) and a  $p$ -set on hydrogen ( $\eta = 0.5$ ), was then added. The orbital exponents  $\eta$  of the polarization functions were determined in optimizing the HF valence shell correlation energy of  $BH_3$ . In order to save computer time it was then investigated whether it is possible to reduce this basis without sacrificing accuracy. It turns out, in fact, that leaving out the boron  $p$ -function with the smallest orbital exponent ( $\eta = 0.070$ ) affects the total  $BH_3$  energy by 0.4 kcal/mole only, whereas the change of  $\Delta E_f$ , equation (1) in the HF approximation is 0.2 kcal/mole.

In order to get an idea of how saturated the present basis set is we make the following remarks. Increasing the  $s$ -basis on boron and hydrogen gives essentially a better description of the nuclear cusp which should not effect  $\Delta E_f$  of reaction (1) or (2). The HF energy of boron obtained with a  $9s, 5p$  basis is anyway only 1.5 kcal/mole higher than the HF limit. Addition of further polarization functions, an  $f$ -set and a second  $d$ -set for boron and a  $d$ -set and a second  $p$ -set for the hydrogen atoms, lowers the HF energy of  $BH_3$  by 1 kcal/mole and the valence shell correlation energy by 9 kcal/mole. The net effect of these additional basis functions on  $\Delta E_f$  is thus expected to be of the order of about 3 kcal/mole. Addition of a second  $p$ -set at the bridge hydrogen atoms lowers the HF energy of  $B_2H_6$  by 0.05 kcal/mole only.

As far as  $LiH$  and  $Li_2H_2$  are concerned, it is no problem to choose the basis large enough to guarantee an accuracy of about 1 kcal/mole for  $\Delta E_f$ . We started with a Huzinaga  $9s$  (5,1,1,1,1) basis for lithium and a  $5s$  (3,1,1) set for hydrogen and then added a set of two  $p$ -functions ( $\eta = 0.14$  and  $0.56$  for  $Li$  and  $\eta = 0.22$  and  $0.66$  for  $H$ ) on either atom, hereafter referred to as basis set I. The orbital exponents  $\eta$  of the  $p$ -sets were determined in minimizing the HF plus valence shell correlation energy of  $LiH$ . KBR [15] used a Huzinaga  $2p$  set (contracted to one group) at the hydrogen atom, which is not suited for molecular computations since it is an approximation of the spectroscopic hydrogen  $2p$ -orbital. The latter has e.g. Bohr-radius of about 4 au whereas the optimized  $p$ -functions, see above, have radii of about 2 au and 1 au. Quite the same comments could be made with respect to the lithium  $p$ -set used by KBR. For these reasons KBR get only 64% of the  $LiH$  valence shell correlation energy as obtained with basis set I. In the final computations, reported in table 3, we added a rather spread out  $s$ -function on hydrogen ( $\eta = 0.03$ ) and a  $d$ -set on  $Li$  ( $\eta = 0.3$ ) and on  $H$  ( $\eta = 0.45$ ), basis set II, which has practically no effect on  $\Delta E_f$  of reaction (2), however (less than 0.14 kcal/mole).

### Discussion of results

$B_2H_6$ : In the present computations we included all  $\Phi_a$  which contribute more than  $10^{-5}$  au to  $\mathcal{E}^{\text{IEPA}}$ , the total number of which is 124 only (counting those that are equivalent on symmetry grounds only once). The energy contributions of the neglected  $\Phi_a$  amounts to  $2 \cdot 10^{-4}$  au in  $BH_3$  and to about  $6 \cdot 10^{-4}$  au in  $B_2H_6$ .

From the results collected in table 1 we get the following values of  $\Delta E_f$  of reaction (1)

$$\text{HF} \quad : \quad \Delta E_f = -20.7 \text{ kcal/mole} \quad (12)$$

$$\text{IEPA} \quad : \quad \Delta E_f = -44.3 \text{ kcal/mole} \quad (13)$$

$$\text{PNO-CI} : \Delta E_f = E^{\text{PNOCI}}(B_2H_6) - 2E^{\text{PNOCI}}(BH_3) \\ = -27.4 \text{ kcal/mole} \quad (14)$$

$$\text{PNO-CI}^* : \Delta E_f = E^{\text{PNOCI}}(B_2H_6) - E^{\text{PNOCI}}(2BH_3) \\ = -34.2 \text{ kcal/mole} \quad (15)$$

$$\text{CEPA} : \Delta E_f = -36.6 \text{ kcal/mole} \quad (16)$$

Our HF result is in good agreement with the recent work of Lipscomb and coworkers [3,13], who obtained  $-19$  kcal/mole. The present HF energies for  $BH_3$  and  $B_2H_6$  are slightly poorer than those of Lipscombe and coworkers, see table 1. This is certainly due to the fact that these authors used a Slater-type basis which gives a better description of the nuclear cusps than a Gaussian basis. Since our basis set appears to be rather saturated for  $BH_3$  as far as flexibility in the bond region is concerned (we have noted above that addition of further polarization functions lowers  $E_{\text{HF}}$  of  $BH_3$  by 1 kcal/mole only) we rather consider our computed  $\Delta E_f$ , see equation (12), as an upper bound to the HF limit. The basis of Lipscomb *et al.* contained two  $s$ -type AO's on hydrogen which were optimized for the  $BH$  molecular fragment [3]. This basis set may be expected to describe terminal bonds better than bridge bonds which would result in a somewhat too small  $\Delta E_f$ . The present basis is more flexible in this

respect since it contains three  $s$ -type AO's on either  $H$ . The difference between terminal and bridge bonded hydrogen atoms may be seen from the coefficients of the hydrogen  $s$ -AO's in the localized MO's, which are (0.191, 0.302, 0.197) for a terminal and (0.187, 0.348, 0.147) for a bridge bond.

The IEPA gives a correlation contribution of  $-23.5$  kcal/mole to  $\Delta E_f$ , see equation (13). Due to the approximation inherent in the IEPA, as explained above, this method is not expected to yield accurate reaction energies.

In equations (14) and (15) we have given the  $\Delta E_f$  values as obtained from the PNO-CI computations. The first one, equation (14), may be called the naive PNO-CI, since we have simply compared  $E^{\text{PNOCI}}(B_2H_6)$  with  $2E^{\text{PNOCI}}(BH_3)$ . This procedure is unsatisfactory since the quality of the PNO-CI depends on the number of electrons involved. This is clearly shown by a comparison of the PNO-CI correlation energies obtained for  $BH_3$  and  $BH_3BH_3$  at large intermolecular distance (50 au), see table 1.

$$\epsilon^{\text{PNOCI}}(BH_3BH_3) = 0.2174 \text{ au} < 0.2282 \text{ au} \\ = 2 \epsilon^{\text{PNOCI}}(BH_3) \quad (17)$$

In order to obtain the equality sign in equation (17),

Table 1: Computed HF and correlation energies of  $BH_3$  and  $B_2H_6$  <sup>a</sup>

	$-E_{\text{HF}}^b$	pair <sup>c</sup>	Valence Shell Correlation Energies		
			IEPA <sup>d</sup>	PNO-CI	CEPA
$BH_3$ <sup>e</sup>	26.39697 (26.4014)	$tt$ (3x)	0.03167 (0.02805)	0.02959	0.03085
		$tt'$ (3x)	0.01128 (0.00796)	0.00844	0.00889
		total	0.12887 (0.10804)	0.11410	0.11921
$BH_3BH_3$ <sup>f</sup>	52.79394	$tt$ (6x)	0.03167	0.02816	0.03085
		$tt'$ (6x)	0.01128	0.00807	0.00889
		total	0.25774	0.21739	0.23843
$B_2H_6$ <sup>g</sup>	52.82699 (53.8331)	$tt$ (4x)	0.03127 (0.02779)	0.02749	0.03034
		$bb$ (2x)	0.03040 (0.02796)	0.02641	0.02915
		$tt'$ (2x)	0.01113 (0.00778)	0.00786	0.00871
		$tb$ (8x)	0.00859 (0.00608)	0.00597	0.00631
		$bb'$ (1x)	0.01443 (0.01154)	0.01020	0.01124
		$tt''$ cis (2x)	0.00100 -	0.00062	0.00070
		$tt''$ trans (2x)	0.00099 -	0.00059	0.00065
total	0.29525 (0.24284)	0.23888	0.26377		

(a) in au

(b) results of Lipscomb and coworkers [3,13] are given in parentheses

(c)  $t$  and  $b$  denote terminal bridge bonds respectively.  $tt'$  denotes a pair of adjacent bonds,  $tt''$  a pair of terminal  $BH$  bonds at different boron atoms

(d) results of GASK [11] are given in parentheses

(e)  $B-H$  distance = 2.25 au, which is the equilibrium distance obtained within the CEPA

(f)  $B-B$  distance was 50 au, each  $BH_3$  in its equilibrium geometry, see (e)

(g) experimental geometry as given in [29]

it would be necessary to include all quadruples which arise from simultaneous double substitutions on either  $BH_3$  in the  $BH_3BH_3$  computation. In the modified PNO-CI, see equation (15), we have compared  $E^{\text{PNO-CI}}(B_2H_6)$  with  $E^{\text{PNO-CI}}(BH_3BH_3)$ , the PNO-CI energy obtained for the system of two separated  $BH_3$  molecules. We have thus consistently neglected the contributions of higher than doubly substituted configurations for  $B_2H_6$  and for 2  $BH_3$ , which certainly gives a more realistic  $\Delta E_f$  than the naive PNO-CI, see equation (14).

This procedure is still not too satisfactory. On the formation of  $B_2H_6$  from 2  $BH_3$  we find significant changes of the pair correlation energies. The intermolecular terms (which give essentially the van der Waals interaction) vanish for two separated  $BH_3$  molecules, whereas the corresponding interpair contributions are by no means negligible for  $B_2H_6$ . These changes are, of course, accompanied by changes of the contributions of quadruples and higher terms to the wavefunction and the total correlation energy. As the number of non negligible interpair terms is larger in  $B_2H_6$ , which has 11 next neighbour bond interactions compared to 6 in 2  $BH_3$ , one expects a larger contribution of quadruples etc. in  $B_2H_6$ . The CEPA accounts for the higher substituted configurations in a consistent although approximate way. (This is e.g. shown by the fact that  $E^{\text{CEPA}}(BH_3BH_3) = 2 E^{\text{CEPA}}(BH_3)$ , see table 1). This explains why the CEPA realistically predicts a larger correlation contribution to  $\Delta E_f$  (-15.9 kcal/mole) than the modified PNO-CI (-13.5 kcal/mole, see equation (15)). We thus consider the CEPA result for  $\Delta E_f$ , equation (16), to be more reliable than those given in equations (12)-(15). If one prefers for some reason to compare variational computations only, the modified PNO-CI, equation (15), is certainly more accurate than (12) or (14).

Let us briefly compare the present results with those of GASK [11]. In the latter treatment we underestimated the HF contribution to  $\Delta E_f$  and also underestimated the corrections to the IEPA contributions which are due to the interaction of correlation functions of different pairs, as was discussed above. The estimated IEPA limit (-25 kcal/mole as compared to -23 kcal/mole obtained now) was not too bad, however, but the IEPA is not accurate enough to predict reaction energies with an accuracy of a few kcal/mole. The present study confirms at least qualitatively the conclusion of GASK that the increase of next neighbour bond interactions on the formation of  $B_2H_6$  results in a considerable contribution to  $\Delta E_f$ , whereas the changes in intrabond correlation energies are almost negligible (2.5 kcal/mole, see table 1). We finally note that even the non neighbour terms, denoted  $tt''$  in table 1, contribute about -1.7 kcal/mole to  $\Delta E_f$  within the CEPA.

$Li_2H_2$ : We first redetermined the geometry of  $Li_2H_2$  in the bridge bonded  $D_{2h}$  symmetry. From the CEPA

results collected in table 2, we obtain the following equilibrium distances

$$d(Li - Li) = 4.28 \text{ au} \quad (18)$$

$$d(H - H) = 5.06 \text{ au} \quad (19)$$

The latter differ slightly from those found by KBR [15] who obtained 4.46 au and 5.16 au. Additional computations for other geometries confirmed the result of KBR that  $Li_2H_2$  has  $D_{2h}$  equilibrium geometry.

Table 2: Potential surface for  $Li_2H_2$  in  $D_{2h}$  geometry <sup>a</sup>

Distance		$-E_{\text{HF}}$	$-E_{\text{IEPA}}$	$-E_{\text{PNO-CI}}$	$-E_{\text{CEPA}}$
<i>Li-Li</i>	<i>H-H</i>				
4.66	5.16	16.04282	16.11241	16.10958	16.11150
4.46	5.16	16.04474	16.11420	16.11141	16.11330
4.26	5.16	16.04607	16.11555	16.11273	16.11462
4.06	5.16	16.04424	16.11350	16.11077	16.11260
4.46	4.96	16.04450	16.11428	16.11141	16.11329
4.46	5.36	16.04398	16.11320	16.11047	16.11236

(a) all quantities in au. Basis set I was used.

Table 3: Computed HF and correlation energies of  $LiH$  and  $Li_2H_2$  <sup>a</sup>

	$-E_{\text{HF}}$	Valence Shell Correlation Energies pair			
		IEPA	PNO-CI	CEPA	
$LiH$ <sup>b</sup>	7.98593 <sup>c</sup> (7.98262)	$tt$ (1x)	0.03523	0.03523	0.03523 (0.02204)
$2LiH$ <sup>d</sup>	15.97185	$tt$ (2x)	0.03523	0.03422	0.03523
		total	0.07047	0.06845	0.07047
$Li_2H_2$ <sup>e</sup>	16.04680 (16.03894)	$bb$ (2x)	0.03449	0.03343	0.03432
		$bb'$ (1x)	0.00464	0.00364	0.00387
		total	0.07361	0.07049	0.07251 (0.04247)

(a) See footnotes of table 1. Basis set II was used. The results reported by KBR [15] are given in parentheses.

(b)  $Li-H$  distance = 3.038 au, which is the equilibrium distance obtained with basis set I.

(c) HF limit:  $E_{\text{HF}} = -7.9867$  au [30]

(d)  $Li-Li$  distance 100 au

(e) Geometry  $D_{2h}$ ,  $Li-Li = 4.28$  au,  $H-H = 5.06$  au, see text



From the final computations reported in table 3 we get the following values for  $\Delta E_f$  of reaction (2), see also equations (12)-(16),

$$\text{HF} \quad : \quad \Delta E_f = -47.3 \text{ kcal/mole} \quad (20)$$

$$\text{IEPA} \quad : \quad \Delta E_f = -49.1 \text{ kcal/mole} \quad (21)$$

$$\text{PNO-CI} \quad : \quad \Delta E_f = -47.0 \text{ kcal/mole} \quad (22)$$

$$\text{PNO-CI}^* \quad : \quad \Delta E_f = -48.3 \text{ kcal/mole} \quad (24)$$

$$\text{CEPA} \quad : \quad \Delta E_f = -48.3 \text{ kcal/mole} \quad (24)$$

A comparison of equations (23) or (24) with (20) shows that electron correlation increases  $\Delta E_f$  by 1 kcal/mole in contrast to the conclusions of KBR [15]. The effect of electron correlations is much smaller than in reaction (1), however. This is due to two reasons,

- (a) in the  $\text{LiH}$  dimer one has just one additional next neighbour bond interaction whereas one has 5 in  $\text{B}_2\text{H}_6$ ;
- (b) due to the rather large  $\text{H-H}$  distance in  $\text{Li}_2\text{H}_2$ , see equation (19), the corresponding interpair correlation energy (0.00387, see table 3) is much smaller than the corresponding term in the  $\text{BH}_3$  dimer (0.01124, see table 1).

## Conclusions

The results reported in the present study demonstrate the importance of electron correlation for the computation of reaction energies even for reactions in which closed shell molecules react and the number of electron pairs remains unchanged. We thus confirm at least qualitatively the conclusion of GASK [11]. The reactions (1) and (2) may be considered as extreme cases since we find a considerable correlation contribution to  $\Delta E_f$  for (1) (-16 kcal/mole), whereas it is rather small for (2) (-1 kcal/mole). This is mainly due to the greater increase of next neighbour bond interactions on the formation of  $\text{B}_2\text{H}_6$  as compared to  $\text{Li}_2\text{H}_2$ .

The author further believes that the present computations are sufficiently accurate to confirm definitely a recent experimental value [13,14] for  $\Delta E_f$  of reaction (1), -34.8 kcal/mole, in contrast to the conclusions of Edmiston and Linder who suggested a  $\Delta E_f$  of -60 kcal/mole [8].

## Programs and Computation Times

The evaluation and further processing of two-electron integrals - which altogether makes up for more than 90% of the total computer time - has been described in a recent paper [27]. Details of the PNO-CI and CEPA parts of the program will be

described elsewhere [28]. The computations were performed in double precision arithmetic with a 65 K-36 bit word program version. The UNIVAC-1108 CPU times for the  $\text{B}_2\text{H}_6$  computation (68 groups) are as follows: integrals: 1.5 h; HF: 20' (12 iterations, starting from a zero density matrix.  $E_{\text{HF}}$  converged to  $10^{-8}$  au), determination of PNO's: 22', matrix elements  $H_{ab}$ : 3.7 h (most of which is required for the case that  $a$  and  $b$  corresponds to the same pair), solution of PNO-CI and CEPA equations, see (8)-(11): 2', total 5.9 h. The corresponding times for the final  $\text{Li}_2\text{H}_2$  calculation (62 groups) are: integrals: 55', HF: 9'; PNO's: 4'; matrix elements  $H_{ab}$ : 30'; PNO-CI and CEPA: 7'', total 100'.

## Acknowledgements

This study would not have been possible without the fruitful cooperation with Mr. F. Driessler, Dr. H. Lischka and Dr. V. Staemmler in developing the present program. The computations were performed at the 'Rechenzentrum der Universität Karlsruhe'. The assistance of the staff of the computation centre is gratefully acknowledged.

## References

- [1] AHLRICHS, R. (1970). *Theoret. Chim. Acta*, **17**, 348.
- [2] ————— (1973). *Chem. Phys. Letters*, **19**, 174.
- [3] LAWS, E., STEVENS, R.M. and LIPSCOMB, W.N. (1972). *J. Am. Chem. Soc.*, **94**, 4461.
- [4] BURNELLE, L. and KAUFMAN, J.J. (1965). *J. Chem. Phys.*, **43**, 3450.
- [5] BUENKER, R.J., PEYERIMHOFF, S.D., ALLEN, L.C. and WHITTEN, J.L. (1966). *J. Chem. Phys.*, **45**, 2825.
- [6] DUKE, B.J. and LINNETT, J.W. (1966). *Trans. Faraday Soc.*, **62**, 2955.
- [7] SWITKES, E., STEVENS, R.M., LIPSCOMB, W.N. and NEWTON, M.D. (1969). *J. Chem. Phys.*, **51**, 2085.
- [8] EDMISTON, C. and LINDER, P. (1973). *Int. J. Quantum Chem.*, **7**, 309.
- [9] See GANGULIN, P.S. and MCGEE, H.A. (1969). *J. Chem. Phys.*, **50**, 4658 (and references therein).
- [10] PALKE, W.E. and LIPSCOMB, W.N. (1966). *J. Am. Chem. Soc.*, **88**, 2384.
- [11] GELUS, M., AHLRICHS, R., STAEMMLER, V. and KUTZELNIGG, W. (1970). *Chem. Phys. Letters*, **7**, 503.
- [12] JUNGEN, M. and AHLRICHS, R. (1970). *Theoret. Chim. Acta*, **17**, 339.
- [13] HALL, J.H., MARYNICK, D.S. and LIPSCOMB, W.N. (1972). *Inorg. Chem.*, **11**, 3126.

- [14] MAPPES, G.W., FRIEDMAN, S.A. and FEHLNER, T.P. (1970). *J. Phys. Chem.*, **74**, 3307. See also [3].
- [15] KOLLMAN, P., BENDER, C.F. and ROTHENBERG, S. (1972). *J. Am. Chem. Soc.*, **94**, 8016.
- [16] VIERS, J.W., HARRIS, F.E. and SHAEFER, H.F. (1970). *Phys. Rev.*, **A1**, 24.  
For a recent discussion see also SHAEFER, H.F. (1972). *The Electronic Structure of Atoms and Molecules*, 134-139, Reading, Massachusetts: Addison-Wesley.
- [17] For a recent review see, for example, DAVIDSON, E.R. (1972). *Adv. Quantum. Chem.*, **6**, 201.
- [18] AHLRICHS, R. and DRIESSLER, F. *Theoret. Chim. Acta*, (in the press).
- [19] KUTZELNIGG, W. (1963). *Theoret. Chim. Acta*, **1**, 327.
- [20] MEYER, W. (1973). *J. Chem. Phys.*, **58**, 1017.
- [21] See, for example, [20] (and references therein).
- [22] See, for example, PRIMAS, H. (1965). *Modern Quantum Chemistry* (ed. O. Sinanoglu), **2**, 45-74, New York: Academic Press.
- [23] MEYER, W., (private communication). AHLRICHS, R., KUTZELNIGG, W., LISCHKA, H. and STAEMMLER, V., (to be published).
- [24] FOSTER, J.M. and BOYS, S.F. (1960). *Revs. Modern Phys.*, **32**, 303.
- [25] DRIESSLER, F. and AHLRICHS, R. (1973). *Chem. Phys. Letters*, **23**, 571.
- [26] HUZINAGA, S. (1965). *J. Chem. Phys.*, **42**, 1293.
- [27] AHLRICHS, R. (1974). *Theoret. Chim. Acta*, **35**, 157.
- [28] AHLRICHS, R., KUTZELNIGG, W., LISCHKA, H. and STAEMMLER, V. *J. Chem. Phys.*, (in the press).
- [29] BARTELL, L.S. and CARROL, B.L. (1965). *J. Chem. Phys.*, **42**, 1135.
- [30] CADE, P.E. and HUO, W.M. (1966). *J. Chem. Phys.*, **44**, 1849.

# Quantum Chemistry and Dynamics: Connections with Experiment

A.C.Wahl\*

The state of the art in computing by *a priori* methods will be discussed. Accurate and chemically useful interaction potentials will be assessed through the use of contemporary calculations on a number of small systems, including *OH*, *ArH*, *LiH<sub>2</sub>* and *NO<sub>2</sub>*. This assessment will be followed by a discussion of the effectiveness of these potential curves and surfaces in the prediction of dynamical behaviour which can then be compared with experiment. The results of specific recent scattering calculations using *ab initio* potentials will be used in example.

## Introduction

The purpose of this brief summary is to outline the 'state of the art' in the calculation of energy curves, surfaces and properties for small molecules and to provide a catalogue of work on such systems performed in our laboratory. This will be followed by a discussion of two recent examples in which *ab initio* potential curves and surfaces have been used to predict dynamical behaviour, and in one case aid experiment in arriving at a 'correct' potential.

Over the past five years an understanding of how to computationally handle the electron correlation problem as a function of changing supermolecular geometry has permitted the evaluation of potential energy curves and surfaces to what is now accepted as chemical accuracy ( $\sim 1$  eV) [1,2].

Several methods are now routinely yielding such results. These methods are straight configuration interaction [3], the first order method (selected configurations combined with the iterative natural orbital technique) [4], the MCSCF technique [5], and the separated electron pair approach [6]. The first three methods, except for the smallest systems, utilize some prescription of configuration selection which results primarily in removing the asymptotic difficulties of the MO model and in evaluating only the *extra* molecular correlation energy.

## Binding Energies and Properties for Diatomic Molecules

The method which we have been developing in our laboratory is the multiconfiguration self consistent field method [5] coupled with a prescription for selecting important molecular configurations (named

optimized valence configurations (OVC)). Over the past several years the application of this scheme to diatomic molecules has been routinely yielding potential curves accurate to approximately .1 eV. Typical recent results obtained by this method are given in table 1. One of the early questions about the configuration selection method (OVC) which we employed was whether or not it would yield accurate results of properties other than the energy. It does indeed seem to yield reliable one electron properties as indicated in table 2 for a number of diatomic molecules.

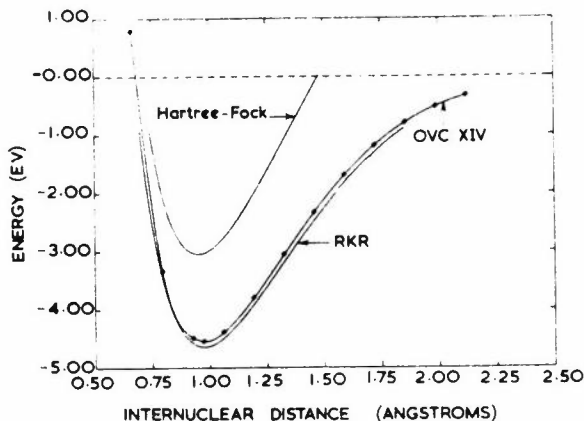


Figure 1: A comparison of theoretical and experimental curves for the potential energy of *OH*. The theoretical values were obtained from a 14 configuration OVC-MCSCF calculation. The experimental potential curve is from a RKR analysis of spectroscopic vibrational data (D. L. Albritton, private communication). The experimental curve lies below the theoretical curve by about 0.1 eV at all points. The shapes of the two curves are the same to about  $\pm 200$  cm<sup>-1</sup>.

\* Chemistry Division, Argonne National Laboratory, 9700 South Cass Avenue, Argonne, Illinois 60439, USA

Table 1: Typical MCSCT results for diatomic molecules utilizing optimized valence configuration selection rules

System	$R_e(\text{bohr})$		$\omega_e(\text{cm}^{-1})$		$D_e(\text{eV})$	
	OVC	Experiment	OVC	Experiment	OVC	Experiment
$H_2$ ( $X^1\Sigma$ ) <sup>b</sup>	1.40	1.40	4398	4400	4.63	4.75
$NaLi$ ( $X^1\Sigma$ ) <sup>c</sup>	5.48	5.45	248.5	251	0.85	unknown
$Li_2$ ( $X^1\Sigma$ ) <sup>d</sup>	5.089	5.051	345.3	351.4	0.99	1.03
$Na_2$ ( $X^1\Sigma$ ) <sup>e</sup>	5.9313	5.818	155.7	159.2	.719	.73
$CH$ ( $X^2\pi$ ) <sup>f</sup>	2.086				3.43	3.65
$NH$ ( $X^3\Sigma$ ) <sup>g</sup>		expt.			3.37	3.40
$OH$ ( $X^2\pi$ ) <sup>h</sup>		expt.			4.53	4.63
$FH$ ( $X^1\Sigma^+$ ) <sup>i</sup>	1.7328 <sup>m</sup>				6.18	6.12
$F_2$ ( $X^1\Sigma^+$ ) <sup>j</sup>		expt.			1.67	1.68
$O_2^-$ ( $X^2\pi$ ) <sup>k</sup>		expt.			4.14	4.16
$CO$ ( $X^1\Sigma^+$ ) <sup>l</sup>	2.132 <sup>m</sup>				11.33	11.38

- (a) All these calculated values are based on a consistent simple model designed to evaluate only changes occurring in the correlation energy with molecular formation. See DAS, G. and WAHL, A.C. (1972). *J. Chem. Phys.*, **56**, 1769.  
 (b) DAS, G. and WAHL, A.C. (1966). *J. Chem. Phys.*, **44**, 87.  
 (c) BERTONCINI, P.J., DAS, G. and WAHL, A.C. (1970). *J. Chem. Phys.*, **52**, 5112.  
 (d) DAS, G. and WAHL, A.C. (1966). *J. Chem. Phys.*, **44**, 87. DAS, G. (1967). *Ibid.*, **46**, 1568.  
 (e) BERTONCINI, P.J. and WAHL, A.C., *J. Chem. Phys.*, (to be submitted).

- (f) NEUMANN, D. and KRAUSS, M., (in preparation).  
 (g) STEVENS, W.J. (1973). *J. Chem. Phys.*, **58**, 1264.  
 (h) STEVENS, W.J., DAS, G., WAHL, A.C., NEUMANN, D. and KRAUSS, M. (1974). *J. Chem. Phys.*, **61**, 3686.  
 (i) NEUMANN, D. and KRAUSS, M. (1974). *Mol. Phys.*, **27**, 917.  
 (j) DAS, G. and WAHL, A.C. (1973). *J. Chem. Phys.*, **56**, 3532.  
 (k) KRAUSS, M., NEUMANN, D., WAHL, A.C., DAS, G. and ZEMKE, W. (1973). *Phys. Rev.*, **A7**, 69. ZEMKE, W., DAS, G. and WAHL, A.C. (1972). *Chem. Phys. Letters*, **14**, 310  
 (l) BILLINGSLEY, F.P. and KRAUSS, M. (1974). *J. Chem. Phys.*, **60**, 4130.  
 (m) Energy calculated at one point, the experimental  $R_e$ .

Table 2: Diatomic dipole moments computed from SCF and OVC wavefunctions. All values are in debyes.

Molecule <sup>a</sup>	SCF	OVC <sup>b</sup>	Experiment
$C^+H^-$ ( $^2\pi$ )	1.570 <sup>c</sup>	1.53 <sup>g</sup>	1.46 ± 0.06 <sup>k</sup>
$N^+H^-$ ( $^3\Sigma$ )	1.627 <sup>c</sup>	1.537 <sup>h</sup>	unknown
$O^+H^-$ ( $^2\pi$ )	1.780 <sup>c</sup>	1.655 <sup>q</sup>	1.660 ± 0.010 <sup>l</sup>
$F^+H^-$ ( $^1\Sigma$ )	1.942 <sup>c</sup>	1.805 <sup>g</sup>	1.797 <sup>m</sup>
$C^+N^-$ ( $^2\Sigma^+$ )	2.301 <sup>d</sup>	1.481 <sup>i</sup>	1.45 ± 0.08 <sup>n</sup>
$C^+O^-$ ( $^1\Sigma^+$ )	-0.274 <sup>e</sup>	0.156 <sup>j</sup>	0.112 ± 0.005 <sup>o</sup>
$Na^+Li^-$ ( $^1\Sigma$ )	0.679 <sup>f</sup>	1.141 <sup>f</sup>	0.47 ± 0.03 <sup>p</sup>

- (a) The dipole moments are given as positive for the indicated polarity.  
 (b) These calculations were all done at or near the experimental equilibrium. Vibrational averaging has not been taken into account except where noted in the footnotes.  
 (c) CADE, P.E. and HUO, W.M. (1966). *J. Chem. Phys.*, **45**, 1063.  
 (d) GREEN, S. (1972). *J. Chem. Phys.*, **57**, 4694.  
 (e) HUO, W.M. (1965). *J. Chem. Phys.*, **43**, 624.

- (f) STEVENS, W.J. and WAHL, A.C., (unpublished work). These results were obtained in an effort to improve previously published values by greatly expanding the STO basis set. The previous values were 0.95D and 1.24D for the SCF and OVC dipole moments respectively. See BERTONCINI, P., DAS, G. and WAHL, A.C. (1970). *J. Chem. Phys.*, **52**, 5112.  
 (g) NEUMANN, D. and KRAUSS, M. (1974). *Mol. Phys.*, **27**, 917.  
 (h) STEVENS, W.J. (1973). *J. Chem. Phys.*, **58**, 1264.  
 (i) DAS, G., JANIS, T. and WAHL, A.C. (1974). *J. Chem. Phys.*, **61**, 1274.  
 (j) BILLINGSLEY, F.P. and KRAUSS, M. (1974). *J. Chem. Phys.*, **60**, 4130. This value has been vibrationally averaged.  
 (k) PHELPS, D.H. and DALEY, F.W. (1966). *Phys. Rev. Letters*, **16**, 3.  
 (l) POWELL, F.X. and LIDE, D.R. (1965). *J. Chem. Phys.*, **42**, 4201.  
 (m) MUENTER, J.S. and KLEMPERER, W. (1970). *J. Chem. Phys.*, **52**, 6033.  
 (n) THOMSON, R. and DALBY, F.W. (1968). *Can. J. Phys.*, **46**, 2815.  
 (o) TOTH, R.A., HUNT, R.H. and PLYLER, E.K. (1969). *J. Mol. Spectroscopy*, **32**, 74.  
 (p) DAGDIGIAN, P.J., GRAFF, J. and WHARTON, L. (1971). *J. Chem. Phys.*, **55**, 4980.  
 (q) STEVENS, W.J., DAS, G., WAHL, A.C., NEUMANN, D. and KRAUSS, M. (1974). *J. Chem. Phys.*, **61**, 3686.

Table 3: STO basis set for *OH*  
(CADE and HUO (1967). *J. Chem. Phys.*, **47**, 614).

	No.	Centre	Exponents
<b>Sigma</b>			
1s	2	O	7.017, 12.385
2s	2	O	1.718, 2.863
3s	1	O	8.646
2p	4	O	1.285, 2.135, 3.760, 8.228
3d	2	O	1.636, 2.824
4f	1	O	2.266
1s	3	H	1.000, 1.314, 2.439
2s	1	H	2.300
2p	1	H	2.805
<b>Pi</b>			
2p	4	O	1.266, 2.115, 3.753, 8.411
3d	1	O	1.913
4f	1	O	2.199
2p	1	H	1.770
3d	1	H	3.325

In order to obtain results of this quality one must utilize an extended basis set (double zeta plus polarization) and also must include all important

'molecular' configurations. The calculation of the *OH* potential curve, figure 1, provides a good example of what is required in these two regards. Table 3 displays the basis set composition and table 4 the classes of configurations required. Discussion of these points has been given in detail recently [5]. Presently these methods have been extended to excited states of the same symmetry yielding satisfactory results, see table 5 [7].

Table 4: OVC configurations for  $X^2\Pi_i$  *OH*

Classification	Occupancies	Number of Couplings
Hartree-Fock	$1\sigma^2 2\sigma^2 3\sigma^2 1\pi^3$	1
Correct Dissociation	$1\sigma^2 2\sigma^2 4\sigma^2 1\pi^3$	1
	$1\sigma^2 2\sigma^2 (3\sigma 4\sigma)_t 1\pi^3$	1
Interpair Split Shells	$1\sigma^2 2\sigma^2 (3\sigma 4\sigma) (1\sigma^2 2\pi)$	7
Intrapair Doubles	$1\sigma^2 2\sigma^2 5\sigma^2 1\pi^3$	1
	$1\sigma^2 2\sigma^2 6\sigma^2 1\pi^3$	1
	$1\sigma^2 2\sigma^2 1\pi^3 3\pi^2$	1
	$1\sigma^2 2\sigma^2 1\pi^3 4\pi^2$	1

Table 5: Spectroscopic constants for the *CN*-states

States	Reference	$D_e$ (eV)	$T_e$ (eV)	$r_e$ (bohrs)	$\omega_e$ ( $\text{cm}^{-1}$ )	$\omega_e x_e$ ( $\text{cm}^{-1}$ )	$B_e$ ( $\text{cm}^{-1}$ )	$\alpha_e$ ( $\text{cm}^{-1}$ )
$X^2\Sigma^+$	This work	7.011		2.20	2079.5	13.00	1.90	.019
	Straight CI <sup>a</sup>	6.178		2.34	1939.2	14.54	1.61	.015
	Exp. <sup>b</sup>	$7.75 \pm .2$		2.22	2068.7	13.14	1.90	.017
$B^2\Sigma^+$	This work	6.280	3.114	2.17	2275.5	24.94	1.97	.022
	Straight CI <sup>a</sup>	4.335	3.765	2.32	1765.2	32.53	1.65	.026
	Exp. <sup>b</sup>		3.193	2.18	2164.1	20.25	1.97	.022
$E^2\Sigma^+$	This work	1.747	7.647	2.45	2074.5	16.83	1.53	.007
	Straight CI <sup>a</sup>	1.745	7.856	2.58	1717.1	30.57	1.32	.015
	Exp. <sup>b</sup>		7.334	2.49	1681.4	3.6	1.49	.006
$A^2\Pi$	This work	5.998	1.013	2.34	1787.2	12.28	1.69	.018
	Straight CI <sup>a</sup>	4.295	1.883	2.50	1621.4	16.74	1.40	.015
	Exp. <sup>b</sup>		1.146	2.33	1814.4	12.88	1.72	.018
$D^2\Pi$	This work	2.943	6.451	2.94	1109	11.99	1.07	.013
	Straight CI <sup>a</sup>	3.008	$\sim 7.593$	3.01	1041.6	6.38	.97	.010
	Exp. <sup>b</sup>		6.755	2.83	1004.7	8.78	1.16	.013
$H^2\Pi$	This work	1.427	7.9673	2.49	2364.3	50.70	1.487	.001
	Straight CI <sup>a</sup>	1.794	7.807	2.67	1651.3	43.84	1.229	.002
	Exp. <sup>b</sup>		$7.556 (=T_0)$	$2.48 (=r_0)$			$1.52 (=B_0)$	

(a) See [3]

(b) See [3] for lists of references on the *CN*-experimental data

Table 6: Configurations used for the VDW calculations for *ArH*

Configurations	
Description	$[1s\sigma_{Ar}^2 2s\sigma_{Ar}^2 2p\sigma_{Ar}^2 2p\pi_{Ar}^4]X$
Hartree-Fock	$(3s\sigma^2 3p\sigma^2 3p\pi^4)_{Ar} 1s\sigma_H$
Overlap-Transfer Excitations	$(3s\sigma^2 4p\sigma 3p\pi^4)_{Ar} 1s\sigma_H^2$ $(3s\sigma^2 3p\sigma 3p\pi^3 4p\pi)_{Ar} 1s\sigma_H^2$
$(3p_{Ar}, 1s_H)$ Dispersion Excitations	$(3s\sigma^2 3p\sigma 3d\sigma 3p\pi^4)_{Ar} 2p\sigma_H$
	$(3s\sigma^2 3p\sigma^2 3p\pi^3 3d\pi)_{Ar} 2p\sigma_H$
	$(3s\sigma^2 3p\sigma^2 3d\sigma 3p\pi^3)_{Ar} 2p\pi_H$
	$(3s\sigma^2 3p\sigma 3d\pi 3p\pi^4)_{Ar} 2p\pi_H$
	$(3s\sigma^2 3p\sigma^2 3p\pi^3 3d\delta)_{Ar} 2p\pi_H$
	$(3s\sigma^2 3p\sigma^2 3p\pi^3 3d\pi)_{Ar} 3d\delta_H$ $(3s\sigma^2 3p\sigma 3d\delta 3p\pi^4)_{Ar} 3d\delta_H$
$(3s_{Ar}, 1s_H)$ Dispersion Excitations	$(3s\sigma 3p\sigma^2 4p\sigma 3p\pi^4)_{Ar} 2p\sigma_H$ $(3s\sigma 3p\sigma^2 4p\pi 3p\pi^4)_{Ar} 2p\pi_H$

Table 7: Calculated and experimentally determined Van der Waals well depths  $\epsilon$  and positions *R*

System	<i>R</i> (bohrs)		$\epsilon$ °K		Reference
	Theory	Experiment	Theory	Experiment	
<i>HeH</i>	6.8	6.97	5.8	4.05	[8]
<i>He<sub>2</sub></i>	5.6	5.6	10.8	10.4 to 11.2	[9]
<i>LiHe</i>	11.8		2.2		[8]
<i>Ne<sub>2</sub></i>	5.82	5.86	39.2	42.0	[10]
<i>NeH</i>	6.65	6.01	16.9	32.6	a
<i>ArH</i>	6.8	6.73	48.2	55.4	[12]
<i>KrH</i>	7.2	6.99	67.3	70.3	a

(a) Work in progress

(b) The disagreement between experiment and theory for *NeH* is under study

Table 8: Comparison of experimental and theoretical well depths for *He<sub>2</sub>*

	$\epsilon$ °K	Reference
Hartree-Fock	Repulsive	
Interatomic terms only included	12	[9]
Inter and Intra computed separately and added	10.8	[9]
Inter and Intra computed simultaneously <sup>a</sup>	8.9	[13]
Experiment <sup>a</sup>	10.6 - 11.2	[9,13]

(a) This discrepancy between theory and experiment has been resolved in recent work by W. Meyer, see [6].

## Van der Waal Interactions

Ideas similar to those which have proven successful in the quantitative evaluation of chemical bond strengths have been applied to the evaluation of Van der Waal's forces (for an example of configurations employed see table 6). Recent MCSCF calculations including only intermolecular excitation have been performed on *HHe* [8], *He<sub>2</sub>* [9], *LiHe* [8], *Ne<sub>2</sub>* [10], *NeH* [11] and *ArH* [12], table 7, and Van der Waal well depths have been obtained in cases where experimental values are well established to an accuracy of approximately 10%. In order to achieve greater accuracy intra-atomic and inter-intra coupling correlation effects must be included. This has been done for the *He<sub>2</sub>* [6,13]. The most complete theoretical results [6] are now in satisfactory agreement with experiment, table 8. In such high accuracy calculations very extended basis sets, table 9, must be employed to avoid expansion errors, dependent on the internuclear distance, which can be of the same order of magnitude as the Van der Waal interaction [12].

Table 9: Basis set used for accurate SCF calculations on the system *ArH*

$\sigma$ -Set			$\pi$ -Set		
n1	Exponent	Centre	n1	Exponent	Centre
1s	20.75	<i>Ar</i>	2p	16.22	<i>Ar</i>
2s	14.9	<i>Ar</i>	2p	8.23	<i>Ar</i>
3s	16.5	<i>Ar</i>	2p	5.0	<i>Ar</i>
3s	10.5	<i>Ar</i>	4p	8.0	<i>Ar</i>
2s	6.206	<i>Ar</i>	3p	2.97	<i>Ar</i>
3s	3.166	<i>Ar</i>	4p	2.211	<i>Ar</i>
3s	1.933	<i>Ar</i>	3p	1.37	<i>Ar</i>
4s	1.933	<i>Ar</i>	4p	1.37	<i>Ar</i>
2p	16.22	<i>Ar</i>	3d	2.97	<i>Ar</i>
2p	8.23	<i>Ar</i>	4d	2.211	<i>Ar</i>
2p	5.0	<i>Ar</i>	3d	1.37	<i>Ar</i>
4p	8.0	<i>Ar</i>	2p	1.0	<i>H</i>
3p	2.97	<i>Ar</i>	2p	1.75	<i>H</i>
4p	2.211	<i>Ar</i>			
3p	1.37	<i>Ar</i>			
4p*	1.37	<i>Ar</i>			
3d*	2.97	<i>Ar</i>			
4d*	2.211	<i>Ar</i>			
3d*	1.37	<i>Ar</i>			
1s	1.0	<i>H</i>			
1s	2.0	<i>H</i>			
2s	1.0	<i>H</i>			
2s	2.5	<i>H</i>			
2p	1.0	<i>H</i>			
2p	1.75	<i>H</i>			

## Triatomic Molecules

The extension of the configuration selection process employed successfully on diatomic molecules could not be straightforwardly applied to the triatomic systems except for the dihydrides in which the various correlation types (in out, left right, angular) are easy to identify. The results of the application of this method to  $H_2O$  and  $NO_2$  are given in figures 2 and 3. The choice of configurations is discussed in several recent papers [14,15].

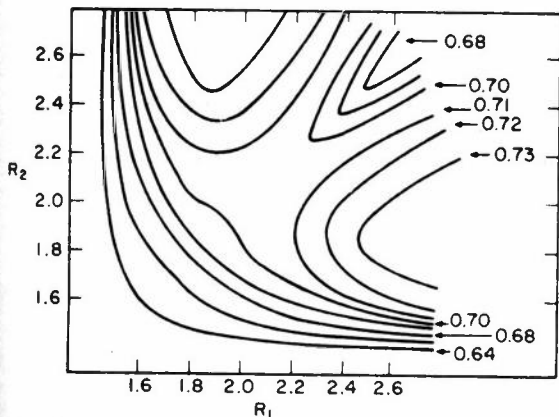


Figure 2: MCSCF potential energy surface for  ${}^3B_1$  state of  $H_2O$  at bond angle of  $105^\circ$ . Energy contours are labelled in atomic units.

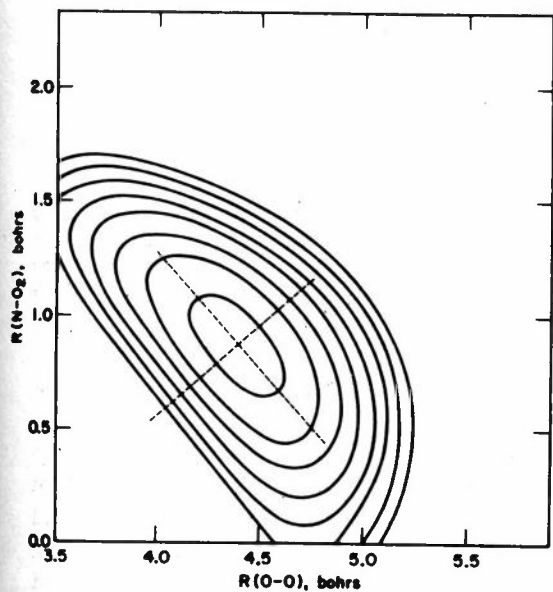


Figure 3: Computed potential surface of  $1^2A_1$  state of  $NO_2$ . Innermost contour is  $-204.10$  au with each succeeding contour  $0.01$  au higher in energy.

## Dynamics and Scattering

With the availability of accurate *ab initio* interaction potentials it becomes possible to compare, at a quantitative level experimentally derived potentials with the calculated ones. For some systems the

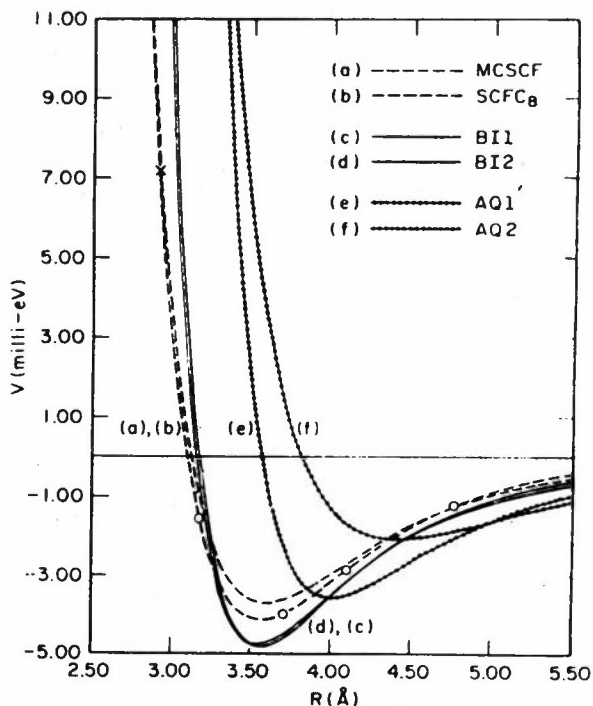


Figure 4:  $V(R)$  versus  $R$ .  $AQ1$  and  $AQ2$  label the two experimentally derived potentials of [17].  $BI1$  and  $BI2$  label the two experimentally derived potentials of [16]. MCSCF and  $SCFC_8$  are the theoretical potentials [12].

uncertainty in the experimentally derived potential is sufficient to warrant serious consideration of the calculated potential. This was the case for  $ArH$  in which the potentials derived from two different experiments [16,17] were in a serious disagreement, figure 4. In this case the theoretically derived potentials agreed with only one of the experimental ones, figure 4. Further the scattering predicted from the theoretical potential also only supported one set of experiments, figures 5-9. Later these disagreements were resolved and it appears that the theoretically evaluated potential was important in catalyzing new experiments [12].

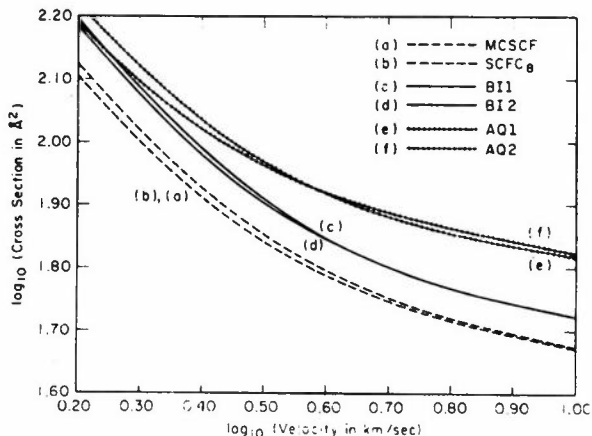


Figure 5: Log of the total elastic cross section versus log of the  $ArH$  relative velocity. The elastic cross sections were calculated from the quantum mechanical phase shifts produced by the six potential curves in figure 4.

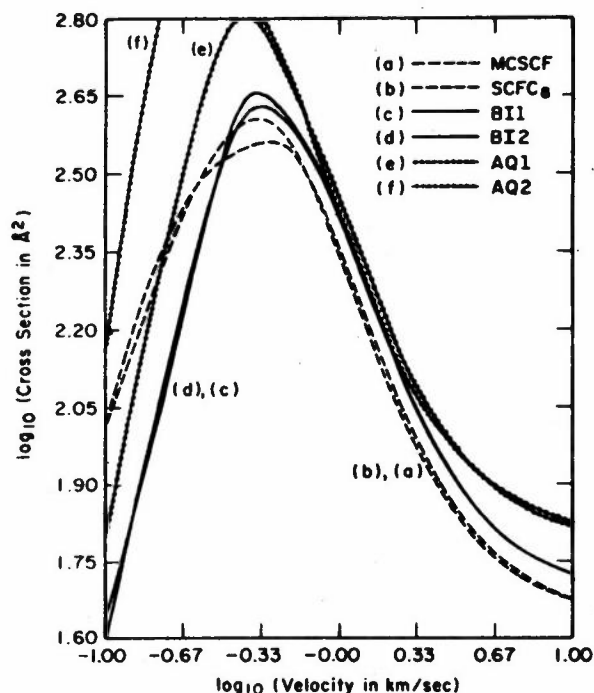


Figure 6: Log of the total elastic cross section versus log of the  $ArH$  relative velocity. The elastic cross sections were calculated from the quantum mechanical phase shift produced by the six potential curves in figure 4.

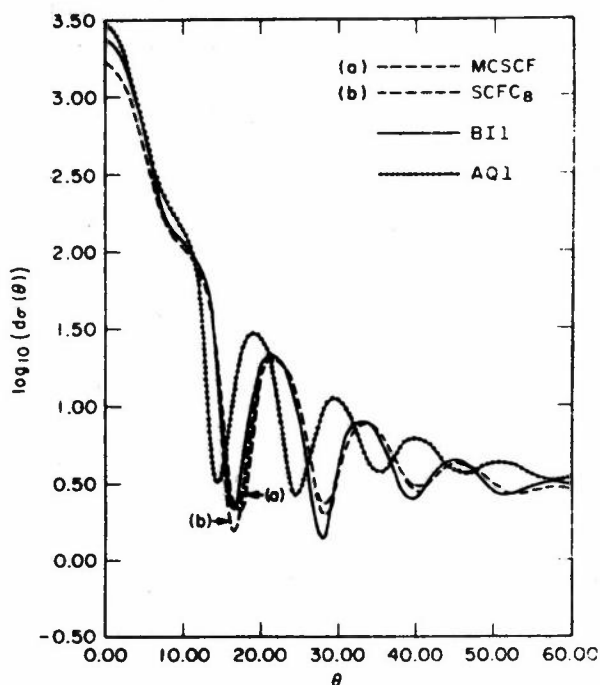


Figure 7: Log of the differential cross section  $d\sigma(\theta)$  versus the angle of scatter  $\theta$ . The  $ArH$  relative velocity is 3.0 km/sec. The differential cross sections were calculated from the quantum mechanical phase shifts produced by four of the six potential curves in figure 4.

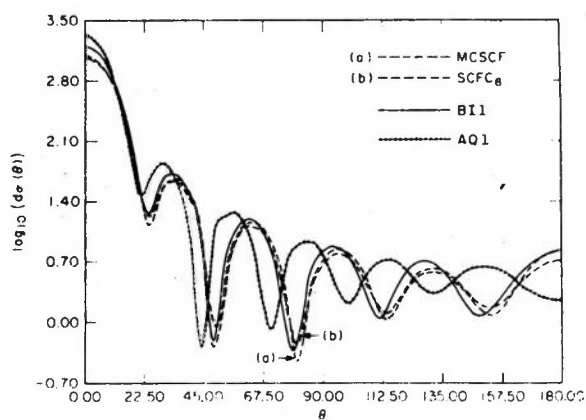


Figure 8: Log of the differential cross section  $d\sigma(\theta)$  versus the angle of scatter  $\theta$ . The  $ArH$  relative velocity is 1.0 km/sec. The differential cross sections were calculated from the quantum mechanical phase shifts produced by four of the six potential curves in figure 4.

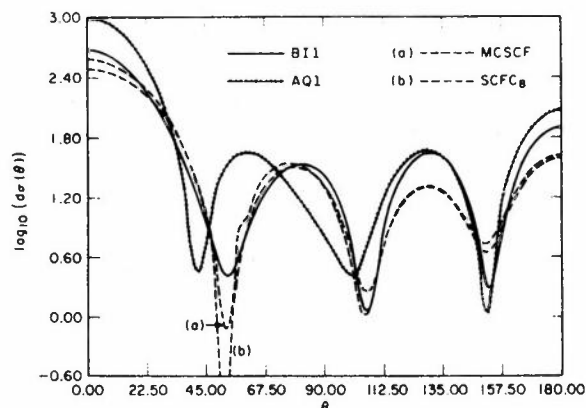


Figure 9: Log of the differential cross section  $d\sigma(\theta)$  versus the angle of scatter  $\theta$ . The  $ArH$  relative velocity is 0.4 km/sec. The differential cross sections were calculated from the quantum mechanical phase shifts produced by four of the six potential curves in figure 4.

We have also performed classical trajectory studies [18] on the  $LiH_2$  surfaces computed at three levels of accuracy. The surfaces were Hartree-Fock, Optimized Valence Configuration, and Hartree-Fock interaction added to a correlated description of the  $H_2$  bond stretching. The OVC surface for 1.4 bohrs is displayed in figure 10. These potential surfaces were computed for three  $H_2$  internuclear distances 1.0, 1.4, and 2.0 bohrs and fitted to the form given in table 10.



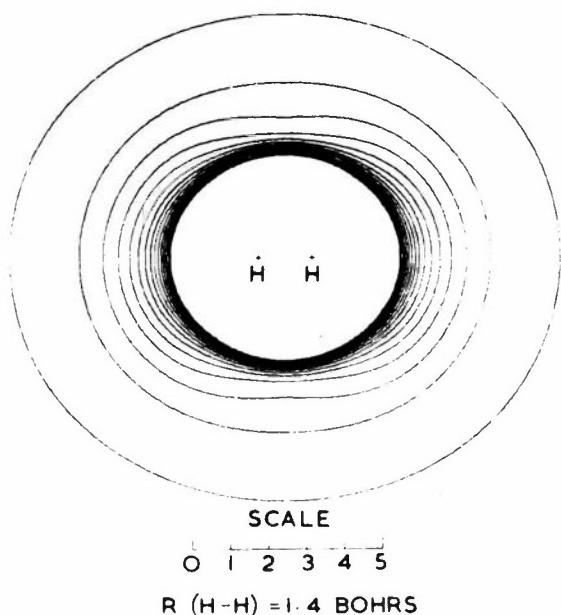


Figure 10: OVC small basis set potential energy surface of  $Li + H_2$  for the  $H_2$  distance frozen at  $1.4a_0$ .

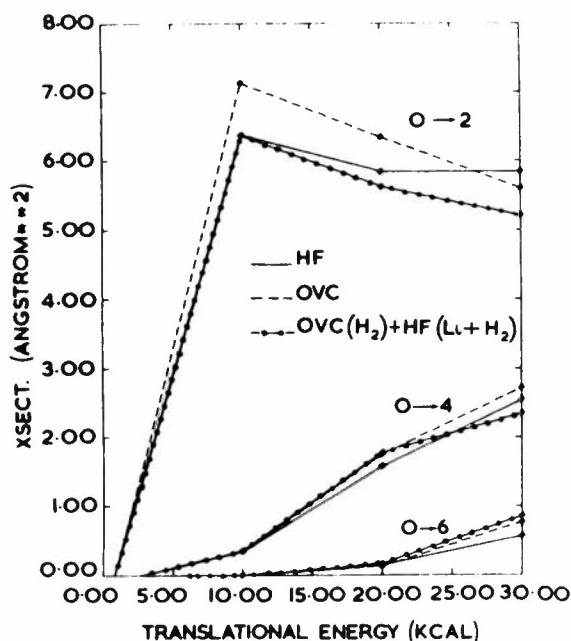
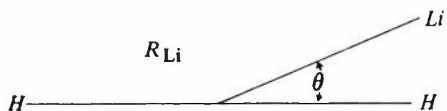


Figure 11: The cross section, as a function of  $Li$  translational energy, for rotational excitation of  $H_2$ . Transitions  $(0 \rightarrow 2)$ ,  $(0 \rightarrow 4)$ , and  $(0 \rightarrow 6)$  are displayed for three different potential energy surfaces: a Hartree-Fock (HF) surface; an OVC surface; and a hybrid surface consisting of the HF interaction energy and the OVC  $H_2$  asymptotic energy.

Table 10: Analytic Potential Form



$$V(R_{Li}, R_{H_2}, \theta) = V_{H_2}(R_{H_2}) + V_{Li-H_2}(R_{Li}, R_{H_2}, \theta)$$

where:

$$V_{H_2}(R_{H_2}) = D \left\{ 1 - \exp(-\beta(R_{H_2} - R_e)) \right\}^2$$

$$V_{Li-H_2}(R_{Li}, R_{H_2}, \theta) = \sum_{\ell=0,2}^4 V_{\ell}(R_{Li}, R_{H_2}) P_{\ell}(\cos \theta)$$

$$V_{\ell}(R_{Li}, R_{H_2}) = Q_{1\ell}(R_{H_2}) \exp(-\alpha_{\ell} R_{Li}) + Q_{2\ell}(R_{H_2}) R_{Li}^{-m_{\ell}} + Q_{3\ell}(R_{H_2}) R_{Li}^{-n_{\ell}}$$

$$Q_{j\ell}(R_{H_2}) = a_{j\ell} + b_{j\ell} R_{H_2} + c_{j\ell} R_{H_2}^2$$

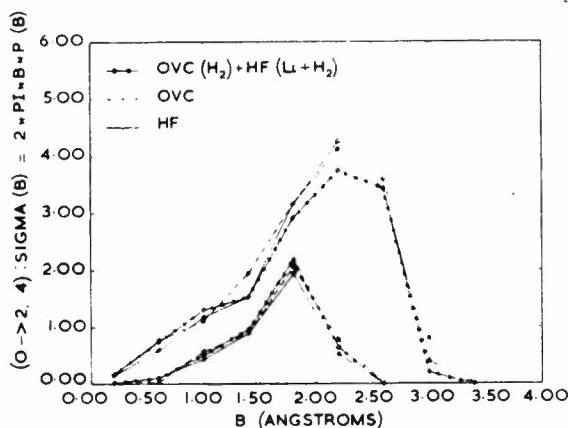


Figure 12: The cross section for the  $(0 \rightarrow 2)$  and  $(0 \rightarrow 4)$  rotational excitation of  $H_2$  as a function of the  $Li$  impact parameter for  $Li$  with an initial translational energy of 20 kcal and for  $H_2$  initially in the ground vibrational state. Results are displayed for the three potential energy surfaces listed in figure 11.

The purpose of these studies was to predict non-reactive collisional behaviour for this system and to assess the effect in the dynamics of the differences in the three potentials employed. As seen in figure 5 11-13 the dynamics obtained from these three potentials are qualitatively indistinguishable. All of them led to negligible vibrational or rotational excitation at the energies studied. Work on the reactive portion of the  $LiH_2$  surface is in progress.

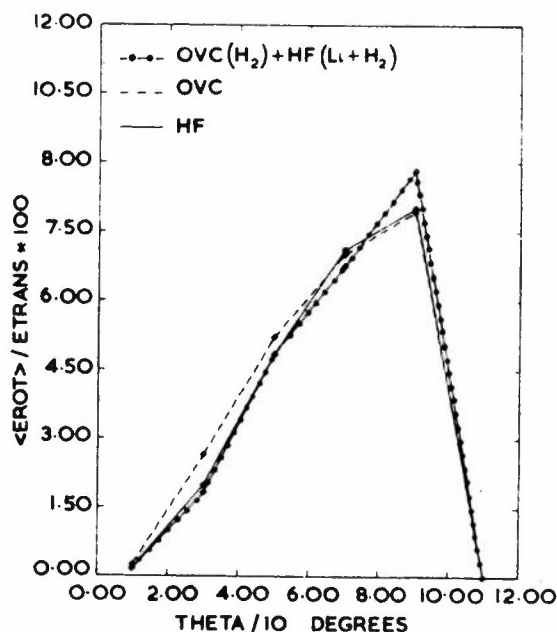


Figure 13: The percentage change in the translational energy of *Li*, as a function of the scattering angle, due to internal excitation of  $H_2$ . *Li* has an initial translational energy of 20 kcal.  $H_2$  is initially in the ground vibrational state. Results are displayed for the three potential energy surfaces listed in figure 11.

## Summary

The purpose of the above presentation has been to give you some idea of the work going on in our laboratory dealing with the evaluation of interaction potentials and their subsequent use in dynamical calculations. These dynamical calculations have served several purposes:

- to aid in developing a unique interatomic potential, as in the *ArH* case,
- to assess the sensitivity of the dynamical results to changes in the potential, as in both the *ArH* and *LiH<sub>2</sub>* cases, and
- to predict collisional behaviour from the *a priori* potential, as in both the *ArH* and *LiH<sub>2</sub>* cases.

With the relatively new capacity for evaluating accurate interatomic and intermolecular potentials for non trivial systems and recent advances in dynamics quantum chemistry can be expected to play an increasingly important role in the establishment of accurate potential energy surfaces and the prediction of dynamical behaviour on them. This process is an iterative one in which regions of the potential surfaces are identified for refinement through dynamical calculations displaying sensitivity to such regions, followed by subsequent improved dynamical calculations.

## References

- SCHAEFFER, H.F. (1972). *The Electronic Structure of Atoms and Molecules*, Reading, Massachusetts: Addison-Wesley.
- WAHL, A.C. (1972). *MTP Int. Rev. of Science*, Volume 2 (ed. W. Byers Brown), London: Butterworths.
- NESBET, R.K. (1968). *Phys. Rev.*, **175**, 2. NESBET, R.K., BARR, T.L. and DAVIDSON, E.R. (1969). *Chem. Phys. Letters*, **4**, 203.
- SCHAEFFER, H.F., KLEIN, R.A. and HARRIS, F.E. (1969). *Phys. Rev.*, **181**, 137.
- DAS, G. and WAHL, A.C. (1972). *J. Chem. Phys.*, **56**, 1769, (and references to previous work therein).
- MEYER, W. (1974). (See this volume, p.97).
- DAS, G. (1973). *J. Chem. Phys.*, **58**, 5104. JANIS, F., DAS, G. and WAHL, A.C. (1974). *J. Chem. Phys.*, (in the press).
- DAS, G. and WAHL, A.C. (1971). *Phys. Rev. A*, **4**, 825.
- BERTONCINI, P. and WAHL, A.C. (1970). *Phys. Rev. Letters*, **25**, 991.
- STEVENS, W., WAHL, A.C., GARDINER, M. and KARO, A. (1974). *J. Chem. Phys.*, **60**, 2195.
- DAS, G. and WAHL, A.C., (in preparation).
- WAGNER, A., DAS, G. and WAHL, A.C. *J. Chem. Phys.*, (in the press).
- LIU, B. and MCLEAN, A.D. (1973). *J. Chem. Phys.*, **59**, 4557.
- HOSTENY, R.P., HINDS, A.R., WAHL, A.C. and KRAUSS, M. (1973). *Chem. Phys. Letters*, **23**, 9.
- GILLESPIE, G., KHAN, A.V., HOSTENY, R.P., WAHL, A.C. and KRAUSS, M., (in preparation).
- BICKES, R.W., LANTZSCH, B., TOENNIES, J.P. and WALASCHEWSKI, K. (1973). *Discussions Faraday Soc.*, **55**, (to be published).
- AQUILANTI, V., LINTI, G., VECCHIO-CATTIVI, F. and VOLPI, G.G. (1972). *Chem. Phys. Letters*, **15**, 305.  
A private communication from F. Vecchio-Cattivi indicates that the above quoted work has been repeated bringing the results in better agreement with that of [16].
- WAHL, A.C. (1974), (to be published).

# On the Direct Configuration Interaction Method from Molecular Integrals

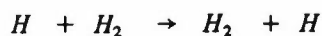
P.Siegbahn\*

The direct configuration interaction method from molecular integrals is investigated in two main directions. The first concerns the use of different diagonalization procedures, and it is shown that a variational form of perturbation theory is most efficient in connection with this CI-method. The other deals with methods of obtaining and sorting the coupling coefficients that appear in the formalism. One such procedure is outlined. Finally a computer program for correlating three valence electrons with full CI, based on these methods, is described. Timings are given from preliminary studies of the  $H_3$  and the  $Li_2H$  systems.

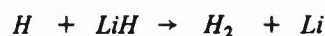
## Introduction

A couple of years ago a basically new method of doing configuration interaction (CI) calculations was introduced [1]. It is the object of this paper to present certain improvements and extensions of this method. One section will put the method in the context of other methods, and the following two parts will concentrate on diagonalization schemes and coupling coefficients respectively. Finally in the last section the performance of a computer program is demonstrated, where the presented algorithms have been used for the case of full CI on three valence electrons.

The decision to make a full CI program for three valence electrons was made for three reasons. The application of the method is particularly simple for the case of full CI. It is a system where it is practical to perform full CI calculations even for large basis sets, and finally there is a big variety of problems of chemical interest where three electrons determine the electronic structure or the potential energy surface. The most striking example of the last point is maybe the classical problem of the exchange-reaction between a hydrogen atom and a hydrogen molecule.



Other examples of reactions involving three electrons are



In the last section of the paper timings for calculations on two of these reactions will be given for a number of different basis sets and symmetries.

## Method of Calculation

To understand the details of the particular method of solving the CI-problem used here, some relevant background has to be given.

Expanding the wavefunction in terms of orthogonal configurations

$$\Psi = \sum_{i=1}^N C_i \Phi_i \quad (1)$$

leads to the secular equation

$$(H - E I) \cdot C = 0 \quad (2)$$

The methods of solving (2) can be divided into two basically different groups. The most commonly used procedure is the iterative scheme where (2) is handled as a set of linear equations and the coefficients and energy are simultaneously updated until convergence [2,3]. The other set of methods are based on perturbation theory [4,5].

The simplest form of the iterative method consists of rewriting (2) as

$$H' \cdot C = A \cdot C \quad (3)$$

where  $H' - A = H - E I$  must hold.

\* Department of Chemistry, University of California, Berkeley, California 94720, USA  
(present address) Institute of Theoretical Physics, University of Stockholm, Vanadisvägen 9, S-113 Stockholm, Sweden

Usually the matrix  $A$  is chosen to be diagonal, with for example  $A_{ii} = E - H_{ii}$ . This leads to the iterative procedure

$$\Delta C_i^{(k)} = \frac{1}{E^{(k-1)} - H_{ii}} \cdot \left[ \sum_{j=1}^N H_{ij} C_j^{(k-1)} - E^{(k-1)} \cdot C_i^{(k-1)} \right] \quad (4)$$

where  $\Delta C_i^{(k)}$  is the increment of coefficient  $i$  in iteration  $k$ , and  $N$  is the number of configurations in the basis set. The energy  $E^{(k-1)}$  is simply the variational energy calculated with the vector from iteration  $k-1$ .

$$E^{(k-1)} = \frac{1}{\sum_{i=1}^N C_i^{(k-1)2}} \cdot \sum_{i=1}^N C_i^{(k-1)} \cdot \sum_{j=1}^N H_{ij} C_j^{(k-1)} \quad (5)$$

In the perturbation approach the usual splitting is made of the Hamiltonian  $H = H_0 + V$ , with the corresponding expansion of the wavefunction  $\Psi = \sum_k \phi^{(k)}$  and energy  $E = \sum_k \mathcal{E}_k$ . Inserting this in the Schrödinger equation and collecting terms of order  $k$  leads to

$$(E_0 - H_0)\phi^{(k)} = V\phi^{(k-1)} - \sum_{m=0}^{k-1} \mathcal{E}_{k-m} \phi^{(m)} \quad (6)$$

After the expansion of  $\phi^{(k)}$  in orthogonal configurations the unperturbed Hamiltonian  $H_0$  is usually, for practical reasons, chosen to be diagonal in this representation. One such choice is:  $H_0 = \sum_{i=1}^N |i\rangle\langle i|H|i\rangle\langle i|$ , where the sum is over all the configurations in the basis set. With this choice (6) can be rewritten in component form as

$$C_i^{(k)} = \frac{1}{E_0 - H_{ii}} \sum_{j=1}^N V_{ij} C_j^{(k-1)} - \sum_{m=0}^N \mathcal{E}_{k-m} C_i^{(m)} \quad (7)$$

The perturbation energies obtained in iteration  $k$  are found to be expressed by [4],

$$\begin{aligned} \mathcal{E}_{2k-1} &= \langle \phi^{(k-1)} | V | \phi^{(k-1)} \rangle - \sum_{m=1}^{k-1} \sum_{n=1}^{k-1} \mathcal{E}_{2k-1-m-n} \langle \phi^{(m)} | \phi^{(n)} \rangle \\ \mathcal{E}_{2k} &= \langle \phi^{(k)} | V | \phi^{(k-1)} \rangle - \sum_{m=1}^k \sum_{n=1}^{k-1} \mathcal{E}_{2k-m-n} \langle \phi^{(m)} | \phi^{(n)} \rangle \end{aligned} \quad (8)$$

Depending on the procedure used to solve the secular equation either (4), (5) or (7), (8) is calculated until convergence. As  $A$  or  $H_0$  are commonly chosen to be diagonal both of these methods in practice basically means calculating the vector  $\sigma$  with components

$$\sigma_i^{(k)} = \sum_{j=1}^N H_{ij} C_j^{(k-1)} \quad (9)$$

B. Roos has shown [1], that for the case of a calculation in a basis of all singly and doubly substituted configurations out of a closed shell reference state,

(9) can be rewritten in terms of integrals and coupling coefficients in a computationally attractive way. The contribution to an element  $\sigma_i^{(k)}$  from the integral  $(ab/cd)$  is then given by

$$\Delta \sigma_i^{(k)} = A \cdot (ab/cd) \cdot C_j^{(k-1)} \quad (10)$$

where  $A$  is the coupling coefficient.

By this procedure the explicit construction of the Hamiltonian matrix is avoided. Instead the updating is made through a sequential reading of the integral list in each iteration. Extensions and modifications of this method will be discussed in the following sections.

### Diagonalization Schemes

A conventional CI-scheme consists of three steps. The generation of formal matrix element expressions, the construction of the Hamiltonian matrix and finally the diagonalization of this matrix. It is clear that the timing with this scheme is less sensitive to

the efficiency of the iteration procedure than the present method, where all work has to be repeated in each iteration. Also with the simultaneous updating of all components of the vector  $\sigma$ , according to (10), some commonly used modifications of the iterative scheme [2,3] cannot be used. With this in mind an investigation of different diagonalization schemes was made, and it will be shown here that a particular choice of perturbation approach is capable of giving rapid convergence in connection with this CI-method.

For the iterative schemes an obvious modification of (4) is the introduction of a damping factor  $\lambda_i$  in

front of the expression on the right hand side. A somewhat different way of introducing damping is obtained by choosing

$$A_{ii} = E - H_{ii} + \alpha_i \quad (11)$$

$\alpha_i$  can be compared to what in Hartree-Fock schemes are called level-shifters [6].

With the introduction of  $\alpha_i$  (4) becomes

$$\Delta C_i^{(k)} = \frac{1}{E^{(k-1)} - H_{ii} + \alpha_i} \left[ \sum_{j=1}^N H_{ij} C_j^{(k-1)} - E^{(k-1)} C_i^{(k-1)} \right] \quad (12)$$

A special case of this procedure is the use of Hartree-Fock orbital energies in the denominator instead of the diagonal elements of the Hamiltonian matrix. One convenient way of using  $\alpha_i$  is to avoid the problems occurring when  $E - H_{ii} \approx 0$ , which may happen in a case of near degeneracy. There is clearly a great variety of possibilities of choosing the  $\alpha_i$ . No effort was here made to map out the advantages of particular choices of  $\alpha_i$ , because certain modifications of the perturbation schemes seemed to show superior convergence patterns in connection with this CI-method.

The corresponding flexibility obtained by choosing the  $\alpha_i$  above is obtained in perturbation theory by the freedom of choosing  $H_0$  according to

$$H_0 = \sum_{i=1}^N |i\rangle \alpha_i' \langle i| \quad (13)$$

where the sum is over all the configurations in the basis set. For the perturbation schemes by far the most efficient choice of  $\alpha_i'$  tried, was the sum of Hartree-Fock orbital energies. In fact with  $\alpha_i'$  equal to the diagonal elements of the Hamiltonian matrix the straightforward perturbation method (7), (8) generally diverges. Having defined  $H_0$ , a choice of different available perturbation schemes are still open.

One can show that simple expressions exist for the matrix elements of the perturbation operator  $V$  between the perturbation functions  $\phi$  according to [4]

$$\begin{aligned} & \langle \phi^{(p)} | V | \phi^{(q)} \rangle \\ &= \epsilon_{p+q+1} + \sum_{k=1}^p \sum_{\ell=1}^q \epsilon_{p+q+1-k-\ell} \langle \phi^{(k)} | \phi^{(\ell)} \rangle \end{aligned} \quad (14)$$

where  $\epsilon$  are perturbation energies.

This means that setting up and solving the secular equation in terms of the perturbation functions is a minor extra work in each iteration. Improved convergence has been demonstrated in some cases with this nonlinear variational perturbation approach [5]. A test calculation on a 1s-hole on  $CO^+$  with 1500 configurations is shown in table 1. The orbitals used were the ground state orbitals of  $CO$  and the  $\alpha_i'$  are chosen to be the sum of the orbital energies for the ion. Also shown in table 1 are various other methods to calculate the energy, easily applied in each iteration. The linear variational perturbation approach [4] is simply the variational energy calculated with the sum of the perturbation functions. For the definitions of  $[N, N-1]$  and  $[N, N]$  Padé approximants used to extrapolate the perturbation energies, see references [5,7]. It should be added that the chosen example was unusually difficult to get to converge, because of the big reorganization effects. Commonly 6 or 7 iterations are needed to get convergence for ground states to 6 decimal figures in the energy with the nonlinear variational method, if there is not a very close lying excited state. Generally even the application of perturbation theory according to (7) (8) with  $H_0$  as the sum of orbital energies converges.

Table 1: Convergence of CI - different procedures calculation on  $CO^+$  Correlation energies in au <sup>a</sup>

Iteration	Linear Perturbation Theory	Linear Variational Perturbation Theory	Non-Linear Variational Perturbation Theory	$[N, N-1]$ Padé-Approximant	$[N, N]$ Padé-Approximant
2	-0.565	-0.357	-0.662859	-0.832297	-0.560801
4	-1.77	-0.703	-0.804137	-0.805747	-0.806888
6	-1.28	-0.547	-0.807554	-0.808230	-0.807879
8	+15.2	+0.332	-0.807884	-0.807320	-0.807734
10	-19.2	+2.22	-0.807975	-0.807966	-0.813891
12	-359	+0.516	-0.807991	-0.807965	-0.807675
14	+1180	+3.28	-0.807993	-0.807994	-0.808027

(a) The correlation energy also includes the reorganization energy

## The Coupling Coefficients

In this section a method for obtaining and sorting the coupling coefficients  $A$  in (10) will be presented, and an example is given for the three electron case. The value of the coupling coefficient  $A$  for a particular integral ( $ab/cd$ ) depends on three independent parameters

- (a) Type of integral
- (b) Spin- (and space-) projection used in the coupled configurations  $i$  and  $j$
- (c) Permutation of the orbitals in these configurations.

To clarify the meaning of 'type of integral' we consider the case of a configuration set of single and double substitutions from a single configuration reference state. Here we can divide the orbitals into three distinct sets

- (a) Doubly occupied in reference state
- (b) Singly occupied in reference state
- (c) Nonoccupied in reference state.

Within each of these sets the orbitals are given a sequential number. The integral is defined in terms of four orbitals  $a, b, c,$  and  $d$ . The 'type of integral' is defined by how many of these four orbitals fall into each of the three groups and the relationship between the sequence number of the orbitals of the same group. As an example, there are 14 different types of integrals which are defined in terms of orbitals all belonging to the same set (table 2). All

Table 2: The fourteen different types of integrals ( $ab/cd$ ) obtained when all orbitals are in the same set

Type No.	Index-relations	Type No.	Index-relations	Type No.	Index-relations
1	$a = b = c = d$	6	$a = b$	11	$b = c$
2	$a = b = c$	7	$c = d, b > c$	12	$b > c$
3	$b = c = d$	8	$c = d, b < c$	13	$b < c, b > d$
4	$a = b, c = d$	9	$a = c$	14	$b < c, b < d$
5	$a = c, b = d$	10	$b = d$		

together there are 53 different types of integrals for a closed shell reference state. With one open shell there are 89 types and with two open shells the number of types has increased to 148. The actual programming work required to use the algorithm (10) in its present form is critically dependent on the number of types of integrals, as each one in principle requires a special subroutine. Therefore, if all orbitals are treated equally, as in the case where all possible configurations generated by the basis set are used in the calculation, full CI, the number of types of integrals is small, 14, and the required programming work moderate.

To obtain the required coupling coefficients a program developed by C. Bender [8] was used, which generates formal matrix-elements between specified configurations. By a specially written program the list of matrix-elements was searched for a specific integral. The coupling coefficients are then ordered by the program according to the indices involved in

Table 3: Full CI for three electrons

Coupling coefficient tables for integral ( $ab/cd$ ) where  $b < c$  and  $b > d$  (Type 13 of table 2)

(a) Interaction elements ( $kda^{(1,2)} || kbc^{(1,2)}$ )

$k$  is the running index and the superindex denotes spin-coupling

Spin-coupling	$k \rightarrow$								
	$d$	$b$			$c$			$a$	
(1  2)	+1/2	0	-1/2	$-\sqrt{6}/2$	-1	$+\sqrt{6}/2$	-1/2	0	+1/2
(1 2)	$-\sqrt{3}/2$	$-\sqrt{2}$	$-\sqrt{3}/2$	0	0	0	$+\sqrt{3}/2$	$-\sqrt{2}$	$+\sqrt{3}/2$
(2  1)	$-\sqrt{3}/2$	0	$+\sqrt{3}/2$	$+\sqrt{2}/2$	0	$+\sqrt{2}/2$	$-\sqrt{3}/2$	0	$+\sqrt{3}/2$
(2 2)	-1/2	0	-1/2	0	+1	0	-1/2	0	-1/2

(b) Interaction elements ( $kca^{(1,2)} || kdb^{(1,2)}$ )

Spin-coupling	$k \rightarrow$								
	$d$	$b$			$c$			$a$	
(1  1)	+1	$+\sqrt{6}/2$	+1/2	0	-1/2	0	+1/2	$-\sqrt{6}/2$	+1
(1 2)	0	0	$+\sqrt{3}/2$	0	$-\sqrt{3}/2$	$-\sqrt{2}$	$-\sqrt{3}/2$	$+\sqrt{2}/2$	0
(2  1)	0	$+\sqrt{2}/2$	$+\sqrt{3}/2$	$-\sqrt{2}$	$+\sqrt{3}/2$	0	$-\sqrt{3}/2$	0	0
(2 2)	+1	0	-1/2	0	-1/2	0	-1/2	0	+1

the interaction. For a three-electron system each configuration is defined in terms of three orbital indices. Each of the two interacting configurations will have two indices – the fixed indices – equal to two of the indices appearing in the investigated integral. The third index – the running index – will appear in both of the configurations but not in the integral. When this last index runs over all orbitals in the basis set a series of configurations that interact through the given integral are generated. A major division of the interactions according to fixed indices and spin-coupling is then made. Within each such group the interactions are ordered after the running index. As an example the list of coupling coefficients obtained in this way for a certain integral is given in table 3. The table contains all the necessary information needed to describe the detailed handling of this type of integral in the CI-calculation. Fourteen such tables have to be generated in this case after which the actual programming is almost trivial. The appearance of a single running index means that each integral runs through a single loop over the number of orbitals ( $m$ ) in the basis set. The full CI for three electrons with this algorithm is consequently an  $m^5$  procedure. For four electrons there will be two running indices which makes the full CI in this case an  $m^6$  problem. For the case of only single and double substitutions in a many electron system each configuration can be defined by four indices with respect to the reference state. This makes the automatic sorting of the coupling coefficients with respect to two running indices possible also in this case.

## The Full CI-Program for Three Valence Electrons

A computer program to correlate three electrons with full CI has been made based on the ideas in the earlier sections. This program was connected to the Gaussian integral part of the MOLECULE-package [9], and the SCF and molecular orbital transformation parts of the ALCHEMY package [10], to form a complete package for three electrons. In all steps of this package full advantage is taken of any available two-fold symmetry.

Since the completion of the program, two applications have been started. One on the system  $H + H_2$  together with B. Liu, and another together with H.F. Schaefer on  $H + Li_2$ . The timings given in tables 4 and 5 are from preliminary studies of these two reactions. A fairly detailed investigation of the timing was made on the largest calculation on  $H_3$  where one iteration takes 4.3 minutes. It was found that only a small fraction of this time, 15 seconds, was spent to read, identify and send the integrals to their proper subroutine. Of the rest one half of the time, 2 minutes, goes into index-handling and the other half goes into the actual floating point operations according to (10). The index-handling per integral is almost independent of the symmetry used, whereas the floating point operations are directly proportional to the number of Hamiltonian matrix elements different from zero, and thereby critically dependent on the symmetry. The increase in time per iteration as the symmetry is reduced, as shown by table 5, is therefore a consequence of both the increasing

Table 4: Timing data – different molecules and basis sets (calculations on IBM 360/195)

Molecule	Symmetry (used)	Number of Orbitals	Number of Configurations	Number of <sup>a</sup> Iterations	Time/Iteration minutes
$Li_2H$	$C_{2v}$ (linear)	25	1378	8	0.08
$Li_2H$	$C_{2v}$ (linear)	32	2928	8	0.25
$Li_2H$	$C_{2v}$ (perpendicular)	32	2593	7	0.21
$Li_2H$	$C_s$ (nonlinear)	32	5175	7	0.55
$H_3$	$D_{2h}$	48	5799	6	0.7
$H_3$	$D_{2h}$	57	9350	6	1.4

(a) This is the number of iterations required to reach convergence on the energy to 6 decimal places

Table 5: Timing data –  $H_3$  different symmetries (calculations on IBM 360/195)

Symmetry (used)	Number of Orbitals	Number of Integrals	Number of Configurations	Number of Matrix-elements Different from Zero	Time/Iteration minutes
$D_{2h}$	48	$0.9 \times 10^5$	5799	$2.3 \times 10^6$	0.7
$C_{2v}$ (linear)	48	$1.7 \times 10^5$	11655	$9 \times 10^6$	1.5
$C_s$ (nonlinear)	48	$3.7 \times 10^5$	20724	$28 \times 10^6$	4.3

number of integrals and the increasing number of Hamiltonian matrix-elements different from zero. The only way to reduce the time per integral, if the same number of orbitals are kept, is to reduce the number of configurations, which would reduce the floating point operations but not the index-handling. A preferable way to reduce the time per iteration would be to reduce the number of integrals by neglecting small integrals. However, in the large calculation of  $H_3$ , of the 370668 integrals, there are only 1534 integrals smaller than  $10^{-5}$ . This is of course due to the delocalized nature of the molecular orbitals obtained from an SCF-calculation. The use of other orbital-sets which would give more small integrals has not been thoroughly investigated.

Two numbers that illustrate the convenience of the present approach as compared to conventional CI in this case, are the number of integrals and the number of nonzero Hamiltonian matrix-elements. The construction and use of 28 million matrix-elements would not only be time consuming but also impractical on most computer installations, whereas the 370 thousand integrals would give no data handling problems.

#### Acknowledgement

I wish to thank Bowen Liu and Björn Roos for many valuable discussions. I am also grateful to Charles Bender, for the use of his program, and to Paul Bagus, Megumu Yoshimine and Ulf Wahlgren for the help to connect the MOLECULE and ALCHEMY programs to the CI-program. Finally I wish to thank the Miller Institute who sponsor my visit to California.

#### References

- [1] ROOS, B. (1972). *Chem. Phys. Letters*, **15**, 153.
- [2] NESBET, R.K. (1965). *J. Chem. Phys.*, **43**, 311.
- [3] SHAVITT, I. (1970). *J. Comp. Phys.*, **6**, 124.
- [4] LÖWDIN, P.O. (1965). *J. Math. Phys.*, **6**, 1341.
- [5] BRÄNDAS, E. and GOSCINSKI, O. (1970). *Phys. Rev.*, **1**, A552.
- [6] SAUNDERS, V.R. and HILLIER, I.H. (1973). *Int. J. Quantum Chem.*, **7**, 699.
- [7] GOSCINSKI, O. and BRÄNDAS, E. (1969). *Proceedings of the Vilnius International Symposium on the Shell Structure of Atoms and Molecules, 1969*.
- [8] BENDER, C., (private communication).
- [9] The MOLECULE package is written by J. Almlöf, B. Roos and P. Siegbahn. A description of the integral part is given in ALMLÖF, J. (1973). *Proceedings of the Second Seminar on Computational Problems in Quantum Chemistry Strasbourg 1972*, München: Max-Planck-Institut für Physik und Astrophysik.
- [10] The ALCHEMY computer programs were written by P. S. Bagus, B. Liu, A. D. McLean and M. Yoshimine of the Theoretical Chemistry Group of IBM Research in San José, California. Preliminary descriptions of the program are given by McLEAN, A. D., *Proceedings of the Conference on Potential Energy Surfaces in Chemistry held at the University of California, Santa Cruz, August 1970*.



# Electron Correlation in $BH$ and $H_4$ : A Numerical Comparison of Various Methods

G.A. van der Velde and W.C. Nieuwpoort\*

The correlation energy of the four valence electrons in  $BH$  and all four electrons of two parallel  $H_2$  molecules has been calculated using six different methods:

- (a) complete CI
- (b) CI based on all singly and doubly excited configurations
- (c) coupled electron-pairs (CEPA) following Kelly
- (d) independent electron-pairs (IEPA)
- (e) independent pair-potential (IPP) following Mehler
- (f) coupled pair-potential (CPPA)

The calculations on  $BH$  were done for several internuclear distances using canonical as well as localized SCF orbitals. The  $H_4$  calculations were carried out for two distances between the  $H_2$  molecules and only localized orbitals were employed.

In comparison with the reference calculation (a) the results of the IPP method are excellent, those of the IPA method poor. The other methods yield intermediate results: (e) > (f) > (c) > (b) > (d)

## Introduction

In most cases some form of configuration interaction (CI) is used for the calculation of correlation corrections to the wavefunction and the energy. However, in order to make numerical calculations feasible one has to truncate the CI expansion. In the literature a number of methods have been proposed to truncate the CI expansion. The approximations in the wavefunction have been justified with qualitative arguments, but to date only a few comparisons exist between rigorous CI results and the results of more approximate methods. In this paper we compare for two four-electron systems the results of a complete CI calculation with the results of the following methods:

- (a) CI calculations with only single and double substitutions with respect to the SCF wavefunction;
- (b) Independent electron pair approximation;
- (c) Coupled electron pair approximation;
- (d) Independent pair potential approximation;
- (e) Coupled pair potential approximation.

## Methods of Calculation

Starting from the closed shell SCF wavefunction  $\Phi_0$  we distinguish the following contributions to the correlated wavefunction of the valence electrons of  $BH$ :

- (a) The orbital polarizations or one-electron clusters  $\chi(2\sigma)$  and  $\chi(3\sigma)$ ;
- (b) The intra-orbital two-electron cluster  $\chi(2\sigma^2)$  and  $\chi(3\sigma^2)$ ;
- (c) The inter-orbital clusters  $\chi(2\sigma 3\sigma_S)$  and  $\chi(2\sigma 3\sigma_T)$  in which the  $2\sigma$  and  $3\sigma$  orbitals are coupled to a singlet and a triplet, state, respectively;
- (d) The three-electron clusters  $\chi(2\sigma^2 3\sigma)$  and  $\chi(2\sigma 3\sigma^2)$ ;
- (e) The four-electron cluster  $\chi(2\sigma^2 3\sigma^2)$ .

In a complete CI calculation all clusters are included in the wavefunction. However, this kind of calculation is very time-consuming because of the large number of terms in the three- and four-electron clusters. Since the two-electron clusters describe the main correlation correction a reasonable method to calculate correlation energies would be to include only the one- and two-electron clusters in the wavefunction. (This method will be denoted as CI(1+2) in the following). This method accounts only for the correlation between two-electrons at a time [1,2]. Consequently, the fraction of the correlation energy that is calculated with this method will become smaller for larger systems [1,2].

To remedy the shortcomings of the CI(1+2) method one has to include the effect of unlinked products of one- and two-electron clusters. Since it is expected that the main contribution to the four-electron cluster consists of a sum of products of two-electron

\* *Chemische Laboratoria der Rijksuniversiteit, Zernikelaan, Paddepoel, Groningen, Netherlands*

clusters [1,2], the interaction between the two-electron clusters and the unlinked product of two-electron clusters can be approximated as [3,4]

$$\langle \chi(2\sigma^2) | \mathcal{H} | \chi(2\sigma^2 3\sigma^2) \rangle \approx \langle \Phi_0 | \mathcal{H} | \chi(3\sigma^2) \rangle \langle \chi(2\sigma^2) | \chi(2\sigma^2) \rangle = \mathcal{E}(3\sigma^2) \langle \chi(2\sigma^2) | \chi(2\sigma^2) \rangle \quad (1)$$

$$\langle \chi(2\sigma 3\sigma; S) | \mathcal{H} | \chi(2\sigma^2 3\sigma^2) \rangle \approx \frac{1}{2} \mathcal{E}(2\sigma 3\sigma; S) \langle \chi(2\sigma 3\sigma; S) | \chi(2\sigma 3\sigma; S) \rangle \quad (2)$$

$$\langle \chi(2\sigma 3\sigma; T) | \mathcal{H} | \chi(2\sigma^2 3\sigma^2) \rangle \approx \frac{1}{6} \mathcal{E}(2\sigma 3\sigma; T) \langle \chi(2\sigma 3\sigma; T) | \chi(2\sigma 3\sigma; T) \rangle \quad (3)$$

$$\langle \chi(3\sigma^2) | \mathcal{H} | \chi(2\sigma^2 3\sigma^2) \rangle \approx \mathcal{E}(2\sigma^2) \langle \chi(3\sigma^2) | \chi(3\sigma^2) \rangle \quad (4)$$

where

$$\mathcal{E}(i) = \langle \chi(i) | \mathcal{H} | \Phi_0 \rangle \quad (5)$$

The interaction between one-electron clusters and three-electron clusters is similarly approximated as

$$\langle \chi(2\sigma) | \mathcal{H} | \chi(2\sigma^2 3\sigma) + \chi(2\sigma 3\sigma^2) \rangle \approx \left\{ \frac{1}{2} \mathcal{E}(2\sigma 3\sigma; S) + \frac{1}{2} \mathcal{E}(2\sigma 3\sigma; T) + \mathcal{E}(3\sigma^2) \right\} \times \langle \chi(2\sigma) | \chi(2\sigma) \rangle \quad (6)$$

$$\langle \chi(3\sigma) | \mathcal{H} | \chi(2\sigma^2 3\sigma) + \chi(2\sigma 3\sigma^2) \rangle \approx \left\{ \mathcal{E}(2\sigma^2) + \frac{1}{2} \mathcal{E}(2\sigma 3\sigma; S) + \frac{1}{2} \mathcal{E}(2\sigma 3\sigma; T) \right\} \times \langle \chi(3\sigma) | \chi(3\sigma) \rangle \quad (7)$$

In the calculation the interaction with three- and four-electron clusters is taken into account by using a different effective Hamiltonian for each one- and two-electron cluster. For instance for the intra-orbital cluster  $\chi(2\sigma^2)$  the effective Hamiltonian is taken to be

$$\mathcal{H}_{\text{eff}} = \mathcal{H} + \mathcal{E}(3\sigma^2) \quad (8)$$

The above method has been used first by Meyer [5], although he uses slightly different effective Hamiltonians. He proposed the name coupled electron pair approximation (CEPA) for his method. In the following we shall use this name also for the method with the above effective Hamiltonians.

In the independent electron pair approximation (IEPA) [6] the correlation energy is calculated for each two-electron cluster separately. For instance the correlation energy for the  $2\sigma^2$  pair is calculated from the trial wavefunction

$$\Phi_0 + \chi(2\sigma) + \chi(2\sigma^2) \quad (9)$$

In the IEPA method the interaction between two-electron clusters is neglected, and the interaction between two-electron clusters and four-electron clusters is overestimated [4].

In the independent pair potential approximation (IPPA) [7] the correlation problem is also split in a number of smaller problems. This method uses trial functions of the form

$$\Phi_0 + \chi(ii) + \chi(i) + \sum_{j(\neq i)} \{ \chi(j) + \chi(ij; S) + \chi(ij; T) \} \quad (10)$$

In this method all interactions are neglected between disjoint two-electron clusters, i.e. clusters which have no indices in common. The coupled pair potential approximation (CPPA) [4] differs from the CEPA

method in that the interactions between disjoint two-electron clusters are neglected.

## Results

**BH with canonical orbitals:** The calculations on *BH* were performed with a small contracted Gaussian basis set (4s- and 2p-functions on *B* and 2s- and 1p-function on *H*) for four internuclear distances. The results of the SCF calculation and the full CI calculation for the valence shells are shown in table 1. In order to test the validity of the approximations (1)-(7) we calculated the quantities

$$\Delta_4(i) = \langle \chi(i) | \mathcal{H} | \chi(2\sigma^2 3\sigma^2) \rangle / \langle \chi_i | \chi_i \rangle \quad (11)$$

and

$$\Delta_3(i) = \langle \chi(i) | \mathcal{H} | \chi(2\sigma^2 3\sigma) + \chi(2\sigma 3\sigma^2) \rangle / \langle \chi(i) | \chi(i) \rangle \quad (12)$$

Table 1: Correlation energy of the valence shell of *BH* in a full CI calculation with canonical SCF orbitals

<i>R</i> (au)	1.836	2.336	2.836	4.336
$E_c$	-0.0721	-0.0727	-0.0761	-0.0991
$\mathcal{E}(2\sigma^2)$	-0.0257	-0.0232	-0.0226	-0.0356
$\mathcal{E}(2\sigma 3\sigma; S)$	-0.0147	-0.0206	-0.0246	-0.0086
$\mathcal{E}(2\sigma 3\sigma; T)$	-0.0044	-0.0042	-0.0040	-0.0033
$\mathcal{E}(3\sigma^2)$	-0.0273	-0.0248	-0.0248	-0.0517

The results are shown in table 2. For reasons of comparison the results of the approximations (1)-(7) are shown in parenthesis. From the results given in

table 2 it is clear that the approximations (1)-(7) underestimate the interactions between two-electron clusters and three- and four-electron clusters. Furthermore it can be concluded that the approximations (6) and (7) overestimate the interaction between one- and three-electron clusters. This is probably due to the fact that the linked three-electron clusters are nearly as important as the unlinked product of one- and two-electron clusters. In the IEPA, IPPA and CPPA methods part of the interaction between two-electron clusters is neglected. These interactions are listed in table 3 ( $\chi(2\sigma3\sigma) = \chi(2\sigma3\sigma;S) + \chi(2\sigma3\sigma;T)$ ). It is seen that these interactions behave rather irregularly as a function of the internuclear distance.

Due to some imperfections in the computer program we were unable to discriminate between the  $\chi(2\sigma3\sigma;S)$  and  $\chi(2\sigma3\sigma;T)$  clusters in the CEPA and CPPA calculations. For these clusters the interactions with the four-electron clusters were taken to be zero instead of  $\frac{1}{2}\chi(2\sigma3\sigma;S)$  and  $\frac{1}{2}\chi(2\sigma3\sigma;T)$  respectively.

Table 2: Mean interaction between one- and two-electron correlation functions and three- and four-electron correlation functions

R(au)	1.836	2.336	2.836	4.336
$\Delta_4(2\sigma^2)$	-0.0341 (-0.0273)	-0.0358 (-0.0248)	-0.0386 (-0.0248)	-0.0528 (-0.0517)
$\Delta_4(2\sigma3\sigma;S)$	-0.0239 (-0.0074)	-0.0246 (-0.0103)	-0.0256 (-0.0123)	-0.0266 (-0.0043)
$\Delta_4(2\sigma3\sigma;T)$	-0.0108 (-0.0015)	-0.0099 (-0.0014)	-0.0101 (-0.0013)	-0.0128 (-0.0011)
$\Delta_4(3\sigma^2)$	-0.0339 (-0.0257)	-0.0338 (-0.0232)	-0.0310 (-0.0226)	-0.0295 (-0.0356)
$\Delta_3(2\sigma^2)$	-0.0152	-0.0201	-0.0237	-0.0117
$\Delta_3(2\sigma3\sigma;S)$	-0.0185	-0.0133	-0.0088	-0.0187
$\Delta_3(2\sigma3\sigma;T)$	-0.0714	-0.0782	-0.0874	-0.1169
$\Delta_3(3\sigma^2)$	-0.0128	-0.0116	-0.0108	-0.0121
$\Delta_3(2\sigma)$	-0.1057 (-0.0368)	-0.0151 (-0.0372)	0.0110 (-0.0391)	-0.0018 (-0.0577)
$\Delta_3(3\sigma)$	-0.0134 (-0.0352)	-0.0176 (-0.0356)	-0.0203 (-0.0369)	-0.0097 (-0.0415)

Table 3: Pair-pair interactions in a full valence-shell CI calculation on BH with canonical orbitals

R(au)	1.836	2.336	2.836	4.336
$\langle\chi(2\sigma^2) H \chi(2\sigma3\sigma)\rangle$	-0.0006	-0.0017	-0.0032	-0.0011
$\langle\chi(2\sigma^2) H \chi(3\sigma^2)\rangle$	0.0007	0.0013	0.0022	0.0013
$\langle\chi(2\sigma3\sigma) H \chi(3\sigma^2)\rangle$	0.0008	-0.0004	-0.0027	0.

Table 4: Results of calculations on BH with canonical orbitals

R(au)	1.836	2.336	2.836	4.336
$E$ (SCF)	-25.0645	-25.1056	-25.0871	-24.9928
$E_C$ (CI) <sup>a</sup>	-0.0721	-0.0727	-0.0761	-0.0991
$E_C$ (CI) <sup>b</sup>	-0.0688	-0.0694	-0.0724	-0.0917
$E_C$ (CEPA)	-0.0703	-0.0706	-0.0736	-0.0973
$E_C$ (IEPA)	-0.0743	-0.0718	-0.0706	-0.0992
$E_C$ (IPPA)	-0.0723	-0.0728	-0.0759	-0.1001
$E_C$ (CPPA)	-0.0716	-0.0731	-0.0779	-0.1002

(a) Full CI calculation

(b) CI calculation with singly and doubly excited configurations

Table 5: Correlation energy of the valence shells of BH in a full CI calculation with localized orbitals

R(au)	2.336	2.836	4.336
$E_C$	-0.0727	-0.0761	-0.0991
$\xi(2\sigma^2)$	-0.0284	-0.0295	-0.0399
$\xi(2\sigma3\sigma;S)$	-0.0057	-0.0070	-0.0096
$\xi(2\sigma3\sigma;T)$	-0.0042	-0.0040	-0.0033
$\xi(3\sigma^2)$	-0.0344	-0.0356	-0.0464

Table 6: Mean interaction between one- and two-electron correlation functions and three- and four-electron correlation functions

R(au)	2.336	2.836	4.336
$\Delta_4(2\sigma^2)$	-0.0375 (-0.0344)	-0.0389 (-0.0356)	-0.0475 (-0.0464)
$\Delta_4(2\sigma3\sigma;S)$	-0.0193 (-0.0029)	-0.0208 (-0.0035)	-0.0219 (-0.0048)
$\Delta_4(2\sigma3\sigma;T)$	-0.0098 (-0.0014)	-0.0101 (-0.0013)	-0.0128 (-0.0011)
$\Delta_4(3\sigma^2)$	-0.0292 (-0.0284)	-0.0313 (-0.0295)	-0.0381 (-0.0399)
$\Delta_3(2\sigma^2)$	-0.0118	-0.0134	-0.0055
$\Delta_3(2\sigma3\sigma;S)$	-0.0368	-0.0311	-0.0246
$\Delta_3(2\sigma3\sigma;T)$	-0.0781	-0.0874	-0.1170
$\Delta_3(3\sigma^2)$	-0.0122	-0.0102	-0.0134
$\Delta_3(2\sigma)$	-0.0224 (-0.0394)	-0.0136 (-0.0411)	-0.0052 (-0.0529)
$\Delta_3(3\sigma)$	-0.0172 (-0.0339)	-0.0139 (-0.0350)	-0.0069 (-0.0464)

Table 7: Pair-pair interactions in a full CI calculation on the valence shells of BH with localized orbitals

R(au)	2.336	2.836	4.336
$\langle\chi(2\sigma^2) H \chi(2\sigma3\sigma)\rangle$	0.0	-0.0004	0.0
$\langle\chi(2\sigma^2) H \chi(3\sigma^2)\rangle$	0.0001	0.0002	0.0006
$\langle\chi(2\sigma3\sigma) H \chi(3\sigma^2)\rangle$	0.0011	0.0009	-0.0032

Table 8: Results of the CEPA, IEPA, IPPA and CPPA calculations with localized orbitals

$R(\text{au})$	1.836	2.336	2.836	4.336
$E_C$ (CEPA)	-0.0707	-0.0714	-0.0746	-0.0971
$E_C$ (IEPA)	-0.0786	-0.0784	-0.0806	-0.0991
$E_C$ (IPPA)	-0.0723	-0.0730	-0.0762	-0.0996
$E_C$ (CPPA)	-0.0708	-0.0716	-0.0749	-0.0982

The results of the CI(1+2), IEPA, CEPA, IPPA and CPPA calculations are listed in table 4. As could be expected, the CI(1+2) calculation underestimates the correlation energy. The difference between the results of the IEPA and the full CI calculation behaves irregularly as a function of the internuclear distance. The IEPA method can certainly not be used with canonical orbitals to calculate potential curves. The CEPA and the CPPA methods underestimate the correlation energy. For these methods it is probably better to follow Meyer's suggestion [5] to use effective Hamiltonians of the form

(13)

$$\mathcal{H}_{\text{eff}} = \mathcal{H} + \sum_{k < \ell} \mathcal{E}(k\ell) \left\{ 1 - \frac{1}{4}(\delta_{ik} + \delta_{i\ell} + \delta_{jk} + \delta_{j\ell}) \right\}$$

The best results are obtained with the IPPA method, but this may be due to a fortunate cancellation of errors.

**BH with localized orbitals:** The calculations for BH were repeated with localized valence orbitals. The results are given in tables 5-8. As could be expected the results of the CEPA, IPPA and CPPA calculations are much less sensitive to localization of the orbitals than the results of the IEPA calculations. In general the results of the CEPA and IPPA calculations differ less than  $10^{-3}$  au from the results obtained with canonical orbitals.

$H_4$ : For the calculations on  $H_4$  the basis set consisted of 2  $s$ - and 1  $p$ - function on each  $H$  atom. The four  $H$  atoms were placed at the corners of a rectangle. The short side was 1.4 au. The calculations were performed for two distances  $d$  between the  $H_2$  molecules. The correlation calculations were carried out with localized orbitals  $\phi_b$  and  $\phi'_b$ . The results of the calculations are shown in tables 9-13. The most striking result of the full CI calculation are the large interactions between the interorbital two-electron clusters and the three-electron clusters, which shows the importance of the inclusion of three-electron clusters for the calculation of Van der Waals interaction.

Table 9: Complete CI calculations on  $H_4$

$d$	3.0	4.0
$E_C$	-0.073769	-0.070348
$\mathcal{E}(b^2)$	-0.035386	-0.034734
$\mathcal{E}(bb';S)$	-0.000952	-0.000314
$\mathcal{E}(bb';T)$	-0.002045	-0.000566

Table 10: Mean interactions between one- and two-electron clusters and three- and four-electron clusters

$d$	3.0	4.0
$\Delta_4(b^2)$	-0.035375 (-0.035386)	-0.034675 (-0.034734)
$\Delta_4(bb';S)$	-0.004773 (-0.000476)	-0.001411 (-0.000157)
$\Delta_4(bb';T)$	-0.011617 (-0.000341)	-0.009830 (-0.000094)
$\Delta_3(b^2)$	-0.003106	-0.001023
$\Delta_3(bb';S)$	-0.048744	-0.051714
$\Delta_3(bb';T)$	-0.078137	-0.076327
$\Delta_3(b)$	-0.039994 (-0.036885)	-0.038824 (-0.035174)

Table 11: CI calculations on  $H_4$  with single and double excitations

$d$	3.0	4.0
$E_C$	-0.072492	-0.069244
$\mathcal{E}(b^2)$	-0.034800	-0.034199
$\mathcal{E}(bb';S)$	-0.000925	-0.000304
$\mathcal{E}(bb';T)$	-0.001967	-0.000542

Table 12: IEPA calculations on  $H_4$

$d$	3.0	4.0
$E_C$	-0.074283	-0.070474
$\mathcal{E}(b^2)$	-0.035416	-0.034748
$\mathcal{E}(bb';S)$	-0.001129	-0.000325
$\mathcal{E}(bb';T)$	-0.002322	-0.000653

Table 13: Results of CEPA calculations on  $H_4$

$d$	4.0
$E_C$	-0.070287
$\mathcal{E}(b^2)$	-0.034722
$\mathcal{E}(bb';S)$	-0.000303
$\mathcal{E}(bb';T)$	-0.000539

## References

- [1] SINANOGLU, O. (1962). *J. Chem. Phys.*, **36**, 706, 3198.
- [2] ————— (1964). *Adv. Chem. Phys.*, **6**, 315.  
————— (1969). *Ibid.*, **14**, 239.
- [3] KELLY, H.P. (1964). *Phys. Rev.*, **A134**, 1450.  
————— (1964). *Ibid.*, **B136**, 896.  
————— (1969). *Adv. Chem. Phys.*, **14**, 129.
- [4] VAN DER VELDE, G.A. (1974). Ph.D. Thesis, Groningen.
- [5] MEYER, W. (1971). *Int. J. Quantum Chem.*, **S5**, 341.  
————— (1973). *J. Chem. Phys.*, **58**, 1017.
- [6] KUTZELNIGG, W. (1972). *Selected Topics in Molecular Physics* (ed. E. Clementi), 91-102, Weinheim: Verlag Chemie.
- [7] MEHLER, E.L. (1973). *Int. J. Quantum Chem.*, **S7**, 437.

# Investigations of Molecular Electronic Structure using Spin Optimised Self Consistent Field Wavefunctions

N.C.Pyper and J.Gerratt\*

The spin optimised self-consistent field (SOSCF) wavefunction for an  $N$  electron system can be described as the best antisymmetrised Hartree product of  $N$  spatial orbitals multiplied by a linear combination of  $N$ -electron spin eigenfunctions.

Some properties of the SOSCF function are discussed. It is shown that such functions are the most general ones yielding an independent particle interpretation, and that unlike the Hartree-Fock function, they can be used to describe the potential energy surface of a molecule. In addition, SOSCF functions can yield a good description of the density of unpaired spin at the nucleus of an atom, even when the unpaired electron occupies a  $p$  orbital. The relation between the SOSCF, HF and VB methods, and the types of correlation described by the SOSCF method are discussed, and it is shown that SOSCF orbitals are, in general, non-orthogonal and have no radial nodes. An expansion of the wavefunction having the SOSCF function as the leading term is used to discuss the errors in properties calculated from SOSCF functions. From this we conclude that one-electron properties are given to second order accuracy, that the calculated binding energies are always less than the observed, and that calculated equilibrium internuclear distances are always greater than the corresponding experimental values.

The computational problems raised by the orbital non-orthogonality are discussed, and useful relations between density matrices presented. These are then used to derive compact expressions for the energy and its first and second derivatives. Techniques for optimising SOSCF functions are discussed from which we conclude that a direct approach using first and second derivatives is efficient and reliable. Results of calculations on  $LiH$ ,  $Li_2$  and  $CH^+$  are presented and discussed.

## Introduction

This paper presents some theoretical properties and model calculations with spin optimised self-consistent field (SOSCF) wavefunctions. For an  $N$  electron system an SOSCF function is of the form

$$\Phi = \sqrt{N!} \mathcal{A} \left( \prod_{i=1}^N \phi_i(i) \sum_k c_k \theta_{SMk}^N \right), \quad (1)$$

where  $\phi_i$  is a purely spatial one electron orbital,  $\theta_{SMk}^N$  an  $N$ -electron spin function, and  $\mathcal{A}$  is the idempotent antisymmetriser. The spatial orbitals and the expansion coefficients  $c_k$  occurring in the spin dependent part of the wavefunction are optimised according to the least energy criterion. The SOSCF function is an eigenfunction of the square of the total

spin,  $\hat{S}^2$ , and of its component along an arbitrary axis  $z$ , with eigenvalues  $S$  and  $M$  respectively.

$$\begin{aligned} \hat{S}_z \theta_{SMk}^N &= M \theta_{SMk}^N \\ \hat{S}^2 \theta_{SMk}^N &= S(S+1) \theta_{SMk}^N \end{aligned} \quad (2)$$

The label  $k$  in this equation distinguishes different linearly independent functions having the same values of  $S$  and  $M$  [1].

The SOSCF method can be regarded as a synthesis of the valence-bond and Hartree-Fock methods since both these classes of wavefunction are subsets of (1). Thus the SOSCF function reduces to a single structure valence-bond function if atomic orbitals are employed, whilst the Hartree-Fock function results if the orbitals are constrained to be identical in pairs. In this case equation (1) becomes

$$\Phi_{HF} = \sqrt{N!} \mathcal{A} \left( \prod_{i=1}^{N/2} \phi_i(2i-1) \phi_i(2i) \sqrt{1/2} (\alpha\beta - \beta\alpha) \sqrt{1/2} (\alpha\beta - \beta\alpha) \dots \right) \quad (3)$$

\* Department of Theoretical Chemistry, University of Bristol, Cantock's Close, Bristol, BS8 1TS

the antisymmetriser causing all other spin functions to vanish. The SOSCF method like the Hartree-Fock method can be given an independent particle interpretation see below. However, in contrast to the Hartree-Fock theory, the SOSCF method for molecules leads to a correct description of dissociation products.

### Calculation and Optimisation of the Energy

The evaluation of the energy is considerably more complicated than in the Hartree-Fock case because SOSCF orbitals are in general non-orthogonal. It is not possible to orthogonalise the orbitals by subjecting them to a linear transformation among themselves without changing the SOSCF wavefunction. It proves convenient to define density matrices  $D^{(1)}$ ,  $D^{(2)}$ , whose elements are such that  $D^{(1)}(ik)$  is the coefficient of  $\phi_k^*(q)\phi_i(q)$  in

$$N \int \Phi^* \Phi d\tau_1 \dots d\tau_{q-1} d\tau_{q+1} \dots d\tau_N d\sigma_1 \dots d\sigma_N, \quad (4a)$$

and  $D^{(2)}(ijkl)$  is the coefficient of  $\phi_k^*(q)\phi_l^*(q')\phi_i(q)\phi_j(q')$  in

$$N(N-1) \int \Phi^* \Phi d\tau_1 \dots d\tau_{q-1} d\tau_{q+1} \dots d\tau_{q'-1} d\tau_{q'+1} \dots d\tau_N d\sigma_1 \dots d\sigma_N, \quad (4b)$$

where  $d\tau$  is a spatial volume element,  $\int d\sigma_i$  represents integration over the spin co-ordinates of the  $i^{\text{th}}$  electron, and  $q$  and  $q' \neq q$  are electronic coordinates.

Defining the usual non-relativistic electronic Hamiltonian  $\hat{\mathcal{H}}$  to be

$$\hat{\mathcal{H}} = \sum_i h(i) + \sum_{i>j} g_{ij} \quad (5)$$

one has by virtue of equations (4)

$$\langle \Phi | \hat{\mathcal{H}} | \Phi \rangle = \sum_{ik} D^{(1)}(ik) \langle k | \hat{h} | i \rangle + \frac{1}{2} \sum_{ijkl} D^{(2)}(ijkl) \langle k\ell | \hat{g} | ij \rangle \quad (6)$$

A useful expression for the normalisation integral can be derived by noting that it is not necessary to antisymmetrise both the bra and the ket. Thus one has

$$\langle \Phi | \Phi \rangle = \langle \phi_1 \phi_2 \dots \phi_N \theta_{SM} | N! \mathcal{A}(\phi_1 \phi_2 \dots \phi_N \theta_{SM}) \rangle = \sum_k D^{(1)}(ik) \langle k | i \rangle \text{ for all } i. \quad (7)$$

By using similar expressions to equation (7), a whole set of recurrence relations between different density matrices can be derived [2]. Thus:

$$D^{(1)}(ik) = \sum_{\ell} D^{(2)}(ijk\ell) \langle \ell | j \rangle \quad \text{for all } j$$

$$D^{(2)}(ijkl) = \sum_n D^{(3)}(ijmkn) \langle n | m \rangle \text{ for all } m \quad (8)$$

etc.

Now the problem of optimising the expectation value of the energy  $W = \langle \Phi | \hat{\mathcal{H}} | \Phi \rangle / \langle \Phi | \Phi \rangle$  subject to the constraint that the orbitals remain normalised, can be replaced by an equivalent problem of minimising the functional

$$F = W - \sum_i \epsilon_i \langle i | i \rangle \quad (9)$$

without constraints. The parameters  $\epsilon_i$  occurring in equation (9) are the usual Lagrange multipliers.

By using the recurrence relations (8), the requirement that  $F$  be stationary with respect to small variations in the orbitals can be expressed as

$$\hat{F}_i | i \rangle = \epsilon_i | i \rangle \quad (i=1,2 \dots N) \quad (10)$$

where  $\hat{F}_i$  is an effective operator for the  $i^{\text{th}}$  orbital. Each orbital is thus an eigenfunction of a distinct effective operator. This is in contrast to the Hartree-Fock method where all the orbitals are eigenfunctions of a single operator. However, the conceptual simplicity of the Hartree-Fock approach is still retained here, since each electron can be regarded as moving in the average field of all the other electrons. One can therefore usefully discuss the changes in the orbital energies  $\epsilon_i$  with nuclear configuration in terms of correlation diagrams.

### Computation of the Wavefunction

All the required density matrices are calculated using the recurrence technique (8) starting from the  $N$ -electron density matrix elements  $D^{(N)}(1\ 2\ 3 \dots N\ 1'2'3' \dots N')$ . In terms of the representation matrices  $U_{SMk}^{SN}(P)$  generated by the basis for the spin functions  $\theta_{SMk}^N$ , these are given by

$$D^{(N)}(1\ 2\ 3 \dots N\ 1'2'3' \dots N') = \sum_{k\ell} c_k c_{\ell} U_{k\ell}^{SN}(P) \quad (11)$$

where  $P$  is the permutation  $(1\ 2\ 3 \dots N\ 1'2'3' \dots N')$  and the  $c_k, c_{\ell}$  are the same coefficients as in equation (1). In the present work, the Young-Yamanouchi-Kotani basis of spin functions [1] were chosen. The advantage of this formulation is that the  $U^{SN}$  matrices are purely group-theoretical quantities and so for a given  $N$  and  $S$  can be calculated once and for all.

A general program has been written for this purpose. The matrices corresponding to the simple transpositions  $P_{12}, P_{23}, \dots, P_{N-1N}$  are computed first as described by Kotani [1], and the other  $U^{SN}$  are obtained by matrix multiplication.

The orbitals  $|i\rangle$  are approximated by an expansion in a finite basis of Slater atomic orbitals  $|x\rangle$

$$|i\rangle = \sum_x c_{xi} |x\rangle \quad (12)$$

The orbital equations (10) are converted by this into a set of finite dimensional matrix equations which could be solved iteratively as in Hartree-Fock theory. However this process converges very slowly since the whole of the operators  $F_i$  change during the minimisation. By contrast, only the two-electron part of the Hartree-Fock operator is modified by iteration, the one-electron (core nucleus) terms remaining unaltered.

The coefficients  $c_{xi}$  and  $c_k$  were therefore optimised by minimising  $W$  directly. Since the absolute values of  $\langle i|i\rangle$  are of no ultimate significance, the uniqueness of the minimisation problem was ensured by fixing one coefficient in each orbital on an arbitrary value. Similarly, since only the ratios of the  $c_k$  parameters are significant, one such parameter was held constant during the iterative process. The orbitals are normalised and the  $c_k$ 's scaled such that  $\sum_k c_k^2 = 1$  after the optimum values have been determined. This procedure is numerically stable provided that the fixed parameters do not make small contributions to the optimised wavefunction. This possibility is always simple to avoid.

The direct minimisation method which was used requires the calculation of the vector ( $\mathbf{g}$ ) of first derivatives of  $W$  with respect to the parameters  $c_{xi}$  and  $c_k$ , and also the corresponding matrix  $\mathbf{G}$  of second derivatives. From these, vectors ( $\delta\mathbf{c}$ ) of corrections to the parameters are calculated from the relation

$$(\mathbf{G} + \lambda\mathbf{I}) \cdot \delta\mathbf{c} = -\mathbf{g}, \quad (13)$$

where  $\mathbf{I}$  is the unit matrix and  $\lambda$  a positive scalar. The scalar  $\lambda$  is set to zero if  $\mathbf{G}$  is positive definite and either all the eigenvalues have changed by less than 1/3 of their values during the previous two iterations, or if the smallest eigenvalue of  $\mathbf{G}$  is greater than  $\bar{D}/10^3$  where  $\bar{D}$  is the average of the moduli of the eigenvalues. In both these circumstances the parameters are close to their optimum values and the iteration reduces to the quadratically convergent Newton-Raphson method. However if the eigenvalues of  $\mathbf{G}$  satisfy neither of these conditions, the parameters are too far from their optimum values for the Newton-Raphson iteration to be stable, and the scalar  $\lambda$  is then set to  $\sum_i g_i^2 / (E_{\text{calc}} - E_{\text{exp}})$ . If the eigenvalues of  $(\mathbf{G} + \lambda\mathbf{I})$  with  $\lambda$  thus calculated do not satisfy the second of the above conditions,  $\lambda$  is set to  $\bar{D}/10^3$  and corrections  $\delta\mathbf{c}$  calculated. If these corrections are unreasonably large,  $\lambda$  is set to  $\bar{D}/5.0$ . These iterations using a non-zero value of  $\lambda$  correspond to a mixture of the Newton-Raphson and steepest descent methods [3]. This minimisation method has the advantage not only that few (usually 10-15) iterations are required, but also that this number is independent of the number

of parameters to be optimised. (This is typically in the range 40-100.) Other direct minimisation techniques, such as that of Davidon [4,5], which require calculation only of  $W$  and the gradient vector ( $\mathbf{g}$ ), were tried and found to be unsatisfactory. This is because such methods require  $\sim 3n$  iterations, where  $n$  is the number of variables. Thus, for example, a calculation on the  $Li$  atom using Davidon's method with 19 parameters required 120 evaluations of  $W$  and of  $\mathbf{g}$  before convergence was reached.

Compact analytic expressions for the elements of the gradient vector and of the second derivative matrix are readily derived using the recurrence relations (8).

Table 1

	$R_e$ (Bohr)		$D_e$ (eV)		
	Calculated	Experiment	HF	SOSCF	Experiment
$LiH$	3.095 (2.6%)	3.015	1.49 (51%)	1.92 (76%)	2.51
$BH$	2.361 (1.3%)	2.329	2.76 (77%)	3.28 (91%)	3.58
$CH^+$	2.157 (0.9%)	2.137	3.17 (76%)	3.88 (94%)	4.10
$Li_2$	5.550 (8.9%)	5.051	0.12 (11%)	0.44 (42%)	1.05

## Results

Calculations have been carried out for the systems  $LiH$ ,  $BH$ ,  $CH^+$ ,  $X^1\Sigma^+$ , and  $Li_2$ ,  $X^1\Sigma_g^+$ . Each SOSCF orbital was expanded in a basis set of Slater orbitals, the basis consisting of 14 of such functions for  $LiH$ , 18 for  $CH^+$  and 22 for  $Li_2$ . The results, together with corresponding ones from Hartree-Fock calculations, are shown in table 1.

The interpretation of these results is aided by noting that to first order the exact wavefunction can be written as a linear combination of the SOSCF function, and terms describing electron pair correlations. Since the SOSCF function is a good approximation to the exact wavefunction for all internuclear distances, it can be shown from this that dissociation energies calculated by the SOSCF method are always less than the experimental values, and that calculated equilibrium internuclear distances are always greater than the observed values. Since the Hartree-Fock function describes dissociation incorrectly, only the first of these two results applies. Neither result holds for a CI wavefunction. The results in table 1 corroborate these theorems and furthermore show that the SOSCF method yields a highly realistic description of the bonding except for the case of  $Li_2$ . It should be noted, however, that Hartree-Fock theory predicts only 11% of the binding energy in this



molecule. One might expect to improve the  $Li_2$  results significantly by adding a second configuration in which the two  $\sigma$  bonding orbitals are replaced by two  $\pi$  orbitals thus introducing some angular correlation. Terms describing this kind of correlation are absent in a single configuration SOSCF function.

A dipole moment function for  $LiH$  has also been calculated. Its calculated value at the calculated equilibrium internuclear distance is  $5.763D$  compared with the experimental value of  $5.828D$  at the experimental internuclear distance. The calculated value of this quantity rises to  $6.760D$  at  $R = 5.0$  Bohrs and drops to  $1.150D$  at  $R = 8.0$  Bohrs.

## References

- [1] KOTANI, M., AMEMIYA, A., ISHIGURO, E. and KIMURA, T. (1963). *Table of Molecular Integrals*, 1.
- [2] GERRATT, J. (1971). *Adv. Atomic Mol. Phys.*, 7, 141.
- [3] POWELL, M.J.D. (1970). *S.I.A.M. Rev.*, 12, 79.
- [4] DAVIDON, W.C. (1959). *A.E.C. research and development report*.
- [5] FLETCHER, R. and POWELL, M.J.D. (1963). *Comp. J.*, 6, 163.

# Molecular Spectroscopic Constants by the Coupled Electron Pair Approach

W.Meyer\*

Highly correlated variational wavefunctions based on a single dominant SCF determinant do not lead to good spectroscopic constants unless they take account of the small but rapidly changing contributions of more-than-doubly substituted configurations. This can be done approximately by the Coupled Electron Pair Approach. Potential energy curves have been calculated for the diatomic hydrides from *LiH* to *HCl* as well as for *H<sub>2</sub>O*, *CH<sub>4</sub>* and *N<sub>2</sub>*. Typical deviations between CEPA spectroscopic constants and observed values for the diatomic hydrides are as follows:

$$R_e \pm 0.003 \text{ \AA}, \omega_e \pm 20 \text{ cm}^{-1}, \omega_e x_e \pm 3 \text{ cm}^{-1}, D_e + 0.25 \text{ eV}, \mu_e + 0.04 \text{ D}.$$

The calculated force constants of *H<sub>2</sub>O* and *CH<sub>4</sub>* are also in very satisfying agreement with observed data except for the experimentally ill-defined stretching constant in *CH<sub>4</sub>*.

## Methods for Calculating Potential Energy Curves

In most cases the traditional one-determinant Hartree-Fock wavefunction does not allow for a correct dissociation into atomic or molecular fractions. That not only makes this method inadequate for calculating potential curves but also renders difficult the treatment of the electron correlation. Ideally, one has to correlate all configurations which are required for a correct dissociation, that is single and double substitutions with respect to all of these configurations should be included in a variational CI calculation. This represents a formidable problem. In order to reduce it, several well known procedures have been proposed: multiconfiguration SCF wavefunctions [1, 2], full CI with respect to a minimal basis set [3], first order wavefunctions coupled with natural orbital iteration [4]. These schemes have drastically improved upon the HF method. However, since they give only a small fraction of the total correlation, the curves corresponding to different electronic states will in general have to be shifted relative to each other by fitting them to data of the fractions. Their success with respect to the shape of the potential curve depends on a critical balance between the neglected parts of the 'extra molecular correlation' (due to restriction of number and type of the configurations) and the parts of the 'atomic correlation' accounted for in the molecule.

Since there seems to be no unambiguous way of separating the extra molecular correlation, one would like to fully treat the valence shell of that part of the molecule involved in the deformation process. For nuclear distances not too far from the equilibrium position the Hartree-Fock configuration is usually the

only dominant one, the coefficients of the additional configurations required for correct dissociation still being small though rapidly increasing with distance. Double substitutions which correlate these configurations are usually quadruple substitutions with respect to the HF configuration. We may therefore argue that a coupled electron pair approach as recently proposed [5,6], which approximately includes those types of configurations, should be able to adequately treat both the extra molecular correlation and the configurations of rapidly increasing importance. We thus expect this approach to yield reasonable spectroscopic constants characterizing the shape of the potential surface around the equilibrium. In comparison with the MC-SCF we may describe the CEPA as follows: instead of assuming large fractions of the correlation

- (a) to be constant during the deformation, and
- (b) to be equal for all explicitly considered configurations,

it keeps only assumption (b) by transferring appropriate parts of the correlation energy calculated for the reference configuration to the other configurations of the CI.

The computational schemes used for the data to be presented here have been discussed in detail in [6] and shall only briefly be characterized.

PNO-CI: for each spin-irreducible electron pair  $P(a,b)$  a set of approximate pseudo-natural orbitals (PNO's)  $i_p$  is calculated perturbationally. All doubly substituted configurations of diagonal form,  $\phi_p^{i_p i_p}$ , contributing more than a certain energy threshold value are treated in a CI along with corresponding

\* Institut für Physikalische Chemie, Universität Mainz, 65 Mainz, POB 3980, West Germany

single substitutions. The particular feature of this CI is the use of partially nonorthogonal orbitals in order to ensure optimal convergence.

CEPA: In the eigenvalue equation for the coefficients  $C_P^i$  we simply replace the total correlation energy  $E^{\text{corr}}$  by the pair correlation energies

$$E_P^{\text{corr}} = \sum (\phi_{\text{HF}} | H | \phi_P^{iP} ) C_P^i$$

which corresponds to shifting the energy of the configuration  $\phi_P^i$  by the correlation contributions of all other pairs  $P' \neq P$  (for a slightly modified version differentiating between distinct and semidistinct pairs see [6]).

### Spectroscopic Constants for the Diatomic Hydrides from LiH to HCl

These hydrides have been investigated systematically in order to establish the quality of CEPA spectroscopic

Table 1: Calculated and experimental spectroscopic constants for diatomic hydrides<sup>a</sup>

Molecule	$r_e$	$B_e$	$\alpha_e$	$\omega_e$	$\omega_e x_e$	$D_e$	$\mu_e$	$d\mu/dr_e$
LiH <sup>b</sup>	1.599	7.48	0.212	1401.5	22.5	2.48	-5.90	-2.15
	1.595	7.51	0.213	1405.7	23.2	2.52	-5.88	-2.14
BeH <sup>b</sup>	1.342	10.33	0.291	2077.2	34.5	2.14	-0.27	-1.95
	1.343	10.32	0.303	2060.8	36.3	(2.30)		
BH	1.238	11.91	0.406	2352.1	46.6	3.49	1.31	-2.90
	1.236	12.02	0.412	2366.9	49.4	3.54	1.27	
CH	1.122	14.40	0.545	2844.5	66.4	3.47	1.44	-1.65
	1.120	14.46	0.534	2858.5	63.0	3.65	1.40	
NH	1.039	16.60	0.648	3269.3	78.8	3.38	1.58	-0.72
	1.040	16.68	0.646	3266.0	78.5	3.67		
OH	0.971	18.85	0.727	3742.2	85.3	4.34	1.69	0.46
	0.971	18.87	0.714	3739.9	86.4	4.63	1.66	0.44
FH	0.917	20.94	0.783	4166.8	89.5	5.83	1.83	1.55
	0.917	20.95	0.795	4138.7	90.1	6.12	1.83	1.60
NaH <sup>b</sup>	1.891	4.88	0.132	1172.2	18.9	1.92	-6.67	-2.60
	1.887	4.90	0.135	1172.2	19.7	2.30		
MgH <sup>b</sup>	1.723	5.87	0.162	1525.6	26.1	1.40	-1.50	-3.05
	1.730	5.82	0.167	1497.0	32.4	(2.10)		
AlH <sup>b</sup>	1.645	6.41	0.185	1691.7	29.6	3.13	-0.18	-3.76
	1.646	6.40	0.188	1682.6	29.1	(3.01)		
SiH	1.526	7.44	0.216	2034.7	36.0	3.09	0.11	-2.48
	1.520	7.50	0.219	2041.8	35.5	3.32		
PH	1.426	8.49	0.251	2365.9	44.8	3.04	0.48	-1.39
	1.422	8.54	(0.27)	(2380.)		3.34		
SH	1.344	9.55	0.285	2676.4	50.0	3.55	0.81	-0.22
	1.340	9.61	(0.30)	(2702.)	(60.0)	3.70		
HCl	1.278	10.54	0.309	2977.2	53.2	4.43	1.13	0.86
	1.275	10.59	0.307	2991.1	52.8	4.62	1.09	0.92

(a) in units of Å, cm<sup>-1</sup>, eV, D and D/Å

(b) including intershell correlation between valence shell and next lower core shell

constants [7]. We used Gaussian type basis sets of the size 11s,6p,2d,1f for the first-row atoms, 13s,8p,2d,1f for the second-row atoms and 6s,2p,1d for hydrogen. Our Hartree-Fock results agree nicely with those of Cade and Huo [8]. By employing an energy threshold of 0.0001 au the variational PNO-CI yielded somewhat above 80% of the valence shell correlation for the first row and probably only few per cent less for the second row.

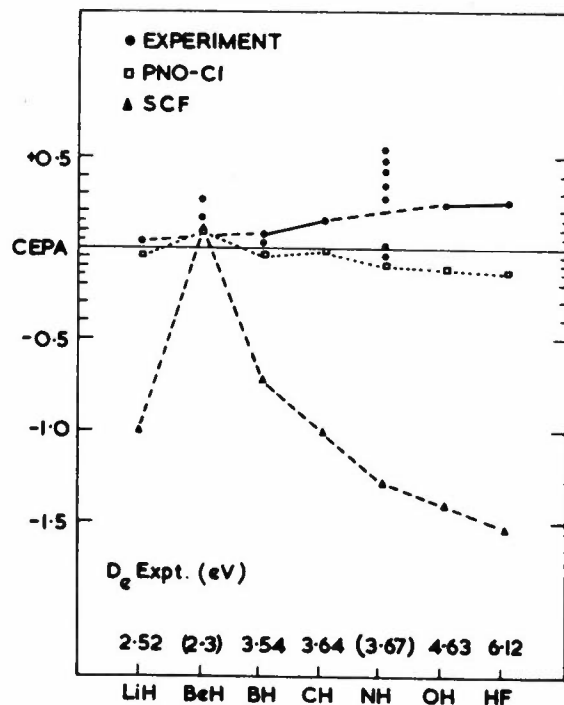


Figure 1: Comparison of  $D_e$  values

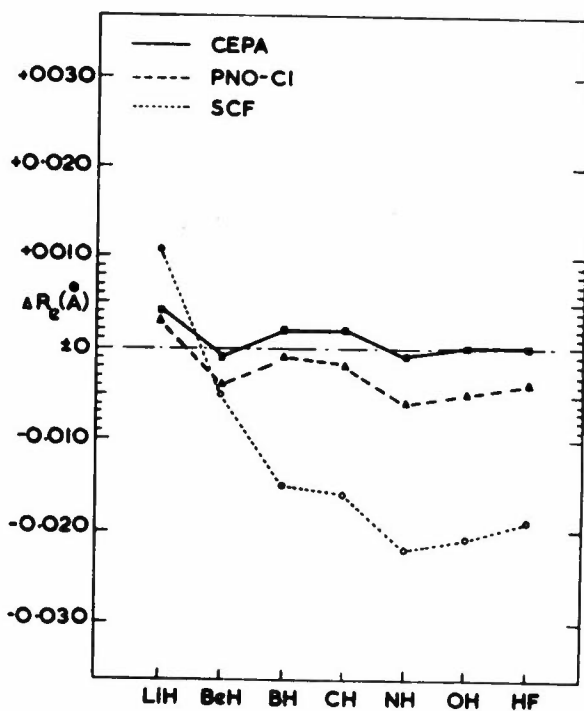


Figure 2: Equilibrium distances ( $R_e$  calc. -  $R_e$  expt.)

The spectroscopic constants obtained by the CEPA are compared with observed values in table 1. Figures 1 to 4 illustrate some of the results including constants from Hartree-Fock and PNO-CI. The average deviations as given in the abstract prove that the CEPA does give rather reliable constants. The systematic behaviour of the  $D_e$  seems to allow for a critical assessment of some experimentally ill-defined dissociation energies.

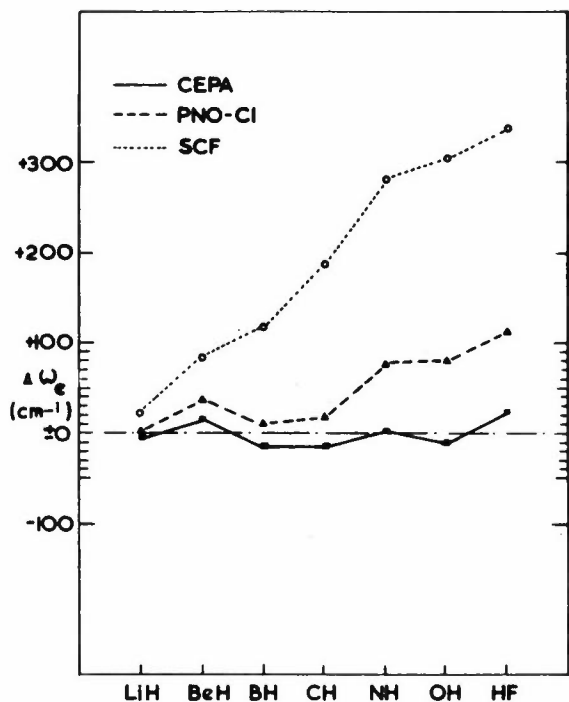


Figure 3: Vibrational constants ( $\omega_e$  calc. -  $\omega_e$  expt.)

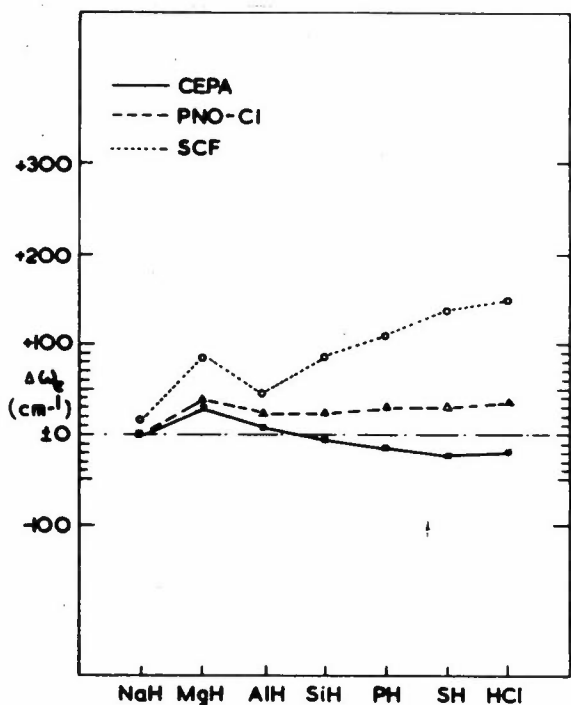


Figure 4: Vibrational constants ( $\omega_e$  calc. -  $\omega_e$  expt.)

## Near Equilibrium Energy Surface for $H_2O$ , $CH_4$ and $N_2$

The results given in tables 2 and 3 [8] show that the surface of the polyatomic hydrides has been reproduced with about the same accuracy as was obtained for the diatomic hydrides. The deviations of the calculated harmonic frequencies from experimental values are around 2% with two exceptions:

- The coupling constant  $f_{r\alpha}$  of the recent force field of Smith and Overend [10] is certainly in error by nearly a factor of 2.
- The anharmonicity correction to the experimental symmetric stretching constant in  $CH_4$ ,  $F_{11}$ , is most probably over estimated. It uses an anharmonicity constant  $X_{11} = 65 \text{ cm}^{-1}$  as compared to our theoretical value of  $13.6 \text{ cm}^{-1}$  which is in line with the  $CH$  anharmonicity of  $63 \text{ cm}^{-1}$  (a factor 1/4 is due to the larger reduced mass [6]).

Table 2: Constants of the near-equilibrium energy surface of  $H_2O$

	Experimental		Theoretical	
	[9]	[10]	HF	CEPA
$r_e$	0.9572		0.9405	0.9550
$\alpha_e$	104.52		106.41	105.07
$f_r$	4.228	4.218	4.842	4.321
$f_\alpha$	0.349	0.371	0.376	0.360
$f_{rr'}$	-0.101	-0.12	-0.061	-0.096
$f_{r\alpha}$	0.246	0.47	0.233	0.243
$f_{\alpha\alpha\alpha}$	-0.127	-0.198	-0.127	-0.112
$f_{rrr}$	-9.98	-9.57	-10.92	-9.81
$f_{rrrr}$	16.8	15.2	15.4	15.7

Table 3: Force constants of  $CH_4$

	Experimental [11]		Theoretical	
	Anharmonic	Harmonic	HF	CEPA
$F_{11}$	5.158	5.842	5.881	5.472
$F_{22}$	0.469	0.486	0.537	0.491
$F_{33}$	5.014	5.383	5.382	5.322
$F_{34}$	0.200	0.206	0.202	0.202
$F_{44}$	0.430	0.458	0.512	0.469
$r_e$	1.094	1.085	1.083	1.091

Table 4: Spectroscopic constants of  $N_2$ 

Method	$r_e$	$B_e$	$\alpha_e$	$\omega_e$	$\omega_e x_e$
HF	1.070	2.102	0.013	2712.2	13.2
PNO-CI	1.090	2.031	0.015	2540.4	14.3
CEPA	1.098	1.997	0.016	2437.1	16.1
Experimental	1.098	1.997	0.018	2358.0	14.2

Table 4 shows some preliminary results on  $N_2$  obtained with a relatively small basis set of size  $10s,5p,1d$ .

We would like to conclude by pointing out that the correlation corrections to  $r_e$  and  $\omega_e$  from the variational PNO-CI and the CEPA have a ratio of about 7/10 with the CEPA showing the much better over-all agreement with experiment.

### References

- [1] DAS, G. and WAHL, A.C. (1966). *J. Chem. Phys.*, **44**, 87.  
 ——— and ——— (1971). *Ibid.*, **56**, 1769.  
 WAHL, A.C. and DAS, G. (1970). *Adv. Quantum Chem.*, **5**, 261.
- [2] LEVY, B. (1970). *Int. J. Quantum Chem.*, **4**, 297.  
 HINZE, J.A. (1972). *J. Chem. Phys.*, **57**, 4928.
- [3] HARRIS, F.E. and MICHELS, H.H. (1967). *Int. J. Quantum Chem.*, **S1**, 329.  
 MICHELS, H.H. and HARRIS, F.E. (1969). *Chem. Phys. Letters*, **3**, 441.
- [4] SCHAEFER, H.F. and HARRIS, F.E. (1968). *Phys. Rev. Letters*, **21**, 1561.  
 PEARSON, P.K., BENDER, C.F. and SCHAEFER, H.F. (1971). *J. Chem. Phys.*, **55**, 5235.  
 BONDYBEY, V., PEARSON, P.K. and SCHAEFER, H.F. (1972). *J. Chem. Phys.*, **57**, 1123.
- [5] MEYER, W. (1971). *Int. J. Quantum Chem.*, **S5**, 341.  
 ——— (1973). *J. Chem. Phys.*, **58**, 1017.
- [7] MEYER, W. and ROSMUS, P., (to be published).
- [8] MEYER, W. and PULAY, P., (to be published).
- [9] KUCHITSU, K. and MORINO, Y. (1965). *Bull. Chem. Soc. Japan*, **38**, 814.
- [10] SMITH, D.F. and OVEREND, J. (1972). *Spectroch. Acta*, **28A**, 471.
- [11] DUNCAN, J.L. and MILLS, I.M. (1964). *Spectroch. Acta*, **20**, 523.

# Calculation of Electron Affinities of Atoms in the Second Long Row

C.Moser\* and R.K.Nesbet†

Results are presented in this paper for the calculation of electron affinities of the ground state of *Al*, *Si*, *P*, *S*, and *Cl*. The contributions to the correlation energies have been calculated using orbital excitations to construct one- and two-particle Bethe-Goldstone equations built on *s*, *p*, *d*, *f* basis sets. The results are in very good agreement with experiment.

## Introduction

As this is a paper which deals with the computation of correlation energies, it may be wise to start out with a definition of this quantity. For our purposes correlation energy will be the difference between the restricted Hartree-Fock energy and the observed non-relativistic energy.

For light atoms, at least, this is a well defined quantity. It is straightforward to calculate the Hartree-Fock energy as well as the relativistic energy and the successive ionizations are known, so the difference is known and can be compared with calculation. For heavier atoms, the successive ionizations are not known all the way to the last 1s electron so in fact calculation is the only way to have an idea of the total energy.

For molecules, the problem is more complex. Except for molecules made up of few light atoms (probably four is the limit) then the Hartree-Fock energy is not known even approximately, calculations of the relativistic energy do not yet exist, and the successive ionizations have not all been observed by any means.

It might be worthwhile for a conference like this one which assembles a large number of experts in the field to decide whether the definition we gave above is suitable for molecules. In particular we think that there is a real problem in many molecular calculations. Using a minimum basis set which gives an SCF energy far higher than the Hartree-Fock energy, then one proceeds to do a configuration interaction calculation presumably to introduce correlation energy effects!

In atoms Hartree-Fock functions are very useful. For example, the ordering of the energies of states belonging to the same configuration is generally correct and the calculated energy differences are of the correct order of magnitude. Excitation energies

in the valence shell are also reasonably well represented and excitations to Rydberg orbitals should be in very good agreement as this is essentially a one-electron phenomenon. Ionization energies are also in reasonable agreement particularly as one goes to a higher number of ionization.

There are a number of observables which are not at all well represented by Hartree-Fock functions and among these is the computed binding energy of the addition of an electron to a neutral atom. As can be seen in table 1, column (A), the agreement between Hartree-Fock and observed binding energies of an electron to the ground state of *Al*, *Si*, *P*, *S*, and *Cl* is in very poor agreement with experiment. The relative error is very large for all atoms. The binding energy for an electron to *P* is predicted to be positive while in fact *P*<sup>-</sup> is quite stable. The prediction for *Al* is so weakly binding that one would not expect *Al*<sup>-</sup> to be stable while in fact it is. Nor is there any agreement even in the relative order of binding energies.

## Bethe-Goldstone Calculations

In view of the success of previous work in the electron affinities of atoms in the first long row [1] we have computed correlation contributions to the electron affinities of these atoms using orbital excitations [2] to construct one- and two-particle Bethe-Goldstone equations built on *s*, *p*, *d*, *f* basis sets.

The use of Bethe-Goldstone equations to calculate correlation energy contributions has been described in detail elsewhere [3,4] and there would be no need to repeat this here. But it might be useful to recall the essential idea.

Instead of calculating a many-electron correlated wavefunction, one calculates the individual independent particle contributions to the correlation energy to as high an order as is necessary.

\* Centre Européen de Calcul Atomique et Moléculaire, Bâtiment 506, Université de Paris XI, 91405 Orsay, France

† IBM Research Laboratory, San José, California 91493, USA

Experience gained up to now has indicated that one- and two-particle equations built on orbital excitations are likely to be reasonably accurate and take relatively small amounts of computer time.

For the atoms *Al*, *Si*, *P*, *S* and *Cl* then the computed electron affinities including correlation contributions thus calculated are in very good agreement with experiment, see table 1, columns (B) and (C). The difference of a few hundredths of an electron-volt are not significant since the 'experimental' results are not those of electron-attachment experiments but the extrapolation of the electron affinity of  $H^-$  by Edlen [5].

Table 1: Electron affinities (eV) from:

- A Hartree-Fock functions
- B Hartree-Fock functions plus correlation contributions obtained from one- and two-particle Bethe-Goldstone equations
- C experiment [5]

Processes	A	B	C
$Al(^2P) \rightarrow Al^-(^3P)$	-0.03	-0.49	-0.52
$Si(^3P) \rightarrow Si^-(^4S)$	-0.96	-1.53	-1.46
$P(^4S) \rightarrow P^-(^3P)$	+0.54	-0.74	-0.77
$S(^3P) \rightarrow S^-(^2P)$	-0.91	-2.10	-2.15
$Cl(^2P) \rightarrow Cl^-(^1S)$	-2.58	-3.79	-3.70

If one compares these results to those obtained for *B*, *C*, *N*, *O* and *F* [1], there is rather better agreement for the second as compared with the first row electron affinities using the same level hierarchy of Bethe-Goldstone equations. It also turns out that the calculations do not take significantly longer computer runs as about 95% of the correlation effect is in the *M* shell. The details will be reported elsewhere.

## References

- [1] MOSER, C. and NESBET, R.K. (1971). *Phys. Rev.*, **A4**, 1336.
- [2] ————— and ————— (1972). *Phys. Rev.*, **A6**, 1710.
- [3] NESBET, R.K. (1968). *Phys. Rev.*, **172**, 2.
- [4] ————— (1969). *Adv. Chem. Phys.*, **14**, 1.
- [5] EDLEN, B. (1960). *J. Chem. Phys.*, **33**, 98.

# Configuration Interaction by the Method of Bonded Functions: Some Preliminary Calculations

G.H.F.Diercksen\* and B.T.Sutcliffe†

A resumé of Boys' approach to configuration interaction calculations is presented, and a program suitable to perform such calculations is described in some detail. The results of a preliminary calculation on water, together with some timings are presented.

## Introduction

If one chooses to attempt approximate solutions of Schrödinger's equation for bound states of atoms and molecules, with the aid of the linear variation theorem, then one begins with the ansatz

$$\psi = \sum_{k=1}^m c_k \Phi_k \quad (1)$$

and is eventually faced with solving the secular problem

$$Hc = ES c \quad (2)$$

Here  $H$  and  $S$  are square matrices with elements

$$H_{ij} = \int \Phi_i^* H \Phi_j d\tau \quad (3a)$$

$$S_{ij} = \int \Phi_i^* \Phi_j d\tau \quad (3b)$$

where  $H$  is the Schrödinger Hamiltonian for the problem

$$H = \sum_i H(i) + \sum_{i>j} H(i,j) \quad (4a)$$

with

$$H(i) = -\frac{1}{2} \Delta_i + \sum_{\lambda} Z_{\lambda} / r_{\lambda i} \quad (4b)$$

$$H(ij) = 1/r_{ij} \quad (4c)$$

The eigenvectors  $c$  consist of those coefficients in (1) which minimize the energy  $E$ .

Nowadays the solution of the eigenvalue problem does not present any particular computational difficulties, but obtaining the matrix elements (3) and

(4) still presents a formidable computational problem.

In quantum chemical problems the  $\Phi_k$  are usually taken to be antisymmetrised products of one particle space and spin functions (*spin orbitals*) and it can be seen at once that with this choice the matrix elements (3) reduce to weighted sums of one- and two-electron (three and six dimensional) integrals. The evaluation of these integrals is again a matter of great computational difficulty, with consequences for the evaluation of the matrix elements to which we shall refer later.

If one chooses the  $\Phi_k$  as antisymmetrised spin-orbital products, then a still further choice is left open, that of choosing the space parts of the functions (orbitals) as members or not, of an orthogonal set.

If one chooses them to form an orthogonal set then many simplifications appear in the formulae for the matrix elements. However, it has not so far been found possible to evaluate directly the integrals involved over any physically meaningful or useful set of orthogonal orbitals. Generally orthogonal orbitals are constructed as linear combinations of primitive functions, by some means. The primitive functions are chosen for the ease with which integrals between them may be evaluated and also on grounds of physical meaning. Thus before one can actually evaluate the matrix elements in an integral basis one has generally to face the problem of transforming the integrals from the primitive basis to the orthogonal basis. Only recently has this problem been solved in a computationally efficient way, and this has been discussed by one of us (G.H.F.D.) in another paper [1].

In this context it is the custom to refer to the primitive functions as atomic orbitals (AO's) and to the orthogonal functions as molecular orbitals (MO's) because the orthogonal functions were often found

\* Max-Planck-Institut für Physik und Astrophysik, Föhringer Ring 6, 8 München 40, West Germany  
† Department of Chemistry, University of York, Heslington, York, YO1 5DD



as solutions of Roothaan's equations. It is also quite customary to refer to the process of constructing the linear variation as *configuration interaction* (CI).

If one does not require the orbitals to form an orthogonal set then one has no transformation problem but the weighting function in the integral sums then involves the evaluation of a rather nasty co-factor expression (see e.g. [2] pp 50-51) and it seems likely that the amount of computational effort involved in evaluating the matrix elements here, may well in fact be very similar to that involved in transforming and evaluating in the orthogonal basis. This is, however, as yet an undecided question.

In this communication we shall confine attention to matrix elements in an orthogonal basis, and because of this we shall be able to consider a somewhat more general functional form for the  $\Phi_k$  than the relatively simple antisymmetrised product. This functional form (which we shall describe in more detail later) we shall, following the usage of Boys, call a *bonded function*. It may be thought as a linear combination of antisymmetrised products, so designed as to be a spin-eigenfunction and to have the required space symmetry properties. Such a functional form has the further advantage that it is easy to generate from any given orbital set all those bonded functions having the same spin-eigenvalue (corresponding to the different canonical structures of classical valence bond theory (see e.g. [2] p 67)) so that one may properly consider all allowed spin-coupling schemes in any problem, in an economical way.

Some of the earliest considerations of the problem of generating bonded functions and calculating matrix elements between them, from the standpoint of computational feasibility, are found in the work of McWeeny [3] and of Boys and his co-workers, [4,5]. Subsequently these approaches were somewhat generalised and extended by McWeeny and Cooper [6] and by Sutcliffe [7] respectively. We shall not concern ourselves here with the problem of generating a suitable set of bonded functions but will regard such a set as given, and concentrate on the computational problems raised by finding the formula for the matrix element between an arbitrary pair of bonded functions and of subsequently substituting the values of the integrals into this formula to obtain the required matrix element. We shall call the first part of this process (again following Boys) the *projective reduction* of a matrix element to yield a *symbolic matrix element*, and the last part that of forming the *numerical matrix element*, by resolving the symbolic references.

From a more general point of view the symbolic matrix element (or indeed a complete list of such elements) can be regarded as a special kind of program, according to the execution of which, the numerical value is computed. The program which generates the symbolic matrix elements can then be regarded as a

compiler, generating from input, the symbolic matrix element regarded as a program, according to the syntax rules and so on of projective reduction. The formation of numerical matrix elements may then be regarded as interpreting the compiled symbolic matrix element program.

In certain cases, as Roos [8] has shown, it is possible to look at this problem from a different viewpoint. If one restricts the structure of the bonded functions in certain ways, then one can so arrange matters that only a small number of possible types of symbolic matrix elements occur. In this kind of situation instead of resolving the references in the symbolic matrix element to the numerical values of the integrals, it is more effective to use the integral type as a symbolic reference and to resolve this reference to all the possible numerical matrix elements. This latter process is very like the technique used, for example, in the POLYATOM [9] and MUNICH [10] SCF routine for making up the  $J$  and  $K$  matrices and the HF-matrix, by tagging each two electron integral according to type and processing it as a potential contributor to a number of matrix elements according to the tag carried. While recognising the outstanding suitability of Roos' technique in particular cases (for example the classical case of configuration interaction involving all single and double substitutions in a closed shell) it is difficult to see how it could be made to operate in the general case of arbitrary bonded functions. We shall therefore not consider it further here since our interest is precisely in this latter situation.

There have, in fact, been quite a number of earlier attempts to treat the problem in the same broad general way that we are proposing, the classical work being that of Boys and Reeves, see [11], and work by others arising from that. However, the present state of the art appears to be that still it is not possible to regard the calculation of a general say 5000 configuration wavefunction as a routine affair, because the computing times involved remain much too great. That this is the case, is almost certainly due (in part) to the fact that no really effective algorithm has been available for interpreting the compiled symbolic matrix element program. Such an algorithm has now been designed, making use of a reordering procedure for large lists of indexed quantities. The algorithm, which will be described later, has been implemented within the scope and framework of the MUNICH program system [10] and has been extensively tested and found to perform well\*.

\* After completing this work the authors found that a very similar algorithm had been developed simultaneously by Yoshimine [12]. The relative merit of this and the procedure described here is still an open question.

## Theory

The bonded functions  $\Phi$  which form the basis of our analysis are defined as follows

(5)

$$\phi = \mathcal{A}[\phi_1 \phi_2] [\phi_3 \phi_4] \dots [\phi_{2p-1} \phi_{2p}] [\phi_{2p+1} \dots \phi_n]$$

where the spin coupled pairs are

$$[\phi_i \phi_j] = \phi_i(i) \phi_j(j) \{ \alpha(i) \beta(j) - \beta(i) \alpha(j) \} \quad \phi_i \neq \phi_j \quad (5a)$$

$$= \phi_i(i) \phi_j(j) \alpha(i) \beta(j) \quad \phi_i = \phi_j \quad (5a')$$

and the unpaired orbital is

$$[\phi_i] = \phi_i(i) \alpha(i) \quad (5b)$$

The symbol  $\mathcal{A}$  denotes an antisymmetrizing operator that produces a normalized, completely antisymmetric wavefunction. The functions  $\phi_i$  are assumed to be orthogonal. If  $\phi_i = \phi_j$ , then the orbitals must occur in the same spin coupled pair or the function vanishes.

A bonded function composed of  $n$  orbitals of which  $c$  are unpaired and containing  $x$  identical orbitals spin coupled (identical pairs) may be written as the sum of  $2^{(n-c)/2-x}$  determinants. A given set of orbitals  $\phi$  may be bracketed together in a number of different ways. A linear independent set of bonded functions (canonical sets) may be formed according to the following rules:

- in each bonded function identical orbitals must be bracketed together (spin coupled);
- to the remaining orbitals the remaining left and right brackets must be assigned.

These have to be assigned one to each orbital in all possible ways consistent with there being at least one more left bracket to the left of any right bracket than there are right brackets. The brackets are associated by the ordinary laws of algebra and the orbitals assigned to each pair of brackets, spin coupled. The excess of left brackets (if any) represents the uncoupled orbitals.

The total number of determinant product terms in the product of two bonded functions  $\Phi_K$  and  $\Phi_{K'}$  containing  $x$  and  $x'$  identical pairs, respectively, is  $2^{(n-c)-(x+x')}$ . These determinant product terms must be enumerated, the required matrix element between the determinants must be found, and all the contributing factors summed to give the final matrix elements between the bonded functions. The matrix elements of the unity and the spinless Hamiltonian operator between the bonded functions  $\Phi_K$  and  $\Phi_{K'}$  are determined to be of the form

$$S_{KK'} = \Gamma \sum_i Q_i \int \phi_i^K(1) \phi_i^{K'}(1) d\tau_1 \quad (6a)$$

$$H_{KK'} = \Gamma \sum_i Q_i \int \phi_i^K(1) H(1) \phi_i^{K'}(1) d\tau_1 \\ + \sum_{i,j} Q_{ij} q'_{ij} \int \phi_i^K(1) \phi_i^{K'}(1) H(1,2) \phi_j^K(2) \phi_j^{K'}(2) d\tau_1 d\tau_2 \\ + q_{ij} \int \phi_i^K(1) \phi_j^{K'}(1) H(1,2) \phi_j^K(2) \phi_i^{K'}(2) d\tau_1 d\tau_2 \quad (6b)$$

The coefficients  $\Gamma$ ,  $Q_i$ ,  $Q_{ij}$ ,  $q_{ij}$  and  $q'_{ij}$  are constants which are independent of the form of the orbitals and of the operators  $H(1)$  and  $H(1,2)$  and depend only on the bracket structure of the bonded functions. The process of reducing the many dimensional integrals  $S_{KK'}$  and  $H_{KK'}$  to a combination of weighted integrals over one- and two-electron coordinate integrals has been termed projective reduction. This projective reduction has to be performed for each matrix element separately according to the following rules:

Let the orbitals  $\phi_i^K$  that compose  $\Phi_K$  be written in a line and the orbitals  $\phi_i^{K'}$  that compose  $\Phi_{K'}$  be written down below them. Now let the orbitals of  $\Phi_K$  and  $\Phi_{K'}$  be rearranged so that

- identical orbitals appear opposite one another as far as possible
- spin coupled pairs are kept adjacent as far as possible.

Rule (a) is applied before rule (b) above, and it will only be the case where the orbitals of  $\Phi_K$  differ from  $\Phi_{K'}$  that identical orbitals will not appear opposite one another. Rule (a) is applied by associating each orbital in  $\Phi_K$  with the same orbital in  $\Phi_{K'}$  until all identical orbitals have been associated. The nonidentical orbitals are then paired and the resulting diagram rearranged so as to conform with rule (b). In particular cases the diagram produced is not unique, but all such diagrams can be shown to be equivalent. It should be noticed that the orbital subscripts in equation (6) refer to the orbital order after this re-ordering has been done. The numerical value of the subscript is, of course, of no consequence, it is simply required that  $\phi_i^K$  be opposite  $\phi_i^{K'}$  and so on after re-ordering.

Patterns are formed by joining orbitals which have been arranged adjacent to each other according to the above rules by a solid line, and connecting all spin coupled pairs by a dotted line. Any diagram consists generally of two types of patterns. Those which begin and end on an unpaired orbital and those which close back on themselves. The former are referred to as chains, the latter as cycles. The chains are of two types: those which begin in one function  $\Phi_K$  and end in the other  $\Phi_{K'}$ , these are called odd chains since they involve an odd number of vertical links; and those which begin in one function and end in the same function are called even chains. It is clear that there must be just as many chains in a diagram as there are unpaired orbitals in a bonded function. If there are even chains then there must be at least two and generally an even number of even chains.

It is necessary to have a convention about where chains begin. The first odd chain is taken to begin at the lowest numbered unpaired orbital in the top of the diagram. The next odd chain starts at the next lowest unpaired orbital and so on. The first even chain is defined like the first odd chain, the second even chain starts from the lowest numbered available unpaired orbital in the bottom line of the diagram and so on.

Inspection shows that if any even chains are present then there must be one spin mismatched for each even chain, between the determinants. By convention this is taken to be at the highest numbered orbital in the chain.

A parity is assigned to each vertical line within a pattern, the lowest numbered line being even, the next odd, the next even, and so on.

Now the patterns can be used to determine the sign of the initial diagram and also to write down the matrix elements between bonded functions in terms of integrals over the orbitals of  $\phi^K$ , and of  $\phi^{K'}$ .

Table 1: Coefficients for two-electron integrals

$i$	$j$	$p_{ij}$	Pattern	$q_{ij}$
cycle	cycle	-1	$D$	$-\frac{1}{2}$
cycle	$o$ chain	+1	$D$	$-\frac{1}{2}$
$o$ chain	cycle	-1	$S$	+1
		+1	$S$	-2
$o$ chain	$o$ chain	-1	$D$	0
		+1	$D$	-1
		-1	$S$	+1
		+1	$S$	-2
$e$ chain	$e$ chain	-1	$D$	-1
		+1	$D$	+1

The results are given by formulas (6) and table 1. The notation convention adopted is as follows: the parity of a given position (+1 or -1) is denoted by  $p_i$ , the product  $p_i p_j$  is written  $p_{ij}$ . If  $i$  and  $j$  occur in different patterns this is denoted by  $D$ , if they occur in the same pattern this is denoted by the letter  $S$ . The function  $Q_i$  is zero, if there exist an  $r \neq i$ , such that  $\phi_r^K \neq \phi_r^{K'}$ , and it is one otherwise. Similarly the function  $Q_{ij}$  is defined to be zero, if there exists an  $r \neq i, j$ , such that  $\phi_r^K \neq \phi_r^{K'}$ , and to be one otherwise. The constant  $\Gamma$  is given by

$$\Gamma = (-1)^{\sigma+\sigma'} (-\frac{1}{2})^{(n-h)/2-m} (-2)^{J/2}$$

where  $n$  is the number of electrons,  $h$  is the total number of (even and odd) chains, and  $m$  is the number of cycles;  $J$  is the number of pairs for which  $\phi_i^K = \phi_i^{K'}$  but  $\phi_i^{K'} \neq \phi_i^{K'}$  or vice versa;  $\sigma$  is the signature of the permutation of the unpaired orbitals of the  $\phi_i^K$

back to their order in  $\Phi_K$  and  $\sigma'$  is the signature of the  $\phi_j^{K'}$  back to their order in  $\Phi_{K'}$ . Odd chain is abbreviated  $o$  chain, and even chain by  $e$  chain.

There are no one-electron terms from diagrams containing two even chains, and there are no terms at all from diagrams containing more than two even chains.

When there are no even chains,  $q_{ij} = 1$ , and if there are two even chains,  $q_{ij} = 0$ . When  $\phi_i^K = \phi_j^K$ , and/or  $\phi_i^{K'} \neq \phi_j^{K'}$ ,  $q_{ij} = 0$ . If there are two even chains and  $i$  and  $j$  are in the same chain,  $q_{ij} = 0$ . Otherwise  $q_{ij}$  is given in table 1.

## Computational Realisation

The 'best', that is the most 'economic' computer algorithm has to minimize the following quantities:

- mathematical operations
- number of processor storage location
- amount of data transferred to or/and from external storage
- number of transferred blocks of data.

An algorithm that fulfils these four conditions uses the minimum of central processor and elapsed time, and therefore is the cheapest. Normally, each algorithm is a compromise with these four conditions, resulting from the characteristics of the computer it is (supposed) to be implemented on.

The calculation of matrix elements between many electron wavefunctions of arbitrary spin states is especially difficult, because normally *not all* one- and two-electron integrals between the functions  $\phi$  used to construct the wavefunction can be held in processor storage simultaneously. In this case data transfer to and from external storage becomes very critical and advanced techniques have to be applied to solve this problem. For the present problem an efficient algorithm has been designed, implemented and extensively tested. It will be described, its relation to similar algorithms will be discussed, and its present implementation will be outlined: for convenience, the number of matrix elements whose numerical values can be formed in processor storage simultaneously is called a *core-load of matrix elements*, the number of symbolic matrix elements that can be held (actually, whose symbolic references can be reordered according to one index) simultaneously on direct access external storage is called a '*disk-load of matrix elements*', and the number of integrals that can be kept in processor storage (actually: directly referenced simultaneously) is called a *core-load of integrals*.

Each symbolic matrix element contains one or more references to one- and/or two-electron integrals. Each of these references is uniquely identified by two numbers: the sequence number of the matrix

Table 2: MUNICH PROGRAM SYSTEM - Configuration Interaction Package Release 0 (March 1973)

Timing Example <sup>a</sup> :	Molecular Orbitals	..	..	..	..	..	..	..	35
	Configurations (all double + single sub. except for the K-Shell)	2063							
	Total SCF energy	..	..	..	..	..	..	..	-76.05199 au
	Total CI energy	..	..	..	..	..	..	..	-76.26620 au

Total Storage (K Bytes)	Data Storage (K Bytes)	Step (b) (min)	Time			Total (min)	Δ Time		Number of Reads of Integral List
			Step (c) (min)	Step (e) (min)	(min)		(%)		
600	453	5.7062	.5947	.5523	6.8573			8	
540	393	5.7088	.6025	.5595	6.8713	.0176	.25	9	
480	333	5.7225	.6085	.5762	6.9075	.0538	.78	11	
420	273	5.7088	.6172	.5928	6.9192	.0655	.96	13	
360	213	5.8029	.6388	.6312	7.0733	.2196	3.2	17	
300	153	5.8167	.7287	.7378	7.2835	.4298	6.3	25	
240	93	5.8940	.8900	.9220	7.7063	.8526	12.4	43	

(a) IBM 360/91

element it contributes to, and the sequence number of the referenced integral. To avoid time consuming searching, these references have to be ordered in such a way, that the quantities who's reference are to be resolved can be processed 'sequentially'. Normally, this makes one or more reorderings of the reference necessary. Based on this general idea an efficient algorithm has been developed for computing numerical matrix elements which essentially consists of the following steps\*:

- Compute a list of symbolic matrix elements
- Order the symbolic contributions, for a *disk-load* of matrix elements at a time, so that consecutive symbolic contributions refer to core loads of integrals in ascending sequence.
- Resolve the references to the integrals.
- Order the numerical contributions, so that consecutive elements refer to *core-loads* of matrix elements in ascending order. Actually, within each sequence of numerical contributions built from the *same* core-load of integrals, the elements are ordered according to matrix elements in ascending order. Therefore re-ordering is not necessary, if the list can be accessed directly (randomly).
- Resolve the references of the numerical contributions to the matrix elements, and compute the matrix elements, a core-load at a time.

It is important to notice, that in this algorithm the list of integrals has only to be read as many times as there are *disk-loads* of matrix elements. As normally the disk (direct access) space available is rather large, one or very few reads of the integral list are necessary.

\* Starting from a different analysis, M. Yoshimine essentially arrived at the same result [12]

At present this algorithm has been implemented in a slightly different way: essentially step (b) of the above sequence is applied to each *core-load* of matrix elements separately, instead to each *disk-load*. This modification of the algorithm needs relatively little disk space, approximately the order of magnitude of processor storage available for the step, and it avoids step (d) completely. But the list of integrals has to be read as many times as there are core-loads of matrix elements, which essentially means more often, because usually core-loads are smaller than disk-loads of matrix elements. But it has been found (compare table 2) that the increase of CPU time with increasing numbers of reads of the integral list is unexpectedly small, while the elapsed time is dependent on the number of reads of the integral list, as is to be expected. Normally, the *complete* list of symbolic matrix elements is generated in step (b). This list can be used to construct the list of numerical matrix elements for any problems where the following quantities agree in number and/or type: molecular symmetry (if explicitly taken into account), electrons, molecular orbitals, and configurations. But with increasing number of electrons and configurations, this list of symbolic matrix elements will become exceedingly large and it might become unreasonable to keep it. In this case the above algorithm, steps (a) to (e), has to be applied to each disk-load of matrix elements separately.

In the following paragraphs some of the approaches used in the present algorithm are discussed in more detail, to show the critical features of their performance:

A very efficient algorithm for the projective reduction of matrix elements has been described by Reeves [11], and has been implemented in the present program with minor (technical) modifications. Timing tests have revealed, that the initial 'pairing' of orbitals between bonded functions is very time consuming, and in the test case actually used up to

65% of the total CPU time necessary for the projective reduction. Therefore this procedure has been carefully analysed.

The procedure consists in 'pairing' the orbitals between two bonded functions one-to-one so as to minimize the number of noncoincidences and to build appropriate cross-reference tables to be used in the actual projective reduction. This 'pairing' may be terminated if the third noncoincidence is found, because if there are three or more noncoincident orbitals between bonded functions the matrix element between these functions is identically zero. This process of pairing has to be done for the orbitals between the first members of all orbital configurations, and in case less than three noncoincidences have been found for the orbitals, between all other members of these orbital configurations.

Two classes of approaches are possible for this 'pairing', one class involving explicit searching, one class involving no searching. We have currently implemented an algorithm with searching gaining speed because it has been programmed in IBM 360 Assembler Language and is largely formed by program sections allowing the computer IBM 360/91 to run in a special state (loop mode). However, we are actively investigating algorithms that do not involve searching in the hope of making further time savings [13].

Throughout the present program *linear indexing* and *table look up* has been used. In particular: all symbolic references are given as to core/disk load number and sequence number (within the load). The variables GAMMA and  $Q$  are identified by entry points to appropriate tables.

Timing examples of the present program release are given in table 2 in which the CI problem is based on a SCF problem solved for the water molecule [14].

### Acknowledgements

The authors are deeply grateful to the NATO Science Committee for a grant in support of this work.

### References

- [1] DIERCKSEN, G.H.F. (1974). *Theoret. Chim. Acta*, **37**, 105.
- [2] McWEENY, R. and SUTCLIFFE, B.T. (1969). *Methods of Molecular Quantum Mechanics*, 51, London: Academic Press.
- [3] McWEENY, R. (1954). *Proc. Roy. Soc. (London)*, **A223**, 63.
- [4] REEVES, C.M. (1957). Ph.D. Thesis, Cambridge.
- [5] BOYS, S.F., REEVES, C.M. and SHAVITT, I. (1956). *Nature*, **178**, 1207.
- [6] COOPER, I.L. and McWEENY, R. (1966). *J. Chem. Phys.*, **44**, 226.
- [7] SUTCLIFFE, B.T. (1966). *J. Chem. Phys.*, **45**, 235.
- [8] ROOS, B. (1972). University of Stockholm Institute of Physics (USIP) Report 72-08. ——— (1972). *Chem. Phys. Letters*, **15**, 153.
- [9] NEUMANN, D.B. *et al.*, *Polyatom Version 2 System Manual*, available from QCPE, Chemistry Department, Indiana University, Bloomington, Indiana 47401, U.S.A.
- [10] DIERCKSEN, G. H. F. and KRAEMER, W. P. *Molecular Program System Reference Manual*, Special Technical Report, Munchen: Max-Planck-Institut für Physik und Astrophysik, (to be published).
- [11] REEVES, C.M. (1966). *Communs, A.C.M.*, **9**, 276.
- [12] YOSHIMINE, M. (1973). *J. Comp. Phys.*, **11**, 449.
- [13] De VRIES, H.L. and DIERCKSEN, G.H.F., (to be published).
- [14] DIERCKSEN, G.H.F. (1971). *Theoret. Chim. Acta*, **21**, 335.

# Self Consistent Groups in Molecular Wavefunctions - An Effective Hamiltonian with Applications to Some Simple Systems

S. Wilson and J. Gerratt\*

The self consistent group function model is examined within the framework of the spin optimised self consistent field method. An effective Hamiltonian is proposed which avoids the introduction of off-diagonal Lagrange undetermined multipliers when optimising the orbitals. Self consistent pair functions are considered as an example of this approach and the necessary conditions for the optimal orbitals are obtained and discussed. Some model calculations are presented and computational aspects of the problem are described.

## Introduction

The determination of the electronic wavefunction for a molecular system can often be simplified if groups of weakly interacting electrons can be recognised [1,2]. To a good approximation, the wavefunction may then be written

$$|\Psi_{S,M;k}\rangle = \sqrt{N!} \mathcal{A} \left( \prod_{\mu}^{N_g} \Phi_{\mu} \Theta_{S,M;k} \right) \quad (1)$$

where  $\mathcal{A}$  is the idempotent antisymmetrising operator [3],  $\Theta_{S,M;k}$  is the spin function [3] and  $\Phi_{\mu}$  the spatial function for the  $\mu$ th group of electrons. It is assumed that these group functions are strongly orthogonal [1]. This is vital to the development of the group function model and is perhaps also its weakest point [4]. However, the group functions do have chemical significance since they may be associated with chemically recognisable entities [8] such as core and valence electrons, lone pairs, bonds, and  $\sigma$ - and  $\pi$ -electrons. It appears that group functions are also transferable, to a certain extent, between molecular systems [5].

Generally, a linear combination of spin functions will be used

$$|\Psi_{S,M;k}\rangle = \sum_{\mathbf{k}} b_{S\mathbf{k}} |\Psi_{S,M;k}\rangle \quad (2)$$

in order to span spin space. This may be important when considering the dissociation of a molecular system or discussing spin properties. In the Spin Optimised Self Consistent Field (S.O.-S.C.F.) method [3,6,7], the optimal coefficients,  $b_{S\mathbf{k}}$ , are determined

by the variation theorem. It is convenient to consider a single spin function initially, however.

The electronic energy expression obtained from wavefunctions of the form (1) or (2) may be written as a sum of intra-group and inter-group terms

$$E = \sum_{\mu} E_{\mu}^{(\text{intra})} + \sum_{\mu > \nu} E_{\mu\nu}^{(\text{inter})} \quad (3)$$

The intra-group contribution to the energy has the form

$$E_{\mu}^{(\text{intra})} = H_{\mu} + J_{\mu} + K_{\mu} \quad (4)$$

where  $H_{\mu}$  is the one-electron energy for the group  $\mu$  while  $J_{\mu}$  is the intra-group Coulomb energy and  $K_{\mu}$  the intra-group exchange energy. The inter-group energy is a sum of the inter-group Coulomb and exchange terms

$$E_{\mu\nu}^{(\text{inter})} = J_{\mu\nu} + K_{\mu\nu} \quad (5)$$

If the group functions are taken to be a product of non-orthogonal orbitals,

$$|\Phi_{\mu}\rangle = \prod_{i \in \mu} |\mu i\rangle \quad (6)$$

they may be given an additional physical interpretation. The wavefunction is then open to discussion within the independent electron model. We shall be entirely concerned with functions of the form (6). General expressions for the terms occurring in equations (4)

\* Department of Theoretical Chemistry, University of Bristol, Cantock's Close, Bristol, BS8 1TS

and (5) when group functions of the form (6) are employed are given in Appendix A.

The wavefunction (1) can be regarded as an eigenfunction of an effective Hamiltonian operator. This is derived in the following section. Its application to the calculation of pair functions is then described. The necessary conditions for the optimal orbitals are given and discussed. Finally, model calculations are presented for some simple systems.

### An Effective Hamiltonian for Group Function Calculations

The electronic Hamiltonian,  $\mathcal{H}$ , within the Born-Oppenheimer approximation, may be written as a sum of one and two electron terms [3]

$$\mathcal{H} = \sum_k \hat{h}_k + \sum_{k>\ell} \hat{g}_{k\ell} \quad (7)$$

where  $k$  and  $\ell$  denote electronic coordinates.

An effective Hamiltonian for group function calculations is obtained as follows. Let  $\mathcal{S}$  denote the space of all wavefunctions, defined by equations (1) and (6), in which the group functions are not subject to any orthogonality restrictions. Let  $\mathcal{S}'$  denote the space of all such wavefunctions in which the group functions are required to be strongly orthogonal.  $\mathcal{S}' \subset \mathcal{S}$ . Let  $\hat{\mathcal{D}}$  denote the projector onto  $\mathcal{S}'$  and  $\mathcal{H}_p$  the projection of the Hamiltonian onto  $\mathcal{S}'$  [9]

$$\mathcal{H}_p = \hat{\mathcal{D}} \mathcal{H} \hat{\mathcal{D}}$$

$\mathcal{H}_p$  is hermitean and transforms any  $|\Psi\rangle \in \mathcal{S}'$  linearly into any  $|\Psi\rangle \in \mathcal{S}'$ .

If the orbitals comprising the group functions are of the same symmetry type, the projection operator,  $\hat{\mathcal{D}}$ , may be derived as follows: Let  $\hat{\mathcal{O}}_\mu$  denote the projector onto the space  $\mathcal{E}_\mu$  spanned by the set of non-orthogonal ket vectors  $|\mu i\rangle$ . Löwdin [10] has shown that this may be written

$$\hat{\mathcal{O}}_\mu = \sum_{i,j \in \mu} |\mu i\rangle (\Delta_\mu^{-1})_{ij} \langle \mu j| \quad (9)$$

where

$$\{\Delta_\mu\}_{ij} = \langle \mu i | \mu j \rangle \quad (10)$$

is the metric matrix. Now  $\mathcal{E}_\mu$  is orthogonal to  $\mathcal{E}_\nu$ , i.e.  $\hat{\mathcal{O}}_\nu \hat{\mathcal{O}}_\mu = \hat{0}$  ( $\mu \neq \nu$ ). This is a necessary and sufficient condition that

$$\hat{P}_\mu = \sum_{\nu \neq \mu} \hat{\mathcal{O}}_\nu \quad (11)$$

is also a projector [11].  $\hat{P}_\mu$  projects onto the direct sum of the subspaces  $\mathcal{E}_1, \mathcal{E}_2, \dots, \mathcal{E}_\alpha, \dots, \mathcal{E}_{N_g}$  ( $\alpha \neq \mu$ ), which we shall denote by  $\mathcal{E}_\mu^{\mu x}$ . The projection operator onto the subspace  $\mathcal{E}_\mu^{\mu x}$  complementary to  $\mathcal{E}_\mu$  is then

$$\hat{\mathcal{D}}_\mu = \hat{I} - \hat{P}_\mu \quad (12)$$

$|\mu i\rangle \in \mathcal{E}_\mu^{\mu x}$  since  $|\mu i\rangle$  is orthogonal to all  $|\nu j\rangle$  ( $\mu \neq \nu$ ). We now impose the condition that  $\hat{\mathcal{D}}_\mu$  acts only on  $|\mu i\rangle, \forall i$ . Hence the required projection operator is

$$\hat{\mathcal{D}} = \prod_\mu \hat{\mathcal{D}}_\mu \quad (13)$$

$[\hat{\mathcal{D}}_\mu, \hat{\mathcal{D}}_\nu] = 0, (\mu \neq \nu)$ , is a necessary and sufficient condition that  $\hat{\mathcal{D}}$  be a projection operator [11].

Assuming that the wavefunction is normalised, the electronic energy for strongly orthogonal group function is

$$E^{\text{Sk}} = \langle \Psi_{S,M;k} | \mathcal{H}_p | \Psi_{S,M;k} \rangle \quad (14)$$

This form of the energy is important when considering the conditions for the optimal group functions. The use of this effective Hamiltonian avoids the introduction of off-diagonal Lagrange multipliers [12].

### The Self Consistent Pair Function Model

The concept of electron pairs is fundamental to a substantial part of the theory of chemical bonding [13]. Such pairs form the simplest example of the application of the group function model. The pair function may be written

$$|\Phi_\mu\rangle = |\mu_1\rangle |\mu_2\rangle \quad (15)$$

Hurley, Lennard-Jones and Pople [14] introduced the pair function as an extension of the molecular orbital theory to include the electrostatic correlation between electrons in the same orbitals. Hay, Hunt and Goddard [21] have considered it as a generalisation of the valence bond method. Effectively each electron pair is described by a function of the type discussed by Coulson and Fischer [15] for the hydrogen molecule. It may be regarded as an extension of the molecular orbital method in which the orbitals are not forced to be doubly occupied or as an extension of the valence bond method in which distorted atomic orbitals are employed.

The Serber basis [16] for the spin functions is particularly suited to pair function calculations. The electron spins are first coupled together in pairs and then the pairs coupled to give the resultant spin. In this basis the representation matrices for the symmetric group have the useful property

$$U_{\mathbf{S},\mathbf{k},\ell}^{\mathbf{N}}(P_{\mu_1\mu_2}) = \pm\delta_{\mathbf{k}\ell}. \quad (16)$$

The energy expression [17], for an arbitrary spin function, then has a particularly simple form. If for convenience we define

$$d_{\mu}^{\mathbf{S}\mathbf{k}} = (1 + U_{\mathbf{S}\mathbf{k}\mathbf{k}}^{\mathbf{N}}(P_{\mu_1\mu_2})\Delta_{\mu}^2)^{-1} \quad (17)$$

the various components of the energy are

$$H_{\mu}^{\mathbf{S}\mathbf{k}} = d_{\mu}^{\mathbf{S}\mathbf{k}} [\langle\mu_1|h|\mu_1\rangle + \langle\mu_2|h|\mu_2\rangle + 2U_{\mathbf{S}\mathbf{k}\mathbf{k}}^{\mathbf{N}}(P_{\mu_1\mu_2})\Delta_{\mu}\langle\mu_1|h|\mu_2\rangle] \quad (18)$$

$$J_{\mu}^{\mathbf{S}\mathbf{k}} = d_{\mu}^{\mathbf{S}\mathbf{k}} \langle\mu_1\mu_2|g|\mu_1\mu_2\rangle \quad (19)$$

$$K_{\mu}^{\mathbf{S}\mathbf{k}} = d_{\mu}^{\mathbf{S}\mathbf{k}} U_{\mathbf{S}\mathbf{k}\mathbf{k}}^{\mathbf{N}}(P_{\mu_1\mu_2}) \langle\mu_1\mu_2|g|\mu_2\mu_1\rangle \quad (20)$$

$$J_{\mu\nu}^{\mathbf{S}\mathbf{k}} = d_{\mu}^{\mathbf{S}\mathbf{k}} d_{\nu}^{\mathbf{S}\mathbf{k}} [\langle\mu_1\nu_1|g|\mu_1\nu_1\rangle + \langle\mu_1\nu_2|g|\mu_1\nu_2\rangle + \langle\mu_2\nu_1|g|\mu_2\nu_1\rangle + \langle\mu_2\nu_2|g|\mu_2\nu_2\rangle + 2U_{\mathbf{S}\mathbf{k}\mathbf{k}}^{\mathbf{N}}(P_{\mu_1\mu_2})\Delta_{\mu}(\langle\mu_1\nu_1|g|\mu_2\nu_1\rangle + \langle\mu_1\nu_2|g|\mu_2\nu_2\rangle) + 2U_{\mathbf{S}\mathbf{k}\mathbf{k}}^{\mathbf{N}}(P_{\nu_1\nu_2})\Delta_{\nu}(\langle\mu_1\nu_1|g|\mu_1\nu_2\rangle + \langle\mu_2\nu_1|g|\mu_2\nu_2\rangle) + 2U_{\mathbf{S}\mathbf{k}\mathbf{k}}^{\mathbf{N}}(P_{\mu_1\nu_2})U_{\mathbf{S}\mathbf{k}\mathbf{k}}^{\mathbf{N}}(P_{\nu_1\nu_2})\Delta_{\mu}\Delta_{\nu}(\langle\mu_1\nu_1|g|\mu_2\nu_2\rangle) + \langle\mu_1\nu_2|g|\mu_2\nu_1\rangle)] \quad (21)$$

$$K_{\mu\nu}^{\mathbf{S}\mathbf{k}} = d_{\mu}^{\mathbf{S}\mathbf{k}} d_{\nu}^{\mathbf{S}\mathbf{k}} U_{\mathbf{S}\mathbf{k}\mathbf{k}}^{\mathbf{N}}(P_{\mu_2\nu_2}) [\langle\mu_1\nu_1|g|\nu_1\mu_1\rangle + \langle\mu_1\nu_2|g|\nu_2\mu_1\rangle + \langle\mu_2\nu_1|g|\nu_1\mu_2\rangle + \langle\mu_2\nu_2|g|\nu_2\mu_2\rangle + 2U_{\mathbf{S}\mathbf{k}\mathbf{k}}^{\mathbf{N}}(P_{\mu_1\mu_2})\Delta_{\mu}(\langle\mu_1\nu_1|g|\nu_1\mu_2\rangle + \langle\mu_1\nu_2|g|\nu_2\mu_2\rangle) + 2U_{\mathbf{S}\mathbf{k}\mathbf{k}}^{\mathbf{N}}(P_{\nu_1\nu_2})\Delta_{\nu}(\langle\mu_1\nu_1|g|\nu_2\mu_1\rangle + \langle\mu_2\nu_1|g|\nu_2\mu_2\rangle) + 2U_{\mathbf{S}\mathbf{k}\mathbf{k}}^{\mathbf{N}}(P_{\mu_1\mu_2})U_{\mathbf{S}\mathbf{k}\mathbf{k}}^{\mathbf{N}}(P_{\nu_1\nu_2})\Delta_{\mu}\Delta_{\nu}(\langle\mu_1\nu_1|g|\nu_2\mu_2\rangle) + \langle\mu_1\nu_2|g|\nu_1\mu_2\rangle)] \quad (22)$$

### Necessary Conditions for Optimal Pair Functions

Consider the determination of the optimal pair functions by the variation theorem [9]. The electronic energy is required to be stationary subject to the constraints that the total wavefunction and the orbitals remain normalised. To this end we form the functional

$$\mathcal{L} = E^{\mathbf{S}\mathbf{k}} - \sum_{\mu i} \epsilon_{\mu i} \langle\mu i|\mu i\rangle \quad (23)$$

where the Lagrange multipliers  $\epsilon_{\mu i}$  maintain orbital normality and  $E^{\mathbf{S}\mathbf{k}}$  is given by equation (14). The variation of the bra vector  $\langle\mu i|$  may always be taken to be independent of the variation of the ket vector  $|\mu i\rangle$  [9]. The requirement that  $\delta\mathcal{L}$  be zero for small, but non-zero,  $\langle\delta\mu i|$ , leads to the necessary conditions for the energy to be a minimum.

$$(\hat{\mathcal{P}}_{\mu} \hat{F}_{\mu i}^{\mathbf{S}\mathbf{k}\mathbf{k}} \hat{\mathcal{P}}_{\mu} - \epsilon_{\mu i})|\mu i\rangle = 0 \quad \forall |\mu i\rangle \quad (24)$$

$$\langle\mu i|\mu i\rangle = 1$$

By using the effective Hamiltonian  $\hat{\mathcal{H}}_{\mu}$  we have avoided the introduction of off-diagonal Lagrange multipliers in these equations. For pair functions the projection operators  $\hat{\mathcal{O}}_{\mu}$  have a simple form

$$\hat{\mathcal{O}}_{\mu} = (1 - \Delta_{\mu}^2)^{-1} (|\mu_1\rangle\langle\mu_1| + |\mu_2\rangle\langle\mu_2| - \Delta_{\mu}\{|\mu_1\rangle\langle\mu_2| + |\mu_2\rangle\langle\mu_1|\}) \quad (25)$$

The orbital operator is

$$\hat{F}_{\mu i}^{\mathbf{S}\mathbf{k}\mathbf{k}} = d_{\mu}^{\mathbf{S}\mathbf{k}} (\hat{P}_{\mu i}^{\mathbf{S}\mathbf{k}} + \hat{Q}_{\mu i}^{\mathbf{S}\mathbf{k}} + \hat{Q}_{\mu i}^{\mathbf{S}\mathbf{k}\mathbf{k}} - \hat{\eta}_{\mu i}^{\mathbf{S}\mathbf{k}\mathbf{k}}) \quad (26)$$

If we define

$$j = j(i) = \begin{cases} 1 & \text{if } i=2 \\ 2 & \text{if } i=1 \end{cases} \quad (27)$$

the intra-pair term is

$$\hat{P}_{\mu i}^{\mathbf{S}\mathbf{k}} = \hat{h} + \hat{\mathcal{J}}(\mu j; \mu j) + U_{\mathbf{S}\mathbf{k}\mathbf{k}}^{\mathbf{N}}(P_{\mu_1\mu_2}) \{|\mu j\rangle\langle\mu j|\hat{h} + \hat{h}|\mu j\rangle\langle\mu j| + \mathcal{X}(\mu j; \mu j)\} \quad (28)$$

where  $\hat{\mathcal{J}}$  and  $\mathcal{X}$  are the Coulomb and exchange operators [22]. The inter-pair Coulomb term is

$$\hat{Q}_{\mu i}^{\mathbf{S}\mathbf{k}} = \sum_{\nu \neq \mu} d_{\nu}^{\mathbf{S}\mathbf{k}} (\hat{\mathcal{O}}_{\nu}^{\mathbf{S}\mathbf{k}} + U_{\mathbf{S}\mathbf{k}\mathbf{k}}^{\mathbf{N}}(P_{\mu_1\mu_2}) \{|\mu i\rangle\langle\mu j|\hat{\mathcal{O}}_{\nu}^{\mathbf{S}\mathbf{k}} + \hat{\mathcal{O}}_{\nu}^{\mathbf{S}\mathbf{k}}|\mu j\rangle\langle\mu j|\}) \quad (29)$$

where the effective operator  $\hat{\mathcal{O}}_{\nu}^{\mathbf{S}\mathbf{k}}$  for the pair  $\nu$  is

$$\hat{\mathcal{O}}_{\nu}^{\mathbf{S}\mathbf{k}} = \hat{\mathcal{J}}(\nu_1, \nu_1) + \hat{\mathcal{J}}(\nu_2, \nu_2) + 2U_{\mathbf{S}\mathbf{k}\mathbf{k}}^{\mathbf{N}}(P_{\nu_1\nu_2})\Delta_{\nu}\hat{\mathcal{J}}(\nu_1; \nu_2) \quad (30)$$

Similarly, the inter-pair exchange term is

$$\hat{Q}_{\mu i}^{\mathbf{S}\mathbf{k}\mathbf{k}*} = \sum_{\nu \neq \mu} d_{\nu}^{\mathbf{S}\mathbf{k}} U_{\mathbf{S}\mathbf{k}\mathbf{k}}^{\mathbf{N}}(P_{\nu_2\mu_2}) (\hat{\mathcal{O}}_{\nu}^{\mathbf{S}\mathbf{k}\mathbf{k}*} + U_{\mathbf{S}\mathbf{k}\mathbf{k}}^{\mathbf{N}}(P_{\mu_1\mu_2}) \{|\mu j\rangle\langle\mu j|\hat{\mathcal{O}}_{\nu}^{\mathbf{S}\mathbf{k}\mathbf{k}*} + \hat{\mathcal{O}}_{\nu}^{\mathbf{S}\mathbf{k}\mathbf{k}*}|\mu j\rangle\langle\mu j|\}) \quad (31)$$



with the effective operator for the pair  $\nu$  given by

$$\hat{O}_\nu^{\text{Skk}^*} = \mathcal{K}(\nu_1;\nu_1) + \mathcal{K}(\nu_2;\nu_2) + U_{\text{Skk}}^{\text{N}}(P_{\nu_1\nu_2}) \Delta_\nu \{ \mathcal{K}(\nu_1;\nu_2) + \mathcal{K}(\nu_2;\nu_1) \} \quad (32)$$

Finally,

$$\eta_{\mu i}^{\text{Skk}} = \eta_{\mu}^{\text{Skk}} |\mu j\rangle \langle \mu j| \quad (33)$$

with

$$\eta_{\mu}^{\text{Skk}} = U_{\text{Skk}}^{\text{N}}(P_{\mu_1\mu_2}) [H_{\mu}^{\text{Sk}} + J_{\mu}^{\text{Sk}} + K_{\mu}^{\text{Sk}} + \sum_{\nu \neq \mu} (J_{\mu\nu}^{\text{Sk}} + K_{\mu\nu}^{\text{Sk}})] \quad (34)$$

The equations (24) are a statement of the Kuhn-Tucker necessary conditions [19] for the minimum of a function subject to equality constraints. The projection of the gradient of the function tangential to the manifold formed by the intersection of the constraints must be zero and the constraints must be obeyed. If the Hessian matrix is positive definite we have the sufficient conditions for a minimum. The Kuhn-Tucker conditions are discussed further in Appendix B.

### Solution of the Orbital Equations

The solution of the integro-differential equations (24) is in practice very difficult. Numerous techniques for the solution of such non-linear equations exist [20]. In this work, following Roothaan [23], the orbitals were expanded in a basis set of Slater functions and an iterative solution attempted in a pseudolinear fashion. The iterations take the following form: for a given partition of the basis set the projector  $\mathcal{P}_\mu$  is formed and the orbital equations for the pair function  $|\Phi_\mu\rangle$  solved until self consistent; the projector  $\mathcal{P}_\nu$  is then formed and  $|\Phi_\nu\rangle$  is varied. This entire process is repeated for all  $\nu$  until self consistent.

The performance of this process is described in the following section together with the results of some model calculations.

### Some Model Calculations

**Lithium hydride:** The ground state of the lithium hydride molecule provides a useful system for an initial calculation using the self consistent pair function model.

In figure 1, the orbitals obtained from a pair function calculation are compared with those obtained by the molecular orbital method and those obtained

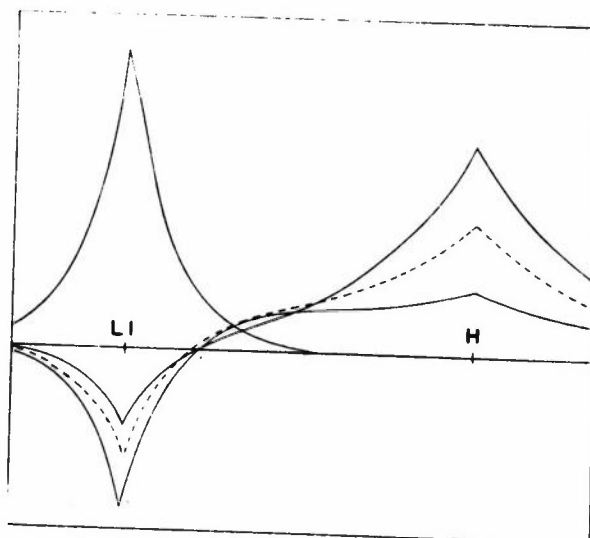


Figure 1(a): Pair function orbitals and valence m.o. (---) for the LiH system

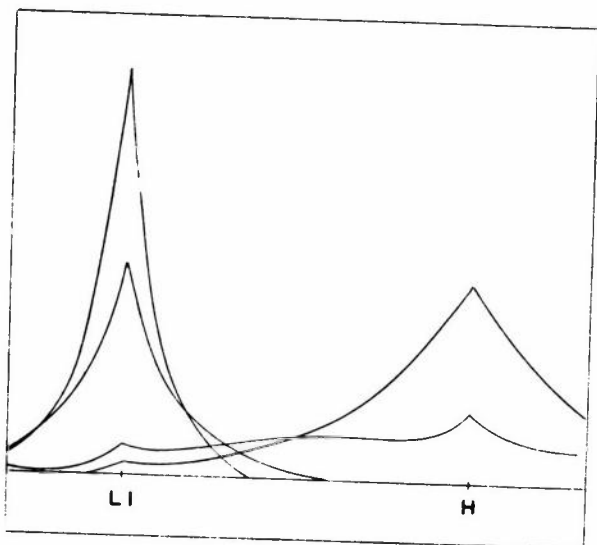


Figure 1(b): Orbitals obtained by relaxing the strong orthogonality constraint for the LiH system

by relaxing the restriction that the pair functions remain strongly orthogonal [30]. The orbitals of the core pair function were found to be virtually identical. The pair function valence orbitals, like the molecular orbital, have a node. This occurs, however, in a region where the core orbitals dominate the electron density. The strong orthogonality constraint has not significantly altered the shape of the orbitals in the chemically important valence region. In the valence pair function, one of the orbitals is dominated by the  $1s$  Slater function on the hydrogen atom, while the other is dominated by the  $2s$  and  $2p_\sigma$  functions of the lithium atom. At the equilibrium internuclear separation, the overlap between the valence orbitals was found to be 0.73810.

The results are compared with those of other relevant calculations in table 1, which also contains specifications of the basis set employed. It was necessary to optimise each pair function three times to obtain overall self consistency.

Table 1: A comparison of M.O., V.B., C.I. and S.C.P.F. calculations for the Lithium Hydride molecule

Description	Reference	Total Energy (au)	Basis Set*	$R(LiH)$ au
S.C.F. Molecular Orbital Calculation	[24]	-7.96992	Li: 1s (2.6909) 2s (0.7075) 2p (0.8449) H: 1s (0.9766)	3.015
Configuration Interaction Calculation (13 configurations)	[25]	-7.98361		
Self Consistent Pair Function Calculation		-7.98350		
Valence Bond Calculation (including all configurations not involving Li 1s excitation)	[26]	-7.98387	Li: 1s (2.6840) 2s (0.6930) 2p (0.7470) H: 1s (1.0830)	3.000
Self Consistent Pair Function Calculation		-7.98479		

\* orbital exponents in parenthesis

**Beryllium dihydride:** Although the  $BeH_2$  system has not been observed experimentally, it provides a simple polyatomic molecule for theoretical studies. It is a prototype of the  $BeF_2$  and  $Be(CH_3)_2$  molecules.

The molecule belongs to the  $D_{\infty h}$  point group and the two valence pair functions are related by symmetry. Generally, symmetrically related pair (group) functions belong to an irreducible representation of a subgroup,  $H$ , of the point symmetry group,  $G$ , of the system. They are transformed into each other by the operations  $R \in G$ ,  $R \notin H$ . Unique pairs (groups) belong to a non-degenerate representation of  $G$ . For the  $BeH_2$  molecule we have  $H = C_{\infty v}$  and  $R = \sigma_h$ .

The equivalent valence molecular orbital and the pair function orbitals are compared in figure 2. The core orbital, which is sketched with a scale five times larger than the orbitals, was taken to be doubly occupied. The second valence pair function was determined by symmetry. Again the valence orbitals have a node, but again these occur in regions where the core orbitals dominate the electron density.

The energies obtained from molecular orbital, valence bond and pair function calculations are compared in table 2. The pair function calculation

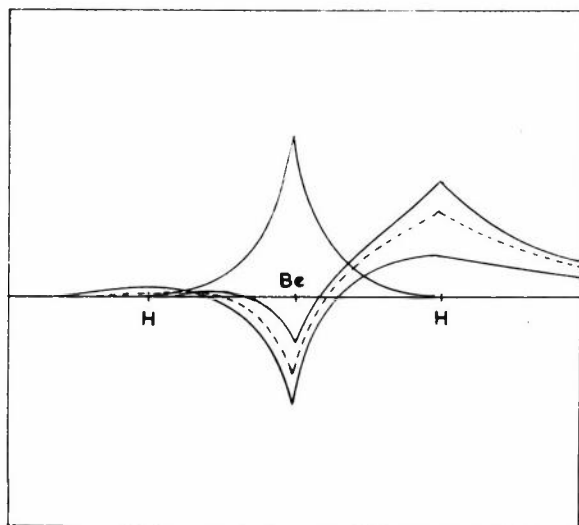


Figure 2: Pair function orbitals and equivalent m.o. (----) for the  $BeH_2$  system with  $R(Be-H) = 2.54$  bohrs

utilised orthogonal hybrids as an initial guess. Self consistency was obtained after varying each pair function twice. The coefficient vectors were consistent to six decimal places.

Table 2: S.C.F.-M.O., V.B. and S.C.P.F. energies for the  $BeH_2$  molecule

Description	Reference	Total Energy (au)	Basis Set*	$R(Be-H)$ au
S.C.F. Molecular Orbital Calculation	[27]	-15.7162	Be: 1s (3.6848) 2s (0.9560) 2p <sub>z</sub> (0.9560) H <sub>a</sub> : 1s (1.0000) H <sub>b</sub> : 1s (1.0000)	2.54
Self Consistent Pair Function Calculation		-15.7363		
Valence Bond Calculation (excluding 1s <sup>2</sup> , Be core, excitation)	[27]	-15.7377		

\* orbital exponents in parenthesis

The water molecule: Finally, the self consistent pair function model has been applied to the water molecule. The total energy of the system has been calculated for various ( $H-O-H$ ) bond angles. The bond length ( $O-H$ ) was fixed at the experimental value, 1.8111 Bohrs [32]. The orbitals of the core pair function were taken to be identical, as were those associated with the two lone pairs.

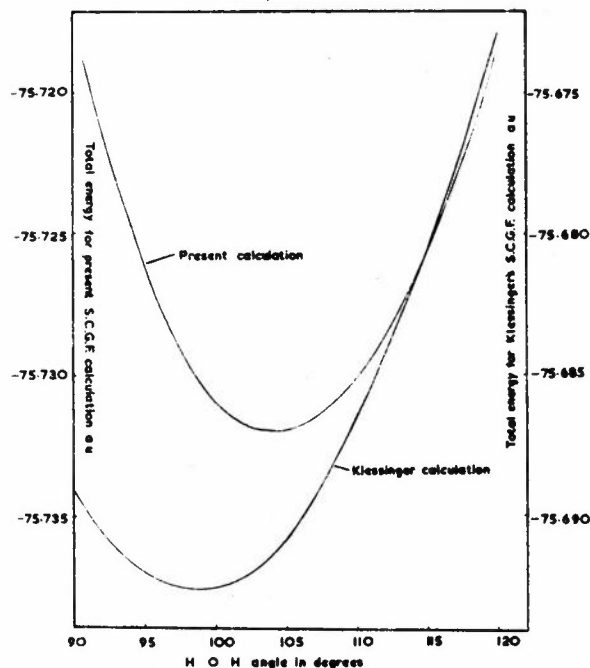


Figure 3: Total energy for the  $H_2O$  system versus  $H-O-H$  angle. (Right hand scale - Klessinger calculation: left hand scale - present calculation.)

The potential curve obtained is compared with that of Klessinger [29] in figure 3. Klessinger fixed the partition of his basis set† before optimising the orbitals. This gives an equilibrium bond angle  $\theta_{min}$  of  $98.1^\circ$ , while optimising the basis set partition, we obtain  $\theta_{min} = 104.27^\circ$ . The experimental value is  $104.45^\circ$  [32]. This illustrates the importance of optimising the basis set partition (cf. the previously reported calculations for the ethane molecule [31]). The potential curve and basis set specifications are given in table 3.

Table 3: Energy of the water molecule as a function of ( $H-O-H$ ) bond angle

$H-O-H$ Angle	- Total Energy (au)
$90.00^\circ$	75.718955
$95.00^\circ$	75.726629
$100.00^\circ$	75.730839
$103.00^\circ$	75.731805
$104.00^\circ$	75.731900
$104.45^\circ$	75.731903
$105.00^\circ$	75.731874
$106.00^\circ$	75.731735
$110.00^\circ$	75.730070
$115.00^\circ$	75.725626
$120.00^\circ$	75.718716

Basis Set (orbital exponents in parenthesis [28])

$O$ :  $1s$  (7.6579),  $2s$  (2.2458),  $2p_x$   $2p_y$   $2p_z$  (2.2266)  
 $H_1, H_2$ :  $1s$  (1.2700)

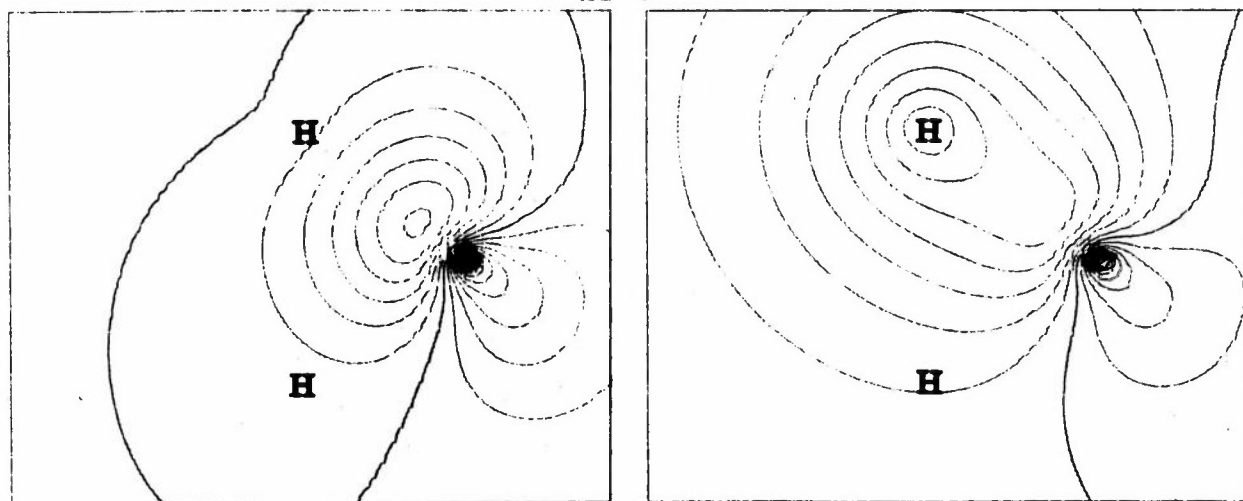


Figure 4: Amplitude of the orbitals in the bonding pair function for the water molecule at the equilibrium configuration.

† Klessinger's basis set was slightly different to that used here

Again starting from orthogonalised hybrids, the optimisation of the orbital coefficients necessitated the variation of each pair function five times. Typical computation times† for this calculation were (with a bond angle of 104°)

- (a) for the evaluation of the integrals over Slater functions‡ - 4.2 seconds;
- (b) for the iterative optimisation of the orbital coefficient vectors - 5.6 seconds.

The orbitals obtained for one of the (*O-H*) bonding pair functions, at the experimental equilibrium configuration, are illustrated in figure 4. The pair function consists of one orbital which is essentially a distorted  $sp^3$ -hybrid and a second which is a distorted hydrogen 1s-function. Electrostatic correlation between the pair of electrons associated with the bond is described. It should be emphasised that, unlike the molecular orbitals, the pair functions may not be subjected to an arbitrary unitary transformation. The chemically and physically appealing interpretation of molecular structure afforded by the pair function model is obtained directly. Localisation procedures are avoided.

### Concluding Remarks

The preliminary results presented in this paper suggest that, if groups of weakly interacting electrons can be recognised in a molecular system, the group function approach may provide a useful description of chemical phenomena. The model retains most of the advantages of the spin optimised S.C.F. method [3], but enables calculations to be made for much larger systems. For example, unlike the molecular orbital wavefunction, the function (2) will *always* behave correctly as the molecule dissociates. The calculations are open to simple physical interpretation within *both* the independent electron model and the group function model [33]. However, the importance of *optimising the partition of the basis set* must be emphasised. The use of a fixed partition of the basis functions, albeit proposed on chemical grounds, is not likely to be very satisfactory. This is particularly true when extended basis sets are employed.

### Acknowledgements

It is a pleasure to acknowledge correspondence with Dr. D. M. Silver (Johns Hopkins University) concerning the diatomic molecule integral programs of Silver, Christoffersen, Ruedenberg and Mehler [34], and the assistance of D.F. Parker (Atlas Computer Laboratory) with the implementation of this and R. M. Steven's integral programs [35] on an IBM 370/195 computer. The S.R.C. kindly provided computer time and financial support for one of us (S.W.).

### Appendix A

The derivation of the electronic energy expression for the present group function model follows closely the discussion given in [3]. (Much of the notation used in [3] will be employed here.)

It is most convenient to use as a basis for the representation of the symmetric group,  $\mathcal{S}_N$ , spin functions in which the electron spins in each group are first coupled together and the resulting spin functions coupled to give the total spin function. This may be represented as follows:

$$(\dots((S_1, S_2)S_{12}, S_3)S_{123}\dots)S \quad (A1)$$

where  $S_1, S_2, \dots, S_\mu, \dots$  are the resultant spins of groups 1, 2,  $\dots, \mu, \dots$ ; and

$S_{12}$  = resultant spin after coupling  $S_1$  and  $S_2$ ;

$S_{123}$  = resultant spin after coupling  $S_{12}$  and  $S_3$ ;

.. .. .. .. .. etc.

In this basis the representation matrices corresponding to the permutation  $P_\mu P_\nu$  ( $P_\mu \in \mathcal{S}_{N\mu}, P_\nu \in \mathcal{S}_{N\nu}$ ) are in fully reduced form [3].

The energy expression is then obtained by the molecular coefficients of fractional parentage technique ([3] and references contained therein). Terms which are zero because of the strong orthogonality of the functions (6) are omitted.

For a single spin function from this basis, the terms in equations (4) and (5) have the form:

$$H_{kk}^S \mu = (\Delta_\mu^{Skk})^{-1} \sum_{p,q}^{N\mu} D_\mu (pq|Skk) \langle p|h|q \rangle; \quad (p,q \in \Phi_\mu) \quad (A2)$$

$$J_{kk; \mu}^S = (\Delta_\mu^{Skk})^{-1} \sum_{p>q,r,s}^{N\mu} D_\mu (pqrs|Skk) \langle pq|g|rs \rangle; \quad (p,q,r,s \in \Phi_\mu) \quad (A3)$$

† IBM 370/195 computer (cycle time = 756 nanoseconds)

‡ Integral package of R. M. Stevens (INT150)

$$K_{kk;\mu}^S = (\Delta_{\mu}^{Skk})^{-1} \sum_{p>q,r>s}^{N_{\mu}} D_{\mu}(qprs|Skk) \langle pq|g|rs\rangle; \quad (p,q,r,s \in \Phi_{\mu}) \quad (A4)$$

$$J_{kk;\mu\nu}^S = (\Delta_{\mu}^{Skk} \Delta_{\nu}^{Skk})^{-1} \sum_{pr}^{N_{\mu}} \sum_{qs}^{N_{\nu}} D_{\mu}(pr|Skk) D_{\nu}(qs|Skk) \langle pq|g|rs\rangle; \quad (p,r \in \Phi_{\mu}, q,s \in \Phi_{\nu}) \quad (A5)$$

$$K_{kk;\mu\nu}^S = (\Delta_{\mu}^{Skk} \Delta_{\nu}^{Skk})^{-1} \sum_{pr}^{N_{\mu}} \sum_{qs}^{N_{\nu}} D_{\mu\nu}(qprs|Skk) \langle pq|g|rs\rangle; \quad (p,r \in \Phi_{\mu}, q,s \in \Phi_{\nu}) \quad (A6)$$

The normalisation integrals and density matrices arising in these expressions are very similar to those discussed in reference [3]. They have the form

$$\Delta_{\mu}^{Skk} = \sum_{P_{\mu} \in \mathcal{S}_{N_{\mu}}} \{U_{Skk}^N(P_{\mu}) \langle \bar{P}^r \Phi_{\mu} | \Phi_{\mu} \rangle\} \quad (A7)$$

$$D_{\mu}(pq|Skk) = \sum_{P_{\mu} \in \mathcal{S}_{N_{\mu}-1}} \{U_{Skk}^N(P_{pN_{\mu}} P_{\mu} P_{qN_{\mu}}) \langle \bar{P}_{\mu}^r \Phi_{\mu p}^{N_{\mu}-1} | \Phi_{\mu q}^{N_{\mu}-1} \rangle\} \quad (A8)$$

$$D_{\mu}(pqrs|Skk) = \sum_{P_{\mu} \in \mathcal{S}_{N_{\mu}-2}} \{U_{Skk}^N(P_{SN_{\mu}} P_{rN_{\mu}-1} P_{\mu} P_{qN_{\mu}-1} P_{pN_{\mu}}) \langle \bar{P}^r \Phi_{\mu pq}^{N_{\mu}-2} | \Phi_{\mu rs}^{N_{\mu}-2} \rangle\} \quad (A9)$$

$$D_{\mu\nu}(qprs|Skk) = \sum_P \{U_{Skk}^N(P_{rN_{\mu}} P_{sN_{\nu}} P P_{N_{\mu}N_{\nu}} P_{qN_{\nu}} P_{pN_{\mu}}) \langle \bar{P}_{\mu}^r \Phi_{\mu p}^{N_{\mu}-1} | \Phi_{\mu r}^{N_{\mu}-1} \rangle \langle \bar{P}_{\nu}^r \Phi_{\nu q}^{N_{\nu}-1} | \Phi_{\nu s}^{N_{\nu}-1} \rangle\} \quad (A10)$$

where

$$P \equiv P_{\mu} P_{\nu} \quad P_{\mu} \in \mathcal{S}_{N_{\mu}-1} \quad P_{\nu} \in \mathcal{S}_{N_{\nu}-1} \quad (A11)$$

$\bar{P}_{\mu}^r$  permutes the orbitals of group  $\mu$  and  $\Phi_{\mu i}^{N_{\mu}-p}$  is defined in [3].

The generalisation of these expressions for wavefunctions of the form (2) is straightforward [18] and follows closely discussions elsewhere [3].

## Appendix B

The Kuhn-Tucker necessary conditions for the solution of optimisation problems subject to constraints have been discussed in numerous works, for example reference [19]. Only a brief outline will be given here for the particular case in which the constraints are equality constraints.

Consider the problem

$$\text{Minimise } F(\mathbf{x}) \quad (B1)$$

subject to the equality constraints

$$C_i(\mathbf{x}) = 0 \quad i = 1, 2, \dots \quad (B2)$$

The Kuhn-Tucker conditions for the solution of this

problem may be written

$$P g = 0; \quad C = 0 \quad (B3)$$

where

$$g = \nabla F \quad (B4)$$

is the gradient vector.  $P$  projects vectors tangential to the manifold formed by the intersection of the constraints.

$$P = 1 - N(N^{\dagger}N)^{-1} N^{\dagger} \quad (B5)$$

where

$$N = \nabla C \quad (B6)$$

For a convex programming problem the conditions (B3) are both necessary and sufficient for the solution of the problem (B1, B2).

## References

- [1] MCWEENY, R. and SUTCLIFFE, B.T. (1969). *Methods of Molecular Quantum Mechanics*, New York: Academic Press.
- [2] MCWEENY, R. (1959). *Proc. Roy. Soc. (London)*, **A253**, 242.
- [3] GERRATT, J. (1971). *Adv. Atomic Mol. Phys.*, **7**, 141.
- [4] SINANOGLU, O. (1960). *J. Chem. Phys.*, **33**, 1212.
- [5] LEVY, M., STEVENS, W.J., SHULL, H. and HAGSTROM, S. (1970). *J. Chem. Phys.*, **52**, 5483.
- [6] KALDOR, U. and HARRIS, F.E. (1969). *Phys. Rev.*, **183**, 1.
- [7] LADNER, R.C. and GODDARD, W.A. (1969). *J. Chem. Phys.*, **51**, 1073.
- [8] ALLEN, L.C. and SHULL, H. (1961). *J. Chem. Phys.*, **35**, 1644.
- [9] MESSIAH, A. (1970). *Quantum Mechanics, Volume II*, Amsterdam: North Holland.
- [10] LOWDIN, P.-O. (1965). *Phys. Rev.*, **A357**, 139.
- [11] MESSIAH, A. (1970). *Quantum Mechanics, Volume I*, Amsterdam: North Holland.
- [12] Cf. the orthogonality constrained basis set expansion (O.C.B.S.E.) techniques of HUNT, W.J., DUNNING, T.H. and GODDARD, W.A. (1969). *Chem. Phys. Letters*, **3**, 606.
- [13] LEWIS, G.N. (1916). *J. Am. Chem. Soc.*, **38**, 762. GILLESPIE, R.J. and NYHOLM, R.S. (1957). *Quart. Rev.*, **11**, 339.
- [14] HURLEY, A.C., LENNARD-JONES, J.E. and POPLE, J. (1953). *Proc. Roy. Soc. (London)*, **A220**, 446.
- [15] COULSON, C.A. and FISCHER, I. (1949). *Phil. Mag.*, **40**, 386.
- [16] SERBER, R. (1934). *Phys. Rev.*, **45**, 461. ——— (1934). *J. Chem. Phys.*, **2**, 697. MATHEISS, L.F. (1959). *Quarterly Progress Report – Solid State and Molecular Theory Group*, Cambridge, Massachusetts: M.I.T.
- [17] GERRATT, J. and LIPSCOMB, W.N. (1968). *Proc. Natl. Acad. Sci. U.S.A.*, **58**, 332.
- [18] WILSON, S. (1974). Dissertation (in preparation).
- [19] HADLEY, G. (1964). *Nonlinear and Dynamic Programming*, Reading Massachusetts: Addison-Wesley. KUHN, H.W. and TUCKER, A.W. (1951). Non-linear programming, in *Proceedings of the Second Berkeley Symposium on Mathematical Statistics and Probability* (ed. J. Neyman), University of California Press.
- [20] ORTEGA, J.M. and RHEINOLDT, W.C. (1970). *Iterative Solution of Non-Linear Equations in Several Variables*, New York: Academic Press.
- [21] HAY, P.J., HUNT, W.J. and GODDARD, W.A. (1972). *J. Am. Chem. Soc.*, **94**, 8293. ———, ——— and ——— (1972). *Chem. Phys. Letters*, **13**, 30. ———, ——— and ——— (1972). *J. Chem. Phys.*, **57**, 738.
- [22] The Coulomb and exchange operators are defined as follows
- $$\hat{J}(\sigma;\tau) \phi_{\mu}(1) = (\int \phi_{\sigma}^*(2) \phi_{\tau}(2) r_{12}^{-1} dr_2) \phi_{\mu}(1)$$
- $$\hat{K}(\sigma;\tau) \phi_{\mu}(1) = (\int \phi_{\sigma}^*(2) \phi_{\mu}(2) r_{12}^{-1} dr_2) \phi_{\tau}(1)$$
- (See [23] for further details)
- [23] Roothaan, C.C.J. (1951). *Revs. Modern Phys.*, **23**, 69.
- [24] Ransil, B.J. (1960). *Revs. Modern Phys.*, **32**, 245.
- [25] Fraga, S. and Ransil, B.J. (1962). *J. Chem. Phys.*, **36**, 1127.
- [26] Murrell, J.N. and Silk, C.L. (1968). *Symp. Faraday Soc.*, **2**, 84.
- [27] MacLagan, R.G.A.R. and Schuelle, G.W. (1971). *J. Chem. Phys.*, **55**, 5431.
- [28] Clementi, E. and Raimondi, D.L. (1963). *J. Chem. Phys.*, **38**, 2686.
- [29] Klessinger, M. (1969). *Chem. Phys. Letters*, **4**, 144.
- [30] Palke, W.E. and Goddard, W.A. (1969). *J. Chem. Phys.*, **50**, 4524.
- [31] Klessinger, M. (1970). *J. Chem. Phys.*, **53**, 225. HUNT, W.J., HAY, P.J. and GODDARD, W.A. (1972). *J. Chem. Phys.*, **57**, 738.
- [32] Herzberg, G. (1945). *Infrared and Raman Spectra of Polyatomic Molecules*, Princeton, New Jersey: Van Nostrand.
- [33] Coulson, C.A. (1973). '... remarks upon the futility of obtaining accurate numbers, whether by computation or by experiment, unless these numbers can provide us with simple and useful chemical concepts; otherwise, one might as well be interested in a telephone directory.' Quoted in *Revs. Modern Phys.*, **45**, 22.
- [34] Silver, D.M. and Ruedenberg, K. (1968). *J. Chem. Phys.*, **49**, 4301, 4306. Christoffersen, R.E. and Ruedenberg, K. (1968). *Ibid.*, **49**, 4285. Mehler, E.L. and Ruedenberg, K. (1969). *Ibid.*, **50**, 2575. Erratum (1972). *Ibid.*, **57**, 3585.
- [35] Stevens, R.M. (1970). *J. Chem. Phys.*, **52**, 1397.

# Studies in the Pair Replacement MC-SCF and Strongly Orthogonal Geminal Theories

V.R.Saunders and M.F.Guest\*

Applications of the pair replacement MC-SCF theory and the method of anti-symmetrized product of strongly orthogonal geminals (APSG) to the systems  $LiH$ ,  $Li_2$ ,  $BH$  and  $NH_3$  are described and contrasted. The inter-pair dispersion energies are computed

(a) by standard CI for the MC-SCF wavefunctions

(b) by the direct interaction of geminal functions in the case of APSG theory.

The methods employed in the minimization of the MC-SCF and APSG energy expressions are briefly described.

## Introduction

In the present work, we shall be concerned with applications and extensions of two methods for obtaining compact electronic wavefunctions of beyond the Hartree-Fock level of accuracy; namely the multiconfigurational self-consistent field (MC-SCF) formalism in its 'pair replacement' form [1] and the method of the antisymmetrized product of strongly orthogonal geminals (APSG) [2-4]. The molecular systems  $LiH$ ,  $BH$ ,  $Li_2$  and  $NH_3$  have been chosen as test cases for numerical work involving these theories, and also for testing extensions designed to give some account of the inter-pair dispersion energies. A practical procedure for obtaining guaranteed convergence of the necessary energy minimizations is described.

## The Pair Replacement MC-SCF Theory

In the 'complete' pair replacement MC-SCF theory [1], we first assume that the  $2N$  electrons of a closed shell system may be distributed amongst  $N$  doubly occupied molecular orbitals,  $\phi_1 \dots \phi_N$ , this set being referred to [5] as the first set molecular orbitals (FSMO). All possible di-excitations from the FSMO to a second set of molecular orbitals (SSMO),  $\phi_{N+1} \dots \phi_M$  are considered. The determinant produced by di-excitation from the  $i^{\text{th}}$  to the  $k^{\text{th}}$  MO will be denoted  $\psi_{ik}$ . The total wavefunction is then written:

$$\psi = a_{00} \psi_{00} + \sum_{i,k} a_{ik} \psi_{ik} \quad (1)$$

where  $\psi_{00}$  is the determinant constructed from the

$N$  FSMO. We shall not concern ourselves greatly with the details of the construction of the MOs, except to say that the total set of  $M$  MOs is normally constrained to be orthonormal, and expanded in terms of a given set of  $M$  linearly independent basis functions. Variants of this 'complete' multiconfigurational (CMC) pair replacement theory are:

- Certain of the FSMO may not be correlated, so that configurations involving excitations from such FSMO are deleted from the expansion, equation (1).
- Certain of the SSMO may not be correlated, so that excitations to such SSMO are deleted from the expansion, equation (1).
- Multiconfigurational wavefunctions can be constructed by grouping the SSMO into disjoint sets, each set being associated with a given FSMO. Thus excitations from a given FSMO into its associated set of SSMO are the only type of pair replacements allowed. In this form the MC-SCF wavefunction is formally identical to the leading terms of an APSG expansion, as discussed by Robb and Csizmadia [6], who use the acronym DS-SEPC (doubly substituted separate electron pair configurations), and Levy [7].

Whatever particular MC expansion is chosen, the aim of the MC-SCF theory is to minimize the electronic energy with respect to variations in the linear coefficients appearing in equation (1) and also with respect to the form of the orbitals. It is this latter aspect which distinguishes the MC-SCF approach from straightforward configuration interaction (CI) calculations.

\* *Atlas Computer Laboratory (Science Research Council), Chilton, Didcot, Oxfordshire, OX11 0QY*

## The APSG Theory

In the APSG theory the total electronic wavefunction for a  $2N$  electron system is written as an antisymmetric product of  $N$  pair functions (geminals):

$$\psi = A' \prod_{r=1}^N \Lambda_r(2r-1, 2r) \quad (2)$$

where  $A'$  is a partial antisymmetrizer interchanging the electron co-ordinates from different pairs only. The geminals are antisymmetric with respect to interchange of the co-ordinates of the two electrons ( $\Lambda_r(1,2) = -\Lambda_r(2,1)$ ), and normalised, so that:

$$\int dV_1 \int dV_2 \Lambda_r(1,2) \Lambda_r^*(1,2) = 1 \quad (3)$$

The APSG theory is distinguished from the more general antisymmetrized product of geminals (APG) theory by the application of the strong orthogonality constraint in the former:

$$\int dV_1 \Lambda_r(1,2) \Lambda_s^*(1,2) = 0 \quad (r \neq s) \quad (4)$$

and under this constraint the geminals are often referred to as separated electron pair functions. Such pair functions are usually written:

$$\Lambda_r(1,2) = \lambda_r(1,2) \theta_r(1,2) \quad (5)$$

where the spin function,  $\theta$ , is given by:

$$\theta(1,2) = (\alpha(1)\beta^*(2) - \beta(1)\alpha^*(2))/\sqrt{2} \quad (6)$$

for a singlet coupling. The spatial functions may be expanded in terms of their natural orbitals [8]:

$$\lambda_r(1,2) = \sum_{\mathbf{k}} a_{r\mathbf{k}} \phi_{\mathbf{k}}(1) \phi_{\mathbf{k}}^*(2) \quad (7)$$

where the  $\phi_{\mathbf{k}}$  form an orthonormal set of molecular orbitals. The strong orthogonality condition means in practice that the total one-electron space spanned by  $\{\phi\}$  is factored into  $N$  disjoint subspaces,  $\{\phi^r\}$ , so that each geminal is written as an expansion over only the one-particle functions belonging to the given geminal's subspace [9].

The central problem of the self-consistent APSG theory is to optimize the energy with respect to variations in the linear expansion parameters and the form of the MOs appearing in equation (7). We note that the generalised valence bond (GVB) method [10] is a restricted form of the APSG theory where each separated pair function is written as a two term self-consistent natural orbital expansion.

## Minimization of the APSG and MC-SCF Energy Expressions

We first note that given a set of molecular orbitals, there is no great difficulty in the optimization of the linear parameters of equations (1) or (7) for the MC-SCF or APSG theories respectively. In the latter case a set of coupled eigen problems result, which may be solved by a method suggested by Silver *et al.* [3], whilst all that is required in the MC-SCF case is the solution of a simple eigen problem. The more difficult problem is concerned with the optimization of the form of the MOs. Consider a variation which mixes orbitals  $\phi_i$  and  $\phi_j$ . Such a variation may be represented:

$$\phi_i \rightarrow \phi_i + X_{ji} \phi_j \quad (8a)$$

$$\phi_j \rightarrow \phi_j + X_{ij} \phi_i \quad (8b)$$

where first order orthonormality is conserved by the requirement that  $X_{ji} = -X_{ij}$ . The standard Newton-Raphson procedure may be invoked for the minimization of the energy functional with respect to the matrix elements of  $X$ , and leads to the set of linear equations:

$$\left( \frac{\partial E}{\partial X_{ji}} \right)_{X=0} + \sum_{k>1} X_{ji} \left( \frac{\partial^2 E}{\partial X_{ji} \partial X_{ik}} \right)_{X=0} = 0 \quad (9)$$

Solution of equation (9) for the  $X_{ji}$  would lead in principle to a quadratically convergent procedure for the optimization of the MOs. Unfortunately the Newton-Raphson equations are not directly of practical value (except for small cases with less than say thirty MOs, 435 independent parameters), largely because the number of second derivatives which must be computed and stored is proportional to the fourth power of the number of molecular orbitals. The necessity for some approximation in the Newton-Raphson procedure is indicated, and we have proceeded by neglecting all off-diagonal second derivatives, giving rise to the decoupled equations:

$$X_{ji} = - \left( \frac{\partial E}{\partial X_{ji}} \right)_{X=0} / \left( \frac{\partial^2 E}{\partial X_{ji}^2} \right)_{R_{X=0}} \quad (10)$$

Unfortunately the quadratic termination properties of the Newton-Raphson scheme are lost, and indeed the approximate procedure may not be convergent. In order to obtain a guarantee of convergence, we have modified equation (10) to the form:

$$X_{ji} = -\alpha \left( \frac{\partial E}{\partial X_{ji}} \right)_{X=0} / \left( \left( \frac{\partial^2 E}{\partial X_{ji}^2} \right)_{X=0} + \beta \right) \quad (11)$$



where  $\alpha$  and  $\beta$  are parameters whose values may be chosen as desired. It is now easy to show that convergence may be guaranteed either:

- (a) by choosing a 'sufficiently' large positive value for  $\beta$ .
- (b) on the assumption that the second derivatives in equation (11) have positive values (which will be the case near a minimum), by choosing a 'sufficiently' small positive value for  $\alpha$ . Far from convergence, where negative second derivatives may be encountered, we have found the use of the absolute value of the second derivative in equation (11) to be occasionally useful.

We shall omit proof of the guaranteed convergence of the present proposals, and content ourselves with the statement that the argument runs along lines closely related to the proof of guaranteed convergence of the 'level shifting' method [11] for converging Hartree-Fock wavefunctions, with  $\alpha$  and  $\beta$  taking the roles of the 'damp factor' and 'level shifter' respectively.

The present method defines improved MOs as linear combinations of the trial MOs, the iterated MOs being orthonormal to first order only. The iterated MOs may be rendered orthonormal to any desired order by an application of the  $S^{-1/2}$  symmetric orthonormalization scheme [12], and re-expressed as linear combinations of the basis functions by means of a linear transformation involving the definition of the trial MOs as linear combinations of the basis functions. We have found that our method is most effective if the linear coefficients of equation (1) or (7) are redetermined after each iteration of the 'quasi-Newton' orbital refinement procedure proposed here. The necessary formulae for the energy derivatives have been collected into the Appendix, and examination of these formulae reveals that all the required derivatives can be evaluated in approximately the same computer time as would be required by methods based on effective Fock operators [1,5,13,14], the most time consuming operation being a partial four-index transformation of the two electron integrals.

It is pertinent to note that Levy [7] has proposed using the formula:

$$X_{ji} = \lambda_{ji} \left( \frac{\partial E}{\partial X_{ji}} \right)_{X=0} \quad (12)$$

where the  $\lambda_{ji}$  are taken to be a set of user supplied parameters whose magnitudes Levy assumed to be based on estimates of the inverse of the appropriate second derivatives. Such a scheme seems to us to be perfectly workable when small basis sets are used (so that comparatively few natural orbitals per electron are involved), but our observations of the magnitude of the second derivatives when large basis sets are used indicate that it becomes increasingly difficult

to make good estimates of those second derivatives involving the more weakly occupied natural orbitals without direct calculation. The full quadratically convergent Newton-Raphson scheme has been used in the optimization of MC-SCF wavefunctions [15] and other correlated wavefunctions [16] for cases of up to six electrons. We believe the present procedure, where the orbital rotations are performed simultaneously, to be considerably more economic than the method of 'two by two rotations' [3], since the latter procedure requires computer time proportional to the sixth power of the basis set size, whilst our method defines an ' $M^5$ ' problem.

### Dispersion Corrections to the DS-SEPC and ASPG Theories

In both the APSG and DS-SEPC theories, electron pairs are described using disjoint sets of natural orbitals. Such theories may be expected to work well only when each set of natural orbitals is strongly localised, so that the differential overlap between any pair of functions belonging to different sets is small, and we proceed on the assumption that these conditions are satisfied.

In the strongly separable limit, the principle correction to the DS-SEPC or APSG wavefunctions arises from the inter-pair dispersion forces first discussed by Eischitz and London [17]. In the DS-SEPC case, such dispersion forces may be allowed for by the inclusion of doubly excited configurations of the type:

$$A' \left( [\phi_i^1 \phi_i^1] \dots [\phi_i^r \phi_k^r] \dots [\phi_i^s \phi_k^s] \dots [\phi_i^N \phi_i^N] \right) \quad (13)$$

where the configuration has been chosen to represent dispersion between pairs  $r$  and  $s$ , and  $\phi_i^r, \phi_k^r$  denote strongly and weakly occupied natural orbitals respectively belonging to the  $r^{\text{th}}$  pair, and:

$$[\phi_i^r \phi_k^r] = \sqrt{1/2} \left( \phi_i^r(2r-1) \phi_k^r(2r) + \phi_i^r(2r) \phi_k^r(2r-1) \right) \cdot \theta \quad (14a)$$

$$[\phi_i^r \phi_i^r] = \phi_i^r(2r-1) \phi_i^r(2r) \cdot \theta \quad (14b)$$

where  $\theta$  denotes the normalised singlet spin function of the co-ordinates of electrons  $2r-1$  and  $2r$ . Such dispersion configurations have been denoted  $[\phi_i^r \phi_k^r]^+$   $[\phi_i^s \phi_k^s]^+$  by Robb and Csizmadia [18] who use the term doubly substituted augmented separated electron pair configurations (DS-ASEPC) to describe the CI wavefunction including the DS-SEPC configurations plus all the inter-pair dispersion functions of the type discussed above. The dispersion configurations may be expected to provide the major correction to the DS-SEPC wavefunction at the strongly separable limit, since all other doubly excited configurations

have Hamiltonian matrix elements with the DS-SEPC function which involve integration over the negligible inter-pair differential overlap distributions, whilst the singly excited configurations either give rise to zero matrix elements because of Brillouin theorem conditions arising out of the self-consistency of the DS-SEPC function (intra-pair one electron excitation), or involve integration over inter-pair differential overlap (in the case of the inter-pair one electron transfer configurations).

In considering the generalization of the ASPG wavefunction to include dispersion effects, we are led to consider a wavefunction expanded as a linear combination of the zero order APSG function plus terms of the form:

$$A' \left( \left[ \phi_i^r \phi_k^s \right] \left[ \phi_i^s \phi_k^r \right] \prod_{p \neq r,s} \Lambda_p \right) \quad (15)$$

In order to determine the optimum form of such a linear combination we shall require Hamiltonian matrix elements between geminal product functions, which may be expected to be more complex than those arising in the more usual forms of CI where Slater determinants (or spin projected Slater determinants) are used as the configurational basis. Fortunately, with the rather restricted class of geminal configurations considered in the present work, the increase in complexity of the relevant matrix elements is not great, and we refer to the work of Kapuy [4] for the necessary formulae. We shall adopt the term augmented separated pair (ASP) [19] to describe the dispersion corrected APSG theory.

### Definition of Pair Energy

When performing calculations beyond the Hartree-Fock limit, it is useful to be able to analyse the computed correlation energy into 'pair contributions'. When such an analysis is carried out, it appears to be inconvenient to use the restricted Hartree-Fock (RHF) energy as a reference point; rather the energy,  $E(\text{PNO})$ , of the single determinant constructed by double occupation of the principal natural orbitals (PNO) of the correlated wavefunction appears to be a more convenient choice. Such a procedure can be justified by the well-known result [7,20-22] that  $E(\text{PNO})$  is usually rather close to  $E(\text{RHF})$ ; we have found differences of 0.001 Hartree maximum in the present work.

We shall first consider the MC-SCF case. Whether in its CMC, DS-SEPC or DS-ASEPC form, we note that the PNO are identical to the FSMO, and that the total wavefunction can be written:

$$\psi = a_0 \psi(\text{PNO}) + \sum_{ij} a_{ij}^{kl} \psi_{ij}^{kl} \quad (16)$$

where  $\psi_{ij}^{kl}$  represents a configuration constructed by di-excitation from the FSMO  $i$  and  $j$  to the SSMO  $k$  and  $l$ . Because the coefficients ( $a_0$  and  $a_{ij}^{kl}$ ) appearing in equation (16) have been determined variationally, we find the relationship:

$$E_{\text{total}} = E(\text{PNO}) + \frac{1}{a_0} \sum_{ij} a_{ij}^{kl} H_{ij}^{kl} \quad (17)$$

where  $H_{ij}^{kl}$  denotes the Hamiltonian matrix element connecting  $\psi_{ij}^{kl}$  with  $\psi(\text{PNO})$ . The correlation energy for the pair of FSMO ( $i,j$ ) is given by:

$$\mathcal{E}_{ij} = \frac{1}{a_0} \sum_{k,l} a_{ij}^{kl} H_{ij}^{kl} \quad (18)$$

so that the total energy may be written:

$$E_{\text{total}} = E(\text{PNO}) + \sum_{ij} \mathcal{E}_{ij} \quad (19)$$

Expressions of this type have been discussed [23] by Nesbet and by Sutton *et al.*

In the case of the APSG model, the factorization of the correlation energy into additive components is not so straightforward. The APSG function can be written as linear combination of  $\psi(\text{PNO})$ , plus configurations produced by double, quadruple, hexuple etc. excitation from  $\psi(\text{PNO})$ . However, the configurational mixing coefficients in such an expansion have not been determined variationally as in a CI calculation, but under the APSG constraint. Fortunately it may be shown [24] that the APSG theory gives rise to configurational mixing coefficients which are closely similar to those which would be produced by a full CI treatment. If we analyse the APSG function along the same lines as the treatment for the MC-SCF function, and ignore the small deviations of the configurational mixing coefficients from the CI variational values, we find the intra-pair correlation energy of the  $r^{\text{th}}$  geminal, whose PNO is orbital  $i$ , is given by:

$$\mathcal{E}_{\pi} = \frac{1}{a_{ri}} \sum_{k \neq i} a_{rk} H_{ii}^{kk} \quad (20)$$

where  $H_{ii}^{kk}$  denotes the Hamiltonian matrix element between  $\psi(\text{PNO})$  and the configuration produced by double substitution of the  $i^{\text{th}}$  PNO by the  $k^{\text{th}}$  weakly occupied natural orbital;  $a_{rk}$  is as defined in the natural orbital expansion of the pair function, equation (7), the summation over  $k$  being over the weakly occupied natural orbitals belonging to the  $r^{\text{th}}$  geminal. Equation (20) has been derived from equation (18) by expressing the configurational mixing coefficients as products of the expansion coefficients

appearing in the natural orbital representations of the geminals, equation (7), and by noting that quadruple and higher order excited configurations have a zero valued Hamiltonian matrix element with  $\psi(\text{PNO})$ . Of course, we cannot expect the APSG total energy to rigorously equal the sum of the intra-pair energies plus  $E(\text{PNO})$ . In practice, such deviations from additivity have been found to be never greater than  $10^{-6}$  Hartree in the present work, and so can be safely ignored.

## Boron Hydride

$BH$  is a system of particular interest, because it is the smallest system for which previous APSG calculations [25] gave disappointing results, only 47% of the total correlation energy being recovered. The present calculations were carried out at an internuclear separation of 2.329 bohr [25], slightly less than the experimental distance of 2.336 bohr [26]. The basis set comprised Slater type orbitals (STO) expressed

as linear combinations of Gaussian type functions (GTF) according to the least squares criterion [27]. The generation of the basis set can be divided into two distinct phases, with the initial generation of a set designed to approach the Hartree-Fock limit, followed by addition of basis functions specifically chosen to account for electronic correlation effects.

The near Hartree-Fock basis was generated from the double zeta set of Huzinaga and Arnau [28], with a hydrogen basis of a  $1s$  and a  $2s$  orbital whose exponents were chain optimized. Certain of the  $1s$  orbitals on  $B$  and  $H$  were finally expanded by scaling the variational expansion of the hydrogenic  $1s$  orbital in six GTF [29]. This double-zeta basis was enlarged by reference to the literature [15,25] together with some energy optimization, to generate an ( $8s$ ,  $3p$ ) on the boron and a ( $4s$ ,  $1p$ ) set on the hydrogen, the added functions being expanded in either three or four GTF depending on their estimated importance in the Hartree-Fock wavefunction, the resulting basis being shown in table 1. A restricted Hartree-Fock (RHF) calculation using this set of 24 STO gave an energy of  $-25.1260$  Hartree, .0054 Hartree above the limit [20].

Table 1: Basis sets<sup>a</sup> for  $BH$ ,  $LiH$ ,  $Li_2$  and  $NH_3$

<i>BH</i>		<i>LiH</i>		<i>Li<sub>2</sub></i>		<i>NH<sub>3</sub></i>	
Orbital	Exponent	Orbital	Exponent	Orbital	Exponent	Orbital	Exponent
<b>Boron</b>		<b>Lithium</b>		<b>Lithium</b>		<b>Nitrogen</b>	
$1s^b$ (6)	4.24477	$2s$ (6)	2.35	$2s$ (6)	2.35	$1s$	10.50
$1s^b$ (6)	6.545	$1s^b$ (6)	2.45	$1s^b$ (6)	2.45	$1s$	6.10
$1s$ (5)	9.8	$1s^b$ (6)	3.70	$1s^b$ (6)	3.70	$2s$	5.90
$2s$ (6)	4.6	$1s^b$ (6)	5.40	$1s^b$ (6)	5.40	$2s$	2.25
$3s$ (4)	5.0	$2s$ (4)	1.00	$2s$ (5)	0.64	$2s$	1.60
$2s$ (6)	0.878793	$2s$ (4)	0.70	$2s$ (5)	1.00	$2s$	1.10
$2s$ (6)	1.41415	$2p$ (4)	6.50	$2s$ (4)	1.77	$2p$	1.10
$2s$ (5)	2.3	$2p$ (4)	4.10	$2p$ (4)	1.05	$2p$	1.90
$2p$ (6)	1.00435	$2p$ (4)	0.75	$3p$ (4)	0.95	$2p$	2.90
$2p$ (6)	2.21163	$3d$ (3)	5.40	$4d$ (3)	1.05	$2p$	6.30
$3p$ (4)	1.9					$3d$	1.95
<b>Hydrogen</b>		<b>Hydrogen</b>				<b>Hydrogen</b>	
$1s^b$ (6)	1.7	$3s$ (4)	1.20			$1s$	2.10
$1s^b$ (6)	1.13	$2s$ (4)	1.15			$1s$	1.30
$2s$ (5)	1.06	$1s^b$ (6)	1.00			$2s$	1.25
$3s$ (4)	1.23	$1s^b$ (6)	1.50			$2p$	1.95
$2p$ (4)	1.7	$3p$ (4)	1.20			<b>Lone Pair Centroid</b>	
		$2p$ (4)	1.05			$3p$	2.70
<b>Lone Pair Centroid</b>		$2p$ (4)	1.55				
$3p$ (4)	1.81	$3d$ (3)	1.70				
$4d$ (3)	2.4						
<b>Bond Centroid</b>							
$2p$ (4)	1.5						
$3p$ (4)	1.8						
$3d$ (3)	2.0						
<b>Boron Inner Shell Correlation</b>							
$2p$ (4)	6.9						
$2p$ (4)	10.4						
$3d$ (3)	9.4						

(a) For  $BH$ ,  $LiH$  and  $Li_2$  the number of GTF/STO is indicated in parentheses

(b) Scaled Variational Hydrogenic orbital, [29]

Basis functions were then added to the 24 STO near Hartree-Fock basis to account for the valence shell correlation effects. The 24 STO of table 1 were retained, with no change in orbital exponents, in a sequence of calculations in which the basis is successively augmented with functions sited at the dipole centroids of the appropriate geminal;  $2p$ ,  $3p$  and  $3d$  STO were placed at the centroid of the bonding geminal (1.7 bohr from the boron),  $3p$  and  $4d$  STO being sited at the lone pair centroid (0.9 bohr from the boron) to yield a 43 STO basis.

the addition of functions to the boron atom, culminating in a 54 STO basis set which gives Hartree-Fock and total APSG energies of  $-25.1302$  and  $-25.2469$  Hartree respectively, the calculated correlation energy being 0.1167 Hartree, or 75% of the total, and the inner shell being described by thirteen natural orbitals ( $5\sigma$ ,  $3\pi$ ,  $1\delta$ ). Our final basis set is thus 0.0010 Hartree above the Hartree-Fock limit; nearly all this error is estimated to arise from inadequacy in the boron inner shell description.

Table 2: Total APSG Energies (Hartree) of  $BH$  during evolution of the basis set

$E(\text{Total})$	$E(\text{PNO})$	$\Delta E^b$	Geminal Pair Energies <sup>a</sup>			Remarks
			Bond	Lone Pair	Inner Shell	
-25.18860	-25.12535	0.0632	0.0267 ( $3\sigma$ , $1\pi$ )	0.0365 ( $2\sigma$ , $1\pi$ )	-	$B(8s$ , $3p)$ ; $H(4s$ , $1p)$
-25.19671	-25.12776	0.0689	0.0307 ( $4\sigma$ , $2\pi$ )	0.0382 ( $2\sigma$ , $1\pi$ )	-	$2p$ ( $\xi=1.5$ ) at bond centroid
-25.20103	-25.12892	0.0721	0.0322 ( $5\sigma$ , $3\pi$ )	0.0400 ( $2\sigma$ , $1\pi$ )	-	$3p$ ( $\xi=1.8$ ) at bond centroid
-25.20810	-25.12937	0.0787	0.0320 ( $5\sigma$ , $3\pi$ )	0.0467 ( $2\sigma$ , $2\pi$ )	-	$3p$ ( $\xi=1.81$ ) at lone pair centroid
-25.20916	-25.12934	0.0798	0.0322 ( $5\sigma$ , $3\pi$ )	0.0477 ( $3\sigma$ , $2\pi$ , $1\delta$ )	-	$4d$ ( $\xi=2.4$ ) at lone pair centroid
-25.21042	-25.12944	0.0810	0.0332 ( $5\sigma$ , $3\pi$ , $1\delta$ )	0.0478 ( $4\sigma$ , $2\pi$ , $1\delta$ )	-	$3d$ ( $\xi=2.0$ ) at bond centroid
-25.22105	-25.12945	0.0916	0.0331 ( $5\sigma$ , $3\pi$ , $1\delta$ )	0.0475 ( $4\sigma$ , $2\pi$ , $1\delta$ )	0.0111 ( $2\sigma$ )	basis as above
-25.24222	-25.12973	0.1125	0.0329 ( $5\sigma$ , $3\pi$ , $1\delta$ )	0.0472 ( $4\sigma$ , $2\pi$ , $1\delta$ )	0.0324 ( $3\sigma$ , $1\pi$ )	$2p$ ( $\xi=6.9$ ) at $B$
-25.24420	-25.12973	0.1145	0.0329 ( $5\sigma$ , $3\pi$ , $1\delta$ )	0.0472 ( $4\sigma$ , $2\pi$ , $1\delta$ )	0.0343 ( $4\sigma$ , $2\pi$ )	$2p$ ( $\xi=10.4$ ) at $B$
-25.24686	-25.12975	0.1171	0.0329 ( $5\sigma$ , $3\pi$ , $1\delta$ )	0.0472 ( $4\sigma$ , $2\pi$ , $1\delta$ )	0.0370 ( $5\sigma$ , $3\pi$ , $1\delta$ )	$3d$ ( $\xi=9.4$ ) at $B$

(a) The quantities in parentheses refer to the number and type of natural orbitals assigned to the appropriate geminal

(b)  $\Delta E = E(\text{PNO}) - E(\text{Total})$

The results of this refinement of the basis set are indicated in table 2. A CMC-MC-SCF calculation using the 24 STO basis indicated that an APSG calculation in which five natural orbitals are assigned to the bond geminal ( $3\sigma$ ,  $1\pi$ ) and four natural orbitals ( $2\sigma$ ,  $1\pi$ ) assigned to the lone pair should be performed: the remaining natural orbitals were found to yield only a minor total contribution (less than  $5 \times 10^{-4}$  Hartree) to the valence shell pair energies. The results of such a two pair APSG calculation are given as the first row of table 2. The experimental total correlation energy of  $BH$  is estimated [25] to be 0.155 Hartree, and the valence shell correlation energy 0.113 Hartree [31]. Using this latter estimate, the present calculation recovers 55% of the valence shell correlation energy. The process of refinement of the valence shell correlating basis culminates in the results of the sixth row, table 2. We see that the bonding geminal is now described by thirteen natural orbitals ( $5\sigma$ ,  $3\pi$ ,  $1\delta$ ), the lone pair by ten natural orbitals ( $4\sigma$ ,  $2\pi$ ,  $1\delta$ ), and the Hartree-Fock energy has improved to  $-25.1299$  Hartree (0.0015 Hartree above the limit). The total APSG energy in this 43 STO basis is  $-25.2104$  Hartree, yielding a valence shell correlation energy of 0.0805 Hartree (71%). Our results indicate that it is the use of  $p$  functions at the geminal centroids which has given the most significant contribution to these improvements. The final stages of the basis set improvement are concerned with the generation of a correlating basis for the boron inner shell, by

The results of a series of calculations using the larger basis sets are summarized in table 3. The one and two pair calculations were performed using the 43 STO basis, the three pair results being derived from the 54 STO basis. Perhaps the most important result is the near invariance of the computed binding energy and dipole moment with the degree of inner shell correlation. The dissociation products of the three pair APSG model of  $BH$  were taken to be hydrogen ( $^2S$ ), (energy =  $-0.49995$  Hartree in our basis), and a non-symmetry equivalences APSG boron atom ( $^2P$ ), with the  $1s$  and  $2s$  shells correlated, (energy =  $-24.6039$  Hartree), leading to a computed dissociation energy of 3.89 eV. The dissociation products of the two pair APSG model were taken to be hydrogen ( $^2S$ ) and a non-symmetry equivalences APSG boron atom ( $^2P$ ) with only the  $2s$  shell correlated (energy =  $-24.5665$  Hartree) leading to a dissociation energy of 3.92 eV. These results should be compared with the experimental value [36] of 3.59 eV. Note that some basis set re-optimization was attempted for the above atomic calculations. We have avoided the computation of dissociation energies for the DS-SEPC and DS-ASEPC theories, because of uncertainty about the nature of dissociation products, noting the omission of certain quadruple excitations which become important at long bond length. The effects of applying a symmetry equivalencing constraint to the APSG model of boron have been discussed by Mehler *et al.* [25]. We note that  $E(\text{PNO})$  is never greater than

Table 3: Energy parameters (Hartree) and dipole moment of *BH*

Calculation	$E(\text{PNO})$	$E(\text{Total})$	$D_e$ $e\text{\AA}$	$\mu_e$ (Debye)	$\Delta E^a$	Pair Energies				Reference
						Bond	Lone Pair	Inner Shell	Bond-Lone Pair	
RHF (54STO)		-25.1302	2.78	1.781						b
RHF (43STO)		-25.1299	2.78	1.778						b
APSG (3 pair)	-25.1298	-25.2469	3.89	1.524	0.1167	0.0329	0.0472	0.0370		b
APSG (2 pair)	-25.1294	-25.2104	3.92	1.517	0.0805	0.0332	0.0478			b
APSG (1 pair)	-25.1299	-25.1670		1.836	0.0371	0.0371				b
APSG (1 pair)	-25.1295	-25.1793		1.416	0.0494		0.0498			b
DS-SEPC (2 pair)	-25.1295	-25.2077		1.549	0.0778	0.0326	0.0456			b
DS-ASEPC (2 pair)	-25.1295	-25.2140		1.556	0.0841	0.0321	0.0443		0.0081	b
Experiment		-25.289	3.59		0.155					[16,36]
RHF limit		-25.1314	2.77	1.733						[30]
CI		-25.2621		1.470	0.1331	0.0356	0.0492	0.0374	0.0199	[37]
GVB-(3 pair)		-25.1777	3.21		0.0495	0.0144	0.0228	0.0124		[10]
G1-(3 pair)		-25.1801	3.24	1.504	0.0519					[42]
IEP-(2 pair)					0.0963	0.0328	0.0458		0.0177	[32]
APSG (2 pair)	-25.1220	-25.1790	4.11		0.0476					[25]
APSG (3 pair)	-25.1220	-25.2053	3.86		0.0739					[25]

(a)  $\Delta E = E(\text{RHF}) - E(\text{Total})$ 

(b) Present work

$E(\text{RHF})$  by more than 0.0009 Hartree in the present calculations, a result in contrast with the findings of Mehler *et al.* [25], who find surprisingly large differences between  $E(\text{PNO})$  and  $E(\text{RHF})$ , of the order of 0.0094 Hartrees. The difference in energy between the two-pair APSG and DS-SEPC results in an estimate of 0.0027 Hartree energy lowering due to the admixing of quadruple excitations in the APSG model.

The DS-ASEPC calculation gives the largest valence correlation energy, 0.0837 Hartree (74%) and an estimate of the inter-pair dispersion energy of 0.0081 Hartree, the latter being much smaller than the independent electron pair (IEP) result [32] of 0.0177 Hartree. In calculations of the latter category, questions arise over the uniqueness of pair correlations and about their additivity [15]. Calculations by Robb and Csizmadia [33] suggest that the IEP model seriously overestimates the correlation energy that may be obtained within the electron pair model. To provide further evidence we have performed APSG calculations where the valence pairs in *BH* are correlated independently. The resulting pair energies are 0.0371 and 0.0499 Hartree for the bond and lone pair respectively, compared with the values of 0.0332 and 0.0456 Hartree (see table 3) obtained from the two-pair APSG calculation, suggesting that an IEP approach overestimates the intrapair APSG correlation energy in *BH* by 11%, compared with a previous estimate of  $\geq 5\%$  [32]. However, it may be more reasonable to compare IEP pair energies with correlation energies calculated in the APG model. Certainly recent two-pair APSG and APG calculations [34] on *LiH* and *BH* indicate that the APG pair energies are considerably larger than those of the APSG model.

The dipole moments (defined so that a positive dipole implies  $B^{\ominus}H^{\oplus}$ ) from the present work and from [16] and GVB [10] calculations are in substantial agreement, all being significantly lower than the RHF estimate [30].

The benefit of careful exponent optimization and a sufficiently large basis set can be seen on comparing the present results with those of Mehler *et al.* [25], who obtained 42% of the valence shell correlation energy in a two-pair APSG treatment, 47% of the total correlation energy in a three-pair calculation, compared with the present results of 71% and 75% respectively.

### Lithium Hydride

A number of calculations using the basis set of 38 STO expanded in GTF reported in table 1, and at the experimental [38] bond length of 3.015 bohr have been carried out. The natural orbital structure of the geminals indicates that the molecular system can be regarded as  $Li^{\oplus}H^{\ominus}$  in first approximation, with an inner shell electron pair closely similar to that found in  $Li^{\oplus}$ , and a 'bonding' geminal looking rather like a  $H^{\ominus}$  system polarized towards the lithium atom. In table 4 we present a pair energy analysis of our APSG wavefunction, and compare the results with similar analyses for isolated  $Li^{\oplus}$  and  $H^{\ominus}$  systems, where the natural orbitals of the molecular system have been placed in maximum correspondence with the isolated ion orbitals. It will be seen that the natural orbital structure of both *LiH* geminals is ( $6\sigma$ ,  $3\pi$ ,  $1\delta$ ).

Table 4: A comparison of the APSG<sup>a</sup> pair energy components (Hartree) of *LiH* ( $R=3.015$  bohr) with  $Li^+$  and  $H^-$

Weakly Occupied Natural Orbital	Pair Energy $Li^+$	Pair Energy, <i>LiH</i> ( <i>Li</i> inner shell geminal)
2s	0.0144	0.0136 ( $\sigma$ )
3s	0.0010	0.0010 ( $\sigma$ )
2p	0.0210	0.0068 ( $\sigma$ ), 0.0140 ( $\pi$ )
3p	0.0019	0.0006 ( $\sigma$ ), 0.0012 ( $\pi$ )
3d	0.0025	0.0005 ( $\sigma$ ), 0.0010 ( $\pi$ ), 0.0010 ( $\delta$ )
Total	0.0408	0.0397

	Pair Energy $H^-$	Pair Energy, <i>LiH</i> (bonding geminal)
2s	0.0231	0.0147 ( $\sigma$ )
3s	0.0009	0.0007 ( $\sigma$ )
2p	0.0135	0.0051 ( $\sigma$ ), 0.0120 ( $\pi$ )
3p	0.0009	0.0003 ( $\sigma$ ), 0.0010 ( $\pi$ )
3d	0.0012	0.0002 ( $\sigma$ ), 0.0006 ( $\pi$ ), 0.0007 ( $\delta$ )
Total	0.0396	0.0353

(a) Basis set for *LiH* and  $Li^+$ , see table 1:  
basis set for  $H^-$  taken from Hinze and Sabelli [15]

The energies of *LiH* at  $R=3.015$  bohr produced by the APSG, DS-SEPC, DS-ASEPC and ASP theories are quoted in table 5, and compared with other theoretical results and experiment. The 38 STO basis set gives an energy within 0.0010 Hartree of the Hartree-Fock limit, most of this error (0.0008 Hartree)

being due to an incomplete valence shell description. The two pair APSG and ASP wavefunctions both give lower energies than the previous best variational result [21], the latter being produced by an iterative natural orbital CI calculation. Indeed the energy of the ASP wavefunction is close to the non-variational transcorrelated wavefunction result of Boys and Handy [44]. The two pair ASP and DS-ASEPC calculations both result in an estimate of 0.0006 Hartree for the dispersion component of the inter-pair correlation energy, whilst the difference in energy between the two-pair APSG and DS-SEPC yields an estimate of 0.0012 Hartree energy lowering due to the admission of certain quadruple excitations in the APSG model.

The results of the present calculations may be used to provide an estimate of the APSG energy limit for *LiH*. From comparison of our isolated  $Li^+$  calculation with an 'exact'  $Li^+$  energy [47], approximately 0.0025 Hartree of the inner shell correlation energy is unaccounted for in the present basis. A further 0.0005 Hartree is likely to be gained by increasing the valence shell correlating basis, which coupled with the known 0.001 error in our Hartree-Fock energy leads to the conclusion that the present APSG calculation lies 0.004 Hartree from an APSG limit of  $-8.065$  Hartree, 94% of the total correlation energy.

A difference of 0.0002 Hartree was found between  $E(\text{PNO})$  and  $E(\text{RHF})$  in all of the present calculations, in agreement with Bender and Davidson [21], but in marked disagreement with Mehler *et al.* [25] who find a difference of 0.0026 Hartree.

Table 5: Calculations on *LiH*,  $R=3.015$  bohr, (energy in Hartree)

Calculation	$E(\text{TOTAL})$	$E(\text{PNO})$	$E(\text{RHF})$	$\mu$ (Debye)	$\Delta E^a$	Reference
RHF			-7.9863	5.979		b
APSG (2 pair)	-8.0611	-7.9861	-7.9863	5.912	0.0748	b
APSG (1 pair)	-8.0220	-7.9861	-7.9863	5.867	0.0357	b
DS-SEPC (2 pair)	-8.0599	-7.9861	-7.9863	5.914	0.0736	b
DS-ASEPC (2 pair)	-8.0605	-7.9861	-7.9863	5.914	0.0742	b
ASP (2 pair)	-8.0617	-7.9861	-7.9863	5.912	0.0754	b
Experiment	-8.0703			5.83		[39,40]
RHF limit			-7.9873	6.002		[30,41]
CI	-8.0606	-7.9871	-7.9873	5.965	0.0733	[21]
GVB (2 pair)	-8.0129		-7.9833		0.0296	[10]
G1 (2 pair)	-8.0137		-7.9833		0.0304	[10]
G1 (2 pair)	-8.0173			5.645		[42]
APSG (2 pair)	-8.0542	-7.9847	-7.9873		0.0669	[25]
APSG (1 pair)	-8.0182		-7.9873		0.0309	[25]
APSG (1 pair)	-8.0213		-7.9873	5.886	0.0340	[43]
Transcorrelated	-8.063					[44]

(a)  $\Delta E = E(\text{RHF}) - E(\text{TOTAL})$

(b) Present work

Table 6: Calculated equilibrium properties of *LiH*

Calculation	$R_e$ bohr	$D_e$ eV	$E(\text{Total})$ Hartree	$\mu$ Debye	$\theta_e$	Reference
RHF	3.044	1.46	-7.9863	6.013	1.66	a
APSG (2 pair)	3.056	2.42	-8.0611	5.953	1.91	a
APSG (1 pair)	3.045	2.44	-8.0221	5.900	1.80	a
DS-SEPC (2 pair)	3.052		-8.0599	5.958	1.74	a
DS-ASEPC (2 pair)	3.047		-8.0605	5.953	1.70	a
Experiment	3.015	2.52	-8.0703	5.83	1.8±0.3	[38-40,45,46]
GVB (2 pair) <sup>b</sup>	3.015	1.89	-8.0129			[10]
GI (2 pair) <sup>b</sup>	3.015	1.89	-8.0137			[10]
GI (2 pair) <sup>b</sup>	3.015	1.90	-8.0173	5.645		[42]
APSG (2 pair)	3.042	2.31	-8.0542			[25]
APSG (1 pair) <sup>b</sup>	3.015	2.35	-8.0182			[25]
APSG (1 pair)	3.049	2.41	-8.0213	5.923	1.86	[43]
RHF limit <sup>b</sup>	3.015	1.49	-7.9873	6.002		[30]

(a) Present work

(b) Result obtained at an assumed  $R_e=3.015$ Table 7: Pair energy analysis of the one pair APSG  $Li_2$  wavefunction,  $R=5.051$  bohr

Weakly Occupied Natural Orbital	Pair Energy (Hartree)
$2\sigma_u$	0.0058
$1\pi_u$	0.0182
$3\sigma_g$	0.0065
$1\pi_g$	0.0002
$4\sigma_g$	0.0001
$1\delta_g$	0.0003
$3\sigma_u$	0.0002
Total pair energy	0.0313
$E(\text{PNO})$	-14.8709
$E(\text{Total})$	-14.9022
$E(\text{RHF})$	-14.8711

A series of calculations was performed at bond lengths of 3.015, 3.05 and 3.08 bohr, and the results interpolated, to yield the predicted equilibrium properties (see table 6). The degree of correlation allowed for the inner shell (compare the one and two pair APSG calculations) has little effect on the computed equilibrium properties, as for *BH*. Particularly gratifying is the close agreement of the computed with experimental dissociation energies, dipole moments and dipole derivative factor,  $\theta_e$ :

$$\theta_e = (\mu_e/R_e) / (\partial\mu/\partial R)_{R_e} \quad (21)$$

the latter being measured from the relative line intensities in the infrared spectrum [46]. Note that the one pair APSG wavefunction dissociates to Hartree-Fock lithium (energy = -7.4326 Hartree after reoptimization of the present valence *s* basis) and

hydrogen (energy = -0.49995 Hartree in the present basis), whilst the two pair APSG function dissociates to an APSG lithium atom (energy = -7.4722 after some reoptimization of the basis) and a Hartree-Fock hydrogen atom.

### The Lithium Molecule

In view of the small influence on the computed properties of *LiH* and *BH* of the amount of inner shell correlation allowed, we have performed calculations on the  $Li_2$  molecule where the lithium inner shells are not correlated, so that only the bonding pair is described by more than one natural orbital. The calculations were performed in a basis of 36 STO expanded in GTF, see table 1, and at the experimental internuclear separation of 5.051 bohr [38], yielding a Hartree-Fock energy of -14.8711 Hartree, 0.0004 Hartree above the limit [48].

The dominant configuration is  $1\sigma_g^2 1\sigma_u^2 2\sigma_g^2$ , and the one pair APSG function was constructed by double substitution of the  $2\sigma_g$  orbital with the orbitals listed in table 7. The bonding geminal thus consists of 11 natural orbitals, and is closely similar to that found by Das [49], except that we have added a  $\delta_g$  natural orbital. From the pair energy analysis, table 7, it is clear that the most significant features of the correlation effect are encapsulated in the  $3\sigma_g$ ,  $2\sigma_u$ , and  $1\pi_u$  weakly occupied natural orbitals.

The self consistent APSG function has an energy of -14.9022 Hartree, and will dissociate into a pair of Hartree-Fock lithium atoms, whose combined energy is -14.8652 Hartree (after reoptimization of the present valence *s* basis), leading to a computed dissociation energy of 1.01 eV, in close agreement with

the experimental result of 1.05 eV [50], and a previous theoretical result of 1.01 eV [49]. In marked contrast, the Hartree-Fock energy of  $Li_2$  gives a dissociation energy of 0.16 eV, only 15% of the experimental result.

## Ammonia

Calculations were performed at the experimental equilibrium geometry, as quoted by Rauk *et al.* [51], using a basis set of 44 STO, as shown in table 1, the 3p 'lone pair correlating' functions being sited 0.7 bohr from the nitrogen atom, on the  $C_3$  axis, at approximately the dipole centroid of the nitrogen lone pair geminal. Molecular integral evaluation was accomplished using a modified version of a program due to Stephens (QCPE 161). The present basis gives a Hartree-Fock energy of  $-56.2222$  Hartree, to be compared with the previous best of  $-56.2219$  Hartree [51], and an estimated Hartree-Fock limit of  $-56.2275$  Hartree [52]. The total correlation energy of ammonia has been estimated at 0.329 Hartree [53], of which perhaps 0.285 Hartree can be attributed to the valence electrons.

the local symmetry of the bond or lone pair with which they are most directly concerned. If this is done, we find an  $N-H$  bonding natural orbital structure of the form  $\{1\sigma, 2\sigma, 3\sigma, \pi, \pi', 4\sigma\}$ , where  $1\sigma$  is the PNO, whilst  $2\sigma$  is the corresponding  $N-H$   $\sigma$  anti-bonding orbital, and  $\pi$  is principally a hydrogen  $2p$  function, tangential to the circle whose locus encompasses the three hydrogen atoms,  $\pi'$  being a hydrogen  $2p$  function whose principal axis is orthogonal to the  $NH$  bond and to the  $\pi$  orbital, thus pointing radially from the hydrogen atom to the  $C_3$  axis. The  $3\sigma$  natural orbital is composed mainly of a hydrogen  $2p$  orbital pointing down the  $NH$  bond, whilst the  $4\sigma$  orbital, which is very weakly occupied, is complex in form, and difficult to describe qualitatively. The structure of the lone pair geminal is  $\{1\sigma, 2\sigma, 3\sigma, \pi_x, \pi_y, 4\sigma\}$ , where  $1\sigma$  is the lone pair PNO, a hybrid of nitrogen  $s$  and  $p$  orbitals, whilst the  $2\sigma$  looks rather like the  $1\sigma$  except that the former has a node bisecting its principal lobe. The largest components of the  $3\sigma$  and  $\pi$  natural orbitals are the 'lone pair correlating'  $3p$  basis functions, whilst  $4\sigma$  is endowed with a complex structure, difficult to describe in qualitative

Table 8: Calculations on  $NH_3$ , including valence shell correlation energy only: energy in Hartree

Calculation	$E(\text{Total})$	$E(\text{PNO})$	$E(\text{RHF})$	$\mu$ Debye	$\Delta E^a$	Reference
APSG	-56.3176	-56.2212	-56.2222	1.717	0.0954	b
DS-SEPC	-56.3151	-56.2213	-56.2222	1.716	0.0929	b
DS-ASEPC	-56.3578	-56.2213	-56.2222	1.718	0.1356	b
CMC-MC-SCF	-56.3168	-56.2214	-56.2222	1.712	0.0946	b
RHF			-56.2222	1.720		b
RHF			-56.2219	1.66		[51]
Estimated RHF limit			-56.2275			[52]
Estimated valence shell $\Delta E$					0.285	b
CI	-56.4155		-56.2122		0.2033	[57]
CMC-MC-SCF	-56.2614		-56.1989		0.0625	c
CMC-MC-SCF	-56.2789		-56.1989		0.0800	d

(a)  $\Delta E = E(\text{RHF}) - E(\text{Total})$

(b) Present work

(c) This CMC-MC-SCF calculation included one localised SSMO per valence FSMO [22]

(d) This CMC-MC-SCF calculation included four localised SSMO and five symmetry adapted SSMO, and appears not to have converged [22]

Calculations within the APSG, DS-SEPC, CMC-MC-SCF and DS-ASEPC frameworks were performed, and the results displayed in table 8. In all of these calculations the nitrogen inner shell was not correlated. The self consistent orbitals, irrespective of the method used, turned out to be localised within the bonds or lone pair, a result which is not surprising in view of the results of Levy [7] and Chu [54]. In view of the localization of the natural orbitals, it seems convenient to classify them according to

terms. In table 9 we present a pair energy analysis of the self consistent APSG orbitals, where the pair energy of the lone pair is seen to be less than the bond, in agreement with Robb and Csizmadia [55], who obtained APSG pair energies of 0.016 and 0.0132 Hartree for the bond and lone pair respectively, considerably less than that obtained in the present work. Such differences can probably be attributed to the larger basis set used in the present work, and also to the fact that the APSG function of Robb and



Csizmadia [55] was not energy optimized, although this latter factor was probably rather small in effect.

Table 9: Pair energies (Hartree) of the  $NH_3$  APSG wavefunction

Bond		Lone Pair	
Natural Orbital	Pair Energy	Natural Orbital	Pair Energy
$2\sigma$	0.0169	$2\sigma$	0.0124
$3\sigma$	0.0040	$3\sigma$	0.0027
$\pi$	0.0022	$\pi_x$	0.0019
$\pi'$	0.0020	$\pi_y$	0.0019
$4\sigma$	0.0007	$4\sigma$	0.0002
Total	0.0258	Total	0.0191

We shall now consider the results displayed in table 8 in greater detail. The computed dipole moment remains essentially at its RHF value of 1.72D, irrespective of the amount of correlation allowed, and in reasonable agreement with a previous RHF estimate of 1.66D [51] and the experimental 1.48D [56]. The CMC-MC-SCF calculation, using the same number of natural orbitals as in the APSG and DS-SEPC calculations, produced an energy only 0.0017 Hartree below the DS-SEPC result, indicating the minor importance of the 'two electron transfer configurations' included in the CMC-MC-SCF wavefunction. The DS-ASEPC model leads to the lowest energy in the present calculations, with a valence correlation energy of 0.1356 Hartree (47.6%), and inter-pair dispersion energies of 0.0093 Hartree (lone pair-bond), 0.0075 Hartree (bond-bond), and to intra-pair energies of 0.0167 Hartree (lone pair) and 0.0231 (bond). We again note the small difference between  $E(\text{PNO})$  and  $E(\text{RHF})$ , of the order of 0.001 Hartree.

## Conclusions

Consider the series  $LiH$ ,  $BH$  and  $NH_3$ , for which our best valence only calculations recover approximately 89%, 74% and 48% of the valence shell correlation energy respectively. We note that as we cross the series, the number of valence shell geminals linked to a common atom increases, and the percentage of the correlation energy recovered decreases. No doubt part of these energy variations can be attributed to variation in the quality of our basis sets, but we do not believe that this is the major factor. For

example, a recent large scale CI calculation [57] yielded a valence correlation energy of 0.2033 Hartree (73%) for  $NH_3$ , using a basis set which is almost certainly inferior to that used in the present work. It is therefore necessary to consider the imperfections of the models we have used, and which are all rooted to some degree in the separated electron pair theory. Reflection on our results has led us to conclude that it is in fact the strong orthogonality constraint which constitutes the principal source of error, and that this constraint becomes ever more untenable as the number of geminals linked to a common atom increases. Thus, for example, a close scrutiny of the more weakly occupied natural orbitals of  $NH_3$  reveals that they possess nodal planes which seem to have little to do with the physics of the situation, and everything to do with the application of the strong orthogonality constraint. It seems worthwhile to consider moving away from models based on the APSG theory, and towards an APG approach. Indeed recent direct numerical work [34] has indicated the considerable improvements which are possible within the APG model, whilst the work of Goddard and co-workers [10,16,35] using the G1 theory (which may be characterised as an APG model in which the pair functions are expanded in two natural orbitals) and GVB theory (characterised as the APSG counterpart to G1) has indicated the potential superiority of the APG approach. Unfortunately APG theory, if directly applied, leads to equations whose solution will be very difficult for all but the smallest systems. A more realistic line of attack has already been attempted by Robb and Csizmadia [18,55], with some success, where the elements of an APG model are generated by successive corrections to the APSG model.

It is not our belief that MC-SCF, APSG and kindred theories will provide adequate compensation at the level of systems the size of  $NH_3$ , if all that is desired is the most accurate wavefunction in the shortest possible computer time, since the methods of large scale CI [57] have become available. If larger systems are to be considered, then APSG/MC-SCF theories will have a significant role to play, and it seems possible that a marriage of the technologies of MC-SCF and large scale CI will produce a workable, accurate and chemically appealing theory, and it is in such directions that we plan future work.

No chemist needs reminding that the computation of total molecular energies is by itself, of little direct value. Instead, the quantities of real interest are always differences in total energies, as reflected, for example, in dissociation energies. The present work has resulted in estimates of 3.89, 2.42 and 1.01 eV for the dissociation energy of  $BH$ ,  $LiH$  and  $Li_2$  respectively, to be compared with the experimental results 3.59, 2.52 and 1.05 eV, indicating that the APSG theory can produce significant improvements over the Hartree-Fock theory estimates (2.78, 1.46 and 0.16 eV respectively).

## Appendix

We are concerned with a parameter space in which a rotation between molecular orbitals  $p$  and  $t$ , which conserves orthonormality to second order in a way which is consistent with the  $S^{-1/2}$  orthonormalization procedure referred to in the main body of the text, may be written:

$$p \rightarrow p + X_{tp}t - \frac{1}{2}X_{tp}^2p$$

$$t \rightarrow t - X_{tp}p - \frac{1}{2}X_{tp}^2t$$

The symbols  $J_{kl}^i$  and  $K_{kl}^i$  will be used to denote the matrix elements connecting molecular orbitals  $k$  and  $l$  over the Coulomb and exchange operators respectively of molecular orbital  $i$ . The symbol  $F_{kl}$  will be used to denote a matrix element of the one electron operator, whilst  $G_{kl}^i = 2J_{kl}^i - K_{kl}^i$ .

**The APSG energy expression:** The electronic energy of the APSG ansatz for a closed shell system may be written:

$$E = 2 \sum_{\pi} \sum_{p \text{ in } \pi} a_{\pi p}^2 F_{pp} + \sum_{\pi} \sum_{p, q \text{ in } \pi} a_{\pi p} a_{\pi q} K_{pq}^p \\ + 2 \sum_{\pi > \tau} \sum_{p \text{ in } \pi} \sum_{t \text{ in } \tau} a_{\pi p}^2 a_{\tau t}^2 G_{tt}^p$$

where  $\pi$  and  $\tau$  are used to denote particular geminals,  $p, q$  denote natural orbitals belonging to geminal  $\pi$ , and  $t$  denotes a natural orbital belonging to geminal  $\tau$ , whilst the  $a_{\pi p}$  are defined by equation (7) of the main body of the text.

We define:

$$Y_{tp} = a_{\pi p}^2 H_{pt} + a_{\pi p} K_{pt}^{\pi} - a_{\pi p}^2 G_{pt}^{\pi}$$

$$Z_{tp} = a_{\pi p}^2 H_{tt} + a_{\pi p} K_{tt}^{\pi} - a_{\pi p}^2 G_{tt}^{\pi}$$

where the orbital  $p$  belongs to geminal  $\pi$ , and:

$$K_{kl}^{\pi} = \sum_{p \text{ in } \pi} a_{\pi p} K_{kl}^p$$

$$G_{kl}^{\pi} = \sum_{p \text{ in } \pi} a_{\pi p}^2 G_{kl}^p$$

$$H_{kl} = F_{kl} + \sum_{\pi} G_{kl}^{\pi}$$

We then find:

$$\frac{\partial E}{\partial X_{tp}} = 4(Y_{tp} - Y_{pt})$$

$$\frac{\partial^2 E}{\partial X_{qp}^2} = 4 \left( Z_{qp} + Z_{pq} - Z_{pp} - Z_{qq} \right. \\ \left. + (a_{\pi p}^2 + a_{\pi q}^2 - 2a_{\pi p} a_{\pi q})(J_{qq}^p + K_{qq}^p) \right)$$

where  $p$  and  $q$  belong to the same geminal,  $\pi$ , and:

$$\frac{\partial^2 E}{\partial X_{tp}^2} = 4 \left( Z_{tp} + Z_{pt} - Z_{pp} - Z_{tt} \right. \\ \left. + (a_{\pi p}^2 + a_{\tau t}^2)(J_{tt}^p + K_{tt}^p) + a_{\pi p}^2 a_{\tau t}^2 (2J_{tt}^p - 6K_{tt}^p) \right)$$

where  $p$  and  $t$  are in different geminals,  $\pi$  and  $\tau$  respectively.

**MC-SCF energy expression:** We first define the quantities:

$$A_{ij} = \sum_k^{\text{SSMO}} a_{ik} a_{jk} \quad (\text{where } i \text{ and } j \text{ are FSMO})$$

$$A_{kl} = \sum_i^{\text{FSMO}} a_{ik} a_{il} \quad (\text{where } k \text{ and } l \text{ are SSMO})$$

where the  $a_{ik}$  were defined by equation (1) of the main body of the text.

The MC-SCF electronic energy may be written:

$$E = \sum_i^{\text{FSMO}} (F_{ii} + (1 - 2A_{ii})H_{ii}) + 2 \sum_k^{\text{SSMO}} A_{kk} H_{kk} \\ + 2 \sum_i^{\text{FSMO}} \sum_k^{\text{SSMO}} (a_{oo} a_{ik} K_{kk}^i - a_{ik}^2 G_{kk}^i) \\ + \sum_k^{\text{SSMO}} \sum_l^{\text{SSMO}} A_{kl} K_{ll}^k + \sum_i^{\text{FSMO}} \sum_j^{\text{FSMO}} A_{ij} K_{jj}^i$$

where:

$$H_{kl} = F_{kl} + \sum_i^{\text{FSMO}} G_{kl}^i$$

We define:

$$Y_{tp} = (1 - A_{pp})H_{pt} + \sum_i^{\text{FSMO}} (A_{ip} K_{pt}^i - A_{ii} G_{pt}^i) \\ + \sum_k^{\text{SSMO}} (A_{kk} G_{pt}^k - a_{pk}^2 G_{pt}^k + a_{oo} a_{pk} K_{pt}^k)$$

$$Z_{tp} = (1 - A_{pp})H_{tt} + \sum_i^{\text{FSMO}} (A_{ip} K_{tt}^i - A_{ii} G_{tt}^i) \\ + \sum_k^{\text{SSMO}} (A_{kk} G_{tt}^k - a_{pk}^2 G_{tt}^k + a_{oo} a_{pk} K_{tt}^k)$$

where  $p$  is an FSMO, and:

$$Y_{tr} = A_{\pi}H_{tt} + \sum_k^{\text{SSMO}} A_{kr}K_{rt}^k + \sum_i^{\text{FSMO}} (a_{oo}a_{ir}K_{rt}^i - a_{ir}^2G_{rt}^i)$$

$$Z_{tr} = A_{\pi}H_{tt} + \sum_k^{\text{SSMO}} A_{kr}K_{tt}^k + \sum_i^{\text{FSMO}} (a_{oo}a_{ir}K_{tt}^i - a_{ir}^2G_{tt}^i)$$

where  $r$  is an SSMO. Then:

$$\frac{\partial E}{\partial X_{tp}} = 4(X_{tp} - X_{pt})$$

and:

$$\frac{\partial^2 E}{\partial X_{qp}^2} = 4 \left( Z_{qp} + Z_{pq} - Z_{pp} - Z_{qq} + (A_{pp} + A_{qq} - 2A_{pq})(J_{qp}^p + K_{qp}^p) \right)$$

where  $p$  and  $q$  are both FSMO, or both SSMO, and:

$$\frac{\partial^2 E}{\partial X_{rp}^2} = 4 \left( Z_{rp} + Z_{pr} - Z_{pp} - Z_{rr} + (A_{rr} + A_{pp})(3J_{pp}^r - 5K_{pp}^r) - a_{pr}^2(2J_{pp}^r - 6K_{pp}^r) - 2a_{oo}a_{pr}(J_{pp}^r + K_{pp}^r) + 3K_{rr}^p - J_{rr}^p \right)$$

if  $r$  is an SSMO, and  $p$  an FSMO.

## References

- [1] VEILLARD, A. and CLEMENTI, E. (1967). *Theoret. Chim. Acta*, **7**, 133.
- [2] HURLEY, A.C., LENNARD-JONES, J. and POPLE, J.A. (1953). *Proc. Roy. Soc. (London)*, **A220**, 446.
- [3] SILVER, D.M., MEHLER, E.L. and RUEDENBERG, K. (1970). *J. Chem. Phys.*, **52**, 1174.
- [4] KAPUY, E. (1966). *Theoret. Chim. Acta*, **6**, 281.
- [5] WOOD, M.H. and VEILLARD, A. (1973). *Mol. Phys.*, **26**, 595.
- [6] ROBB, M.A. and CSIZMADIA, I.G. (1970). *Int. J. Quantum Chem.*, **4**, 36.
- [7] LEVY, B. (1970). *Int. J. Quantum Chem.*, **4**, 297.
- [8] LOWDIN, P.O. (1955). *Phys. Rev.*, **97**, 1474.
- [9] ARAI, T. (1960). *J. Chem. Phys.*, **33**, 95.
- [10] HUNT, W.J., HAY, P.J. and GODDARD, W.A. (1972). *J. Chem. Phys.*, **57**, 738.
- [11] SAUNDERS, V.R. and HILLIER, I.H. (1973). *Int. J. Quantum Chem.*, **7**, 699.

- [12] LOWDIN, P.O. (1950). *J. Chem. Phys.*, **18**, 365.
- [13] DAS, G. (1967). *J. Chem. Phys.*, **46**, 1568.
- [14] KUPRIEVICH, V.A. and SHRAMKO, O.V. (1972). *Int. J. Quantum Chem.*, **6**, 327.
- [15] SABELLI, N. and HINZE, J. (1969). *J. Chem. Phys.*, **50**, 684.
- [16] BLINT, R.J. and GODDARD, W.A. (1972). *J. Chem. Phys.*, **57**, 5296.
- [17] EISENSCHITZ, R. and LONDON, F. (1930). *Z. Physik*, **60**, 491.
- [18] LONDON, F. (1930). *Z. phys. Chem.*, **B11**, 222.
- [19] ROBB, M.A. and CSIZMADIA, I.G. (1970). *Int. J. Quantum Chem.*, **4**, 36.
- [20] MILLER, K.J. and RUEDENBERG, K. (1968). *J. Chem. Phys.*, **48**, 3444.
- [21] DAVIDSON, E.R. and JONES, L.L. (1962). *J. Chem. Phys.*, **37**, 2966.
- [22] BENDER, C.F. and DAVIDSON, E.R. (1966). *J. Chem. Phys.*, **70**, 2675.
- [23] DEJARDIN, P., KOCHANSKI, E., VEILLARD, A., ROOS, B. and SIEGBAHN, P. (1973). *J. Chem. Phys.*, **59**, 5546.
- [24] NESBET, R.K. (1965). *Adv. Chem. Phys.*, **9**, 1965.
- [25] SUTTON, P., BERTONCINI, P., DAS, G., GILBERT, T.L. and WAHL, A.C. (1970). *Int. J. Quantum Chem.*, **53**, 479.
- [26] STAMPER, J.G. (1968). *Theoret. Chim. Acta*, **11**, 459.
- [27] SINANOGLU, O. (1961). *J. Chem. Phys.*, **36**, 706.
- [28] MEHLER, E.L., RUEDENBERG, K. and SILVER, D.M. (1970). *J. Chem. Phys.*, **52**, 1181.
- [29] BAUER, S.H., HERZBERG, G. and JOHNS, J.W.C. (1964). *J. Mol. Spectroscopy*, **13**, 256.
- [30] STEWART, R.F. (1970). *J. Chem. Phys.*, **52**, 431.
- [31] HUZINAGA, S. and ARNAU, C. (1970). *J. Chem. Phys.*, **53**, 451.
- [32] DITCHFIELD, R., HEHRE, W.J. and POPLE, J.A. (1970). *J. Chem. Phys.*, **52**, 5001.
- [33] CADE, P.E. and HUO, W.M. (1967). *J. Chem. Phys.*, **47**, 614.
- [34] HOULDEN, S.A. and CSIZMADIA, I.G. (1973). *Theoret. Chim. Acta*, **30**, 209.
- [35] JUNGEN, M. and AHLRICHS, R. (1970). *Theoret. Chim. Acta*, **17**, 339.
- [36] ROBB, M.A. and CSIZMADIA, I.G. (1971). *J. Chem. Phys.*, **54**, 3646.
- [37] NICELY, V.A. and HARRISON, J.F. (1971). *J. Chem. Phys.*, **54**, 4363.
- [38] GODDARD, W.A. (1967). *Phys. Rev.*, **157**, 81.
- [39] WILKINSON, P.G. (1967). *Astrophys. J.*, **138**, 614.
- [40] BENDER, C.F. and DAVIDSON, E.R. (1969). *Phys. Rev.*, **183**, 23.
- [41] HERZBERG, G. (1966). *Molecular Spectra and Molecular Structure I: Spectra of Diatomic Molecules*, Princeton, New Jersey: Van Nostrand.
- [42] RANSIL, B. (1960). *Revs. Modern Phys.*, **32**, 239.
- [43] WHARTON, L., GOLD, L.P. and KLEMPERER, W. (1962). *J. Chem. Phys.*, **37**, 2149.

- [41] GREEN, S. (1971). *J. Chem. Phys.*, **54**, 827.
- [42] PALKE, W.E. and GODDARD, W.A. (1969). *J. Chem. Phys.*, **50**, 4524.
- [43] DOCKEN, K.K. and HINZE, J. (1972). *J. Chem. Phys.*, **57**, 4928, 4936.
- [44] BOYS, S.F. and HANDY, N.C. (1969). *Proc. Roy. Soc. (London)*, **A311**, 309.
- [45] VELASCO, R. (1957). *Can J. Phys.*, **35**, 1204.
- [46] JAMES, T.C., NORRIS, W.G. and KLEMPERER, W. (1960). *J. Chem. Phys.*, **32**, 728.
- [47] FRANKOWSKI, K. and PEKERIS, C.L. (1966). *Phys. Rev.*, **146**, 146.
- [48] RANSIL, B. and SINAI, J.J. (1967). *J. Chem. Phys.*, **46**, 4050.
- [49] DAS, G. (1967). *J. Chem. Phys.*, **46**, 1568.
- [50] VELASCO, R., OTTINGER, C. and ZARE, R.N. (1969). *J. Chem. Phys.*, **51**, 5522.
- [51] RAUK, A., ALLEN, L.C. and CLEMENTI, E. (1970). *J. Chem. Phys.*, **52**, 4133.
- [52] STEVENS, R.M. (1971). *J. Chem. Phys.*, **55**, 1725.
- [53] KARI, R. E. and CSIZMADIA, I. G. (1972). *J. Chem. Phys.*, **56**, 4337.
- [54] CHU, S.Y. (1970). *Chem. Phys. Letters*, **7**, 569.
- [55] ROBB, M.A. and CSIZMADIA, I.G. (1971). *Int. J. Quantum Chem.*, **5**, 605.
- [56] DANN, A. and REGNIEW, J.F. (1960). *Compt. rend.*, **255**, 2417.
- [57] ROOS, B. (1972). *Chem. Phys. Letters*, **15**, 153.

# Numerical Solution of First-Order Correlation Equations for Atoms

C.S.Sharma\* and G.Bowtell†

A method has recently been developed in which the first-order Schrödinger wavefunction of a many electron atom can be written as a sum of solutions of a certain set of differential equations. The first member of this set is the first-order Hartree-Fock equation and the remaining members are the first-order correlation equations. Each first-order correlation function brings in the *exact* contribution to the second-order energy from infinitely many hydrogenic configurations. A method for the analytic solution of a correlation equation, provided it does not represent the contribution of the doubly ionized continuum, has been developed. This paper reports a numerical method for the solution of these correlation equations. Estimates of contributions to the second-order energy obtained by the numerical method are compared with the exact values obtained by the analytic method. The agreement is found to be excellent.

## Introduction

Sharma and Bowtell [1-3] have recently developed an algorithm for calculating the non-relativistic energy of an atom including the correlation energy. The correlated wavefunction is expanded in powers of the inverse of the nuclear charge, the sum of the inter-electronic interactions is treated as the perturbation and the first-order correction to the wavefunction is written as a sum of Hartree-Fock and correlation terms. In terms of the basis provided by the hydrogenic states, the Hartree-Fock part represents the exact lowest order contribution from interactions between the state under consideration and all states which are singly excited relative to the initial state (for a definition of relative excitation, see [2]). The correlation part thus consists of the contribution from interactions with the doubly excited states; triply and other multiply excited states do not contribute anything to the first-order correction to the wavefunctions because the interelectronic interactions (the perturbing potential) are made up of two particle interactions only. Incidentally the first-order correction to the wavefunction determines the energy exactly up to the third-order. In our scheme the doubly excited states are divided into subsets corresponding to a fixed excitation of one of the electrons and an arbitrary excitation of a second electron giving rise to a state of required symmetry. Each set of first-order correlation equations calculates exactly the first-order correction to the wavefunction arising from one such subset. In our earlier work [1,2] we have described how exact analytic solutions of these equations can be found by expanding the

solutions in terms of a suitable Hilbert basis and how the corresponding contributions to the second-order energy can be calculated exactly. The advantages of our algorithm are described in [3], the chief of which is that the solutions for a complex atom can be built up from solutions of the helium problem. Thus the solution of each set of correlation equations finds application not only for calculating the energy of a particular state of the helium isoelectronic sequence but of all atoms and ions having the configuration of the helium state under consideration as a subconfiguration.

We have now developed a numerical procedure for the solution of the first-order correlation equations. The availability of both analytic and numerical methods enables one to put infallible checks on the accuracy of these calculations. We first describe the procedure for the solution of a particular set of correlation equations and then consider the general case.

## A Particular Set of First-Order Correlation Equations

We consider the contributions to the first-order correction functions for the  $1s2p\ ^{1,3}P$  states of helium arising from the lowest order interaction with the  $2snp\ ^{1,3}P$  states where  $n$  takes all discrete and continuum values in the hydrogen spectrum. From our earlier work [2] and some elementary calculations with known hydrogenic  $1s$ ,  $2s$  and  $2p$  eigenfunctions, it follows that this contribution is exactly given in terms of the solutions of the following set of differential equations:

\* Department of Mathematics, Birkbeck College, University of London, Malet Street, London, WC1E 7HX

† Department of Mathematics, The City University, St John Street, London, EC1V 4PB

$$(L_1 + \frac{1}{2})\Phi_1 = F_1 \quad (1)$$

$$(L_1 + \frac{1}{2})\Phi_2 = F_2 \quad (2)$$

where

$$L_1 = -\frac{1}{2} \frac{d^2}{dr^2} - \frac{1}{r} \frac{d}{dr} - \frac{1}{r} + \frac{1}{r^2} \quad (3)$$

$$F_1 = \frac{1}{108\sqrt{3}} e^{-r} r(3r+4) \quad (4)$$

$$F_2 = \frac{e^{-r}}{r^2\sqrt{3}} \left( \frac{r^4}{16} + \frac{r^3}{2} + 3r^2 + 12r + 24 \right) - \frac{8\sqrt{3}}{r^2} e^{-r/2} \quad (5)$$

If we denote by  $\mathcal{H}$  the Hilbert space of normed functions on  $\square 0, \infty \square$  with the inner-product defined by

$$\langle f, g \rangle = \int_0^\infty f(r)g(r)r^2 dr \quad (6)$$

then it is known that  $L_1$  is an essentially self-adjoint operator on  $\mathcal{H}$  [4] and its spectrum  $\Lambda(L_1)$  is given by:

$$\Lambda(L_1) = \left\{ \lambda: -\lambda = \frac{1}{2(n+1)^2}, n \in \mathbb{Z}^+ \text{ or } 0 \leq \lambda \leq \infty \right\} \quad (7)$$

It is evident that  $F_1 \in \mathcal{H}$  and it is not difficult to prove that  $F_2$  also belongs to  $\mathcal{H}$ , then since  $-\frac{1}{2} \notin \Lambda(L_1)$  it follows that solutions  $\Phi_1, \Phi_2$  belonging to  $\mathcal{H}$  exist. We have already proved that such solutions are unique [2]. We now wish to find a numerical procedure for obtaining square integrable, in the sense of equation (6), solutions of equations (1) and (2). Since the required solutions are superpositions of  $p$ -states we want solutions which satisfy

$$\Phi_1(0) = \Phi_2(0) = 0 \quad (8)$$

The general solutions, that is solutions not necessarily belonging to  $\mathcal{H}$  are undetermined by arbitrary multiples of the solution of the corresponding homogeneous equation:

$$(L_1 + \frac{1}{2})\Phi = 0 \quad (9)$$

It is known [5] that the homogeneous equation has two solutions one of which has a pole at the origin and the other is zero at the origin but diverges exponentially at infinity. The desired solutions go to zero at infinity as negative exponentials. It follows that the numerical solutions  $\tilde{\Phi}_i$  and  $\Phi$  of equations (1), (2) and (9) obtained by setting, for  $i = 1, 2$

$$\tilde{\Phi}_i(0) = \Phi(0) = 0 \quad (10)$$

and

$$\tilde{\Phi}'_i(0) = \Phi'(0) = 1 \quad (11)$$

are related to the square integrable solutions  $\Phi_i$  by

$$\Phi_i = \tilde{\Phi}_i - \alpha_i \Phi \quad (12)$$

where

$$\alpha_i = \lim_{r \rightarrow \infty} \frac{\tilde{\Phi}_i(r)}{\Phi(r)} \quad (13)$$

With these initial values we solved the homogeneous and the two inhomogeneous equations numerically by using the Runge-Kutta routine on a computer and the numerical integrations were continued till  $\frac{\tilde{\Phi}_i(r)}{\Phi(r)}$  had acquired constant values. Formulae (12) and (13) were then used to determine  $\Phi_1$  and  $\Phi_2$ . In order to calculate the corresponding contributions to the second-order correlation energies of the  $1s2p \ ^1,^3P$  states of helium we needed the values of the following integrals:

$$I_i = \int_0^\infty \Phi_i(r) F_i(r) r^2 dr \quad (i=1,2) \quad (14)$$

$$I_3 = \int_0^\infty \Phi_1(r) F_2(r) r^2 dr = \int_0^\infty \Phi_2(r) F_1(r) r^2 dr = I_4 \quad (15)$$

The four integrals were evaluated by numerical integrations. From the self-adjointness of  $L_1$  it follows that two of these integrals should have the same value. All the values are presented in table 1 in comparison with those obtained from exact analytic calculations. The agreement is satisfying!

Table 1: Value of integrals

	$I_1$	$I_2$	$I_3$	$I_4$
Analytic	- 0.000 592 23	- 0.000 736 21	0.000 598 02	0.000 598 02
Numerical	- 0.000 592 23	- 0.000 736 21	0.000 598 02	0.000 598 02

## The General Case

In the general case the first-order correlation equations are of the type

$$(L_{\ell} + \lambda)\Phi = F \quad (16)$$

where

$$L_{\ell} = -\frac{1}{2} \frac{d^2}{dr^2} - \frac{1}{r} \frac{d}{dr} - \frac{1}{r} + \frac{\ell(\ell+1)}{2r^2}, \quad (17)$$

$F \in \mathcal{H}$  and  $\lambda$  is a real number such that  $-\lambda \notin \Lambda(L_{\ell})$  and we require a solution  $\Phi \in \mathcal{H}$ . As in the particular case of the previous section it is easy to prove that such a solution exists and is unique. Since  $\Phi$  behaves as  $r^{\ell}$  near the origin, for  $\ell \neq 1$  the initial values of the previous sections cannot be used. However, if we make the substitution

$$\Phi(r) = r^{\ell-1}\Psi(r) \quad (18)$$

equation (16) takes the form

$$\left( -\frac{1}{2} \frac{d^2}{dr^2} - \frac{1}{r} \frac{d}{dr} - \frac{1}{r} + \frac{\ell}{r^2} + \lambda \right) \Psi = r^{1-\ell} F \quad (19)$$

The procedure of the previous section is now directly applicable without any further modifications.

When one considers the doubly excited states, the calculation of the level-shifts involves solving equations similar to equation (16) but with  $-\lambda$  belonging to the continuous spectrum of  $L_{\ell}$ . In this case  $F$  is such that solutions belonging to  $\mathcal{H}$  do not exist. Such equations have been dealt with in [3].

## The Hartree-Fock Case

A first-order Hartree-Fock equation is also of type (16) but in this case  $-\lambda$  belongs to the point spectrum of  $L_{\ell}$ . In this case the desired solution belongs to the orthogonal complement of the eigenspace of  $-\lambda$  and the solution of the homogeneous problem is an eigenfunction of  $L_{\ell}$  belonging to the eigenvalue  $-\lambda$  and is exactly known.  $\Phi$  is obtained from the numerical solution  $\tilde{\Phi}$  with the initial values given above by orthogonalizing it to the homogeneous solution by the Gram-Schmidt process. The analytic solution of such equations is described in [6].

## Concluding Remarks

We have developed a very simple yet very accurate method for finding square integrable solutions of differential equations of type (16). The numerical

method is in fact substantially easier than the analytic one. Due to lack of facilities and resources, however, we have been unable to carry the work to the actual computation of correlation energies of atoms and had to content ourselves with the development of the algorithm. As already pointed out each set of equations yields numbers which are useful for calculating energy levels of many complex atoms and ions and the values obtained are *exact* contributions from a particular set of interactions. We should like to persuade colleagues looking for computational problems that here we have an almost inexhaustible supply of good and meaningful problems which they might find worth their while to solve.

## References

- [1] SHARMA, C.S. and BOWTELL, G. (1971). *Nature Phys. Sci.*, **233**, 34.
- [2] ————— and ————— (1972). *J. Phys. B*, **5**, 1062.
- [3] ————— and ————— (1973). *Can. J. Phys.*, **51**, 1637.
- [4] KATO, T. (1966). *Perturbation Theory for Linear Operators*, Heidelberg: Springer.
- [5] BETHE, H.A. and SALPETER, E.E. (1957). *Handbuch der Physik*, **35**, 88.
- [6] SHARMA, C.S. and WILSON, R.G. (1968). *J. Phys. B*, **1**, 1.

# The Calculation of Three- and Four- Body Correlation Energies

M.A.Robb\*

The calculation of three- and four-body correlation energies in Many-Body Perturbation Theory is discussed. It is shown that the four-body diagrams where only the spin label is changed by the intermediate interaction can be accounted for by the use of 'spin-irreducible' pairs and that the remainder of the three- and four-body terms may be evaluated directly from the 'pair-pair' repulsions. Some numerical results are presented for the water molecule in a basis of canonical and localised orbitals.

## Introduction

The method of 'independent spin-orbital correlations' as formulated by Sinanoglu [1] or Nesbet [2] is equivalent [3,4] to an infinite summation of a certain class of diagrams arising in many-body perturbation theory. These diagrams are the so called [3] diagonal hole-line 'ladders' and are shown in figure 1. Each diagram is formed by making 'ladder' type insertions into the basic diagram, subject to the constraint that the hole-line label is unchanged by an intermediate interaction.

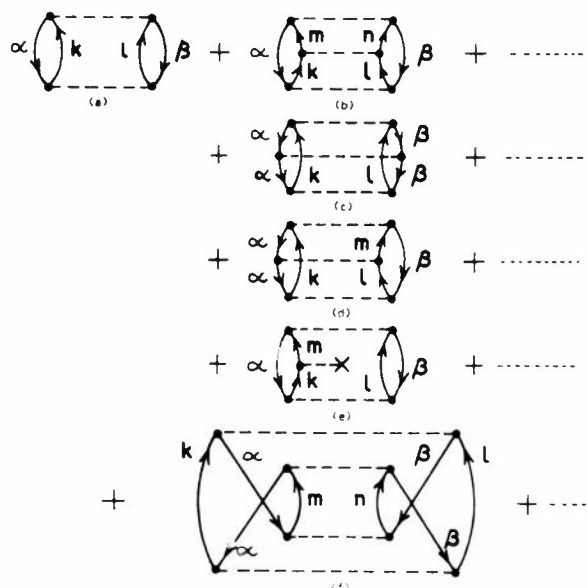


Figure 1

This 'sum of pairs' method usually overestimates the correlation energy by 10 to 15 percent in small

molecules. This error is due to three- and four-body correlation effects and may be separated into two terms:

- (a) rearrangements [5] effects
- (b) exclusion [1] effects

In Nesbet's [2] method of 'higher order Bethe-Goldstone increments' these two effects are treated equally; however, in many-body perturbation cal-

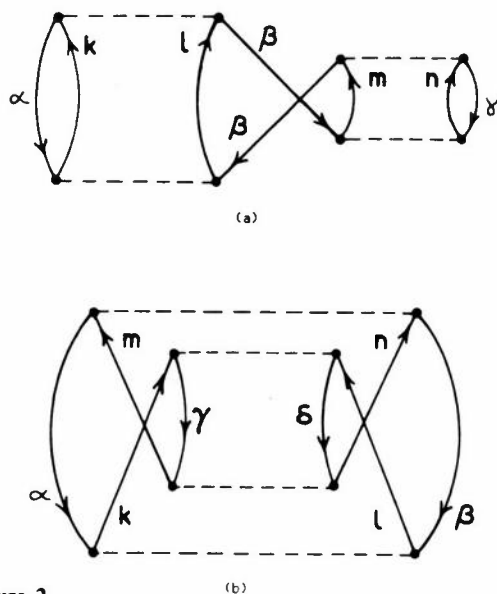


Figure 2

culations [6] certain rearrangement effects (figure 2a) are included in first order using shifted energy denominators. One hopes, that by including the rearrangement effects at first order by solving the resulting coupled pair equations [7], one can eliminate

\* Department of Chemistry, Queen Elizabeth College, University of London, Campden Hill, Kensington, London, W8 7AH



the need to solve 'higher order Bethe-Goldstone equations' by correcting for 'exclusion' effects by evaluating the pair-pair interactions directly from the repulsions of the independent pairs.

### Theory

There are three types of three- and four-body diagrams which give rise to exclusion effects and these are shown in figure 3. Diagram 3a is a 'ring' diagram and there are seven others corresponding to various exchanges. Diagram 3b involves an off-diagonal matrix element of the Hartree-Fock operator and vanishes for canonical molecular orbitals (CMO). Diagram 3c is a hole-line 'ladder'. All these diagrams have no more than two electrons excited at a time and thus we refer to them as three- and four-orbital two-body diagrams. The most important correction results from figure 3c where only the spin labels of the hole states are changed by the intermediate interaction. This term is included if one uses 'spin-irreducible' pairs where the particle and hole pairs are coupled to give two-particle singlets or triplets. All of our calculations are carried out in this basis.

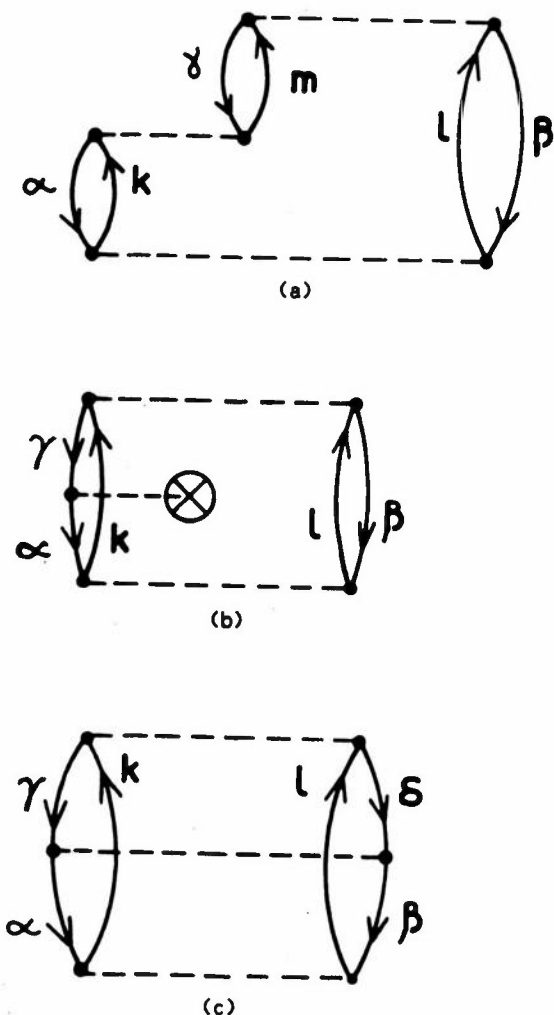


Figure 3

Once one has determined the independent pairs (including the rearrangement effects), the correlation energy may be corrected to first order in exclusion effects, figure 3, by computing the pair-pair repulsions between all pairs  $U_{a\beta}/U_{\gamma\delta}$  from

$$\Delta E_{\text{exclusion effects}} = \sum_{a\beta \neq \gamma\delta} \langle U_{a\beta} | V_{\text{dh}\ell} | U_{\gamma\delta} \rangle \quad (1)$$

where

$$\begin{aligned} V_{\text{dh}\ell} = & \sum_{a\beta, \gamma\beta} \left\{ |U_{a\beta}\rangle \langle U_{a\beta}| \left( \sum_{\mu=1,2} J_{a\gamma}(\mu) - K_{a\gamma}(\mu) \right. \right. \\ & \left. \left. - \epsilon_{a\gamma} + \langle [a\beta]_{12} | r_{12}^{-1} | [\gamma\beta]_{12} \rangle \right) |U_{\gamma\beta}\rangle \langle U_{\gamma\beta}| \right\} \\ & + \sum_{a\beta, a\gamma} \left\{ |U_{a\beta}\rangle \langle U_{a\beta}| \left( \sum_{\mu=1,2} J_{\beta\gamma}(\mu) - K_{\beta\gamma}(\mu) \right. \right. \\ & \left. \left. - \epsilon_{\beta\gamma} + \langle [a\beta]_{12} | r_{12}^{-1} | [a\gamma]_{12} \rangle \right) |U_{a\gamma}\rangle \langle U_{a\gamma}| \right\} \\ & + \sum_{a\beta, \gamma\delta} \left\{ |U_{a\beta}\rangle \langle U_{a\beta}| \left( \langle [a\beta]_{12} | r_{12}^{-1} | [\gamma\delta]_{12} \rangle \right) \right. \\ & \left. |U_{\gamma\delta}\rangle \langle U_{\gamma\delta}| \right\} \quad (2) \end{aligned}$$

and  $\epsilon_{a\gamma}$  is an off-diagonal matrix element of the Hartree-Fock operator.

### Results and Discussion

The results of this analysis for the  $H_2O$  molecule, in a contracted Gaussian basis [8] of double zeta quality, are shown in table 1 along with the variational result of Shavitt [9]. For both CMO and localized molecular orbitals (LMO) almost all of the correction for exclusion effects is due to diagrams of the type

Table 1: Pair correlation energies of  $H_2O$  in DZ basis

	CMO	LMO
Sum of spin irreducible pairs	-0.1472	-0.1397
Diagonal rearrangement effects figure 2a	-0.1459	-0.1376
Pair-pair repulsions (first order correction)	-0.1407	-0.1287
3-orbital 2-body effects figure 4a	+0.0032	+0.0078
figure 4c	+0.0101	+0.0097
figure 3b	-0.0064	-0.0004
	-	-0.0015
4-orbital 2-body effects figure 4b	+0.0021	+0.0011
	+0.0022	+0.0008
Variational result		-0.132

shown in figure 4. It is remarkable that they involve at most two different spacial orbitals  $i$  and  $j$ .

For the CMO, the contribution of diagrams 4a and 4c are of opposite sign and it is likely that convergence has not been obtained. In contrast, for LMO, the contribution of diagram 4c is very small and the contribution of diagram 4a dominates. Further, the small contribution of diagram 4b is almost cancelled by diagram 3b.

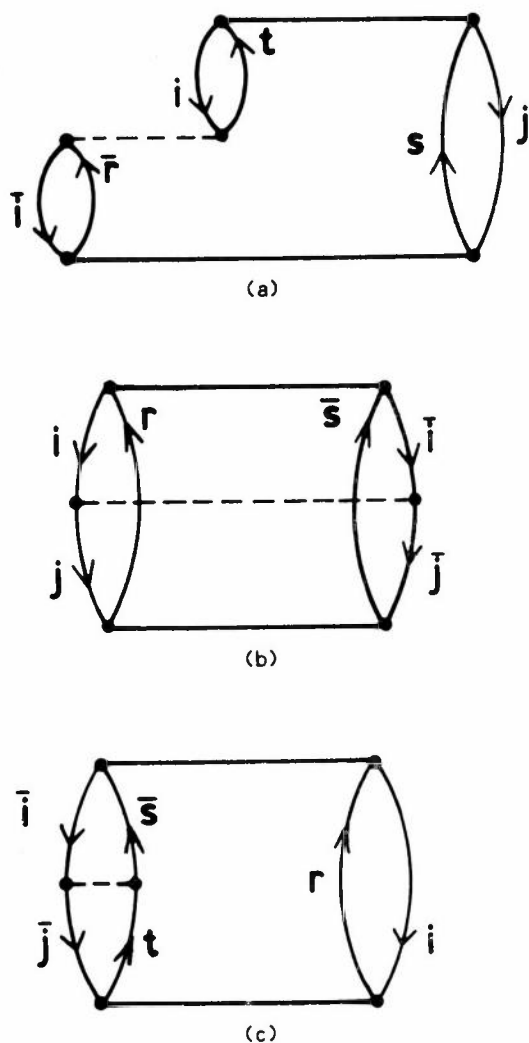


Figure 4

It would be premature to draw extensive conclusions from this simple calculation. However, the transformation to LMO certainly appears to remove most of the coupling between semi-disjoint pairs of the types  $U_{ii}^{\bar{i}}/U_{ij}^{\bar{i}}$ . It is only pairs such as  $U_{ij}^{\bar{i}}/U_{ij}$  that are strongly coupled and no orbital transformation can remove this. Further, the fact that the contribution of diagram 3b is not large implies that coupled first order equations for LMO pairs [10] may not be necessary.

## References

- [1] SINANOGLU, O. (1969). *Adv. Chem. Phys.*, **14**, 239.
- [2] NESBET, R.K. (1969). *Adv. Chem. Phys.*, **14**, 1.
- [3] FREED, K.F. (1968). *Phys. Rev.*, **173**, 1.
- [4] KELLY, H.P. and SESSLER, A.M. (1963). *Phys. Rev.*, **132**, 2091.
- [5] BRUEKNER, K.A. and GOLDMAN, D.T. (1960). *Phys. Rev.*, **117**, 307.
- [6] KELLY, H.P. (1968). *Adv. Theoret. Phys.*, **2**, 75.
- [7] ROBB, M.A. (1973). *Chem. Phys. Letters*, **20**, 274.
- [8] HUZINAGA, S. and SAKAI, Y. (1969). *J. Chem. Phys.*, **50**, 1371.
- [9] HOSTENEY, R.P., GILMAN, R.R., DUNNING, T.H. and SHAVITT, I. (1970). *Chem. Phys. Letters*, **7**, 325.
- [10] AMOS, A.T., MUSER, J.I. and ROBERTS, H.G.Ff. (1969). *Chem. Phys. Letters*, **4**, 93.

# Valence-Bond Calculations on $HF$ and $LiH$

R.N. Yardley and G.G. Balint-Kurti\*

*Ab initio* multi-structure valence-bond calculations are presented for the molecules  $HF$  and  $LiH$ . The atomic basis sets used in these calculations were contracted Gaussian minimum orbital basis sets of double zeta quality, augmented by a few extra  $s$  and  $p$  type orbitals. The extra orbitals permit a reasonably accurate description of  $F^-$  and  $H^-$  relative to their neutral atoms and also provide extra flexibility to the molecular wavefunction. The calculated potential energy curves behave correctly at large internuclear separations and yield dissociation energies which are within 11% of the experimental values. These calculations are intended only as preliminary studies for larger triatomic calculations, but they nevertheless demonstrate the capabilities of valence-bond calculations using limited orbital basis sets.

## Introduction and Description of Method

The distinctive feature of the valence-bond method is that, in contrast to the molecular orbital method, it regards a molecule as being built up from its constituent atoms. Suppose that we wish to describe a diatomic molecule  $AB$ . We first define approximate atomic eigenfunctions such as  $\Phi_i^A$  and  $\Phi_j^B$  which refer respectively to the  $i^{\text{th}}$  state of atom  $A$  and the  $j^{\text{th}}$  state of atom  $B$ . These functions are antisymmetric with respect to interchange of any two electron coordinates and are eigenfunctions of  $S^2$ ,  $S_z$  and  $L^2$  for the atoms.

The basis set, in terms of which the molecular wavefunction is to be expanded, is now constructed by multiplying together approximate atomic eigenfunctions for atoms  $A$  and  $B$  and antisymmetrising the product:

$$\chi_a = A'[\Phi_i^A \Phi_j^B] \quad (1)$$

where  $A'$  is a partial antisymmetriser and antisymmetrises the product with respect to the interchange of electrons originally assigned to different atoms. These antisymmetrised products of atomic eigenfunctions were first introduced by Moffitt [1] and are called composite functions (CF's). They are not, in general, eigenfunctions of the total spin angular momentum ( $S^2$ ) for the molecule, but it is simple to form linear combinations of them which are. The molecular wavefunction ( $\Psi_i$ ) is expanded in terms of the CF's (or linear combinations of them):

$$\Psi_i = \sum_a C_{ia} \chi_a \quad (2)$$

Use of the variational theorem to find the  $C_{ia}$ 's leads to a set of secular equations

$$\sum_{\beta} (H_{\alpha\beta} - E_i S_{\alpha\beta}) C_{i\beta} = 0 \quad (3)$$

which may be solved in the standard manner.

A composite function may be expressed as a linear combination of Slater determinants built up from nonorthogonal orbitals

$$\chi_a = \sum_A R_{aA} \Phi_A \quad (4)$$

where

$$\Phi_A = (N!)^{-1/2} \det|\phi_{a_1}(\vec{r}_1) \phi_{a_2}(\vec{r}_2) \dots \phi_{a_N}(\vec{r}_N)| \quad (5)$$

and  $\phi_{a_i}(\vec{r}_i)$  etc. are atomic orbitals. The main difficulty which has been encountered in the past in performing *ab initio* valence-bond calculations has been the nonorthogonality problem. Several methods of handling this problem have been proposed. We use a method which was introduced by Hurley [2,3] and is outlined below:

- (a) The nonorthogonal orbitals ( $\phi_j(\vec{r})$ ) are first transformed to a set of orthogonal orbitals ( $\psi_i(\vec{r})$ ).

$$\phi_j(\vec{r}) = \sum_i \psi_i(\vec{r}) \gamma_{ij} \quad (6)$$

- (b) The Slater determinants over the nonorthogonal orbitals,  $\Phi_A$  of equation (5), are expanded in terms of Slater determinants over orthogonal orbitals.

(7)

$$\Psi_K = (N!)^{-1/2} \det|\psi_{k_1}(\vec{r}_1) \psi_{k_2}(\vec{r}_2) \dots \psi_{k_N}(\vec{r}_N)|$$

\* School of Chemistry, University of Bristol, Cantock's Close, Bristol, BS8 1TS

The relationship between the two sets of Slater determinants is given by:

$$\Phi_A = \sum_K T_{AK} \Psi_K \quad (8)$$

where

$$T_{AK} = \begin{vmatrix} \gamma_{k_1 a_1} & \gamma_{k_1 a_2} & \dots & \gamma_{k_1 a_N} \\ \gamma_{k_2 a_1} & \gamma_{k_2 a_2} & \dots & \gamma_{k_2 a_N} \\ \dots & \dots & \dots & \dots \\ \gamma_{k_N a_1} & \dots & \dots & \gamma_{k_N a_N} \end{vmatrix} \quad (9)$$

The number of orthogonal Slater determinants appearing in the sum over  $K$  can be minimised by using the Schmidt orthogonalisation technique and a judicious ordering of the nonorthogonal orbitals.

- (c) The Hamiltonian matrix between the orthogonal Slater determinants is calculated

$$H_{KL} = \langle \Psi_K | H | \Psi_L \rangle \quad (10)$$

- (d) The Hamiltonian matrix is transformed into the CF basis using equations (4) and (8).

$$\begin{aligned} H_{\alpha\beta} &= \langle \chi_\alpha | H | \chi_\beta \rangle \\ &= \sum_{AB} \sum_{KL} R_{\alpha A} T_{AK} H_{KL} T_{BL} R_{\beta B} \end{aligned} \quad (11)$$

The equations for the overlap matrix are considerably simpler than those for the Hamiltonian matrix:

$$\begin{aligned} S_{\alpha\beta} &= \langle \chi_\alpha | \chi_\beta \rangle \\ &= \sum_{AB} \sum_K R_{\alpha A} T_{AK} T_{BK} R_{\beta B} \end{aligned} \quad (12)$$

### Potential Energy Curve for Ground State of HF

The atomic orbitals were represented as linear combinations of Gaussian type orbitals (GTO's). For fluorine the 1s, 2s and 2p orbitals were taken from Ditchfield, Hehre and Pople [4] and were each made up from five GTO's. These orbitals gave an energy for the ground state of fluorine which was just a little worse than the double zeta SCF energy. A more diffuse 2s and a set of 2p orbitals were added to provide an adequate description of the  $F^-$  ion. For hydrogen the 1s orbital was a linear combination of five GTO's (as given by Huzinaga) [5], a more diffuse s orbital was added to provide a better

description of  $H^-(1S)$  and a more contracted one to allow for distortion in the molecule. A set of p orbitals was also added to allow for polarisation. Finally a 1s orbital, which was an uncontracted GTO, was placed in the centre of the bond to provide extra flexibility for the molecular wavefunction.

Table 1<sup>a</sup>

Atomic State	Number of Functions of Correct Symmetry used to represent Atomic or Ionic State	Calculated Energy	Experimental <sup>b</sup> Energy
$F(2P^0)$	2	-99.3698	-99.8060
$F(2S)$	2	-98.4845	-99.0386
$F^-(1S)$	3	-99.4738	-99.9333 <sup>c</sup>
$F^+(3P)$	1	-98.6891	-99.1654
$F^+(1D)$	1	-98.5976	-99.0711
$F^+(1S)$	1	-98.6433	-98.9615
$F^+(3P^0)$	1	-97.8855	-98.4146
$F^+(1P^0)$	1	-97.5264	-98.0744
$H(2S)$	3	-0.4998	-0.50
$H^-(1S)$	3	-0.5226 <sup>d</sup>	-0.5278 <sup>e</sup>
$Li(2S)$	1	-7.4248	-7.4779
$Li(2P^0)$	1	-7.3560	-7.4100
$Li^+(1S)$	1	-7.2306	-7.2798
$Li^-(1S)$	2	-7.4168	-7.4999 <sup>f</sup>

(a) All energies are in atomic units: 1 au =  $4.359828 \times 10^{-18}$  Joules

(b) Experimental energies are from MOORE, C. (1949), *Natl. Bur. Standards*, Circular No. 467

(c) See [6]

(d) This was the calculated energy of  $H^-$  using p orbital exponents optimised for this ion. If the exponents which were found to be optimal for describing HF and LiH are used, then the calculated energy is -5.2175 and -5.2221 respectively.

(e) STEWART, A.L. and TEMKIN, A. (1966), *Bull. Am. Phys. Soc.*, 11, 722

(f) WEISS, A.W. (1968), *Phys. Rev.*, 166(1), 70

These atomic orbitals were used to construct approximate atomic eigenfunctions for the atoms and ions involved in the calculation. In many cases several functions of the same symmetry were constructed. These were then subjected to an atomic configuration interaction calculation and the lowest and excited approximate atomic eigenfunctions which resulted were then used as building blocks in the construction of the CF basis set. In table 1 the calculated and experimental energies of the atomic and ionic states which were used to construct the CF's are listed. Only the lowest state of a given symmetry is listed. Several states of  $H^-$  and  $Li^-$ , which lie above the energy of the neutral atom plus an electron and which were used to construct CF's are not included in the table (i.e.  $H^-(3P)$ ,  $H^-(3P^0)$ ,  $H^-(3S)$ ,  $H^-(1P^0)$ ,  $H^-(1D)$ ,  $Li^-(3P^0)$ ,  $Li^-(1P^0)$ ,  $Li^-(1D)$  and  $Li^-(3P)$ ). Of special interest is the calculated electron affinity of F which is 0.1040 au as compared with an

experimental value of 0.1273 au [6]. This is much better than the Hartree-Fock estimate of this quantity which is [7] 0.05 au.

For HF 113 CF's were constructed from the approximate atomic eigenfunctions and these composite functions were combined into 57 functions of  $^1\Sigma^+$  symmetry. Calculations were then performed at the experimental equilibrium separation of HF [8] ( $R_e = 1.7328$  au) and the exponents of the central  $s$  orbital and then of the  $p$  type orbitals on the hydrogen atom were scaled in order to approximately minimise the calculated energy. These scaled exponents were then used in the calculations at other internuclear separations.

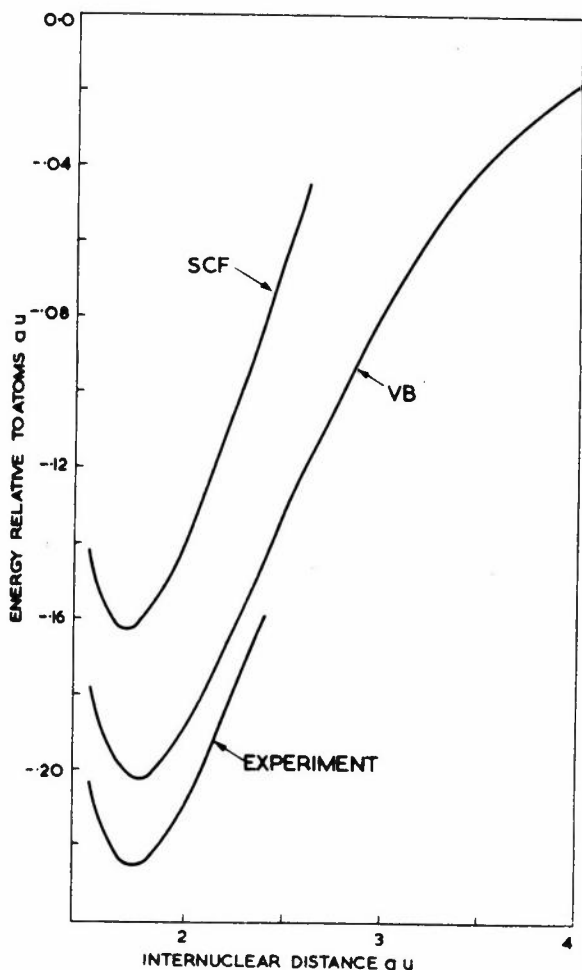


Figure 1: Calculated potential energy curve for HF(VB). Also shown are the SCF curve of Cade and Huo [9] and the experimental curve [10]. The zero of energy is taken to be the calculated or experimental energy of  $F(^2P^0) + H(^2S)$  as appropriate. The VB curve is drawn on the basis of calculations at 16 different internuclear separations.

The calculated potential energy curve is shown in figure 1. Also shown are the best SCF calculations for HF [9] and the experimental curve [10]. The calculated dissociation energy is 90% of the experimental value (i.e. 0.2021 au calculated as compared to 0.2249 au experimental). The calculated equilibrium distance of 1.74 au is also very close to the

experimental one of 1.733 au. This is, however, at least partly due to the way in which the exponents were optimised. The present results are of comparable accuracy to those of Bender and Davidson [11] whose calculated potential energy curves were the best previously available. The results they give do not permit the estimation of a dissociation energy, so we cannot unfortunately make a numerical comparison on that basis. On the basis of total energies our calculated total energy at the lowest point on the potential energy curve is  $-100.0718$  au (as compared with their value of  $-100.0438$  au. It should also be noted that the present calculations use only  $s$  and  $p$  type orbitals while Bender and Davidson's basis set included  $d$  orbitals. In order to check that the calculated potential energy curve dissociates smoothly to the calculated atomic energies, a calculation was performed at 20 au. The calculated energy at this separation agreed to within one digit in the sixth decimal place with the sum of the calculated energies of  $F(^2P^0) + H(^2S)$ .

Table 2: Effect of Omitting One Type of Orbital at a Time on the Calculated Energy of HF at  $R = 1.6$  au

Orbital(s) Omitted	Amount by which Molecular Energy was Raised (au)
Contracted $s$ orbital on hydrogen	0.0333
Diffuse $s$ orbital on hydrogen	0.0004
$p$ orbitals on hydrogen	0.0325
Diffuse $2s$ orbital on fluorine	0.0019
Diffuse $2p$ orbitals on fluorine	0.0041
$s$ orbital in centre of bond	0.0165

A preliminary analysis of the wavefunction has been carried out by performing a number of calculations in which certain of the orbitals were completely omitted from the basis set. The effect on the calculated molecular energy at  $R = 1.6$  au of omitting one orbital at a time is shown in Table 2. It is clear from the table that omitting either the diffuse  $s$  orbital on the hydrogen (chosen to describe  $H(^1S)$ ) or the additional diffuse  $2s$  orbital on F (chosen to improve the description of  $F^-$ ) has little effect on the calculated energy. Omitting either the  $s$  orbital in the centre of the bond or the  $p$  orbitals on hydrogen, both of whose exponents were scaled to minimise the molecular energy has a much larger effect. Omitting the contracted  $s$  orbital on hydrogen also has a large effect.

### The Low Lying $^1\Sigma^+$ States of LiH

The orbital basis set for lithium consisted of a  $1s$ ,  $2s$  and a set of  $2p$  orbitals. The  $1s$  orbital was a linear combination of five GTO's and was taken from

an exponent optimised SCF calculation on  $Li^+$  performed by Whitman, Leyshon and Hornback [12]. The  $2s$  orbital was a linear combination of four GTO's and was taken from a similar calculation for  $Li(2S)$  and was then scaled so as to give the best possible energy for  $Li(2S)$  when combined with the  $1s$  orbital just described. The  $2p$  orbital was made up of two GTO's and chosen to give as good an energy as possible for  $Li(2P^0)$ . The hydrogen orbitals were the same as those described in the previous section. As with  $HF$  a  $1s$  type GTO was placed in the centre of the bond. Its exponent and those of the  $p$  orbitals on the hydrogen were scaled to give the lowest possible energy for the ground state of  $LiH$  at the experimental equilibrium separation.

These atomic orbitals were used to construct approximate atomic eigenfunctions for  $Li$ ,  $Li^+$ ,  $Li^-$ ,  $H$  and  $H^-$ . The calculated and experimental energies corresponding to most of these atomic states are given in table 1. The more highly excited states of  $Li^-$  and  $H^-$  are not included in the table (see above). The approximate atomic eigenfunctions were then used to construct the CF basis set for the molecular calculation. This basis set consisted of 37 CF's which were combined to give 21 functions of  $1\Sigma^+$  symmetry.

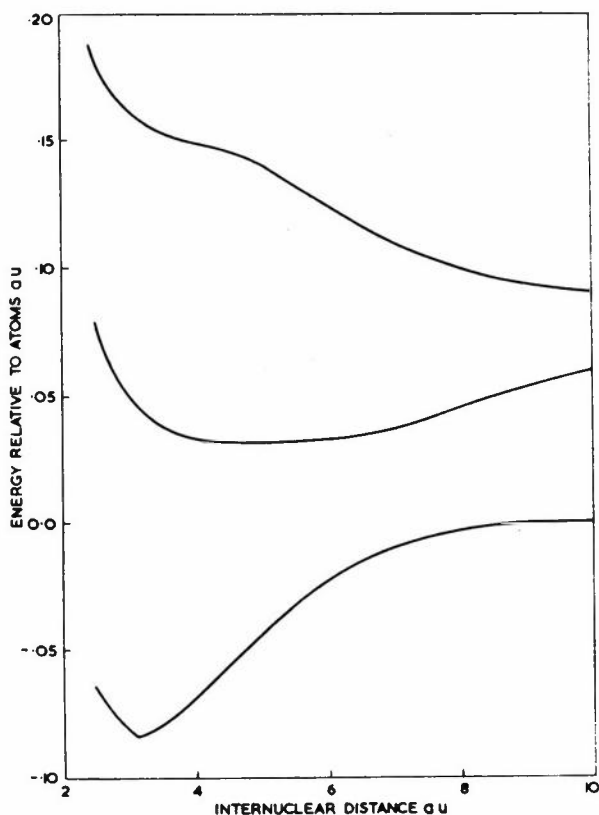


Figure 2: Lowest three  $1\Sigma^+$  curves for  $LiH$  as calculated by valence-bond method. The zero of energy is taken to be the calculated energy of  $Li(2S) + H(2S)$ . The curves are drawn on the basis of calculations at 30 different internuclear separations.

The lowest three calculated  $LiH$  potential energy curves of  $1\Sigma^+$  symmetry are shown in figure 2. For the ground state the calculated dissociation energy and equilibrium distance are  $D_e = 0.0822$  au,  $R_e = 3.116$  au as compared with the experimental [13] values of  $D_e = 0.0924$  au and  $R_e = 3.015$  au. For the first excited  $1\Sigma^+$  state the calculated and experimental dissociation energies and equilibrium separations are; Calculated [14]:  $D_e \approx 0.03698$  au,  $R_e \approx 5.095$  au; Experimental:  $D_e = 0.03956$  au,  $R_e = 4.906$  au.

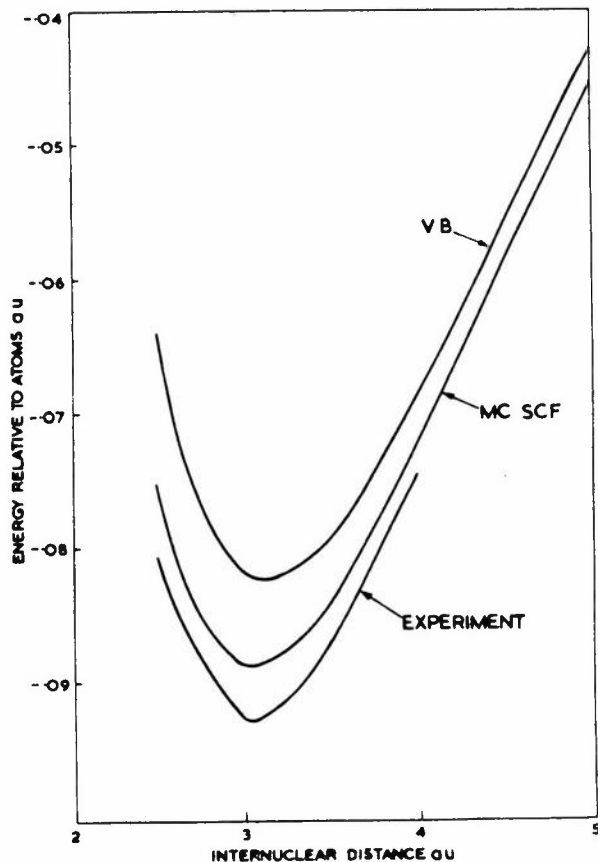


Figure 3: Potential energy curves for  $LiH 1\Sigma^+$  ground state. The VB curve is shown together with the MC-SCF curve of Docken and Hinze [15] and the experimental curve [16]. The zero of energy is taken to be the calculated or experimental energy of  $Li(2S) + H(2S)$  as appropriate.

The present calculations for  $LiH$  yield 89% of the experimental dissociation energy for the ground state. This is not as good as the best available calculated potential energy curve which was calculated by Docken and Hinze [15] using the MC-SCF method. Their calculation gave 96% of the experimental ground state dissociation energy. To achieve this result they used a much larger basis set and performed a more extensive exponent optimisation at the experimental equilibrium separation. Their results for the ground state potential energy curve are compared with the present VB calculations and with the experimental [16] curve in figure 3.

## Discussion

The valence-bond calculations presented here have been performed using relatively small orbital basis sets. Despite this limitation the calculations have yielded potential energy curves of comparable accuracy to the best ones calculated by other methods. It should be possible to extend the valence-bond method to treat small triatomic systems with wavefunctions of similar accuracy to those used in the present calculations.

## Acknowledgement

The authors are indebted to the Science Research Council for a grant of computer time and would like to express their gratitude to the staff of the Atlas Computer Laboratory for their assistance. In particular we are grateful for the provision of the ATMOL 2 integral evaluation package which was used in this work. R.N.Y. also wishes to thank the Science Research Council for financial support.

## References

- [1] MOFFITT, W. (1954). *Rep. Prog. Phys.*, **17**, 173.
- [2] HURLEY, A.C. (1960). *Rev. Modern Phys.*, **32**, 400.
- [3] BALINT-KURTI, G.G. and KARPLUS, M. (1969). *J. Chem. Phys.*, **50**, 478.
- [4] DITCHFIELD, R., HEHRE, W.J. and POPLE, J.A. (1970). *J. Chem. Phys.*, **52**, 5001.
- [5] HUZINAGA, S. (1965). *J. Chem. Phys.*, **42**, 1293.
- [6] BERRY, R.S. and REINMAN, C.W. (1963). *J. Chem. Phys.*, **38**, 1540.
- [7] CLEMENTI, E. and MCLEAN, A.D. (1964). *Phys. Rev.*, **133A**, 419.
- [8] HERZBERG, G. (1950). *Spectra of Diatomic Molecules*, 2nd ed., Princeton, New Jersey: Van Nostrand.
- [9] CADE, P.E. and HUO, W.M. (1967). *J. Chem. Phys.*, **47**, 614.
- [10] This is taken to be a Morse curve with the parameters  $R_e = 1.7325$  au,  $D_e = 0.2247$  au and  $\omega_e = 0.01886$  au. See JOHNS, J.W.C. and BARROW, R.F. (1959). *Proc. Roy. Soc. (London)*, **A251**, 504.
- [11] BENDER, C.F. and DAVIDSON, E.R. (1968). *J. Chem. Phys.*, **49**, 4989.
- [12] WHITMAN, D.R., LEYSHON, K. and HORNBACK, C.J., (private communication).
- [13] VELASCO, R. (1957). *Can. J. Phys.*, **35**, 1204.
- [14] These values are the result of approximate interpolation and are not completely accurate. (Found by fitting 3rd order polynomial to the 5 points nearest the minimum).
- [15] DOCKEN, K.K. and HINZE, J. (1972). *J. Chem. Phys.*, **57**, 4928.
- [16] This was taken to be a Morse curve with the parameters  $R_e = 3.0147$  au,  $D_e = 0.09246$  au,  $\omega_e = .006406$  au. See [13] and WHARTON, L., GOLD, L.P. and KLEMPERER, W. (1962). *J. Chem. Phys.*, **37**, 2149. BENDER, C.F. and DAVIDSON, E.R. (1968). *Ibid.*, **49**, 4222.

# Studies of Correlation Effects on Hydrogen Bonding and Ion Hydration

G.H.F.Diercksen, W.P.Kraemer\* and B.O.Roos†

## Introduction

MO-SCF-CI calculations have been performed for the systems:  $H_2O$ ,  $H^+(H_2O)$ ,  $Li^+(H_2O)$ ,  $F^-(H_2O)$  and  $(H_2O)_2$ . The main purpose of the work has been to investigate the effect of electron correlation in hydrogen bonded systems and hydrated ions. It is generally believed that the Hartree-Fock approximation gives an adequate description of this type of interaction and that electron correlation is only of minor importance. This has, however, not yet been tested by actual CI-calculations on hydrogen bonded systems.

The calculations have been performed using the MUNICH program systems for the SCF part and for the transformation of the two-electron integrals to a molecular orbital basis [1]. The MOLEUCLE-CI program, developed in Stockholm, was used for the actual CI-calculations [2].

The molecular orbitals are expanded in a set of contracted Gaussian atomic orbitals. The basis set consists of (11, 7, 1) contracted to [5, 4, 1] for oxygen and fluorine, (11, 2) contracted to [5, 2] for lithium and (6, 1) contracted to [3, 1] for hydrogen.

The CI expansion of the wavefunction includes all singly and doubly excited configurations with respect to a closed shell HF reference state, with the

exception of excitations out of the 1s orbitals for oxygen and fluorine. For the larger systems this gives rise to a large number of spin-symmetrised configurations - 56000 for the water dimer. The special technique employed in the MOLEUCLE program makes it, however, possible to solve the corresponding secular equation with a reasonable use of computer time also for such large matrices (one full CI calculation on the water dimer takes around three hours CPU time on an IBM 360/91 computer). The number of molecular orbitals and configurations for the different systems are listed in table 1.

## Results and Discussions

A number of calculations were first performed on the water molecule in order to test the reliability of data computed with the present method, and also to have theoretical data available for comparison with the results for the ion hydrates and the water dimer. Calculations were made for a number of different OH distances and HOH angles, keeping the  $C_{2v}$  symmetry. The results are presented in table 2. Calculated values for the bond distance, the bond angle and the symmetric force constants are all in good agreement

Table 1: Number of orbitals and configurations for the CI-calculations

	$n^a_{\text{occupied}}$	$n^b_{\text{virtual}}$	$N^c_{\text{configuration}}$
$H_2O$	4	29	1917
$H^+(H_2O)$	4	35	10010
$Li^+(H_2O)$	5	39	10101
$F^-(H_2O)$	8	46	36204
$(H_2O)_2$	8	58	56000

(a) Number of non-frozen occupied orbitals

(b) Number of virtual orbitals

(c) Number of spin- and space-symmetrized configurations

Table 2: Predicted geometries and force constants for  $H_2O$ . The parameters have been obtained with the expansion:

$$V = V_e + f_r(\Delta r)^2 + (2/r_e) f_{rrr}(\Delta r)^3 + \frac{1}{2} f_{\alpha} r_e^2 \Delta \alpha^2$$

	SCF	CI	Experiment [3]
Bond distance (Å)	0.944	0.960	0.957
Bond angle, $\alpha$ (degrees)	105°3	103°8	104°5
Stretching force constant, $f_r$ (md/Å)	9.50	8.44	8.35
Anharmonicity, $f_{rrr}$ (md/Å)	-10.00	-9.84	-9.55
Bending force constant, $f_{\alpha}$ (md/Å)	0.816	0.752	0.76

\* Max-Planck-Institut für Physik und Astrophysik, Föhringer Ring 6, 8 München 40, West Germany

† Institute of Theoretical Physics, University of Stockholm, Vanadisvägen 9, S-113 46 Stockholm, Sweden



with experiment. The potential surface around the equilibrium geometry therefore seems to be well described with the present CI-scheme and basis set.

The calculations on  $H_3O^+$  were restricted to geometries having  $C_{3v}$  symmetry. The  $HOH$  angle and the  $OH$  distance were varied independently. The minimum energy was found for a pyramidal structure with  $d(OH) = 0.979$  (0.963) Å and  $\angle(HOH) = 111.6$  ( $113.5$ ). Values within parentheses were obtained at the SCF-level. The inversion barrier was calculated to be 2.1 (1.3) kcal/mole. Thus correlation favours the pyramidal structure and increases the inversion barrier by 0.8 kcal/mole. The correlation energy is smaller in magnitude for  $H_3O^+$  than for  $H_2O$  (cf. table 3). The difference is 1.5 kcal/mole at the equilibrium geometries. The calculated total energy difference was 172.8 (174.3) kcal/mole. The zero-point energy difference should be added to this value in order to estimate the proton affinity of water. The computed energy surface at the CI-level for  $H_3O^+$  was used in a variational calculation of the vibrational energy corresponding to the symmetrical stretching and bending modes. The contribution to the zero-point energy from the two degenerate modes were obtained using the valence force method [4]. For water this method gave a zero-point energy in complete agreement with the experimental values. The contribution to the binding energy from the variational energy obtained in this way was  $-5.3$  kcal/mole. This gives a proton affinity of 167.5 kcal/mole in excellent agreement with recent experimental values [5].

Table 3: SCF, correlation and CI energies for the systems  $X(H_2O)$  (in atomic units)<sup>a</sup>

$X$	$E_{SCF}$	$E_{correlation}^c$	$E_{CI}$
b	-76.051998	-0.214473	-76.266471
$H^+$	-76.329776	-0.212027	-76.541803
$Li^+$	-83.345706	-0.240108	-83.585814
$F^-$	-175.541213	-0.414810	-175.956023
$H_2O$	-152.112148	-0.409535	-152.521683

- (a) At the calculated equilibrium geometry  
 (b) The isolated water molecule  
 (c) Valence electron correlation energies

The monohydrate of the lithium positive ion was studied both in a planar geometry with  $Li^+$  on the symmetry axis of the water molecule and in some non-planar geometries keeping one plane of symmetry. The lowest energy was obtained for a planar complex with an  $LiO$  distance of 1.842 (1.831) Å. The calculated binding energy at the SCF-level was 36.1 kcal/mole in good agreement with other recent HF studies [6,7], which also report the same equilibrium geometries. At the CI-level we find a binding energy

of 34.1 kcal/mole in excellent agreement with the experimental value [8]. The calculated binding energy includes a vibrational contribution of  $-2.0$  kcal/mole. The zero-point energy was estimated by using the valence force approximation. The force constant for the stretching of the  $OH$  bonds and the variation of the  $HOH$  angle were taken from the CI calculations on the free water molecule. The force constants for the  $LiO$  stretching and the out of plane motion of the lithium ion has been deduced from the present CI calculations. The same procedure has been used to estimate the vibrational corrections to the binding energy for the systems  $F^-(H_2O)$  and  $(H_2O)_2$  (cf. table 4).

Qualitatively the effect of correlation is the same in  $Li^+(H_2O)$  and  $H^+(H_2O)$ . Delocalisation of electronic charge onto the positive ion diminishes the effective nuclear charge seen by the electrons. This leads to a decrease in the magnitude of the correlation energy. The situation is similar to what has been observed for the isoelectronic series of first row hydrides ( $CH_4$  ...  $HF$ ), where the correlation energy increases in magnitude along the series.

The situation is different for the complexes  $F^-(H_2O)$  and  $(H_2O)_2$ . The two interacting systems have in this case a filled shell structure with no empty valence orbitals. The intermolecular correlation energy is therefore mainly describing a Van der Waals type interaction.

The calculations on  $F^-(H_2O)$  assumed a planar structure with an almost linear fluorine-oxygen hydrogen bond. The  $FO$  distance and the  $FHO$  angle were varied. The most stable structure was found to have an  $FO$  distance of 2.471 (2.509) Å and an  $FHO$  angle of  $176.4$  ( $175.7$ ). The SCF values are close to the geometry reported in a recent HF calculation with a larger basis set [9]. A binding energy of 24.2 kcal/mole was obtained at the SCF-level. Correlation increases the binding energy by almost 2 kcal/mole and also decreases the  $FO$  equilibrium bond distance by 0.04 Å.

Calculations on the water dimer were made only for the most stable linear hydrogen bond:

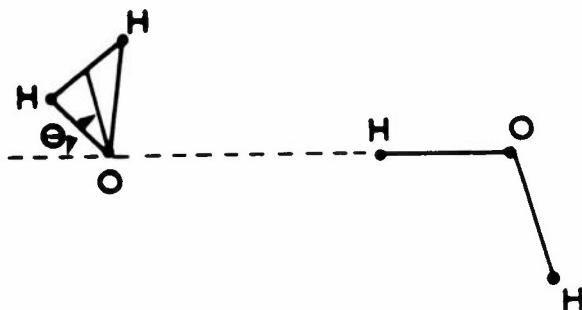


Figure 1: Most stable geometry for the water dimer

The  $OO$  distance and the angle  $\Theta$  were varied. The calculated values for these parameters were

found to be 2.92 (3.00) Å and 42°4 (41°5). Thus the effect of correlation on the bond distance is comparatively large in this weakly bonded system. Actually correlation energy was found to account for almost 20% of the binding energy, or 1.0 kcal/mole (cf. table 4). The final calculated binding energy, including an estimate of the vibrational correction of 0.2 kcal/mole, was 5.9 kcal/mole. This is very close to the energy per *H*-bond found in ice (5.7 kcal/mole) but somewhat larger than the gas phase value of 5.0 kcal/mole reported by Rowlinson in 1949 [10].

Table 4: Binding energies for some ion hydrates and the water dimer (kcal/mole)

	$\Delta E_{SCF}$	$\Delta E_{CI}$	$(\Delta E_{CI} - \Delta E_{SCF})$	$\Delta E_{2p}^a$	B.E. <sup>b</sup>	Experiment
$H^+(H_2O)$	174.3	172.8	-1.5	5.3	167.5	166±2 <sup>c</sup>
$Li^+(H_2O)$	36.1	34.9	-1.2	2.0	32.9	34.0 <sup>d</sup>
$F^-(H_2O)$	24.2	26.2	1.9	3.2	23.0	23.3 <sup>e</sup>
$(H_2O)_2$	5.1	6.1	1.0	~1.0	5.1	5.0 <sup>f</sup>

(a) Estimated increase in zero-point energy for the complex

(b) Binding energy ( $E(X) + E(H_2O) - E(X \cdot H_2O)$ ) calculated at the CI level and including the zero-point energy

(c) COTTER, R.J. and KOSKI, W.S. (1973), *J. Chem. Phys.*, **59**, 784

(d) DZIDIC, I. and KEBARLE, P. (1970), *J. Phys. Chem.*, **74**, 1466

(e) ARSHADI, M., YAMADAGNI, R. and KEBARLE, P. (1971), *J. Phys. Chem.*, **74**, 3308

(f) ROWLINSON, J.S. (1949), *Trans. Faraday Soc.*, **45**, 974: the *H*-bond energy in ice is 5.7 kcal/mole

Dispersion effects have thus been found to account for 1.9 and 1.0 kcal/mole of the binding energy for the two systems  $F^-(H_2O)$  and  $(H_2O)_2$ , respectively. These effects have a considerable influence on the geometry of the systems, especially the bond distance which is shortened by as much as 0.08 Å in the water dimer. It is interesting to notice that if the London formula

$$\Delta E = -K/R^6$$

is used, a dispersion energy of 1.1 kcal/mole is obtained for  $R = 2.92$  Å [11, 12]. A somewhat smaller value was obtained by Hankins *et al.* using the same formula but estimating  $K$  from the experimental value for the neon dispersion attraction, corrected for the water-neon polarizability ratio, (0.9 kcal/mole at  $R = 2.76$  Å) [13].

The present calculations account for approximately 70% of the valence electron correlation energy. For the water molecule this means that the error is around 0.1 au (60 kcal/mole). The HF error is around 0.015 au (~10 kcal/mole). Errors in relative quantities (binding energies, bond distances, etc.) should be

some orders of magnitude smaller. This is also found to be the case when experimental data is available for comparison. We therefore believe that the binding energies reported in the present paper have an accuracy of around ±1 kcal/mole and that calculated bond distances are less than ±0.01 Å in error.

A more detailed account of the work presented here is under preparation and will be published in the near future. This will also include a discussion of two possible sources of error in the present work. One is the so called superposition error. This is due to the fact that with an incomplete basis set the monomer energies themselves might be affected when they approach each other. This will occur both at the SCF- and the CI-level if a too small basis set is used, and lead to errors in the binding energy. An investigation of the size of the superposition error in the present calculations is under way and will be discussed in the forthcoming publication.

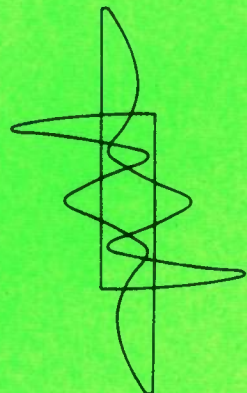
Table 5: Bond distances *X-O* for the systems  $X(H_2O)$  (Å)

<i>X</i>	SCF	CI	difference
$H^+$	0.963	0.979	0.016
$Li^+$	1.831	1.842	0.011
$F^-$	2.509	2.471	-0.038
$H_2O$	3.003	2.919	-0.084

## References

- [1] DIERCKSEN, G.H.F. and KRAEMER, W.P. (1973). *Munich Molecular Program System Reference Manual*, Special Technical Report, München: Max-Planck-Institut für Physik und Astrophysik.
- [2] ROOS, B. (1972). *Chem. Phys. Letters*, **15**, 153.
- [3] KUCHITS, K. and MORINO, Y. (1965). *Bull. Chem. Soc. Japan*, **38**, 814.
- [4] HERZBERG, G. (1951). *Infrared and Raman Spectra*, New York: Van Nostrand.
- [5] COTTER, R.J. and KOSKI, W.S. (1973). *J. Chem. Phys.*, **59**, 784.
- [6] DIERCKSEN, G.H.F. and KRAEMER, W.P. (1972). *Theoret. Chim. Acta*, **23**, 387.
- [7] CLEMENTI, E. and POPKIE, H. (1972). *J. Chem. Phys.*, **57**, 1077.
- [8] DZIDIC, I. and KEBARLE, P. (1970). *J. Phys. Chem.*, **74**, 1466.
- [9] KISTENMACHER, H., POPKIE, H. and CLEMENTI, E. (1973). *J. Chem. Phys.*, **58**, 5627.
- [10] ROWLINSON, J.S. (1949). *Trans. Faraday Soc.*, **45**, 974.
- [11] LONDON, F. (1937). *Trans. Faraday Soc.*, **33**, 8.
- [12] MARGENAU, H. (1939). *Revs. Modern Phys.*, **11**, 1.
- [13] HANKINS, D., MOSKOWITZ, J.W. and STILLINGER, F.H. (1970). *J. Chem. Phys.*, **53**, 4544.

HARTREE-FOCK  
THEORY  
AND  
APPLICATIONS



# Cusped-Gaussian Molecular Wavefunctions

E.Steiner and B.C.Walsh\*

A cusped-Gaussian basis is made up of the conventional Gaussian functions supplemented by a small number of cusp functions of the form

$$\begin{cases} r^{n+l}(\rho-r)^l Y_{lm}(\theta, \phi) & \text{if } r < \rho \\ 0 & \text{if } r > \rho \end{cases}$$

which are included to improve the quality of the Gaussian basis at and near a nucleus. In this paper we present the results of some simple molecular SCF calculations, and a brief description of the molecular integrals and of the general technique used for their evaluation.

## Introduction

The calculation of molecular wavefunctions in terms of a basis of Gaussian functions has in recent years become a very well established technique, particularly for polyatomic molecules. The main advantage of Gaussians over the more traditional Slater functions is the ease of computation of the multicentre integrals in a molecular calculation. The main disadvantage is that Gaussians are not suitable functions for an accurate description of a wavefunction near a nucleus. A Slater function like  $\exp(-\zeta r)$  has a non-zero derivative at  $r = 0$ , and this 'cusp' is a characteristic property of a molecular wavefunction at a nucleus. The corresponding Gaussian  $\exp(-\gamma r^2)$  has zero derivative at  $r = 0$ , and this behaviour can be corrected only by a substantial increase in the number of functions included in the basis. The problem of evaluating a relatively small number of difficult integrals over Slater functions is therefore replaced by that of evaluating a much larger number of simple integrals over Gaussian functions, and by the consequent computational problems of storing and manipulating this large number of integrals.

In this paper, we present some results of an investigation into the possibility of finding an alternative set of simple functions for the construction of molecular wavefunctions which is to satisfy two requirements:

- that the number of basis functions required to produce a given accuracy be comparable to the number of Slater functions required to give the same accuracy;
- that the molecular integrals be considerably easier to evaluate than those over Slater functions.

## The Cusped-Gaussian Basis

It is proposed that a basis of Gaussian functions

$$r^{n+l} e^{-\gamma r^2} Y_{lm}(\theta, \phi) \quad (1)$$

supplemented by a small number of *cusp functions*

$$\begin{cases} r^{n+l}(\rho-r)^l Y_{lm}(\theta, \phi) & \text{if } r < \rho \\ 0 & \text{if } r > \rho \end{cases} \quad (2)$$

Table 1

Atom	N	$\rho/B$	E/H
H	2	5.56	-0.499801
	3	4.84	-0.4999984
	4	4.78	-0.4999997
			Exact -0.5
He	3	2.33	-2.861421
	4	2.12	-2.861674
	5	2.09	-2.861679
		Slater double-zeta	-2.86167
		Hartree-Fock	-2.86168
Be	4	1.39	-14.56348
	5	1.15	-14.57264
	6	1.14	-14.57286
		Slater double-zeta	-14.57237
		10-Gaussian	-14.57258
	Hartree-Fock	-14.57302	

\* Department of Chemistry, University of Exeter, Stocker Road, Exeter, EX4 4QD

where  $\rho$  and  $t$  are parameters, may go some way towards satisfying the requirements of accuracy and relative simplicity of the integrals. The cusp functions, particularly for  $s$ -orbitals, are designed to improve the quality of a Gaussian basis in the region near a nucleus. Integrals involving Gaussians are simple to evaluate only if the number  $n$  in equation (1) is an even integer or zero. In the same way, molecular integrals involving at least two cusp functions centred on different nuclei are tractable only if the cusp functions on different nuclei do not overlap. For most systems, this implies cusp sizes  $\rho$  of the order  $1 B$  or less †. Some results for the ground states of the atoms  $H$ ,  $He$  and  $Be$  are shown in table 1. These have been obtained with a normalised basis of  $(N - 1)$   $1s$  Gaussians supplemented by a single  $1s$  cusp function with value of the parameter  $t = 6$  [1]. The energies demonstrate that the addition of the cusp function leads to a considerable enhancement of the quality of a Gaussian basis, at least for  $s$ -orbitals. For example, the 5-function cusped-Gaussian basis for  $He$  gives an SCF energy which is almost identical to that obtained from four or five Slater functions. Of greatest significance are the results for  $Be$ . A basis of four Gaussians plus the cusp function gives better than double-zeta (two Slater functions per atomic orbital) accuracy, and at the same time satisfies the condition  $\rho \approx 1 B$ . Similar results are obtained for the  $s$ -orbitals of the atoms beyond  $Be$  [2]. At least double-zeta accuracy is obtained with a basis no larger than two  $1s$  Gaussians per  $s$ -orbital plus the  $1s$  cusp function, with optimum cusp size  $\rho \approx 1 B$  when  $t \approx Z + 1$ , where  $Z$  is the atomic number. The accuracy requirement is therefore satisfied for the  $s$ -orbitals of atoms other than  $H$  (and possibly  $Li$ ). The  $1s$  orbital of  $H$  has its maximum radial density at  $1 B$  so that the cusp function cannot make a significant contribution to this orbital if  $\rho$  is restricted to a small value. This is typical of valence orbitals with no corresponding inner shells. Thus, a  $2p$  cusp function does not make a significant contribution to the  $2p$  orbitals of the atoms  $B$  to  $Mg$ . For subsequent atoms, double-zeta accuracy is obtained with a basis no larger than three  $2p$  Gaussians per  $p$ -orbital plus the  $2p$  cusp function.

### The Molecular Integrals

We consider a basis of  $1s$  Gaussians and cusp functions, with not more than one cusp function centred on any one nucleus in a molecule. Such a basis is suitable for the construction of molecular wavefunctions if:

- (a) the molecular orbitals are expressed in terms of 'nuclear-centred' functions, but the  $p$ ,  $d$ , ... Gaussians are represented by suitable

combinations of  $1s$  Gaussians (Gaussian lobe functions [3]); or

- (b) the molecular orbitals are constructed by the floating spherical Gaussian orbital method (FSGO) introduced by Frost [4] and modified by Christoffersen (for example [5]), with the addition of a cusp function on each atom other than hydrogen.

A full discussion of the evaluation of the molecular integrals will be published elsewhere. We restrict ourselves here to a presentation of the formulae for just a few of the integrals containing both cusp and Gaussian functions, and to a brief discussion of the general methods proposed for their evaluation and use. These integrals involve the modified spherical Bessel function of the first kind

$$i_{\ell}(x) = \frac{1}{2} \int_{-1}^{+1} e^{x \cos \theta} P_{\ell}(\cos \theta) d(\cos \theta)$$

which satisfy the recurrence relation

$$i_{\ell-1}(x) - i_{\ell+1}(x) = \frac{(2\ell+1)}{x} i_{\ell}(x)$$

with

$$i_0(x) = [e^x - e^{-x}]/2x$$

$$i_1(x) = [e^x + e^{-x} - i_0(x)]/2x$$

Except for some special simpler cases, all the integrals can be expressed in one of the forms

$$\int_0^1 f(x) (1-x)^m x^n dx \quad (3)$$

$$\int_0^1 \left\{ \int_0^1 f(x,y) (1-x)^m x^n dx \right\} (1-y)^p y^q dy \quad (4)$$

It is proposed that such integrals are most conveniently evaluated numerically using the Gauss-Jacobi quadrature formula [6]

$$\int_0^1 f(x) (1-x)^m x^n dx \approx \sum_{i=1}^N A_i f(x_i) \quad (5)$$

**The overlap integral:** Let  $C_A$  be a normalised  $1s$  cusp function centred on  $A$ , with cusp size  $\rho = 1 B$  for simplicity, and let  $G_B$  be a normalised  $1s$  Gaussian on centre  $B$ :

† Distances and energies are expressed in terms of the 'atomic units'  $B$  and  $H$  respectively, where  $B = \epsilon_0 h^2 / \pi m e^2$  is the Bohr radius and  $H = m e^4 / 4 h^2 \epsilon_0^2$  is the Hartree energy.

$$C_A = \frac{N_A}{(4\pi)^{1/2}} (1 - r_A)^t \quad \text{if } r_A < 1 \left. \vphantom{\frac{N_A}{(4\pi)^{1/2}}} \right\}$$

$$= 0 \quad \text{if } r_A > 1 \left. \vphantom{\frac{N_A}{(4\pi)^{1/2}}} \right\}$$

$$G_B = \frac{N_B}{(4\pi)^{1/2}} e^{-br_B^2}$$

where

$$N_A = [(2t+1)(t+1)(2t+3)]^{1/2}$$

$$N_B = [8b(2b/\pi)^{1/2}]^{1/2}$$

are normalisation factors. Then

$$\langle C_A | G_B \rangle = N_A N_B e^{-bR_{AB}^2} \int_0^1 e^{-br^2} i_0(2bR_{AB}r) (1-r)^t r^2 dr \quad (6)$$

This integral can be evaluated using the Gauss-Jacobi formula (5) with  $m = t$  and  $n = 2$ . The number of integration points  $N$  required for a given accuracy is strongly dependent on the values of the parameters  $t$ ,  $b$ , and  $R_{AB}$ , and on the required accuracy. In figure 1 are shown the number of points required for an accuracy to at least 12 decimal places for  $t = 10$  and  $t = 30$  and a range of values of  $b$  and  $R_{AB}$ . Integrals whose values are less than  $10^{-12}$  have been set equal to zero ( $N = 0$ ).

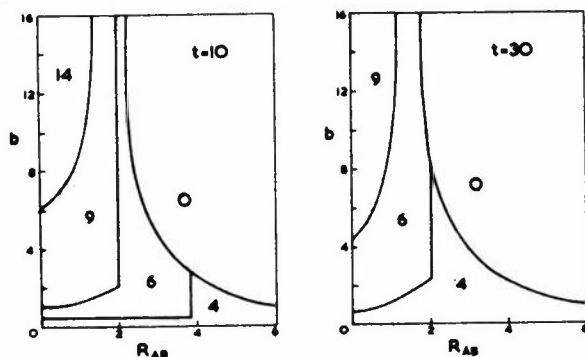


Figure 1

Two types of Gaussian functions may be distinguished:

- (a) Valence-shell (and bond) functions, for which  $b \lesssim 1$ . The corresponding overlap integrals very seldom require more than six integration points. The computational labour per point is approximately the same as that for two (double-precision) exponentials.

- (b) Inner-shell functions, for which  $b \gtrsim 1$ . Such a function is centred on a nucleus (or very close to a nucleus in the case of a lobe function), and the distance  $R_{AB}$  between cusp and Gaussian is therefore either zero or equal to an inter-nuclear separation ( $\gtrsim 2B$ ). Only for the one-centre integrals does the number of points become large.

These observations are generally valid for all the integrals which involve both cusp and Gaussian functions. In particular, and in direct contrast to the Slater-function case, the atomic integrals may often be considerably more difficult to evaluate (difficulty being measured by the amount of computational labour) than the molecular integrals. This need not however be a serious obstacle to the use of the cusped-Gaussian basis. In the first place, the number of difficult atomic integrals is expected to be relatively small. In the second place, their evaluation in a molecular calculation may be avoided altogether if, as is the most widely-used approach, fixed basis sets of atomic orbitals are used to construct molecular orbitals. The corresponding atomic integrals need be evaluated only one for each atom, and stored for future use.

The most difficult integrals for a Slater-function basis are the two-electron integrals

$$(\phi_1 \phi_2 | \phi_3 \phi_4) = \iint \frac{\phi_1^*(1) \phi_2(1) \phi_3^*(2) \phi_4}{r_{12}} dv_1 dv_2$$

when the atomic orbitals are centred on three or four non-colinear nuclei. All but two of the various different types of two-electron integrals for the cusped-Gaussian basis can be reduced to the simple form (3).

The three-centre integral  $(C_A C_A | G_B G_C)$ : We have

$$(C_A C_A | G_B G_C) = \langle G_B | G_C \rangle (C_A C_A | G_D G_D) \quad (7)$$

where  $G_D$  is a normalised 1s Gaussian with exponent  $d = (b+c)/2$  and position  $R_D = (bR_B + cR_C)/(b+c)$ , and

$$(C_A C_A | G_D G_D) = \frac{1}{R_{AD}} \operatorname{erf}((2d)^{1/2} R_{AD}) - N_D^2 e^{-2dR_{AD}^2} \int_0^1 e^{-2dr^2} i_0(4dR_{AD}r) [1 + (t+1/2)r] \times (1-r)^{2t+2} r dr \quad (8)$$

where

$$\operatorname{erf}(x) = (4/\pi)^{1/2} \int_0^x e^{-t^2} dt$$

The integral can be evaluated using the Gauss-Jacobi formula (5) with  $m = 2t + 2$  and  $n = 1$ . Of significance here is that the factor  $\langle G_B | G_C \rangle$  in (7) means that a given accuracy of the three-centre integral can often be obtained with a lower accuracy of the corresponding two-centre integral (8). In figure 2 are shown the number of points, for  $t = 10$  and a range of values of  $d$  and  $R_{AD}$ , required for accuracies to 12 and 8 decimal places of the two-centre integral (8). It is seen that the computational labour is significantly reduced on going from double- to single-precision accuracy. The molecular integrals seldom require more than four integration points for single-precision accuracy.

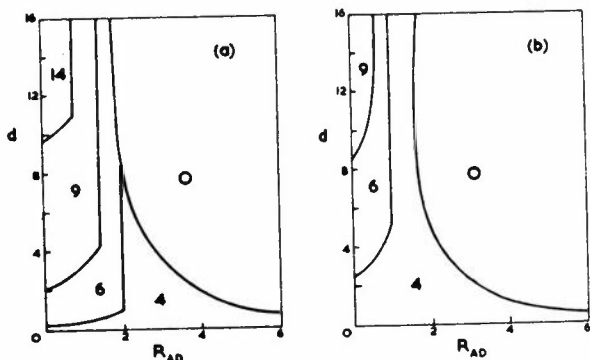


Figure 2: (a) error  $10^{-12}$  (b) error  $10^{-8}$

The three- and four-centre integrals  $\langle C_A | 1/r_B | G_C \rangle$ ,  $\langle C_A G_C | C_B C_B \rangle$ ,  $\langle C_A G_C | C_B G_D \rangle$ : The three-centre nuclear attraction integral is:

$$\langle C_A | \frac{1}{r_B} | G_C \rangle = \frac{N_A N_C}{R_{AB}} e^{-cR_{AC}^2} \int_0^1 e^{-\alpha^2} \times \left\{ \sum_{\ell=0}^{\infty} \left( \frac{r}{R_{AB}} \right)^\ell P_\ell(\cos\theta) i_\ell(2cR_{AC}r) \right\} (1-r)^t r^2 dr \quad (9)$$

where  $\theta = \widehat{CAB}$ , and  $R_{AB}$  is greater than the cusp size. This may be evaluated in the same way as (and simultaneously with) the overlap integral  $\langle C_A | G_C \rangle$ . When  $R_{AC} = 0$ ,  $\langle C_A | 1/r_B | G_C \rangle = \langle C_A | G_C \rangle / R_{AB}$ . For  $R_{AB} \gtrsim 2$  or  $c \lesssim 1$ , the maximum value of  $\ell$  required for an accuracy to twelve decimal places is seldom greater than 10, and the sum creates no difficulties.

The integrals  $\langle C_A G_C | C_B C_B \rangle$  and  $\langle C_A G_C | C_B G_D \rangle$  are the only non-zero integrals which involve cusp functions on different nuclei. We have

$$\langle C_A G_C | C_B C_B \rangle = \langle C_A | \frac{1}{r_B} | G_C \rangle \quad (10)$$

and

$$\begin{aligned} \langle C_A G_C | C_B G_D \rangle &= \langle C_A | G_C \rangle \langle C_B | \frac{1}{r_A} | G_D \rangle \\ &+ \langle C_A | \frac{1}{r_B} | G_C \rangle \langle C_B | G_D \rangle \\ &- \langle C_A | G_C \rangle \langle C_B | G_D \rangle / R_{AB} \\ &+ \sum_{\ell_1=1}^{\infty} \sum_{\ell_2=1}^{\infty} X_{\ell_1, \ell_2} I_{\ell_1}^{AC} I_{\ell_2}^{BD} \quad (11) \end{aligned}$$

where, in terms of the angles shown in figure 3,

$$\begin{aligned} X_{\ell_1, \ell_2} &= \sum_{m=\ell}^{\ell} \frac{(\ell_1 + \ell_2)!}{(\ell_1 + |m|)! (\ell_2 + |m|)!} \\ &\times P_{\ell_1}^m(\cos\theta_A) P_{\ell_2}^m(\cos\theta_B) e^{im(\phi_A - \phi_B)} / R_{AB}^{\ell_1 + \ell_2 + 1} \end{aligned}$$

and, for example

$$I_{\ell}^{AC} = N_A N_C e^{-cR_{AC}^2} \int_0^1 e^{-cr^2} i_\ell(2cR_{AC}r) (1-r)^t r^2 dr$$

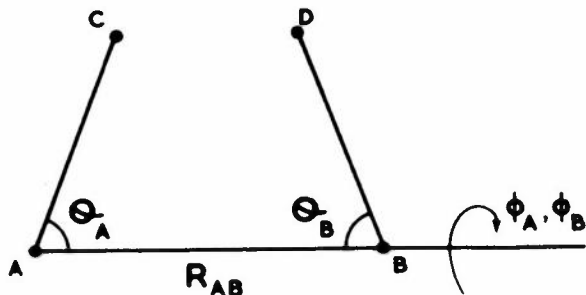


Figure 3

The quantities  $I_{\ell}^{AC}$  can be obtained as a by-product in the evaluation of the nuclear attraction integral (9):

$$\langle C_A | \frac{1}{r_B} | G_C \rangle = \sum_{\ell=0}^{\infty} P_{\ell}(\cos\theta_A) I_{\ell}^{AC} / R_{AB}^{\ell+1}$$

If  $R_{AC} = 0$ ,

$$\langle C_A G_C | C_B G_D \rangle = \langle C_A | G_C \rangle \langle C_B | \frac{1}{r_A} | G_D \rangle$$

The four-centre integral  $\langle C_A G_B | G_D G_E \rangle$ : This is one of the two types (the other is  $\langle C_A G_B | C_A G_C \rangle$ ) which may

require a double numerical integration. We have

$$(C_A G_B | G_D G_E) = \langle G_D | G_E \rangle (C_A G_B | G_C G_C) \quad (12)$$

where  $c = (d + e)/2$ ,  $R_C = (d R_D + e R_E)/(d + e)$ , and

$$(C_A G_B | G_C G_C) = N_A N_B \left( \frac{2c}{\pi} \right)^{1/2} e^{-b R_{AB}^2} \times \int_{x=0}^1 e^{-2cx^2 R_{AC}^2} \left\{ \int_{r=0}^1 e^{-(b+2cx^2)r^2} i_0(2Rr)(1-r)^t r^2 dr \right\} dx \quad (13)$$

$$= \langle C_A | \frac{1}{r_C} | G_B \rangle - N_A N_B \left( \frac{2c}{\pi} \right)^{1/2} e^{-b R_{AB}^2} \times \int_{x=1}^{\infty} e^{-2cx^2 R_{AC}^2} \left\{ \int_{r=0}^1 e^{-(b+2cx^2)r^2} i_0(2Rr)(1-r)^t r^2 dr \right\} dx \quad (14)$$

where

$$R = [b^2 R_{AB}^2 + 4c^2 x^4 R_{AC}^2 + 4bcx^2 R_{AB} \cdot R_{AC}]^{1/2}$$

When  $R_{AC} = 0$ ,

$$(C_A G_B | G_C G_C) = N_A N_B e^{-b R_{AB}^2} \times \int_0^1 e^{-br^2} i_0(2b R_{AB} r) \operatorname{erf}((2c)^{1/2} r) (1-r)^t r dr \quad (15)$$

The form (13) is appropriate when  $c R_{AC}^2$  is small, the form (14) when  $c R_{AC}^2$  is large (and  $R_{AC}$  greater than the cusp size).

### First Row Atom Hydrides

A model, which may be called the cusped-FSGO model, has been used for a molecular-orbital description of the ground states of the first row atom hydrides *LiH*, *BeH<sub>2</sub>*, *BH<sub>3</sub>*, *CH<sub>4</sub>*, *NH<sub>3</sub>*, *H<sub>2</sub>O* and *HF*. The model is identical to the FSGO model proposed by Frost [4,7] being made up of 1s Gaussians whose centres are determined variationally, plus a 1s cusp function on the heavy atom. The simplest description of *LiH* then consists of the cusp function on *Li* and a Gaussian centred on the bond axis. The simplest description of *CH<sub>4</sub>* consists of the cusp function on *C* and four equivalent Gaussians on the bond axes. Additional Gaussians are added to improve the description.

The variation of the total energy of *LiH* with increasing number of basis functions is compared in

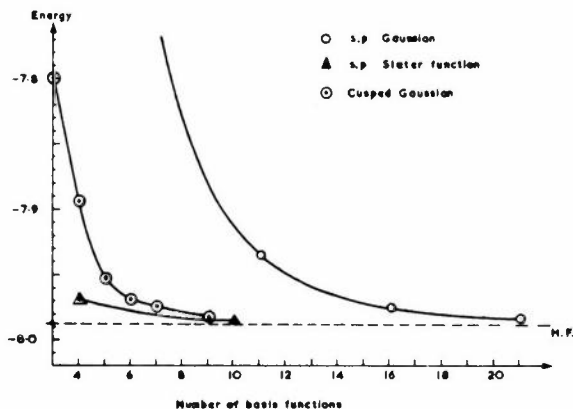


Figure 4

figure 4 with an (*s,p*) basis of Gaussians [8] and an (*s,p*) basis of Slater functions [9,10]. The basis sets of two to nine functions, and the corresponding energies, internuclear distances, and values of the cusp parameter  $t$  are shown in table 2. The basis sets are made up of

- the minimal basis of the cusp function on *Li* (cusp size fixed at 1 *B*) and a Gaussian which is allowed to float on the bond axis;
- additional Gaussians fixed on *Li* and *H*; and
- for the bases of seven and nine functions, a 'polarisation' Gaussian on *Li* which is allowed to float off the nucleus.

Table 2:  $C$  denotes the cusp function,  $G$  a nuclear-centred Gaussian,  $G'$  a floating Gaussian

Number of Functions	<i>Li</i>	Bond	<i>H</i>	$E/H$	$R/B$	$t$
2	$C$	$G'$		-5.2577	2.952	2
3	$C+G$	$G'$		-7.8016	3.162	3
4	$C+G$	$G'$	$G$	-7.8932	3.172	3
5	$C+G$	$G'$	$2G$	-7.9011	3.160	4
5	$C+2G$	$G'$	$G$	-7.9528	3.152	4
6	$C+2G$	$G'$	$2G$	-7.9690	3.164	4
7	$C+2G+G'$	$G'$	$2G$	-7.9742	3.095	5
9	$C+3G+G'$	$G'$	$3G$	-7.9830	3.024	5
Hartree-Fock [11]				-7.9873	3.034	

It is clear from figure 4 that the cusped-Gaussian basis quickly becomes almost as efficient as the Slater-function basis. The *Li* inner-shell is accurately described by the cusp and two Gaussians of the 6-function basis, the error being due wholly to the very poor description of the bonding orbital. The 9-function basis is very much more accurate, and the addition of up to three more Gaussians is expected to give results close to the Cade and Huo [11] values.



**Timing:** The time (on the ICL 4-50 at Exeter) required to evaluate the integrals for the cusped-Gaussian basis is compared in figure 5 with that required to give the same energy with an all-Gaussian basis. The all-Gaussian curve has been estimated

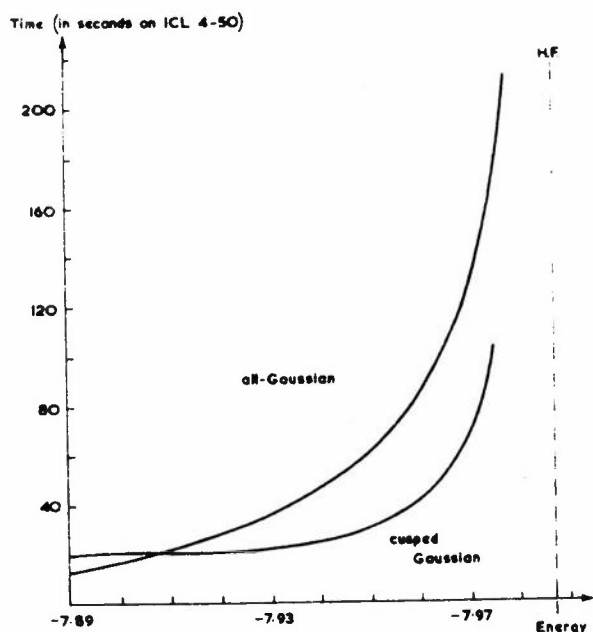


Figure 5

from the average time per two-electron integral (0.018 seconds on the ICL 4-50), with each integral evaluated separately as in the cusped-Gaussian case. Figure 5 suggests that the cusped-Gaussian basis may be superior to the all-Gaussian basis with respect not only to the size of basis required to produce a given accuracy of the energy and wavefunction of a molecular system, but also to the computational time required.

For the series of hydrides *LiH* to *HF*, the simplest basis, made up of the cusp function plus one Gaussian for each pair of electrons in the valence shell, gives energies which vary from 66% of the Hartree-Fock value for *LiH* to 98% for *HF*, with a more or less constant error of about 2.2 *H* (except for *LiH*).

## References

- [1] STEINER, E. and SYKES, S. (1972). *Mol. Phys.*, **23**, 643.
- [2] STEINER, E. (1972). *Mol. Phys.*, **23**, 657, 669.
- [3] WHITTEN, J.L. (1966). *J. Chem. Phys.*, **44**, 359.
- [4] FROST, A.A. (1968). *J. Phys. Chem.*, **72**, 1289.
- [5] CHRISTOFFERSEN, R.E. and MAGGIORA, G.M. (1969). *Chem. Phys. Letters*, **3**, 419.
- [6] STROUD, A.H. and SECREST, D. (1966). *Gaussian Quadrature Formulas*, Eaglewood Cliffs, New Jersey: Prentice-Hall.
- [7] FROST, A.A. (1967). *J. Chem. Phys.*, **47**, 3707.
- [8] CSIZMADIA, I.G. (1966). *J. Chem. Phys.*, **44**, 1849.
- [9] KAHALAS, S.L. and NESBET, R.K. (1963). *J. Chem. Phys.*, **39**, 529.
- [10] RANSIL, B.J. (1960). *Revs. Modern Phys.*, **32**, 250.
- [11] CADE, P.E. and HUO, W.M. (1967). *J. Chem. Phys.*, **47**, 614.

# The Simulated *Ab Initio* Molecular Orbital (SAMO) Method

B.J.Duke\* and B.O'Leary†

The simulated *ab initio* molecular orbital (SAMO) method will be reviewed and recent developments reported. This method relies on the transferability of matrix elements over the Fock operator from *ab initio* calculations on small molecules to the matrix for a larger molecule.

Particular attention will be given to the use of different basis sets and the application to organic molecules containing *OH*, *NH<sub>2</sub>* and *CHO* groups. The relationship with other approaches will be briefly mentioned.

## Introduction

The molecular orbital method, with its use of delocalised orbitals, loses the chemists intuitive insight that organic molecules in particular are, to a first approximation, the sum of their constituent functional groups. This insight must be hidden within the molecular orbital approach. It can be uncovered by a transformation to localised orbitals which describe the various bonds, lone pairs and core orbitals. Many workers [1-7] have suggested or shown that such localised orbitals are approximately transferable between molecules. It should however be possible to use the chemists insight to approximate molecular wavefunctions for large molecules by utilising information from more accurate calculations on smaller molecules. Von Niessen [8] with the 'molecules in molecules' method has developed one such approach, localised orbitals are transferred from smaller molecules and only a few orbitals are recalculated. By the use of some approximations his wavefunction can be partially optimised and the total electronic energy evaluated without the need to evaluate all the electron repulsion integrals over the basis set. The resulting saving in effort, although significant, is not as substantial as one would hope.

Other workers have concentrated on transferring features of small molecule wavefunctions other than localised orbitals. Particular attention has been given to the matrix elements over the Fock operator. Fitts and Orloff [9] used transferability of matrix elements in  $\pi$  electron theory, an approach that was extended to all valence calculations by Lipscomb and coworkers [10] in the non-empirical molecular orbital (NEMO) scheme. In the NEMO method diagonal Fock matrix elements are transferred from *ab initio*

calculations on small molecules and off-diagonal elements are obtained partially by a semi-empirical scheme. In a combined approach Dugand, Leroy and Peeters [7] utilise transferability of both localised orbitals and Fock matrix elements. They expand their molecular orbitals as a linear combination of localised orbitals and then transfer both diagonal and off diagonal Fock matrix elements over the localised orbital basis.

The simulated *ab initio* molecular orbital (SAMO) technique, which was originated by Eilers and Whitman [11] and extended in collaboration with the present authors, is similar in that it utilises transferability of both diagonal and off-diagonal Fock matrix elements. The basis set employed is one of hybrid orbitals plus 1s orbitals on hydrogen and first row atoms. The method has been successfully applied to chain hydrocarbons [11], aromatic rings [12], simple polymers [13], certain organic radicals using a spin unrestricted open shell formalism [14], cyclohexane [15], one large system of biological interest [16] and molecules containing a polar functional group [17]. A suite of four computer programs for closed shell calculations, open shell calculations, polymer calculations and the automatic transfer of matrix elements from libraries of *ab initio* results will shortly be available from the Quantum Chemistry Program Exchange [18]. The SAMO method has a wider applicability than the work of Dugand, Leroy and Peeters [7] since it can be used in cases such as benzene where it would not be possible to transfer localised orbitals from smaller molecules.

\* Department of Chemistry, University of Lancaster, Bailrigg, Lancaster, LA1 4YA

† Theoretical Chemistry Department, University of Oxford, 1 South Parks Road, Oxford, OX1 3TG  
(present address) Department of Chemistry, University of Alabama in Birmingham, Alabama 35294, USA

## The SAMO Method

As an example of the SAMO method we briefly discuss the as yet unpublished results for molecules containing a polar group [17]. This example is of particular importance since, as previous work has been restricted to hydrocarbon molecules, the method has been open to the criticism that it would be inapplicable to polar molecules. We shall conclude by discussing some unpublished work dealing with variation of the basis set. We first summarise the method for closed shell molecules.

The SAMO method for closed-shell molecules generates the molecular orbitals and orbital energies for large molecules by a single solution of the eigenvalue problem

$$FC = SC\lambda$$

where  $S$  is the matrix of overlap integrals (all of which are evaluated explicitly),  $\lambda$  is the diagonal matrix of eigenvalues or orbital energies,  $C$  is the matrix whose columns are the eigenvectors (LCAO expansion coefficients) and  $F$  is the matrix over the Hartree-Fock operator. The SAMO method obtains the elements of  $F$  by transferring values, truncated to four decimal places, from *ab initio* calculations on similar small molecules known as 'pattern' molecules. In those cases where interactions between distant orbitals are unavailable from the 'pattern' molecules, the Fock matrix elements are usually small and can consequently be set to zero when constructing the Fock matrix for the large molecules. The total energy is given by

$$E_T = \sum_{\text{OCC}} (\epsilon_i^{(0)} + \lambda_i) + V_{\text{NN}}$$

where the  $\epsilon_i^{(0)}$  are the expectation values of the one-electron operator, the  $\lambda_i$  are the eigenvalues of the Hartree-Fock operator,  $V_{\text{NN}}$  is the nuclear repulsion energy and the summation is over occupied molecular orbitals.

### Polar Molecules

In order to test the applicability of the SAMO technique to polar molecules a detailed study of molecules of type  $R-X$  has been carried out. We report here results obtained in the simplest SAMO approach where  $X = OH, NH_2$  and  $CHO$  and  $R$  is the butyl hydrocarbon group. Our ultimate aim is to produce wavefunctions of near *ab initio* accuracy for molecules where the group  $R$  is very large and consequently an *ab initio* calculation on  $R-X$  would be prohibitively expensive. We expect

- (a) to be able to use 'pattern' molecules of the form  $R'-X'$ , where although  $R'$  is small it is

nevertheless large enough to include all relevant Fock matrix elements involving orbitals on or close to the functional group;

- (b) to obtain other Fock matrix elements involving orbitals located on the hydrocarbon chain from a pattern molecule  $R''$ : (Again, although  $R''$  is much smaller than  $R$ , it is chosen to be of sufficient size to include all relevant Fock matrix elements involving orbitals on that part of the hydrocarbon chain.)
- (c) to be able to neglect Fock matrix elements involving orbitals on a functional group and orbitals further out along the chain and thus not included in  $R'-X$ .

Our selection of molecules for this test was motivated by the following:

- (a) all molecules studied should be of such size as to lend themselves to economical *ab initio* calculations;
- (b) all pattern molecules chosen should be of optimum size for simulation, i.e. they should contain all those Fock matrix elements necessary to the adequate simulation of the target molecule (molecule of interest -  $R-X$ ).

Requirements (a) and (b) result in the target and pattern molecules used in this study being of comparable size. In no way does this limit our investigation; there are matrix elements present in the target molecule, and absent in the pattern molecules, which can be neglected. Increasing the size of the target molecule would simply add an increased number of even smaller Fock elements, whose magnitude is smaller than those neglected in this study.

As in previous work the geometries are idealised and all *ab initio* calculations are performed using the ATMOL2 system [19] and a  $5s3p$  Whitman-Hornback basis set [20]. This basis is, prior to the SCF stage, transformed to a basis of  $1s, sp^2$  and  $sp^3$  hybrids on carbon, oxygen and nitrogen.

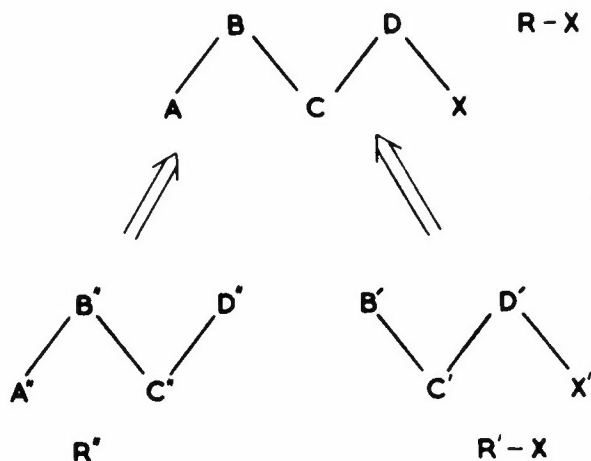


Figure 1: A, B, C, D and X represent the set of basis orbitals centred on  $CH_3, CH_2$  and the appropriate functional group centre respectively

In figure 1 we illustrate the simulation of the target molecule  $R-X$  from the pattern molecules  $R'-X$  and  $R''$ .

In the present study transferability has been investigated as follows:

- (a) The Fock matrix elements over the following centres of the target molecule –

$XX, XD, XC, XB, DD, DC, DB, CC, CB$   
are obtained from

$X'X', X'D', X'C', X'B', D'D', D'C', D'B', C'C', C'B'$   
respectively, in  $R'-X$ . The nomenclature  $AB$  implies set  $\{F_{ij} : i \in A, j \in B\}$  where  $A$  and  $B$  are the sets of orbitals on groups  $A$  and  $B$  respectively (figure 1)

- (b) The Fock matrix elements over the centres  $AA, AB, AC, AD, BB$

are obtained from

$A''A'', A''B'', A''C'', A''D'', B''B''$   
respectively, in  $R''$

- (c) Fock matrix elements over the terminal centres  $AX$  are set to zero. The one exception to this occurs for elements involving the functional group and the  $sp^3$  hybrid orbital situated on the terminal methyl group  $A$  and directed towards the methylene group  $B$ . These Fock matrix elements are set equal to those arising for elements over the terminal  $X$  group and the hydrogen orbital lying in the plane of  $R'-X$  and attached to the terminal  $B'$  group. This approach has been successfully employed in other work [14].

Table 1

	AO Basis	OAO Basis
Butanol	0.0011	0.0014
Butyl amine	0.0010	0.0013
Pentanol	0.0010	0.0013

In the first column of table 1, we present the results of our transferability study by giving the root mean square of the errors in the simulated Fock matrix elements when compared with the corresponding elements obtained from *ab initio* calculations. In the second column of table 2, we give, in addition to total energies and dipole moments, the errors for occupied orbital energies and gross orbital populations for butanol, butyl amine and pentanol. From the results presented in table 2, one can conclude that total energies, orbital energies and orbital populations are reproduced by the SAMO method in as satisfactory

Table 2: Summary of results for polar molecules

		<i>Ab Initio</i>	SAMO-AO	SAMO-OAO
Butanol	$E$	-231.107	-231.117	-231.113
	$\mu$	1.726	1.773	1.798
root mean square error - occupied orbital energies		–	0.0016	0.0021
root mean square error - orbital populations		–	0.0032	0.0025
Butyl amine	$E$	-211.336	-211.351	-211.348
	$\mu$	1.555	1.599	1.515
root mean square error - occupied orbital energies		–	0.0017	0.0022
root mean square error - orbital populations		–	0.0026	0.0021
Pentanol	$E$	-268.799	-268.805	-268.800
	$\mu$	2.225	2.287	2.293
root mean square error - occupied orbital energies		–	0.0018	0.0024
root mean square error - orbital populations		–	0.0035	0.0025

and accurate a manner as those obtained for the previously studied hydrocarbons. Dipole moment results using the SAMO technique are presented here for the first time. The simulated results are in satisfactory agreement with the *ab initio* results.

A slight improvement in the results can be obtained if some of the elements in the set  $CB$  are transferred from butane rather than the pattern molecule  $R'-X$ . Full details of this method (which we designate SAMO( $\beta$ )), along with

(a) results for butanoic acid

(b) results where  $X$  in  $R-X$  is an ionic group will be reported elsewhere [17]. For (b) the simple SAMO technique is inapplicable and a new, slightly less accurate, extension of the method has been developed. For comparison we present in table 3 a summary in the total energy and the occupied orbital energies for the best SAMO result for all molecules where *ab initio* results, using the same basis set, are available. Not only do these figures demonstrate that SAMO calculations on molecules containing polar functional groups are at least as accurate as the calculations reported in our previous studies, they clearly show that, with respect to orbital energies, the present work is significantly better. These results allow us to confidently predict that, provided suitable pattern molecules are chosen, the SAMO technique can successfully be applied to other molecules of general form  $R-X$ .

The perhaps surprising conclusion is that the SAMO method has a wider applicability than could have been predicted. The SAMO technique has many applications for organic molecules giving results close to *ab initio* accuracy at considerably less cost.

Table 3: Comparison of errors in total energy and orbital energies

	Total Energy $ \Delta E/E  \times 10^4$	Occupied Orbital Energy root mean square $\times 10^3$
Butane [11]	0.80	3.1
Benzene <sup>a</sup>	8.20	16.8
Cyclohexane [15]		
- chair - method III (PA) <sup>b</sup>	0.91	3.4
- boat - "	1.29	3.7
Butyl radical [14] - method (ii)	0.45	2.7( $\lambda^a$ ) 2.8( $\lambda^b$ )
Pentyl radical - method a(i)	0.67	5.4( $\lambda^a$ ) 5.7( $\lambda^b$ )
Butanol - method ( $\beta$ )	0.26	1.6
Butyl amine - method ( $\beta$ )	0.55	1.6
Pentanal - method ( $\beta$ )	0.03	1.8
Butanoic acid - method ( $\beta$ )	1.78	4.5
Butyl cation - method ( $\beta$ )	2.64	5.8
Butyl anion - method ( $\beta$ )	4.45	12.8

(a) Benzene comparison is with unpublished *ab initio* result using the same basis set as the SAMO results [12].

(b) Method labels are as in original references.

### Variation of the Basis Set

All the SAMO calculations reported so far use the same Whitman-Hornback [20] basis set of contracted Gaussian-type orbitals. This raises the question whether Fock matrix elements are transferable between two calculations if different basis sets are used. This has been tested using calculations on butane and propane with a Slater-type orbital (STO) basis. The following orbital exponents were used:

C1s 5.6727 C2s 1.6083 C2p 1.5679 H1s 1.2

These STO's were, firstly, transformed into an orthogonal basis on each atom by Schmidt orthogonalising the C2s orbital to the C1s orbital, and, secondly, transformed into a basis of C1s, Csp<sup>3</sup> hybrids and H1s orbitals. The errors in simulating the Fock matrix elements for butane using propane as pattern molecule are shown in table 4.

Table 4: Transferability root mean square errors for Fock matrix elements

Butane - Whitman-Hornback GTO basis	0.0010
Butane - STO basis	0.0012

The slightly higher value for the root mean square error using the STO basis is due to the fact that the STOs used are more diffuse than the Whitman-Hornback contracted GTOs. The terminal CH<sub>3</sub> to terminal CH<sub>3</sub> matrix elements in butane, which can not be obtained from propane, are accordingly larger. The matrix elements in the STO basis are, however,

quite different from the equivalent elements in the GTO basis. Different basis sets have different overlap matrices and hence different Fock matrices. We must therefore conclude that the same basis set must be used both for all pattern molecules and for the final SAMO calculation. Earlier Eilers [21] had suggested that this conclusion might not be necessary.

With this point in mind and with the need to find a basis set where long range Fock matrix elements are small, we have commenced a study of Löwdin [22] symmetric orthogonalised orbitals [23]. The Fock matrix in such a basis might be expected to have smaller off-diagonal matrix elements than the similar matrix in the non-orthogonalised basis. The Löwdin orthogonalised orbitals X' (OAO basis) are formed from the non-orthogonalised orbitals X (AO basis) by

$$X' = X T$$

where

$$T = S^{-1/2}$$

and S is the overlap matrix

$$S_{ij} = \langle \chi_i | \chi_j \rangle$$

The Fock matrix F' in the new basis is related to the one in the old basis F by

$$F' = T^\dagger F T$$

Using the same atomic basis as was used for the polar molecules discussed above, we have studied the transferability of elements of F' for these molecules. The errors of transferability have already been shown in table 1, compared with those using the AO basis. Transferability of the elements of F' has been independently observed by Leroy and co-workers [24].

The OAO basis is slightly less transferable than the AO basis. The reason is that although many off-diagonal elements are smaller in the OAO basis than in the AO basis, the long range elements which have no counterpart in the pattern molecules are surprisingly larger. This appears to be due to the fact that the terms in F'\_{ij}, for these orbitals, arising from the negative outer part of the OAOs (and hence incorporating terms F\_{pq} where  $\chi_p$  and  $\chi_q$  are AOs between AOs  $\chi_i$  and  $\chi_j$ ) are more important than the long-range terms F\_{ij} in F'\_{ij} even though  $\chi_i$  and  $\chi_j$  are the dominant terms in the expansions of  $\chi_i$  and  $\chi_j$  respectively. We have thus to neglect terms which are larger in the OAO basis than in the AO basis.

A SAMO technique in the OAO basis can be developed as follows -

- (a) Transfer elements of F' for the target molecule from elements of F' for the pattern molecules in a manner exactly analogous to the SAMO method in the AO basis.

(b) Solve

$$F' C' = C' \lambda$$

to give orbital energies and eigenvectors in the OAO basis.

(c) For convenience transform the eigenvectors to the AO basis by

$$C = T C'$$

(d) Use  $C$  to give population density terms, dipole moments and energies as in the SAMO technique using AOs.

Such calculations have been carried out for butanol, butyl amine and pentanal. Results are summarised earlier in table 2, along with the results obtained by using the AO basis directly.

Although the increase in the error of transferability leads to an increase in the error in the occupied orbital energies, the OAO basis set gives a better density matrix. This results in a better total energy and better orbital populations. The errors in the orbital populations using the OAO basis set are more evenly spread than those arising from the use of an AO basis. In an AO basis there are particularly large errors in the orbitals corresponding to the terminal C-C bond in the pattern molecule  $R'-X$  and very small errors elsewhere. In general, however, the use of the OAO basis set is disappointing. We are currently investigating whether the elements of  $F'$  are less sensitive to the original choice of AO basis (e.g. STO's or contracted GTO's) than elements of  $F$ .

We acknowledge the collaboration with J. E. Eilers and M. Pickering on the polar molecules work, and the Science Research Council for the provision of computer time at the Atlas Computer Laboratory and a Fellowship to one of us (B.O'L.). The assistance of the staff of the Atlas Computer Laboratory and the Lancaster and Oxford University Computing Services is also gratefully acknowledged.

## References

- [1] BOYS, S.F. (1960). *Revs. Modern Phys.*, **32**, 296.
- [2] EDMISTON, C. and RUEDENBURG, K. (1963). *Revs. Modern Phys.*, **35**, 457.  
——— and ——— (1965). *J. Chem. Phys.*, **43S**, 97.  
RUEDENBURG, K. (1973). *Computational Methods for Large Molecules and Localised States in Solids* (ed. F. Hermann, A.D. McLean and R.K. Nesbet), 149, New York: Plenum Press.  
ROTHENBERG, S. (1969). *J. Chem. Phys.*, **51**, 3389.
- [3] PETERS, D. (1963). *J. Chem. Soc.*, 2003, 2015, 4017.  
——— (1964). *Ibid.*, 2901, 2908, 2916.  
——— (1966). *Ibid.*, 644, 652, 656.
- [4] ADAMS, W.H. (1965). *J. Chem. Phys.*, **42**, 4030.  
——— (1961). *Ibid.*, **34**, 89.  
——— (1962). *Ibid.*, **37**, 2009.
- [5] GILBERT, T.L. (1964). *Molecular Orbitals in Chemistry, Physics and Biology* (ed. P-O Löwdin and B. Pullman), 405, New York: Academic Press.
- [6] MAGNASCO, V. and PERICO, A. (1967). *J. Chem. Phys.*, **47**, 971.  
——— and ——— (1968). *Ibid.*, **48**, 800.
- [7] DEGAND, P., LEROY, G. and PEETERS, D. (1973). *Theoret. Chim. Acta*, **30**, 243;
- [8] VON NIESSEN, W. (1971). *J. Chem. Phys.*, **55**, 1948.  
——— (1973). *Theoret. Chim. Acta*, **31**, 111, 297.  
——— (1973). *Ibid.*, **32**, 13.
- [9] ORLOFF, M.K. and FITTS, D.D. (1963). *J. Am. Chem. Soc.*, **85**, 3721.
- [10] NEWTON, M.D., BOER, F.P. and LIPSCOMBE, W.N. (1966). *J. Am. Chem. Soc.*, **88**, 2353, 2361, 2367.
- [11] EILERS, J. E. and WHITMAN, D. R. (1973). *J. Am. Chem. Soc.*, **95**, 2067.
- [12] EILERS, J.E., O'LEARY, B., LIBERLES, A. and WHITMAN, D.R. *J. Am. Chem. Soc.*, (in the press).
- [13] DUKE, B.J. and O'LEARY, B. (1973). *Chem. Phys. Letters*, **20**, 459.
- [14] DUKE, B.J., EILERS, J.E. and O'LEARY, B. (1974). *J. Chem. Soc. (Faraday II)*, **70**, 386.
- [15] EILERS, J. E., O'LEARY, B., DUKE, B. J., LIBERLES, A. and WHITMAN, D.R. *J. Am. Chem. Soc.*, (in the press).
- [16] O'LEARY, B., DUKE, B.J., EILERS, J.E. and ABRAHAMSON, E.W. (1973). *Nature*, **246**, 166.
- [17] DUKE, B.J., PICKERING, M., O'LEARY, B. and EILERS, J.E., (to be published).
- [18] O'LEARY, B., DUKE, B.J. and EILERS, J.E. *Program SAMOS*, Program 263, Quantum Chemistry Program Exchange (QCPE), Chemistry Department, University of Indiana.
- [19] SAUNDERS, V.R. (1973). *ATMOL2 Program*, Atlas Computer Laboratory, Chilton, Oxfordshire, England.
- [20] WHITMAN, D.R. and HORNBACK, C.J. (1969). *J. Chem. Phys.*, **51**, 398.
- [21] EILERS, J.E. (1971). *Ph.D. Thesis*, Case Western Reserve University.
- [22] LÖWDIN, P-O. (1950). *J. Chem. Phys.*, **18**, 365.
- [23] This approach was suggested by R. McWeeny following a research colloquium given by one of us (B.J.D.) in the University of Sheffield.
- [24] LEROY, G., (private communication).  
DEPLUS, A., LEROY, G. and PEETERS, D. (1974). *Theoret. Chim. Acta.*, **36**, 109.

# Approximate *Ab Initio* Calculations and the Method of Molecular Fragments

D.F.Brailsford\*

A two stage approach to performing *ab initio* calculations on medium and large sized molecules is described. The first step is to perform SCF calculations on small molecules or molecular fragments using the OPIT program. This employs a small basis set of spherical and *p*-type Gaussian functions. The Gaussian functions can be identified very closely with atomic cores, bond pairs, lone pairs, etc. The position and exponent of any of the Gaussian functions can be varied by OPIT to produce a small but fully optimised basis set.

The second stage is the molecular fragments method. As an example of this, Gaussian exponents and distances are taken from an OPIT calculation on ethylene and used unchanged in a single SCF calculation on benzene. Approximate *ab initio* calculations of this type give much useful information and are often preferable to semi-empirical approaches, since the nature of the approximations involved is much better defined.

## Introduction

All-electron atomic and molecular *ab initio* calculations have been possible for about fifteen years now, and have underlined the importance of electronic computers in sustaining the momentum of quantum chemistry research. Such calculations offer a way of avoiding the many uncertainties and pitfalls that bedevil semi-empirical calculations. For this reason most *ab initio* calculations have tried to obtain high accuracy for molecular energies and properties by solving the SCF equations using a large basis set of suitably chosen functions. Little effort is usually expended in optimising such non-linear parameters as basis function exponents, because the basis is usually so large that energies better than 99% of the SCF limit can be obtained simply from the automatic determination of linear parameters (molecular orbital coefficients) that takes place in the SCF procedure. Calculations of this sort can be further refined by configuration interaction methods if required.

However, we now have a situation where there is a great difference between the accuracy and reliability of semi-empirical calculations and accurate *ab initio* work. In an attempt to bridge this gap I should like to review the work that we have been doing at Nottingham over the past five years in what might be called approximate *ab initio* calculations. By 'approximate', in this context, I mean that we are satisfied with energies that are about 95% of the SCF limit. The reason for this approach can best be summed up in a remark once made by the late Professor Coulson. He said that he was often asked by chemists to give them a clear description of

familiar chemical concepts such as lone pairs and bond pairs, in the language of modern quantum mechanics. His reply was always to the effect that a 90% correct description is very easy to give in this way, but that describing the extra 10% is much more difficult to do and the wavefunction tends to become almost unrecognisable in chemical terms. For this reason we at Nottingham have long been interested in seeing whether a viable model for closed shell atoms and molecules can be set up using a small basis set of very simple functions.

## The Frost Model

This consists of modelling a closed shell molecule using a single floating spherical gaussian function for each pair of electrons in a molecule. Thus for a  $2n$  electron system there are  $n$  spherical gaussians of the form:—

$$g_i = N_i e^{-\alpha_i(r-R_i)^2}$$

where

$N_i$  is the normalisation factor

$\alpha_i$  is the exponent (size factor) of the gaussian

$R_i$  is the position of the centroid of the  $i^{\text{th}}$  gaussian relative to some centre of co-ordinates.

It is usual in the Frost [1,2] method to optimise the exponents  $\alpha_i$  and positions  $R_i$  of all the gaussian functions involved. In most cases one of the gaussians will come to rest on each heavy nucleus in the molecule and can be kept fixed there. Figure 1 shows

\* Department of Mathematics, University of Nottingham, University Park, Nottingham, NG7 2RD

Frost model basis sets for methane and ethylene. In the case of methane the  $CH$  bond functions are equivalent by symmetry and so the number of independent non-linear parameters is only three i.e. the core and bond gaussian exponents, and the distance of the bond gaussian along the  $CH$  bond (denoted  $\alpha_C$ ,  $\alpha_{CH}$  and  $d_{CH}$  respectively). In ethylene we have five independent parameters,  $\alpha_C$ ,  $\alpha_{CH}$ ,  $d_{CH}$ ,  $\alpha_{\pi}$ , and  $d_{\pi}$ . The last two parameters denote the exponents, and distance from the internuclear axis, of the two spherical gaussian functions that model the  $\pi$  electron system.

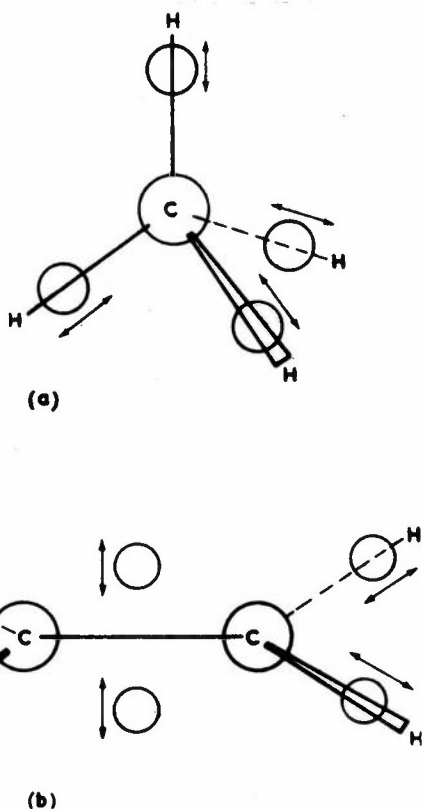


Figure 1: Frost models for (a) methane and (b) ethylene; arrows show the direction of movement of the floating gaussians

For each setting of the non-linear parameters indicated by the optimisation routine an energy is calculated. This is extremely easy in the Frost model, for the number of basis functions is equal to the number of electron pairs, and there is no need for an iterative scheme to find the energy. In fact, the density matrix in the Frost model turns out to be just the inverse of the overlap matrix [1]. Also, the choice of spherical gaussians makes all integrals easy to evaluate [3]. When non-linear parameters are optimised the Frost model gives, typically, 85% of the SCF energy limit. This low accuracy, however, is not so much of a drawback as the inherent instability of the model under certain circumstances. The main contribution to the molecular energy arises from the 'heavy' carbon atoms in the molecule. It follows,

therefore, that if the optimisation routine can improve the description of the heavy atoms then a lower energy will probably be obtained. This is achieved by moving the bond pairs in methane (say) closer in to the carbon nucleus. If they coalesce, with equal exponents, then the overlap matrix becomes singular with off-diagonal elements of unity. This extreme form of behaviour does not usually occur in saturated systems, but is almost certain to occur in unsaturated molecules. For example, the gaussian functions simulating the  $\pi$  orbital system in ethylene will coalesce if their positions are allowed to optimise fully.

## OPIT

The first version of this program was written in 1969 for a KDF9 computer. As its name implies it is both optimising and iterative. It has recently been completely rewritten and implemented on ICL 1900 series computers and the CDC 7600 machine [4,5]. The program is a general SCF-MO floating gaussian program capable of giving single determinant closed shell wavefunctions to any required degree of accuracy provided a large enough basis set is specified. However, its main use so far has been to extend the scope of the Frost model by using two independently optimised spherical gaussians at each 'heavy' nucleus. Under these conditions the cusp condition at the nucleus is much better approximated, and the energy obtained is now 95% of the SCF limit. The extra core gaussian greatly reduces the tendency of lone pair or bond pair gaussians to coalesce on the nucleus during the

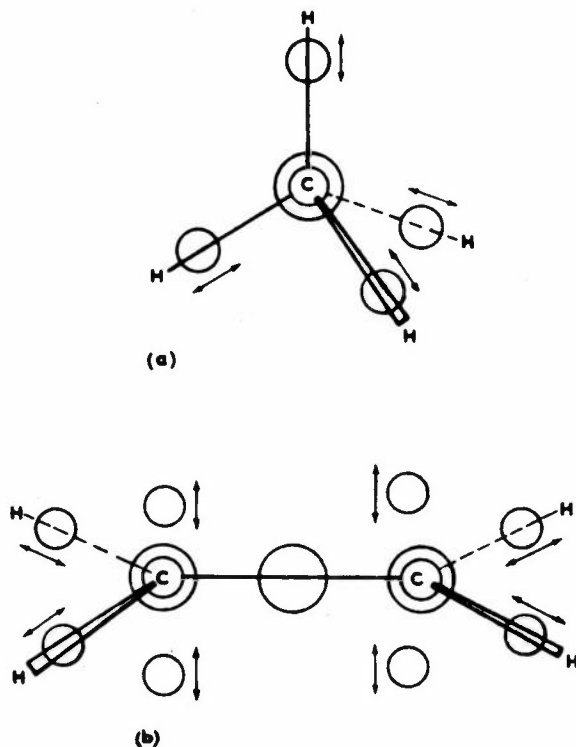


Figure 2: OPIT models for (a) methane and (b) ethylene



optimisation. But, since the basis set is now larger than the Frost minimal set, a SCF calculation is needed to calculate the energy for every setting of the non-linear parameters. Possible OPIT models for methane and ethylene are shown in figure 2 and calculations of this type are reported in the paper by Ford, Hall and Packer [6]. A coherent description of saturated organic molecules can be obtained from models of this sort. Bond lengths and molecular angles are predicted semi-quantitatively. The energy ordering of conformers e.g. the staggered and eclipsed forms of ethane, is given correctly but the predicted barrier heights are rather high. However, when one studies OPIT values for barrier heights, geometrical features and other first order properties [7] a pleasing pattern emerges that the predicted values are a constant fraction of the true values.

Despite the many advantages of OPIT over a simple Frost treatment, the problem of modelling  $\pi$  electron systems still remains. For, even with an extra core gaussian, any attempt to model a molecule such as ethylene, in the manner depicted in figure 2b, would still fail due to the tendency of the spherical gaussians representing the  $\pi$  system to coalesce, with identical exponents, on to the carbon nuclei. In fact, figure 3 shows the effect of fixing all ethylene parameters at the values shown, except for the distance,  $d$ , of the ' $\pi$ ' spherical gaussians from the carbon atoms. This distance is then allowed to optimise and the best result is clearly obtained as  $d \rightarrow 0$ ! Study of the molecular orbital eigenfunctions and the behaviour of the overlap matrix for small  $d$  [8], shows a clear tendency for the two pairs of gaussians to combine antisymmetrically to give functions of  $p$  type symmetry.

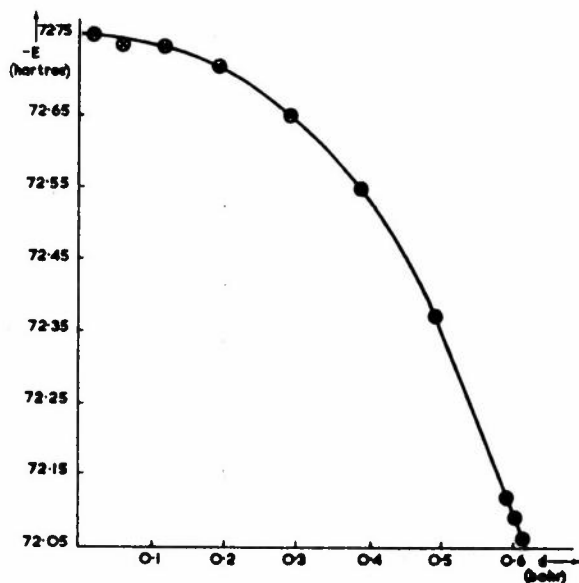


Figure 3: Plot of energy versus distance ( $d$ ) of the ' $\pi$ ' spherical gaussian from the C atom, in the OPIT ethylene model. The remaining parameter values are fixed at:  $\alpha_C$  (inner) = 40.0,  $\alpha_C$  (outer) = 10.0,  $\alpha_{CH}$  = 0.45,  $\alpha_{CC}$  = 0.5,  $\alpha_{\pi}$  = 1.0,  $d_{CH}$  = 1.336

The symmetric combination of the functions, however, also contributes more strongly to the  $\sigma$  system around the C-C bond, as  $d$  becomes small. This helps to lower the total energy of the system and, thus, configurations with small  $d$  values are favoured by the optimisation routine.

For this reason an attempt was made to add into the Fock matrix only the antisymmetric contributions from these functions. This, unfortunately, only had the effect of slowing down the coalescence of the functions, and gives a worse energy for the system because of the extra constraint. Now it has always been part of the OPIT philosophy that there should be no constraint in optimising *any* non-linear parameter, if it is desired to do so. Faced with this situation we had to capitulate and include 'genuine'  $p$ -type gaussians as defined by Boys [9] into the program. The integrals over these functions were performed using the relationships given by Huzinaga *et al.* [10] but in the form of the specific formulae given by Clementi and Davis [11]. Note that, in the interests of keeping the basis set small, we include only those  $p_z$  type orbitals that are essential for describing the  $\pi$  orbital system.

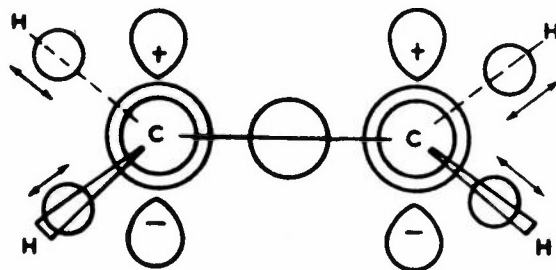


Figure 4: OPIT model for ethylene using  $p$ -type gaussians

Table 1: Ethylene molecular orbital energies \*

Species	OPIT	Moskowitz <i>et al.</i> [12]
1a <sub>g</sub>	-11.064	-11.240
1b <sub>1u</sub>	-11.052	-11.238
2a <sub>g</sub>	-1.019	-1.040
2b <sub>1u</sub>	-0.759	-0.780
1b <sub>2u</sub>	-0.495	-0.655
3a <sub>g</sub>	-0.405	-0.581
1b <sub>3g</sub>	-0.392	-0.514
1b <sub>3u</sub> ( $\pi$ )	-0.207	-0.374
1b <sub>2g</sub> ( $\pi$ )	+0.354	
Total Energy	-74.6083	-78.0062

\* All energies in hartree

The model for our ethylene calculation is now shown in figure 4. In accordance with the philosophy of full optimisation, the  $p$  functions were even left free to drift off the carbon nuclei. However, the amount of drift was found to be negligible, and so in this, and all subsequent calculations using  $p$  functions, they are anchored to the heavy nuclei. The results for this ethylene calculation are shown in table 1, the ordering of the orbital energies agrees with that obtained in a much more accurate calculation performed by Moskowitz *et al.* [12].

Similar calculations, with full optimisation, were performed on *cis* and *trans* butadiene with basis sets

Table 2: Total energies\* for *cis* and *trans* butadiene

	OPIT	Buenker and Whitten [13]
<i>cis</i>	-148.2463	-154.7023
<i>trans</i>	-148.2609	-154.7103
$\Delta E$	0.0146 (9.1 kcal mole <sup>-1</sup> )	0.0080 (5 kcal mole <sup>-1</sup> )

\* Energies are in hartree except where stated. Geometry is as described in [13]

Table 3: Total energies for benzene

OPIT	Buenker <i>et al.</i> [14]
-221.027 hartree	-230.375 hartree

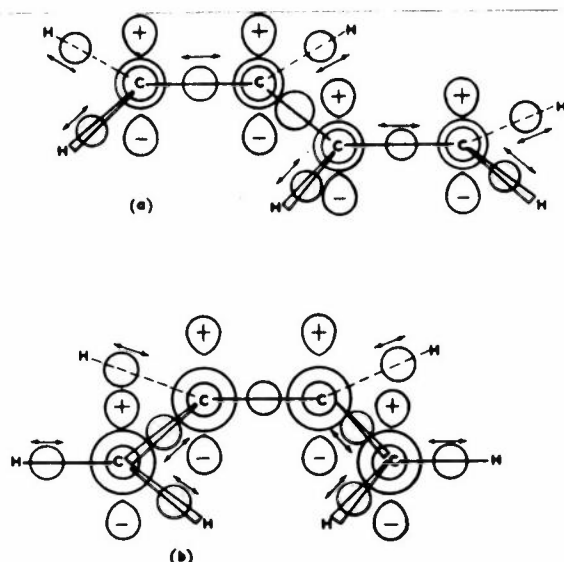


Figure 5: OPIT models for (a) *trans* and (b) *cis* butadiene

as shown in figure 5, and also for benzene. The energies obtained are shown in tables 2 and 3. Note how the energies obtained are about 95% of those obtained in the accurate *ab initio* calculations that are included for comparison. In agreement with our general experience of OPIT, we predict the energy difference between the *cis* and *trans* conformers of butadiene to be too high by a factor of two.

The most interesting aspect of these calculations on simple  $\pi$  orbital systems, lies in the values of the optimised non-linear parameters. These results are collected in table 4. To a good approximation the core and bond exponents do not vary from molecule to molecule, with the exception of the  $p$  orbital exponents. We see a clear effect, for the  $p$  functions, in the case of butadiene, to become less diffuse on the central carbon atoms than they would have been in ethylene, while those on the terminal carbon atoms become more diffuse. The difference between the central atom and terminal atom  $p$  orbital exponents is greater in *trans* than in *cis* butadiene reflecting, perhaps, the different steric factors in the two molecules. As might be expected, the greater delocalisation of the  $\pi$  electron system in benzene leads to the  $p$  orbital being rather more diffuse than in ethylene and its exponent value differs from ethylene by 10%.

Table 4: OPIT optimal parameter values for ethylene, butadiene and benzene

	Ethylene	Butadiene		Benzene
		<i>cis</i>	<i>trans</i>	
$\alpha_C$ (inner)	45.90	45.945 45.915	45.958 45.918	45.93
$\alpha_C$ (outer)	6.63	6.639 6.635	6.642 6.635	6.64
$\alpha_\pi$	0.33	0.333 0.458	0.290 0.493	0.36
$\alpha_{CC}$	0.40	0.433 0.386	0.436 0.386	0.41
$\alpha_{CH}$	0.377	0.377 0.379 0.378	0.378 0.377	0.377
$d_{CH}$	1.255	1.254 1.255 1.279	1.239 1.244 1.280	1.276
$d_{CC}$	-	1.251	1.249	

$\alpha$  Values are optimal gaussian exponents

$d$  Values are optimal distances (in bohrs) measured from the heavy atom along the bond direction

The multiple parameter values for butadiene reflect the number of symmetrically distinct parameters of each type in the molecule; parameters for the terminal atoms and bonds are given first in each set followed by the values for central atoms or bonds

These calculations confirm my earlier remark that 95% accurate calculations can fit in with chemical notions in a very simple and straightforward way. Table 4 shows us the importance of  $\pi$  orbitals, the amount of their delocalisation and lends weight to the hypothesis of  $\sigma$ - $\pi$  separability, since the  $\sigma$  systems remain essentially constant while the  $\pi$  systems alter appreciably. It is particularly pleasing that these results arise from an all electron *ab initio* calculation.

The high degree of parameter transferability that is evident so far, prompts the use of OPIT as a tool for optimising non-linear parameters in small molecules, with a view to their later use in the method of molecular fragments described by Christoffersen *et al.* [15,16]. The idea here is that, as molecules become bigger, it is neither necessary nor desirable to optimise fully all the non-linear parameters. Instead, one fixes the parameters at values obtained from smaller species and then a 'one-off' SCF calculation is performed without any attempt at reoptimising the non-linear parameters. As the larger molecules have little or no symmetry, a special program (SCOFF - Self Consistent Calculation Using Optimised Fixed Fragments) has been developed. In essence it resembles the very first function evaluation of OPIT but with special techniques to cope with low symmetry, and the large number of near-zero integral values that occur simply because of large inter-atomic distances. The essential features of OPIT modelling (i.e. single spherical gaussians for lone pairs and bond pairs; two spherical gaussians on each heavy nucleus with  $p$  type gaussians for  $\pi$  systems) are retained in SCOFF.

### Work Performed with SCOFF

As a check on the viability of the SCOFF method we have recalculated many systems that had previously been done with OPIT. As an example of this, table 5 shows the results of recalculating *cis* and *trans* butadiene and benzene using ethylene parameters and

Table 5: Comparison of energies\* for butadiene and benzene obtained from a full parameter optimisation (OPIT) and a molecular fragments approach using ethylene parameters (SCOFF)

	OPIT	SCOFF
butadiene		
$E_{cis}$	-148.2463	-148.2317
$E_{trans}$	-148.2609	-148.2440
$\Delta E$	0.0146	0.0123
	(9.1 kcal mole <sup>-1</sup> )	(7.7 kcal mole <sup>-1</sup> )
benzene		
$E$	-221.0268	-221.0145

\* Energies are in hartree except where stated. Effects due to bond length differences between butadiene, benzene and the ethylene fragment have been ignored

ignoring the effects such as differing C-C bond lengths in the species involved. We see that the energies obtained by the two methods are in remarkably good agreement although, of course, the better values are given by OPIT. The stabilities of the butadiene conformers are still predicted in the correct order and the energy difference is close to that obtained by OPIT.

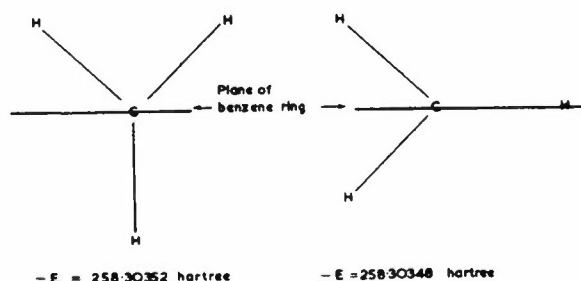


Figure 6: Energies for two toluene conformers obtained from SCOFF

Finally, as examples of the possibilities opened up by a molecular fragments program like SCOFF, I shall quote two recently obtained results. The first is summarised in figure 6 and shows the energies of two toluene conformers. The form in which the  $CH_3$  group is fully staggered with respect to the benzene ring is predicted to be fractionally more stable than the one in which a hydrogen atom is eclipsed. Secondly, we have looked at the drug amphetamine in its protonated form. The important torsional angles  $\tau_1$ ,  $\tau_2$  and  $\tau_3$  are shown in figure 7. We have calculated energies for this molecule for  $\tau_1 = 90^\circ$  and various  $\tau_2$ . The relative stabilities of the various rotated forms are shown in figure 8 together with interpolated results for the same species calculated by Pullman *et al.* [17] using semi-empirical methods. The overall shape of the plot is the same, but SCOFF appears to differentiate between the three equivalent minima predicted by the PCILO method and indicates that the rotamer with the  $NH_3^+$  group folded back over the benzene ring, but the  $CH_3$  group extended away from the ring, will be fractionally more stable.

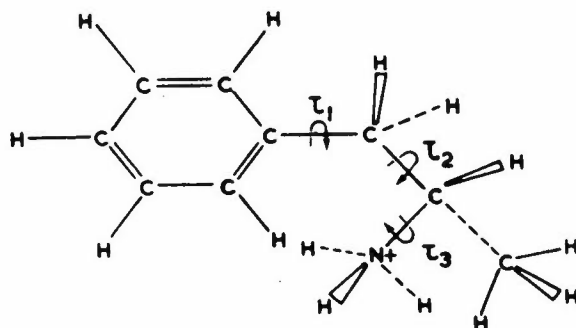


Figure 7: The amphetamine ion

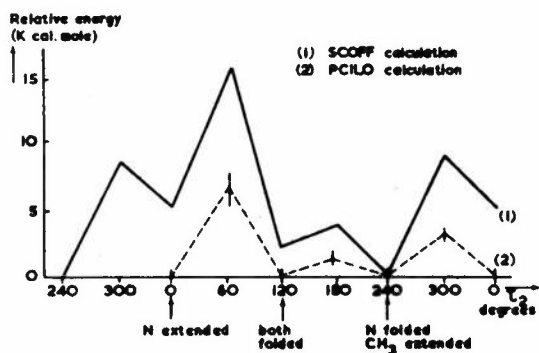


Figure 8: Relative energy of rotameric forms of amphetamine as a function of the angle  $\tau_2$ .  $\tau_1$  is fixed at  $90^\circ$  (see figure 7): the PCILO calculation is reported in [17]

## Conclusions

Although we have used OPIT in many contexts to obtain a simple and readily understandable wavefunction, the emphasis in this paper has been on its use for obtaining molecular fragment parameters for later use in the SCOFF program. Approximate *ab initio* calculations of this type give about 95% of the Hartree-Fock SCF limiting energy. Most of the remaining energy deficit can be ascribed to the poor description of atomic nuclei in this model. In general, valence electron and bond properties are well predicted, but even when such properties are given incorrectly, the results obtained are usually a constant fraction of the true values. The wavefunction obtained, being of *ab initio* type is much more amenable to error analysis than semi-empirical results.

The place of semi-empirical and accurate *ab initio* calculations is already well established in quantum chemistry. We believe that approximate *ab initio* molecular fragment techniques are well suited to bridge the gap between these extreme approaches in areas such as the study of medium sized molecules of biological interest.

## Acknowledgements

In a review paper of this sort I have had to draw heavily on the experience and research work of other colleagues. I should like to thank Professor G.G. Hall for his continued interest in this project, and also Brian Ford, Jane Hylton, Colin Miller, Gary Schnuelle (who wrote the SCOFF program) and Andrew Tait. These colleagues have all contributed in some measure to the results reported here. We thank the Cripps Computer Centre, University of Nottingham, and the Science Research Council Atlas Computer Laboratory, Chilton, for allocations of computer time.

## References

- [1] FROST, A.A. (1967). *J. Chem. Phys.*, **47**, 3707.
- [2] ——— (1967). *J. Chem. Phys.*, **47**, 3714.
- [3] SHAVITT, I. (1963). *Methods Comp. Phys.*, **2**, 1.
- [4] PACKER, J.C. and BRAILSFORD, D.F. (1973). *Comp. Phys. Comm.*, **5**, 123.
- [5] BRAILSFORD, D.F. and PRENTICE, J.A. (1973). *Comp. Phys. Comm.*, **5**, 136.
- [6] FORD, B., HALL, G.G. and PACKER, J.C. (1970). *Int. J. Quantum Chem.*, **4**, 533.
- [7] DIXON, M. and TAIT, A.D. *Mol. Phys.*, (submitted for publication).
- [8] FORD, B. and HALL, G.G. (1974). *Comp. Phys. Comm.*, **8**, 337.  
SCHNUELLE, G.W., (unpublished work).
- [9] BOYS, S.F. (1950). *Proc. Roy. Soc. (London)*, **A200**, 542.
- [10] TAKETA, H., HUZINAGA, S. and O-OHATA, K. (1966). *J. Phys. Soc. Japan*, **21**, 2313.
- [11] CLEMENTI, E. and DAVIS, D.R. (1966). *J. Comp. Phys.*, **1**, 223.
- [12] SCHULMAN, J.M., MOSKOWITZ, J. and HOLLISTER, C. (1967). *J. Chem. Phys.*, **46**, 2759.
- [13] BUENKER, R.J. and WHITTEN, J.L. (1968). *J. Chem. Phys.*, **49**, 5381.
- [14] BUENKER, R.J., WHITTEN, J.L. and PETKE, J.D. (1968). *J. Chem. Phys.*, **49**, 2261.
- [15] CHRISTOFFERSEN, R.E., GENSON, D.W. and MAGGIORA, G. (1971). *J. Chem. Phys.*, **54**, 239.
- [16] CHRISTOFFERSEN, R.E. (1971). *J. Am. Chem. Soc.*, **93**, 4104.
- [17] PULLMAN, B., COUBEILS, J-L., COURRIERE, P. and GERVOIS, J-P. (1971). *J. Medicinal Chem.*, **15**, 17.

# The Electronic Structure of Cadmium Dichloride by the Multiple Scattering $X\alpha$ Method

N.V.Richardson, A.F.Orchard\* and M.A.Whitehead†

The results of an MS- $X\alpha$  treatment of  $CdCl_2$  are presented and the ionisation potentials calculated using Slater's transition state concept are compared with the available experimental data.

## Introduction

Cadmium dichloride has been studied as a member of the group IIB dihalides, which form a relatively simple but chemically interesting series of compounds because of the interplay between spin orbit coupling effects and other bonding effects. A current point of interest here for the inorganic chemist is the degree of involvement in bonding of the 'inner'  $d$  electrons. Experimental photo-ionisation data on these compounds has only recently become available [1,2] with the development of high temperature photoelectron spectroscopy.

The multiple scattering (MS)  $X\alpha$  model has been invoked for the calculation of molecular ionisation energies because of the ease with which molecules containing heavy atoms can be investigated, for a relatively small expenditure of computer time.

## Details of the Calculation

All the calculations detailed here were performed on the University computer, an ICL 1906A, using the basic MS- $X\alpha$  programme of Johnson and Slater [3].

Calculations were carried out on cadmium chloride at the experimental geometry [4], with the atomic sphere radii chosen as covalent radii suitable scaled such that the cadmium and chlorine spheres were touching. An outer sphere enclosing the entire molecule was also incorporated, as shown in figure 1. Table 1 shows these radii and the values of the exchange parameter  $\alpha$  [5-7] within the various regions of the molecule. Inside the cadmium and chlorine spheres,  $\alpha$  was given the values tabulated by Schwarz [8], for the outer sphere region the  $\alpha$  value for chlorine was used and in the intersphere region an

arithmetic mean of a cadmium and two chlorine  $\alpha$  values was used.

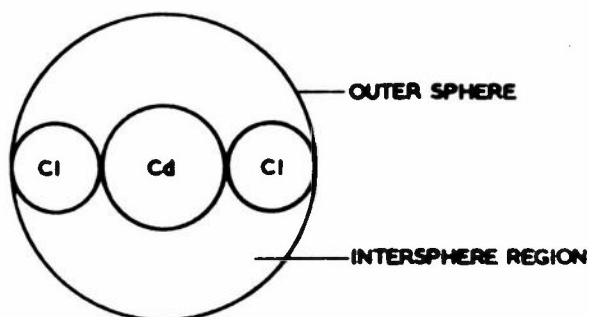


Figure 1: Diagrammatic representation of the  $CdCl_2$  molecule

Table 1: Bond length, sphere radii and exchange parameters for the MS- $X\alpha$  calculation on  $CdCl_2$

Bond length				
$Cd-Cl$	au	4.23	$\alpha_{III}^a$	0.72277
Sphere radius				
$Cd$	au	2.54	$\alpha_{Cd}$	0.70084
Sphere radius				
$Cl$	au	1.69	$\alpha_{Cl}$	0.72277
Outer sphere				
radius	au	5.92	$\alpha_{I}^b$	0.71546

(a)  $\alpha_{III}$  denotes the exchange parameter in the outer-sphere region

(b)  $\alpha_{I}$  denotes the exchange parameter in the inter-sphere region

\* *Inorganic Chemistry Laboratory, University of Oxford, South Parks Road, Oxford, OX1 3QR*

† *Theoretical Chemistry Department, University of Oxford, 1 South Parks Road, Oxford, OX1 3TG*

The MS- $X\alpha$  method consists of superposing atomic charge densities using the chosen geometry and hence deriving a molecular potential field. A secular determinant is then constructed within the 'muffin tin' and exchange approximations. The symmetry of the molecule can be exploited to factorise this determinant, which is subjected to an energy search in the valence region, in order to find the molecular energy levels. In utilising the symmetry ( $D_{\infty h}$ ) of the cadmium dichloride system, spherical harmonics of  $L = 0, 1, 2$  and  $3$  for cadmium and  $L = 0, 1$  and  $2$  for chlorine were used. Using these non-SCF eigenvalues in the valence region and the atomic eigenvalues in the core region as starting energies, an SCF calculation was then performed. Fifteen iterations, each taking about three minutes, were needed to produce a degree of self-consistency of  $1.7 \times 10^{-5}$  Ry. in the potential and  $1.5 \times 10^{-5}$  Ry. in the orbital energies.

Slater has introduced in connection with the MS- $X\alpha$  model the concept of a transition state [9,10], in which half an electron is removed from a particular orbital. The energy of this orbital, on re-attaining self-consistency, is then taken as the negative of the ionisation potential of the doubly occupied orbital. This concept allows one to take some account of relaxation processes during ionisation. Further SCF calculations were carried out on transition states derived from each of the valence orbitals. In these cases only five iterations were necessary, using the potential from the ground state SCF calculation as the starting potential.

The total time for the calculations indicated here was ninety minutes.

### The Photoelectron Spectrum

The He I (21.21 eV) photoelectron spectrum shows four bands in the region of 11-14 eV [1,2], which are expected to arise from orbitals of  $\pi_g, \pi_u, \sigma_g$  and  $\sigma_u$  symmetry (no ordering implied). The photoelectron spectrum of the chlorine molecule shows three bands in this region [11], assigned such that the ordering of orbital energy levels is  $\pi_g > \pi_u > \sigma_g$ . The inclusion of a cadmium atom is not expected to change this order but it is not clear where the  $\sigma_u$  orbital will appear in this order. It is unlikely that the  $\sigma_u$  orbital, of Cl-Cl antibonding and Cd 5p character will lie below the  $\sigma_g$  orbital which has Cl-Cl bonding and Cd 5s character. Cocksey *et al.* [1] prefer the ordering  $\pi_g > \pi_u > \sigma_u > \sigma_g$ , on intensity grounds and by comparison with the spectra of other group IIB dihalides which show the splitting of  $\pi$  bands due to spin orbit coupling effects.

Ionisations which could be assigned to cadmium 4d electrons have not been observed, though they might be expected to occur in the 18-20 eV region (bands at 17.5 eV and 18.2 eV in cadmium metal and at 18.9 eV in cadmium di-iodide) [12]. This may be

due to instrumental factors which make the observation of bands in the region 19-21 eV rather difficult.

### Discussion of the Results

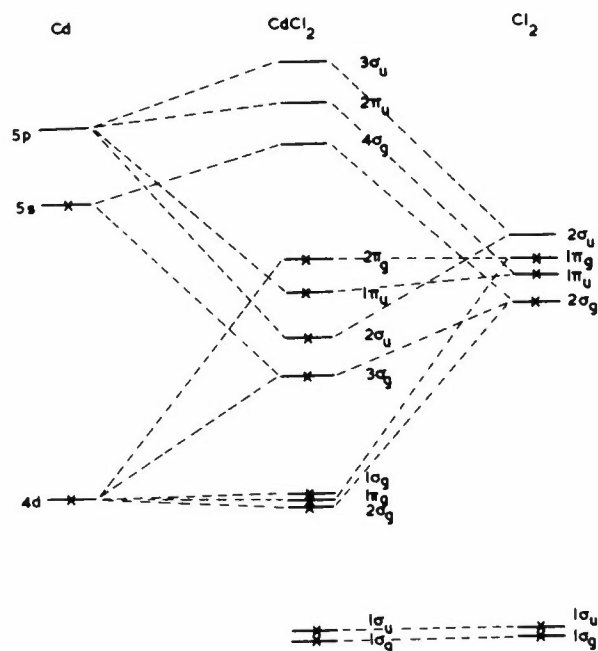
The pattern of ionisation potentials for cadmium chloride is well reproduced by this calculation, with the levels of predominantly chlorine 3p character well separated from those of cadmium 4d character. The atomic, non-SCF and SCF electronic energy levels are shown in table 2. The order of levels in the low I.P. region, as shown by the non-SCF calculation is  $2\pi_g > 2\sigma_u > 1\pi_u > 3\sigma_g$  but during the SCF procedure the transfer of charge from cadmium to chlorine causes the  $2\sigma_u$  and  $1\pi_u$  levels to invert, such that the SCF ordering of levels is in agreement with experiment. On application of the transition state concept, the predicted ionisation energies are found to be in close agreement with the experimental values (table 3). The predicted I.P.'s in the region below 14 eV are uniformly about 0.8 eV too low. In contrast, the cadmium 4d electrons are predicted to ionise at 22.6 eV, which is rather higher than expected.

Table 2: Atomic, non-SCF and SCF  $X\alpha$  electronic energy levels of  $CdCl_2$

	Atomic Orbital Energy (Ry.)	Non-SCF Orbital Energy (Ry.)	SCF Orbital Energy (Ry.)
Cd (1s)	1884.2	-	1884.6
Cd (2s)	273.95	-	274.25
Cd (2p)	255.58	-	255.89
Cd (3s)	50.80	-	51.09
Cd (3p)	43.31	-	43.60
Cd (3d)	29.40	-	29.69
Cd (4s)	7.141	-	7.444
Cd (4p)	4.738	-	5.043
Cl (1s)	201.35	-	201.14
Cl (2s)	18.45	-	18.44
Cl (2p)	14.16	-	14.13
$1\sigma_g$	-	1.306	1.575
$1\sigma_u$	-	1.283	1.551
$2\sigma_g$	-	0.905	1.181
$1\pi_g$	-	0.913	1.187
$1\delta_g$	-	0.909	1.185
$3\sigma_g$	-	0.488	0.670
$2\sigma_u$	-	0.398	0.623
$1\pi_u$	-	0.426	0.604
$2\pi_g$	-	0.384	0.583

Table 3: Comparison of the calculated and experimental photoionisation data for the valence region of  $CdCl_2$

SCF Orbital Energy (eV)	Transition State Energy (eV)	Experimental I.P. (eV)	
		[1]	[2]
$2\sigma_g$	16.05		
$1\pi_g$	16.16		
$1\delta_g$	16.10		
$3\sigma_g$	9.31	13.12	13.31
$2\sigma_u$	8.67	12.53	12.48
$1\pi_u$	8.41	11.93	11.92
$2\pi_g$	7.92	11.44	11.48



x DENOTES A COMPLETELY FILLED ORBITAL

Figure 2: Diagrammatic representation of the electronic structure of  $CdCl_2$

The splitting of the cadmium  $4d$  levels by the linear field of the chlorine atoms is predicted to be very small ( $0.04 eV$ ) and considerably less than the spin orbit coupling effect which splits the  $4d$  levels of the cadmium atom by  $0.7 eV$ .

## Conclusion

The multiple scattering  $X\alpha$  model gives an electronic structure for cadmium dichloride which is in close agreement with data available from UV photoelectron spectroscopy.

## References

- [1] COCKSEY, B.G., ELAND, J.H.D. and DANBY, C.J. (1973). *J. Chem. Soc. (Faraday II)*, **69**, 1558.
- [2] FERNER, R.E., WATSON, P.R. and RICHARDSON, N.V., (to be published).
- [3] JOHNSON, K.H. (1973). *Adv. Quantum Chem.*, **7**, 142, (and references therein).
- [4] SUTTON, L.E. (1965). *Chem. Soc. special publication 11 and supplement 18*.
- [5] SLATER, J.C., WILSON, T.M. and WOOD, J.H. (1969). *Phys. Rev.*, **179**, 28.
- [6] SLATER, J.C., MANN, J.B., WILSON, T.M. and WOOD, J.H. (1969). *Phys. Rev.*, **184**, 672.
- [7] SLATER, J.C. and WOOD, J.H. (1971). *Int. J. Quantum Chem.*, **45**, 3.
- [8] SCHWARZ, K. (1972). *Phys. Rev.*, **B5**, 2466.
- [9] SLATER, J.C. (1971). *Computational Methods in Band Theory* (ed. P.M. Marcus, J.F. Janak and A.R. Williams), 447, New York: Plenum Press.
- [10] ——— (1971). *Advances in Quantum Chemistry* (ed. P-O. Löwdin), Chapter 6, New York: Academic Press.
- [11] EVANS, S. and ORCHARD, A.F. (1971). *Inorg. Chim. Acta*, **5**, 81.
- [12] MOORE, C.E. (1952). *Atomic Energy Levels*, circular 467, Natl. Bur. Standards.

# Recent Developments in Hartree-Fock Theory

J.P.Dahl\*

A review is given of some recent theoretical developments in open-shell Hartree-Fock theory. Particular emphasis is given to the role played by the off-diagonal (Lagrange) multipliers, and some existing theories are rectified and extended so as to include all necessary conditions on the Hartree-Fock orbitals. In conclusion, a simple computational scheme is developed and applied to the stability problem in the allyl radical.

## Introduction

The corner-stone in open-shell Hartree-Fock theory is the classical paper by Roothaan [1], dating back to 1960. This paper has during the past years been followed up by several others, in which the original treatment is extended and elaborated on, and sophisticated computer programs have, in turn, led to the determination of many accurate wavefunctions for open-shell systems, atoms and molecules alike.

Nevertheless, each additional system that is taken up tends to present itself as a new case, with its own mischievous characteristics. These include, in particular, convergence problems and ambiguities as regards the selection of open shell orbitals from one iterative step to the next. It is not very likely that such difficulties can be eliminated in a completely mechanical way, but an understanding of their origin may help to circumvent them in an intelligible manner.

In the present paper we shall consider the rôle which the off-diagonal (Lagrange) multipliers play in Hartree-Fock theories, since many of the difficulties mentioned are associated with these quantities. We shall review some of the latest theoretical developments and deduce an alternative computational scheme, distinguished by its conceptual simplicity.

## Necessary Conditions on Hartree-Fock Orbitals

In Hartree-Fock theory one writes the wavefunction  $\Psi$  for a given state of an  $N$ -electron system as a fixed linear combination of a small number of Slater determinants, built over  $\alpha$  and  $\beta$  spin functions and an orthonormal set of spatial orbitals  $\phi_1, \phi_2, \dots, \phi_n$ . The coefficients of the linear combination are determined by the equivalence and symmetry restrictions on the system. The expectation value of the energy

$$E = \langle \Psi | H | \Psi \rangle, \quad (1)$$

with  $H$  being the  $N$ -electron Hamiltonian, is thus a functional of the orbitals  $\phi_1, \phi_2, \dots, \phi_n$ , and the Hartree-Fock problem consists in determining  $\phi_1, \phi_2, \dots, \phi_n$  in such a way that

$$\delta E = 0. \quad (2)$$

The orthonormality of the orbitals must be retained during the variation, and this imposes the orthonormality constraints

$$\delta \langle \phi_i | \phi_j \rangle = 0 \quad (i, j = 1, 2, \dots, n) \quad (3)$$

The conditions (2) and (3) lead to the Hartree-Fock equations.

In an open-shell system it takes two or more degenerate wavefunctions to describe an electronic state, and one must then replace the energy value in (1) with the average of the expectation values of the degenerate components. The variation of the energy may then be written in the form

$$\delta E = \sum_{i=1}^n \{ \langle \delta \phi_i | F_i | \phi_i \rangle + \langle \phi_i | F_i | \delta \phi_i \rangle \}, \quad (4)$$

where  $F_i$  is the Hartree-Fock one-electron operator for orbital  $\phi_i$ .

The constraints (3) become

$$\langle \delta \phi_i | \phi_j \rangle + \langle \phi_i | \delta \phi_j \rangle = 0 \quad (i, j = 1, 2, \dots, n), \quad (5)$$

and we shall now sketch how the Hartree-Fock equations may be obtained from equations (4) and (5) along the lines described elsewhere [2,3].

For this purpose we introduce a complete orthonormal set of functions by augmenting the set defined by the Hartree-Fock orbitals. Let

\* Department of Chemical Physics, Technical University of Denmark, DTH 301, DK-2800 Lyngby, Denmark



$$\{\phi_1, \phi_2, \dots, \phi_n, \phi_{n+1}, \dots, \phi_\mu, \dots\}$$

be such a set, and let the occupied orbitals be denoted by Roman subscripts, the unoccupied orbitals by Greek subscripts. All functions of the type

$$\psi_I = \sum_{i=1}^n c_i \phi_i \quad (6)$$

may be said to constitute a function space  $\Omega_I$  [4]. All functions of the type

$$\psi_{II} = \sum_{\mu=n+1}^{\infty} c_\mu \phi_\mu \quad (7)$$

will then constitute the complementary function space  $\Omega_{II}$ . Any function in  $\Omega_I$  is, of course, orthogonal to all functions in  $\Omega_{II}$ , and vice versa.

Equation (2) must be satisfied for all possible variations  $\{\delta\phi_1, \delta\phi_2, \dots, \delta\phi_n\}$  which are consistent with (5). Let us consider two variations of an especially simple form.

As the first choice we take a variation of the type

$$\delta\phi_k = c\phi_\lambda, \quad \delta\phi_j = 0, \quad j \neq k \quad (8)$$

with  $c$  being an infinitesimal but otherwise arbitrary complex number. The conditions (5) are obviously satisfied for this type of variation, and we obtain from equation (4):

$$c^* \langle \phi_\lambda | F_k | \phi_k \rangle + c \langle \phi_k | F_k | \phi_\lambda \rangle = 0. \quad (9)$$

When  $c$  is replaced by  $ic$ , and the resulting equation compared with (9), we obtain

$$\langle \phi_\lambda | F_k | \phi_k \rangle = \langle \phi_k | F_k | \phi_\lambda \rangle = 0 \quad (10)$$

as a first necessary condition on the Hartree-Fock orbitals.

The second type of variation to be considered is chosen to be

$$\delta\phi_k = c\phi_\ell, \quad \delta\phi_\ell = -c^*\phi_k, \quad \delta\phi_j = 0, \quad j \neq k, \ell, \quad (11)$$

a variation which is again in accord with (5). Equation (4) becomes in this case

$$c^* \{ \langle \phi_\ell | F_k | \phi_k \rangle - \langle \phi_\ell | F_\ell | \phi_k \rangle \} + c \{ \langle \phi_k | F_k | \phi_\ell \rangle - \langle \phi_k | F_\ell | \phi_\ell \rangle \} = 0. \quad (12)$$

By comparison with the equation obtained by replacing  $c$  by  $ic$  we get

$$\langle \phi_\ell | F_k | \phi_k \rangle = \langle \phi_\ell | F_\ell | \phi_k \rangle, \quad (13)$$

plus a similar equation with  $k$  and  $\ell$  interchanged. Equation (13) is a second necessary condition on the Hartree-Fock orbitals. It states that the elements defined as

$$\theta_{k\ell} = \langle \phi_k | F_\ell | \phi_\ell \rangle \quad (14)$$

must form a Hermitian matrix, that is

$$\theta_{k\ell} = \theta_{\ell k}^* \quad (15)$$

The most general allowed variation may apparently be built by combining variations of the form (8) and (11). Hence, (10) and (13) constitute the complete set of necessary conditions for the energy to be stationary under variations satisfying the constraints (3).

Let us now expand  $F_k \phi_k$  on the complete orthonormal set of functions  $\{\phi_1, \phi_2, \dots, \phi_n, \phi_{n+1}, \dots, \phi_\mu, \dots\}$

$$F_k \phi_k = \sum_{j=1}^n a_{jk} \phi_j + \sum_{\mu=n+1}^{\infty} a_{\mu k} \phi_\mu, \quad (16)$$

and take the inner product with  $\phi_\ell$  and  $\phi_\lambda$ , to obtain

$$a_{jk} = \langle \phi_j | F_k | \phi_k \rangle; \quad (17)$$

$$a_{\mu k} = \langle \phi_\mu | F_k | \phi_k \rangle. \quad (18)$$

A comparison with (10) and (14) then shows that

$$F_k \phi_k = \sum_{j=1}^n \theta_{jk} \phi_j, \quad k = 1, 2, \dots, n. \quad (19)$$

These are the Hartree-Fock equations which the orbitals  $\phi_1, \phi_2, \dots, \phi_n$  have to satisfy. The coefficients  $\theta_{jk}$  are the Lagrange multipliers in the ordinary nomenclature, and our second necessary condition, as expressed through (15), requires that these be the elements of a Hermitian matrix.

We have thus reached the object of the present section, to derive the Hartree-Fock equations from equations (4) and (5). In the following sections we shall comment on the actual problem of solving these equations.

### The Coupling Operator Method

This commonly applied method was introduced in Roothaan's original paper [1], and further developments are, in particular, due to Huzinaga [5,6,8]

and Birss and Fraga [7]. The present status of the method has recently been discussed by Huzinaga [8] and by Hirao and Nakatsuji [9]. We shall introduce the elements involved in four steps, and begin by rewriting the Hartree-Fock equations (19) in a ket notation

$$F_k |\phi_k\rangle = \sum_{j=1}^n \theta_{jk} |\phi_j\rangle. \quad (20)$$

Equation (20) may be transferred into a pseudo-eigenvalue equation by inserting the expression for  $\theta_{jk}$  from (14)

$$F_k |\phi_k\rangle = \sum_{j=1}^n |\phi_j\rangle \langle \phi_j | F_k | \phi_k \rangle, \quad (21)$$

and including the non-diagonal terms in the left hand side

$$\{F_k - \sum_{j \neq k} |\phi_j\rangle \langle \phi_j | F_k | \phi_k \rangle\} |\phi_k\rangle = \theta_{kk} |\phi_k\rangle. \quad (22)$$

The quantity

$$C_k'' = \sum_{j \neq k} |\phi_j\rangle \langle \phi_j | F_k | \phi_k \rangle \quad (23)$$

is called a coupling operator. As it stands, it is non-Hermitian, and we shall therefore replace it by the Hermitian operator

$$C_k' = \sum_{j \neq k} \{ |\phi_j\rangle \langle \phi_j | F_k | \phi_k \rangle + F_k | \phi_j \rangle \langle \phi_j | \}, \quad (24)$$

whereby we obtain the pseudo-eigenvalue equation

$$\{F_k - C_k'\} |\phi_k\rangle = \theta_{kk} |\phi_k\rangle. \quad (25)$$

When solving the  $n$  coupled equations represented by (25) one usually follows Roothaan [1] by limiting the considerations to a finite function space, with basis functions  $\chi_1, \chi_2, \dots, \chi_M$ , say. The Hartree-Fock orbitals are then expanded on these basis functions

$$\phi_k = \sum_{s=1}^M c_{sk} \chi_s, \quad (26)$$

whereby the equations (25) are converted into equations for the expansion coefficients. These equations are of the fifth order in the coefficients.

The construction of the pseudo-eigenvalue equation (25) defines the first step in our presentation. The second step takes account of the condition (15) on the Lagrange multipliers. This is done by noting that

the equation

$$F_k |\phi_k\rangle = \sum_{j=1}^n |\phi_j\rangle \langle \phi_j | F_j | \phi_k \rangle \quad (27)$$

is equivalent with (20), whenever equation (15) is fulfilled. We may therefore replace equation (20) with the equation

$$F_k |\phi_k\rangle = \sum_{j=1}^n |\phi_j\rangle \langle \phi_j | G_{jk} | \phi_k \rangle \quad (28)$$

where the operator  $G_{jk}$  has the form

$$G_{jk} = \lambda_{jk} F_j + (1 - \lambda_{jk}) F_k. \quad (29)$$

The  $\lambda_{jk}$ 's are arbitrary numbers, and in general

$$\lambda_{jk} \neq \lambda_{kj}. \quad (30)$$

We see, by taking the inner product of (28) with  $\phi_k$ , that the solutions of the  $n$  equations represented by (28) will automatically satisfy the conditions (15) for any choice of the constants  $\lambda_{jk}$  excepting  $\lambda_{jk}=0$ .

The operator (29) was introduced by Huzinaga [8], and it is again possible to include the non-diagonal terms in (28) in the left hand side of that equation and obtain a pseudo-eigenvalue equation similar to (25)

$$\{F_k - C_k\} |\phi_k\rangle = \theta_{kk} |\phi_k\rangle. \quad (31)$$

The steps are straightforward and obtained in Huzinaga's paper. The  $n$  equations represented by (31) are again of the fifth order when the expansion method is adopted.

The two steps so far described are the essential and necessary steps in the operator coupling method. Two further steps may, however, be introduced. The first of these, i.e. step three of our outline, was introduced by Birss and Fraga [7] so far as equation (25) is concerned, and described in the general case of equation (31) by Hirao and Nakatsuji [9].

These authors argue that an equation like (22) only has meaning as long as the operators to the left act on  $|\phi_k\rangle$ . When the expansion method is used they suggest, therefore, that this operator be replaced by the operator

$$F_k |\phi_k\rangle \langle \phi_k | - \sum_{j \neq k} |\phi_j\rangle \langle \phi_j | F_k | \phi_k \rangle \langle \phi_k |.$$

The introduction of the projection operator  $|\phi_k\rangle \langle \phi_k |$  is, of course, a consistent step, and it adds a certain flavour to the theory. On the other hand, it increases

the order of the equations to be solved from five to seven, and it is, as has been stressed by Huzinaga [8], not really necessary. The full implication of using projection operators in connection with equation (31) is, however, worked out in reference [9].

The fourth step that may be introduced in the analysis consists in summing the left hand sides of the  $n$  equations represented by (25), so as to obtain a unified operator for all orbitals. The possibility of this step was already pointed out by Roothaan [1], and it was incorporated in the expansion method by Birss and Fraga [7]. Hirao and Nakatsuji [9] have described it for the general case of equation (31). Again, this step is not necessary, and it does not seem to have any real advantages from a computational point of view either.

Having introduced the various elements of the coupling operator method we shall proceed by adding some comments concerning the solution of the equations involved, i.e. the equations represented by (31) – or their counterparts obtained by adding step three and/or step four.

These  $n$  coupled equations are usually solved by the expansion method in connection with an iterative SCF technique, and symmetry restrictions are, of course, utilized to the extent they are present. It is the rule rather than the exception, however, that one encounters convergence difficulties in this process, and it is not really hard to see from where such difficulties stem. The source is undoubtedly to be found in the fact that one is trying to satisfy  $\frac{1}{2}n(n+1)$  conditions by solving only  $n$  equations. The  $\frac{1}{2}n(n+1)$  conditions are, of course, the  $n$  conditions represented by equation (19) and the  $\frac{1}{2}n(n-1)$  conditions of equation (15).

Whether or not a chosen iterative scheme converges for a given set of input orbitals is apparently tied up with the choice of the  $\lambda_{jk}$ 's in equation (29). One might argue that only half of these, i.e.  $\frac{1}{2}n(n-1)$  quantities, should be considered as independent. A fortunate guess of these might then allow a proper solution of the  $n$  equations, and this would then reflect that a total of  $\frac{1}{2}n(n+1)$  conditions has in some way been taken care of. This point of view is consistent with a suggestion by Hirao and Nakatsuji [9], according to which one takes

$$\lambda_{jk} - \lambda_{kj} = 1 \quad (32)$$

for all  $k, j$ -pairs.

It should be clear by now that any set of functions  $\phi_1, \phi_2, \dots, \phi_n$  satisfying the  $n$  equations represented by equation (31) will meet all the necessary conditions associated with the Hartree-Fock problem. They are therefore Hartree-Fock orbitals. The solutions associated with (25) do not automatically have this property, however, and one must assume that many false

solutions of the Hartree-Fock problem may be generated from (25). This is in accordance with a recent study of Albat and Gruen [10], who analysed the  $^1S(1s)(2s)$  state of  $He$  and obtained a variety of false solutions by using (25) and starting the iteration procedure with different orbitals. In particular, they pointed out that the orbitals obtained for the same state by Birss and Fraga [11] represent a false solution of the Hartree-Fock problem, in agreement with the fact that the theory by these authors [7] is based upon (25) alone.

In this context it is worth-while noting, as it is also done in [8] and [10], that the coupling operators occurring in Roothaan's paper [1] actually do have the form (29) for the specific example treated there.

The content of the present section reflects the fact that the coupling operator method must be used with great care and a sense of the problem under study, if the convergence difficulties are to be avoided. Additional difficulties are associated with the problem of identifying the filled orbitals from one step of the iteration to the next. This type of problem is usually dealt with by introducing some maximum overlap criterion.

In the next section we shall consider an alternative way of treating the  $\frac{1}{2}n(n+1)$  equations (13) and (19).

### The Direct Method

In this section we shall describe a new method for solving the open-shell Hartree-Fock problem, which we propose to call the direct method, because the necessary conditions (10) and (11) are attacked as they stand without any recourse to coupling operators. The method may be seen as an extension and a rectification of a method introduced by Hunt *et al.* [12] and by Peters [13], and called by them the Orthogonality Constrained Basis Set Expansion (OCBSE) Method and the Superiteration Method respectively. Thus, the direct method represents a completely consistent procedure, whereas the method by Peters and Hunt *et al.* generally leads to false solutions of the Hartree-Fock problem because the second of the necessary conditions, equation (15), is neglected. Examples of such false solutions for the  $^2S(1s)^2(2s)$  state of  $Li$  have, in fact, been presented by Albat and Gruen [10].

Let us rewrite the conditions (10) and (13) in the following form

$$\begin{aligned} \langle \phi_\lambda | F_i | \phi_i \rangle &= 0, & i &= 1, 2, \dots, n; \\ \lambda &= n+1, \dots, M \end{aligned} \quad (33)$$

$$\langle \phi_i | F_i - F_j | \phi_j \rangle = 0, \quad i, j = 1, 2, \dots, n \quad (34)$$

and recall that we use Roman subscripts for the

occupied orbitals, Greek subscripts for the unoccupied orbitals. We assume, in harmony with most other calculational schemes, that the Hartree-Fock orbitals are to be sought within a finite function space,  $\Omega$ , of dimension  $M$ , and  $\phi_1, \phi_2, \dots, \phi_M$  are thus all represented as in (26). The analysis concerning the necessary conditions for Hartree-Fock orbitals is unaffected by the restriction to a finite dimension, with the obvious proviso that all variations must be limited to  $\Omega$  also.

Rather than describe the direct method for the general case we shall illustrate it by a specific example which, in fact, contains the characteristics of the general case in it. Let us assume that occupied orbitals fall in two sets, such that

$\phi_1, \phi_2, \dots, \phi_m$  all correspond to the Hartree-Fock operator  $F_a$ ,

$\phi_{m+1}, \dots, \phi_n$  all correspond to the Hartree-Fock operator  $F_b$ .

The conditions (33) become in this case

$$\langle \phi_\lambda | F_a | \phi_i \rangle = 0, \quad \begin{array}{l} i = 1, 2, \dots, m; \\ \lambda = n+1, \dots, M \end{array} \quad (35a)$$

$$\langle \phi_\lambda | F_b | \phi_j \rangle = 0, \quad \begin{array}{l} j = m+1, \dots, n; \\ \lambda = n+1, \dots, M \end{array} \quad (35b)$$

and the conditions (34) may be written as

$$\langle \phi_i | F_a - F_b | \phi_j \rangle = 0, \quad \begin{array}{l} i = 1, 2, \dots, m; \\ j = m+1, \dots, n \end{array} \quad (36)$$

Let us proceed from here in two steps.

In step one we direct our attention to equations (35a) and (35b) alone, and begin by constructing an orthonormal set of functions

$$\phi_1^{(0)}, \phi_2^{(0)}, \dots, \phi_M^{(0)}.$$

The symbols  $\Omega_a^{(0)}$ ,  $\Omega_b^{(0)}$  and  $\Omega_{II}^{(0)}$  are introduced for the function spaces spanned by the sets

$$\{\phi_1^{(0)}, \dots, \phi_m^{(0)}\}, \{\phi_{m+1}^{(0)}, \dots, \phi_n^{(0)}\}, \{\phi_{n+1}^{(0)}, \dots, \phi_M^{(0)}\}$$

respectively. We then consider  $\phi_1^{(0)}, \dots, \phi_n^{(0)}$  as zero order approximations to  $\phi_1, \dots, \phi_n$  and go through the following iterative scheme:

(a) Solve the SCF problem

$$F_a \phi = \epsilon_a \phi \quad (37)$$

within the subspace  $\Omega_a^{(0)} \oplus \Omega_{II}^{(0)}$ , keeping the orbitals  $\phi_{m+1}^{(0)}, \dots, \phi_n^{(0)}$  fixed. The  $m$  lowest eigenvalues of  $F_a$  define the occupied orbitals

$\phi_1^{(1)}, \dots, \phi_m^{(1)}$  and a function space  $\Omega_a^{(1)}$ ; the remaining  $M-n$  eigenvalues define the unoccupied orbitals  $\phi_{n+1}^{(1a)}, \dots, \phi_M^{(1a)}$  and the function space  $\Omega_{II}^{(1a)}$ . The orbitals obtained in this way satisfy the conditions (35a).

(b) Solve the SCF problem

$$F_b \phi = \epsilon_b \phi \quad (38)$$

within the subspace  $\Omega_b^{(0)} \oplus \Omega_{II}^{(1a)}$ , keeping the orbitals  $\phi_1^{(1)}, \dots, \phi_m^{(1)}$  fixed. The  $n-m$  lowest eigenvalues of  $F_b$  define the occupied orbitals  $\phi_{m+1}^{(1)}, \dots, \phi_n^{(1)}$  and the function space  $\Omega_b^{(1)}$ ; the remaining  $M-n$  eigenvalues define the unoccupied orbitals  $\phi_{n+1}^{(1)}, \dots, \phi_M^{(1)}$  and the function space  $\Omega_{II}^{(1)}$ . The orbitals obtained in this way satisfy the conditions (35b).

(c) Redefine  $\phi_1^{(1)}, \dots, \phi_M^{(1)}$  as  $\phi_1^{(0)}, \dots, \phi_M^{(0)}$  and go back to (a) until the solutions converge. The orbitals obtained in this way are self-consistent solutions of (35a) and (35b), and step one is thus completed.

The iterative procedure described as step one constitutes the method introduced by Hunt *et al.* and by Peters, but the formulation is somewhat simpler. Reference [12] describes in detail how the matrices of the operators  $F_a$  and  $F_b$  may be constructed in an economical way. The result of step one is, however, dependant on the choice of starting orbitals, a point which was overlooked in [12] and [13].

We must therefore continue our endeavours and introduce a step two which goes as follows:

Solve the SCF problem

$$(F_a - F_b) \phi = \epsilon \phi \quad (39)$$

within the subspace  $\Omega_a^{(1)} \oplus \Omega_b^{(1)}$ , as defined by the self-consistent output from step one. The orbitals obtained by solving equation (39) are denoted  $\phi_1, \dots, \phi_n$ . They satisfy the conditions (36).

Finally we take these output orbitals together with the orbitals  $\phi_{n+1}^{(1)}, \dots, \phi_M^{(1)}$  from (c) as new input orbitals for step one, and cycle through step one and two until convergence is reached. The resulting set of orbitals will then satisfy (35) as well as (36) in a self-consistent manner, and they are therefore the Hartree-Fock orbitals.

This direct method of obtaining the Hartree-Fock orbitals is of an appealing simplicity. All SCF equations involved are of the third order in the expansion coefficients, and there are no ambiguities as to the identification of the occupied orbitals. The method is easy to program; all that is required is, in fact, a few additions to any already existing closed-shell Hartree-Fock program. It remains, however, to be examined whether or not the method is computationally cheaper than the usual coupling

operator method in the cases where both methods work, but there is no *a priori* reason to believe that it should be inferior in this respect. In the following section we shall demonstrate how the direct method may be applied with confidence in cases where the coupling operator method is a very insecure procedure to use.

The extension to cases with more than two different Hartree-Fock operators is straightforward. The problem does arise, however, of choosing the order in which the various operators should be diagonalized. This order will presumably be a determining factor for the total number of iterations that it is necessary to perform in order to reach self-consistency.

### Doublet Instability in the Allyl Radical

To illustrate the potential of the direct method we shall analyse the ground state of the allyl radical within the Pariser-Parr-Pople approximation. The function space  $\Omega$  is three-dimensional, with the  $2p_z$  atomic orbitals  $\pi_1$ ,  $\pi_2$  and  $\pi_3$  on the three carbon atoms as basis functions.

The ground state is a doublet, represented by the two wavefunctions

$$\Psi(M_S = \frac{1}{2}) = |\phi_a^+ \phi_a^- \phi_b^+|, \quad \Psi(M_S = -\frac{1}{2}) = |\phi_a^+ \phi_a^- \phi_b^-|. \quad (40)$$

The corresponding energy expression is easily written down, and its variation evaluated to be

$$\begin{aligned} \delta E = & \langle \delta \phi_a | F_a | \phi_a \rangle + \langle \phi_a | F_a | \delta \phi_a \rangle \\ & + \langle \delta \phi_b | F_b | \phi_b \rangle + \langle \phi_b | F_b | \delta \phi_b \rangle, \end{aligned} \quad (41)$$

where the Hartree-Fock operators  $F_a$  and  $F_b$  have the form

$$F_a = F\uparrow + F\downarrow \quad (42)$$

$$F_b = F\uparrow \quad (43)$$

with

$$F\uparrow = h + 2J_a + J_b - K_a - K_b \quad (44)$$

$$F\downarrow = h + 2J_a + J_b - K_a. \quad (45)$$

$h$  is the one-electron core operator, and the  $J$ 's and  $K$ 's the usual Coulomb and exchange operators.

The step one conditions (35) become in this case

$$\langle \phi_c | F\uparrow + F\downarrow | \phi_a \rangle = 0 \quad (46a)$$

$$\langle \phi_c | F\uparrow | \phi_b \rangle = 0 \quad (46b)$$

with  $\phi_c$  being the unoccupied orbital.

The condition (36) is

$$\langle \phi_a | F\downarrow | \phi_b \rangle = 0. \quad (47)$$

The allyl radical has  $C_{2v}$  symmetry, and we may therefore look for symmetry adapted solutions of (46) and (47) of the form

$$\phi_a = c_1 \chi_1 + c_2 \chi_2 \quad (48)$$

$$\phi_b = \chi_3 \quad (49)$$

with  $\chi_1$ ,  $\chi_2$  and  $\chi_3$  being the symmetry adapted basis functions

$$\chi_1 = \sqrt{\frac{1}{2}}(\pi_1 + \pi_3), \quad \chi_2 = \pi_2, \quad \chi_3 = \sqrt{\frac{1}{2}}(\pi_1 - \pi_3). \quad (50)$$

$F\uparrow$  and  $F\downarrow$  are totally symmetric operators in this case, and the conditions (46b) and (47) are therefore automatically satisfied. All that remains is to solve equation (46a) within the subspace spanned by  $\chi_1$  and  $\chi_2$ , and this is a fairly simple matter.

With the following values for the usual Pariser-Parr-Pople parameters

$$\begin{aligned} \alpha &= 0, \quad \beta = -2.38 \text{ eV} \\ \gamma_{11} &= \gamma_{22} = \gamma_{33} = 11.08 \text{ eV} \\ \gamma_{12} &= \gamma_{23} = 5.36 \text{ eV} \\ \gamma_{13} &= 3.88 \text{ eV} \end{aligned} \quad (51)$$

we obtain

$$\phi_a^s = 0.5334\pi_1 + 0.6565\pi_2 + 0.5334\pi_3 \quad (52)$$

$$\phi_b^s = 0.7071\pi_1 - 0.7071\pi_3 \quad (53)$$

and a corresponding energy

$$E^s = 11.5258 \text{ eV} \quad (54)$$

The superscript  $s$  has been added to indicate that the solution is symmetry adapted.

Paldus and Cizek [14] have shown, from general considerations, that this solution is doublet unstable. This implies that there exists another Hartree-Fock solution, having a lower energy, which is a pure doublet state, i.e. of the form (40). The orbitals  $\phi_a$  and  $\phi_b$  are no longer symmetry adapted, however.

The direct method is very suitable for investigating this new solution. We have determined it in the following way.

To begin with, step one was carried through for several choices of the input orbitals  $\phi_a^{(0)}$  and  $\phi_b^{(0)}$ . These choices were taken as a function of a single parameter  $w$ , viz.

$$\phi_a^{(0)} = (\phi_a^s + w\phi_b^s)/(1 + w^2)^{1/2} \quad (55)$$

$$\phi_b^{(0)} = (\phi_b^s - w\phi_a^s)/(1 + w^2)^{1/2} \quad (56)$$

with  $\phi_a^s$  and  $\phi_b^s$  as determined above. The following table shows how the resulting energies  $E$  and Lagrange multipliers

$$\theta_{ba} = \langle \phi_b | F \uparrow + F \downarrow | \phi_a \rangle, \quad \theta_{ab} = \langle \phi_a | F \uparrow | \phi_b \rangle \quad (57)$$

vary with  $w$ .

Table 1

$w$	$E(eV)$	$\theta_{ba}(eV)$	$\theta_{ab}(eV)$	$\theta_{ba} - \theta_{ab}(eV)$
0	11.5258	0	0	0
0.04	11.5253	-0.2674	-0.2797	0.0123
0.08	11.5241	-0.5361	-0.5499	0.0138
0.12	11.5236	-0.8060	-0.8025	-0.0035
0.16	11.5252	-1.0750	-1.0312	-0.0438
0.30	11.5707	-1.9514	-1.6035	-0.3479
0.50	11.7874	-2.8334	-1.8566	-0.9768

From table 1 it is apparent that an unsymmetrical solution does exist. The full set of iterations within the direct method were therefore carried out with input orbitals corresponding to  $w = 0.12$ . The new Hartree-Fock orbitals were thus found to be

$$\phi_a = 0.4465\pi_1 + 0.6568\pi_2 + 0.6076\pi_3 \quad (58)$$

$$\phi_b = 0.8059\pi_1 - 0.00004\pi_2 - 0.5921\pi_3 \quad (59)$$

with the corresponding energy

$$E = 11.5235 \text{ eV}. \quad (60)$$

The new Hartree-Fock orbitals are seen to be rather different from the symmetry adapted ones, but the energies of the two solutions differ very little, about  $20\text{cm}^{-1}$ . This is a result of considerable interest, especially when it is realized that we have to

do with a two-fold degenerate solution, for the orbitals obtained from (58) and (59), by interchanging the indices 1 and 3, are also Hartree-Fock orbitals due to the symmetry of the problem. The implication must be that a single Slater determinant provides a poor representation of the true ground state wavefunction.

The direct method is clearly superior to the coupling operator method when a problem of the present kind is to be investigated. (We assume that nothing is known about the actual doublet instability from the outset.) A near degeneracy is involved, and one may imagine that this could lead to oscillatory behaviour during the iteration process of the coupling operator method. And because there would be no simple way of setting up a table like the one above, it would be difficult to decide whether the oscillations should be taken as an indication of the presence of more than one solution, or whether they should be considered as reflections of certain awkward 'convergence difficulties' associated with a single solution.

## Conclusions

The direct method has been introduced as an alternative to the coupling operator method in Hartree-Fock theory. The method may be used alone or in conjunction with the coupling operator method; and it must be considered as a very useful tool, for instance in connection with studies of the Hartree-Fock stability problem.

## References

- [1] Roothaan, C.C.J. (1960). *Revs. Modern Phys.*, **32**, 179.
- [2] Dahl, J.P., Johansen, H., Truax, D.R. and Ziegler, T. (1970). *Chem. Phys. Letters*, **6**, 64.
- [3] Dahl, J.P. (1972). *The Independent-Particle Model*, Lyngby: Polyteknisk Forlag.
- [4] Nesbet, R.K. (1961). *Revs. Modern Phys.*, **33**, 28.
- [5] Huzinaga, S. (1960). *Phys. Rev.*, **120**, 866
- [6] ——— (1961). *Phys. Rev.*, **122**, 131.
- [7] Birss, F.W. and Fraga, S. (1963). *J. Chem. Phys.*, **38**, 2552.
- [8] Huzinaga, S. (1969). *J. Chem. Phys.*, **51**, 3971.
- [9] HiraO, K. and Nakatsuji, H. (1973). *J. Chem. Phys.*, **59**, 1457.
- [10] Albat, R. and Gruen, N. (1973). *Chem. Phys. Letters*, **18**, 572.
- [11] Fraga, S. and Birss, F.W. (1964). *J. Chem. Phys.*, **40**, 3203.
- [12] Hunt, W.J., Dunning, T.H. and Goddard, W.A. (1969). *Chem. Phys. Letters*, **3**, 606.
- [13] Peters, D. (1972). *J. Chem. Phys.*, **57**, 4351.
- [14] Paldua, J. and Cizek, J. (1969). *Chem. Phys. Letters*, **3**, 1.

# On Constrained Variational Calculations on Molecules

M.A.Whitehead\* and G.D.Zeiss†

The accurate calculation of the expectation values of one-electron molecular properties is considered, and suggested methods reviewed. Alternatives to the energy as a measure of the accuracy of a wavefunction are proposed and the constrained variational method is described.

A systematic investigation of the accuracy of this method for diatomic molecules within the minimum basis set Roothaan-Hartree-Fock method (RHF) is reviewed.

Several basis sets, involving weighted and unweighted least squares expansions of Slater type functions in terms of Gaussian type functions are compared and their behaviour within the CVM analysed.

The CVM is applied to the NDDO method, the maximum overlap method and to RHF with configuration interaction and the calculated one-electron expectation values are compared to the constrained and unconstrained RHF results, and experimental values.

The constrained variational method is very sensitive to the basis set, and unreliable as a method to give accurate one-electron molecular properties, except *via* the MOM.

## Introduction

A constrained variational method determines a wavefunction for a molecule that satisfies an energy variational extremum condition and a finite number of imposed conditions [1-8]. If there is a true energy extremum, the constraints reduce the variational degrees of freedom of the wavefunction and raise the energy, and the success of a constrained true energy extremum method in improving the overall quality of the wavefunction measures how unreliable the energy is as a measure of the overall quality of a wavefunction to give good one-electron expectation values.

Only diagonal constraints are considered, where for a trial wavefunction  $\Psi$

$$\delta \mathcal{E} \equiv \delta \langle \Psi | H | \Psi \rangle = 0$$

with

$$\langle \Psi | \Psi \rangle = 1$$

and constraint conditions

$$\langle \Psi | M_i | \Psi \rangle = \mu_i \quad i = 1, \dots, s$$

with  $M_i$  the set of molecular electronic operators, and  $\mu_i$  a set of externally determined (theoretical or experimental) expectation values. Introducing the

Lagrange multipliers  $\lambda_q$  and replacing the real Hamiltonian by a fictitious Hamiltonian [1,2,7]

$$H' = H + \sum_q \lambda_q (M_q - \mu_q)$$

gives *constrained*-RHF equations,

$$\sum_j^m F'_{ij} c'_{j\mu} = \sum_\nu^n \sum_j^m \langle \chi_i | \chi_j \rangle c'_{j\nu} \mathcal{E}'_{\nu\mu}$$

where

$$F'_{ij} = F_{ij} + \sum_q \lambda_q \langle \chi_i | M_q - \frac{\mu_q}{2n} | \chi_j \rangle$$

and the Lagrange Multipliers are determined from

$$2 \sum_\nu^n \sum_{ij}^m \langle \chi_i | M_q - \frac{\mu_q}{2n} | \chi_j \rangle c'_{i\nu} c'_{j\nu} = 0.$$

The  $M_q$  are assumed Hermitean and  $\mathcal{E}'_{\mu\nu}$  is required to be diagonal so the constrained-RHF equations become

$$\sum_j^m F'_{ij} c'_{j\mu} = \sum_j^m \langle \chi_i | \chi_j \rangle c'_{j\mu} \mathcal{E}'_{\mu\mu} \quad (1)$$

and the unconstrained basis set  $\{\chi_i\}$  is transformed

\* *Theoretical Chemistry Department, University of Oxford, 1 South Parks Road, Oxford, OX1 3TG*

† *Department of Chemistry, McGill University, Montreal 110, Quebec, Canada (also present address for M.A.W.)*

to an orthonormal basis set  $\{\theta_i\}$ , so that

$$\sum_j^m \bar{F}_{ij} \bar{c}_{j\mu} = \bar{c}_{i\mu} \epsilon_{\mu}$$

gives the pseudo-eigenvalue problem to be solved iteratively. The solution is complicated by the  $\lambda_q$  constraints.

The *parameterization technique* [8] is used. An initial set of  $\lambda_q$  are chosen, and the *totally* determined equations

$$\sum_j^m \bar{F}'_{ij} \bar{c}'_{j\mu} = \bar{c}'_{i\mu} \epsilon'_{\mu}$$

solved, where

$$\bar{F}'_{ij} = \bar{F}_{ij} + \sum_q^s \lambda_q \langle \theta_i | M_q - \frac{\mu_q}{2n} | \theta_j \rangle.$$

The equations are solved iteratively using the quantity

$$2 \sum_{\nu}^n \sum_{ij}^m \langle \theta_i | M_q - \frac{\mu_q}{2n} | \theta_j \rangle \bar{c}'_{i\nu} \bar{c}'_{j\nu}$$

for each constraint operator to determine the new  $\lambda_q$ . Each constraint is solved for an optimum  $\lambda_q$ , and then  $\lambda_{q+1}$  calculated with  $\lambda_q$  constant [9].

Very few constrained-RHF wavefunctions have been reported, and no conclusion about the effectiveness of the method could be arrived at [1,5,10,11]. Therefore a systematic investigation was undertaken to study the effect of a number of one-electron constraints on minimum basis, single configuration wavefunctions of several small molecules, *HF*, *LiH*, *N<sub>2</sub>* and *CO*, in the hope of arriving at definite conclusions about the usefulness of the method in producing good one-electron expectation values.

### The Constraints

- (a) Kinetic energy  $\langle T \rangle$ , with experimental reference values from [12]

$$\langle T \rangle = -E$$

where  $E$  is the total energy;

- (b) Dipole moment  $\mu$  where  $\langle x_n \rangle = \langle \sum_i^{2n} x_{ni} \rangle$ ,

and  $x_{ni}$  is the  $x$ -co-ordinate of electron  $i$  from the centre of nuclear charge, and the  $\mu$  are experimental [13-15];

- (c) Nuclear diamagnetic shielding constant  $\sigma_{\alpha}^d(\alpha)$

where  $\langle r_{\alpha}^{-1} \rangle = \langle \sum_i^{2n} r_{i\alpha}^{-1} \rangle$  and  $r_{i\alpha}$  is the

distance between the  $\alpha$  nucleus and the  $i^{\text{th}}$  electron; the  $\sigma_{\alpha}^d(\alpha)$  are either theoretical or experimental [16,17];

- (d) Nuclear electronic attraction energy  $V_{ne}$  where

$$\langle V_{ne} \rangle = -\sum_{\alpha} Z_{\alpha} \langle \sum_i^{2n} r_{i\alpha}^{-1} \rangle,$$

and the values are calculated using (c);

- (e) Total single electron energy

$$\langle T + V_{ne} \rangle = \langle \sum_i^{2n} (-\frac{1}{2} \nabla^2 - \sum_{\alpha} Z_{\alpha} r_{i\alpha}^{-1}) \rangle;$$

- (f) Electric field at a nucleus

$$\langle E_{\alpha} \rangle = \langle \sum_i^{2n} \frac{x_{i\alpha}}{r_{i\alpha}^3} \rangle - \frac{Z_{\beta}}{R_{\beta\alpha}^2} = E_{\alpha}^e + E_{\alpha}^n$$

where  $\alpha$  nucleus is the origin,  $R_{\beta\alpha}$  the inter-nuclear distance, and  $x_{i\alpha}$  is  $x_i - x_{\alpha}$ , the difference between the electron and nuclear co-ordinates; constraint condition,  $\langle E_{\alpha} \rangle = 0$ .

- (g) Hellman-Feynman forces [18,19],  $F$ , where  $\langle F \rangle = -Z_{\alpha} \langle E_{\alpha} \rangle - Z_{\beta} \langle E_{\beta} \rangle$ . The approximate wavefunctions, unlike Hartree-Fock wavefunctions, do not satisfy  $\langle F \rangle = 0$  hence it is a constraint;

- (h) Electric field gradient at a nucleus [6]  $q_{\alpha}$ , with

$$q_{\alpha} = \frac{2Z_{\beta}}{R_{\beta\alpha}^3} - \langle \sum_i^{2n} \frac{3x_{i\alpha}^2 - r_{i\alpha}^2}{r_{i\alpha}^5} \rangle = q_{\alpha}^e + q_{\alpha}^n$$

and the expectation values are experimental [6] for *Li*, *H*, *O* and *N* but theoretical [6] for *F* and *C*;

- (i) Molecular quadrupole moments  $\theta$ . For a diatomic molecule

$$\theta = \theta_{\gamma}^e + \theta_{\gamma}^n,$$

and by choosing the origin at the centre of nuclear charge, the molecular quadrupole moment becomes  $\theta_n^e + \theta_n^n$  [20]. The values are experimental [6];

- (j) Diamagnetic susceptibility,  $\chi_{\gamma}^d$  is chosen so that

$$\chi_{\gamma}^d = -\langle \sum_i^{2n} r_{\gamma i}^2 \rangle = -\langle r_{\gamma}^2 \rangle$$

where  $r_{\gamma i}$  is the distance from co-ordinate origin to electron  $i$ . With the origin at centre of nuclear charge  $\chi_{\gamma}^d$  becomes



$$\chi_n^d = -\langle r_n^2 \rangle$$

The expectation values are experimental [6] and theoretical.

### Basis Sets

Most previous calculations used Slater type functions (STO) or Gaussian type functions (GTO), or

STO expanded in GTO [21,22], in which case the problem of weighting occurs. Herein several expectation values were calculated for HF using RHF wavefunctions with minimum basis set STO expanded in GTO:—

- (a) PL-4G weighted expansions from Page and Ludwig [24];
- (b) HSP-4G and HSP-2G unweighted expansions of four- and two-GTO from Hehre *et al.* [23];

Table 1: Comparison of constrained Roothaan-Hartree-Fock wavefunctions of HF in a BLMO basis

Constraint Operator	Criterion	Rank <sup>c</sup> with respect to			Number <sup>d</sup> of Properties Improved	C' <sub>C</sub>	C' <sub>B</sub>	-E(au)
		C' <sub>C</sub>	C' <sub>B</sub>	E				
—	—	8	13	0	—	6.429	2.312	104.469
-½V <sup>2</sup>	a	24	24	23	2/9	8.667	3.558	104.329
	b	21	16	22	3/9	7.548	2.565	104.401
r <sub>F</sub> <sup>-1</sup>	a	20	18	20	3/9	7.491	2.587	104.414
	b	15	0	11	5/9	6.695	1.933	104.453
r <sub>H</sub> <sup>-1</sup>	a	11	3	8	6/9	6.631	2.002	104.462
	b	17	8	13	5/9	6.847	2.069	104.452
χ <sub>n</sub>	a	10	6	6	6/9	6.584	2.040	104.465
	b	12	5	7	6/9	6.663	2.020	104.462
θ <sub>n</sub> <sup>e</sup>	a	23	23	23	3/9	7.906	3.105	104.388
	b	19	15	15	4/9	7.226	2.444	104.426
r <sub>n</sub> <sup>2</sup>	a	25	25	24	1/9	9.880	6.830	104.329
	b	26	26	26	1/9	10.824	7.718	104.277
x <sub>F</sub> r <sub>F</sub> <sup>3</sup>	a	0	17	18	1/9	5.583	2.570	104.420
	b	1	19	19	1/9	5.594	2.591	104.417
3x <sub>F</sub> <sup>2</sup> -r <sub>F</sub> <sup>2</sup> r <sub>F</sub> <sup>5</sup>	a	6	14	4	2/9	6.417	2.434	104.470
	b	9	9	3	7/9	6.450	2.222	104.469
x <sub>H</sub> r <sub>H</sub> <sup>3</sup>	a	14	4	12	6/9	6.694	2.006	104.453
	b	18	10	14	5/9	6.986	2.223	104.438
3x <sub>H</sub> <sup>2</sup> -r <sub>H</sub> <sup>2</sup> r <sub>H</sub> <sup>5</sup>	a	4	7	5	7/9	6.385	2.043	104.467
	b	5	11	1	7/9	6.416	2.266	104.469
V <sub>ne</sub>	a	22	22	21	4/10	7.572	2.662	104.408
	b	16	1	9	6/10	6.701	1.967	104.454
T+V <sub>ne</sub>	a	13	2	10	6/10	6.689	1.995	104.453
	b	7	12	2	7/10	6.424	2.275	104.469
F	a	2	20	16	2/10	5.612	2.643	104.425
	b	3	21	17	2/10	5.619	2.658	104.422

Note: This is an example of the type of table used in the analysis discussed in the text. Notes (a) and (b) give an idea of the overall sensitivity of the various criteria of wavefunction quality to various reference values of the constraining operators.

- (a) Values of the criteria calculated with theoretical reference values from the best available recently determined wavefunctions.
- (b) Values of the criteria calculated with experimental reference values from the best available experimental results with the

$$C_C^{\ell'} = \left[ \sum_i \left\{ \frac{m_i^{\rho} - \mu_i}{\sigma_i^C} \right\}^2 \right]^{1/2}$$

which excludes the constrained  $j$  term which constrains  $\Psi^{(\ell)}$ . Similarly for  $C_B^{\ell'}$ . For unconstrained wavefunctions  $C = C'$ .

- (c) Number of improved properties: fraction of the total number of independent unconstrained properties which are improved.
- (d) The numerical rank indicates the number of wavefunctions with lower values of  $C'_C$ ,  $C'_B$  or  $E$ .

(c) OTH-4G, *unweighted* expansions of four-GTO from O-hata *et al.* [25].

The results [6] show that a weighting [26,27] of  $\omega = r^{-1}$  improves  $\langle r_F^{-1} \rangle$  and  $\langle r_H^{-1} \rangle$ ;  $\omega = r^{-2}$  improves  $\langle \frac{3x_F^2 - r_F^2}{r_F^5} \rangle$ ; but best value of  $q_H$  is from the *unweighted* HSP-4G, as are the  $\langle x_n \rangle$ ,  $\langle \theta_{CM} \rangle$  and  $\langle r_{CM}^2 \rangle$  best values; weightings of  $\omega = r$  and  $\omega = r^2$  are poor for all molecular expectation values.

The Slater orbital exponents also effect the significance of the weightings. A series of calculations on *HF* using a GTO expansion of STO's with Burns [27], Slater [28] and BLMO [29] (table 1) exponents with weighted and *unweighted* expansions showed that

- the most accurate  $\langle -\frac{1}{2}\nabla^2 \rangle$ ,  $\langle r_F^{-1} \rangle$  and  $\langle r_H^{-1} \rangle$  are given by Slater's  $\zeta$ , the worst by Burns'  $\zeta$  and poor by BLMO  $\zeta$ ;
- for  $\langle x_n \rangle$ ,  $\langle \theta_n^e \rangle$  and  $\langle r_n^2 \rangle$  the best are with Burns  $\zeta$ , the worst are with Slater  $\zeta$ ;
- for  $\langle \frac{x_F}{r_F^3} \rangle$ ,  $\langle \frac{3x_F^2 - r_F^2}{r_F^5} \rangle$  and the equivalent H expectation values, BLMO  $\zeta$  are the best; the worst results are for Slater  $\zeta$ ;
- there is only a rough correlation between  $\omega$  and expectation values in the same region of wavefunction;
- Two-GTO wavefunctions are always very poor;
- The best *overall* RHF wavefunction is a BLMO  $\zeta$  basis and *unweighted* or  $r^{-1}$  weighted GTO.

In *CO* however quite *different* trends were discovered! They were different again in *LiH*! Analysing all the results suggested

- for  $\langle -\frac{1}{2}\nabla^2 \rangle$ ,  $\langle r^{-1} \rangle$ ,  $\langle -V_{ne} \rangle$  and  $\langle T + V_{ne} \rangle$  use Slater  $\zeta$ ,
- for  $\langle x^3/r^3 \rangle$ ,  $\langle \frac{3x^2 - r^2}{r^5} \rangle$  use BLMO  $\zeta$ ,
- for  $\langle x_n \rangle$ ,  $\langle \theta_n^e \rangle$  and  $\langle r_n^2 \rangle$  no exponent is successful, because the wavefunction with a basis set suiting these expectation values is distorted by the RHF calculation which depends explicitly on

$$\langle \chi_i | -\frac{1}{2}\nabla^2 | \chi_j \rangle \quad \text{and} \quad \langle \chi_i | r^{-1} | \chi_i \rangle.$$

#### Sensitivity of a Constrained Wavefunction to the Accuracy of the Expectation Value of the Constraint Operator

If the error in the experimental value of  $\langle -\frac{1}{2}\nabla^2 \rangle$  is  $\pm 1\%$ , the error in the  $\langle r_n^2 \rangle$  is 9% on Slater  $\zeta$  or BLMO  $\zeta$ , but the distribution among the various expectation values is non-uniform. Small variations in  $\langle -\frac{1}{2}\nabla^2 \rangle$ ,  $\langle r_F^{-1} \rangle$ ,  $\langle r_H^{-1} \rangle$ ,  $\langle V_{ne} \rangle$ ,  $\langle T + V_{ne} \rangle$ ,

$\langle x_H/r_H^3 \rangle$  and  $\langle 3x_H^2 - r_H^2/r_H^5 \rangle$  give large variations in the unconstrained expectation values: while errors in  $\langle x_F/r_F^3 \rangle$ ,  $\langle \theta_n^e \rangle$  and  $\langle F \rangle$  give only small changes.

Variations in the reference value of the constraint also effect the resulting one-electron expectation values; all properties are insensitive to changes in  $\langle x_F/r_F^3 \rangle$  and  $\langle F \rangle$  and *vice versa*, but these constraints are interdependent;  $\langle T + V_{ne} \rangle$  and  $\langle x_H/r_H^3 \rangle$  exert a strong effect on all property values due to the inflexible nature of the wavefunction at the *H* nucleus.

The effect of imposing a constraint on a *minimum* basis set wavefunction is to cause changes of the same order of relative magnitude in the *unconstrained* expectation values as in the expectation value of the constraining operator; constraints do *not* lead to significant improvement in the *overall* quality of the RHF wavefunctions.

#### Constrained RHF Wavefunctions for *LiH*, *FH*, *CO* and *N<sub>2</sub>* [6]

If the average percentage error and energy were not good criteria for the overall quality of a wavefunction, what could be used? A *similarity function* can be defined by [6,30]

$$C^\ell = \left[ \sum_i^{N_p} \left\{ \frac{m_i^\ell - \mu_i}{\sigma_i} \right\}^2 \right]^{1/2}$$

in which  $m_i^\ell$  is the value of the  $i^{\text{th}}$  property from the  $\ell^{\text{th}}$  wavefunction,  $m_i^\ell = \langle \Psi^{(\ell)} | M_i | \Psi^{(\ell)} \rangle$ , and  $\mu_i$  is the reference value. The  $\sigma_i^{-1}$  are arbitrary and here using  $(\sigma_i^B)^2$  as the second moment about  $\mu_i$  or  $\sigma_i^C$  as the standard deviation in the distribution of the  $m_i^\ell$

$$\sigma_i = \left[ \sum_\ell^{N_i} (m_i^\ell - \eta)^2 / N_i' \right]^{1/2}$$

where for  $\sigma_i^C$ ,  $\eta = \bar{m}_i$  or for  $\sigma_i^B$ ,  $\eta = \mu_i$ , giving two  $\sigma_i$  and hence two  $C^\ell$  and

$$\bar{m}_i = \frac{N_i'}{\sum_\ell m_i^\ell / N_i'}$$

and  $N_i'$  is the number of wavefunctions *not constrained* with respect to the  $i^{\text{th}}$  property. The summations are over *all* wavefunctions. The properties used in calculating the  $C^\ell$  are  $-\frac{1}{2}\nabla^2$ ,  $\langle r^{-1} \rangle$ ,  $x_n$ ,  $\theta_n$ ,  $r_n^2$ ,  $x/r^3$  and  $(3x^2 - r^2)/r^5$ ; i.e. ten properties for *LiH*, *FH* and *CO*, and six for *N<sub>2</sub>*;  $V_{ne}$ ,  $(T + V_{ne})$  and  $F$  are not included as they contain directly the values of two or more of the other properties. A statistical analysis [31] was also performed, but distribution analyses [10] were not attempted since they require an accurate reference distribution.

Armed with  $C$  and the  $\sigma$ , we can statistically analyse the numerical results [6,33]:

- (a) in  $LiH$ ,  $(x_H/r_H^3)$  and  $\left(\frac{3x_H^2 - r_H^2}{r_H^5}\right)$  are incapable of giving good expectation values with a Slater basis, as is  $(r_H^{-1})$  in  $HF$  due to the Slater  $\zeta$  of the  $1s$  orbital; and  $(r_C^{-1})$  and  $(r_O^{-1})$  in  $CO$  with Burns  $\zeta$ 's which differ widely from the energy optimised exponents.
- (b)  $\sigma_i^B$  is 3 times larger than  $\sigma_i^C$  due to the poor behaviour of RHF wavefunctions at large  $r$ , and often becomes even bigger with a Burns  $\zeta$  due to the poor behaviour of a Burns basis at small  $r$ .
- (c) Correlation between ranking according to energy and according to the  $C$  is most alike when an energy optimized basis is used.
- (d) As a criterion of overall quality a wavefunction for one-electron operators with minimum basis set, energy is *inferior* to the  $C$ . A very good energy in a poor basis often gives a wavefunction poor for calculating one-electron properties.
- (e) Constrained RHF wavefunctions do not exhibit significant improvement in overall quality over the *unconstrained* RHF wavefunctions, except where the basis selected is very poor. When there is improvement the cost in energy is insignificant for energetically good bases, and substantial when the basis is energetically poor, when it is best to ignore the energy and to determine the wavefunction directly from the constraint conditions [32].
- (f)  $\langle -\frac{1}{2}\nabla^2 \rangle$  correlates poorly with any criteria of overall quality of the wavefunction, and correlates with  $\langle r^{-1} \rangle$  in 9 out of 12 constrained wavefunctions;  $\langle r^{-1} \rangle$  and  $\langle \theta_n^e \rangle$  correlate;  $\langle r^{-1} \rangle$  correlates with  $\langle \frac{3x^2 - r^2}{r^5} \rangle$  at the nucleus opposite to the  $\langle r^{-1} \rangle$  constraint;  $x_n$  improves >50% of the unconstrained properties;  $\theta_n^e$  improves  $\langle -\frac{1}{2}\nabla^2 \rangle$  and  $\langle x/r^3 \rangle$ ;  $\langle r_n^2 \rangle$  correlates badly with criteria of overall quality of the wavefunction; etc. Multiple constraints are no more effective than single constraints, and cause a large increase in the energy and in computer time [9].

### Constrained Neglect of Diatomic Differential Overlap (NDDO-RHF) Method [6,33]

The expectation values are sensitive to the weighting function used to determine the GTO expansions of STO, as well as the STO exponents,  $\zeta$ . Calculations were performed on  $HF$  for different STO exponents and GTO weightings:

- (a) for  $\langle -\frac{1}{2}\nabla^2 \rangle$  and  $\langle r_F^{-1} \rangle$ , expectation values

are best with STO and Slater  $\zeta$  (as for RHF wavefunctions); but for  $\langle r_H^{-1} \rangle$  the expectation values is best with BLMO wavefunctions);

- (b)  $\langle \theta_n^e \rangle$  and  $\langle r_n^2 \rangle$  are best with Burns wavefunctions;
- (c)  $\langle x_F/r_F^3 \rangle$ ,  $\langle (3x_F^2 - r_F^2)/r_F^5 \rangle$  and the hydrogen equivalents are best with STO, whereas STO is the worst for RHF expectation values of these operators;
- (d) there is a rough correlation between the weighting functions for the GTO expansion and expectation values of properties weighted in the same region of the wavefunction;
- (e) 2-GTO are much worse than 4-GTO expansions;
- (f) The best overall NDDO-RHF wavefunction has an STO basis, with either *unweighted*, or  $r^{-1}$  or  $r^{-2}$  weighted GTO expansions;
- (g) The deviation of predicted expectation values from experiment is much greater with NDDO-RHF than with RHF wavefunctions, except for the dipole moment,  $\mu$ , which is excellently predicted by constrained NDDO-RHF wavefunctions.

Similar results are obtained with  $CO$  and  $LiH$ , and overall the best basis for *constrained* NDDO-RHF is one of STO's with Slater  $\zeta$ . In contrast the RHF wavefunction best basis was one with BLMO exponents.

**Constrained NDDO-RHF with RHF expectation values as constraint reference values [6]:** The  $1e$  expectation values calculated with lowest energy Slater determinant wavefunction for a given basis are used as reference values; these are the *unconstrained* RHF values.

Constrained NDDO-RHF calculations on  $LiH$  used Slater and BLMO bases, on  $CO$  used Slater (table 2) and Clementi bases and on  $N_2$  a Slater basis. The number of *variational* degrees of freedom in each case is 4, 6 and 2, always less than the number of properties contributing to the statistical survey. With the RHF expectation values as constraints, the energy variation is a good criterion of the overall quality of the wavefunction, and a constraint improves the expectation values of over 50% of the constraint operators. Multiple constraints give more improvement in contrast to the behaviour of constrained RHF wavefunctions:

- (a)  $(\frac{1}{2}\nabla^2, r_n^2)$ ,  $(r_n^{-1}, \theta_n^e)$  and  $(r_n^{-1}, r_n^2)$  lead to constrained NDDO-RHF wavefunctions that give the RHF expectation values and energy;
- (b) In no case did a constrained NDDO-RHF wavefunction converge to the exact RHF wavefunction or energy;
- (c)  $(-\frac{1}{2}\nabla^2, \theta_n^e, r_n^2)$  on  $LiH$  with Slater basis gives 99.99% of the RHF energy, while  $(x_{Li}/r_{Li}^3)$  is 96%, and  $r_{Li}^{-1}$ ,  $r_H^{-1}$  and  $x_n$  are 99.8% of the RHF value;

Table 2: Constrained NDDO-RHF wavefunctions for CO. Basis: Slater

	Constraint	Rank <sup>d</sup>		Rank <sup>d</sup>	E	Percentage Properties Improved <sup>e</sup>	Property Rank <sup>a</sup>											
		C <sub>C</sub>	C <sub>B</sub>				1	2	3	4	5	6	7	8	9	10		
	0 0 0	69	5.75	70	3.01	47	-134.2322	0	56	78	72	72	60	1	76	51	48	55
Kinetic energy	1 0 0	67	5.57	50	2.33	75	-134.0243	66	b	38	36	44	54	19	84	17	88	12
diamagnetic shielding	2 0 0	30	4.42	0	1.89	28	-134.3501	77	44	b	50	46	45	21	34	28	57	5
	3 0 0	43	4.80	14	2.03	40	-134.2730	77	10	13	b	9	38	46	57	10	71	16
dipole moment	4 0 0	36	4.63	12	2.02	29	-134.3253	77	20	34	10	b	34	56	55	5	62	26
molecular quadrupole moment	5 0 0	18	3.87	55	2.41	21	-134.3801	77	28	46	44	16	b	80	23	88	45	37
diamagnetic susceptibility	6 0 0	64	5.39	61	2.66	41	-134.2723	88	53	72	71	66	56	b	71	48	49	41
field (at C)	7 0 0	24	4.20	36	2.19	52	-134.2063	66	69	59	60	53	28	9	b	50	50	30
field gradient (at C)	8 0 0	55	5.15	24	2.10	42	-134.2632	66	27	27	46	41	76	17	73	b	61	18
field (at O)	9 0 0	83	6.76	87	4.09	65	-134.0963	0	85	92	93	81	61	16	83	67	b	72
field gradient (at O)	10 0 0	48	4.98	44	2.24	30	-134.3193	77	49	56	64	55	49	4	65	35	55	b
nuclear attraction	11 0 0	50	5.01	25	2.10	49	-134.2242	80	5	7	7	10	41	45	66	7	75	15
total electronic	12 0 0	38	4.63	3	1.96	27	-134.3555	80	37	19	48	43	39	23	58	25	53	1
F	13 0 0	74	6.27	78	3.46	50	-134.2206	10	68	88	75	78	67	10	89	55	41	68
c	2 3 0	47	4.96	22	2.08	44	-134.2364	75	8	b	b	13	42	43	62	11	72	11
	1 2 3	60	5.25	37	2.19	61	-134.1120	71	b	b	b	18	47	36	70	9	84	2
	1 11 0	62	5.33	43	2.22	64	-134.1067	66	b	5	5	21	46	35	78	13	81	0
	1 4 0	54	5.12	42	2.21	56	-134.1757	75	b	28	32	b	36	53	64	1	77	22
	1 6 0	80	6.54	68	2.98	88	-133.7227	62	b	73	61	60	73	b	92	38	90	51
c	4 11 0	41	4.74	18	2.06	34	-134.2968	77	13	32	18	b	35	58	56	3	67	23
	11 5 0	20	3.94	54	2.40	24	-134.3591	66	15	10	11	3	b	93	21	84	51	19
	11 6 0	81	6.58	67	2.95	87	-133.8138	55	0	63	56	58	91	b	94	26	85	69
c	1 6 5	95	7.64	95	5.13	96	-132.8535	0	b	94	78	84	b	b	87	96	94	95
	6 5 0	84	6.81	92	4.94	77	-133.9970	25	62	97	85	92	b	b	50	97	40	90
	4 5 0	15	3.82	52	2.36	18	-134.3857	75	21	18	25	b	b	91	15	85	46	20
	4 13 0	42	4.75	17	2.06	31	-134.3174	77	55	21	42	b	32	61	80	0	32	25
	4 10 8	49	4.98	20	2.07	45	-134.2338	57	11	36	15	b	69	47	60	b	63	b
c	10 8 0	61	5.32	35	2.17	48	-134.2251	50	30	42	51	50	82	15	79	b	59	b
	7 9 0	51	5.04	72	3.09	68	-134.0674	62	94	47	81	64	24	0	b	63	b	47
	4 7 9	27	4.30	63	2.70	58	-134.1243	57	86	81	67	b	20	71	b	21	b	27
	1 13 0	82	6.63	60	2.65	84	-133.8904	55	b	17	2	23	64	32	97	6	54	29
	1 10 0	65	5.50	48	2.29	70	-134.0533	62	b	26	27	38	52	24	82	14	87	b
	4 10 0	34	4.57	8	1.99	32	-134.3074	75	18	40	14	b	31	60	53	15	58	b

K  
E  $r_o^{-1}$   $\theta$   $x_c/r_3$   $x_o/r_3$   
 $r_c^{-1}$   $\chi_{co}$   $r_n^2$   $q_c$   $q_o$

Note: This is an example of the type of table used to develop the analysis in the text: i.e. constrained NDDO-RHF wavefunctions for CO.

(a) The rankings are relative to all unconstrained and constrained RHF, NDDO-RHF and MOM wavefunctions with the same basis set.

A property rank close to unity means that constraining property A will give a good expectation value for property B.

(b) Signifies the constraint.

(c) Signifies incomplete convergence, with a divergence in the 5th significant figure compared to the reference value.

(d) The rank is the number of wavefunctions with lower values of C<sub>B</sub>, C<sub>C</sub> or E, expressed as a percentage of the total number of wavefunctions in the set.

(e) The percentage of properties improved over their values when unconstrained is expressed as the total number of independent unconstrained expectation values, for each constrained wavefunction, which are improved.

(d)  $(-\frac{1}{2}\nabla^2, \theta_n^e, r_n^2)$  on CO with Slater basis gives 99.93% of the RHF energy, while  $r_c^{-1}$  and  $r_o^{-1}$  are 99.9%, and  $(x_c/r_c^3)$  and  $((3x_c^2 - r_c^2)/r_c^5)$  are 98% of the RHF value. All other expectation values are quite inaccurate.

Constrained NDDO-RHF calculations with empirical or theoretical expectation values for the constraints [6,34]: While the unconstrained NDDO-RHF wavefunction gives a high energy for LiH, HF, CO and N<sub>2</sub>, the constrained NDDO-RHF gives comparable results to

the RHF theory, and 75% of all  $\langle 1e \rangle$ , with single and multiple constraints, are improved. There is a significant improvement in the energy prediction.

In *LiH* and *CO* for BLMO or Clementi basis,  $(x_n)$  gives a constrained NDDO-RHF wavefunction superior to RHF, while *CO* (Burns) gives lowest energy singly constrained wavefunction and a good quality wavefunction. However  $(\theta_n^2)$  is a good constraint in *N<sub>2</sub>* and *CO*, but very bad in *LiH* and *FH*;  $(-\frac{1}{2}\nabla^2)$  is always a poor constraint, as is  $x/r^3$ ;  $r_H^{-1}$ ,  $r_C^{-1}$  and  $r_O^{-1}$  are good constraints in *LiH* and *CO* and  $((3x^2 - r^2)/r^5)$  lowers the energy; the Hellman-Feynman operator ( $F$ ) is ineffective.

Multiple constraints do not significantly improve the effect of the constraints individually in contrast to the results for multiple constraints from RHF wavefunctions, above. This behaviour is caused by the incompatibility of the constraint conditions when applied to severely limited basis sets. Therefore a method could be developed to optimize a function dependent on several constraints to give the exact values of the constraints. The wavefunction would then be as accurate as an extended basis set.

### Constrained Maximum Overlap Method [6, 35]

While [37]

$$\langle \chi_i | F | \chi_j \rangle \equiv K \langle \chi_i | \chi_j \rangle$$

has been suggested, the maximum overlap method (MOM) [38] is not an energy extremum method. The method is poor for atomic orbitals of different energies [39], and for heteratomic diatomics using  $p_\pi$ -orbitals. The use of constraints is to overcome these failures: a *complete minimum* basis set was used for each molecule; inclusion of 1s orbitals permits direct comparison of constrained MOM results with those from RHF and NDDO-RHF.

Method:

The constrained MOM finds the Slater determinant  $\Psi$ 's which optimize the total overlap [40]

$$\delta \Gamma = 0$$

with

$$\langle \Psi | \Psi \rangle = 1$$

and

$$\langle \Psi | M_q | \Psi \rangle = \mu_q \quad q = 1, \dots, s$$

where  $M_q$  are a set of operators dependent on the

co-ordinates of the electrons, and  $\mu_q$  are the expectation values.

By analogy with the RHF and NDDO-RHF equations, the operator

$$G = \sum_k^{2n} g(\bar{r}_k) = \sum_k^{2n} \left( \sum_i^m |\chi_i(\bar{r}_k)\rangle \langle \chi_i(\bar{r}_k)| \right)$$

where  $\bar{r}_k$  represents  $(x_k, y_k, z_k)$ , the  $k^{\text{th}}$  electron co-ordinates; hence

$$\Gamma = \langle \Psi | G | \Psi \rangle$$

giving canonical maximum overlap equations

$$\sum_j^m g_{ij} c_{j\mu} = \sum_j^m \langle \chi_i | \chi_j \rangle c_{j\mu} d_\mu$$

which is identical with equation (1).

Defining a fictitious total overlap operator  $G'$

$$G' = G + \sum_q^s \lambda_q (M_q - \mu_q)$$

requiring

$$d\Gamma = \delta \langle \Psi | G' | \Psi \rangle = 0$$

with

$$\langle \Psi | M_q - \mu_q | \Psi \rangle = 0; \quad q = 1, \dots, s$$

gives

$$\sum_j^m g'_{ij} c'_{j\mu} = \sum_j^m \langle \chi_i | \chi_j \rangle c'_{j\mu} d'_\mu$$

Since maximum overlap equations are true eigenvalue equations, no iterative self-consistent step is required and hence the time consuming parts of the RHF and NDDO-RHF methods are avoided.

The unconstrained problem is solved giving canonically orthonormal functions  $\theta_\sigma$ , and all operators expressed as a matrix in the basis  $\{\chi_i\}$  are transformed to the basis  $\{\theta_\sigma\}$ . The matrix

$$\begin{aligned} \langle \theta_\sigma | g' | \theta_\sigma \rangle &= \langle \theta_\sigma | g | \theta_\sigma \rangle + \lambda \langle \theta_\sigma | M - \frac{\mu}{2n} | \theta_\sigma \rangle \\ &= \delta_{\sigma\tau} d_\sigma + \lambda \langle \theta_\sigma | M - \frac{\mu}{2n} | \theta_\sigma \rangle \end{aligned}$$

is evaluated for  $\lambda$ , and diagonalized to give the eigenvectors  $\phi_\mu$  as linear combinations of  $\{\theta_\sigma\}$ .

$$2 \sum_{\mu}^n \sum_{\sigma, \tau}^m \bar{c}'_{\sigma\mu} \bar{c}'_{\tau\mu} \langle \theta_{\sigma} | M - \frac{\mu}{2n} | \theta_{\tau} \rangle$$

is solved to give a new  $\lambda$ , and the process repeated until the constraint condition is satisfied.

Constrained MOM calculations: RHF expectation values as reference values for the constraints (table 3): While the *unconstrained* MOM wavefunction gives a much poorer energy and expectation values than the *unconstrained* NDDO-RHF method, all constraints improve the MOM wavefunction, and *multiple constraints* give better wavefunctions than single constraints.

Table 3: Constrained (RHF reference values) maximum overlap wavefunctions for CO. Basis: Slater RHF expectation values as constraint

	Constraint	Rank <sup>d</sup> <sub>C<sub>C</sub></sub>		Rank <sup>d</sup> <sub>C<sub>B</sub></sub>		Rank <sup>d</sup>	E	Percentage Properties Improved <sup>e</sup>	Property Rank <sup>a</sup>											
		1	2	3	4				5	6	7	8	9	10						
	0 0 0	98	8.00	98	5.31	93	-134.0155	0	93	96	98	97	91	97	60	16	38	96		
Kinetic Energy	1 0 0	89	7.49	89	4.79	98	-133.8908	66	b	98	76	83	83	82	98	3	94	83		
diamagnetic shielding	2 0 0	91	7.50	93	4.85	96	-133.9046	66	97	b	90	85	95	85	78	1	29	88		
	3 0 0	71	4.85	66	2.81	83	-134.1318	77	14	62	b	20	81	57	45	56	92	66		
dipole moment	4 0 0	35	3.62	33	2.16	38	-134.3543	88	72	50	54	b	33	27	38	62	3	39		
molecular quadrupole moment	5 0 0	81	6.05	84	4.37	74	-134.2081	77	87	90	84	75	b	63	49	94	41	84		
diagramagnetic susceptibility	6 0 0	15	1.89	15	1.18	15	-134.4308	88	48	35	25	27	4	b	34	30	0	54		
field (at C)	7 0 0	94	7.72	94	5.04	94	-133.9855	66	95	74	94	91	85	91	b	24	36	98		
field gradient (at C)	8 0 0	96	7.93	96	5.24	91	-134.0208	66	91	94	96	93	97	95	63	b	40	86		
field (at O)	9 0 0	93	7.51	91	4.81	86	-134.0764	88	82	92	92	95	93	93	56	15	b	92		
field gradient (at O)	10 0 0	72	5.24	76	3.60	61	-134.2946	88	80	76	80	68	70	72	58	71	12	b		
nuclear attraction	11 0 0	74	5.43	71	3.36	84	-134.0796	70	68	47	29	47	68	59	87	49	98	69		
total electronic	12 0 0	28	3.25	23	1.87	18	-134.4207	90	12	56	35	25	22	12	0	66	18	32		
F	13 0 0	88	7.24	88	4.54	88	-134.0643	90	85	80	86	89	89	89	23	20	5	90		
	2 3 0	69	4.81	62	2.78	81	-134.1550	75	59	b	14	16	72	55	43	52	96	62		
	c 1 2 3	45	3.93	32	2.14	45	-134.3461	71	b	b	b	8	62	44	27	54	63	56		
	1 11 0	30	3.28	25	1.88	20	-134.4170	89	b	54	41	22	25	14	3	64	30	33		
	1 4 0	33	3.58	27	1.98	44	-134.3473	75	b	23	7	b	27	25	7	60	60	43		
	1 6 0	11	1.87	5	1.10	11	-134.4335	87	b	27	11	31	0	b	9	28	21	52		
	c 4 2 3	50	4.00	45	2.40	64	-134.2896	57	42	b	b	b	20	31	72	50	80	45		
	4 11 0	42	3.89	42	2.25	57	-134.3022	77	25	17	5	b	29	23	40	58	76	47		
	11 5 0	47	3.94	55	2.59	79	-134.1909	66	63	49	37	16	b	17	74	47	90	77		
	11 6 0	8	1.85	8	1.11	8	-134.4345	100	2	33	19	43	6	b	10	5	25	41		
	1 5 6	10	1.87	6	1.10	10	-134.4335	85	**	29	13	39	b	b	12	26	20	50		
	6 5 0	13	1.87	13	1.18	13	-134.4310	87	46	37	21	41	b	b	36	18	1	49		
	4 5 0	18	2.40	18	1.48	28	-134.3986	87	70	9	58	b	b	8	5	39	7	64		
	4 9 10	5	1.43	10	1.12	0	-134.4812	85	57	1	52	b	8	0	61	b	9	b		
	8 10 0	64	4.50	72	3.48	59	-134.2955	100	76	88	82	81	12	70	25	b	10	b		
	7 9 0	86	7.21	86	4.51	89	-134.0447	87	89	70	88	87	87	87	b	22	b	94		
	c 11 5 6	6	1.82	11	1.12	6	-134.4367	100	6	41	28	50	b	b	20	0	16	37		

K  
E  $r_o^{-1}$   $\theta$   $x_c/r^3$   $x_o/r^3$   
 $r_c^{-1}$   $X_{co}$   $r_n^2$   $q_c$   $q_o$

Note: Another example of the type of table used in the development of the analysis in the text; this time, constrained MOM wavefunctions for CO.

- (a) The rankings are relative to all unconstrained and constrained RHF, NDDO-RHF and MOM wavefunctions with the same basis set. A property rank close to unity means that constraining property A will give a good expectation value for property B.
- (b) Signifies the constraint.
- (c) Signifies incomplete convergence, with a divergence in the 5th significant figure compared to the reference value.
- (d) The rank is the number of wavefunctions with lower values of C<sub>B</sub>, C<sub>C</sub> or E, expressed as a percentage of the total number of wavefunctions in the set.
- (e) The percentage of properties improved over their values when unconstrained is expressed as the total number of independent unconstrained expectation values, for each constrained wavefunction, which are improved.

The double constraint  $(r_n^e, \theta_n^e)$  gives  $\psi$  identical with that from  $\langle \theta_n^e \rangle$ ; but  $(r_n^{-1}, \theta_n^e)$  gives the RHF energy and expectation value; the  $\psi$  is completely determined. In several cases multiple constraints give the RHF energy and expectation values:  $(-\frac{1}{2}\nabla^2, \theta_n^e, r_n^e)$  on *LiH* with STO gives 99.98% of RHF

energy. While expectation values are comparable to those from NDDO-RHF, the energy is always better; and compared to their effectiveness in NDDO-RHF, the operators  $(-\frac{1}{2}\nabla^2)$ ,  $(r^{-1})$ ,  $(V_{ne})$  and  $(T+V_{ne})$  are very effective in MOM for STO, BLMO or Burns basis in all molecules yielding 99.9% of the RHF

Table 4: Constrained maximum overlap wavefunctions for CO. Basis: Slater  
Best available experimental or theoretical values as constraint

	Constraint	Rank <sup>d</sup> <sub>C<sub>C</sub></sub>		Rank <sup>d</sup> <sub>C<sub>B</sub></sub>		E	Percentage Properties Improved <sup>e</sup>	Property Rank <sup>a</sup>										
		1	2	3	4			5	6	7	8	9	10					
	0 0 0	89	7.03	90	4.45	76	-134.0155	0	88	89	94	95	89	52	43	72	2	81
Kinetic Energy	1 0 0	90	7.11	80	3.56	92	-133.4439	77	b	82	68	73	78	6	93	47	96	76
diamagnetic shielding	2 0 0	72	6.26	84	3.82	81	-133.9193	66	92	b	86	86	90	34	0	61	9	79
	3 0 0	35	4.60	38	2.19	60	-134.1168	88	31	75	b	33	68	28	1	31	74	40
dipole moment	4 0 0	16	3.85	15	2.03	25	-134.3562	77	65	68	38	b	27	65	2	23	33	6
molecular quadrupole moment	5 0 0	52	5.12	81	3.61	51	-134.2132	66	73	85	76	61	b	38	39	90	3	86
diamagnetic susceptibility	6 0 0	45	4.90	64	2.75	36	-134.2940	88	76	51	73	67	43	b	24	52	16	66
field (at C)	7 0 0	78	6.44	85	4.02	85	-133.8224	55	97	30	88	89	80	41	b	77	5	84
field gradient (at C)	8 0 0	77	6.34	76	3.44	74	-134.0275	77	84	69	84	75	97	13	51	b	1	54
field (at O)	9 0 0	92	7.43	91	4.75	82	-133.9105	22	95	90	98	96	84	54	47	71	b	83
field gradient (at O)	10 0 0	68	5.72	75	3.27	43	-134.2392	88	78	77	82	76	72	8	42	42	14	b
nuclear attraction	11 0 0	63	5.33	47	2.25	69	-134.0586	80	2	6	6	35	58	27	74	34	80	38
total electronic	12 0 0	25	4.22	1	1.92	16	-134.4036	90	60	11	55	47	50	20	28	40	42	31
F	13 0 0	85	6.81	88	4.24	71	-134.0529	80	82	86	90	93	86	50	38	78	16	80
	2 3 0	56	5.19	40	2.20	67	-134.0693	75	1	b	b	32	57	30	61	32	79	36
	c 1 2 3	58	5.24	45	2.25	80	-133.9349	71	b	b	b	36	65	26	48	27	89	44
	1 11 0	57	5.20	41	2.20	63	-134.1094	77	b	2	3	30	53	31	69	36	76	33
	c 1 4 0	75	6.31	77	3.46	95	-133.2742	50	b	48	21	b	13	98	46	81	98	56
	1 6 0	76	6.33	69	2.99	90	-133.6869	75	b	71	63	63	63	b	88	46	93	70
	c 4 2 3	44	4.81	27	2.12	54	-134.2030	57	7	b	b	b	19	57	75	43	70	13
	4 11 0	29	4.39	10	2.00	35	-134.2960	77	14	50	30	b	26	69	33	30	66	9
	11 5 0	31	4.45	62	2.69	55	-134.1859	66	4	44	22	12	b	83	35	89	64	73
	c 11 6 0	88	6.97	74	3.13	91	-133.5846	66	17	60	47	56	95	b	96	2	83	77
	c 1 6 5	96	7.69	94	5.12	97	-132.7965	28	b	93	77	83	b	b	91	93	92	97
	c 6 5 0	91	7.16	96	5.18	83	-133.9010	37	81	96	96	87	b	b	67	94	0	93
	4 5 0	14	3.69	56	2.46	23	-134.3605	62	57	15	52	b	b	87	8	86	18	58
	4 13 0	22	4.00	23	2.10	38	-134.2883	77	75	55	59	b	21	68	17	19	7	4
	4 10 8	28	4.31	34	2.16	37	-134.2932	85	71	76	40	b	75	40	5	b	31	b
	10 8 0	70	5.84	71	3.07	57	-134.1658	62	79	67	80	69	94	2	52	b	10	b
	7 9 0	87	6.86	89	4.36	89	-133.7065	50	98	22	97	90	79	42	b	75	b	87
	4 7 9	32	4.51	65	2.82	72	-134.0363	71	91	84	69	b	23	64	b	21	b	8
	1 13 0	97	8.13	83	3.80	94	-133.3636	66	b	64	65	70	83	5	98	44	68	88
	9 10 0	71	6.12	82	3.65	62	-134.1107	75	89	80	89	80	71	12	44	39	b	b
	4 10 0	17	3.86	11	2.01	22	-134.3642	75	63	65	39	b	30	63	3	18	35	b

K  
E  $r_o^{-1}$   $\theta$   $x_c/r^3$   $x_o/r^3$   
 $r_c^{-1}$   $\chi_{co}$   $r_n^2$   $q_c$   $q_o$

Note: Another example of the type of table used in the analysis discussed in the text. Compare carefully with table 3 which used RHF expectation values as the constraint, while table 4 uses the best available experimental or theoretical values for the constraint.

- (a) The rankings are relative to all unconstrained and constrained RHF, NDDO-RHF and MOM wavefunctions with the same basis set. A property rank close to unity means that constraining property A will give a good expectation value for property B.
- (b) Signifies the constraint.
- (c) Signifies incomplete convergence, with a divergence in the 5th significant figure compared to the reference value.
- (d) The rank is the number of wavefunctions with lower values of  $C_B$ ,  $C_C$  or  $E$ , expressed as a percentage of the total number of wavefunctions in the set.
- (e) The percentage of properties improved over their values when unconstrained is expressed as the total number of independent unconstrained expectation values, for each constrained wavefunction, which are improved.

energy and the RHF expectation values. The operators  $\left(\frac{x}{r^3}\right)$  and  $\left(\frac{3x^2 - r^2}{r^5}\right)$  and  $(F)$  are ineffective. as are multiple constraints based on them.

In general, the MOM augmented by suitable choice of constraint operators gives wavefunctions of as good quality as the constrained NDDO-RHF wavefunctions.

**Constrained MOM calculations: empirical and theoretical reference values (table 4):** Except for *LiH* and a BLMO basis, there is one or more singly constrained MOM wavefunction with a lower energy than the unconstrained NDDO-RHF wavefunction. For all molecules and all bases, every constraint results in an improved wavefunction, and lower energy.

- the operators  $(-\frac{1}{2}\nabla^2)$ ,  $r^{-1}$ ,  $V_{ne}$  and  $(T+V_{ne})$  are very effective constraints, more effective than in NDDO-RHF or RHF calculations;
- $r_{Li}^{-1}$  in *LiH* for Slater  $\zeta$ ,  $r_H^{-1}$  in *FH* for Slater  $\zeta$ ,  $r_F^{-1}$  in *FH* for BLMO  $\zeta$  and  $r_O^{-1}$  in *CO* for Slater  $\zeta$  greatly improved wavefunctions;
- $V_{ne}$  is one of the best constraints in *LiH*, *FH* and *CO* for all bases;
- $(T+V_{ne})$  gives the lowest energy in *N<sub>2</sub>*, *LiH*, *FH* and *CO* for most bases;
- $x_n$ ,  $\theta_n^e$ ,  $r_n^2$  give slight improvements in all bases;
- $x/r^3$  is a poor constraint, worse than  $\left(\frac{3x^2 - r^2}{r^5}\right)$  while  $F$  is totally ineffective;
- in multiple constraints,  $(x_\alpha/r_\alpha^3, x_\beta/r_\beta^3)$  is poor;  $(r_\alpha^{-1}, r_\beta^{-1})$  is good in *LiH* for BLMO  $\zeta$  and  $\left(\frac{3x_\alpha^2 - r_\alpha^2}{r_\alpha^5}, \frac{3x_\beta^2 - r_\beta^2}{r_\beta^5}\right)$  is good in *FH* only; in general multiple constraints are not better than single constraints; this was true of NDDO-RHF and RHF constrained calculations also when theoretical or empirical reference values were used.

In all cases,  $(T+V_{ne})$  constrained MOM calculations are superior to  $(T+V_{ne})$  constrained NDDO-RHF calculations; this is also true of  $r_n^2$  constrained calculations.

Thus MOM with a proper choice of constraint operators generates a wavefunction superior to a similarly constrained NDDO-RHF wavefunction. This is surprising when one remembers how much more approximate MOM is generally believed to be than the NDDO-RHF method.

### Constrained Configuration Interaction Method on CO [6, 36]

The constrained CI method requires finding  $\psi_{CI}$  with a fictitious Hamiltonian  $\mathcal{H}$  defined in terms of the Lagrange multipliers

$$\mathcal{H} = H + \sum_i^s \lambda_i (M_i - \mu_i)$$

with

$$\delta \langle \psi_{CI} | \mathcal{H} | \psi_{CI} \rangle = 0$$

and the  $\lambda_i$  defined from

$$\langle \psi_{CI} | M_i - \mu_i | \psi_{CI} \rangle = 0$$

with  $i = 1$  through  $s$ .

Only single constraints were used;  $\langle T+V_{ne} \rangle$  was required to equal the estimated theoretical expectation value and  $\langle x_n \rangle$ ,  $\langle \theta_n^e \rangle$  and  $\langle r_n^2 \rangle$  to equal the experimental expectation values. Three types of constrained CI calculations were performed.

- First Excitation CI: all symmetry allowed single excitation configurations were included; 15 Slater determinants and 8 contributing configurations.
- Iterative Natural Orbital [41] first excitation CI: after constraining by (a) the first order spinless density matrix is diagonalized to give spinless natural orbitals [42], and the natural orbitals of highest occupation number are used to give a new dominant configuration. The remaining natural orbitals are used to construct single excitation configurations. The constraint is applied and the method iterated until a change of less than  $1 \times 10^{-4}$  in the spinless density matrix is reached, usually 5 iterations. This is an alternate method for obtaining a constrained RHF wavefunction.
- First and Second Excitation CI: all symmetry allowed singly and doubly excited configurations are included: 108 Slater Determinants and 47 contributing configurations ( $S^2$  eigenfunctions).

### Results:

There is a decrease in energy due to CI but the *unconstrained* singly and doubly excited CI wavefunction yields poorer expectation values than the *unconstrained* RHF wavefunction for 6 out of 10 properties.

When *constraints* are introduced:—

- CI does not improve the prediction of  $\langle 1e \rangle$  by the constrained RHF wavefunctions: CI cannot compensate for a poor basis set.
- The close agreement between the expectation values from *constrained* first excitation CI wavefunction and the *constrained* RHF wavefunction permits either to be used for most rapid convergence.

The same results are obtained using CI with NDDO and maximum overlap wavefunctions.



(c) With the constraint operators ( $T+V_{ne}$ ),  $x_n$  and  $\theta_n^e$ , the iterative natural orbital first excitation CI procedure converges to the RHF wavefunction. In  $r_n^2$  the iterative natural orbital wavefunction gives a much lower energy than the constrained RHF wavefunction, and this is because of the large difference between the expectation value of the constraint operator calculated with the *unconstrained* wavefunction and the reference value of the constraint operator. When this occurs great care should be used in determining wavefunctions with the constrained RHF method.

theory and configuration interaction theory, suggests that the behaviour of the constrained variational method of RHF is so erratic as to make it valueless. It only *appears* to have reasonable behaviour for a *selected* basis in a *selected* molecule for *selected* constraints, see table 5 and figure 1. The real interest lies in the MOM; perhaps here we can fully describe a true MO wavefunction and then minimize the energy, avoiding all problems of basis sets, exponents and types of atomic orbitals.

## Conclusion

This analysis of four molecules, with three basis sets for each, thirteen one-electron operators and seven multiple one-electron operators, several orbital exponents and weighting factors, within the RHF theory, the NDDO-RHF theory, the maximum overlap

Table 5: Expectation values of some properties of CO calculated with constrained wavefunctions with a Slater basis. Constraint operator:  $T + V_{ne}$

	RHF <sup>a</sup>	First Excitation CI	First and Second Excitation CI	Reference
Kinetic Energy	111.675 1.704	111.706 1.673	111.894 1.485	113.379
diamagnetic shielding	18.4465 -0.0745	18.4517 -0.0797	18.4521 -0.0801	18.372
diamagnetic shielding	24.7292 0.2688	24.7291 0.2689	24.7524 0.2456	24.998
dipole moment	-0.83059 0.78652	-0.84900 0.80493	-0.83545 0.79138	-0.04407
$\theta$ molecular quadrupole moment	18.1671 -1.0961	18.1354 -1.0644	18.1073 -1.0363	17.071
$\chi$ magnetic susceptibility	38.9527 0.9343	38.9401 0.9469	38.9145 0.9725	39.887
field (at C)	1.46847 0.29154	1.46690 0.29312	1.46660 0.29341	1.76001
field gradient (at C)	1.87829 0.67171	1.86993 0.68007	1.79786 0.75214	2.5500
field (at O)	-0.96767 -0.35233	-0.97088 -0.34912	-0.96909 -0.35091	-1.32001
field gradient (at O)	1.75176 0.27124	1.72605 0.29695	1.81532 0.20768	2.023
nuclear attraction	308.513 1.703	308.543 1.673	308.731 1.435	310.216
total energy	-196.837 0.000	-196.837 0.000	-196.837 0.000	-196.837
Hellman-Feynman	1.06940 -1.06940	1.03430 -1.03430	1.04686 -1.04686	0
Energy	-134.5221	-134.5309	-134.6545	

(a) RHF wavefunction determined using an iterative natural orbital first excitation CI procedure

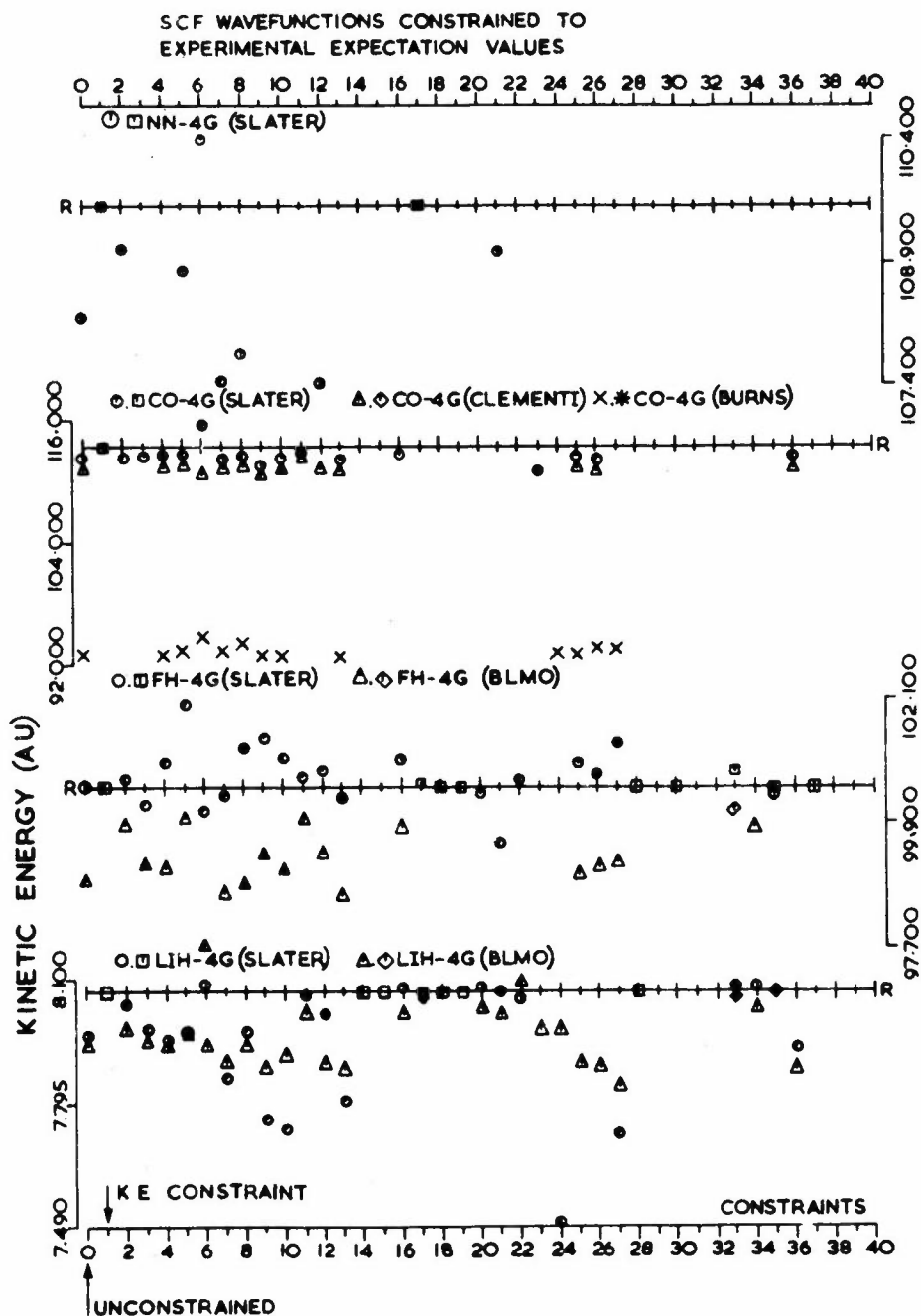


Figure 1: A typical plot of the behaviour of the various expectation values for  $N_2$ ,  $CO$ ,  $FH$  and  $LiH$  with particular basis sets:

- $N_2$  - 4 gaussian with Slater orbitals;
- $CO$  - 4 gaussian with (i) Slater  
(ii) Clementi  
and (iii) Burns exponents;
- $FH$  - 4 gaussian with (i) Slater  
and (ii) BLMO exponents;
- and  $LiH$  - 4 gaussian with (i) Slater  
and (ii) BLMO exponents.

The horizontal dashed line represents the expectation value of the kinetic energy. Two different symbols are used for each basis in each molecule for the expectation value:

- (a) the expectation values of wavefunctions constrained with constraints other than the kinetic energy; and  
(b) the constrained expectation values of wavefunctions constrained to give the kinetic energy.

Thus  $\Delta$ ,  $\circ$  or  $\times$  represents the expectation values from the wavefunction constrained by constraint other than kinetic energy; and  $\diamond$ ,  $*$  or  $\square$  represents the expectation values when the kinetic energy is the constraint.

A good constraint would put  $\Delta$ ,  $\circ$  or  $\times$  along the line, or closer to the line than the unconstrained value, constraint 0.

## References

- [1] MUKHERJI, A. and KARPLUS, M.J. (1963). *J. Chem. Phys.*, **38**, 44.
- [2] RASIEL, Y. and WHITMAN, D.R. (1965). *J. Chem. Phys.*, **42**, 2124.
- [3] CHONG, D.P. and BENSTON, M.L. (1968). *Theoret. Chim. Acta*, **12**, 175.
- [4] HENDERSON, G.A. and ZARUN, J. (1971). *Bull. Am. Phys. Soc.*, **16**, 647.
- [5] BJORNA, N. (1972). *Mol. Phys.*, **24**, 1.
- [6] ZEISS, G.D. (1974). *Ph.D. Dissertation*, Canada: McGill University.
- [7] BYERS-BROWN, W. (1966). *J. Chem. Phys.*, **44**, 567.
- [8] CHONG, D.P. and RASIEL, Y. (1966). *J. Chem. Phys.*, **44**, 1819.
- [9] LOEB, R.J. and RASIEL, Y. (1970). *J. Chem. Phys.*, **52**, 4995.
- [10] KERN, C.W. and KARPLUS, M. (1964). *J. Chem. Phys.*, **40**, 1374.  
 ——— and ——— (1965). *Ibid*, **43**, 2926.
- [11] SCHERR, C.W. (1955). *J. Chem. Phys.*, **23**, 569.
- [12] SLATER, J.C. (1933). *J. Chem. Phys.*, **1**, 687.
- [13] WHARTON, L., GOLD, L.P. and KLEMPERER, W. (1960). *J. Chem. Phys.*, **33**, 1255.
- [14] WEISS, R. (1963). *Phys. Rev.*, **131**, 659.
- [15] ROSENBLUM, B., NETHERCOT, A.A. and TOWNES, C.H. (1958). *Phys. Rev.*, **109**, 400.
- [16] FLYGARE, W.H. and GOODISMAN, J. (1968). *J. Chem. Phys.*, **49**, 3122.
- [17] KOLOS, W. and WOLNIEWICZ, L. (1964). *J. Chem. Phys.*, **41**, 3674.
- [18] HELLMAN, H. (1937). *Einführung in die Quantenchemie*, 285, Leipzig: Deuticke.
- [19] FEYNMAN, R.P. (1939). *Phys. Rev.*, **56**, 340.
- [20] BUCKINGHAM, A.D. (1970). *Physical Chemistry*, Volume 4 (ed. D. Henderson), New York: Academic Press.
- [21] BOYS, S.F. (1950). *Proc. Roy. Soc. (London)*, **A200**, 542.
- [22] MATSUOKA, O. (1973). *Int. J. Quantum Chem.*, **8**, 365.
- [23] HEHRE, W.J., STEWART, R.F. and POPLE, J.A. (1969). *J. Chem. Phys.*, **51**, 2657.
- [24] PAGE, G. and LUDWIG, O.G. (1972). *J. Chem. Phys.*, **56**, 5626.
- [25] O-OHATA, K., TAKETA, H. and HUZINAGA, S. (1966). *J. Phys. Soc. Japan*, **21**, 2306.
- [26] EHRENSON, S. (1971). *Chem. Phys. Letters*, **9**, 521.
- [27] BURNS, G. (1964). *J. Chem. Phys.*, **41**, 1521.
- [28] SLATER, J.C. (1930). *Phys. Rev.*, **36**, 51.
- [29] RANSIL, B.J. (1960). *Revs. Modern Phys.*, **32**, 245.
- [30] CROW, E.L., DAVIS, F.A. and MAXFIELD, M.W. (1960). *Statistics Manual*, New York: Dover.
- [31] YUE, C.P. and CHONG, D.P. (1968). *Theoret. Chim. Acta*, **12**, 431.
- [32] CLINTON, W.L., GALLI, A.J. and MASSA, L.J. (1969). *Phys. Rev.*, **177**, 7.
- [33-36] ZEISS, G.D. and WHITEHEAD, M.A., (to be published). These papers will contain full details of the results, analysis and detailed conclusions.
- [37] MULLIKEN, R.S. (1952). *J. Phys. Chem.*, **56**, 295.
- [38] FEINBERG, M.J., RUEDENBERG, K. and MEHLER, E.L. (1970). *Adv. Quantum Chem.*, **5**, 27.
- [39] BARTLETT, R.J. and ÖHRN, Y. (1971). *Theoret. Chim. Acta*, **21**, 215.
- [40] LYKOS, P.G. and SCHMEISING, H.N. (1961). *J. Chem. Phys.*, **35**, 288.
- [41] BENDER, C.F. and DAVIDSON, E.R. (1966). *J. Phys. Chem.*, **70**, 2675.
- [42] LÖWDIN, P.O. (1955). *Phys. Rev.*, **97**, 1474.

# Direct Minimisation Schemes - Some Difficulties and Possible Resolutions

B.T.Sutcliffe and D.Garton\*

If one wishes to minimise the electronic energy of a molecule, considered as a function of the linear coefficients (basis function coefficients), then some of the more modern direct minimisation methods, are obviously extremely attractive, particularly in the context of energies found from complicated wavefunctions like LCAO-MO-SCF functions.

Some results will be presented which indicate that the methods are not so attractive as might at first be thought, and an analysis of the reasons for their relative failure will be presented together with some methods of remedying their defects.

## Introduction

Recently interest has been revived in 'direct' methods of minimising the energy with respect to such parameters as nuclear position, orbital exponents and orbital (linear) coefficients, following the pioneering work of McWeeny [1,2] using the steepest descent methods. In particular Fletcher [3] showed how it was possible to use one of the more modern conjugate-direction techniques in such direct minimisation, and an approach similar to that of Fletcher was later exploited by Kari and Sutcliffe [4] and by Claxton and Smith [5]. Claxton and Smith concentrated on optimising the linear coefficients in an unrestricted Hartree-Fock (UHF) approach for systems which had proved convergent only with difficulty using more conventional techniques. Though Claxton and Smith were able to obtain convergence using a direct method (in fact the Fletcher-Reeves method [6]), they commented that the method proceeded only very slowly and could not compete with conventional methods when these methods worked. The object of this paper is to try to explain why it is that direct methods have so far proved so disappointing for linear coefficients in closed and in unrestricted LCAO-MO-SCF calculations, to see how far we may anticipate similar difficulties in LCAO-MO-MC-SCF calculations, and to suggest possible methods for their resolution.

## Direct Methods of Minimisation

Most modern direct minimisation techniques are based on choosing a sequence of directions in the co-ordinate space in which the function  $f(\mathbf{x})$  is to be minimised, and finding a sequence of points by minimising, or at least decreasing, the function value

along the chosen direction until a minimum point is found. The most effective of the modern methods are based on the supposition that sufficiently close to the minimum the objective function  $f(\mathbf{x})$  can be expanded in a Taylor series to second order.

$$f(\mathbf{x}) = u + \mathbf{b}^\dagger \mathbf{x} + \frac{1}{2} \mathbf{x}^\dagger \mathbf{H} \mathbf{x} \quad (1)$$

where  $\mathbf{x}$  is a column vector of co-ordinates and the matrix  $\mathbf{H}$  (the Hessian matrix at the minimum) is assumed to be a real symmetric, positive-definite, non-singular matrix. If this is possible the gradient of the function  $\mathbf{g}(\mathbf{x})$  may be written

$$\mathbf{g}(\mathbf{x}) = \mathbf{b} + \mathbf{H}\mathbf{x} \quad (2)$$

with  $g_i(\mathbf{x}) = \partial f / \partial x_i$ , and hence the minimum point  $\mathbf{a}^0$  may be found from any arbitrary point  $\mathbf{a}$  as

$$(\mathbf{a}^0 - \mathbf{a}) = -\mathbf{H}^{-1} \mathbf{g}(\mathbf{a}) \quad (3)$$

provided that  $\mathbf{H}$  is non-singular.

It can be shown that this problem can be solved in just  $n$  steps without having to invert  $\mathbf{H}$  or indeed without explicit knowledge even of  $\mathbf{H}$ , by constructing a sequence of conjugate-directions, that is a sequence of directions  $\mathbf{p}_i$  such that

$$\mathbf{p}_i^\dagger \mathbf{H} \mathbf{p}_j = 0 \quad i \neq j \quad (4)$$

$$\mathbf{g}_{i+1}^\dagger \mathbf{p}_i = 0 \quad (5)$$

and minimising the function along these directions. That is, if at any point  $\mathbf{x} = \mathbf{a}$ , one knows the direction  $\mathbf{p} \equiv \mathbf{p}(\mathbf{a})$ , then one constructs the function

\* Department of Chemistry, University of York, Heslington, York, YO1 5DD

$$F(\lambda) = f(a + \lambda p) \quad (6)$$

and finds the value of  $\lambda$ ,  $\alpha$  say, that minimises  $F(\lambda)$  and then the next point in the descent sequence,  $\hat{a}$ , is chosen according to

$$\hat{a} = a + \alpha p. \quad (7)$$

It is easy to see that at the point  $\hat{a}$

$$\hat{g}^\dagger p = 0 \quad (8)$$

where

$$\hat{g} \equiv g(\hat{a}) \quad (9)$$

and that therefore

$$f(\hat{a}) - f(a) = - (g^\dagger p)^2 / 2 p^\dagger H p \quad (10)$$

and that

$$\alpha = -g^\dagger p / p^\dagger H p. \quad (11)$$

Many methods are available for choosing such conjugate direction, examples are the method of Powell [7] which does not use the gradient matrix, the method of Fletcher and Reeves [6] which uses the gradient matrix and Fletcher and Powell's modification of Davidon's method [8], which uses the gradient matrix and also yields an estimate of the inverse Hessian at the minimum. A general discussion of such methods in the case of quadratic functions may be found in Huang [9] see also Dixon [10].

It is clear however from the above discussion that considerable difficulties may arise in utilising one of these methods if the Hessian matrix is not positive definite. Thus in this case it is possible that the denominators in (10) and (11) become zero so that the location of a minimum in the direction  $p$  is just not possible. Even if the methods do not fail overtly because of this, it is the case that proof of quadratic termination for the methods depends on the positive definiteness of  $H$  so that one might well expect poor convergence even when the method does not fail outright.

We shall now show that the Hessian at the minimum in the closed shell SCF problem is indeed singular and we suggest that this may be the origin of the difficulties experienced by Claxton and Smith and others. The demonstration we use may be generalised immediately to the UHF method, and a similar approach used in the general LCAO-MO-MC-SCF problem.

## The LCAO-MO Closed Shell Problem

Using the notation of McWeeny and Sutcliffe [11] the energy function in the closed shell problem may be written as

$$E = 2 \text{tr } hR + \text{tr } G(R)R \quad (12)$$

where  $h$  is the matrix of one electron integrals and  $G(R)$  the usual electron interaction matrix, both in the atomic orbital basis. The matrix  $R$  is defined as

$$R = TT^\dagger \quad (13)$$

where  $T$  is the  $m$  by  $n$  matrix that relates the  $n$  doubly-occupied molecular orbitals to the chosen atomic orbital basis ( $\eta$ ).

This function as it stands is not a suitable object for use in a direct minimisation procedure since the variables of the problem, the linear coefficients,  $T_{ir}$ , are constrained by the orthonormality requirements among the molecular orbitals, namely

$$T^\dagger S T = I \quad (14)$$

where  $S$  is the overlap matrix in the atomic orbital basis and  $I$  is the  $n$  dimensional unit matrix.

These constraints can be incorporated, as was first shown by Fletcher [3], by writing

$$T = Y U \quad (15)$$

where  $Y$  is an  $m$  by  $n$  matrix of unconstrained variables and the  $n$  by  $n$  matrix  $U$  is chosen to supply the constraints. In terms of (14) it is seen that  $U$  must satisfy the equation

$$U U^\dagger = (Y^\dagger S Y)^{-1} \quad (16)$$

and for the sake of brevity we denote  $(Y^\dagger S Y)$  by  $A$ . It follows therefore that we may write

$$R = Y A^{-1} Y^\dagger \quad (17)$$

and since the energy depends only on  $R$ , we see that it is unnecessary to specify  $U$  more closely than by (16).

Following Fletcher [3] (see also Kari and Sutcliffe [12]) we may determine the gradient of  $E$  with respect to the variables  $Y_{ir}$  by noting that under the change  $Y \rightarrow Y + \delta Y$  such that  $E \rightarrow E + \delta E$ , then

$$R \rightarrow R + Y A^{-1} \delta Y^\dagger (I - SR) + (I - RS) \delta A^{-1} Y^\dagger \quad (18)$$

$$A^{-1} \rightarrow A^{-1} - A^{-1} \delta A A^{-1} \quad (19)$$

where

$$\delta A = \delta Y^\dagger S Y + Y^\dagger S \delta Y \quad (20)$$

and that

$$G(R) \rightarrow G(R) + G(\delta R). \quad (21)$$

After a little manipulation it may be shown that for real  $Y$ , that

$$\delta E = 4 \operatorname{tr} (I - SR) f Y A^{-1} \delta Y^\dagger \quad (22)$$

where

$$f = h + G(R), \quad (23)$$

and hence,

$$\frac{\partial E}{\partial Y_{ir}} = 4 \left\{ (I - SR) f Y A^{-1} \right\}_{ir} \quad (24)$$

so that the gradient can in this case be represented by an  $m$  by  $n$  matrix

$$W = 4 (I - SR) f Y A^{-1} \quad (25)$$

with the row indices labelling the atomic, and the column indices the molecular orbitals.

It would thus seem that choice of the elements of  $Y$  as the variables of minimisation according to (15) is an extremely good choice since one is able to express the gradient of the energy in a compact manner in terms of them. Furthermore, they are peculiarly suitable for a direct minimisation procedure precisely because they are unconstrained variables and so do not need to be modified to satisfy an ancillary condition at each iteration. As was pointed out by Fletcher [3] if one chooses a variable set subject to an ancillary condition which one needs to restore at the end of an iteration (for example if one chose  $T$ ) and restored orthonormality one cannot use a direct minimisation process because the information from the previous iteration is 'spoiled' by the restoration of constraints and so the advantages of direct minimisation are lost. However the advantages of many direct minimisation procedures may well be lost if the Hessian at the minimum turns out to be singular, and as we shall now show, unfortunately in the basis provided by the elements of  $Y$  the Hessian at the minimum is indeed singular.

To determine the Hessian of the problem we must find the second variation in  $E$ , and it is easy to see that under a variation  $Y \rightarrow Y + \delta Y$  we get  $W \rightarrow W + W^1$  where:

$$\begin{aligned} W^1 &= 4 \{ -S \delta R f Y A^{-1} \\ &\quad + (I - SR) (f \delta Y A^{-1} - f Y A^{-1} \delta A A^{-1}) \\ &\quad + (I - SR) G (\delta R) Y A^{-1} \} \quad (26) \\ &= 4 \{ (I - SR) (f \delta Y A^{-1} - f Y A^{-1} \delta A A^{-1}) \\ &\quad - S(Y A^{-1} \delta Y (I - SR)) \\ &\quad + (I - RS) \delta Y A^{-1} Y) f Y A^{-1} \\ &\quad + \sum_{j=1}^m \sum_{r=1}^n X^{jr} \delta Y_{jr} \} \quad (27) \end{aligned}$$

where

$$\begin{aligned} X_{is}^{jr} &= \sum_{klqp=1} (I - SR)_{iq} (I - SR)_{jp} (B_{pl,qk} + B_{lp,qk}) \\ &\quad \times (Y A^{-1})_r (Y A^{-1})_{ks} \quad (28) \end{aligned}$$

where  $B_{pl,qk}$  is the electron-repulsion supermatrix with elements.

$$B_{pl,qk} = 2 \langle qp | g | kl \rangle - \langle qp | g | lk \rangle \quad (29)$$

where the integral notation is that of McWeeny and Sutcliffe [11].

Since we are interested only in the Hessian at the minimum, we can use the fact that at the minimum  $W = 0$ , to simplify (27) somewhat, and it is easily seen that at the minimum the second and third terms in (27) vanish to give

$$\begin{aligned} W^1 &= 4 \{ (I - SR) (f \delta Y A^{-1} - S \delta Y A^{-1} Y f Y A^{-1}) \\ &\quad + \sum_{j=1}^m \sum_{r=1}^n X^{jr} \delta Y_{jr} \} \quad (30) \end{aligned}$$

that is

$$\begin{aligned} \frac{\partial^2 E}{\partial Y_{jr} \partial Y_{is}} &= 4 \{ ((I - SR) f)_{ij} A_{rs}^{-1} - ((I - SR) S)_{ij} \\ &\quad (A^{-1} Y^\dagger f Y A^{-1})_{rs} + X_{is}^{jr} \} \quad (31) \end{aligned}$$

so that the Hessian at the minimum has elements given by (31) where it is understood that all quantities dependent on  $Y$  in (31) are given in terms of the minimising  $Y$ , though this is not explicitly indicated in the equation.

From (25) it is easy to see that at the minimum

$$f R S - S R f R S = 0 \quad (32)$$

and that

$$SRf - SRfRS = 0 \quad (33)$$

so that the matrix  $(I - SR)f$  is symmetric at the minimum and hence the Hessian itself is symmetric, as required. We can therefore write the Hessian as a partitioned matrix of dimension  $n$  by  $n$  in blocks of dimension  $m$  by  $m$ , the MO's labelling the blocks and the AO's labelling the rows and columns within a block. The  $r,s$  block clearly has the structure

$$H^{rs} = 4A_{rs}^{-1}(I - SR)f - 4\bar{A}_{rs}^{-1}(I - SR)S + 4Z^{rs} \quad (34)$$

where

$$\bar{A} = A(Y^\dagger f Y)^{-1} A \quad (35)$$

and

$$Z_{ji}^{rs} = X_{is}^{jr} \quad (36)$$

Now let us suppose that we have found a matrix  $T$ , that minimises  $E$  by satisfying the usual equations

$$fT = ST \& \quad (37)$$

$$T^\dagger ST = I \quad (38)$$

Then we know that we can write the minimising  $R$  as  $T T^\dagger$  and the minimum  $f$  as the one obtained from (37). Consider now the  $mn$  by 1 column matrix  $t$  whose first  $m$  rows are  $T_1$  whose second  $m$  rows are  $T_2$ , and so on, where  $T_r$  is the  $r^{\text{th}}$  column of  $T$ . We can then construct

$$\hat{t} = Ht \quad (39)$$

where  $\hat{t}$  is a column matrix whose first  $m$  rows are

$$\hat{t}^1 = \sum_{s=1}^n H^{1s} T_s \quad (40)$$

and so on. If we write out the expression for  $\hat{t}^r$  explicitly we get

$$\hat{t}^r = 4 \sum_{s=1}^n A_{rs}^{-1} (I - SR)fT - \bar{A}_{rs}^{-1} (I - SR)ST + Z^{rs} T_s \quad (41)$$

But

$$\begin{aligned} (I - SR)fT_s &= fT_s - STT^\dagger fT_s \\ &= fT_s - \&_s ST_s \\ &= 0 \end{aligned} \quad (42)$$

$$(I - SR)ST_s = ST_s - STT^\dagger ST_s$$

$$= ST_s - ST_s$$

$$= 0$$

(43)

and

$$\begin{aligned} (Z^{rs} T_s)_j &= \sum_{i=1}^m Z_{ji}^{rs} T_{is} \\ &= \sum_{ip=1}^m X_{rs,ip} (I - SR)_{ip} T_{is} \end{aligned} \quad (44)$$

where

$$\begin{aligned} X_{rs,ip} &= \sum_{k,l,q=1}^m (I - SR)_{ik} (B_{pl,ik} + B_{pl,kp}) \\ &\quad \times (YA^{-1})_{lr} (YA^{-1})_{ks} \end{aligned} \quad (45)$$

so that

$$\begin{aligned} (Z^{rs} T_s)_j &= \sum_{i,p=1}^m X_{rs,ip} (\delta_{ip} T_{is} - \sum_l R_{pl} S_{li} T_{is}) \\ &= \sum_{p=1}^m X_{rs,ip} (T_{ps} - \sum_{i=1}^m \sum_{u=1}^n T_{pu} T_{lu} S_{li} T_{is}) \\ &= \sum_{p=1}^m X_{rs,ip} (T_{ps} - \sum_{u=1}^n \delta_{us} T_{pu}) \\ &= 0 \end{aligned} \quad (46)$$

We therefore conclude that  $\hat{t}^r = 0$ , so that we can write:

$$Ht = 0t \quad (47)$$

and hence we conclude that  $t$  is an eigenvector of  $H$  with zero eigenvalue so that  $H$  is singular and not positive definite.

In fact the above demonstration may easily be extended to show that the Hessian at the minimum has precisely  $n^2$  zero roots, by the following means. We can regard the Hessian as being defined in an  $mn$  dimensional vector space and we can define a basis in this space by choosing  $n^2$  vectors  $t_p$ ,  $p=1,2,\dots,mn$ , according to the following specification. Select one column  $T_q$  from the  $n$  possible columns of  $T$ . Let  $t_p$  be the vector that has  $T_q$  as its first  $m$  rows and is null elsewhere, let  $t_{p+1}$  have  $T_q$  as the second  $m$  rows and be null elsewhere and so on. It is easy to see that the  $n^2$  vectors so chosen are linearly independent since they are orthonormal in a metric specified by the matrix partitioned as is  $H$  but with  $S$  forming the diagonal blocks and with null blocks elsewhere. It follows at once from (40) to (45) that these  $n^2$  vectors are eigenvectors of  $H$  with null eigenvalues. The vector  $t$  that we chose in

equation (39) is of course just the linear combination of degenerate eigenvectors

$$t = t_1 + t_{n+2} + t_{2n+3} + \dots + t_{n^2} \quad (48)$$

### The Origin of the Zero Roots in the Hessian

Let us suppose for the moment that we had formulated our energy expression originally in terms of a set of non-orthonormal orbitals related to the atomic basis  $\eta$  by the matrix  $Y$ . Then it is easy to see, using the formulae for matrix elements between determinants of non-orthonormal orbitals (see e.g. [11] pages 49-51) that the energy expression obtained is just (12) but now with  $R$  defined directly by (17). Thus had we worked without any constraints at all, we would have obtained precisely the same equations as we have already for the gradient and for the Hessian and would, in consequence, have encountered precisely the same difficulties. In the light of this it is perhaps misleading to regard  $U$  in equation (15) as a constraint supplying matrix, but rather as a constraint removing matrix. One can therefore regard the minimisation problem we have so far formulated as the one of determining the non-orthonormal molecular orbital at any stage and then, using the freedom that one has in the one-determinant approximation, performing a linear transformation among them to produce an orthonormal set. It would seem likely therefore that it is precisely because we have, even at the minimum, this freedom to perform an arbitrary  $n$  by  $n$  linear transformation among the solution vectors that we have a Hessian with  $n^2$  degenerate zero roots. It further seems likely that if instead of removing the constraints we had used the constraints to remove variables from the problem and hence effectively to remove the freedom to perform an arbitrary linear transformation among the solution vectors, then we should not have a singular Hessian for the problem.

In this context it is clearly interesting now to investigate the full LCAO-MO-MC-SCF problem for which the energy expression is (in the notation of [11])

$$E = \sum_{r,s} \sum_{i,j} T_{ir}^* h_{ij} T_{js} P_{1sr} + \frac{1}{2} \sum_{rstu} \sum_{ijkl} T_{ir}^* T_{js}^* g_{ijkl} T_{kt} T_{lu} P_{2tu,rs} \quad (49)$$

In this notation the gradient matrix was shown by Kari and Sutcliffe [12] to take the form

$$W = 2(XU^\dagger - SYVBV^\dagger Y^\dagger) \quad (50)$$

assuming a symmetric orthogonalisation procedure, and one of the present authors (D.G.) was able to show that  $W$  took precisely the same form as (50) (though

it was not equivalent to it) if a Schmidt orthogonalisation procedure was used. Here  $X$  is the MC-SCF equivalent of the Fock Matrix

$$X = hTP_1 + Z \quad (51)$$

with  $Z$  the equivalent of the  $G$  matrix

$$Z_{ir} = \sum_{stu} \sum_{kjl} (T^\dagger)_{sj} g_{ijkl} (T \times T)_{kl,tu} P_{2tu,rs} \quad (52)$$

and  $V$  is the orthogonal matrix that diagonalises  $S$ .  $B$  is a rather complicated matrix involving the eigenvalues of  $S$  and details of it can be found in the paper of Kari and Sutcliffe [12].

It is an extremely difficult (if not impossible) matter to determine from (49) a general expression for the Hessian, particularly in the case of symmetric orthogonalisation. However it is possible (see [13]) though even then, extremely tedious, to determine the form that the Hessian will take at a point in configuration space where the orbitals are in fact orthogonal, that is where

$$U = I_n, \quad Y^\dagger S Y = I_m \quad (53)$$

It is possible further to specialise this result by transforming it (much in the spirit of Hillier and Saunders' work [14]) to a 'temporary solution' basis, that is a basis in which we have conditions (53) obeyed but in which we also have

$$S = I \quad (54)$$

and in which we can write

$$Y = \begin{pmatrix} I_n \\ O \end{pmatrix} \quad (55)$$

implying that we are expressing the Hessian at the given point in terms of the orbitals found at that point (which are not of course the solution orbitals) and in this basis it is convenient to write

$$W = \begin{pmatrix} \lambda \\ \Delta \end{pmatrix}_{m-n} \quad (56)$$

where  $\Delta \rightarrow 0$ ,  $\lambda \rightarrow \lambda^\dagger$ , as a solution is achieved.

In this basis it is possible to show that the Hessian can again be regarded as blocked, with elements in



each block:

$$\begin{aligned}
 H_{pq}^{sr} = & -1/8(\lambda + \lambda^\dagger)_{rs} \delta_{pq} - 1/8(\lambda + \lambda^\dagger)_{pq} \delta_{rs} \\
 & + 3/8(\lambda + \lambda^\dagger)_{rp} \delta_{qs} + 3/8(\lambda + \lambda^\dagger)_{sq} \delta_{pr} \\
 & - 1/2 \lambda_{rp}^\dagger \delta_{qs} - 1/2 \lambda_{sq}^\dagger \delta_{pr} \quad (57a) \\
 & + 1/4(K_{pq}^{sr} + K_{sr}^{pq} - K_{pr}^{sq} - K_{sq}^{pr}) \quad \text{for } p, q \leq n
 \end{aligned}$$

$$\begin{aligned}
 H_{pi}^{sr} = & 1/2(K_{pi}^{sr} - K_{si}^{pr}) - 1/2(\delta_{rs} \Delta_{ip} + \delta_{rp} \Delta_{is}) \\
 & \text{for } p \leq n, i > n \quad (57b)
 \end{aligned}$$

$$H_{jq}^{sr} = H_{qj}^{rs} \quad (57c)$$

$$H_{ji}^{sr} = -1/2(\lambda^\dagger + \lambda)_{rs} \delta_{ij} + K_{ji}^{sr} \quad \text{for } i, j > n \quad (57d)$$

and where this expression

$$\partial^2 E / \partial T_{js} \partial T_{ir} = K_{ji}^{sr} \quad (58)$$

And it is very easy to see from these expressions that at the solution point ( $\Delta = 0$ ,  $\lambda = \lambda^\dagger$ ) that:

$$H_{si}^{sr} = H_{ir}^{sr} = 0 \quad i = 1, 2, \dots, m \quad (59)$$

Thus there are in general precisely  $n$  rows and columns in the Hessian at the solution point which consist only of zeros, so that the Hessian has even for the most general case  $n$  zero roots, so that it is only positive semi-definite and we may assert that the 'reason' for the occurrence of these  $n$  zero roots is precisely the arbitrary nature of the orbital normalisation conditions. There is of course in general in this case no energy invariance under linear transformations among these  $n$  orbitals. It is clear also from this discussion that in any particular LCAO-MO-MC-SCF if there are sub-groups of orbitals which, when subjected to linear transformations, leave the energy invariant, then even more than  $n$  zero roots may occur in the Hessian. It is also clear however that 'natural' orthogonality due to symmetry will not in itself increase the number of zero roots.

### Minimising in the Presence of Zero Roots in the Hessian

The work described in this section was begun before the authors were aware explicitly of the presence of zero roots in the Hessian. The method used was the Fletcher-Reeves method (F-R method) [6] which commends itself to anyone interested in large minimisations because it does not make use

explicitly of the Hessian or an estimate of it. In this method the descent direction are chosen according to

$$\mathbf{p}_{i+1} = -\mathbf{g}_{i+1} + \beta_i \mathbf{p}_i, \quad \beta_i = \mathbf{g}_{i+1}^\dagger \mathbf{g}_{i+1} / \mathbf{g}_i^\dagger \mathbf{g}_i \quad (60)$$

and it is easy to show of equation (11) that in the quadratic case  $\beta_i$  may be written as

$$\beta_i = \mathbf{g}_{i+1}^\dagger \mathbf{H} \mathbf{p}_i / \mathbf{p}_i^\dagger \mathbf{H} \mathbf{p}_i \quad (61)$$

Thus in the F-R method it is only necessary to retain the gradient matrix from the previous iteration in order to construct the next descent direction.

The F-R method derives from a conjugate gradient method first proposed by Hestenes and Stiefel [15] for the solution of linear equations, and in the original paper Hestenes and Stiefel consider the positive semi-definite case explicitly and show that in that case the method converges, if minima are found along each search direction, and the method converges to at least squares minimum of the problem. Straightforward extensions of their argument show this to be true for the F-R method also. Thus the presence of zero roots in the Hessian is not fatal to the F-R method unless one happens to have a genuinely quadratic function and alight by accident on a direction which is an eigenvector of the Hessian with zero eigenvalue, in which case as can be seen from (11)  $\alpha$  increases without limit, that is a minimum cannot be found in the direction of search. However the proof of quadratic convergence for the F-R method depends on the fact that the conjugacy condition (4) implies that the set of directions  $\mathbf{p}_0$  through  $\mathbf{p}_{n-1}$  are linearly independent. However this is clearly not necessarily so unless  $\mathbf{H}$  is positive definite. Thus quadratic convergence cannot be guaranteed even in a nominally quadratic function in this case.

The initial trials of the F-R method were undertaken using the UHF approach in the INDO approximation on some large organic free radicals, which had failed to respond to the conventional Roothaan treatment. The behaviour of these first trials was so favourable to the F-R method that nothing would be gained from detailing the results here beyond saying that the F-R method always worked but was always slightly slower than the conventional method (when both worked), but it always approached an accurate minimum of the problem very slowly indeed, that is if one wanted to refine the results past the acceptable conventional limit, the process was very slow. Furthermore the energy surface appeared to be very quadratic almost from the start of the problem (which was always the equivalent set of Hückel vectors) in the sense that if the energy was plotted as function of distance along the search line the plot was a parabola in good approximation. The fact that the surface was so

quadratic meant that the minimum along the line could always be found accurately and quickly by cubic interpolation, in the results obtained by calculating the energy along the line in steps of length

$$k = 2(E_m - E_i) / p_i^\dagger g_i \quad (62)$$

where  $E_m$  is an estimate of the minimum energy of the problem and  $E_i$  the energy at the current iteration. If  $E_m$  were the true minimum along the line and the section along the line a true parabola then  $k$  would be  $\alpha$ , the optimum step length. If  $E_m$  was fed in as a reasonable lower bound to the final energy,  $k$  was nearly always an over-estimate of  $\alpha$ , but a single interpolation between the point reached using  $k$  and the original part always gave a very good estimate of the minimum.

This work was followed up by some non-empirical work also using the UHF method, even in 'closed' shells to allow for the possibility of splitting if it was energetically favourable to do so. In tables 1 and 2 a summary of results on the  $HF$  molecule is presented. The calculation here was performed in  $4s$   $6p$  basis on  $F$  and  $2s$  on  $H$ , the orbitals being contracted from Huzinaga's ( $9s$ ,  $5p$ ) basis for  $F$  and  $4s$  for  $H$ . In table 3 a summary of the results on the  $F$  atom is shown, the calculation being a repeat of Huzinaga's  $9s$   $5p$  uncontracted calculation. In the  $HF$  problem there are 56 non-zero elements in the  $Y$  matrix and there are 16 constraints not supplied by symmetry. In the  $F$  problem there are 61 non-zero elements in the  $Y$  matrix and 9 constraints not supplied by symmetry. Thus one might hope that at worst the  $HF$  molecule would converge in 40 to 60 iterations and the  $F$  problem in 50 to 60 iterations if the surfaces were truly quadratic.

Table 1:  $HF$  molecule

Cycle	$E_R$	$E_{FR}$	$(g^\dagger g)$	$\alpha$
1	-100.561227	-100.617807	50.57	0.003
2	-102.783456	-104.127781	529.199	0.167
3	-104.439168	-104.563877	51.61	0.001
4	-104.908306	-104.697114	45.93	0.005
5	-105.113306	-104.792196	44.81	0.004

Table 2:  $HF$  molecule

Cycle	$E$	$(g^\dagger g)$	$\alpha$
30	-105.173754	2.659	0.022
40	-105.191753	0.135	0.002
50	-105.199341	0.029	0.002
60	-105.202825	0.090	0.023

Table 3:  $F$  atom

Cycle	$E_R$	$E_{FR}$	$(g^\dagger g)$	$\alpha$
1	-85.913583	-88.613314	15240.23	0.00475
2	-94.460655	-88.918065	1728.04	0.00004
3	-98.353704	-89.200206	341.09	0.00033
4	-99.197832	-89.285109	4169.67	0.000498
5	-99.364629	-91.477661	1216.27	0.00106

If  $HF$  is considered first, it is clear that on a simple iteration for iteration basis the Roothaan method is superior to the F-R method, but this is in fact not a fair comparison because the average time for an F-R iteration in this system is about twice that for an iteration of the Roothaan method, chiefly because it proves extremely difficult to locate the linear minima in this calculation. This difficulty arises not because the surface is not quadratic, for it seems to be on the basis of tests such as those described above, but rather because the formula (62) now seems to fail to estimate a step length adequately. This problem persists right through to the end of the calculation and the termination behaviour is clearly reminiscent of the termination behaviour of a steepest-descent procedure.

The results of the  $F$  atom calculation are clearly pathological in the extreme, and yet tests again indicate that the surface is highly quadratic at all stages. It should also be mentioned that even after 40 iterations of the F-R procedure here the results are still appreciably far from the minimum.

The authors believe that these two calculations are fairly representative of the behaviour of the F-R method in non-empirical UHF-SCF calculations, in the sense that we have found few calculations to proceed better than the  $HF$  one and none worse than the  $F$  calculation.

The source of the difficulty clearly cannot lie in actually having chosen a direction in which  $\alpha$  increases without limit, for the  $\alpha$  values are not in any case excessively large, nor has a minimum ever failed to be located along the line of search. However, the fact that the termination of the process is very like a steepest descent termination perhaps provides a clue to the difficulty. In the steepest descent case it is known that as the iterations proceed one becomes trapped in a subspace of the full  $n$ -dimensional space and there is reason to believe that this is a two dimensional subspace. Now if in the F-R procedure at some early stage in the process, a direction linearly dependent on the preceding directions has been chosen, one would move back into a subspace of the full search space. Furthermore one would be in a subspace that has already been at least partially searched so that only a very small further lowering in energy could be expected. Of course if one moved into such a subspace by accident one might also move

out of it by accident, but as the sequence of iterations continue one might expect the linear dependence problem, if incipient, to become more acute simply from accumulated rounding error. Thus one would expect to end up trapped and to experience slow final convergence at very least.

Now it is easy to see a simple circumstance in which linear dependence, at least to machine accuracy, could well arise; that is the case in which  $g_1$  is very small compared with  $g_{i+1}$  so that  $\beta_i$  is very big, and if  $p_i$  is of the order of  $g_{i+1}$  then

$$p_{i+1} \approx c p_i. \quad (63)$$

and clearly something like this can arise at iteration 2 in the *HF* problem and at iteration 4 in the *F* problem. However linear and near-linear dependence can be much more sophisticated than this and it is quite tricky to test for in detail. However, the behaviour observed is consistent with the presence of linearly dependent directions, and while recognising that this may not be the source of all the trouble encountered in using the F-R method, it is clearly worthwhile investigating the possibilities of modification of the method to try specifically to avoid such a possibility. In passing it should be said that the authors are not yet clear as to why the F-R method did so well in the semi-empirical calculations, but this may be because of a relatively better starting point in these calculations.

### Choosing Linearly Independent Descent Directions

As far as the theoretical properties of the F-R algorithm are concerned (or indeed any related algorithm) to avoid linear dependencies it would seem likely that it is sufficient to use the orbital constraints (see equation (14)) to eliminate redundant variables from the basis and if the minimisation procedure is cast in terms of the non-redundant variables then the Hessian of that reduced problem should be non-singular and hence the F-R method should work. It appears to be quite difficult to show in detail however that such a step is sufficient to achieve a positive definite Hessian (though one of us [16] has attempted a more detailed discussion in the closed shell case). It is also not at all clear that it is necessary to take this step.

In a discussion of the use of the Powell [7] method of minimisation, Raffinetti and Ruedenberg [17] develop a procedure for eliminating the redundant variables. However it is extremely difficult to get closed expressions for the gradient in terms of the non-redundant variables in this approach so that its use appears to be confined to methods like Powell's method which do not utilise the gradient explicitly.

Fletcher and Bradbury [18] also consider the possibility of elimination in the case of solving the ordinary secular problem for a single root by the F-R method. They advocate the arbitrary fixing of one component of the eigenvector. This device effectively confines the possible solutions of the problem to those lying on the faces of hypercube and the face of the hypercube along which minimisation is to occur is determined by the choice of element fixed. However it is not known in advance whether a minimum exists on this face. If a minimum does not exist on the chosen face then this should be shown up by an element other than that chosen becoming greater than the chosen element, in which case the vector must be renormalised so that the emerging element is now fixed, and the minimisation process must be started afresh along the newly chosen face.

In the general case the equivalent tactic would be to fix  $\frac{1}{2}n(n+1)$  values of *Y* and then to attempt to minimise the energy. Presumably the equivalent behaviour in the event of no minimum existing would be for the matrix *A* (cf. equation (16)) to become singular. If this occurred then one would simply have to choose a new set of fixed values that avoided this. Alternatively, of course, there is the possibility that fixing elements of *Y* makes the closest stationary point of the function, one other than the lowest minimum sought (an 'excited state'). In this case also one would have simply to restart the process from with a new choice of fixed elements.

It is clearly not possible to specify any general strategy in respect of choosing the elements of *Y* to be fixed, beyond saying that of course no more than *n* elements and no less than one element should be fixed in any one column. It seems a case where numerical trials alone can decide whether a general strategy is possible for the problem. It should also be remembered that such a strategy may not even be necessary, thus in the MC-SCF case it seems quite likely that it may well be sufficient just to fix one element in each column of *Y*.

However this may be, the analysis so far does suggest another method of tackling the problem which we illustrate below simply in the closed shell case.

Suppose that at any stage of a minimisation process we have a matrix

$$T_1 = YU, \quad T_1^\dagger S T_1 = I_n \quad (64)$$

and from the matrix *f* evaluated at  $T_1$  we construct a matrix  $\bar{f}$  such that

$$\bar{f} = T_1^\dagger f T_1 \quad (65)$$

and find a matrix  $Q_1$  which diagonalises  $\bar{f}$  such that

$$\bar{f} Q_1 = Q \mathfrak{E}_1, \quad Q_1^\dagger Q_1 = I_n \quad (66)$$

and define a matrix  $Z_1 = T_1 Q_1$ . Let us also invent an  $m$  by  $m-n$  matrix  $Z_2$  and define a new basis

$$\phi = (\phi_1 : \phi_2) = \eta(Z_1 : Z_2) \quad (67)$$

such that in this basis

$$f \rightarrow \bar{f} = \begin{pmatrix} \mathfrak{E}_1 & \vdots & \bar{f}_{12} \\ \vdots & \ddots & \vdots \\ \bar{f}_{21} & \vdots & \mathfrak{E}_2 \end{pmatrix}, \quad \bar{f}_{ij} = Z_1^\dagger f Z_j \quad (68)$$

where  $\mathfrak{E}_2$  is diagonal and

$$S \rightarrow \bar{S} = I_m. \quad (69)$$

In this basis clearly

$$T_1 \rightarrow \bar{T} = \begin{pmatrix} I_n \\ \vdots \\ O \end{pmatrix} \quad (70)$$

It then follows immediately from (25), (68), (69) and (70) that the gradient matrix with respect to the elements of  $\bar{T}$  is just

$$\bar{W} = 4 \begin{pmatrix} O \\ \vdots \\ \bar{f}_{21} \end{pmatrix} \quad (71)$$

We can find the Hessian at the point  $\bar{T}$  (that is, *not* at the minimum) by noting from (26) that in general we must add to (31) a term for the ( $j$ ,  $r$ ) element

$$-(S Y A^{-1})_{ir} W_{js} + (S Y A^{-1})_{js} W_{ir} + (W Y^\dagger S)_{ij} (A^{-1})_{rs} \quad (72)$$

where  $W$  is given by (25).

After some manipulation it can be shown that the Hessian with respect to the elements of  $T$  at  $\bar{T}$  is blocked (*cf.* equation (34)) with blocks of the form

$$H^{rs} = 4 \delta_{rs} \begin{pmatrix} O & \vdots & B_{ir}^{(1)} \\ \vdots & \ddots & \vdots \\ B_{ir}^{(2)} & \vdots & H_r \end{pmatrix} + 4 \begin{pmatrix} O & \vdots & B_{rs}^{(1)} \\ \vdots & \ddots & \vdots \\ B_{rs}^{(2)} & \vdots & H_{rs} \end{pmatrix} \quad (73)$$

where  $H_r$  is diagonal with elements.

$$(H_r)_i = (\mathfrak{E}_{n+1} - \mathfrak{E}_r) + 3 \langle (n+i)r | g | r(n+i) \rangle - \langle (n+i)r | g | (n+i)r \rangle \quad (74)$$

and  $(H_{rs})_{ij}$  contains similar off-diagonal terms.

The matrix  $B_{rs}^{(1)}$  is null but for its  $r^{\text{th}}$  row which is the  $s^{\text{th}}$  row of  $f_{12}$  and  $B_{rs}^{(2)}$  is similarly null except for its  $s^{\text{th}}$  column which is the  $r^{\text{th}}$  column of  $\bar{f}_{21}$ .

Now we have seen in equation (10) that it is always possible to decrease the value of locally quadratic function if we choose a direction  $p$  such that  $g^\dagger p \neq 0$  and  $p^\dagger H p \geq 0$ , even if  $H$  is not positive definite. Now if we choose our direction vector in this problem so that its  $r^{\text{th}}$  group of  $m$  rows is given by

$$p_r = -\frac{1}{4} \begin{pmatrix} O & \vdots & O \\ \vdots & \ddots & \vdots \\ O & \vdots & H_r^{-1} \end{pmatrix} \bar{W}_r \quad (75)$$

where  $\bar{W}_r$  is the  $r^{\text{th}}$  column of  $\bar{W}$ , then it follows at once that, if we can neglect terms in  $H_{rs}$ ,

$$g^\dagger p = p^\dagger H p \simeq -4 \sum_{r=1}^m \sum_{j=n+1}^m \bar{f}_{jr} (H_r^{-1})_j \bar{f}_{jr} \quad (76)$$

and since  $H_r$  is certain to be positive definite we have achieved the desired result, in the following sense. We have ensured that the  $p_r$  are directions of descent at least for locally quadratic functions and we have also ensured that near the end of the procedure when  $H_r$  is effectively constant then we can show that the directions chosen are conjugate with respect to  $H_r$  and hence linearly independent. That the directions so chosen are effective minimisation directions depends of course on the legitimacy of neglecting terms in  $H_{rs}$  and on the assumption of quadraticity near the minimum. Furthermore the point reached along  $p$  will not satisfy the orthonormality conditions, so that the discussion of direction conjugacy is somewhat problematic.

We can rewrite (75) in terms of a rectangular  $m$  by  $n$  matrix  $P$  with elements

$$P_{ir} = 0, \quad i \leq n$$

$$(f_{21})_{i-n,r} / ((\mathfrak{E}_r - \mathfrak{E}_i) - 3 \langle ir | g | ri \rangle + \langle ir | g | ir \rangle), \quad i > n \quad (77)$$

and then the next point in the descent is found by constructing

$$\hat{T} = \bar{T} + \lambda P$$

and minimising the energy with respect to  $\lambda$ . Using (63) we can write the change in terms of the  $Z_i$  as

$$\hat{Z}_1 = Z_1 + \lambda Z_2 P_b \quad (78)$$

where  $P_b$  is just the non-zero part of  $P$  written as an  $(m-n)$  by  $n$  matrix.

The matrix  $Z_1$  does not of course satisfy the orthonormality constraints, so it should be regarded as a next estimate of  $Y$  and treated accordingly to determine  $\lambda$ . It violates the constraints only by terms of order  $(P_{ir})^2$  which vanish as the minimum is reached.

The up-dating equation (78) is seen at once to be of precisely the same form as that proposed by Hillier and Saunders [14] and indeed our up-dating matrix  $P_b$  differs from the up-dating matrix  $B$  proposed by these authors only in the presence in  $P_b$  of electron interaction terms in the denominator. Since these terms are probably in most instances small compared with the orbital energy differences, it is perhaps legitimate to neglect them and we can regard this method as being essentially equivalent to that of Hillier and Saunders, a method which is known to work extremely well in practice.

It seems worthwhile therefore to look for a method analogous to the Hillier and Saunders method for use in the MC-SCF case, and work is at present in progress here. However in the MC-SCF case it is by no means as clear as here what one may neglect in order to avoid storing too much of the Hessian. We are also currently investigating the fixing of elements in the  $Y$  matrix in a simplified MC-SCF scheme.

It would appear therefore that it might well be possible to construct schemes which are appropriate and effective in particular problems in Quantum Chemistry, using the general considerations applied in direct minimisation.

### Acknowledgement

B.T.S. would like to thank Professor C.J. Ballhausen of the University of Copenhagen and Dr. J.P. Dahl of the Technical University of Denmark very much indeed for the hospitality at their respective institutions, during which some of this work was performed. D.G. would like to acknowledge the receipt of a Science Research Council studentship.

### References

- [1] McWEENY, R. (1956). *Proc. Roy. Soc. (London)*, **A235**, 496.
- [2] ——— (1960). *Revs. Modern Phys.*, **32**, 335.
- [3] FLETCHER, R. (1970). *Mol. Phys.*, **19**, 55.
- [4] KARI, R. and SUTCLIFFE, B.T. (1970). *Chem. Phys. Letters*, **7**, 149.
- [5] CLAXTON, T. and SMITH, W. (1971). *Theoret. Chim. Acta*, **22**, 399.
- [6] FLETCHER, R. and REEVES, C. M. (1964). *Comp. J.*, **7**, 149.
- [7] POWELL, M.J.D. (1964). *Comp. J.*, **7**, 155.

- [8] FLETCHER, R. and POWELL, M.J.D. (1963). *Comp. J.*, **6**, 163.
- [9] HUANG, H.Y. (1970). *J. Opt. Th. Appl.*, **5**, 405.
- [10] DIXON, L.C.W. (1972). *Math. Programming*, **2**, 383.
- [11] McWEENY, R. and SUTCLIFFE, B.T. (1969). *Methods of Molecular Quantum Mechanics*, London and New York: Academic Press.
- [12] KARI, R. and SUTCLIFFE, B.T. (1973). *Int. J. Quantum Chem.*, **7**, 459.
- [13] SUTCLIFFE, B.T. and GARTON, D., *Theoret. Chim. Acta*, (to be published).
- [14] HILLIER, I.H. and SAUNDERS, V.R. (1970). *Proc. Roy. Soc. (London)*, **A320**, 161.
- [15] HESTENES, M. R. and STIEFEL, E. (1951). *J. Research Natl. Bur. Standards*, **49**, 409.
- [16] SUTCLIFFE, B.T. (1974). *Theoret. Chim. Acta*, **33**, 201.
- [17] RAFFENETTI, R. and RUEDENBERG, K. (1971). *Int. J. Quantum Chem.*, **35**, 625.
- [18] BRADBURY, W. and FLETCHER, R. (1966). *Num. Math.*, **9**, 259.

# The Theoretical Interpretation of the Low Energy Photoelectron Spectra of Transition Metal Complexes

M.F.Guest\* and I.H.Hillier†

The He(I) photoelectron spectra of a number of transition metal complexes containing different ligands are interpreted by means of *ab initio* SCF-MO calculations. It is found that ionization potentials calculated assuming Koopmans' theorem are seriously in error due to the considerably greater orbital relaxation accompanying ionization from metal than from ligand orbitals. When such allowance is made for orbital relaxation by performing RHF calculations on the ionic states the experimental spectra can be satisfactorily interpreted.

## Introduction

Low energy (He(I), He(II)) photoelectron (p.e.) spectroscopy is potentially a very powerful method of studying the electronic structure of transition metal complexes. It is often possible, especially in the case of molecules of high symmetry, to assign the p.e. spectra using chemical arguments and comparisons with spectra of related molecules. Such assignments are usually made in terms of molecular orbitals (m.o.s) arising from either mainly metal or ligand atomic orbitals. If Koopmans' theorem is not greatly in error then the one-to-one correlation between the order and relative energy of the valence ionic states and filled m.o.s allows inferences to be made concerning the bonding in the metal complex. For most molecules composed of first and second row atoms Koopmans' theorem applied to *ab initio* wavefunctions of approximately double zeta quality is successful in calculating the observed ionization potentials (i.p.s). There are of course situations such as  $N_2$  where there are closely spaced m.o.s in the molecular ground state so that more accurate calculations including both relaxation and correlation effects are necessary to predict the ordering of the ionic states. We have previously found that even for core ionizations where the orbital relaxation energy is large, Koopmans' theorem is accurate in predicting the variation of core i.p. with chemical environment (ESCA chemical shifts), the relaxation energy being independent of chemical environment [1].

In our study of the p.e. spectra and electronic structure of transition metal complexes containing a variety of ligands we have found that assignment of the p.e. spectra and the associated deductions

concerning the bonding in the complexes are complicated by serious deviations from Koopmans' theorem and that quite detailed calculations are necessary to obtain a correct interpretation of the experimental data. In this paper we review our findings for a number of molecules in order to establish trends of behaviour rather than to discuss in detail the bonding in individual molecules.

## Computational Details

All electron *ab initio* self-consistent field m.o. calculations were performed in bases of contracted gaussian type functions (g.t.f.s). The core, metal 4s and ligand 2s orbitals were Slater type orbitals (s.t.o.s) with best atom exponents fitted by 3 g.t.f.s/s.t.o. Ligand 2p orbitals were Hartree-Fock orbitals fitted by 4 g.t.f.s and hydrogen 1s and metal 4p orbitals were s.t.o.s having exponents of 1.2 and near 1 respectively each fitted by 3 g.t.f.s/s.t.o. [2,3]. For dibenzene chromium and chromium tricarbonyl benzene an expansion of the metal 3d orbitals in 5 g.t.f.s was used [4], whilst in the other molecules a double zeta basis of metal 3d s.t.o.s expanded in 3 g.t.f.s/s.t.o. was used.

The valence i.p.s were calculated in two approximations. Firstly from the ground state wavefunction using Koopmans' theorem, and secondly by performing a restricted Hartree-Fock (RHF) calculation on each valence ionic state and obtaining the i.p.s directly as the energy difference between the doublet ionic state and singlet ground state ( $\Delta$ SCF method). This latter procedure thus allows for orbital relaxation to occur, accompanying the ionization process. We

\* Atlas Computer Laboratory (Science Research Council), Chilton, Didcot, Oxfordshire, OX11 0QY

† Department of Chemistry, University of Manchester, Brunswick Street, Manchester, M13 9PL

now discuss the bonding and p.e. spectra of a number of transition metal complexes.

### Nickel Tetracarbonyl, Cobalt Tricarbonyl Nitrosyl, Iron Dicarbonyl Dinitrosyl [5]

The isoelectronic series  $Ni(CO)_4$ ,  $Co(CO)_3NO$ ,  $Fe(CO)_2(NO)_2$  were studied in order to see if a comparison of the ligand properties of  $CO$  and  $NO$  could be made from an investigation of the p.e. spectra of these molecules. In figure 1 we show the low energy regions of the  $He(I)$  spectra of these molecules. It can be seen that there is a close resemblance between all three spectra. The interpretation of the spectrum of  $Ni(CO)_4$  is straightforward in terms of the i.p.s calculated from Koopmans' theorem (table 1), the two peaks with approximate intensity ratio 3 : 2 arising from the highest filled  $t_2$  and  $e$  m.o.s of mainly nickel  $3d$  character. The similarity of the spectra of  $Co(CO)_3NO$  and  $Fe(CO)_2(NO)_2$  to that of  $Ni(CO)_4$  implies an approximate metal  $d^{10}$  configuration for these two complexes, the increase in the number of peaks for  $Fe(CO)_2(NO)_2$  being due to the reduced molecular symmetry. Such metal configurations with their associated negative

Table 1: Ionization potentials (eV) of  $Fe(CO)_2(NO)_2$ ,  $Co(CO)_3NO$ ,  $Ni(CO)_4$

	Experimental	Calculated			Symmetry and Character of Ground State m.o. (%)
		KT	$\Delta$ SCF		
<b><math>Ni(CO)_4</math></b>					
${}^2T_2$	8.90	11.7	7.0		$5t_2$ ; 65 (3d)
${}^2E$	9.77	13.5	7.8		$2e$ ; 90 (3d)
<b><math>Co(CO)_3NO</math></b>					
${}^2E$	8.90	8.7	6.7		$8e$ ; 57 (3d)
${}^2A_1$		12.9	6.7		$8a_1$ ; 78 (3d)
${}^2E$	9.82	14.1	7.8		$7e$ ; 86 (3d)
<b><math>Fe(CO)_2(NO)_2</math></b>					
${}^2B_1$	8.97	8.7	7.9		$6b_1$ ; 15 (3d), 74 (NO)
${}^2A_1$		9.1	8.1		$10a_1$ ; 19 (3d), 70 (NO)
${}^2B_2$	8.56	12.6	7.5		$6b_2$ ; 64 (3d)
${}^2A_1$	9.74	15.1	9.4		$9a_1$ ; 83 (3d)
${}^2A_2$		16.0	9.6		$3a_2$ ; 77 (3d)

$Co$  and  $Fe$  charges are in disagreement with the calculated ground state charge distribution (table 2) which give substantial positive charges in both molecules. In addition these low energy i.p.s cannot be correlated with the values given by Koopmans' theorem (table 1). In both  $Co(CO)_3NO$  and  $Fe(CO)_2(NO)_2$  the two highest filled m.o.s ( $8e$ , and  $6b_1$  and  $10a_1$  respectively) have large ligand contributions ( $8e$ , 43%;  $6b_1$ ,  $10a_1$   $\sim$  70%) and are

Table 2: Charge distribution in  $Ni(CO)_4$ ,  $Co(CO)_3NO$ ,  $Fe(CO)_2(NO)_2$

	$Ni(CO)_4$	$Co(CO)_3NO$	$Fe(CO)_2(NO)_2$
Metal 3d population	9.2	7.9	6.6
Atomic Charge			
Metal	+0.5	+0.6	+1.0
Carbon	+0.2	+0.2	+0.2
Oxygen (CO)	-0.4	-0.3	-0.3
Nitrogen		0.0	-0.2
Oxygen (NO)		-0.2	-0.2

followed by three mainly metal m.o.s ( $8a_1$  and  $7e$  for  $Co(CO)_3NO$ ;  $6b_2$ ,  $9a_1$  and  $3a_2$  for  $Fe(CO)_2(NO)_2$ ). The energy spread of the five m.o.s is calculated to be  $\sim 5$  eV and 7 eV in the  $Co$  and  $Fe$  complex respectively, so that no assignment of the p.e. spectra can be made using these values. When the RHF calculations on the ions are performed it is found that there is a striking variation of relaxation energy with the atomic orbital character of the m.o. from which ionization occurs. Thus, for ionization from the highest filled m.o. of  $Co(CO)_3NO$  ( $8e$ ) having substantial ligand character the relaxation energy is 2 eV whilst for the mainly metal  $8a_1$  and  $7e$  m.o.s it is 6.2 eV. This result places the  ${}^2E$  and  ${}^2A_1$  states derived from the  $8e$  and  $8a_1$  m.o.s at the same energy, followed by the  ${}^2E$  state arising from the  $7e$  m.o. at 1.1 eV higher energy. The two peaks in the p.e. spectrum of  $Co(CO)_3NO$  with intensity ratios near 3 : 2 are thus explained as arising from the first  ${}^2E$  and  ${}^2A_1$  states and the second  ${}^2E$  state respectively.

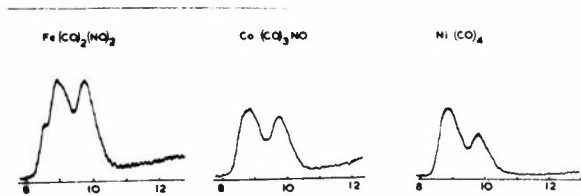


Figure 1:  $He(I)$  p.e. spectra of  $Ni(CO)_4$ ,  $Co(CO)_3NO$  and  $Fe(CO)_2(NO)_2$

A similar situation is found for  $Fe(CO)_2(NO)_2$ . The relaxation energy associated with the  $6b_1$  and  $10a_1$  m.o.s having considerable  $NO$  character ( $\sim 1$  eV) is considerably less than the values for the  $6b_2$  and  $3a_2$  m.o.s (5-6 eV) having mainly metal  $3d$  character. Such variations in the relaxation energies reduces the spread of the first five i.p.s from  $\sim 7$  eV given by Koopmans' theorem to  $\sim 2$  eV and allows

an assignment of the p.e. spectrum of  $Fe(CO)_2(NO)_2$ . Thus, the first i.p. arises from ionization of the third highest-lying  $6b_2$  orbital (mainly metal), the second from ionization of the  $6b_1$  and  $10a_1$  m.o.s having a large ligand character and the third from ionization of the other two metal orbitals,  $9a_1$  and  $3a_2$ .

### Dibenzene Chromium and Chromium Tricarbonyl Benzene [4]

The  $He(I)$  p.e. spectrum of dibenzene chromium ( $CrBz_2$ ) has been reported by Evans, Green and Jackson [6], and shows two low energy bands at 5.4 and 6.4 eV with intensity ratio 1 : (3.5-4). If a chromium  $d^6$  configuration is assumed for the complex then these two peaks may be assigned to the mainly metal  $a_{1g}$  and  $e_{2g}$  m.o.s. As in the iso-electronic series previously described there are further bands in the p.e. spectrum which may be assigned to mainly ligand m.o.s. The corresponding p.e. spectrum for chromium tricarbonyl benzene  $BzCr(CO)_3$  [4] shows but a single peak in the region where metal  $3d$  ionizations are expected at 7.5 eV, implying that there is no splitting between the metal  $e$  and  $a_1$  m.o.s. The experimental i.p.s for these two molecules are compared with the calculated values in table 3. On the basis of Koopmans' theorem the lowest  ${}^2E_{2g}$  state is calculated to be below the lowest  ${}^2A_{1g}$  state of dibenzene chromium, in contradiction to a simple interpretation of the p.e. spectrum. However, inspection of the atomic orbital composition of the  $8a_{1g}$  and  $4e_{2g}$  m.o.s shows that whereas the former is essentially localized on the chromium atom, the  $4e_{2g}$  has nearly equal contributions from the metal- $3d$  and benzene  $\pi$  orbitals. Indeed, the  $4e_{2g}$  orbital provides the largest contribution to the chromium- $3d$  benzene- $2p\pi$  bond, this interaction arising from  $\pi$  back-donation into the  $1e_{2u}\pi^*$  m.o. of benzene. The  $\Delta$ SCF calculations reveal substantially more relaxation energy associated with the  $8a_{1g}$  m.o. (6.2 eV), and reduce the calculated separation of the  ${}^2A_{1g}$  and  ${}^2E_{2g}$  states from the 3.8 eV given by Koopmans' theorem to 0.2 eV. However, the

experimental ordering of these two levels is still incorrectly given, although the calculated splitting is in error by only 1.2 eV. It is anticipated that a better basis, particularly a more flexible  $3d$  one, would remove this inaccuracy.

In the case of  $BzCr(CO)_3$ , Koopmans' theorem predicts a splitting of 2.7 eV between the lowest  ${}^2E$  and  ${}^2A_1$  states although none is observed experimentally. As in  $CrBz_2$ , the  $e$  m.o. is calculated to have  $\sim 50\%$  ligand contribution, whereas the  $a_1$  m.o. is mainly metal  $3d$  (79%). The  $\Delta$ SCF calculations give greater orbital relaxation associated with the  $a_1$  (5 eV) than with the  $e$  m.o. (2.3 eV), so that the  ${}^2E$  and  ${}^2A_1$  states are calculated to have the same energies in agreement with the single line observed in the p.e. spectrum of this molecule.

### Iron Tricarbonyl Butadiene [3]

The mode of bonding of butadiene in transition metal complexes has been the subject of much discussion. As a result of our *ab initio* calculation of this complex we predict there is greater metal  $\rightarrow$  ligand  $\pi$  donation into the first virtual  $2b_1$  m.o. of butadiene than  $\pi$  back-bonding from the highest filled  $1a_2$  m.o. of the ligand, so that the charge distribution in complexed butadiene bears some resemblance to that of the butadiene anion. The low energy p.e. spectrum of this complex (figure 2) is considerably

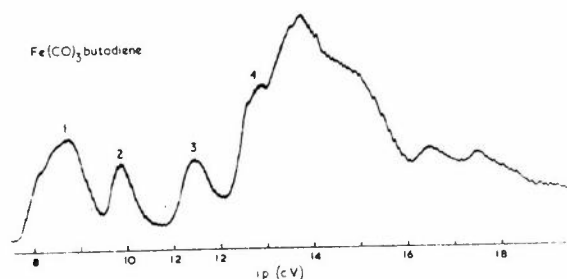


Figure 2:  $He(I)$  p.e. spectrum of  $Fe(CO)_3C_4H_6$

Table 3: Ionization potentials (eV) of  $Cr(Bz)_2$  and  $BzCr(CO)_3$

		Experi- mental	Calculated	KT $\Delta$ SCF		Symmetry and Character of Ground State m.o. (%)
$Cr(Bz)_2$	${}^2A_{1g}$	5.4	11.3	5.1		$8a_{1g}$ ; 92 (3d)
	${}^2E_{2g}$	6.4	7.5	4.9		$4e_{2g}$ ; 53 (3d)
$BzCr(CO)_3$	${}^2E$	7.5	8.4	6.1		$17e$ ; 51 (3d)
	${}^2A_1$	7.5	11.1	6.1		$17a_1$ ; 79 (3d)

more complicated than those of the other molecules discussed here, and without the aid of a suitable calculation any assignment would appear rather difficult. However, a comparison of the intensities of the various bands in a p.e. spectrum using both  $He(I)$  and  $He(II)$  radiation can often provide some empirical information of the atomic character of the orbitals giving rise to the bands. With the aid of a  $He(II)$  spectrum of iron tricarbonyl butadiene, together with information obtained from  $He(I)$  and



He(II) spectra of simpler carbonyls where the assignment is rather more certain, the following tentative conclusions emerge concerning the origin of the first four bands of figure 2.

- Band 1 contains three essentially metal levels, together with one possessing significant butadiene character;
- Band 2 arises from an orbital also possessing significant metal character;
- Bands 3 and 4 arise from orbitals largely localized on the butadiene entity.

Table 4: Ionization potentials (eV) of  $Fe(CO)_3C_4H_6$

Orbital	Metal 3d Character (%)	Koopmans' Theorem	$\Delta$ SCF Method	Band Assignment	Experimental
$31a'$	33	8.1	6.5	1	8.8
$18a''$	10	10.8	9.9	2 ?	9.9
$30a'$	51	12.6	7.7	1	8.8
$17a''$	66	13.8	10.8	1	8.8
$29a'$	34	14.1	13.4	3 ?	11.5
$28a'$	65	14.7	9.0	1	8.8
$16a''$	13	15.4		4	12.9

We first review this interpretation of the low energy p.e. spectra in the light of the ground state m.o.s of table 4. Amongst the first seven filled m.o.s there are indeed three with large metal character ( $30a'$ ,  $17a''$  and  $28a'$ ), two with quite significant metal character ( $31a'$ ,  $29a'$ ) and two with rather small metal character ( $18a''$ ,  $16a''$ ) which are mainly butadiene in origin. Although an assignment of the p.e. spectrum based upon orbital character can thus be made which is consistent with the deductions based upon intensity arguments, the calculated ordering of the m.o.s is not in line with such an assignment. In particular, those m.o.s of mainly metal character lie below the top two m.o.s of mainly butadiene character. From our previous discussion of other metal complexes we would thus expect a reordering of the ionic states obtained from Koopmans' theorem due to the different relaxation energies associated with the m.o.s of different atomic orbital character. This is in fact found, and the i.p.s calculated by the  $\Delta$ SCF method are shown in table 4, which now allow a fairly satisfactory assignment of the p.e. spectrum. Thus band 1 is associated with the mainly metal  $30a'$ ,  $17a''$  and  $28a'$  m.o.s and with the  $31a'$  m.o. having substantial butadiene character. We correlate bands 2 and 3 with the  $18a''$  and  $29a'$  m.o.s respectively of mainly butadiene character and band 4 with the  $16a''$  butadiene m.o. The order of the ionic states

calculated by the  $\Delta$ SCF method is in line with this assignment except for the relative positions of the two  $2A''$  states arising from the  $18a''$  and  $17a''$  m.o.s. Furthermore, it should be noted that using arguments based upon correlations between orbital character and band intensities the assignment of bands 2 and 3 would probably be interchanged from that given in table 4. These discrepancies are however to be expected for a molecule of this size in view of the limited basis used and the neglect of correlation effects.

### Iron Tricarbonyl Cyclobutadiene [7]

The low energy p.e. spectrum of iron tricarbonyl cyclobutadiene (figure 3) is considerably simpler than that of the butadiene complex although its interpretation is no more obvious. Only two peaks are resolved below 12 eV, (at 8.4 and 9.2 eV), although

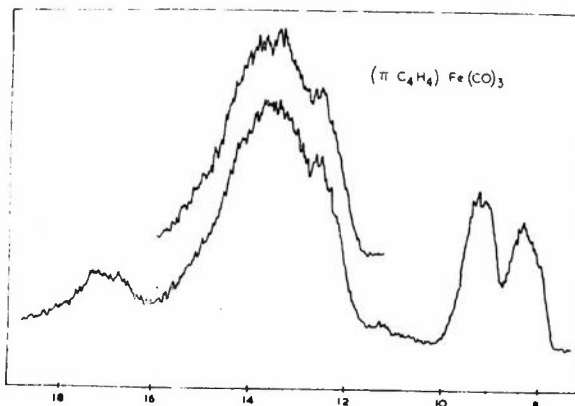


Figure 3: He(I) p.e. spectrum of  $Fe(CO)_3C_4H_4$

a number of metal orbitals and those m.o.s giving rise to the metal-cyclobutadiene bonds are expected to occur in this region of the spectrum. The two highest filled m.o.s of the complex are seen to be nearly degenerate (table 5) and involve the metal 3d orbitals ( $\sim 20\%$ ) and the partially filled  $e_g \pi$  m.o.s

Table 5: Ionization potentials (eV) of  $Fe(CO)_3C_4H_4$

Orbital	Metal Character (%)	Koopmans' Theorem	$\Delta$ SCF Method	Experimental
$17a''$	21	9.2	8.1	} 9.2
$31a'$	22	9.3	8.2	
$30a'$	50	13.8	8.4	} 8.4
$16a''$	65	13.9	8.5	
$29a'$	44	13.9		

of cyclobutadiene. The next three m.o.s are also nearly degenerate and have larger (~50%) metal 3d components. The remaining m.o.s are largely ligand in character. From this data it is plausible that the two bands in the p.e. spectrum arise from these two groups of m.o.s. A comparison of the band intensities using both He(I) and He(II) radiation suggests that band 2 has mainly ligand character, and band 1 mainly metal character, and from the shapes it seems likely that band 1 has more contributing ionizations than band 2. Thus Koopmans' theorem fails to provide a satisfactory explanation for the low i.p. region, since the calculations of table 5 would predict that band 1 arises from the  $17a''$  and  $31a'$  m.o.s of mainly cyclobutadiene character, and that band 2 arises from the closely spaced metal orbitals ( $30a'$ ,  $16a''$  and  $29a'$ ). The results of the  $\Delta$ SCF calculations show that there is much more orbital relaxation accompanying ionization from the mainly metal orbitals than from the ligand m.o.s. As with dibenzene chromium, the calculated differential relaxation is not quite sufficient to invert the order of these two groups as required by the experimental data, but we consider band 2 is best assigned to the two ligand  $\pi$  ionizations and band 1 to the three mainly metal ionizations.

## Conclusions

It is clear that an assignment of the low energy p.e. spectrum of many transition metal complexes cannot be made on the basis of Koopmans' theorem since we have found that orbital relaxation accompanying ionization from the mainly metal 3d m.o.s is much larger than that from m.o.s having a large ligand component. A similar situation has also been found for ferrocene [8] and bis-( $\pi$ -allyl) nickel [9]. When this difference is taken into account the experimental spectra are much better reproduced. We note that greater orbital relaxation is associated with the *localized* metal orbitals than with the relatively *delocalized* ligand m.o.s. In an attempt to obtain a semiquantitative relationship between the spatial extent of a m.o. and the relaxation energy we have computed expectation values of the second moment operator  $r^2$ , for the occupied m.o.s of the molecular ground state and we find that variations in  $\langle r^2 \rangle$  and the reciprocal of the relaxation energies follow a similar trend. A similar result has been found in the study of core hole states when there is greater relaxation energy associated with localized core holes than with delocalized ones [1,10].

## Acknowledgements

Thanks are due to the Science Research Council for supporting this research.

## References

- [1] AARONS, L.J., GUEST, M.F., HALL, M.B. and HILLIER, I.H. (1973). *J. Chem. Soc. (Faraday II)*, **69**, 563.
- [2] HILLIER, I.H. and SAUNDERS, V.R. (1971). *Mol. Phys.*, **22**, 1025.
- [3] CONNOR, J.A., DERRICK, L.M.R., HALL, M.B., HILLIER, I.H., GUEST, M.F., HIGGINSON, B.R. and LLOYD, D.R. (1974). *Mol. Phys.*, **28**, 1193.
- [4] GUEST, M.F., HILLIER, I.H. and LLOYD, D.R. (1975). *Mol. Phys.*, **29**, 113.
- [5] HILLIER, I.H., GUEST, M.F., HIGGINSON, B.R. and LLOYD, D.R. (1974). *Mol. Phys.*, **27**, 215.
- [6] EVANS, S., GREEN, J.C. and JACKSON, S.E. (1972). *J. Chem. Soc. (Faraday II)*, **68**, 249.
- [7] HALL, M.B., HILLIER, I.H., CONNOR, J.A., GUEST, M.F. and LLOYD, D.R. (1975). *Mol. Phys.*, (submitted for publication).
- [8] COUTIERE, M.M., DEMUYNCK, J. and VEILLARD, A. (1972). *Theoret. Chim. Acta*, **27**, 281.
- [9] ROHMER, M.-M. and VEILLARD, A. (1973). *Chem. Comms.*, 250.
- [10] BAGUS, P.S. and SCHAEFER, H.F. (1972). *J. Chem. Phys.*, **56**, 224.

# Ab Initio Calculations of Transition Metal Complexes and Organometallics

A. Veillard\*

Some features of *ab initio* calculations which are specific to systems involving transition metals will be discussed briefly: use of large basis sets involving many *d*-functions, possibility of recognizing negligible integrals, how to take advantage of the usually high symmetry. A short description of the possible organization of the programs will be given. Some problems connected with the calculation of ionized and excited states will be mentioned. Physical or chemical results which may be obtained will be surveyed in the light of recent calculations carried out in Strasbourg:

- calculation of ionization and excitation energies;
- calculation of binding energies and linkage isomerism;
- possible mechanisms of stereochemical nonrigidity;
- binding of molecular oxygen by metal complexes.

*Ab initio* calculations of transition metal complexes raise the following questions:

- what type of complexes<sup>†</sup> are presently amenable to *ab initio* calculations and what are the technical requirements on this type of calculations?
- why *ab initio* calculations for complexes? In other words, what benefit in the field of physical chemistry or chemistry can we expect from *ab initio* calculations?

Transition metals start with the filling of the *3d* orbitals. This implies that *3d* functions in the LCAO basis set are now essential to the description of the bonding instead of accounting solely for the polarization effects. A fair description of the polarization effects for the first and second row atoms can be achieved usually with only one *d* function. Experience has shown that in order to describe satisfactorily the *3d* valence shell, one needs at least four or five *d* gaussian functions for each *d* orbital. Since we work with a set of six *d* functions *XX*, *XY*, *XZ*, *YY*, *YZ*, *ZZ*, this implies for each metal atom a total of between 24 and 30 *d* gaussian functions. The basis set for relatively simple complexes being usually in the range of 250 to 300 basis functions, *d* functions represent of the order of 10% of the basis set. Then about 35% of the two-electron integrals will involve at least one *d* function. The calculation of these integrals involving *d*-functions being one order of magnitude slower than for integrals involving only *s* and *p* functions, we see that most of the two-electron integral calculation time is spent over integrals involving the *d* functions.

There are two major possibilities to cut down the time for integral calculation. The first one is based on the grouping of integrals which have certain terms in common. This has been found an efficient procedure for integrals involving only *s* and *p* functions [1,2]. However, this represents a much more complicated task for integrals involving *d*-functions. The other way is to take advantage of the relatively high symmetry of many complexes, as proposed first in POLYATOM [3]. We have reported in table 1 some systems investigated recently in Strasbourg together with their molecular point group. Most of them have relatively high symmetry and this results in a large number of integrals being zero by symmetry or being equal to within a sign. We use an algorithm similar to the one of the POLYATOM program [3] in order to generate a list of unique non-zero integrals. From table 1 one may see that this results in an appreciable time saving.

Many transition metal complexes have an open-shell configuration in their ground state or in the excited states. We deal with open-shell systems through the restricted Hartree-Fock procedure of Roothaan with two hamiltonians [4]. However, this is a relatively expensive procedure for large basis sets. Either the one hamiltonian procedure of Roothaan [4] or the orthogonality constrained basis set expansion method for treating off-diagonal Lagrange multipliers [5] might lead to more economical *large* SCF calculations. Each excited state is obtained through an independent SCF calculation, since one major conclusion reached was that electronic relaxation is a

\* Centre National de la Recherche Scientifique, Université Louis Pasteur, BP 296R8, 67 Strasbourg, France

† In what follows, the word complex will be taken in a very broad sense, including an assembly of ions like  $NiF_6^{2-}$  or some molecular species like  $NiN_2$ .

Table 1: Some representative calculations of transition metal complexes

System	Molecular Point Group	Point group used in Integral Evaluation Highest Symmetry <sup>a</sup>	Point group used in Evaluation Highest Symmetry <sup>b</sup>	Number of Gaussian Functions	Number of Contracted Functions	Number of Two-electron Integrals ( $\times 10^6$ )	Number of Unique Non-zero Integrals ( $\times 10^6$ )	Integral Computation Time <sup>c</sup>
$MnO_4^-$	$T_d$	$C_{2v}$	$C_{2v}$	142	61	1.788	0.463	3h 44'
$NiN_2$ End-on	$C_{\infty v}$	$C_{4v}$	$C_{4v}$	102	43	0.447	0.073	35'
$NiN_2$ Side-on	$C_{2v}$	$C_{2v}$	$C_{2v}$	102	43	0.447	0.120	1h 5'
$Cu(H_2O)_4^{2+}$	$C_{2v}$	$C_{2v}$	$C_{2v}$	174	77	4.510	1.145	5h 11'
$Cu(H_2O)_5^{2+}$	$C_{2v}$	$C_{4v}$	$C_{2v}$	202	90	8.386	1.258	-
$CuCl_3^-$	$D_{3h}$	$C_{4v}$	$C_{2v}$	202	90	8.386	1.938	6h 20'
	$C_{4v}$	$C_{4v}$	$C_{4v}$	202	90	8.386	1.040	-
$Fe(CO)_5$	$D_{3h}$	$C_{2v}$	$C_{2v}$	212	115	17.703	5.520	$\sim 11$ h
$Co(acacen)^d$	$C_{2v}$	$C_{2v}$	$C_{2v}$	236	83	6.077	1.715	$\sim 13$ h
$Co(acacen)O_2$	$C_s$	$C_{2v}$	$C_s$	268	93	9.555	3.716	$\sim 13$ h
$[Co(acacen)O_2CN]^-$	$C_s$	$C_{2v}, C_{4v}$	$C_s$	300	103	14.346	5.871	$\sim 22$ h

(a) For a subset of the system  
 (b) For the whole system

(c) On the Univac 1108  
 (d) *acacen* stands for  $(HNCHCHCHO)_2$

prime factor in determining the sequence of excited states [6,7]. However, when one has to deal with many excited states, it may become more economical to perform a configuration interaction calculation limited to the monoexcited configurations and based on the virtual orbitals from the ground-state SCF calculation [8].

Among the questions which one may try to answer is the electronic configuration of the ground state for some complexes. The degeneracy of the 3d orbitals is lifted in the complex but the energy splitting between the 3d orbitals may remain small. This results in several electronic configurations with close energy values when the number of d electrons is different from zero or ten. The species  $CoN_2$  [9] has a  $3d^9$  configuration which may result in the electronic configurations  $^2\Sigma$ ,  $^2\Pi$  or  $^2\Delta$  for the end-on conformation<sup>†</sup> ( $C_{\infty v}$  point group) and  $^2A_1$ ,  $^2B_1$ ,  $^2A_2$

or  $^2B_2$  for the side-on conformation ( $C_{2v}$  point group) (figure 1 and figure 2). Calculation at the SCF level predict a  $^2\Sigma$  ground-state [10]. Settling the electronic configuration of the ground state represents for  $CoN_2$  a prerequisite to a discussion of the possible linkage isomerism (cf. below).

A similar situation occurs for  $FeCO$  or  $FeN_2$  ( $FeN_2$  has been reported recently in matrix isolation experiments [11] and  $Fe(CO)^+$  has been identified in ion cyclotron resonance experiments [12]). With a  $3d^8$  configuration, the most probable electronic configurations for a linear molecule are  $^1\Sigma$  or  $^3\Sigma$  (figure 3). SCF calculations give the  $b^3\Sigma$  ( $\sigma^2 \pi^4 \delta^2$  configuration) as the ground state, followed by the other triplet state  $a^3\Sigma$  ( $\sigma^2 \delta^4 \pi^2$  configuration). Similar results should hold for the isoelectronic system  $FeN_2$ , recently observed, for which the ground state is then expected to be a triplet.

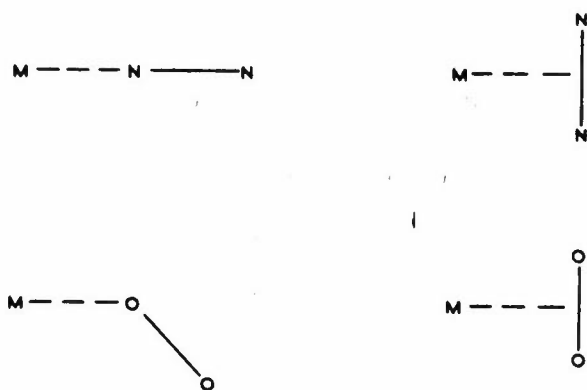


Figure 1: End-on (left) and side-on (right) bonding of the  $N_2$  and  $O_2$  ligands

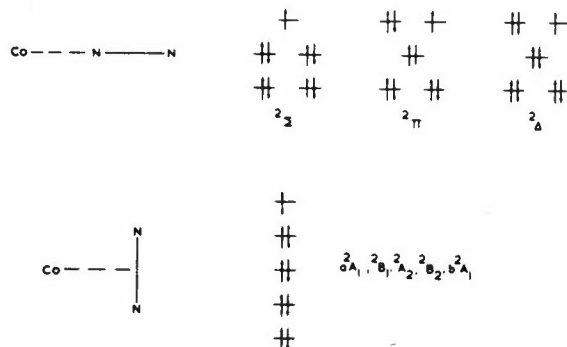


Figure 2: Possible electronic configurations for  $CoN_2$  (end-on or side-on)

<sup>†</sup> In order to avoid any confusion with the electronic configuration, we use here the word conformation to denote the geometric configuration.

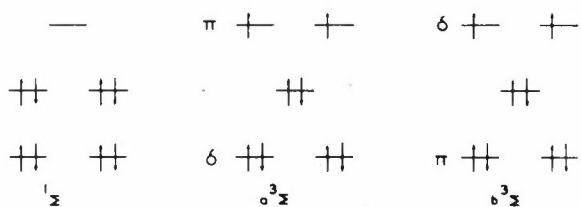


Figure 3: Possible electronic configurations for linear  $FeCO$  or  $FeN_2$

Transition metal complexes usually display a rich electronic absorption spectrum in the visible and near UV, since there are several possibilities of electronic excitations, either  $d \rightarrow d$  (ligand-field) excitations or charge-transfer excitations from ligand to metal but also from metal to ligand. One of the major difficulties which the experimentalists face is the assignment of the observed transitions. In this respect the calculation of excitation energies will be helpful to the experimentalists if SCF calculations of excitation energies may be shown to lead to the right sequence of excitation energies (even if the computed excitation energies are in error by several thousands  $cm^{-1}$ ).

Table 2: Computed excitation energies (in  $cm^{-1}$ ) for the  $D_{4h}$  configuration of the  $CuCl_4^{2-}$  ion<sup>a</sup>

Excited State and Transition	Excitation Energy	Nature of the Transition	Type of the Transition
${}^2B_{2g}(2b_{2g} \rightarrow 6b_{1g})$	8 100	$d_{xy} \rightarrow d_{x^2-y^2}$	} $d \rightarrow d$
${}^2E_g(2e_g \rightarrow 6b_{1g})$	9 900	$d_{xz,yz} \rightarrow d_{x^2-y^2}$	
${}^2A_{1g}(8a_{1g} \rightarrow 6b_{1g})$	10 500	$d_{z^2} \rightarrow d_{x^2-y^2}$	
${}^2A_{2g}(2a_{2g} \rightarrow 6b_{1g})$	32 200	$\pi_L \rightarrow d_{x^2-y^2}$	} charge transfer
${}^2E_u^*(9e_u \rightarrow 6b_{1g})$	37 700	$\pi_L \rightarrow d_{x^2-y^2}$	
${}^2B_{2u}^*(2b_{2u} \rightarrow 6b_{1g})$	40 400	$\pi_L \rightarrow d_{x^2-y^2}$	
${}^2A_u(4a_{2u} \rightarrow 6b_{1g})$	48 100	$\pi_L \rightarrow d_{x^2-y^2}$	
${}^2E_u^*(8e_u \rightarrow 6b_{1g})$	50 900	$\sigma_L \rightarrow d_{x^2-y^2}$	

\* Excited states corresponding to allowed transitions

(a) Experimental (in  $cm^{-1}$ , with previous assignment):  
 10 900 ( $d_{z^2} \rightarrow d_{x^2-y^2}$ ), 13 100 ( $d_{xy} \rightarrow d_{x^2-y^2}$ ),  
 14 300 ( $d_{xz,yz} \rightarrow d_{x^2-y^2}$ ), 24 000 ( $\pi \rightarrow d_{x^2-y^2}$ ),  
 33 300 ( $\pi \rightarrow d_{x^2-y^2}$ ), 38 500 ( $\pi \rightarrow d_{x^2-y^2}$ ),  
 49 000 ( $\sigma \rightarrow d_{x^2-y^2}$ ) [14]

In table 2 we have reported the computed excitation energies [7] together with the experimental transitions and previous assignments (based on crystal field calculations) [13,14] for the square planar  $CuCl_4^{2-}$  ion ( $D_{4h}$  point group). For the  $d-d$  excitations our calculation leads to a different assignment from

the previous one, namely

$${}^2B_{2g}(d_{xy} \rightarrow d_{x^2-y^2}) < {}^2E_g(d_{xz,yz} \rightarrow d_{x^2-y^2}) < {}^2A_{1g}(d_{z^2} \rightarrow d_{x^2-y^2}).$$

This is supported by the experimental evidence from the polarized spectra and magnetic circular dichroism (MCD) spectra, leading to a similar assignment, for  $PdCl_4^{2-}$  and  $PtCl_4^{2-}$  [15,16]:

$${}^1A_{2g}(d_{xy} \rightarrow d_{x^2-y^2}) < {}^1E_g(d_{xz,yz} \rightarrow d_{x^2-y^2}) < {}^1B_{1g}(d_{z^2} \rightarrow d_{x^2-y^2}).$$

Our computed excitation energies for the two allowed charge-transfer transitions to the states  ${}^2E_u(\pi 9e_u \rightarrow 6b_{1g})$  and  ${}^2B_{2u}(2b_{2u} \rightarrow 6b_{1g})$  are very close with a difference of about  $2500 cm^{-1}$  and fall at longer wavelengths than the excitation to the state  ${}^2E_u(\sigma 8e_u \rightarrow 6b_{1g})$ . This is supported by the following sequence for  $PdCl_4^{2-}$  inferred from the polarized and MCD spectra [16]:

$${}^1A_{2u}(\pi b_{2u} \rightarrow b_{1g}) \sim a {}^1E_u(\pi e_u \rightarrow b_{1g}) < b {}^1E_u(\sigma e_u \rightarrow b_{1g}).$$

The electronic spectrum of the anion  $Ni(CN)_4^{2-}$  has been the subject of many experimental investigations. The sequence of excited states assumed on the basis of the experimental work (electronic absorption spectrum and MCD spectrum) was the following in 1972 [17]

$${}^1A_{2g}(d_{xy} \rightarrow d_{x^2-y^2}) < {}^1B_{1g}(d_{z^2} \rightarrow d_{x^2-y^2}) < {}^1E_g(d_{xz,yz} \rightarrow d_{x^2-y^2}) < {}^1B_{1u}(d_{xy} \rightarrow \pi^*) < {}^1A_{2u}(d_{z^2} \rightarrow \pi^*) < {}^1E_u(d_{xz,yz} \rightarrow \pi^*)$$

while the sequence based on the computed excitation energies was found [6]

$${}^1B_{1g} < {}^1E_g \sim {}^1A_{2g} < {}^3A_{2u}(d_{z^2} \rightarrow \pi^*) < {}^1A_{2u} < {}^3E_u(d_{xz,yz} \rightarrow \pi^*) < {}^1E_u$$

with the  ${}^3, {}^1B_{1u}$  states at much higher energies. Gray and Ballhausen have recently proposed a new assignment of the experimentally observed transition [18], which is quite different from the previous one and much closer to the theoretical sequence

$${}^1B_{1g} < {}^1E < a A_{2u}({}^1A_{2u}, {}^3E_u) < ({}^3E_u, {}^3B_{1u}, {}^3A_{2u}, {}^1E_u) < b A_{2u}({}^3E_u, {}^1A_{2u}) < {}^1E_u$$

(the bracket notations refer to spin-orbit mixed states). One will notice particularly that the transition to

the  ${}^1B_{1u}$  state, which was considered previously to be the lowest charge-transfer transition, has now been discarded.

Table 3: Computed binding energy (in kcal/mole) for the aquo ions  $Cu(H_2O)_n^{2+}$

$n$	Molecular Point Group <sup>a</sup>	Binding Energy
4	$T_d$	338
	$D_{4h}$	348
5	$D_{3h}$	381
	$C_{4v}$	381
6	$D_{4h}$	409

(a) For the skeleton of  $Cu$  and  $O$  atoms

The chemistry of metal ions in solution is determined by the properties of their aquo ions, namely the complexes  $M(H_2O)_n^{m+}$ . Calculation of the binding energy associated with these ions should give some insight into their structure. In table 3 we have reported the binding energies computed for the ions  $Cu(H_2O)_n^{2+}$  ( $n = 4, 5, 6$ ) [10]. The largest binding energy of 409 kcal/mole is associated with a coordination number of six, the species  $Cu(H_2O)_6^{2+}$  assuming the configuration of a distorted octahedron due to the Jahn-Teller effect. Since the experimental hydration energy of the  $Cu^{2+}$  ion amounts to 502 kcal/mole [19], this means that the solvation energy corresponding to the outer-shell molecules of water represents of the order of 20% of the hydration energy. It is generally believed that exchange of water molecule from the first coordination sphere of the metal ion occurs through an  $SN_1$  mechanism with an intermediate  $M(H_2O)_5^{m+}$  assuming a square pyramid structure [20]. The computed binding energies of table 3 indicate that the square pyramid and the trigonal bipyramid structures have comparable stabilities and that a lower limit to the activation energy for the exchange reaction would be 28 kcal/mole, the difference between the binding energies for  $n = 6$  and  $n = 5$ .

Linkage isomerism corresponds to the ability of certain ligands to bind to the metal atom in more than one way. Both the dinitrogen ligand  $N_2$  and the dioxygen ligand  $O_2$  may display two different bonding types, either end-on or side-on (figure 1) [11]. The dinitrogen ligand in most transition metal-dinitrogen complexes studied to date (like  $Ni(N_2)_4$ ) is bonded end-on with a linear or near-linear  $M...N...N$  skeleton. However two cases have been reported recently with the dinitrogen molecule bonded in a

sideways fashion [9,21]. An extremely intriguing finding (based on the pattern of  $NN$  stretching modes in the matrix infrared spectrum) was the conclusion of Ozin and colleagues that, for the monodinitrogen complexes  $M(N_2)$ , both  $NiN_2$  and  $FeN_2$  correspond to end-on bonding while the bonding in  $CoN_2$  would be in a sideways fashion [11]. They emphasized that 'these three compounds were synthesized under virtually identical matrix conditions and that the observed structural variations from end-on to side-on bonded  $N_2$  must reflect properties characteristic of the metal atom' (*id est* electronic factors).

We have reported in table 4 the total energy computed for the ground state of  $NiN_2$  and  $CoN_2$  both end-on and side-on bonded. Given the lack of any structural data, a full geometry optimization, with respect to both the  $Ni-N$  and  $N-N$  distances, was carried for  $NiN_2$ . For  $CoN_2$  we optimized only the  $Co-N$  distance. Our results support the hypothesis of Ozin that the difference of bonding between  $NiN_2$  and  $CoN_2$  arise from electronic factors and not from matrix effects. For  $NiN_2$  we find the end-on structure to be more stable than the side-on by 7 kcal/mole<sup>†</sup>. For  $CoN_2$  this value is reduced to 0.7 kcal/mole, still in favour of the end-on structure. However such a small energy difference is probably beyond the accuracy of this calculation. A significant result is the increase in the relative stability of the side-on complex when going from  $Ni$  to  $Co$ .

Table 4: Energy results for the species  $CoN_2$  and  $NiN_2$  (with geometry optimization)

Species	Ground State	Computed Energy	
$NiN_2$	End-on	$1\Sigma^+$	-1612.3704 <sup>a</sup>
	Side-on	$1A_1$	-1612.3585 <sup>a</sup>
	Difference		7.4 <sup>b</sup>
$CoN_2$	End-on	$2\Sigma^+$	-1487.0891 <sup>a</sup>
	Side-on	$2A_1$	-1487.0880 <sup>a</sup>
	Difference		0.7 <sup>b</sup>

(a) In au

(b) In kcal/mole

There is a strong experimental interest in oxygen carriers complexes, *id est* complexes which can bind molecular oxygen in a reversible way. Some synthetic oxygen carrier cobalt complexes have been recently characterized, and they are sometimes considered as models for the haemoglobin and myoglobin molecules which carry reversible oxygenation in life processes.  $Co(acacen)$  is such a synthetic carrier, with the oxygen adduct written usually  $Co(acacen)LO_2$ , with

<sup>†</sup> This relatively small energy difference makes understandable that complexes have been reported with dinitrogen bonded to the  $Ni$  atom in a sideways fashion [21], possibly because of the electronic effect of the other ligands or because of packing effects in the crystal.

$L$  the second axial ligand ( $L$  may be a solvent molecule) (figure 4) [22]. In these complexes, the  $O_2$  molecule binds in an end-on fashion, the  $CoO_1O_2$  angle being of the order of  $126^\circ$ . Binding of dioxygen has been previously discussed either in a qualitative way [23] or through extended Hückel calculations [24] but only in the case of linear ( $CoO_1O_2 = 180^\circ$ ) or perpendicular (sideways) bonding. The degenerate  $\pi$  and  $\bar{\pi}$  orbitals of the dioxygen molecule are split in these complexes (while similar  $FeII$  complexes are diamagnetic, these  $CoII$  complexes are experimentally known to have one unpaired electron) and there are four possible electronic configurations for the ground state of the dioxygen adduct (figure 5) (assuming that the unpaired electron for the  $Co(acacen)L$  complex is in the  $3d_{z^2}$  orbital), of which three denoted  $S_1$ ,  $S_2$  and  $S_3$  belong to the symmetric representation and one denoted  $A$  belongs to the antisymmetric one (the symmetry plane of the complex is the plane  $xOz$  and includes the dioxygen ligand (figure 4)). These four electronic configurations of figure 5 correspond to the different possibilities regarding

- the relative order of the  $\pi_g^a$  and  $\pi_g^b$  orbitals of the dioxygen ligand in the complex ( $\pi_g^a$  and  $\pi_g^b$  are related to the  $\pi_g$  and  $\bar{\pi}_g$  orbitals of  $O_2$ , we denote  $\pi_g^b$  the one made from the  $2p_y$  orbitals of the oxygen atoms, which is antisymmetrical with respect to the symmetry plane  $xOz$ );
- the relative location of the  $3d_{z^2}$  orbital with respect to  $\pi_g^a$  and  $\pi_g^b$ ;
- the relative magnitudes of  $\Delta_1$ , the splitting between  $\pi_g^a$  and  $\pi_g^b$ , and  $\Delta_2$ , the energy gap between the  $3d_{z^2}$  and  $\pi_g^a$  orbitals after interaction.

One will notice that the formal oxidation number of  $Co$  remains II in  $S_1$  and  $S_2$ , while  $A$  and  $S_3$  correspond

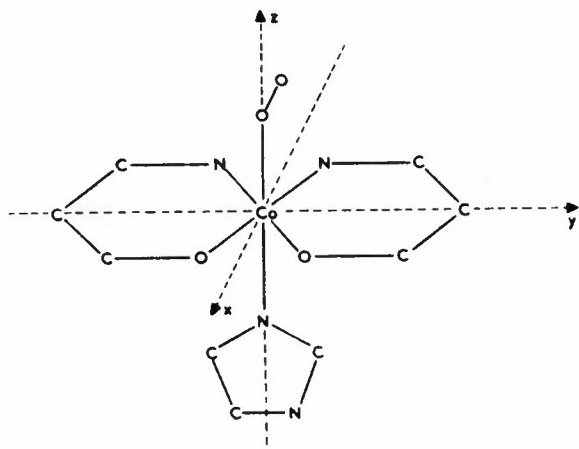


Figure 4: The  $Co(acacen)O_2Im$  molecule

† Since there are three  $S$  configurations which are close in energy, one may expect that configuration interaction will stabilize comparatively more the lowest  $S$  configuration than the  $A$  configuration.

‡ This conclusion should not be affected by the effect of configuration interaction, since the lowest  $S$  configuration (except for  $L = \text{none}$ ) is found to be the  $S_3$  configuration which corresponds to a charge-transfer configuration  $Co(III)O_2^-$ .

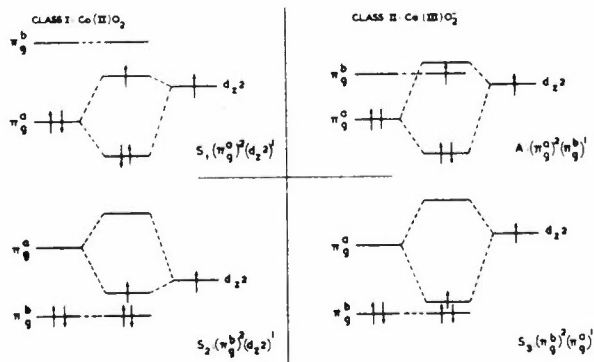


Figure 5: Possible electronic configurations for a dioxygen adduct  $Co(acacen)LO_2$

to a charge transfer configuration  $Co(III)O_2^-$  (although population analysis will probably lead to a different order of magnitude for the change in the atomic populations).

We have reported in table 5 the energy values obtained for these four configurations, with  $L = \text{none}$ ,  $H_2O$ ,  $CN^-$  or imidazole ( $Im$ ) [28], using a basis set (10,6,4/7,3/3) contracted to a minimal set (except for the  $3d$  functions which are split). A first conclusion is that none of these configurations should be discarded *a priori*, since they have comparable values. However, in each case, we find the  $A$  configuration to be the most stable one<sup>†</sup>. This seems to be in agreement with the general conclusion from RPE experiments for oxygen adducts of  $CoII$  complexes (*acacen*, *salen*, porphyrin or vitamin  $B_{12r}$ ) that the unpaired electron is largely delocalized on the oxygen atoms and that these adducts should rather be formulated as  $Co(III)O_2^-$  complexes<sup>‡</sup> [25]. The relative stabilities of  $A$  with respect to  $S_1$  and of  $S_3$  with respect to  $S_2$  increase along the series  $L = \text{none}$ ,  $H_2O$ ,  $Im$ ,  $CN^-$ , hence with the  $\sigma$  donor ability of the fifth ligand. This is easily rationalized on the basis of the change induced in the orbital energy of the  $3d_{z^2}$  orbital as a function of the fifth ligand  $L$  in  $Co(acacen)L$  (table 5). We have also reported in table 5 the computed enthalpies for the oxygenation reaction. These are also found to vary as both the  $\sigma$ -donor ability of the fifth ligand  $L$  and the energy of the  $3d_{z^2}$  orbital. This is in agreement with the suggestion of Ibers that 'ligands which stabilize cobalt(III) relative to cobalt(II) would give systems with the highest affinity for oxygen' [26], as confirmed recently by Basolo *et al.* [27].

Table 5: Energy values (in au) for the four possible configurations of  $Co(acacen)LO_2$  and computed enthalpies (in kcal/mole) for the oxygenation reaction<sup>a</sup>

$L$	$S_1$	$S_2$	$S_3$	$A$	$\epsilon(3d_{z^2})^b$
none	-2013.630 (+12.)	-2013.619 (+19.)	-2013.611 (+24.)	-2013.635 (+9.)	-0.574
$H_2O$	-2089.382 (+12.)	-2089.373 (+18.)	-2089.388 (+8.)	-2089.406 (-3.)	-0.533
$Im$	-2237.589 (+16.)	-2237.583 (+19.)	-2237.615 (-1.)	-2237.634 (-12.)	-0.507
$CN$	-2105.626 (+16.)	-	-2105.720 (-43.)	-2105.735 (-53.)	-0.299

(a) Computed with respect to  $O_2 \ ^1\Delta$  (the computed stabilization for  $O_2 \ ^3\Sigma$  with respect to  $O_2 \ ^1\Delta$  is 37 kcal/mole)

(b) Energy (in au) of the  $3d_{z^2}$  orbital in  $Co(acacen)L$

## Acknowledgements

I wish to thank my collaborators in Strasbourg for their contributions in the course of this work. Special thanks are due to Drs. A. Dedieu and J. Demuyneck and to my wife, H. Veillard, for making some results available prior to publication. This work has been made possible through a grant of computer time from the C.N.R.S. It is a pleasure to acknowledge the assistance given by the staff of the Centre de Calcul de Strasbourg-Cronenbourg. Part of this work was supported by the A.T.P. N° 219903 of the C.N.R.S.

## References

- [1] DIERCKSEN, G.H.F. and KRAEMER, W.P. (1973). *Munich Molecular Program System Reference Manual*, Special Technical Report, München: Max-Planck-Institut für Physik und Astrophysik.
- [2] BENARD, M., (private communication).
- [3] CSIZMADIA, I.G., HARRISON, M.C., MOSKOWITZ, J.W., SEUNG, S., SUTCLIFFE, B.T. and BARNETT, M.P. *The POLYATOM system*, Technical Note No. 36, Co-operative Computing Laboratory, M.I.T.
- [4] ROTHAAAN, C.C.J. (1960). *Revs. Modern Phys.*, **32**, 179.
- [5] HUNT, W.J., DUNNING, T.H. and GODDARD, W.A. (1969). *Chem. Phys. Letters*, **3**, 606.
- [6] DEMUYNECK, J. and VEILLARD, A. (1973). *Theoret. Chim. Acta*, **28**, 241.
- [7] DEMUYNECK, J., VEILLARD, A. and WAHLGREN, U. (1973). *J. Am. Chem. Soc.*, **95**, 5563.
- [8] POPLE, J.A. (1955). *Proc. Phys. Soc. (London)*, **A68**, 81.
- [9] OZIN, G.A. and VANDER VOET, A. (1973). *Can. J. Chem.*, **51**, 637.
- [10] VEILLARD, H. and VEILLARD, A., (unpublished work).
- [11] OZIN, G.A. and VANDER VOET, A. (1973). *Acc. Chem. Res.*, **6**, 313.
- [12] FOSTER, M.S. and BEAUCHAMP, J.L. (1971). *J. Am. Chem. Soc.*, **93**, 4924.
- [13] HATFIELD, W.E. and PIPER, T.S. (1964). *Inorg. Chem.*, **3**, 841.
- [14] WILLETT, R.D., LILES, O.L. and MICHELSON, C. (1967). *Inorg. Chem.*, **6**, 1885.
- [15] MASON, W.R. and GRAY, H.B. (1968). *J. Am. Chem. Soc.*, **90**, 5721.
- [16] MCCAFFERY, A.J., SCHATZ, P.N. and STEPHENS, P.J. (1968). *J. Am. Chem. Soc.*, **90**, 5730.
- [17] References may be found in [6].
- [18] COWMAN, C.D., BALLHAUSEN, C.J. and GRAY, H.B. (1973). *J. Am. Chem. Soc.*, **95**, 7873.
- [19] COTTON, F.A. and WILKINSON, G. (1972). *Advanced Inorganic Chemistry*, 644 and following, New York: Interscience.
- [20] BASOLO, F. and PEARSON, R.G. (1967). *Mechanisms of Inorganic Reactions*, 124 and following, New York: Wiley.
- [21] JONAS, K. (1973). *Angew. Chem. Int. Ed. Engl.*, **12**, 997.
- [22] See, for instance, HENRICI-OLIVE, G. and OLIVE, S. (1974). *Angew. Chem. Int. Ed. Engl.*, **86**, 1.
- [23] GRIFFITH, J.S. (1956). *Proc. Roy. Soc. (London)*, **A235**, 23.
- [24] ZERNER, M., GOUTERMAN, M. and KOBAYASHI, H. (1966). *Theoret. Chim. Acta*, **6**, 363.
- [25] HOFFMAN, B.M., DIEMENTE, D.L. and BASOLO, F. (1970). *J. Am. Chem. Soc.*, **92**, 61.
- [26] STYNES, D.V., STYNES, H.C., JAMES, B.R. and IBERS, J.A. (1973). *J. Am. Chem. Soc.*, **95**, 1796.
- [27] CARTER, M.J., RILLEMA, D.P. and BASOLO, F. (1974). *J. Am. Chem. Soc.*, **96**, 392.
- [28] DEDIEU, A. and VEILLARD, A., (unpublished work).



# Accurate Hartree-Fock Calculations on the Structure and Stability of Hydrated Diatomic Ions

W.P.Kraemer\*

The equilibrium geometrical structures and stabilities of the monohydrated nitrosyl cation,  $NO^+ \cdot H_2O$ , and cyanide anion,  $CN^- \cdot H_2O$ , are studied within the single determinant Hartree-Fock method using an extended gaussian basis set to approximate the molecular wavefunctions. The interaction energies between the molecular ions and the water molecule are calculated for a number of different structures of the monohydrates in which the water is attached to the ions through their  $\sigma$  or  $\pi$  electron systems. The difference between the interaction energies of the different structures are found to be very small. In the equilibrium geometry of  $CN^- \cdot H_2O$  the water is bound to the nitrogen centre *via* a linear hydrogen bond involving the  $\sigma$  electrons while in  $NO^+ \cdot H_2O$  the interaction of the water with the  $\pi$  electrons leads to the most stable structures. The corresponding binding energies are found to be:  $B(CN^- \cdot H_2O) = 14.5$  kcal/mole,  $B(NO^+ \cdot H_2O) = 19.8$  kcal/mole. The binding energy value of the  $NO^+$ -monohydrate is used together with the preliminary results for the dihydrated system to discuss the energetics of some charge transfer reactions leading possibly to the production of hydronium hydrates which have been observed in the earth's upper ionosphere.

## Introduction

Accurate Hartree-Fock SCF studies on the phenomenon of ion solvation published in the past few years have mostly been concerned with the hydration of atomic ions [1,2]. In these studies it has been shown that the interaction between the ions and the solvent molecules takes place *via* a linear or almost linear hydrogen bond if *negative ions* are solvated in polar solvents like water or ammonia, and that there exists a corresponding weak interaction between a *positive ion* and the lone pair electrons of the solvent molecules. The numerical results of these studies are in general agreement with some early qualitative investigations by Buckingham on the structure of ion-solvent complexes on an entirely classical electrostatic model [3]. A comparison of the theoretically determined equilibrium geometrical parameters and of the solvation energies (which have been calculated within the single determinant SCF approximation as the difference between the energy of the composed system and the sum of the energy values of the non-interacting subsystems) show a surprisingly good agreement with the corresponding experimental data obtained by Kebarle and coworkers from mass spectroscopic measurements in the gas phase [4]. The accuracy of the SCF results has been found to be within  $\pm 0.03 \text{ \AA}$  for the intersystem bond distances and about 2-5% for the solvation energies.

Recently in an extensive study of the correlation energy effects on hydrogen bonding and ion hydration

[5] it has been shown that in the case of *H-bond* interactions between closed shell systems two different effects, i.e. the correlation energy contribution to the bond energy and the change in the zero-point vibrational energy during bond formation, which are both of the same order of magnitude, compensate each other to some extent. In the case of the weak interactions between a positive ion and water, on the other hand, it has been demonstrated that by far the most dominating contribution to the bond formation is due to a pure electrostatic interaction. Any other effects, e.g. delocalization and correlation, have only very small influences. With these findings it has been possible to explain the success of pure SCF studies on the structures and stabilities of weak interacting closed shell systems.

With this background it seemed to be of some interest to extend the present series of accurate Hartree-Fock SCF calculations on ion hydration to a particular class of molecular ions in which two types of electrons, the  $\sigma$  as well as the  $\pi$  electrons, are both well suited to interact with the solvent molecule. For this purpose two simple diatomic ionic species have been selected, the nitrosyl cation  $NO^+$  and the cyanide anion  $CN^-$ . These ions have also been expected to occur in the earth's ionosphere. Recent rocket-borne mass spectroscopic observations for positive ions in the ionosphere [6] have established that the water clustered  $NO^+$ -ion plays among others a decisive role in the D-region chemistry [7]. In this context some preliminary calculations and estimates

\* Max-Planck-Institut für Physik und Astrophysik, Föhringer Ring 6, 8 München 40, West Germany

have been performed on the structure and the hydration energies of some higher hydrates of the nitrosyl cation as well.

The SCF wavefunctions and energies have been calculated within the single determinant Hartree-Fock approximation using the Roothaan SCF LCAO MO formalism. The actual calculations have been carried out with the program system MUNICH [8] on an IBM 360/91 computer taking a rather extended and flexible gaussian basis set into account. The basis set consists of (11s, 7p, 1d) functions centred at the heavier nuclei (C, N, O) (contracted to a [5s, 4p, 1d]-set to reduce the number of linear parameters in the SCF iteration process) and of (6s, 3p) functions at the hydrogen atoms (contracted to a [3s, 1p]-set) [9]. The basis functions have essentially been taken from the literature [10]. Only the exponents of the polarization functions (the *d*-functions at the heavier centres and the *p*-functions at the hydrogens) have been optimized in calculations on the relevant subsystems  $CN^-$ ,  $NO^+$ , and  $H_2O$ . No symmetry reduction has been used. The timings for each calculation are as follows in IBM 360/91 central processor time:

production of gaussian integral list	73.1 min.
time per SCF iteration step	0.8 min.

Employing the appropriate starting vectors for the iteration process SCF convergence has normally been achieved within 10-15 iteration steps.

## Results

**Monohydrated cyanide anion,  $CN^- \cdot H_2O$ :** From previous studies on the hydration of atomic ions it can be concluded that the interaction between the cyanide anion and a water molecule takes place *via* a hydrogen bond. Thus the following five geometrical structures have been studied:

- (1) linear structure  $(CN...HOH)^-$  in which the water molecule has been attached to the nitrogen atom with the centres  $CN...HO$  on a straight line;
- (2) bent structure  $(CN...HOH)^-$  with the water again at the nitrogen and where the  $CN$  bond axis and the  $N...HO$  hydrogen bond axis are perpendicular to each other;
- (3) linear structure  $(HOH...CN)^-$  with the water attached to the carbon atom and the collinear centres  $OH...CN$ ;
- (4) bent structure  $(HOH...CN)^-$  corresponding to (2) with the water molecule at the carbon atom;
- (5) the water molecule being attached through the  $\pi$  electron system in a position midway between (2) and (4).

Structures with a non-linear hydrogen bond (except the structure (5)) or with the water molecule rotated around the *H*-bond axis have not been considered

in the present study. In all the structures described above the geometrical parameters of the two subsystems,  $CN^-$  and  $H_2O$ , have been kept fixed at their previously determined equilibrium values:  $d(CN) = 1.16 \text{ \AA}$ ,  $d(OH) = 0.96 \text{ \AA}$ , angle  $(HOH) = 104.52^\circ$ . Thus the geometry of the monohydrate has only been optimized with respect to the intersystem separation in the five configurations (1)-(5) representing different steps on the path of the water molecule around the  $CN^-$ -ion from the nitrogen to the carbon side.

The intermolecular hydrogen bond can formally be described as an interaction between a region of high electron density in one molecule and an electron deficient hydrogen in the other one. Assuming that in the  $CN^-$ -ion the nitrogen atom is more electronegative than carbon, the structures (1) and (2) would be expected to be the most stable ones. The numerical results determining the relative stabilities of the five different geometrical structures are summarized as follows:

structure (1):	$R = 2.88 \text{ \AA}$ ;	$B_1 = -14.5 \text{ kcal/mole}$
structure (2):	$R = 3.15 \text{ \AA}$ ;	$B_1 = -10.9 \text{ kcal/mole}$
structure (3):	$R = 3.04 \text{ \AA}$ ;	$B_1 = -13.1 \text{ kcal/mole}$
structure (4):	$R = 3.29 \text{ \AA}$ ;	$B_1 = -9.7 \text{ kcal/mole}$
structure (5):	$R = 3.33 \text{ \AA}$ ;	$B_1 = -10.3 \text{ kcal/mole}$

where  $R$  represents the optimized intersystem distance and  $B_1$  the SCF stabilization energy of the monohydrate:  $B_1 = E^{\text{SCF}}(CN^- \cdot H_2O) - E^{\text{SCF}}(CN^-) - E^{\text{SCF}}(H_2O)$ . These data show, indeed, that the structure (1) with the water attached to the nitrogen atom is the most stable configuration. But the five stabilization energy values are found to be quite similar. The difference between structures (1) and (3) with the water molecule bond through the  $\sigma$  electron system to the nitrogen and carbon centres, respectively, is only about 1 kcal/mole. The three structures in which the water interacts with  $CN^-$ -ion through the ionic  $\pi$  electrons are found to be less stable. Apparently the  $\pi$  electrons are already too diffuse in the cyanide anion.

The partial enthalpy for the first hydration step of the  $CN^-$ -ion has been determined in a recent experimental study by Kebarle and co-workers [11]. They have deduced a value of  $\Delta H_{1,0} = -13.8 \text{ kcal/mole}$  from their mass spectroscopic measurements. The discrepancy between the theoretically calculated and the experimental binding energy is thus less than 5%. Recently Clementi and co-workers have performed Hartree-Fock SCF calculations to compare the structures and stabilities of the ionic compounds  $LiNC$  and  $LiCN$  [12]. According to the small energy difference between these two compounds (about 6 kcal/mole) and because they have not found any energy barrier for the path of the lithium cation around the  $CN^-$ -ion, they have referred to this bond as a 'polytopic bond' to stress its equality in energy for substantially different geometrical configurations. These findings fit with the present results for the

monohydrated cyanide anion where the energy differences have been found to be even smaller according to the fact that the interaction is much weaker. On the other hand, Clementi's data seem to indicate that the equilibrium structure of  $LiNC$  would be slightly non-linear (angle ( $LiNC$ ) approximately  $160^\circ$ ).

**The monohydrated nitrosyl cation,  $NO^+ \cdot H_2O$ :** The geometrical structures studied for this complex are defined in analogy to the structures (1)-(5) described above, replacing the carbon and nitrogen centres in  $CN^-$  by nitrogen and oxygen, respectively. However, as the nitrosyl ion is a positive ion, a stable hydrate can only be found if the attached water molecule points with the oxygen centre against the  $NO^+$ -ion in the positions (1)-(5). Again the geometrical parameters of the subsystems,  $NO^+$  and  $H_2O$ , have been kept fixed at the previously determined equilibrium values:  $d(NO) = 1.04 \text{ \AA}$ , and only the intersystem distance  $R$  has been optimized in the five different structures.

The numerical SCF results determining the relative stabilities may be summarized as follows:

- structure (1):  $R = 2.69 \text{ \AA}$ ;  $B_1 = -14.5 \text{ kcal/mole}$
- structure (2):  $R = 2.48 \text{ \AA}$ ;  $B_1 = -19.8 \text{ kcal/mole}$
- structure (3):  $R = 2.59 \text{ \AA}$ ;  $B_1 = -13.8 \text{ kcal/mole}$
- structure (4):  $R = 2.59 \text{ \AA}$ ;  $B_1 = -18.2 \text{ kcal/mole}$
- structure (5):  $R = 2.61 \text{ \AA}$ ;  $B_1 = -19.2 \text{ kcal/mole}$

There are no experimental data available for a comparison.

The SCF hydration energy values listed above show that in the nitrosyl monohydrate the binding between the water molecule and the  $\pi$  electron system in  $NO^+$  is definitely preferred. The stability of the hydrated system increases slightly moving the water from the oxygen to the nitrogen centre. The shorter bond length in position (2) indicates that in the region around the nitrogen atom the  $\pi$  electrons are less diffuse, particularly compared to the  $CN^-$  anion.

**The dihydrated nitrosyl cation,  $NO^+ \cdot 2H_2O$ :** There has been recently some speculation in the literature about the structure of the higher hydrates of the nitrosyl cation,  $NO^+ \cdot nH_2O$  ( $n = 2,3,4$ ) [13]. In order to explain charge transfer reactions leading from these hydrates to a production of hydronium-water clusters it has been postulated that instead of forming a classical spherical water cluster the nitrosyl hydrates prefer a so-called 'chain structure' where  $NO^+$  is attached to a chain of hydrogen bonded water molecules. From this structure the reactions can simply be visualized as a proton transfer process in the hydrogen bond next to the  $NO^+$ -ion.

To have a rough estimate on the associated reaction heats some preliminary SCF calculations on the  $NO^+$ -dihydrate have been performed. For this purpose three different geometrical structures

have been considered which are briefly described as follows:

- (1) structure  $(ON \cdot 2OH_2)^+$ , in which the two water molecules have been attached to the nitrogen atom through the  $\pi$  electron system of the  $NO^+$ -ion;
- (2) structure  $(H_2O \cdot ON \cdot OH_2)^+$ , in which the two water molecules have been attached to the oxygen and to the nitrogen centres, respectively, in the positions that have been determined in the monohydrate to be the most stable ones;
- (3) structure  $(ON \cdot (H_2O)_2)^+$  where the  $NO^+$  has been attached to the water dimer through the  $\pi$  electron system of the  $NO^+$ -ion. This structure represents the smallest possible 'chain structure'.

Because the SCF calculations on the dihydrated system are quite time consuming a complete optimization of these geometrical structures has not been possible. The total SCF binding energies  $B_T$  ( $B_T = E^{SCF}(NO^+ \cdot 2H_2O) - E^{SCF}(NO^+) - 2E^{SCF}(H_2O)$ ) characterizing the relative stabilities have been found to be:

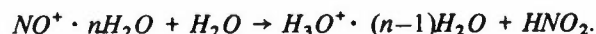
- structure (1):  $B_T = -37 \text{ kcal/mole}$
- structure (2):  $B_T = -35.5 \text{ kcal/mole}$
- structure (3):  $B_T = -33 \text{ kcal/mole}$

These numerical results show that the pure chain structure has not been found to be the most stable one at least in the case of the dihydrate. But as the differences in the above binding energies are quite small it might well be possible that for the tri- and tetrahydrates the energy gain from the additional hydrogen bond formations offsets the lowering of the energy from the direct ion-water interactions.

Subtraction of the first hydration energy from the  $B_T$ -value gives the hypothetical second hydration energy  $B_2$ . In the present case  $B_2$  is found to be about  $-17 \text{ kcal/mole}$ . The decrease from  $B_1$  to  $B_2$  is surprisingly small for the  $NO^+$  hydrates compared to the corresponding values found for atomic ions [14].

**Reaction heats of some charge transfer reactions:** With these theoretically determined binding energy values available a quantitative estimate can be made of the reaction heats of some chemical reactions which are expected to be of considerable importance in the D-region aeronomy. In this region of the earth's ionosphere the  $NO^+$  and  $O_2^+$  ions are the major positive ions produced. In mass spectroscopic measurements, however, hydrated hydronium ions,  $H_3O^+ \cdot nH_2O$ , have been observed to be by far the most abundant ionic species, while the nitrosyl hydrates as well as the  $O_2^+$ -hydrates are of small abundance [6]. The direct production of  $H_3O^+$  and its hydrates, on the other hand, from  $H_2O^+$ -ions has to be excluded under atmospheric conditions

because of a very fast reaction of  $H_2O^+$  with  $O_2$ . To solve this dilemma Fehsenfeld and Ferguson have proposed a reaction scheme [7] in which the nitrosyl cation is hydrated stepwise to the trihydrated level. The trihydrate finally reacts with a further water molecule according to ( $n = 3$ ):



This reaction has been predicted to be fast and exothermic for  $n = 3$ , and to be endothermic for  $n = 2$ . A similar reaction scheme has been discussed for the  $O_2^+$ -ion [13].

The reaction heat of the charge transfer reaction with  $n = 2$  can easily be estimated because the SCF energies of all the molecular systems involved have been calculated. For  $HNO_2$  in its experimental geometry a SCF energy of  $E^{SCF} = -204.69594$  au has been obtained. Within the SCF level of accuracy the reaction turns out to be endothermic by about 26 kcal. Although this result is in agreement with qualitative predictions, it can only be accepted as an estimate of the energy balance in the above equation of reaction. If the assumption is correct that the whole reaction can be described just as a proton transfer process, the above energy value would have to be corrected only by the energy barrier of the proton potential. On the other hand, correlation and vibration effects might change this SCF result considerably.

An analogous direct estimate of the energy balance in the charge transfer reaction with  $n = 3$  can only be performed using an extrapolated value for the SCF energy of the  $NO^+$ -trihydrate because the system  $NO^+ \cdot 3H_2O$  is already too big for SCF calculations of the accuracy to be claimed in the present study. With a reasonable extrapolated energy value a slightly exothermic energy balance of approximately 10 kcal is obtained.

A very similar reaction has been studied recently by Fehsenfeld and Ferguson with the flowing after-glow technique [15]:



The direct estimate of the energy balance for  $n = 1$  based on the corresponding SCF energy values gives a very small exothermicity of about 2.5 kcal. In analogy to the previously discussed reactions it can be expected, however, that the reactions involving the higher  $NO^+$ -hydrates ( $n > 1$ ) become more exothermic because of the strong hydrogen bonds that are formed in the  $NH_4^+$ -water clusters.

As has already been pointed out the estimated energy balances have to be considered very carefully, particularly if the charge transfer reaction consists of a number of different concerted basic reactions and if it cannot be described as a single proton transfer process.

## References

- [1] DIERCKSEN, G.H.F. and KRAEMER, W.P. (1970). *Chem. Phys. Letters*, **5**, 570.  
————— and ————— (1972). *Theoret. Chim. Acta*, **23**, 287.
- [2] CLEMENTI, E. and POPKIE, H. (1972). *J. Chem. Phys.*, **57**, 1077.  
KISTENMACHER, H., POPKIE, H. and CLEMENTI, E. (1973). *Ibid.*, **58**, 1689, 5627.  
—————, ————— and ————— (1973). *Ibid.*, **59**, 5842.
- [3] BUCKINGHAM, A.D. (1957). *Discussions Faraday Soc.*, **24**, 151.
- [4] KEBARLE, P. (1972). *Ion Molecule Reactions*, (ed. J. L. Franklin), Chapter 7, New York: Plenum Press.
- [5] DIERCKSEN, G.H.F., KRAEMER, W.P. and ROOS, B., (to be published).
- [6] NARCISI, R. S. and BAILEY, A. D. (1965). *J. Geophys. Research*, **70**, 3787.
- [7] FEHSENFELD, F.C. and FERGUSON, E.E. (1969). *J. Geophys. Research*, **74**, 2217.  
FERGUSON, E.E. and FEHSENFELD, F.C. (1969). *Ibid.*, **74**, 5743.
- [8] DIERCKSEN, G.H.F. and KRAEMER, W.P. (1973). *Munich Molecular Program System Reference Manual*, Special Technical Report, München: Max-Planck-Institut für Physik und Astrophysik.
- [9] For a definition of the basis set notation used, see MOSKOWITZ, J.W. and HARRISON, M.C. (1965). *J. Chem. Phys.*, **43**, 3550.
- [10] SALEZ, C. and VEILLARD, A. (1968). *Theoret. Chim. Acta*, **11**, 441.
- [11] PAYSANT, J.D., YAMDAJNI, R. and KEBARLE, P. (1971). *Can. J. Chem.*, **49**, 3308.
- [12] CLEMENTI, E., KISTENMACHER, H. and POPKIE, H. (1973). *J. Chem. Phys.*, **58**, 2460.
- [13] FEHSENFELD, F.C., MOSESMAN, M. and FERGUSON, E.E. (1971). *J. Chem. Phys.*, **55**, 2115, 2120.  
LINEBERGER, W.C. and PUCKETT, L.J. (1969). *Phys. Rev.*, **187**, 286.  
PUCKETT, L.J. and TEAGUE, M.W. (1971). *J. Chem. Phys.*, **54**, 2564.  
HOWARD, C.J., RUNDLE, H.W. and KAUFMAN, F. (1971). *Ibid.*, **55**, 4772.  
GOOD, A., DURDEN, D.A. and KEBARLE, P. (1970). *Ibid.*, **52**, 222.
- [14] KRAEMER, W.P. and DIERCKSEN, G.H.F. (1972). *Theoret. Chim. Acta*, **23**, 393.  
————— and ————— (1972). *Ibid.*, **27**, 265.
- [15] FEHSENFELD, F.C. and FERGUSON, E.E. (1971). *J. Chem. Phys.*, **54**, 439.

# Can Hartree-Fock Limit Wavefunctions be calculated with Gaussian Basis Functions? - *FH* again

W.von Niessen\*, G.H.F.Diercksen and W.P.Kraemer†

Wavefunctions which give the Hartree-Fock limit of the total energy have been calculated so far only with Slater-type functions for atoms and for linear molecules. Whether Gaussian-type basis functions are capable of giving the same accuracy has been investigated in the case of the *FH* molecule. It has been demonstrated that the Hartree-Fock limit of the energy can be reached, but that the required size of the basis set exceeds any which has been used until now. The potential curve for *FH* computed with Gaussian basis functions is compared to the results of Cade and Huo.

## Introduction

The well-known division of the total energy of an atomic or molecular system within the Born-Oppenheimer approximation into the Hartree-Fock (HF) energy, correlation energy, and relativistic corrections according to

$$E_{\text{tot}} = E_{\text{HF}} + E_{\text{cor}} + E_{\text{rel}}$$

is based on a computational scheme; only the total energy is an experimentally observable quantity. The exact solution of the Schrödinger equation would give as energy eigenvalue the first two terms in the above equation. The exact solution of the corresponding HF equation, i.e. the best one-particle approximation, would give the first term,  $E_{\text{HF}}$ , only. The HF wavefunction is in itself of particular importance because a number of useful theorems hold for it. E.g. the Hellmann-Feynman forces [1] are equal to the forces calculated as derivatives of the total energy with respect to some nuclear displacement coordinate [2]. Expectation values of single-particle operators for closed shell systems calculated with a HF wavefunction are correct to second order of perturbation theory [3]. This is a consequence of Brillouin's theorem. The virial theorem holds [4] as well. The HF limit is of importance still from another point of view. To calculate the effect of electronic correlation one subtracts the computed (or estimated) relativistic corrections from the experimental total energy, but one still has to know the HF limit of the energy. Hollister and Sinanoğlu have made semi-empirical estimates of the HF energies

for a series of molecules [5], these have in general been regarded as somewhat too low. The exact solution of the HF equation would involve a numerical integration, which until now has proven to be possible only for atomic systems where the equations can be decoupled [6,7]. The numerical accuracy of the total energy values calculated in this way can be doubted at least for the atoms beyond *Ne* [8]. This finds its expression in the slightly different energy values given by Froese-Fischer [6] and by Mann [7]. For molecular systems one has to take recourse to the Roothaan LCAO approximation [9]. But since this involves an additional approximation beyond the one-particle approximation in any actual calculation using a finite basis set, one has to prove that a wavefunction has reached the HF limit. For two- and four-electron atoms a very systematic investigation has been performed by Weiss [10]. On the whole the analytic atomic wavefunctions of Bagus and Gilbert [11] and Clementi [12], which are based on Slater-type functions are regarded to be of the same accuracy as the numerically calculated ones [6,7]. For molecular systems the procedure of Weiss does not appear to be applicable or useful as has been discussed by Cade and Huo [13]. In their investigations of molecular wavefunctions close to the HF limit they used convergence arguments which are inductive and appeared to be the best practical approach [13-15]. No methodical advances have been made since then. The levelling-off of the energy values as the basis set size is increased, however, remains a major concern despite all optimizations of the nonlinear parameters. The wavefunctions of Cade and Huo remain still a standard

\* Lehrstuhl für Theoretische Chemie der Technischen Universität München, Arcisstrasse 21, 8 München 2, West Germany

† Max-Planck-Institut für Physik und Astrophysik, Föhringer Ring 6, 8 München 40, West Germany

of accuracy. The re-examination of the wavefunctions for *FH* and *CIH* by McLean and Yoshimine [16] proved that the corresponding energy values are well within the claimed limits of 0.001 au and 0.005 au, respectively. These authors claim that their *FH* wavefunction, which uses an augmented basis set compared to the work of Cade and Huo, is within 0.0002 au of the HF limit for this molecule. Wavefunctions which meet these standards of accuracy become available for larger classes of linear molecules due to advances in computational methods in particular for the evaluation of integrals over Slater-type functions [17,18].

Recently, however, wavefunctions have been published for nonlinear molecules which claim to be near Hartree-Fock wavefunctions [19-22]. In general they are based on Gaussian basis functions. The question naturally arises, whether this claim is justified. Slater-type functions (STF) are superior to Gaussian-type functions (GTF) and many more GTF's are needed to obtain the same accuracy as a given set of STF's. E.g. for the *He* atom two *s*-type STF's are superior to 10 GTF's [23], although this represents one of the worst cases known. For molecules GTF's have been shown to give in general the same accuracy as STF's if about three times as many basis functions are employed. But the question whether Gaussian functions can lead to HF limit wavefunctions has not been answered as yet. In view of the fact that most studies on molecules will be based on GTF's and because more calculations are made which aim at incorporating a large fraction of the correlation energy it would be invaluable to know which size of a basis set of GTF's can claim to give the HF limit of the energy.

To answer these two questions detailed investigations have been performed on the *FH* molecule, where a comparison with the highly accurate calculations of Cade and Huo [13] and McLean and Yoshimine [16] can be made. In addition the potential curve has been calculated at the same points as done by Cade and Huo to compare the relative flexibility of STF's and GTF's as a function of internuclear distance. These investigations are described in the subsequent sections, in the second section the atomic calculations, in the third section the molecular ones.

### Atomic Calculations

A basis set which for a molecule is to give the HF limit of the energy must do this also for the constituting atoms, also in the case the basis consists of Gaussian functions. Any significant error in the atomic calculation will persist in the molecular calculation. The wavefunctions of greatest accuracy calculated for the *F* atom in its ground  $^2P$  state are the analytical ones of Clementi  $E_{\text{HF}} = -99.409284$

au [12] and of Bagus and Gilbert  $E_{\text{HF}} = -99.409334$  au [11] and the numerical ones of Froese-Fischer  $E_{\text{HF}} = -99.40959$  au [6] and of Mann  $E_{\text{HF}} = -99.40935$  au [7]. Several basis sets of GTF's were obtained starting with a basis set of 13 *s*-type and 8 *p*-type GTF's as the smallest one leading to the basis set of 15 *s*-type and 12 *p*-type functions as the final set. The calculations have been performed with the SCF program of Roos *et al.* [24]. The final basis set was generously optimized, the other ones were only superficially optimized. The energy values calculated with the different basis sets are listed in table 1. Table 2 contains the final set of GTF's. The contraction coefficients are given in brackets, they are taken from the atomic calculations, but it was only determined for the *s*-type functions from the atomic calculation which functions were grouped together, for the *p*-type functions this was determined from a molecular calculation on *FH* involving no polarization functions. It was demanded that contraction of the functions affected the energy to less than  $10^{-6}$  au. The contracted basis set consists of 11 *s*-type and 8 *p*-type functions. The total SCF energy values, virial ratio, and Hartree-Fock eigenvalues for  $F(^2P)$  and  $F(^1S)$  are given in table 3 both for the uncontracted and contracted basis sets. The results of Bagus and Gilbert [11] and of Froese-Fischer [6] are given for comparison as well. The total HF energy calculated with this basis,  $E_{\text{HF}} = -99.409290$  au, is between the energy values of Clementi and of Bagus and Gilbert, which will be used as a standard. The error with respect to the slightly lower value of Bagus and Gilbert is  $4.0 \cdot 10^{-5}$  au. The electron affinity of *F* is calculated to be  $A = 1.357$  eV, the the experimental quantity is  $A = 3.448 \pm 0.005$  eV [25]. It has frequently been noted that in the process of optimizing a basis set the problem of multiple minima is likely to arise [23]. In the present investigation involving a large number of parameters the trapping of the energy in a minimum above the true minimum obtainable with a given number of functions can easily occur, but because of the agreement of the results with those of other authors it is unlikely that a significant improvement in the

Table 1: SCF energies and virial ratios for  $F(^2P)$  calculated with different Gaussian basis sets

Basis	$E^{\text{SCF}}$ (au)	Virial Ratio
13s8p	-99.408836	-2.0000169
13s9p	-99.409079	-2.0000062
13s10p	-99.409115	-2.0000051
14s10p	-99.409235	-2.0000022
14s11p	-99.409241	-2.0000022
15s11p	-99.409265	-2.0000022
15s12p	-99.409290	-2.0000017

energy expectation value could be achieved. Other basis sets of the same size and composition, but involving different exponential parameters could give inferior, but only very slightly superior results.

Table 2: Gaussian basis set for  $F(^2P)$ ; contraction coefficients, if different from unity, are given in brackets

Number	$\alpha(s)$	$\alpha(p)$
1	230,000.0 (0.232592 · 10 <sup>-4</sup> )	912.666 (0.958295 · 10 <sup>-4</sup> )
2	34,691.4 (0.177908 · 10 <sup>-3</sup> )	241.152 (0.656870 · 10 <sup>-3</sup> )
3	8,000.97 (0.920639 · 10 <sup>-3</sup> )	88.9807 (0.286130 · 10 <sup>-2</sup> )
4	2,254.64 (0.398335 · 10 <sup>-2</sup> )	37.4194 (0.104154 · 10 <sup>-1</sup> )
5	712.481 (0.151150 · 10 <sup>-1</sup> )	16.4422 (0.328709 · 10 <sup>-1</sup> )
6	247.4398	7.55273
7	94.0899	3.66352
8	38.90768	1.81879
9	17.30389	0.888741
10	8.197460	0.422592
11	4.08440	0.197102
12	1.73599	0.089545
13	0.769575	
14	0.339900	
15	0.147270	

A further point observed in the optimization process should be mentioned. Cade and Huo stressed the 'ineffectiveness of exponent optimization compared to simply having a large and versatile basis set composition' [13]. A reasonably chosen set of  $n$  STF's led to a lower energy value than a completely optimized set of  $n-1$  functions. This is not the case in the optimization of GTF's, simply because it is

much more difficult to give a reasonable guess for fifteen parameters than for five and because any additional function has a much smaller weight. With GTF's an optimized set of  $n-1$  or  $n-2$  functions is superior to an unoptimized but reasonably chosen set of  $n$  functions (i.e. chosen on the basis of the optimized smaller sets).

Table 4: Gaussian basis set for  $H(^2S)$ ; contraction coefficients, if different from unity, are given in brackets

Number	$\alpha(s)$	
1	1170.498	(0.00007)
2	173.5822	(0.00058)
3	38.65163	(0.00318)
4	10.60720	(0.01380)
5	3.379649	
6	1.202518	
7	0.463925	
8	0.190537	
9	0.0812406	
10	0.0285649	

No basis sets were optimized for the  $H$  atom. Instead the basis sets determined by Huzinaga were employed in the calculations [23]. The smallest set consists of 8 functions of s-type contracted to 6 functions, the larger one of 10 functions of s-type contracted to 7 functions. For completeness the larger basis set, which was used in the final calculations, is given in table 4. It leads to a total HF energy of  $E_{\text{HF}} = -0.4999986$  au, potential energy of  $E_{\text{pot}} = -0.9999939$  au, kinetic energy of  $E_{\text{kin}} = -0.4999953$  au, and virial ratio of  $-2.0000066$ , whereas the smaller set leads to a HF energy of  $E_{\text{HF}} = -0.4999913$  au, potential energy of  $E_{\text{pot}} = -0.9999698$  au, kinetic energy of  $E_{\text{kin}} = 0.4999657$  au, and virial ratio of  $-2.0000511$ .

Table 3: HF energy, virial ratio, and Hartree-Fock eigenvalues for  $F(^2P)$  and  $F(^1S)$

	$F(^2P)$				$F(^1S)$	
	Bagus-Gilbert	Froese-Fischer	(15s12p)	(15s12p)/[11s8p]	(15s12p)	(15s12p)/[11s8p]
$E_{\text{HF}}$	-99.409334	-99.40959	-99.409290	-99.409290	-99.459171	99.459171
$E_{\text{pot}}$			-198.818407	-198.818409	-198.920798	-198.920783
$E_{\text{kin}}$			99.409117	99.409119	99.461627	99.461612
V.T.	-1.999996		-2.0000017	-2.0000017	-1.9999753	-1.9999755
$\epsilon_{1s}$	-26.38265	-26.38281	-26.38274	-26.38274	-25.82785	-25.82785
$\epsilon_{2s}$	-1.57245	-1.572535	-1.57253	-1.57253	-1.07321	-1.07321
$\epsilon_{2p}$	-0.72994	-0.730015	-0.73002	-0.73002	-0.17983	-0.17983

## Molecular Calculations

The atomic basis sets for the atoms *F* and *H* were employed without change in the molecular calculations except that for the *p*-type functions on *F* and the *s*-type functions on *H* it was determined in a calculation on *FH* which basis functions were contracted. The basis sets determined in this way were also left isotropic, although it may be anticipated that an anisotropic basis set would lead to a better description for *FH*. Cade and Huo [13] and McLean and Yoshimine [16] used anisotropic basis sets optimized in the molecule. With the large number of nonlinear parameters it was regarded as computationally too expensive to vary the exponents in the molecule and even more so to vary the  $\sigma$ - and the  $\pi$ -type basis functions independently to obtain an anisotropic set, but the atomic set was considered to be flexible enough to describe molecules with an equal accuracy as the constituting atoms. For this reason too the basis was left nearly uncontracted. To verify these assumptions some of the basis functions on the *F* atom with small exponential parameters were varied on *FH* in the absence of polarization functions. The improvement was less than  $10^{-6}$  au and was regarded as immaterial. A variation towards an anisotropic basis set was not undertaken.

Table 5: SCF energies of *FH* at intermediate stages of the basis set determination

Basis	$E_{\text{tot}}^{\text{SCF}}$ (au)
(15s12p 8s)/[11s8p 6s]	-100.043570
(15s12p 8s3p)/[11s8p 6s3p]	-100.062266
(15s12p3d 8s)/[11s8p3d 6s]	-100.063411
(15s12p3d 8s3p)/[11s8p3d 6s3p]	-100.068907
(15s12p3d1f 8s3p1d)/[11s8p3d1f 6s3p1d]	-100.070004
(15s12p3d1f 10s3p1d)/[11s8p3d1f 7s3p1d]	-100.070023
(15s12p 10s4p)/[11s8p 7s4p]	-100.062333
(15s12p4d 10s)/[11s8p4d 7s]	-100.063812
(15s12p4d 10s4p)/[11s8p4d 7s4p]	-100.069279
(15s12p4d1f 10s4p)/[11s8p4d1f 7s4p]	-100.070302
(15s12p4d1f 10s4p1d)/[11s8p4d1f 7s4p1d]	-100.070459

The basis set [11s8p|6s] gives at the experimental distance  $R = 1.7328$  au a total SCF energy of  $E_{\text{SCF}} = -100.043570$  au. The polarization functions were determined in the way described below. A set of *d*-type functions on *F* was optimized without any polarization functions on the *H* atom. Then a set of *p*-type functions was determined for the *H* atom without any *d*-type functions on the *F* atom. These sets of functions were then combined and not varied further. One function of *f*-type on *F* and one function of *d*-type on *H* were added with

exponential parameter estimated on the basis of the results of Cade and Huo and were not optimized. The energy values calculated with these intermediate basis sets are listed in table 5. First a set of 3 *d*-type functions on *F* and 3 *p*-type functions on *H* was optimized. The exponential parameters are given in table 6. Adding a *f*-type function on *F* and a *d*-type function on *H* to the basis set [11s8p3d|6s3p] leads to a SCF energy of  $E_{\text{SCF}} = -100.070004$  au higher than the result of Cade and Huo by 0.0003 au. This was regarded as insufficient. The basis of *s*-type functions on the *H* atom was consequently enlarged to 10 *s*-type functions contracted to 7 functions. The basis set (15s12p3d1f|10s3p1d)/[11s8p3d1f|7s3p1d] gives a total SCF energy of  $E_{\text{SCF}} = -100.070023$  au a small but insufficient improvement. It was concluded that the set of *d*-type functions on *F* and *p*-type functions on *H* was incomplete. Consequently a set of 4 polarization functions of each type was optimized. The intermediate results are given in table 5. This enlargement proves to be the essential one. Upon adding one *f*-type function on *F* and one *d*-type function on *H* a HF energy of  $E_{\text{HF}} = -100.070459$  au is obtained which surpasses the value obtained by Cade and Huo and is higher than the value of McLean and Yoshimine by only  $3 \cdot 10^{-5}$  au, their value being  $E_{\text{HF}} = -100.07049$  au. The basis set of polarization functions is given in table 6 as well. It can thus be stated that GTF's are capable of giving molecular energies to the HF limit and that the present wavefunction for *FH* as the one of McLean and Yoshimine can be claimed to be within 0.0002 au of the HF limit. The remaining difference of  $3 \cdot 10^{-5}$  au is nearly the same as the defect in the atomic basis set as compared to the result of Bagus and Gilbert [11] ( $4 \cdot 10^{-5}$  au). It may be that it is this small defect in the atomic calculation which persists in the molecular calculation, but it may also be the incomplete optimization of exponents (in particular the *f*-type function on *F* and the *d*-type function on *H*) or the isotropy of the basis set which may give rise to this small energy difference. Since this difference is regarded as immaterial this point was not examined further.

Table 6: Exponential parameters for polarization functions in *FH*

Type	$\alpha$			
<i>p</i> ( <i>H</i> )	1.261	0.70	0.27	
<i>d</i> ( <i>F</i> )	1.554	0.65	0.217	
<i>d</i> ( <i>H</i> )	1.25			
<i>f</i> ( <i>F</i> )	1.25			
<i>p</i> ( <i>H</i> )	3.5	1.15	0.75	0.26
<i>d</i> ( <i>F</i> )	4.5	1.1	0.5	0.22
<i>d</i> ( <i>H</i> )	1.25			
<i>f</i> ( <i>F</i> )	1.25			



Table 7: Energy quantities for  $FH$  as a function of internuclear separation. The results of Cade and Huo are given in brackets

$R$ (au)	$E^{\text{HF}}$ (au)	$\Delta^{\text{a}}$	$\epsilon_{1\sigma}$	$\epsilon_{2\sigma}$	$\epsilon_{3\sigma}$	$\epsilon_{1\pi}$
1.325	-99.986829 (-99.98645)	-0.000379	-26.284268 (-26.28459)	-1.707307 (-1.70772)	-0.856174 (-0.85620)	-0.674895 (-0.67492)
1.65	-100.070108 (-100.06996)	-0.000148	-26.293549 (-26.29331)	-1.617748 (-1.61745)	-0.785912 (-0.78583)	-0.654901 (-0.65471)
1.696	-100.070925 (-100.07077)	-0.000155	-26.294216 (-26.29391)	-1.608225 (-1.60795)	-0.776120 (-0.77590)	-0.652334 (-0.65211)
1.7328	-100.070459 (-100.07030)	-0.000159	-26.294593 (-26.29428)	-1.601053 (-1.60074)	-0.768341 (-0.76810)	-0.650310 (-0.65008)
2.606	-99.954875 (-99.95391)	-0.000965	-26.287436 (-26.28480)	-1.506173 (-1.50411)	-0.614373 (-0.61268)	-0.613147 (-0.61150)

(a)  $\Delta = E^{\text{HF}} - E^{\text{HF}}(\text{Cade-Huo})$

The final basis set used in the calculations is so large that problems of linear dependence may arise. The lowest eigenvalue of the overlap matrix, which measures the degree of linear dependence [26], was found to be  $0.5 \cdot 10^{-6}$ . Since all calculations were performed in double precision arithmetic on an IBM 360/91 computer no particular precautions were regarded as necessary.

The binding energy of the  $FH$  molecule with respect to the atoms in their respective ground states ( $F(^2P)$ ,  $H(^2S)$ ) calculated with the same basis sets as used for the molecule is  $B = 4.4 \text{ eV}$ . Cade and Huo [13] and McLean and Yoshimine [16] obtained the same value. The experimental result is  $B = 6.12 \text{ eV}$  [13]. (For a discussion of the related problems see [13].)

The basis set determined for the  $H$  atom was used in a calculation for  $H_2$  at the experimental distance of  $R = 1.4 \text{ au}$  as well. The computed HF energy is  $E_{\text{HF}} = -1.133602 \text{ au}$  which is again within  $3 \cdot 10^{-5} \text{ au}$  of the HF energy of Kolos and Roothaan:  $E_{\text{HF}} = -1.13363 \text{ au}$  [27], although the polarization functions have been determined for the very polar molecule  $FH$ . This result demonstrates again that the Gaussian basis used in these studies is of HF limit accuracy. The basis set used by Schulman and Kaufman [28] in their study of the spin-spin coupling in  $HD$  is larger – it consists of 10  $s$ -type, 5  $p$ -type, and 1  $d$ -type function, left completely uncontracted – but it gives a higher energy of  $E_{\text{HF}} = -1.133554 \text{ au}$ .

With the basis sets for the  $F$  and  $H$  atoms a few points were calculated on the potential curve, those points which among others have been computed by Cade and Huo [13]. Table 7 contains some energy quantities computed with the basis set of Cade and Huo, the present results, and the corresponding energy difference. At the experimental distance of  $R = 1.7328 \text{ au}$ , for which both basis sets were determined this difference is  $E_{\text{HF}}$  (this work) –  $E_{\text{HF}}$  (Cade-Huo) =  $\Delta = -0.000159 \text{ au}$ . For the

distances  $R = 1.696 \text{ au}$  for which the minimum of the potential curve is reached, and  $R = 1.65 \text{ au}$ , i.e. close to the experimental distance, this energy difference retains approximately the same value, but for the smaller and larger internuclear separations this energy difference significantly increases in magnitude to  $\Delta = -0.000379 \text{ au}$  for  $R = 1.325 \text{ au}$  and  $\Delta = -0.000965 \text{ au}$  for  $R = 2.606 \text{ au}$ . It is thus concluded that basis sets of GTF's become relatively better than the corresponding sets of STF's for smaller and especially for larger internuclear distances probably because the larger number of basis functions provides an additional flexibility. All molecular calculations have been performed with the program system MUNICH [29].

## Conclusions

It has been demonstrated in the present work that basis sets of GTF's can be determined which are as accurate as the best sets of STF's both for atoms and for molecules, in other words basis sets of GTF's are capable of giving the energy to the HF limit. But the size of the basis sets required to achieve this goal is larger than any set employed in the literature until now. The wavefunction calculated for the atoms  $F$  and  $H$  and the molecules  $FH$  and  $H_2$  lead to a HF energy which is always within  $4 \cdot 10^{-5} \text{ au}$  of the best analytical results and are thus expected to be within 0.0002 au of the HF limit for the respective systems. It may be argued that the presently determined sets of functions are not optimal and that smaller sets are capable of giving the same accuracy. But, although this cannot be excluded, the experience gained in the investigations renders it highly improbable.

In this context a comment on some recent articles on near-HF wavefunctions and estimation of some HF limit energies is appropriate. Ermler and Kern [22] employed a Gaussian basis set –  $(9s5p1d|4s1p)/$

[4s2p1d|2s1p] – to calculate properties of the benzene molecule near the HF limit. It is the opinion of the authors that this basis set is the smallest one which can be regarded to lead to accurate wavefunctions, but it is too small, too contracted, and too deficient in polarization functions to be capable of approaching the HF limit close enough to deserve the title 'near-HF limit', Dunning, Pitzer and Aung published a number of wavefunctions for the water molecule, some based on STF's, others on GTF's [20]. Their best wavefunction calculated with a (5s4p1d|3s1p) Slater basis, which incorporates the atomic basis set of Bagus and Gilbert [11], leads to a SCF energy of  $E_{\text{SCF}} = -76.06309$  au. On this basis they estimated the HF energy of water to be  $E_{\text{HF}} = -76.066 \pm 0.002$  au. However, compared to the work of Cade and Huo [13] and McLean and Yoshimine [16] their basis set is deficient in polarization functions. In fact Clementi and Popkie using a large basis of Gaussian functions – (13s8p3d1f|6s2p1d)/[8s5p3d1f|4s2p1d] already reached this value of the energy for the water molecule, their best result being  $E_{\text{HF}} = -76.06587$  au [21]. The HF limit thus has to be lowered once more. According to the experience gained in the present investigations the basis set of Clementi and Popkie is somewhat too contracted and somewhat deficient in functions of *p*- and *d*-type on the *O* atom and of *s*- and *p*-type on the *H* atom so that it does not give results as accurate as the ones of Cade and Huo [13], although their results have to be regarded as highly accurate. The claim that their results are within 0.002 au of the HF limit for water, however, appears not to be unreasonable. Cade and Huo claimed an accuracy of 0.001 au which is probably exceeded. The semi-empirical estimates of the HF limit energies by Hollister and Sinanoglu [5] are generally believed to be somewhat too low [19-22] – for *FH* e.g. their estimate is  $E_{\text{HF}} = -100.0751$  au. This is probably the case, but it must be admitted that the levelling-off of the energy as the basis set size is increased has not been resolved in an entirely satisfactory manner until now. Somewhat more care in assigning the HF limit of the energy based on more or less complete calculations appears thus to be appropriate.

#### Acknowledgement

One of the authors (W.vN.) would like to acknowledge support from the Deutsche Forschungsgemeinschaft.

#### References

- [1] HELLMAN, J. (1937). *Einführung in die Quantenchemie*, Leipzig: Deuticke.  
FEYNMAN, R.P. (1939). *Phys. Rev.*, **56**, 340.
- [2] HURLEY, A.C. (1954). *Proc. Roy. Soc. (London)*, **A226**, 170, 179.  
HALL, G.G. (1961). *Phil. Mag.*, **6**, 249.  
STANTON, R.E. (1962). *J. Chem. Phys.*, **36**, 1298.  
For a review, see DEB, B.M. (1973). *Revs. Modern Phys.*, **45**, 22.
- [3] MOLLER, C. and PLESSET, M.S. (1934). *Phys. Rev.*, **46**, 618.  
GOODISMAN, J. and KLEMPERER, W. (1963). *J. Chem. Phys.*, **38**, 721.  
EPSTEIN, S.T. (1971). University of Wisconsin Report No. WIS-TGI-437.
- [4] FOCK, V. (1930). *Z. Physik*, **63**, 855.  
LOWDIN, P.O. (1959). *J. Mol. Spectroscopy*, **3**, 46.
- [5] HOLLISTER, C. and SINANOGLU, O. (1966). *J. Am. Chem. Soc.*, **88**, 13.
- [6] FROESE-FISCHER, C. (1968). *Some Hartree-Fock Results for the Atoms Helium to Radon*, special report from the Department of Mathematics, University of British Columbia, Vancouver.  
————— (1972). *Atomic Data*, **4**, 301.
- [7] MANN, J.B. (1967). *Atomic Structure Calculations: Hartree-Fock Energy Results for the Elements Hydrogen to Lawrencium*, Los Alamos Scientific Laboratory Report LA-3690.  
————— (1973). *Atomic Data*, **12**, 1.
- [8] TREFFTZ, E., (private communication).
- [9] ROOTHAAN, C.C.J. (1951). *Revs. Modern Phys.*, **23**, 69.  
————— (1960). *Ibid.*, **32**, 179.
- [10] WEISS, A.W. (1961). *Phys. Rev.*, **122**, 1826.  
ROOTHAAN, C.C.J., SACHS, L.M. and WEISS, A.W. (1960). *Revs. Modern Phys.*, **32**, 186.
- [11] BAGUS, P.S. and GILBERT, T.L., (unpublished work), cited partially in McLEAN, A.D. and YOSHIMINE, M. (1968). *Tables of Linear Molecule Wavefunctions*, Supplement to *IBM J. Research Develop.*, **12**, 206.  
BAGUS, P.S., GILBERT, T.L. and ROOTHAAN, C.C.J. (1972). *J. Chem. Phys.*, **56**, 5195.
- [12] CLEMENTI, E. (1965). Supplement to *IBM J. Research Develop.*, **9**, 2.  
CLEMENTI, E., ROOTHAAN, C.C.J. and YOSHIMINE, M. (1962). *Phys. Rev.*, **127**, 1618.
- [13] CADE, P.E. and HUO, W.M. (1967). *J. Chem. Phys.*, **47**, 614.
- [14] ————— and ————— (1967). *J. Chem. Phys.*, **47**, 649.
- [15] ————— and ————— (1966). *J. Chem. Phys.*, **45**, 1063.
- [16] McLEAN, A.D. and YOSHIMINE, M. (1967). *J. Chem. Phys.*, **47**, 3256.
- [17] A system of programs developed by B. Liu, M. Yoshimine, P.S. Bagus and A.D. McLean. For a description, see:  
McLEAN, A.D. (1971), in *Proceedings of the Conference on Potential Energy Surfaces in*

- Chemistry*, RA18, 87, IBM Research Laboratory, San José, California; and  
 BAGUS, P.S. (1972), in *Selected Topics in Molecular Physics*, 187, Weinheim: Verlag Chemie.
- [18] WAHL, A.C., BERTONCINI, P., KAISER, K. and LAND, R. (1970). *Int. J. Quantum Chem.*, **S3**, 499.  
 \_\_\_\_\_, \_\_\_\_\_, \_\_\_\_\_ and \_\_\_\_\_ (1968). USAEC Report ANL 7271.
- [19] MEYER, W. (1971). *Int. J. Quantum Chem.*, **S5**, 341.
- [20] DUNNING, T.H., PITZER, R.M. and AUNG, S. (1972). *J. Chem. Phys.*, **57**, 5044.
- [21] CLEMENTI, E. and POPKIE, H. (1972). *J. Chem. Phys.*, **57**, 1078.
- [22] ERMLER, W. C. and KERN, C. W. (1973). *J. Chem. Phys.*, **58**, 3458.
- [23] HUZINAGA, S. (1965). *J. Chem. Phys.*, **42**, 1293.
- [24] ROOS, B., SALEZ, C., VEILLARD, A. and CLEMENTI, E. (1968). *A General Program for Calculation of Atomic SCF Orbitals by the Expansion Method*, IBM Technical Report RJ518.
- [25] BERRY, R.S. and REIMANN, C.W. (1963). *J. Chem. Phys.*, **38**, 1540.
- [26] LOWDIN, P.O. (1967). *Int. J. Quantum Chem.*, **S1**, 811.
- [27] KOLOS, W. and ROTHAAAN, C.C.J. (1960). *Revs. Modern Phys.*, **32**, 219.
- [28] SCHULMAN, J. and KAUFMAN, N.D. (1970). *J. Chem. Phys.*, **53**, 477.
- [29] DIERCKSEN, G.H.F. and KRAEMER, W.P. (1973). *Munich Molecular Program System Reference Manual*, Special Technical Report, München: Max-Planck-Institut für Physik und Astrophysik.

# Ground State Wavefunctions for Aromatic and Heteroaromatic Molecules

M.H.Palmer, A.J.Gaskell, R.H. Findlay, S.M.F.Kennedy, W.Moyes and J.Nisbet\*

Near to Hartree-Fock wavefunctions have been obtained for a wide variety of benzenoid hydrocarbons and benzene derivatives, as well as 5- and 6-membered ring heterocycles containing varying numbers of first and second row elements. Trends in the computed properties derived from the wavefunctions are described with particular reference to the correlation with magnetic susceptibility and photoelectron spectroscopy. The effect of basis set upon molecular properties and energies within this range of molecules is discussed.

We have been interested in the ground state electronic structures of aromatics and heterocycles, and in their reactivity for some years [1]. Thus it is appropriate that we should have studied a range of these molecules by non-empirical means. In the early days we had very limited computing facilities, but with large amounts of time available on an IBM 360/50, we endeavoured to arrive at a compromise between size of molecule that could be studied and basis set that it would be practicable to use. The obvious starting point was the work of Clementi *et al.* [2] on pyridine and pyrrole etc., and subsequently that of Berthier *et al.* [3] on benzene and related species. We took the view that a wide number of studies comparatively close to the Hartree-Fock limit would be more valuable than just a few molecules very near the limit. Furthermore there appeared to be no case for just trying to marginally leapfrog the work cited above by minor extensions of the basis. In fact most one-electron properties for these molecules are virtually unaffected by change in basis set beyond our present level. We used in our studies [4] on the 5- and 6-membered ring heterocycles a best atom basis consisting of 7 *s*-type and 3 *p*-type for first row elements [5], with three *s*-type for hydrogen. Subsequent studies [6] showed that the addition of polarisation functions [7] lowered the energy slightly, but scaling of best atom sets to better represent molecular environments became widespread and we contributed to this with our work on small model molecules where the molecular energy was optimised [6]. Certainly if one's only desire is to lower the molecular energy obtained, then scaling is more cost effective than the addition of extra basis functions; it also lowers the valency shell binding energy and leads to better numerical agreement with photoelectron spectra when Koopmans'

Theorem is used. Scaling does not have any effect upon the orbital ordering, but in some cases it can effect the one-electron properties. For example using our best atom bases and evaluating the dipole moments leads to generally very good agreement with experiment, see table 1 [8]. When scaled bases are used the dipole moments often show a significant change, and since our work usually leads to random scatter near the experimental value this can lead to poorer results. Examples are furan (experimental 0.6D) where we obtain 1.0D for the scaled basis but 0.6D for the unscaled one, similarly 1,2,5-oxadiazole is worse on scaling. In contrast pyrrole is improved both by scaling and by the addition of polarisation functions [6]. Many other 1-electron properties are less sensitive than dipole moments to scaling.

In none of the cases that we have studied with both best atom and scaled bases have the orbital orderings been significantly changed. Furthermore, in carbocyclic and heterocyclic aromatic compounds it is true to say that virtually all orbital orderings become stable once one passes the threshold of reasonable size in minimal basis sets. By this we mean that extended bases offer little additional change. For example, in the azines with over 70 correlations, the ordering is unchanged between minimal and double zeta bases [9] in all except two cases; in these cases near degeneracy is observed in any event. The computational cost of extended bases can be rarely justified at this point in time. Amongst others, Lipscomb *et al.* [10] found that minimal Slater based calculations were as reliable as extended sets for many operators on boranes. Thus we decided to work with a firmly based single basis set for a very wide range of molecules – the scaled best atom basis. We now do upgrading to

\* Department of Chemistry, University of Edinburgh, West Mains Road, Edinburgh, EH9 3JJ

Table 1: Dipole moments ( $\mu/D$ ) and vector components in five-membered rings<sup>a,b</sup>

Name	Experimental Value	LCGO				
		Total $\mu$	$\mu_{\perp}$	$\mu_{\parallel}$	$\mu\sigma$	$\mu\pi$
Pyrrole	1.80	2.01	+2.01	0.0	-0.53	+2.54
Pyrazole	2.21	2.85	+2.23	+1.77	+1.65	+3.07
Imidazole	3.8	4.41	+4.31	+0.96	(-30.1°)	(+83.0°)
1 <i>H</i> -1,2,4-Triazole	3.20	3.56	+3.50	+0.65	+1.46	+3.15
1 <i>H</i> -1,2,3-Triazole		4.50	+3.26	+3.10	(+52.4°)	(+95.3°)
2 <i>H</i> -1,2,3-Triazole		-3.24	-3.26	0.0	1.14	2.91
1 <i>H</i> -1,2,3,4-Tetrazole	5.15	5.17	+4.72	+2.11	(+54.0°)	(+86.6°)
2 <i>H</i> -1,2,3,4-Tetrazole	(2.30)	2.54	+2.24	+1.22	2.79	2.87
Furan	0.67	-0.64	-0.64	0.0	(+81.7°)	(+83.0°)
Thiophen ( <i>sp</i> basis)	0.53	-1.25	-1.25	0.0	1.57	2.71
( <i>sp</i> + 3 <i>s'</i> + 3 <i>d</i> basis)		-0.44	-0.44	0.0	(-25.8°)	(+94.1°)
1,2,5-Oxadiazole	3.38	-2.96	-2.96	0.0	-2.77	2.13
1,3,4-Oxadiazole	3.04	2.75	+2.75	0.0	-3.22	1.97
1,2,4-Oxadiazole	1.2	1.18	-0.16	+1.17	-2.49	2.05
1,2,3-Oxadiazole		3.70	-0.22	+3.69	0.26	2.49
1,3,4-Thiadiazole ( <i>sp</i> basis)	3.28	3.38	3.38	0.0	-2.45	2.21
( <i>sp</i> + <i>d</i> basis)	3.28	4.23	4.23	0.0	(-70.6°)	(+80.0°)
1,2,5-Thiadiazole ( <i>sp</i> basis)	1.57	-2.53	-2.55	0.0	-3.96	-2.16
( <i>sp</i> + <i>d</i> basis)	1.57	-1.75	-1.75	0.0	(-35.8°)	(+77.2°)
Phosphole (planar)		1.40	1.40	0.0	-0.70	2.23
Phosphole ( <i>PH</i> out-of-plane)		1.14	-0.54	1.00( $\mu_2$ )		
1,6,6a-Trithiapentalene ( <i>sp</i> basis)	3.01	-3.87	-3.87	0.0		
( <i>sp</i> + <i>d</i> basis)	3.01	-2.17				
1,6a,6-Dithiaoxapentalene ( <i>sp</i> basis)	3.78	-4.32	-3.78	-2.09		
( <i>sp</i> + <i>d</i> basis)	3.78	-3.70				
6a,1,6-Thiadioxapentalene ( <i>sp</i> basis)		-3.22	-3.22	0.0		
( <i>sp</i> + <i>d</i> basis)		-2.75				
1,6a,6-Dithiaazapentalene ( <i>sp</i> basis)		-4.23	-1.59	-3.92		
( <i>sp</i> + <i>d</i> basis)		-3.02				

(a) see [8]

(b) Angles with respect to positive direction of  $\mu_{\parallel}$  and measured anticlockwise; the sign of the dipole moment is taken with the negative end in the positive cartesian direction as positive

split valency shell or double zeta basis on a selective procedure in order to confirm that our hypothesis is reasonable, or to deal with particularly polar molecules. As a matter of practice all of our work with second row elements we include *d*-orbitals to see whether they are significantly populated in the ground state. This is uniformly not the case in all examples that we have studied where the element *S* or *P* is in a planar state, such as in the dithiolium salts (1) and trithiapentalenes (2) (thiathiophthens) [11]. The 3*d* orbitals are of course extensively utilised in the tetrahedral sulphur compounds, such as the thiophene mono- and di-oxides (3) [12].



Our interest in wavefunctions in the first instance has been to obtain:

- an interpretation of photoelectron spectra;
- to evaluate the moments and compare with experimental data;
- to evaluate the diamagnetic susceptibility and compare with experimental microwave data;
- to try to investigate that controversial subject in organic chemistry – aromatic character and resonance energy.

If it was possible to calculate the molecular *g*-value non-empirically then we would be able to calculate the total magnetic susceptibility. As we will see we have made progress on all of (a) to (d). We would also like to study the electronic spectra of the aromatic and heteroaromatic systems; we have done a little work on the first excited states, but again

within the single configuration procedure. One or two results of this are of particular significance, but in general the subject is not well described by this type of investigation so we will not cover this further.

Our work covers various systems. There is in fact surprisingly little work on conjugated olefins, particularly if floating spherical gaussian calculations are ignored. The justification for the latter view is not just based upon the fact that for molecules, such as hexatriene the FSGO energy is 33 au above our LCGO one, or that for naphthalene the difference is 54 au [13] but also that properties evaluated and (some) described below are unsatisfactory. We are working on both cyclic polyolefins including the annulenes, and acyclic systems. In the aromatic series we have an extensive study of molecules of type  $C_6H_4XY$  where  $X$  and/or  $Y$  are all the common substituents;  $H$ ,  $OH$ ,  $F$ ,  $NH_2$ ,  $NO_2$ ,  $CN$ ,  $CHO$  etc. As you will see this is an extensive triple triangular array since there are three isomers in each case. Although much of this work is complete, and we

have assigned the photoelectron spectra – rather well as it turns out – we would not gain much from looking at extensive tables of data. From the fragmentary data, the correlation with experiment is not improved by larger basis sets, and the rather smaller bases by Pople and others [14] which lead to energies several au higher in energy are sure to be considerably poorer. Indeed we have repeated several of their computations and note that it is common to find eigenvalues in the 5-7 eV region. The other areas where we have made major studies are in the 6-membered ring heterocycles containing various numbers of nitrogen atoms with or without one atom of sulphur or phosphorus. Again the photoelectron data is very good. These studies are practicable with quite large systems as seen for indole, benzofuran, benzothiophene and naphthalene, see figure 1.

We have already referred to the dipole moment studies on heterocycles when discussing the subject of basis sets. In the substituted benzenes the conformations of unsymmetrical substituents ( $X$  or  $Y$ ) in the system  $C_6H_4XY$  bring about additional problems. We are active in this and have endeavoured to determine the most favoured geometry on the basis of energy, and then compare the dipole moment with the experimental one. Thus we find that in the case 1,2- $C_6H_4(NO_2)_2$  the best geometry is probably one in-plane and another perpendicular. These results are not complete and we don't want to commit ourselves to the final answer. For many simple aromatics we calculate a dipole moment relatively close to the experimental one. We reproduce trends within the isomers and the effects do show vector addition for substituents as has long been known experimentally. The results are not perfect and this can be attributed to several factors:

- the geometry of the ring; if not known from a gas phase determination this was taken as that of benzene;
- that the energy optimised scaling on oxygen and fluorine compounds generally leads to poorer dipole moments than best atom bases for these systems;
- that some of the dipole moments are anyway very high and this really calls for additional model compounds for the scaling.

One of the very controversial subjects of organic chemistry has been resonance and resonance energy. We feel that we may have made a contribution here. It is clear that one of the virtues of keeping to a standard basis is that small trends become apparent unexpectedly. Thus in trying to evaluate resonance energy one is in difficulty with a definition and a classical analogue on which to measure heats of hydrogenation etc. Strain energy is very important and so on. We felt that the results of Hartree-Fock studies are unlikely to lead to good heats of formation. We need to return to the classical definition of

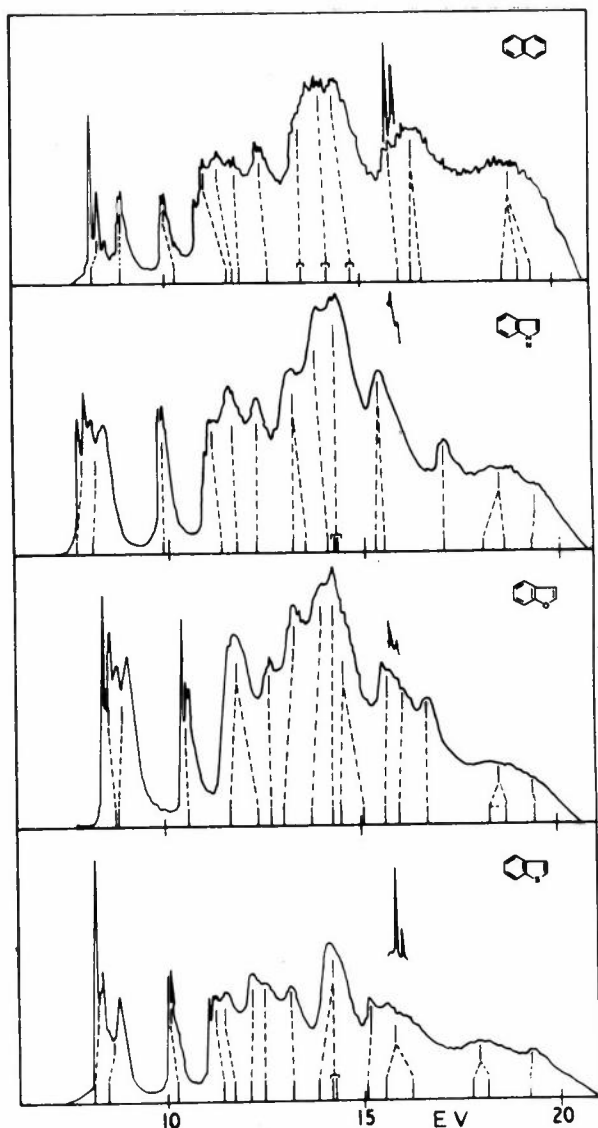


Figure 1

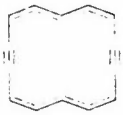
resonance energy if we are to study the subject at all. It was apparent to us that if we take a series of small molecules, the total energies are additive in bonds, table 2; so we propose to use the thermochemists approach, but *not* to equate the atom energies to zero. Thus the energy of the *C-H* bond  $E_{C-H}$  is  $E_{CH_4}/4$ , that of the  $E_{C=C}$  is obtained from  $E_{C-H}$  and the energy of ethylene. In this way, with a series of classical molecules we arrive at a set of bond energies, which are of course on a very different energy scale to those of the thermochemist. Firstly we observed that they work for a number of non-aromatic systems, and then we apply them, table 3, to conjugated molecules.

pyrrole is also reasonable, and the fusion of the rings with benzene even more so; thus while benzofuran (or indole) are only about the same in aromaticity as benzene, the iso series are markedly less. The result with hexa fluorobenzene is a direct result of trying to obtain the *C-F* bond energy from vinyl fluoride. We are unable to stop the  $\pi$ -systems mixing, and hence some interaction energy is being lost in  $C_6F_6$ . However, even using the *C-F* bond energy from  $CH_3F$  fails to alter the low resonance energy. Thus we must either accept the value, or question whether the *C-F* length (we used that from  $C_6H_5F$ ) was optimal in  $C_6F_6$ . All of the systems so far are nearly strain free; if we operate

Table 2: Analysis of molecular total energy in aromatics

Model Molecules (-Energy au)					
$CH_4$	40.10180	$NH_3$	56.0199	$H_2O$	75.79999
( <i>CH</i> )		( <i>NH</i> )		( <i>OH</i> )	
$C_2H_4$	77.83143	$CH_3CH=CH_2$	116.77453	$CH_2=CH-CH=CH_2$	154.50920
( <i>C=C</i> )		( <i>C-C</i> )		Perpendicular ( <i>C-C</i> )	
$CH_2=CH-NH_2$	132.70390	$CH_2=CH-OH$	152.46202	$CH_2CH-F$	176.40569
Perpendicular ( <i>C-N</i> )		Perpendicular ( <i>C-O</i> )		( <i>C-F</i> )	
$CH_3CN$	131.55927	$CH_2=O$	113.51009		
( <i>C-N</i> )		( <i>C=O</i> )			

Table 3: 'Resonance energies' (kcal/mole)

$C_6H_6$	$C_{10}H_8$	<i>PhF</i>	<i>PhCHO</i>	<i>PhOH</i>	<i>PhNH_2</i>	$C_6F_6$
50.8	85.4	50.7	53.7	43.9	48.6	16.6
Furan	Pyrrole					
21.2	21					
Benzofuran	Isobenzofuran	Indole	Isoindole			
55.6	35.2	56.7	43.3			
						
						77.7
<i>trans</i> Butadiene		<i>cis, cis</i> Hexatriene	Cyclooctatetraene (experimental geometry)		Barrelene	
5.5		7.8	6.1		-114	

As is seen from the table we here quote just a few examples. The figures for the hydrocarbons, ethylene 0.0, butadiene 5.5, hexatriene 7.8, cyclopentadiene 16.3, benzene 50.8 kcal/mole follow a logical pattern. Naphthalene is less than twice benzene in agreement with thermochemical data. The substituted benzenes (with the exception of hexafluoro benzene to be described elsewhere) are normally in the 55-40 kcal region. In most cases adding  $\pi$ -electrons increases the resonance energy above that of benzene. The data for furan and

with strained systems then we must expect to obtain strange results. We have been studying other members of the  $C_nH_n$  series for various charged states; for cyclobutadiene the best square triplet (Hückel) state is preferred over the best square or rectangular singlet and neither has any resonance energy (i.e. resonance energy positive). Thus they are antiaromatic even before strain energy is included. Planar alternating cyclooctatetraene would have a resonance energy of -8 kcal/mole, so it is antiaromatic anyway, but the strain energy has not been

Table 4: Bond population moments

$\sigma$ System							
Azines ( $X^{\delta+} - Y^{\delta-}$ )							
$X-Y$	$H-C$	$C-N$	$N-N$	$C-C$			
	0.241	0.121	0.004	0.007			
Number of Points	29	30	7	11			
Maximum deviation	0.023	0.015	0.003	0.003			
Azoles $X^{\delta+} - Y^{\delta-}$							
$X-Y$	$C_{\alpha}-O$	$N_{\alpha}-O$	$C_{\alpha}-N(H)$	$N_{\alpha}-N(H)$	$C_{\alpha}-N_{\beta}$	$C_{\beta}-N_{\alpha}$	$N_{\beta}-N_{\alpha}$
	0.317	0.200	0.244	0.133	0.070	0.159	0.034
Number of points	7	4	8	6	6	6	4
Maximum deviation	0.010	0.070	0.015	0.016	0.018	0.026	0.019
$X-Y$	$H-N$	$C_{\beta}-N_{\beta}$	$N_{\beta}-N_{\beta}$				
	0.386	0.115	0.007				
Number of points	7	6	2				
Maximum deviation	0.050	0.004	0.007				
$\pi$ System Azines							
$X-Y$	$C-N$	$C-C$	$N-N$				
	0.004	0.008	0.012				
Number of points	30	11	7				
Maximum deviation	0.03	0.010	0.010				
Azoles ( $X^{\delta+} - Y^{\delta-}$ )							
$X-Y$	$O-C_{\alpha}$	$(H)N-C_{\alpha}$	$(H)N-N_{\alpha}$	$O-N_{\alpha}$	$C_{\alpha}-C_{\beta}$	$N_{\alpha}-C_{\beta}$	
	0.142	0.195	0.219	0.148	0.103	0.087	
Number of points	6	8	6	3	8	6	
Maximum deviation	0.014	0.023	0.030	0.030	0.026	0.020	
$X-Y$	$C_{\alpha}-N_{\beta}$	$N_{\alpha}-N_{\beta}$	$C_{\beta}-C_{\beta}$	$N_{\beta}-C_{\beta}$	$N_{\beta}-N_{\beta}$		
	0.107	0.089	0.0	0.006	0.0		
Number of points	6	4	1	6	1		
Maximum deviation	0.029	0.030	0.0	0.008			

included. In the nearly strain-free experimental geometry (which has a dihedral angle of about  $50^{\circ}$ ) there is still 6.1 kcal/mole of resonance energy showing that there is still an interaction between the olefinic systems, as is clear from photoelectron spectra of this type of system.

The Mulliken population analysis of heterocycles might be expected to lead to net atomic populations which vary markedly

- from molecule to molecule, and
- with basis set.

From a comparison of our minimal data with larger basis set calculations we find that this is far from the case; it is just the relative populations in the constituent atomic functions which differ. For example if our thiopene data is compared with Gelius *et al.* [15] the direct transference of our  $3d_{\sigma}$  to their  $3s$  leads to very similar results. We then noted that the populations at the atomic centres could be separated into bond population moments, see table 4, and that these are almost constant, with the sole exceptions of  $CH$  and  $NH$  which act as electron sinks for the whole system [8].

A further idea consistent with basic organic chemical notions is of the aromatic sextet behaving as a sextet i.e. having the same average position.

If the average positions of the electrons vary markedly then the  $\pi$ -system is not behaving as a unit, and this should lower the aromatic character. Studies of this both in mono and bicyclic systems are very revealing [8,12,13]. Of course there are difficulties in applying this approach to molecules with a centre of symmetry.

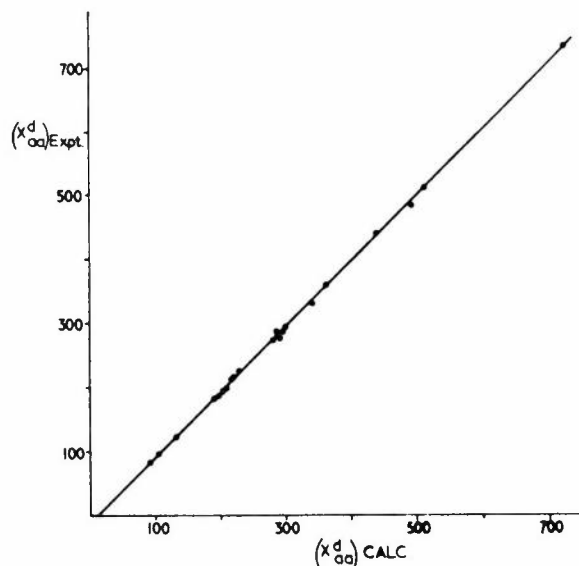


Figure 2: Diamagnetic susceptibility



Lastly we want to mention that we are able to compute the diamagnetic susceptibility, figure 2, for carbocyclic and heterocyclic aromatics within the experimental accuracy in almost all cases [16]. Whether the total magnetic susceptibility anisotropy can be regarded as a characteristic of aromaticity remains unproven. Certainly Flygare's own data, figures 3 and 4, shows that the out of plane term is related to the average in plane irrespective of whether the system is aromatic or not. Our work on the diamagnetic term in annulenes should provide some interesting results here. Preliminary results for some Hückel annulenes suggest that they are showing strong diamagnetic susceptibility anisotropy, but that the paramagnetic term less the  $g$ -factor portion already makes the sign of the sub-total opposite to that required by Flygare's proposal. There appears to be a linear correlation between the computed binding energy and the diamagnetic susceptibility anisotropy in isoelectronic series, see figure 5.

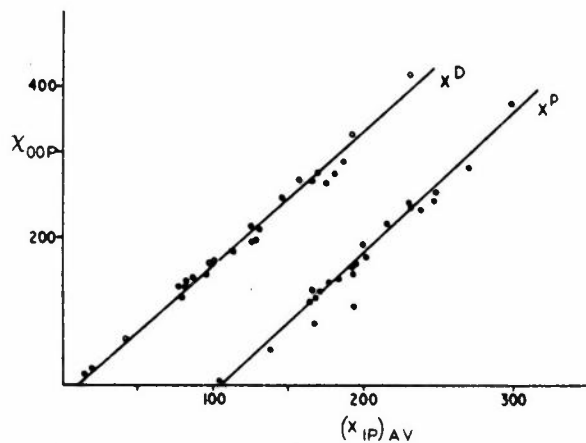


Figure 3: Magnetic susceptibility of acyclic systems (Flygare)  $\chi_p$  offset

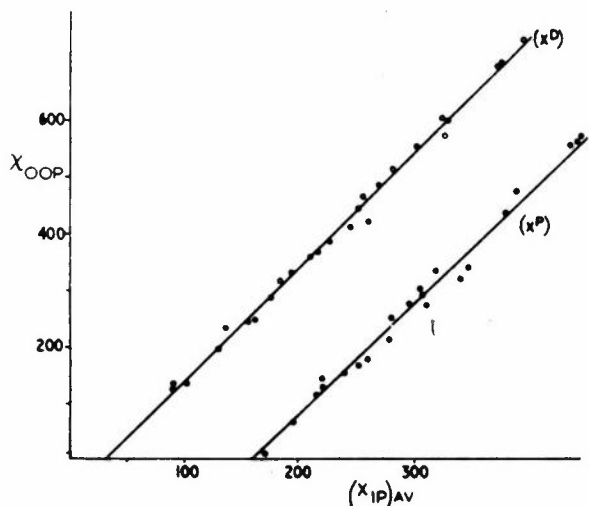


Figure 4: Magnetic susceptibility of cyclic systems (Flygare)  $\chi_p$  offset

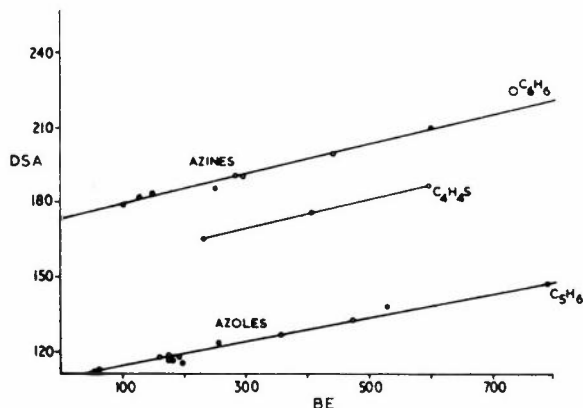


Figure 5: Diamagnetic susceptibility anisotropy and binding energy

## References

- [1] PALMER, M.H. (1967). *Structure and Reactions of Heterocyclic Compounds*, London: Arnold.
- [2] CLEMENTI, E. (1967). *J. Chem. Phys.*, **46**, 4725, 2731, 2737.
- [3] BERTHIER, G., PRAUD, L. and SERRE, J. (1969). *Quantum Aspects of Heterocyclic Compounds in Chemistry and Biochemistry*, Israel Academy of Sciences and Humanities Symposium, 40, New York: Academic Press.
- [4] PALMER, M.H. and GASKELL, A.J. (1971). *Theoret. Chim. Acta*, **23**, 52.
- [5] ROOS, B. and SIEGBAHN, P. (1970). *Theoret. Chim. Acta*, **17**, 209.
- [6] PALMER, M.H., GASKELL, A.J. and BARBER, M.S. (1972). *Theoret. Chim. Acta*, **26**, 357.
- [7] ROOS, B. and SIEGBAHN, P. (1970). *Theoret. Chim. Acta*, **17**, 199.
- [8] PALMER, M.H., FINDLAY, R.H. and GASKELL, A.J. (1974). *J. Chem. Soc. (Perkin II)*, 420.
- [9] ALMLOF, J., ROOS, B., WAHLGREN, U. and JOHANSEN, H. (1973). *J. Electron Spectroscopy*, **2**, 51.
- [10] PALMER, M.H., GASKELL, A.J. and FINDLAY, R.H. (1974). *J. Chem. Soc. (Perkin II)*, 778.
- [11] LAWS, E.A., STEVENS, R.M. and LIPSCOMB, W.N. (1972). *J. Am. Chem. Soc.*, **94**, 4661.
- [12] PALMER, M.H. and FINDLAY, R.H. (1971). *Tetrahedron Letters*, 4165.
- [13] ——— and ——— (1974). *J. Chem. Soc. (Perkin II)*, 1885.
- [14] ——— and ——— (1974). *J. Chem. Soc. (Perkin II)*, (in the press).
- [15] PALMER, M.H. and KENNEDY, S.M.F. (1974). *J. Chem. Soc. (Perkin II)*, 1893.
- [16] HEHRE, W.J., RADOM, L. and POPLE, J.A. (1972). *J. Am. Chem. Soc.*, **94**, 1496.
- [17] GELIUS, U., ROOS, B. and SIEGBAHN, P. (1972). *Theoret. Chim. Acta*, **27**, 171.
- [18] PALMER, M.H. and FINDLAY, R.H. (1974). *Tetrahedron Letters*, 253.

# Non Empirical LCAO SCF MO Investigations of Electronic Reorganizations accompanying Core Ionizations

D.T.Clark, I.Scanlan, J.Muller and D.B.Adams\*

Calculations have been carried out on an extensive series of molecules for both the neutral species and core ionized states. Substituent effects on  $C_{1s}$ ,  $N_{1s}$ ,  $O_{1s}$  and  $F_{1s}$  levels have been investigated and where available comparison has been drawn with experiment. Comparison with Koopmans' Theorem has allowed a relatively detailed study of change in relaxation energies as a function of substituent effect on a given core level. For  $C_{1s}$  levels the computed shifts in core binding energies are approximately linearly related to difference in relaxation energies. The empirical correction of Koopmans' Theorem for difference in relaxation energies at different sites has been investigated for large molecules. The results compared well with direct hole state calculations.

## Introduction

Theoretical interpretations of molecular core binding energies, measured by ESCA, within the Hartree-Fock formalism have centred around five models namely: core hole state calculations [1], Koopmans' Theorem [2], equivalent core model [3], potential at an atom model and the charge potential model [4]. The extensive discussions of experimental data utilizing these models have assumed that nuclear relaxation is slow compared with the typical lifetimes of core hole states. On the other hand the importance of electronic reorganizations accompanying photoionization of core electrons has clearly been established. However, theoretical studies in which electronic reorganization has been specifically incorporated have been confined to relatively simple molecules and few systematic studies are available in which the importance of differences in electronic relaxation energies for different core holes has been investigated. The data currently available does suggest however, that for atoms of similar bonding environment, relaxation energies are closely similar.

Our objectives in this paper are four-fold:

- (a) to investigate the importance of nuclear relaxation accompanying core ionization on both absolute and relative binding energies;
- (b) to investigate, with a common basis set, substituent effects on shifts in core binding energies for a large range of compounds and bonding types;
- (c) to investigate systematically the relative importance of relaxation energy contributions to shifts in core binding energies;

- (d) consequent on (b) and (c), to investigate the possibility of making systematic corrections to Koopmans' Theorem, thus enabling shifts for relatively large systems to be obtained from ground state calculations.

## Computational Details

The calculations discussed in this work were performed with STO 4-31G basis sets [5], Clementi's best atom exponents [6] were used for C, N, O and H. The deficiencies of an STO basis set for fluorine dictated the use of a comparable gaussian expansion of Hartree-Fock orbitals (HF4,31G) [7]. For the more detailed studies in (a) an STO 6-1,1,1,1G basis gave added flexibility to the valence basis. The calculations were performed using the ATMOL system of programs [8] implemented on an IBM 370/195. Experimental geometries have been used where these were known, in other cases geometries were estimated from standard tables.

## Results and Discussion

- (a) **An investigation of nuclear relaxation in the core hole state of methane:** In the Hartree-Fock formalism the binding energy corresponding to photoionization of a core electron is given by:

$$BE = (\Delta E)_{HF} + (\Delta E)_{rel} + (\Delta E)_{corr}$$

where

\* Department of Chemistry, University of Durham, South Road, Durham, DH1 3LE

$$\Delta E = E_{(\text{ion})} - E_{(\text{ground state})}$$

Recent theoretical and experimental studies have indicated that at least for first and second row atoms the absolute magnitudes of the relativistic and correlation energy differences are very small [9]. Our previous studies have indicated the relative importance of basis set dependence of computed binding energies (as a difference between the neutral molecule and the ion) and this is of some importance since most calculations have by necessity employed basis sets a long way from the HF limit. Good agreement in general is obtained between calculated and observed binding energies on the assumption that nuclear relaxation is unimportant. The success of the equivalent cores model (employing either experimental or theoretically generated thermodynamic data) also suggests that nuclear relaxation during photoionization is unimportant. Experimental evidence to date suggests that the lifetimes of core hole states are typically in the range  $10^{-13}$ - $10^{-17}$  secs. Of particular interest as far as this work is concerned, is the observation that some Auger transitions involving carbon have a halfwidth of the order of .1 eV. This suggests therefore that under appropriate conditions, the natural linewidth of a carbon 1s core level might be of the same order of magnitude. If this is so then from the uncertainty principle one might expect the lifetime for a carbon 1s hole state to be of the same order of magnitude as a vibrational frequency (i.e.  $\sim 10^{-13}$  sec.). Indeed it has been demonstrated recently by Siegbahn and coworkers [10] (employing a high resolution spectrometer based on a fine focus X-ray monochromatization scheme), that the carbon 1s spectra for  $CH_4$  (in the gas phase), exhibits a marked degree of asymmetry. This has been attributed to a Frank Condon envelope and clearly provides the first evidence for a change in geometry in going to the hole state.

It is of some interest therefore to investigate the energy minimised geometries for  $CH_4$  and for its  $C_{1s}$  hole state and for comparison (since it is of some importance with respect to the equivalent cores approximation) the equivalent cores species  $NH_4^+$ . For such small systems, extended basis set calculations become feasible. Geometry minimizations have therefore been carried out for the three species using an STO 6,1,1,1,G basis set, with exponents optimized for a molecular environment, being taken from the extensive studies of Pople and coworkers. The resultant potential energy curves are shown in figure 1. For the optimum ground state geometry the binding energy is calculated to be 290.8 eV in excellent agreement with the experimental (290.8 eV).

There are several interesting features which emerge from this. Firstly, it can be seen qualitatively (and demonstrated quantitatively by fitting to a quadratic), that the three curves are very similar, with the hole state and equivalent cores species being displaced by

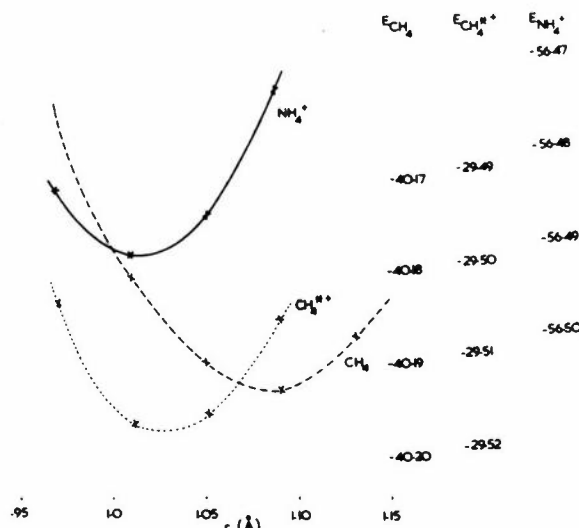


Figure 1: Variation of total energy with bond length for methane and its core hole and equivalent core states

$\sim 0.06$  Å to shorter bond length. The minimised geometries are in excellent agreement with experiment [11],  $C-H$  1.09 (1.09 Å) for  $CH_4$  and  $N-H$  1.03 (1.03 Å) for  $NH_4^+$ , the experimental values being given in parenthesis. Taking a typical vibrational frequency ( $\sim 3000$   $cm^{-1}$ ) the observed band envelope for the  $C_{1s}$  level of methane may readily be accounted for. The calculated binding energy corresponding to the minima for neutral molecule and hole state differs by only  $\sim 0.3$  eV from that computed from the geometry appropriate to the neutral molecule. It is clear therefore that the assumption of an unchanged nuclear framework on core ionization is a good approximation. This possibility has also been discussed recently in a different context by Meyer [12]. In the remainder of this work therefore, nuclear relaxation has been ignored.

(b) **Substituent effects:** As we have previously indicated there have been numerous theoretical and experimental studies of substituent effects on core binding energies. There has been no previous systematic theoretical study however of a large range of substituent effects on different core levels studied with a comparable basis set. In an attempt to rectify this deficiency we have investigated substituent effects on  $C_{1s}$ ,  $N_{1s}$ ,  $O_{1s}$  and  $F_{1s}$  core levels in a range of both saturated and unsaturated systems. Calculations have been carried out within the RHF formalism with a 4.31G basis set. Since a variety of experimental and theoretical studies have shown that on the ESCA timescale core holes are localised [13], the calculations reported refer only to the localised core hole states. Experimental geometries were employed where available but preliminary studies indicated that the binding energies were virtually unchanged for subtle variations in the geometry.

The emphasis in these particular calculations has been on shifts in binding energies rather than absolute values and therefore the limitations of such a basis set are to some extent relatively minor as has been previously shown in calculations on the fluoromethanes [14]. As a preliminary check the absolute binding energy for the  $C_{1s}$  levels  $CH_4$  is calculated to be 294.3 eV. In the next sub-section a detailed discussion of relaxation energies will be given but at this stage it should be emphasized that by comparison with the results from Koopmans' Theorem the basis underestimates the magnitude of the relaxation energy. Considerable evidence is available that this relaxation energy is associated almost solely with the valence electrons and the underestimation of this quantity with the 4-31G basis is readily understandable since the exponents are optimised with respect to the neutral species. That this is the case may be readily demonstrated by re-computing the total energy for the hole state with exponents appropriate for the valence atomic orbitals of the equivalent core (*viz.*  $N$  for  $CH_4$ ). The excellent agreement (table 1) for the absolute binding energies for the molecules studied by this approach is most encouraging and indicates a computationally less expensive means of calculating absolute binding energies, as compared to a large basis set computation.

Table 1: Effect of optimised core valence atomic orbital exponents on core binding energies

X	Unoptimised	Optimised <sup>a</sup>	Experimental <sup>b</sup>
$C^*H_4$	294.18	290.71	290.8
$H_2O^*$	545.49	539.12	539.4
$CO^*$	548.47	541.89	542.3
$C^*O$	300.78	296.71	296.2

(a) In this context optimised is taken to mean that the valence atomic orbital exponents correspond to the equivalent core species for the hole state.

(b) THOMAS, T.D. (1970). *J. Chem. Phys.*, 53, 1744.

It is convenient in discussing these results to consider the effect of substituents on a given core level in different bonding environments and then proceed to a comparison as outlined in (b). Where results are available comparison has been made with experimental data.

(i) *Binding energies in saturated systems:* The range of substituents which have been studied is indicated in tables 2 and 3 with the primary substituent effect with respect to the methyl substituent taken as standard. This is more reasonable than employing

hydrogen substituent as reference since it is not clear in cases where strong hydrogen bonding is possible that the experimental results refer to the free molecule. Where direct experimental data is available or where it may be inferred the agreement between theory and experiment is good. The shifts in the binding energies are in accord with chemists intuitive ideas concerning the nature of substituent effects *viz.* at the two extremes replacing  $H$  by  $Me$  or  $F$  results in a shift to lower and higher binding

Table 2: Substituent effects on carbon core binding energies

	X	Calculated	Experimental <sup>a</sup>
$C^*H_3-X$	$CH_3$	(0)	(0)
	$H$	0.23	0.2
	$CH_2F$	0.61	
	$CHF_2$	1.26	
	$CF_3$	1.96	2.2 <sup>b</sup>
	$CHO$	0.57	0.8
	$NH_2$	0.89	0.9 <sup>c</sup>
	$OH$	1.55	1.8
	$F$	3.46	3.0
$C^*H_2=X$	$CH_2$	0.22	0.3
	$CHF$	0.80	
	$CF_2$	1.54	
	$NH$	1.97	
	$O$	3.87	3.4
$HC\equiv C^*-X$	$H$	1.18	0.6
	$F$	4.46	
$XC^*HO$	$CH_3$	3.40	3.4
	$H$	3.87	3.4
	$NH_2$	4.30	
	$OH$	5.32	5.2
	$F$	7.28	
$CH_3C^*H_2F$		2.96	
$CH_3C^*HF_2$		6.04	
$CH_3C^*F_3$		9.13	
$F_2C^*O$		10.73	
$HC^*CF$		2.03	
$FCC^*F$		5.29	
$CH_2C^*HF$		3.17	
$CH_2C^*F_2$		6.29	

(a) SCHWARTZ, and SWITALSKI, (1972). *J. Am. Chem. Soc.*, 94, 6298. Collection of experimental data from references as follows:

DAVIS, D.W., SHIRLEY, D.A. and THOMAS, T.D. (1970). *J. Chem. Phys.*, 92, 4184.

THOMAS, T.D. (1970). *J. Am. Chem. Soc.*, 92, 4184.

DAVIS, D.W., HOLLANDER, J.M., SHIRLEY, D.A.

and THOMAS, T.D. (1970). *J. Chem. Phys.*, 52, 3295.

SIEGBAHN, K. *et al.* (1969). *ESCA Applied to Free Molecules*, Amsterdam: North Holland.

(b) Estimated from thin film measurements on benzotrifluoride and benzene: cf. CLARK, D.T., KILCAST, D. and MUSGRAVE, W.K.R. (1971). *J. Chem. Soc. D*, 516.

(c) Estimated from thin film measurements on pyrrole: cf. CLARK, D.T. and LILLEY, D.M.J. (1971). *Chem. Phys. Letters*, 9, 234.

Table 3: Substituent effects on nitrogen, oxygen and fluorine core binding energies

	X	Calculated	Experimental <sup>a</sup>
Nitrogen:			
$N^*H_2\cdot X$	CH <sub>3</sub>	(0)	(0)
	H	0.78	0.5
	CHO	1.17	1.0
	NH <sub>2</sub>	0.88	
	OH	1.44	
	F	3.75	
$CH_2N^*H$		0.40	
Oxygen:			
$HO^*\cdot X$	CH <sub>3</sub>	(0)	(0)
	H	1.0	0.8
	CHO	1.77	1.5
	NH <sub>2</sub>	0.49	
	OH	1.30	
	F	4.52	
$CH_2O^*$		0.60	-1.3
$CF_2O^*$		3.12	
$CH_3CHO^*$		-0.30	-1.3
$NH_2CHO^*$		-1.37	
$OHCHO^*$		-0.17	-0.1
$O^*HCHO$		1.78	1.5
$FCHO^*$		1.84	
Fluorine:			
$F^*\cdot X$	CH <sub>3</sub>	(0)	
	H	2.24	1.6 <sup>b</sup>
	CH <sub>2</sub> CH <sub>3</sub>	-0.28	
	CHFCH <sub>2</sub>	0.77	0.9 <sup>c</sup>
	CF <sub>3</sub> CH <sub>3</sub>	1.84	1.4 <sup>c</sup>
	CHO	1.41	
	NH <sub>2</sub>	0.58	
	OH	0.89	
	F	4.0	4.3 <sup>b</sup>
	$F^*_2CO$		3.16
$CH_2CHF^*$		0.40	
$CH_2CF^*_2$		1.78	
$HCCF^*$		2.84	
$FCCF^*$		3.29	

(a) See footnote (a) of Table 2

(b) SHAW, R.W. and THOMAS, T.D. (1973). *Chem. Phys. Letters*, 22, 127.

(c) Extrapolated from experimental data on fluoromethanes (see text)

energies respectively for all core levels. Of some interest is the fact that substituent effects are such that in progressing across the series from  $C_{1s}$  to  $F_{1s}$  core levels there is generally relatively little variation due to Me, NH<sub>2</sub>, OH and F substituents. The net effect is that the difference in shifts arising from these substituents remains relatively constant for the different core levels.

There is sufficient data available to consider both primary and secondary substituent effects on core

binding energies and these results are shown in the case of fluorine substitution in table 4. The marked consistency of primary and secondary shifts at carbon of  $\sim 3.0$  eV and 0.7 eV respectively are in excellent agreement with available experimental data obtained from studies of simple homopolymers [15]. It is clear that for fluorine, the primary and secondary substituent effects, in not only saturated but also unsaturated systems are essentially constant in accord with the observed shifts in the fluorobenzenes [16]. By employing appropriate primary and secondary shift data it is possible to estimate shifts in core binding energies for other systems. In difluoroacetylene for example, a shift of 4.15 eV is anticipated with respect to acetylene in accord with a calculated value of 4.12 eV. The experimentally observed gas phase shifts in the fluoromethane by comparison with the fluoroethanes are also well reproduced by this data.

Table 4: Effect of fluorine substitution on  $\alpha$  and  $\beta$  core binding energies

	Primary ( $\alpha$ )	Secondary ( $\beta$ )
CH <sub>3</sub> -CH <sub>3</sub>	(0)	(0)
CH <sub>2</sub> F-CH <sub>3</sub>	2.96 (2.96)	0.61 (0.61)
CHF <sub>2</sub> -CH <sub>3</sub>	6.04 (3.08)	1.26 (0.65)
CF <sub>3</sub> -CH <sub>3</sub>	9.13 (3.09)	1.96 (0.70)
CH <sub>2</sub> =CH <sub>2</sub>	(0)	(0)
CHF=CH <sub>2</sub>	2.95 (2.95)	0.58 (0.58)
CF <sub>2</sub> =CH <sub>2</sub>	6.07 (3.12)	1.32 (0.74)
H-C $\equiv$ C-H	(0)	(0)
F-C $\equiv$ C-H	3.20	0.86
H <sub>2</sub> C=O	(0)	(0)
HFC=O	3.41 (3.41)	1.24 (1.24)
F <sub>2</sub> C=O	6.86 (3.45)	2.40 (1.16)
H-C $\equiv$ N	(0)	(0)
F-C $\equiv$ N	3.3	1.09

For the  $F_{1s}$  levels the computed primary and secondary shifts for a methyl substituent are 2.2 eV and 0.3 eV respectively. It is interesting to note that by contrast, the primary effect of methyl for  $C_{1s}$  levels is only 0.4 eV and this large difference in substituent effects at different core levels is also reproduced by the experimental data. The two sets of results for the effect of fluorine on  $C_{1s}$  levels and of methyl on fluorine 1s levels emphasizes once again the short range nature of substituent effects in saturated systems.

(ii) *Binding energies in unsaturated atoms:* A similar analysis has been undertaken for some unsaturated species. Reasonable agreement is again evident

between the calculated and experimental results where available. Introduction of a double or triple bond to the core ionised centre is seen to have little effect on the primary and secondary shifts with the notable exception of the  $O_{1s}$  shifts in the carbonyl compounds. The primary shifts at the carbonyl carbon correlate quite well with those observed at a saturated carbon, the shifts (with respect to  $CH_3$ ) being slightly larger.

(c) **Relaxation energies:** The computational expense etc. of performing calculations on core hole states for each core level has meant that considerable emphasis in the literature has been placed on the interpretation of shifts using Koopmans' Theorem. As we have already indicated the energy lowering due to the relaxation of the valence electrons in going from the neutral molecule to the core ionised species is quite appreciable in absolute terms (of the order of 10-20 eV for first row atoms). Previous investigation in which comparisons have been made between Koopmans' Theorem and hole state calculations have shown that the relaxation energies are closely similar for a given core level in a closely related series of molecules [14]. Experimental data is available however which suggests that for different bonding environments there may be significant contributions to shifts in core binding energies arising from differences in relaxation energies. A particular example is the shift in carbon  $1s$  levels for the methyl and carbonyl carbons in acetaldehyde. Experimental measurements both in the gas and solid phase give a shift of between 2.7 and 2.9 eV [17]. The shift however computed from Koopmans' Theorem is always smaller by approximately .4 eV, independent of the basis set, provided a suitably balanced basis is employed. By contrast the hole state calculations reported here are in excellent agreement with the measured shift in  $C_{1s}$  levels for acetaldehyde thus suggesting a small but significant difference in relaxation energy at the two carbon atoms. In studying an extensive series of molecules covering a number of core levels and a variety of bonding situations we may investigate the importance of differences in relaxation energy in contributing to these shifts.

Figure 2 shows a plot of calculated shifts in binding energies *versus* differences in relaxation energies covering  $C_{1s}$  levels in both saturated and unsaturated systems. It is interesting to note that the relaxation energies span a range of  $\sim 1.5$  eV whilst the corresponding range for the shift is  $\sim 7$  eV, there is a clear trend established between shift and relaxation energy and this has also been noted recently for a very limited series of molecules by Hillier and coworkers [18]. Good linear correlations are observed for the four individual series of molecules studied. The relaxation energies are obviously lowest for those core levels corresponding to the largest shift in binding energy. This is not unreasonable

since the valence electron clouds will already be somewhat contracted in the neutral molecule. The good overall correlation between shift and relaxation energy goes some way to rationalizing why in general the charge potential model works so well. Indeed this is not so unexpected in the light of a recent analysis [19] of the contributions to relaxation energies of local and neighbouring atom contributions with both the former and latter containing charge dependent terms.

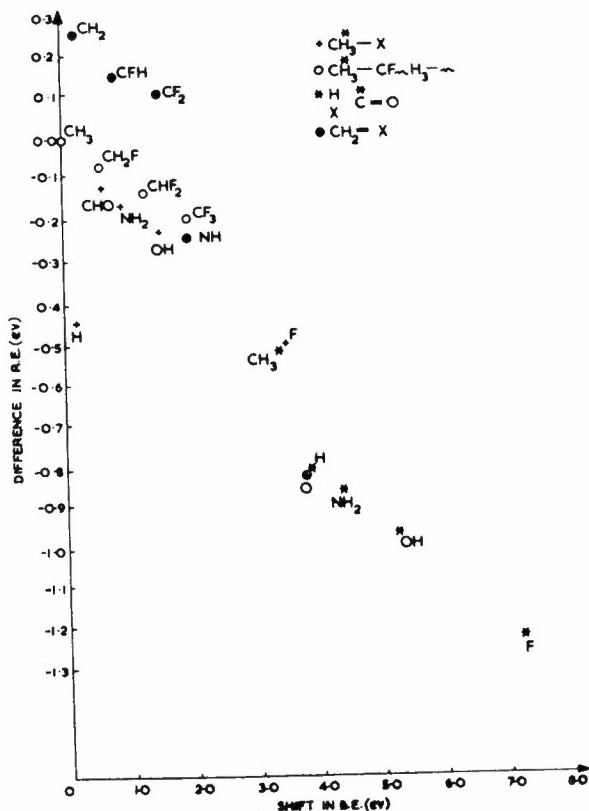


Figure 2: Plot of computed differences in relaxation energy *versus* shifts in binding energy (both with respect to ethane as standard) for some  $C_{1s}$  levels

In a previous investigation we have discussed in detail the constancy of the relaxation energy in the case of the fluoromethanes [14]. In this case the constancy was attributed to the cancellation of charge dependent terms arising from local and nearest neighbour charge distributions.

For the particular case of the simple fluoro-substituted ethanes we have pursued a similar analysis. The data are collected in table 5. Considering firstly the effect of substituents on the  $C^*H_3$  core levels in proceeding from  $CH_3$  to  $CF_3$  as substituent the binding energy increases by 1.96 eV and the relaxation energy decreases by 0.19 eV. From Mulliken population analyses the changes in valence electron population in going from neutral molecule to the hole state have been computed for both the

Table 5

Core	$\Delta BE^a$	$\Delta RE^b$	$\Delta(\Delta_{pop})^c$	$\Delta(\Delta n_i)^d$
$C^*H_3-CH_3$	(0)	(0)	(0)	(0)
$C^*H_3-CFH_2$	0.6	-0.07	.026	0.004
$C^*H_3-CF_2H$	1.26	-0.13	.048	-0.005
$C^*H_3-CF_3$	1.96	-0.19	.060	-0.021
$C^*FH_2-CH_3$	2.96	-0.14	-.033	0.029
$C^*F_2H-CH_3$	6.04	-0.21	-.088	0.089
$C^*F_3-CH_3$	9.13	-0.19	-.169	0.183

(a)  $\Delta BE$  shift in binding energies(b)  $\Delta RE$  difference in relaxation energy(c)  $\Delta_{pop}$  = electronic population  $C^*$  - electronic population  $C$ (d)  $\Delta n_i$  = sum over bonded atoms (populations  $X^*$  - population  $X$ )

atom on which the core hole is located and the nearest neighbour atoms. Whilst the change in nearest neighbour populations are effectively constant in this series there is considerably less electron flow in the case of  $CF_3$  as substituent than for  $CH_3$  and the relaxation energy therefore decreases. By contrast the effect of a methyl substituent in the series  $C^*F_nH_{3-n}-CH_3$  is such that the change in population at the atom concerned and on the nearest neighbours are similar in magnitude and opposite in sign.

(d) Estimation of shifts in binding energies from Koopmans' Theorem and relaxation energy corrections: We have stressed above the importance of electronic relaxation concomitant upon core ionisation and that between certain core holes there is an appreciable calculated error in their shift if this is not taken into consideration. There appears however in these small molecules to be fairly systematic variations in the reorganisation energies of a particular atom in similar environments which may be quite general for the nearest neighbour environment. The possibility then arises of making systematic corrections to core level ionisation energies as calculated from Koopmans' Theorem to estimate the core binding energies. This is of considerable importance for comparison with ESCA studies of larger molecules since computations with a basis set of comparable size would require considerable central processor unit expenditure if the individual core hole states were to be studied. As a suitably complex test case we have studied the biologically important 5-azauracil. Experimental studies [20] of the core binding energies for an extensive range of pyrimidine bases has allowed by direct correlation an assignment of core binding energies in the order:

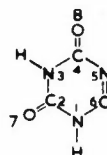
$$C_{1s} \quad C2 > C4 > C6$$

$$N_{1s} \quad N1 > N3 > N5$$

The charge potential model (CNDO/2 charges) and Koopmans' Theorem correctly predict the ordering of  $N_{1s}$  levels, however the shift between  $C4$  and  $C6$  is calculated to be small and in both cases in the opposite sense to that inferred from the experimental correlations. It should be emphasized of course that the measurements refer to the solid phase and that extensive hydrogen bonding may modify the pattern of binding energies that might be expected from the free molecule. This will be discussed in detail elsewhere [20].

In studying relaxation energies as a function of structural type however, it is clear that significant differences in relaxation energies might be expected at different sites within the molecule. Direct hole state calculations have therefore been carried out and, from the series of small molecules exhibiting the appropriate structural features, estimates have been made of differences in relaxation energies, which may be used as corrections to Koopmans' Theorem. The results are presented in table 6. The corrected Koopmans' Theorem results are in excellent agreement with the direct hole state calculations and in complete agreement with the experimentally determined ordering of  $C_{1s}$  and  $N_{1s}$  levels.

Table 6: Shifts in core binding energies (eV) in 5-azauracil



Core	Koopmans' Theorem	Hole State	Estimated RE	Estimated BE <sup>a</sup>
$N1$	2.08	2.52	-0.43 <sup>b</sup>	2.51
$N3$	1.15	1.82	-0.43 <sup>b</sup>	1.58
$N5$	(0)	(0)	(0) <sup>c</sup>	(0)
$C2$	0.83	1.70	-0.60 <sup>d</sup>	1.43
$C4$	-0.19	0.54	-0.60 <sup>d</sup>	0.41
$C6$	(0)	(0)	(0)	(0)
$O7$	0.54	0.92		
$O8$	(0)	(0)		

(a) BE = Koopmans' Theorem - RE

(b) Estimated from  $N^*H_2CHO$  (14.29)(c) Estimated from  $N^*H=CH_2$  (14.72)(d) Estimated from  $NH_2C^*HO$  (10.56)(e) Estimated from  $HN=C^*H_2$  (11.16)

The agreement between the estimated and calculated binding energies is most encouraging and we are currently engaged in further investigations

of a more extensive series encompassing  $C_{1s}$ ,  $N_{1s}$ ,  $O_{1s}$  and  $F_{1s}$  core hole states in comparable chemical environments.

## Acknowledgements

I. Scanlan and J. Muller wish to thank the Science Research Council for research studentships. Thanks are due to the Science Research Council for provision of computing facilities and to Atlas Computer Laboratory personnel for their help in making this investigation possible.

## References

- [1] BAGUS, P.S. (1965). *Phys. Rev.*, **A139**, 619.
- [2] KOOPMANS, T.A. (1933). *Physica*, **1**, 104.
- [3] JOLLY, W.L. and HENDRICKSON, D.N. (1970). *J. Am. Chem. Soc.*, **92**, 1863.
- [4] SIEGBAHN, K., NORDLING, C., JOHANSSON, G., HEDMAN, J., HEDEN, P.F., HAMRIN, K., GELIUS, U., BERGMARK, T., WERME, L.O., MANNE, R. and BAER, Y. (1969). *ESCA Applied to Free Molecules*, Amsterdam: North Holland.
- [5] DITCHFIELD, R., HEHRE, W.J. and POPLE, J.A. (1971). *J. Chem. Phys.*, **54**, 724.
- [6] CLEMENTI, E. and RAIMONDI, D.L. (1963). *J. Chem. Phys.*, **38**, 2686.
- [7] STEWART, R.F. (1969). *J. Chem. Phys.*, **50**, 2485.
- [8] HILLIER, I.H. and SAUNDERS, V.R. (1973). Atlas Computer Laboratory.
- [9] CLEMENTI, E. and POPKIE, H. (1972). *J. Am. Chem. Soc.*, **94**, 4057.
- [10] GELIUS, U., BASILIER, E., SVENSSON, S., BERGMARK, T. and SIEGBAHN, K. (1974). *J. Electron Spectroscopy*, **2**, 405.
- [11] HERZBERG, G. (1966). *Molecular Spectra and Molecular Structure*, Princeton, New Jersey: Van Nostrand.
- [12] MEYER, W. (1973). *J. Chem. Phys.*, **58**, 1017.
- [13] Cf. references [1] and [9].
- [14] ADAMS, D.B. and CLARK, D.T. (1973). *Theoret. Chim. Acta*, **31**, 171.
- [15] CLARK, D.T., FEAST, W.J., KILCAST, D. and MUSGRAVE, W.K.R. (1973). *J. Polymer Sci A1*, **11**, 389.
- [16] CLARK, D.T., KILCAST, D., ADAMS, D.B. and MUSGRAVE, W.K.R. (1972). *J. Electron Spectroscopy*, **1**, 227.
- [17] Unpublished work: cf. reference [4].
- [18] GUEST, M.F., HILLIER, I.H., SAUNDERS, V.R. and WOOD, M.H. (1973). *Proc. Roy. Soc. (London)*, **A333**, 201.
- [19] GELIUS, U. and SIEGBAHN, K. (1972). *Discussions Faraday Soc.*, **54**, 257.
- [20] CLARK, D.T. and LILLEY, D.M.J., (in preparation).



# Localised versus Delocalised Descriptions of the $n-\pi^*$ Excitations in $p$ -Benzoquinone

H.T.Jonkman, G.A.van der Velde and W.C.Nieuwpoort\*

Results of restricted SCF calculations on the closed shell ground-state and open shell  $n-\pi^*$  excited states of  $p$ -benzoquinone will be presented and discussed. The basis set for  $C$  and  $O$  consisted of 6/3 sets of primitive gaussian orbitals contracted to 4/2 sets. For  $H$  2 Gaussians contracted from 3 primitive ones were employed.

In the groundstate the oxygen 'n' orbitals can be described in two equivalent ways: delocalized m.o.'s of odd and even symmetry or m.o.'s localized essentially on each oxygen. In the excited state these two descriptions are no longer equivalent. The SCF excitation energies calculated for the two situations differ drastically, the localized results being some 2.5 eV less than the delocalized ones and in much better agreement with experiment.

## Introduction

In recent work [1,2,3] on the spectroscopy of  $p$ -benzoquinone it is established that the observed lowest triplet and singlet states are all of the  $n-\pi^*$  type. A typical feature of the spectrum is the small splitting between the states corresponding respectively to the excitations  $4b_{1g}(n^2) \rightarrow 2b_{2g}(\pi)$  and  $5b_{2u}(n^2) \rightarrow 2b_{2g}(\pi)$ :  ${}^3A_u - {}^3B_{3g} \sim 0.04$  eV,  ${}^1A_u - {}^1B_{3g} \sim 0.03$  eV. The splitting between corresponding singlet and

triplet states of  $\sim 0.2$  eV is also relatively small. (The  $x$  and  $y$  axis are chosen in the plane of the molecule, the  $x$  axis coinciding with the carbonyl bonds,  $x=b_{3u}, y=b_{2u}, z=b_{1u}$ ). As the existing theoretical treatments [4,5] leave room for improvement we have undertaken a series of *ab initio* SCF-MO calculations on the groundstate as well as on a variety of excited and ionised states of  $p$ -benzoquinone. The calculations were carried out with the program SYMOL written by one of the authors (G.A. vd V.). This program solves the conventional restricted closed and open shell SCF equations in terms of cartesian basis functions and is especially constructed to deal efficiently with molecular symmetry. The contracted basis set employed is listed in table 1. The molecular geometry was taken from [6]. In the following we briefly report and discuss the results obtained for a number of excited states from two sets of calculations. In the first one  $D_{2h}$  symmetry was imposed on the molecular orbitals, in the second one the symmetry was lowered to  $C_{2v}$  with the long axis of the molecule as the  $C_2$  axis.

Table 1: Exponents and contraction coefficients

Atom	Function	Exponent	Coefficient		
C	s	490.404	0.03330498		
		73.7839	0.23233429		
		16.4654	0.81681938		
		4.36231	1.		
		0.565720	1.		
		0.178954	1.		
	p	4.19582	0.21144665		
		0.856630	0.87965386		
		0.200293	1.		
		O	s	898.8000	0.03289584
				135.5780	0.23002992
30.4306	0.81844867				
8.14235	1.				
1.15450	1.				
0.350681	1.				
p	8.17771		0.22416168		
	1.69320		0.87017089		
	0.376417	1.			
	H	s	4.46834	0.15699764	
0.678538			0.90407691		
0.151055			1.		

## Results and Discussion

In table 2 calculated and measured excitation energies are listed. The most striking feature is the large discrepancy between the calculated and experimental positions of the  $n-\pi^*$  excited states when the molecular orbitals are constrained to transform according to the irreducible representations of  $D_{2h}$ . In particular the lowest triplet state is calculated as  $\pi-\pi^*$  and although the lowest singlet states correspond to  $n-\pi^*$  their calculated excitation energies as well as those of the  $n-\pi^*$  triplet states

\* *Chemische Laboratoria der Rijksuniversiteit, Zernikelaan, Paddepoel, Groningen, Netherlands*

are 2 eV larger than the measured values. The calculated splittings between the  $n-\pi^*$  states are about three times larger than observed:  ${}^3A_u-{}^3B_{3g}=0.13$  eV,  ${}^1A_u-{}^1B_{3g}=0.082$  eV, the singlet-triplet splittings are about 0.35 eV.

Table 2: Computed and experimental excitation energies of *p*-benzoquinone (in eV)

Transitions	States	$\Delta_{SCF}^a$		Experi <sup>b</sup> mental
		$D_{2h}$	$C_{2v}$	
$2b_{1u}-2b_{2g}(\pi\pi^*)$	${}^3B_{3u}$	2.49	2.49	
$4b_{1g}-2b_{2g}(n,\pi^*)$	${}^3B_{3g}$	4.21	1.85	2.279
$1b_{3g}-2b_{2g}(\pi\pi^*)$	${}^3B_{1g}$	4.25	4.25	
$5b_{2u}-2b_{2g}(n,\pi^*)$	${}^3A_u$	4.34	(1.85)	2.318
$1b_{3g}-1a_u(\pi\pi^*)$	${}^3B_{3u}$	6.75	6.75	
$2b_{1u}-1a_u(\pi\pi^*)$	${}^3B_{1g}$	7.39	7.39	
$4b_{1g}-2b_{2g}(n,\pi^*)$	${}^1B_{3g}$	4.59	2.08	2.458
$5b_{2u}-2b_{2g}(n,\pi^*)$	${}^1A_u$	4.67	(2.08)	2.516
$1b_{3g}-2b_{2g}(\pi\pi^*)$	${}^1B_{1g}$	5.42	5.24	4.069
$2b_{1u}-2b_{2g}(\pi\pi^*)$	${}^1B_{3u}$	7.13	(5.24)	5.127

(a)  $E_{ground} = -378.392087$  au

(b) See [1,2]

There is no doubt that this situation can be improved substantially by carrying out extensive configuration interaction calculations. However, such an approach at this stage might obscure an important physical origin of the discrepancies observed. The completely filled pair of  $n_g$  and  $n_u$  orbitals obtained in the groundstate calculation (i.e.  $4b_{1g}$  and  $5b_{2u}$ ) consist mainly of  $2p_y$  orbitals centred on the oxygen atoms and they can in fact be transformed to a set of equivalent orbitals  $n_1$  and  $n_2$  that are well localised on the oxygen atoms  $O_1$  and  $O_2$  respectively. In the groundstate there is of course no physical difference between the delocalised and localised representation. They are, however, quite different when states are considered where one  $n$ -electron is excited as in the  $n-\pi^*$  transitions considered. At first sight this difference may not seem very meaningful because the localised hole states which may be indicated by  $\Phi_1 \sim |\dots n_1 n_2 \bar{n}_2 \dots|$  and  $\Phi_2 \sim |\dots n_1 \bar{n}_1 n_2 \dots|$  do not have the required  $g$  or  $u$  symmetry. This property can be recovered by forming  $\Phi_{g,u} \sim \Phi_1 \pm \Phi_2$  which can be seen to be equivalent to the delocalised descriptions  $\Phi_g \sim |\dots n_g n_u \bar{n}_u \dots|$ ;  $\Phi_u \sim |\dots n_g \bar{n}_g n_u \dots|$  as long as the localised orbitals  $n_1$  and  $n_2$  are equivalent i.e. they transform in to each other under inversion as is the case for the localised groundstate orbitals. The equivalence of localised and delocalised descriptions is, however, lost when the localised orbitals in each determinant are no longer related by symmetry:  $\Phi_1' \sim |\dots n_1' n_2 \bar{n}_2 \dots|$ ,  $\Phi_2' \sim |\dots n_1 \bar{n}_1 n_2' \dots|$ ,  $I n_1 = n_2 \neq n_2' = I n_1'$ . For this to occur the orbital

relaxation or polarisation effects that take place on excitation should be significantly different for the two descriptions of the excited states. Exactly this is expected to happen when the equivalent orbitals in the groundstate are found to be well localised because the polarising influence of a localised hole will be larger than that of a distributed one. Since in that case also the matrix element between  $\Phi_1'$  and  $\Phi_2'$  will be small an open shell SCF calculation based on either one of the equivalent determinants  $\Phi_1'$ ,  $\Phi_2'$  should be indicative. In other words if our reasoning is basically correct a calculation in which the symmetry is lowered to  $C_{2v}$  should yield inequivalent localised  $n$ -orbitals instead of delocalised  $g$  and  $u$  symmetry orbitals and it should lower the  $n-\pi^*$  excitation energies by an amount which is much larger than half the splitting of the  $n-\pi^*$  states found in the  $D_{2h}$  calculations ( $\approx 0.1$  eV). At the same time no significant changes are expected for the  $\pi-\pi^*$  excitations because the  $\pi$  orbitals cannot be very well localised.

The data in table 2 show that these expectations are born out quite well, the calculated  $n-\pi^*$  excitation energies are lowered by  $\sim 2.5$  eV with respect to the delocalised results. The singlet-triplet separation is reduced to 0.23 eV again in closer agreement with experiment. The 'n-hole' is strongly localised on one of the oxygen atoms, the  $\pi^*$  orbital stays delocalised. In table 3 the Mulliken gross charges on the atoms are displayed. These numbers indicate

Table 3: Mulliken gross atomic charges in ground and  $n-\pi^*$  excited states

	$O_1$	$C_1'$	$C_2'$	$H_2'$	$H_2$	$C_2$	$C_1$	$O_2$
groundstate	-0.47	0.39	-0.21	0.28	0.28	-0.21	0.39	-0.47
$n-\pi^*(D_{2h})^a$	-0.44	0.36	-0.21	0.28	0.28	-0.21	0.36	-0.44
$n-\pi^*(C_{2v})^a$	-0.52	0.37	-0.21	0.27	0.26	-0.21	0.28	-0.27

(a) averaged over all states of excited configuration

Table 4: Some computed and experimental ionisation energies of *p*-benzoquinone (in eV)

Orbitals	$(D_{2h})^a$	$\Delta_{SCF}$ $D_{2h}$	$C_{2v}$	Experi <sup>b</sup> mental
$2b_{1u}(\pi)$	10.91	10.42	10.06	10.12
$1b_{3g}(\pi)$	11.37	10.53	(10.06)	10.42
$4b_{1g}(n_y^y)$	11.75	11.04	8.60	11.04
$5b_{2u}(n_x^y)$	12.35	11.23	(8.60)	11.51
$1b_{2g}(\pi)$	14.91	14.20	14.20	13.44
$8a_g(n_x^x)$	16.02	15.45	13.40	14.69
$7b_{3u}(n_x^x)$	16.84	16.08	(13.40)	16.10

(a) orbital energies

(b) [8], assignments not conclusive

that the polarisation is of short range and essentially confined to the oxygen atom where the  $n$ -hole is created and its neighbouring carbon atom. We note that in a geometry optimization the nuclear configuration of lowest energy may in fact correspond to  $C_{2v}$  symmetry on the basis of our results which would give rise to static or dynamic (pseudo) Jahn-Teller phenomena in the  $n-\pi^*$  states. In this connection it is of interest that recent Stark measurements on  $p$ -benzoquinone have been interpreted by assuming a double minimum potential for the  $^3B_{3g}$  and  $^1B_{3g}$  states.

The same effects are expected and in fact found in calculations on ionised states (table 4). This has been noted earlier by Bagus and Schaeffer [7] in their calculation on the  $1s$  core excitations of the  $O_2$  molecule. These authors invoke  $C_{\infty v}$  symmetry instead on  $D_{\infty h}$  for  $O_2^+$  in order to obtain restricted HF results that agree with the ESCA data.

We have also carried out calculations on a variety of excited and ionised states of pyrazine where similar results are obtained. The energy shifts are somewhat smaller here as is expected from the fact that the  $n$ -orbitals are found to be less localised in this molecule.

## References

- [1] TROMSDORFF, H.P. (1972). *J. Chem. Phys.*, **56**, 5358.
- [2] VEENVLIET, H. and WIERSMA, D.A. (1973). *Chem. Phys.*, **2**, 69.
- [3] ————— and ————— (1973). *Chem. Phys. Letters*, **22**, 87.
- [4] HUG, W., KUHN, J., SEIBOLD, K., LABHART, H. and WAGNIERE, G. (1971). *Helv. Chim. Acta*, **54**, 1451.
- [5] MERIENNE-LAFORE, M.F., quoted in reference [1].
- [6] TROTTER, J. (1960). *Acta Cryst.*, **13**, 86.
- [7] BAGUS, P.S. and SCHAEFFER, H.F. (1972). *J. Chem. Phys.*, **56**, 224.
- [8] BRUNDLE, C.R., ROBIN, M.R. and KUEBLER, N.A. (1972). *J. Am. Chem. Soc.*, **94**, 1466.  
TURNER, D.W., BAKER, C., BAKER, A.D. and BRUNDLE, C.R. (1970). *Molecular Photoelectron Spectroscopy*, 262, London: Wiley-Interscience.

# The Shapes of $AX_2$ Molecules

J.C.Dobson\*

The theoretical prediction of the shapes of molecules of type  $AX_2$  is reviewed. LCAO-SCF-MO calculations on  $Na_2S$ ,  $Li_2S$  and  $Li_2O$  show that these molecules are linear; while  $H_2S$  is bent, as predicted by the Walsh rules. The SCF results for these four molecules are related to a simple 'ionic' model, and the changing character of their bonding discussed.

The classic work on the shapes of molecules is that of Mulliken [1] and Walsh [2]. They rationalise the shape of various classes of molecule by considering the sum of certain 'molecular orbital energies', identified by Walsh with binding energies or ionisation potentials. But as Coulson and Neilson [3] point out, this is not valid for Hartree-Fock m.o. theory, since the total electronic energy is not equal to the sum of the ionisation potentials, and since the nuclear potential energy must also be considered.

Buenker and Peyerimhoff [4] have recently discussed the theoretical basis of the Mulliken-Walsh rules. They show that the total Hartree-Fock energy may be written

$$E_{\text{tot}} = E_{\text{orb}} + (V_{\text{nn}} - V_{\text{ee}}) \quad (1)$$

where  $E_{\text{orb}}$  is the sum of orbital energies,  $V_{\text{nn}}$  the nuclear repulsion and  $V_{\text{ee}}$  the electron-electron repulsion. For  $AX_2$  molecules, the variation of  $E_{\text{orb}}$  with apex angle  $\theta$  determines the geometry as long as the variation of  $(V_{\text{nn}} - V_{\text{ee}})$  is of the same sign, or smaller in magnitude, at all  $\theta$ . This condition is approximately satisfied for many molecules; but it fails for  $Li_2O$ , which from their SCF-LCAO calculations Buenker and Peyerimhoff predict to be linear in contradiction to the Mulliken-Walsh rules. They ascribe this to its 'ionic' character.

How would we expect an 'ionic' molecule to behave, within the framework of Hartree-Fock theory? Consider a simplified model of the molecule  $M_2L$ , where  $M$  is an element in Group I and  $L$  in Group VI. Let us suppose that the molecular orbitals of  $M_2L$  consist either of pure atomic orbitals for  $L^{2-}$  or for  $M^+$ ; that these orbitals do not change in form as the apex angle  $\theta$  changes; and that electron exchange is unimportant. With these deliberately extreme assumptions, we can estimate the change of the total energy with  $\theta$ . The only changing terms are those describing  $M-M$  interactions, i.e.:

$$V_{\text{ee}}(M-M) = (Z_M - 1)^2(e^2/r) \quad (2)$$

$$V_{\text{nn}}(M-M) = Z_M^2(e^2/r) \quad (3)$$

$$V_{\text{en}}(M-M) = -2Z_M(Z_M - 1)(e^2/r) \quad (4)$$

Here  $V_{\text{en}}$  is the potential energy of the electrons on one  $M^+$  ion in the field of the other  $M$  nucleus,  $r$  is the distance between the  $M$  nuclei, and  $Z_M$  the atomic number of  $M$ ;  $V_{\text{ee}}$  and  $V_{\text{nn}}$  have the same significance as above.

Now the total Hartree-Fock energy can be partitioned as follows:—

$$E_{\text{tot}} = E_e^{(1)} + V_{\text{ee}} + V_{\text{nn}} \quad (5)$$

where  $E_e^{(1)}$  is the total one-electron energy, i.e. the sum of electron kinetic energy and electron-nucleus potential energy. We can therefore test the predictions of the ionic model, equations (2)-(4), against the corresponding SCF quantities. This is shown in table 1 for calculations on  $Li_2O$  and  $Li_2S$ .

For  $Li_2O$ , the ionic model is remarkably successful in predicting the components of the energy: only for the total energy, which is the difference of larger quantities, is there an appreciable error. For  $Li_2S$  the relative error in the components of the energy is still fairly small, but the total energy is badly in error, over-estimating the SCF values for  $\partial E_{\text{tot}}/\partial\theta$  by a factor of 5-10. The deviations are such as to favour a bent configuration, i.e. they tend towards the behaviour predicted by the Walsh rules. Indeed, my calculations suggest that if the  $Li-S$  bond length is increased by about 0.6 au above its equilibrium value  $Li_2S$  should go over to a bent configuration with an apex angle of about  $130^\circ$ .

I have extended this treatment to a number of other molecules: a very brief summary is shown in

\* Department of Chemistry, University of Manchester Institute of Science and Technology, PO Box 88, Manchester, M60 1QD

Table 1: The change with apex angle of the total energy of  $Li_2X$ , as estimated from equations (2)-(4); SCF values in brackets

$f(\theta)$	$f(150)-f(180)$	$f(120)-f(150)$	$f(90)-f(120)$
$Li_2O^a$			
$E_e^{(1)}$	-0.072 (.074)	-0.245 (.253)	-0.532 (.546)
$V_{ee}$	+0.024 (.023)	+0.081 (.083)	+0.177 (.183)
$V_{nn}$	+0.054	+0.183	+0.399
$E_{tot}$	+0.006 (.003)	+0.020 (.014)	+0.044 (.036)
$Li_2S$			
$E_e^{(1)}$	-0.053 (.064)	-0.180 (.207)	-0.392 (.423)
$V_{ee}$	+0.018 (.025)	+0.060 (.074)	+0.131 (.136)
$V_{nn}$	+0.040	+0.135	+0.294
$E_{tot}$	+0.0045 (.0006)	+0.015 (.002)	+0.033 (.088)

(a) SCF values for  $Li_2O$  from [4]; all values in atomic units

table 2, which compares the calculated curvature ( $\partial^2 E_{tot}/\partial\theta^2$ ) at  $\theta = 180^\circ$  for the 'ionic model' and the SCF computations. In the upper part, we see that a restricted  $sp$ -basis set for  $Li_2S$  gives a calculation in better agreement with the ionic model than the original calculation with polarisation functions on  $S$ . In the lower part of the table, we see that the ionic model fails completely for  $H_2S$  (as might be expected); for  $Na_2S$  it appears to be about as successful as for  $Li_2S$ , although the details suggest that the comparison chosen is an even more stringent test of the ionic model in this case.

Table 2: A comparison of the curvature ( $\partial^2 E_{tot}/\partial\theta^2$ ) at  $\theta = 180^\circ$ , estimated from the 'ionic model' and from the SCF calculations

Molecule	Basis Set	$(\partial^2 E_{tot}/\partial\theta^2)_{180} \times 10^{-6} \text{ au deg}^{-2}$		
		SCF	ionic	SCF/ionic
$Li_2O^a$	$sp$	5.8	12.2	0.48
$Li_2S$	$sp$	3.2	9.6	0.33
$Li_2S$	$spdf$	1.4	9.6	0.15
$H_2S$	$spdf$	-129.	+15.2	-8.5
$Na_2S$	$sp$	2.9	8.3	0.35

(a) SCF value from [4]

I do not intend to develop this method as yet another scale of 'ionic' versus 'covalent' behaviour. But it does seem to be a rather sensitive device for detecting deviations from 'perfect ionic behaviour' in compounds which, according to chemical intuition, we would expect to be rather well described by an ionic model. It also helps to rationalise the shape of those molecules for which the Mulliken-Walsh rules break down.

## References

- [1] MULLIKEN, R.S. (1942). *Revs. Modern Phys.*, **14**, 204.
- [2] WALSH, A.D. (1953). *J. Chem. Soc.*, 2260.
- [3] COULSON, C.A. and NEILSON, A.H. (1963). *Discussions Faraday Soc.*, **35**, 71.
- [4] BUENKER, R.J. and PEYERIMHOFF, S.D. (1966). *J. Chem. Phys.*, **45**, 3682.

# A Study of the Structure and Properties of Clusters of Lithium Atoms

A.D.Tait\*

An optimised Floating Gaussian Orbital model has been used in the study of  $(Li)_{2n}$  and  $(Li)_{2n-1}^+$  for  $1 \leq n \leq 3$ . The nuclear geometry of the smaller systems has been optimised. Multipole moments, potential, electric field, and electric field gradients have been evaluated at an  $Li^-$  nucleus in each system studied. Trends in the behaviour of these properties and in the optimised orbital parameters have been observed.

## Introduction

The process of condensation in expanding vapour beams has been known for some time [1]. Several observations of this process occurring in molecular beams of alkali metal vapours have been made in recent years [2,3]. Clusters of from two to twelve atoms, produced during condensation have been detected in sodium vapour [3] and the ionisation potentials have been measured for these and some other clusters. The structure of such clusters and the number of atoms required to produce a metallic cluster is still in doubt.

The lightest of the alkali metals is lithium and it is the most difficult to examine experimentally [3]. However lithium is very amenable to theoretical study. A wide range of calculations on  $Li_2$  [4-11] and one or two on larger systems have been reported [12-14]. This paper contains the results of preliminary studies on a number of the smaller lithium clusters. The neutral molecules  $Li_2$ ,  $Li_4$ ,  $Li_8$ , and the ions  $Li^+$ ,  $Li_3^+$ ,  $Li_5^+$  have been studied using a Floating Spherical Gaussian (FSGO) model [15]. The equilibrium geometries of  $Li_2$  and  $Li_3^+$  have been determined. Optimum internuclear distances for highly symmetric arrangements of the nuclei of the other systems are also presented. Multipole moments, potentials, electric fields, and electric field gradients evaluated at a nucleus are also given.

This work is continuing with the aim of establishing the equilibrium nuclear geometry of each species. An examination of larger clusters is being undertaken with a view to determining when the metallic structure becomes apparent.

## Theory

The basis of the FSGO model [15-18] is the expansion of a set of orthonormal molecular orbitals in terms of a set of spherical gaussian orbitals, each of the form

$$\omega_{\mu}(\alpha_{\mu}, R_{\mu}) = (2\alpha_{\mu}/\pi)^{3/4} \exp(-\alpha_{\mu}(r-R_{\mu})^2) \quad (1)$$

In equation (1)  $R_{\mu}$  is the position vector of orbital  $\omega_{\mu}$  with exponent  $\alpha_{\mu}$ .  $r$  is the electronic position vector. The total molecular energy corresponding to a single determinant wavefunction composed of the orthonormal molecular orbitals is then minimised with respect to some or all of the orbital position vectors and exponents within the usual Hartree-Fock-LCAO-SCF method [19].

In the simplest application of the FSGO model [15] each pair of electrons in a closed shell molecule is associated with a single gaussian orbital  $\omega_{\mu}$ . As the associated density matrix is the inverse of the overlap matrix between the basis orbitals no iteration is required to minimise the molecular energy with respect to the coefficients of these orbitals in the molecular orbitals [15]. In this form a single spherical gaussian function is associated with each heavy nucleus (i.e. not with protons) and the remaining orbitals are distributed amongst the bonds (and lone pairs if present).

An extension of the method [16-18] is the use of two spherical gaussians situated on each heavy nucleus. This improves the description of the electron density at the nuclei and causes a substantial lowering of the molecular energy [18]. However the density matrix is no longer the inverse of the overlap matrix and an iterative solution of the SCF equations is necessary to determine the orbital coefficients and electronic energy.

\* Department of Mathematics, University of Nottingham, Nottingham, NG7 2RD  
(present address) Control Data Canada Limited, 1855 Minnesota Court, Streetsville, Mississauga, Ontario, Canada

The operators required in the calculation of multipole moments, the potential and its derivatives are defined in a paper of Neumann and Moskowitz [20]. Atomic units are used throughout the present work. All the calculations were performed using the OPIT system developed at the University of Nottingham [21-23].

## Calculations

$Li^+$ : The wavefunction for this ion was constructed from two spherical gaussian orbitals situated at the nucleus. The optimised exponents, corresponding energy and non-zero one-electron properties are given in table 1.

Table 1: Optimised exponents, energy and non-zero one-electron properties for the  $Li^+$  ion

Electronic energy	-6.980429
Orbital exponents	
$\alpha_1$	10.1246
$\alpha_2$	1.3902
One-electron properties	
$Q_{YY}$	-0.2694
$\langle r^2 \rangle$	0.8081
$\langle \frac{1}{r} \rangle$	5.2050
potential	-5.2050

$Li_2$ : A basis of five FSGOs was used for this molecule. Initially the orbitals were distributed with two at each nucleus and one at the mid-point of the internuclear axis. The optimisation was constrained so that the orbitals lay on the internuclear axis. The optimised exponents, orbital positions, energy and non-zero one-electron properties

Table 2: Optimised exponents and orbital positions, energies and non-zero one-electron properties for the  $Li_2$  molecule at its equilibrium bond length

Total energy	-14.354331
Equilibrium bond length	5.24
Optimised orbital parameters	
$(\alpha_1, Z_1)$	10.2335, $\pm 2.6200$
$(\alpha_2, Z_2)$	1.4056, $\pm 2.6239$
$(\alpha_3, Z_3)$	0.0426, 0.0000
One-electron properties evaluated at (0,0,2.62)	
$Q_{XX}, Q_{YY}$	-12.6971
$Q_{ZZ}$	1.4644
$\langle r^2 \rangle$	106.303
$R_{YYZ}, R_{XXZ}$	33.2664
$R_{ZZZ}$	-11.5105
$\langle \frac{1}{r} \rangle$	6.1381
potential	-5.5656
$q_{XX}, q_{YY}$	$1.46 \times 10^{-3}$
$q_{ZZ}$	$-2.92 \times 10^{-3}$

at the equilibrium bond length of 5.24 bohr are shown in table 2.

$Li_3^+$ : The equilibrium geometry of this molecular ion was found to be an equilateral triangle with a side of 5.84 bohr. The basis of seven FSGOs was arranged with two functions at each nucleus and one at the centroid of the triangle. Only the orbital exponents were optimised. The results of this calculation are summarised in table 3.

Table 3: Energy, optimised exponents, and non-zero one-electron properties for  $Li_3^+$  at its equilibrium geometry. The spherical polar co-ordinates of the nuclei are (0,0,0), (5.84,30,0), and (5.84,30,180)

Total energy	-21.400171
Optimised orbital exponents	
$\alpha_1$ (at nuclei)	10.2042
$\alpha_2$ (at nuclei)	1.4014
$\alpha_2$ (at centroid)	0.05274
One-electron properties evaluated at (0,0,0)	
$\mu_Z$	3.3717
$Q_{XX}$	6.8313
$Q_{YY}$	-10.6692
$Q_{ZZ}$	18.1998
$\langle r^2 \rangle$	190.272
$R_{YYZ}$	-35.9735
$R_{ZZZ}$	77.9819
$R_{XXZ}$	52.4831
$\langle \frac{1}{r} \rangle$	6.4142
potential	-5.3869
$E_Z$	0.03077
$q_{XX}$	$-8.05 \times 10^{-3}$
$q_{YY}$	$-2.8 \times 10^{-4}$
$q_{ZZ}$	$8.33 \times 10^{-3}$

Table 4: Energy, optimised exponents, and non-zero one-electron properties for  $Li_4$ . The nuclei are situated at (2.85,0,2.85), (2.85,0,-2.85), (-2.85,0,-2.85), and (-2.85,0,2.85)

Total energy	-28.577996
Optimised orbital exponents	
$\alpha_1$ (at nuclei)	10.3726
$\alpha_2$ (at nuclei)	1.4269
$\alpha_3$ (at mid-point of side)	0.04986
$\alpha_4$ (at centroid)	0.03632
One-electron properties evaluated at (2.85,0,2.85)	
$Q_{XX}, Q_{ZZ}$	-17.7682
$Q_{YY}$	-21.9947
$\langle r^2 \rangle$	447.411
$R_{XXX}, R_{ZZZ}$	151.918
$R_{XYY}, R_{YYZ}$	62.6849
$R_{XXZ}, R_{XZZ}$	50.6392
$\langle \frac{1}{r} \rangle$	6.9516
potential	-5.5268
$E_X, E_Z$	0.1250
$q_{XX}, q_{ZZ}$	30.0743
$q_{YY}$	29.9281
$q_{XZ}$	$-8.59 \times 10^{-5}$

$Li_4$ : Previous calculations [13,14] on this molecule indicate that the equilibrium geometry is a square. In the present work the energy of a square arrangement of the nuclei is a minimum when the square has a side of length 5.70 bohrs. A basis of thirteen FSGOs permitted each  $Li_2$  fragment of  $Li_4$  in a square geometry to be represented by five FSGOs. The arrangement being two per nucleus, one at the mid-point of each side and one at the centroid. And again only the orbital exponents were optimised and these together with the other results for  $Li_4$  are presented in table 4.

$Li_5^+$ : The square planar geometry chosen for this ion is one of several possible nuclear geometries. Four nuclei are situated at the corners of a square and the fifth at the centroid. The basis of fourteen spherical gaussians was arranged as for  $Li_4$ , and an additional orbital was placed on the nucleus at the centroid. Only the orbital exponents were optimised. A square of side 7.40 bohrs produced the lowest energy, and the results are given in table 5.

Table 5: Energy, optimised exponents, and non-zero one-electron properties for  $Li_5^+$ . The nuclei are situated at (0,0,0), (R,0,R), (R,0,-R), (-R,0,-R), and (-R,0,R), with  $R = 3.7$

Total energy	-35.563010
Optimised orbital exponents	
$\alpha_1$ (at centroid)	10.2883
$\alpha_2$ (at centroid)	1.4148
$\alpha_3$ (at remaining nuclei)	10.2460
$\alpha_4$ (at remaining nuclei)	1.4077
$\alpha_5$ (at mid-point of sides)	0.05946
One-electron properties evaluated at (R,0,R)	
$\mu_X, \mu_Y$	-3.7000
$Q_{XX}, Q_{ZZ}$	16.2808
$Q_{YY}$	-18.5813
$Q_{XZ}$	13.6900
$\langle r^2 \rangle$	725.280
$R_{XXX}, R_{ZZZ}$	-79.4105
$R_{XYY}, R_{YYZ}$	68.7509
$R_{XXZ}, R_{XZZ}$	-60.2388
$\langle \frac{1}{r} \rangle$	7.0602
potential	-5.3893
$E_X, E_Z$	0.1516
$q_{XX}, q_{ZZ}$	0.2473
$q_{YY}$	0.1703
$q_{XZ}$	-0.03533

$Li_6$ : The hexagonal arrangement of the nuclei chosen for  $Li_6$  exhibited a minimum energy at a 'nearest neighbour' distance of 5.55 bohr. A basis of eighteen spherical gaussians was arranged with two at each nucleus and one at the mid-point of each side of the hexagon. Optimised exponents, energies and properties are given in table 6.

Table 6: Energy, optimised exponents, and non-zero one-electron properties for  $Li_6$ . The spherical polar co-ordinates of the nuclei are (R,0,0), (R,60,0), (R,120,0), (R,180,0), (R,120,180), and (R,60,180) with  $R = 5.55$  bohr, i.e. a hexagon of side 5.55 bohr

Total energy	-43.070259
Optimised orbital exponents	
$\alpha_1$ (at nuclei)	10.3193
$\alpha_2$ (at nuclei)	1.4182
$\alpha_3$ (at mid-point of side)	0.04363
One-electron properties evaluated at (R,0,0)	
$Q_{XX}, Q_{ZZ}$	-12.5003
$Q_{YY}$	-37.3195
$\langle r^2 \rangle$	1171.2
$R_{YYZ}$	207.123
$R_{ZZZ}$	208.130
$R_{XXZ}$	69.3765
$\langle \frac{1}{r} \rangle$	7.5445
potential	-5.5690
$E_Z$	0.1780
$q_{XX}$	30.1983
$q_{YY}$	30.1375
$q_{ZZ}$	30.2342

## Discussion

Both  $Li^+$  and  $Li_2$  have singlet ground states and these can be properly described by a single determinant wavefunction [19]. The energies obtained for these systems using an FSGO wavefunction are 96% of the values obtained using much more accurate implementation of the one-particle approximation [4,25]. The experimentally observed value of the  $Li_2$  equilibrium bond length is 5.05 bohr [24]. The present value of 5.24 bohr represents an increase of about 4% in accordance with previous calculations using FSGOs [15].

Of the other systems examined, only  $Li_3^+$  and  $Li_6$  are stable with respect to dissociation to  $Li_2 + Li^+$  and  $3Li_2$  respectively. Earlier calculations on  $Li_4$  [13,14] predict the equilibrium geometry to be a square of side 5.47 bohr which is barely stable (-0.02 hartrees) relative to dissociation to  $2Li_2$ . The present calculations indicate that  $Li_4$  has a square conformation with a side of 5.70 bohr giving a minimum energy. However this is not stable relative to  $2Li_2$ . The cause of this result is probably due to the non-optimisation of the orbital positions. The same argument applies to  $Li_5^+$  which is predicted to be unstable relative to  $2Li_2 + Li^+$ .

The optimised exponents given in tables 1-6 exhibit very small variations from one system to another. This variation could well be reduced by the optimisation of the orbital positions.



Of the properties presented it is seen that the value of  $\langle \frac{1}{r} \rangle$  is tending slowly towards a limit. The values of  $\langle \frac{1}{r} \rangle$ , the potential, and electric field gradients divide the systems into two groups. Smooth curves can be drawn through either the ionic values or the molecular values of  $\langle \frac{1}{r} \rangle$ , the potential is reasonably constant at about 5.5 au for the molecules and is less than 5.4 au for the ions. For the ions the electric field gradients are small, and large for the molecules with the exception of  $Li_2$ . It is interesting to note that  $E_z$ , the z-component of the force on the nucleus increases from 0 for  $Li^+$  and  $Li_2$  to 0.178 au for  $Li_6$ . The value of the electric field at a nucleus should be zero at the equilibrium geometry. The calculated values indicate that although the energy minimum has been reached some further optimisation of the basis is required to reduce the electric field to zero. The values of the potential and its derivatives are susceptible to the electron density at the nucleus, and it is poorly described by the FSGO model. However there is evidence [26] to support the suggestion that the given values are about 60% of the result of more accurate calculations.

It is important to acknowledge the possible existence of molecules and ions with different geometries to those studied and that these may have lower energies [14]. It is also true that non-singlet states may have lower energies.

## Conclusion

The FSGO model with two orbitals on the heavy nuclei predicts stable configurations of  $Li_3^+$ ,  $Li_4$ ,  $Li_5^+$ , and  $Li_6$ . However only  $Li_3^+$  and  $Li_6$  are stable with respect to combinations of  $Li_2$  and  $Li^+$ . It is felt that the instability of  $Li_4$  and  $Li_5^+$  is due to the non-optimisation of the orbital positions. The optimisation of the orbital positions will produce a lower energy for all of the systems examined. These calculations are currently in progress. In addition a search for different stable configurations continues. The size of clusters examined is being increased with the intention of determining when the three dimensional geometry becomes desirable and when an energy band structure in the orbital eigenvalues becomes apparent. Relatively crude calculations [27] indicate that a cluster of at least forty atoms is required before a metallic structure will be observed.

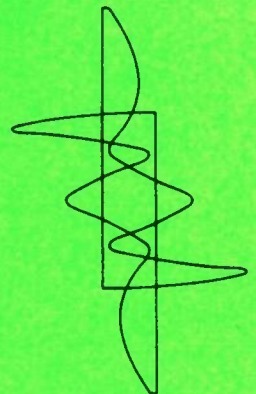
## Acknowledgements

It is a pleasure to acknowledge the keen interest taken by Professor G.G. Hall in this work and to thank the Science Research Council for financial support.

## References

- [1] OSWATITSCH, K.L. (1942). *Z. Angew. Math. Mech.*, **22**, 1.
- [2] ROBBINS, E.J., LECKENBY, R.E. and WILLIS, P. (1967). *Adv. Phys.*, **16**, 739.
- [3] FOSTER, P.J., LECKENBY, R.E. and ROBBINS, E.J. (1969). *J. Phys. B*, **2**, 478.
- [4] RICHARDS, W.G., WALKER, T.E.H. and HINKLEY, R.K. (1971). *A Bibliography of ab initio Molecular Wavefunctions*, 54, Oxford: Clarendon Press.
- [5] KOCKEL, B. and GRUN, N. (1969). *Z. Naturforsch.*, **24**, 731.
- [6] KUTZELNIGG, W. and GELUS, M. (1970). *Chem. Phys. Letters*, **7**, 296.
- [7] RUSSEGER, P., LISCHKA, H. and SCHUSTER, P. (1971). *Chem. Phys. Letters*, **12**, 292.
- [8] YDE, P.B., THOMSON, K. and SWANSTROM, P. (1972). *Mol. Phys.*, **23**, 691.
- [9] CHANDRA, A.K. and SUNDAR, R. (1972). *Chem. Phys. Letters*, **14**, 577.
- [10] HERNANDEZ, A. and LUDENA, E.V. (1972). *J. Chem. Phys.*, **57**, 5350.
- [11] PFEIFFER, G.V. and ELLISON, F.O. (1965). *J. Chem. Phys.*, **43**, 3405.
- [12] RAY, N.K. (1970). *J. Chem. Phys.*, **52**, 463.
- [13] COMPANION, A.L. (1969). *J. Chem. Phys.*, **50**, 1165.
- [14] PICKUP, B.T. (1973). *Proc. Roy. Soc. (London)*, **A333**, 69.
- [15] FROST, A.A. (1967). *J. Chem. Phys.*, **47**, 3707.
- [16] ROUSE, R.A. and FROST, A.A. (1969). *J. Chem. Phys.*, **50**, 1705.
- [17] CHU, S.Y. and FROST, A.A. (1971). *J. Chem. Phys.*, **54**, 764.
- [18] FORD, B., HALL, G.G. and PACKER, J.C. (1970). *Int. J. Quantum Chem.*, **4**, 533.
- [19] MCWEENY, R. and SUTCLIFFE, B.T. (1969). *Methods of Molecular Quantum Mechanics*, 110, London: Academic Press.
- [20] NEUMANN, D. and MOSKOWITZ, J.W. (1968). *J. Chem. Phys.*, **49**, 2056.
- [21] PACKER, J.C. and BRAILSFORD, D.F. (1973). *Comp. Phys. Comm.*, **5**, 123.
- [22] BRAILSFORD, D.F. and PRENTICE, J.A. (1973). *Comp. Phys. Comm.*, **5**, 136.
- [23] BRAILSFORD, D.F. and HYLTON, J. (1973). *Chem. Phys. Letters*, **18**, 595.
- [24] HERZBERG, G. (1950). *Spectra of Diatomic Molecules*, 546, London: Van Nostrand Reinhold.
- [25] WEISS, A.W. (1961). *Phys. Rev.*, **122**, 1826.
- [26] TAIT, A.D. and DIXON, M., (to be published).
- [27] LASAROV, D. and MARKOV, P. (1969). *Surface Sci.*, **14**, 320.

# PARTICIPANTS



## PARTICIPANTS

- ADAMS, D.B. Department of Chemistry, University of Durham, South Road,  
Durham, DH1 3LE
- AHLRICHS, R. Institut für Physikalische Chemie und Elektrochemie, Universität  
Karlsruhe, Kaiserstrasse 12, 75 Karlsruhe, West Germany
- BALINT-KURTI, G.G. School of Chemistry, University of Bristol, Cantock's Close,  
Bristol, BS8 1TS
- BELL, R.J. Division of Quantum Metrology, National Physical Laboratory,  
Teddington, Middlesex, TW11 0LW
- BISHOP, D.M. Chemistry Department, University of Ottawa, Ottawa, K1N 6N5,  
Canada
- BOSANAC, S. School of Chemistry, University of Bristol, Cantock's Close,  
Bristol, BS8 1TS
- BRAILSFORD, D.F. Department of Mathematics, University of Nottingham, University  
Park, Nottingham, NG7 2RD
- BRANDSEN, B.H. Department of Physics, University of Durham, South Road,  
Durham, DH1 3LE
- BROWN, J. Atlas Computer Laboratory (Science Research Council), Chilton,  
Didcot, Oxfordshire, OX11 0QY
- CHILD, M.S. Theoretical Chemistry Department, University of Oxford, 1 South  
Parks Road, Oxford, OX1 3TG
- CHIU, M.F. Atlas Computer Laboratory (Science Research Council), Chilton,  
Didcot, Oxfordshire, OX11 0QY
- CLARK, A.P. Department of Physics, University of Stirling, Stirling, FK9 4LA,  
Scotland
- COLLINS, M.P.S. Department of Theoretical Chemistry, University of Lancaster,  
Bailrigg, Lancaster, LA1 4YA
- CONNELLY, M.J. Centre for Computer Studies, University of Leeds, Leeds, LS2 9JT
- CONNOR, J.N.L. Department of Chemistry, University of Manchester, Brunswick  
Street, Manchester, M13 9PL
- DAHL, J.P. Department of Chemical Physics, Technical University of Denmark,  
DTH 301, DK-2800 Lyngby, Denmark
- DARKO, T. Department of Chemistry, University of Manchester, Brunswick  
Street, Manchester, M13 9PL

- DAVIES, D.W. Department of Chemistry, Haworth Building, University of Birmingham, Birmingham, B15 2TT
- del CONDE, G. Department of Chemistry, Haworth Building, University of Birmingham, Birmingham, B15 2TT
- DIERCKSEN, G.H.F. Max-Planck-Institut für Physik und Astrophysik, Föhringer Ring 6, 8 München 40, West Germany
- DOBSON, J.C. Department of Chemistry, University of Manchester Institute of Science and Technology, PO Box 88, Manchester, M60 1QD
- DUKE, B.J. Department of Chemistry, University of Lancaster, Bailrigg, Lancaster, LA1 4YA
- ELLIS, D.J. Department of Physics, University of Leicester, Leicester, LE1 7RH
- GERRATT, J. Department of Theoretical Chemistry, University of Bristol, Cantock's Close, Bristol, BS8 1TS
- GIANTURCO, F.A. Istituto di Chimica Fisica, Università di Pisa, via Risorgimento 35, 56100 Pisa, Italy
- GITTINS, M.A. School of Molecular Sciences, University of Warwick, Coventry, CV4 7AL
- GOPINATHAN, M.S. Theoretical Chemistry Department, University of Oxford, 1 South Parks Road, Oxford, OX1 3TG
- GRANT, I.P. Mathematical Institute, University of Oxford, 24 St. Giles, Oxford, OX1 3LB
- GREENWOOD, H.H. Computer Centre, University of Keele, Keele, North Staffordshire, ST5 5BG
- GUEST, M.F. Atlas Computer Laboratory (Science Research Council), Chilton, Didcot, Oxfordshire, OX11 0QY
- HAIGH, C.W. Department of Chemistry, University College of Swansea, Singleton Park, Swansea, SA2 8PP, Wales
- HILLIER, I.H. Department of Chemistry, University of Manchester, Brunswick Street, Manchester, M13 9PL
- HIRST, D.M. Department of Molecular Sciences, University of Warwick, Coventry, CV4 7AL
- JONATHAN, N.B.H. Department of Chemistry, University of Southampton, Southampton, SO9 5NH
- KENDRICK, J. Department of Chemistry, University of Manchester, Brunswick Street, Manchester, M13 9PL
- KENNEDY, N.F. Department of Chemistry, University of Glasgow, Glasgow, G12 8QQ, Scotland

- KRAEMER, W.P. Max-Planck-Institut für Physik und Astrophysik, Föhringer Ring 6,  
8 München 40, West Germany
- LAVERY, R. Theoretical Chemistry Department, University of Manchester,  
Brunswick Street, Manchester, M13 9PL
- LAWLEY, K.P. Department of Chemistry, University of Edinburgh, West Mains  
Road, Edinburgh, EH9 3JJ, Scotland
- LEWIS, J.W.E. Atlas Computer Laboratory (Science Research Council), Chilton,  
Didcot, Oxfordshire, OX11 0QY
- LIEBMANN, S.P. Department of Molecular Sciences, University of Warwick, Coventry,  
CV4 7AL
- MACKRODT, W.C. ICI Corporate Laboratory – Bozodown, Bozodown House, Whit-  
church Hill, Reading, RG8 7PF
- MADDEN, P.R. School of Molecular Sciences, University of Sussex, Falmer,  
Brighton, BN1 9QJ
- MALLION, R.B. Theoretical Chemistry Department, University of Oxford, 1 South  
Parks Road, Oxford, OX1 3TG
- MASHAT, M.M. Department of Physics, University of Leicester, Leicester, LE1 7RH
- MEYER, W. Institut für Physikalische Chemie, Universität Mainz, 65 Mainz,  
POB 3980, West Germany
- MILLER, W.H. Inorganic Material Research Division, Lawrence Berkeley Labora-  
tory and Department of Chemistry, University of California,  
Berkeley, California 94720, USA
- MOSER, C. Centre Européen de Calcul Atomique et Moléculaire, Bâtiment 506,  
Université de Paris XI, 91405 Orsay, France
- MULLER, J. Department of Chemistry, University of Durham, South Road,  
Durham, DH1 3LE
- MURPHY, S.P. Department of Physical Chemistry, University of Cambridge,  
Lensfield Road, Cambridge, CB2 1EP
- NALEWAY, C.A. Department of Chemistry, University of Manchester, Brunswick  
Street, Manchester, M13 9PL
- NIEUWPOORT, W.C. Chemische Laboratoria der Rijksuniversiteit, Zernikelaan, Padde-  
poel, Groningen, Netherlands
- O'LEARY, B. Theoretical Chemistry Department, University of Oxford, 1 South  
Parks Road, Oxford, OX1 3TG
- OVERILL, R.E. Department of Chemistry, University of Leicester, University Road,  
Leicester, LE1 7RH

- PALMER, M.H. Department of Chemistry, University of Edinburgh, West Mains Road, Edinburgh, EH9 3JJ, Scotland
- PEEL, J.B. Department of Chemistry, University of Southampton, Southampton, SO9 5NH
- PERCIVAL, I.C. Department of Physics, University of Stirling, Stirling, FK9 4LA, Scotland
- POMPHREY, N. Department of Physics, University of Stirling, Stirling, FK9 4LA, Scotland
- PYPER, N.C. Department of Theoretical Chemistry, University of Bristol, Cantock's Close, Bristol, BS8 1TS
- RICHARDS, D. Mathematics Department, Open University, Walton Hall, Milton Keynes, Buckinghamshire, MK7 6AA
- RICHARDSON, N.V. Inorganic Chemistry Laboratory, University of Oxford, South Parks Road, Oxford, OX1 3QR
- ROBB, M.A. Department of Chemistry, Queen Elizabeth College, University of London, Campden Hill, Kensington, London, W8 7AH
- ROBERTS, H.G. FF. Glamorgan Polytechnic, Llantwit Road, Treforest, Pontypridd, Glamorgan, CF37 1DL, Wales
- RØEGGEN, I.A. Theoretical Chemistry Department, University of Oxford, 1 South Parks Road, Oxford, OX1 3TG
- ROOS, B.O. Institute of Theoretical Physics, University of Stockholm, Vanadisvägen 9, S-113 46 Stockholm, Sweden
- SAUNDERS, V.R. Atlas Computer Laboratory (Science Research Council), Chilton, Didcot, Oxfordshire, OX11 0QY
- SCANLAN, I.W.S. Department of Chemistry, University of Durham, South Road, Durham, DH1 3LE
- SCHAEFER, H.F. III Lawrence Berkeley Laboratory and Department of Chemistry, University of California, Berkeley, California 94720, USA
- SCOTT, J. Department of Chemistry, University of York, Heslington, York, YO1 5DD
- SHARMA, C.S. Department of Mathematics, Birkbeck College, University of London, Malet Street, London, WC1E 7HX
- SHENTON, I.C. Department of Chemistry, University of Manchester, Brunswick Street, Manchester, M13 9PL
- SIEGBAHN, P.E.M. Department of Chemistry, University of California, Berkeley, California 94720, USA

- SMITH, K. Centre for Computer Studies, University of Leeds, Leeds, LS2 9JT
- STEINER, E. Department of Chemistry, University of Exeter, Stocker Road,  
Exeter, EX4 4QD
- SUTCLIFFE, B.T. Department of Chemistry, University of York, Heslington, York,  
YO1 5DD
- SUTCLIFFE, F.K. Department of Colour Chemistry and Dyeing, University of Leeds,  
Leeds, LS2 9JT
- TABOR, M. School of Chemistry, University of Bristol, Cantock's Close,  
Bristol, BS8 1TS
- TAIT, A.D. Department of Mathematics, University of Nottingham, Notting-  
ham, NG7 2RD
- THOMSON, C. Department of Chemistry, University of St Andrews, North Haugh,  
St Andrews, KY16 9ST, Scotland
- van der VELDE, G.A. Chemische Laboratoria der Rijksuniversiteit, Zernikelaan, Padde-  
poel, Groningen, Netherlands
- VEILLARD, A. Centre National de la Recherche Scientifique, Université Louis  
Pasteur, BP 296R8, 67 Strasbourg, France
- von NIESSEN, W. Lehrstuhl für Theoretische Chemie der Technischen Universität  
München, Arcisstrasse 21, 8 München 2, West Germany
- WAHL, A.C. Chemistry Division, Argonne National Laboratory, 9700 South  
Cass Avenue, Argonne, Illinois 60439, USA
- WALSH, B.C. Department of Chemistry, University of Exeter, Stocker Road,  
Exeter, EX4 4QD
- WESTON, G.J. School of Studies in Chemistry, University of Bradford, Bradford,  
Yorkshire, BD7 1DP
- WHITEHEAD, M.A. Theoretical Chemistry Department, University of Oxford, 1 South  
Parks Road, Oxford, OX1 3TG
- WILLIAMS, D.J. School of Studies in Chemistry, University of Bradford, Bradford,  
Yorkshire, BD7 1DP
- WILSON, S. Department of Theoretical Chemistry, University of Bristol,  
Cantock's Close, Bristol, BS8 1TS
- WISHART, B.J. Department of Chemistry, University of St Andrews, North Haugh,  
St Andrews, KY16 9ST, Scotland
- YARDLEY, R.N. School of Chemistry, University of Bristol, Cantock's Close,  
Bristol, BS8 1TS